The palaeodietary and morphometric responses of Pleistocene spotted hyaena (*Crocuta crocuta* Erxleben, 1777) to environmental changes in Europe

Volume I

Angharad Kathrine Jones

Royal Holloway University of London

PhD Geography

i. Declaration of authorship

I, Angharad Jones, hereby declare that this thesis and the work presented in it is entirely my own. Where I have consulted the work of others, this is always clearly stated.

Signed: _____ Date: _____

ii. Abstract

Spotted hyaena (*Crocuta crocuta* Erxleben, 1777) are today restricted to sub-Saharan Africa, yet during the Pleistocene, they ranged throughout Eurasia and were subject to widely fluctuating climatic and environmental conditions. This study assesses palaeodietary and morphometric variability in the spotted hyaena against this backdrop of Pleistocene palaeoenvironmental change in Europe. The study comprises first a detailed examination of modern *Crocuta* from sub-Saharan Africa, in order to establish baseline parameters of body mass variation, sexual dimorphism, tooth wear/breakage and the impact of competition and local environment. It is followed by a detailed examination of fossil *Crocuta* from the Middle and Late Pleistocene of Britain, paired with a study of Late Pleistocene *Crocuta* from Ireland, Belgium, Spain, Italy, Austria, the Czech Republic and Serbia.

Influences upon present-day *C. crocuta* population biomass were compared with those of its main competitor, the lion (*Panthera leo*), revealing a stronger relationship between environmental conditions and *C. crocuta* biomass, than between the environment and *P. leo*. Morphometric analysis of present-day *C. crocuta* revealed ontogenetic variation in the craniodental and post-cranial elements, in addition to a lack of sexual size dimorphism in many features. Finally, the frequency of broken teeth varied according to sex and age. The results of these analyses were then used to aid interpretation of the fossil assemblages.

Reconstructed Pleistocene body masses of *C. crocuta*, coupled with the morphometric analyses, indicated a lack of consistent body size response to environmental changes (in contrast to patterns seen in other large carnivores), although the Island Rule was manifested in individuals from Sicily. Body mass, morphometrics and tooth breakage frequencies suggested palaeodietary variation, particularly regarding the degree of bone consumption and predation behaviours. Finally, the reasons for *C. crocuta* extirpation from Europe focussing on climate, vegetation, presence of prey species, and competition for food and shelter were examined.

iii. Acknowledgements

I would first like to thank Danielle Schreve for her supervision, advice, support and knowledge throughout and also prior to this PhD. It was during Danielle's lectures during the MSc that I first became interested in Quaternary mammals. Without Danielle I would probably be doing something very different today.

Secondly, I thank Chris Carbone for his supervision and guidance, and particularly his insight into modern carnivore ecology. I also enjoyed exploring London Zoo every time I visited Chris for meetings!

Many thanks to Simon Blockley for advice on statistics and OxCal, and for being my unofficial life coach. Additional thanks go to my advisor, Alice Milner. I am also grateful to Roula Pappa, Jane Ford and Christine Frischauf for additional advice.

Additional thanks to Clare Mayers, Jen Thornton, Raymon Aung, Adrian Palmer and Marta Perez for additional support.

I am grateful to the CQR and the wider Department of Geography, and in particular the following people for supportive and often amusing company in EMU and the computer room: Ash Abrook, Lizzy Peneycad, Amy Walsh, Poppy Harding, Dave Arnold, Emily Wiesendanger, Rachel Devine, Alice Carter-Champion, Jacob Bendal and Ben Newman.

I am also indebted to the many institutions that I visited in order to carry out this research. I would therefore like to thank the follow people for granting me access to their institution's collections: Eileen Westwig and Brian O'Toole (Department of Mammalogy, American Museum of Natural History New York), Deborah Hutchinson (Geology, Bristol Museum and Art Gallery, Bristol), Paul Shepherd and colleagues (Palaeontology, British Geological Survey, Keyworth), Hannah Boddy (Creswell Crags Museum and Heritage Centre, Worksop), Johannes Tuzar (Krahuletz-Museum, Eggenburg), Vesna Dimitrijević (Laboratorija za bioarheologiju, Univerzitet u Beogradu, Belgrade), Neil Owen (Leeds Discovery Centre, Leeds), Tom Lord (Lower Winskill, Settle), David Gelsthorpe, Kate Sherburn and Rachel Petts (Earth Science Collections, Manchester Museum, Manchester), Laura Bonfiglio (Museo della Fauna, Università degli Studi di Messina, Messina), Susana Fraile Gracia (Colección de Paleontología de Vertebrados y de Prehistoria, Museo Nacional de Ciencias Naturales, Madrid), Vincent Vicedo (Museu de Geologia, Museu de Ciències Naturals de Barcelona, Barcelona), Steffen Bock (Recent Mammals, Museum für Naturkunde, Berlin), Nigel Monaghan (Natural History, National Museum of Ireland, Dublin), Elizabeth Walker and colleagues (Palaeolithic and Mesolithic Archaeology, National Museum of Wales, Cardiff), Pip Brewer and Roula Pappa (Fossil Mammals, Natural History

Museum, London), Roberto Portela Miguez and Louise Tomsett (Mammal Section, Natural History Museum, London), Ursula Göhlich (Vertebrate Palaeontology, Naturhistorisches Museum Wien, Vienna), Adam Smith (Nottingham Natural History Museum, Wollaton Hall, Nottingham), Eliza Howlett (Oxford University Museum of Natural History, Oxford), Jan Freedman (Plymouth City Museum and Art Gallery, Plymouth), Annelise Folie and colleagues (Palaeontology, Royal Belgian Institute of Natural Sciences, Brussels), Terry Walschaerts and colleagues (Recent Vertebrates, Royal Belgian Institute of Natural Sciences, Brussels), Emmanuel Gilissen and colleagues (Royal Museum for Central Africa, Tervuren), Matt Riley (Sedgwick Museum of Earth Sciences, Cambridge), Darrin Lunde (Division of Mammals, Smithsonian Institution National Museum of Natural History, Washington DC), Dennis Parsons (South West Heritage Trust, Taunton), Barry Chandler (Torquay Museum, Torquay), Linda Wilson (University of Bristol Spelaeological Society museum, Bristol), Matt Lowe (University Museum of Zoology, Cambridge), Barry Lane (Wells and Mendip Museum, Wells), and Stuart Ogilvy (Yorkshire Museum, York).

I am incredibly grateful to NERC and the London NERC DTP for funding this thesis. Additional funds came from three SYNTHESYS grants, which allowed me to visit the Museo Nacional de Ciencias Naturales in Madrid, the Museum für Naturkunde in Berlin, and the Naturhistorisches Museum Wien in Vienna. I therefore thank the SYNTHESYS administrators at each institution for arranging my visits: Josefina Cabarga (Madrid), Manja Voß (Berlin) and Astrid Hille (Vienna). Additional grants from SVP and QRA allowed me to attend the SVP conference in 2017.

Finally, I would like to thank my friends and family for being so understanding during this PhD.

Contents

List of tables

List of figures

1 Introduction

1.1 Background

This thesis will explore the responses of the spotted hyaena (*Crocuta crocuta*, Erxleben 1777) to Pleistocene environmental changes in Europe. The first known occurrence of *C. crocuta* in Europe was around 850-780,000 years ago (Garcia and Arsuaga, 2001). The spotted hyaena is an excellent model for studying the impacts of palaeoclimatic change on a major predator, since they were present in both warm and cold-climatic periods (e.g. Currant and Jacobi, 2011), and in a diverse range of habitats. Furthermore, there are abundant remains, particularly from the Late Pleistocene, with some sites yielding hundreds of *C. crocuta* specimens (Ehrenberg, 1966a; Currant, 1998), together with abundant remains of their prey (e.g. Currant and Jacobi, 2011). During the Pleistocene, *C. crocuta* had an extremely wide distribution outside Africa, from Portugal at the western margin of Europe (e.g. Davis *et al.*, 2007) across to Ukraine and further east into Asia (Baryshnikov, 1999), and from in Britain in the north (Currant and Jacobi, 2011) through to southern Italy (Bonfiglio *et al.*, 2001).

Despite ranging across Eurasia during the Pleistocene, *C. crocuta* are now restricted to sub-Saharan Africa (Hofer and Mills, 1998a). Today, they demonstrate considerable behavioural flexibility, including generalist diets (Mills, 1990; Holekamp *et al.*, 1997; Hayward, 2006), the ability to obtain food from both predation and scavenging (e.g. Henschel and Skinner, 1990; Gasaway *et al.*, 1991; Cooper *et al.*, 1999) and the ability to alter the areas they preferentially occupy in response to disturbance (Boydston *et al.*, 2003). They are capable of successfully competing against other larger carnivores in direct interactions (Mills, 1990; Volmer and Hertler, 2016) or through environmental partitioning (e.g. Schaller, 1972; Hayward and Kerley, 2008). They are also capable of consuming bone, an act that is particularly important during periods of low food availability (Kruuk, 1972; Egeland *et al.*, 2008), and to which they are morphologically well-suited (e.g. Werdelin and Solounias, 1991; Raia, 2004; Therrien, 2005; Ferretti, 2007). Except for two other hyaenids (striped hyaena, *Hyaena hyaena* and brown hyaena, *Parahyaena brunnea*), the bone-cracking behaviour exhibited by *C. crocuta* is not seen in their competitors (Werdelin and Solounias, 1991). *C. crocuta* are also morphologically responsive to environmental conditions such as temperature, evidenced by variation in the size of some craniodental measurements across Africa (Roberts, 1951; Klein, 1986). These characteristics will be discussed in more detail in Chapters 2 and 3.

Given the aforementioned characteristics of *C. crocuta*, it is therefore interesting to explore how the species withstood a wider range of environmental conditions in Pleistocene Europe than

those experienced today, particularly whether their body size varied, whether certain conditions created dependency on scavenging to obtain food, and whether they experienced periods of dietary stress leading to increased bone consumption. Although morphometric and body size variation in Pleistocene *C. crocuta* has already been explored, particularly by Turner (1981) and Collinge (2001), this thesis will present a reassessment of the evidence, including samples from a wider geographical area and utilising additional methods.

Finally, given the apparent behavioural adaptations and morphological robustness of *C. crocuta*, it is relevant to examine the conditions that eventually led the species to disappear from Europe during the Late Pleistocene. Although a chronology of the extirpation of *C. crocuta* has recently been constructed by Stuart and Lister (2014), the publication of an updated radiocarbon calibration curve (Reimer *et al.*, 2013) and more stringent date selection criteria necessitate a reanalysis of these data.

This thesis will therefore focus on *C. crocuta* from Britain throughout much of its presence in the country, coupled with Late Pleistocene *C. crocuta* from Austria, Belgium, the Czech Republic, Ireland, Italy, Serbia and Spain, thus covering much of the species' European geographical range. Specifically, changes in body mass and morphometrics of craniodental and post-cranial elements of *C. crocuta* will be examined, in order to assess changes in size, palaeodiet (with a particular focus on bone consumption) and predation behaviours. Any changes, or lack thereof, in these features may have affected the ability of *C. crocuta* to withstand the changes in environment and competition from other members of the large carnivore guild in Europe. This may in turn shed new light on the potential reasons behind the final extirpation of *C. crocuta* from Europe.

1.2 Aims

The aims of this thesis are as follows:

- To assess the body mass and morphometric responses of *C. crocuta* to Pleistocene environmental changes in Europe
- To assess the palaeodiet of *C. crocuta* from Pleistocene Europe, with a particular focus on bone consumption and frequency of predation versus scavenging
- To reassess the timing and potential reasons for the extirpation of *C. crocuta* from Europe

These aims will be accomplished first through an investigation of present-day *C. crocuta* in Africa. The influences affecting the population biomass of *C. crocuta* will be examined and

compared to those of a competitor, the lion (*Panthera leo*), which will aid in understanding the potential environmental influences upon Pleistocene *C. crocuta* populations. The changes through ontogeny (of cranial and post-cranial measurements) and sexual size dimorphism (in body mass, craniodental and post-cranial elements) of *C. crocuta* will also be assessed. This is an important step prior to the Pleistocene morphological analysis as it will highlight any areas that might otherwise be misinterpreted as reflecting a climatic influence, for example whether some elements are larger in females or males, or whether some elements continuously change in size through life. Environmental correlates with body mass, craniodental and post-cranial elements will be established in order to aid interpretation of any changes in the Pleistocene material. Finally, the degree of tooth breakage will be assessed in present-day *C. crocuta* to highlight how this signal increases with age, and to examine any differences between males and females.

Secondly, the Pleistocene material will be assessed, including the identification of any temporal and spatial changes in body mass, craniodental and post-cranial across Europe. This will highlight any morphological responses to environmental changes.

Conclusions regarding palaeodietary and predation behaviour will be drawn from the body mass reconstructions, in addition to some of the morphometric measurements, reconstructions of bite force and mandibular bending strength, and degree of tooth breakage.

Finally, investigation of the causes of *C. crocuta* extirpation from Europe will be undertaken through a reassessment of the timing of the species' occupation of Europe during Marine Oxygen Isotope Stage (MIS) 3 and its final known appearance. This will be coupled with a reassessment of the chronologies of a potential competitor, the cave lion (*Panthera leo* (*spelaea*)), and three prey species, woolly rhinoceros (*Coelodonta antiquitatis*), red deer (*Cervus elaphus*) and reindeer (*Rangifer tarandus*). Information will be taken from the literature about the environmental conditions experienced by *C. crocuta* during the Pleistocene, including temperature, precipitation, vegetation, presence of competitor species, presence of prey species, and competition for the use of caves. This information will complement the biomass, morphometric and palaeodiet results and allow reassessment of the probable causes of *C. crocuta* extirpation from Europe.

1.3 Thesis structure

The structure of the thesis is as follows:

- Chapter 2 reviews the literature on both present-day and Pleistocene *C. crocuta*, focusing on diet, competition, denning, important factors influencing mortality, and theories behind the species' extirpation from Europe.

- Chapter 3 established influences upon body mass and sexual size dimorphism. The functional features of the craniodental and post-cranial elements are then discussed, including those related to the brain, the senses, diet, predation and locomotion.
- Chapter 4 first outlines details of the sites yielding present-day and Pleistocene data. Methods are then presented, including explanation of the morphometric measurements, reconstruction of bite force and mandibular bending strength, the calculation of post-cranial indices, and records of dental macrowear, tooth loss and tooth breakage. Finally, the statistical analyses are explained.
- Chapter 5 presents the results of the investigations of present-day *C. crocuta* biomass, body mass, morphometrics and tooth breakage. Along with an assessment of the environmental influences upon these data, there will be analyses of sexual dimorphism and ontogenetic change, where relevant.
- Chapter 6 comprises the results of analyses of Pleistocene *C. crocuta* body mass, morphometrics and tooth breakage. This will involve investigations of the palaeoenvironmental influences upon these data. Predation behaviours and palaeodietary information will be drawn from these data.
- Chapter 7 focuses on the timing and potential causes of the extirpation of *C. crocuta* from Europe, putting forward new radiocarbon models of *C. crocuta*, *P. leo* (*spelaea*) and selected prey species, and discussing these in the context of information presented previously in the thesis.
- Chapter 8 summarises the findings of this thesis and provides conclusions relating these to the aims.

2 Review of *Crocuta crocuta*

2.1 Introduction

This chapter will first cover the taxonomy of *C. crocuta* and the relationship between present-day and Pleistocene *C. crocuta*. Second, the ecology of present-day *C. crocuta* will be covered, including the species' distribution and habitat, controls on population density, denning habits and factors leading to mortality. Finally, Pleistocene *C. crocuta* will be reviewed, focussing on current knowledge of its temporal and spatial presence in Europe, denning and cave use, diet and competition, body size and morphometrics, and the timing and possible reasons for its extirpation from Europe.

2.2 Hyaenidae systematics

2.2.1 Crocuta crocuta taxonomy

The taxonomy of the spotted hyaena (*Crocuta crocuta*) is outlined below, following Werdelin and Solounias (1991) and Bohm and Höner (2015).

Kingdom: Animalia Linnaeus, 1758

Phylum: Chordata Haeckel, 1847

Class: Mammalia Linnaeus, 1758

Order: Carnivora Bowdich, 1821

Suborder: Feliformia Kretzoi, 1945

Family: Hyaenidae Gray, 1821

Genus: *Crocuta* Kaup, 1828

Species: *Crocuta crocuta* (Erxleben, 1777)

In addition to the Hyaenidae, the suborder Feliformia includes the extant families Felidae, Viverridae, Herpestidae, Eupleridae, Prionodontidae and Nandiniidae (Werdelin and Solounias, 1991; Zhou *et al.*, 2017). The family Hyaenidae includes four extant species: *C. crocuta*, brown hyaena (*Parahyaena brunnea*, Thunberg 1820), striped hyaena (*Hyaena hyaena*, Linnaeus 1758), and aardwolf (*Proteles cristata*, Sparrman 1783; Werdelin and Solounias, 1991). Many studies

have attempted to determine the relationships between the species of Hyaenidae, using both morphological and DNA evidence (see reviews in Werdelin and Solounias, 1991; Jenks and Werdelin, 1998; Koepfli *et al.*, 2006), something that has evidently proved difficult. As Koepfli *et al.* (2006, p.605) stated, '[t]aken together, previous morphological and molecular phylogenetic analyses have supported every possible combination of relationships between extant bone-cracking hyaenids.'

2.2.2 Variation within present-day Crocuta crocuta

At least 19 species or subspecies of extant *Crocuta* have been proposed (reviewed by Matthews, 1939; Jenks and Werdelin, 1998), although this variability is contested. Matthews (1939) disputed that different species and subspecies could be identified, as the morphological features that differentiated them were present in a single population in the Balbal plains, Tanganyika Territory (now Tanzania). The only feature that was not present in the Balbal population was the large size of *Crocuta crocuta fortis* in the Belgian Congo (now Democratic Republic of the Congo), as discussed by Allen (1924). However, Matthews (1939) suggested that as only 13 specimens of the subspecies were acquired from an expedition of nearly two years, there may have been collection bias in favour of large specimens.

Nevertheless, there is now genetic evidence for different clades of present-day *C. crocuta* within Africa, although the clades all belong to a single species. Mitochondrial DNA (mtDNA) analyses revealed four clades of *C. crocuta*, with two surviving into the present day (Rohland *et al.*, 2005, Table 2.1). Clade A is found in northern Africa while Clade C is found in southern Africa. There is some overlap at the equator, with both clades found in Sudan and Tanzania (Rohland *et al.*, 2005). Clade A was also found in Europe during the Pleistocene along with Clade B, while Clade D was found in Asia (Rohland *et al.*, 2005; Bon *et al.*, 2012; Dodge *et al.*, 2012; Sheng *et al.*, 2014, Table 2.1).

Table 2.1: Clades and haplotypes of present day *C. crocuta*, Pleistocene *C. c. ultima* in Asia, and *C. crocuta* in Europe, along with their known distributions.

Clade	Haplotype	Location	Reference
Present-day			
A		Cameroon, Eritrea, Ethiopia, Rwanda, Senegal, Somalia, Sudan, Tanzania, Togo, Uganda	Rohland *et al.* (2005)
C		Angola, Kenya, Namibia, South Africa, Sudan, Tanzania, Zimbabwe	Rohland *et al.* (2005)
Pleistocene			
A	A1	Austria (Teufelslucken, Winden Cave), Czech Republic (Vypustek), France (Les Plumettes), Germany (Irpfel Cave), the North Sea	Rohland *et al.* (2005)
	A2	Belgium (Goyet Cave), Britain, (Church Hole), France (Coumère, Les Roches de Villeneuve), Romania (Igric), Ukraine (Bukovina Cave)	Rohland *et al.* (2005), Bon *et al.* (2012), Dodge *et al.* (2012)
B	B1	Hungary (Kiskevelyi), Slovakia (Tmavaskala)	Rohland *et al.* (2005)
	B2	Czech Republic (Sveduvstul), Germany (Lindenthal Cave), Slovakia (Certovapec)	Rohland *et al.* (2005)
D		China (Da'an Cave, Tonghe Bridge), Russia (Geographical Society Cave)	Rohland *et al.* (2005), Sheng *et al.* (2014)

2.2.3 Relationship between present-day and Pleistocene Crocuta crocuta

There is debate about whether the European Pleistocene *C. crocuta* should be regarded as a subspecies (*Crocuta crocuta spelaea*) or a separate species (*Crocuta spelaea*), commonly referred to as the cave hyaena (Kurtén, 1956; Werdelin and Solounias, 1991; Baryshnikov, 1995, cited in Baryshnikov, 1999). The Late Pleistocene equivalent in Asia has been attributed to a further subspecies, *Crocuta crocuta ultima* (Kurtén, 1956; Sheng *et al.*, 2014). The evidence for this stems from morphological differences, namely that the European Pleistocene hyaena were supposedly larger than present-day African individuals, and differed in their limb proportions. In Pleistocene *C. crocuta*, the humerus and femur were longer and the metapodials shorter, while the radius and tibia were of similar lengths to the present-day individuals (Kurtén, 1956). The dentition of the European Pleistocene representatives was more specialised for carnivory than present-day *C. crocuta* (Baryshnikov, 1995, cited in Baryshnikov, 1999).

From mtDNA data, Rohland *et al.* (2005) concluded that there is no evidence that the Pleistocene spotted hyaena in Europe was either a separate species or a sub-species of the present-day *C. crocuta* in Africa. This conclusion was also drawn by Bon *et al.* (2012) based on the similarity

of mtDNA and nuclear genes in coprolites from Coumère Cave, France, to DNA from present-day *C. crocuta*.

The genetic evidence further suggests that Pleistocene *C. c. ultima* in Asia were members of clade D, based on analyses of specimens from eastern Russia and China (Rohland *et al.*, 2005; Sheng *et al.*, 2014). Pleistocene *C. crocuta* in Europe were split into four mtDNA haplotypes from two clades (A and B), with overlapping ranges (Hofreiter *et al.*, 2004; Rohland *et al.*, 2005), see Table 2.1.

Despite the genetic evidence, many recent authors continue to identify specimens as *C. spelaea* or *C. c. spelaea* (e.g. Magniez and Boulbes, 2014; Diedrich, 2015; Fourvel *et al.*, 2015). However, it is not the intention of this thesis to attempt to resolve this debate and the conclusions of the genetic studies will be followed here. Henceforth, all spotted hyaenas from Pleistocene Europe and present-day Africa will be referred to as the same species, *Crocuta crocuta*.

2.3 Present-day Crocuta crocuta

2.3.1 Distribution and habitat

C. crocuta currently live in sub-Saharan Africa. They are more widespread in eastern than western Africa (Hofer and Mills, 1998a, and references therein). In some areas, there are very few records of their presence. For example, a single *C. crocuta* was seen within closed forest of Equatorial Guinea (Juste and Castroveijo, 1992), and only tracks of *C. crocuta* have been seen in the rainforest of Gabon (Bout *et al.*, 2010). A review by Hofer and Mills (1998b) indicated that the population status of *C. crocuta* is threatened in many western Africa countries, but also in Rwanda, some areas of South Africa, and outside protected areas in Kenya. They may now be locally extinct from Togo and Algeria (Hofer and Mills, 1998a; Bohm and Höner, 2015). Their population is in decline, particularly outside protected areas, due to human persecution, loss of habitat, loss of prey and drought (Hofer and Mills, 1998b, and see Section 2.2.6). The IUCN Red List categorisation of *C. crocuta* population is Least Concern, but Decreasing (Bohm and Höner, 2015).

They are present in many habitats including open savannahs, woodland and semi-deserts, dense forests, tropical forests, coastal areas, dense thicket, around human settlements, and at altitudes up to 4000m (Kruuk, 1972; Sillero-Zubiri and Gottelli, 1992; Hofer, 1998a).

The distribution of *C. crocuta* has been severely impacted by humans and the species is now largely located in only protected areas and surrounding land (Hofer and Mills, 1998a). The distribution of *C. crocuta* within the Talek region of the Maasai Mara National Reserve, Kenya has altered along with increased human use of the area, particularly the grazing of livestock (Boydston *et al.*, 2003). Prior to increased human use, *C. crocuta* occupied short, open grassland where prey abundance was highest. Subsequent to increased human use, *C. crocuta* frequently stayed close to areas of closed vegetation, even though there was no decrease in prey abundance in the short grassland. This change occurred in less than ten years, with no associated decrease in *C. crocuta* population density, leading Boydston *et al.* (2003) to suggest that *C. crocuta* are able to alter rapidly their behaviour in response to changing environmental conditions. This behavioural plasticity may have been useful during the Pleistocene, and is an important consideration when assessing the responses of *C. crocuta* to past environmental changes.

2.3.2 Population density

Carnivore density is primarily controlled by prey biomass, with higher carnivore density in areas of high prey biomass (Carbone and Gittleman, 2002). Indeed, *C. crocuta* density is positively correlated with prey density (Cooper, 1989) and prey biomass (Périquet *et al.*, 2015). There is a scaling relationship across many different ecosystems, including the African savannah, whereby predator biomass increases at a lower rate to prey biomass (Hatton *et al.*, 2015). Population size may also be influenced by competition (Carbone and Gittleman, 2002), with lack of preferred prey resulting in sub-optimal foraging (Hayward and Kerley, 2008), enhanced predation and susceptibility to disease (Kissui and Packer, 2004).

Cooper (1989) found that in areas such as the Maasai Mara National Reserve in Kenya or the Savuti region in the Chobe National Park in Botswana, there is sufficient resident prey to support *C. crocuta* year-round, with migratory prey providing supplementary food periodically. The relationship between *C. crocuta* density and prey density is complicated when migratory prey is the major food source, such as in the Serengeti, Tanzania. In these cases, the size and nature of *C. crocuta* territories must be flexible in order to obtain sufficient food (Cooper, 1989).

In addition to high density of resident prey populations, Cooper (1989) found that *C. crocuta* population density is higher in areas of reliable water sources. In arid areas, *C. crocuta* may obtain much of their water requirement from fresh carcasses (Cooper, 1990). However, Gasaway *et al.* (1991) suggested that arid conditions may reduce *C. crocuta* populations if prey is scarce and most of the food comes in the form of desiccated carcasses.

Finally, the influence of disease upon *C. crocuta* population density has been seen through short-term population decrease in the Ngorongoro Crater (Höner *et al.*, 2012, see Section 2.3.5 for further details).

The factors influencing *C. crocuta* populations across Africa will hence be assessed within Chapter 5. This is important in determining potential reasons for the extirpation of *C. crocuta* from Europe during the Pleistocene.

2.3.3 Diet and competition

C. crocuta derive their food from both predation and scavenging, the ratio of which varies between locations. For example, in the Maasai Mara National Reserve, 95 % of the total biomass consumed by *C. crocuta* constituted fresh kills, with only 0.5 % of this total scavenged (Cooper *et al.* 1999). In the Etosha National Park in Namibia, 75 % of *C. crocuta* food derived from their

kills (Gasaway *et al.*, 1991) but in the Kruger National Park in South Africa, biomass from *C. crocuta* kills constituted only 51 % of the diet (Henschel and Skinner, 1990), thereby highlighting considerable variation in behaviour, the reasons for which will be addressed below.

Cooper *et al.* (1999) stated that scavenging is an unreliable food source. This is because carcass availability is dependent upon factors such as disease, drought, and kills by other predators (Henschel and Skinner, 1990; Gasaway *et al.*, 1991). Furthermore, scavenged carcasses contain less energy, nutrients and water than fresh kills, and are therefore not a preferred food source in the Maasai Mara (Cooper *et al.,* 1999).

The main prey of *C. crocuta* are herbivores weighing between 56 – 182 kg (Hayward and Kerley, 2008). Larger species such as buffalo (*Syncerus caffer*), giraffe (*Giraffa camelopardalis*) or African elephant (*Loxodonta africana*) are consumed either as a result of scavenging, or because the prey individuals are injured, incapacitated or young (Cooper, 1990; Cooper *et al.,* 1999; Henschel and Skinner, 1990). In the Maasai Mara National Reserve, *C. crocuta* more frequently attempted solo hunts of ungulates, however, a greater proportion of hunts were successful when they hunted in groups (Holekamp *et al.*, 1997). By contrast, in the Comoé National Park (Côte d'Ivore), rodents made up more than 60 % of *C. crocuta* diet. In this area, *C. crocuta* did not range in groups (Korb, 2000). Additional species consumed include termites, caterpillars, crayfish, ostriches and hares (Tilson *et al.*, 1980; Holekamp and Dloniak, 2010). Remains of Chacma baboon (*Papio cynocephalus ursinus*) have been found in *C. crocuta* dens in Mashatu Game Reserve, Botswana (Kuhn, 2012), whereas remains of other mammalian carnivores (*P. leo*, leopard *Panthera pardus*, caracal *Caracal caracal*, black-backed jackal *Canis* cf. *mesomelas*) have also been found in dens (Faith, 2007). They may also dig up human remains from cemeteries (Sutcliffe, 1970). *C. crocuta* do not show marked preference towards particular species, rather individual clan preference reflects local availability of prey species, prior hunting experience and the ease by which prey can be captured (Mills, 1990; Holekamp *et al.*, 1997; Hayward, 2006). Seasonal variability influences targeted prey species. In the Serengeti, Tanzania, wildebeest (*Connochaetes taurinus*) migrate into the area for part of the year, during which time they are the species most frequently targeted by *C. crocuta*. Prior to the migration, resident Thomson's gazelle (*Gazella thomsonii*) is the most abundant ungulate species, and is targeted most frequently by *C. crocuta* (Cooper *et al.*, 1999).

C. crocuta may also consume the bones of a carcass. As will be discussed in Section 3.3.6, the craniodental morphology of *C. crocuta* is well-suited to bone consumption. Bone consumption may occur when there is greater interspecific competition (Egeland *et al.*, 2008). Intraspecific competition at carcasses may also lead to bone consumption, driven by established dominance hierarchies. Females will dominate carcasses over males. The only exception to this is the male

cubs of a high ranking female. The high rank of a mother will be passed onto its young, who will then dominate all individuals of a lower rank than the mother (Frank *et al.*, 1989). It is therefore the lower ranking individuals that are left with the less preferential parts of a carcass, and may therefore have to consume the bones. This intraspecific competition is evidenced in the Ngorongoro, where *C. crocuta* density is high, and most carcasses are completely consumed. By contrast, in areas of the Serengeti National Park, there are large ungulate populations and low *C. crocuta* density so bone are often not eaten (Kruuk, 1972).

Exploitation competition (the use of the same resource by different species) between *C. crocuta* and other large carnivores is apparent in the overlap of targeted prey species. For example, in the Faro National Park, Cameroon, there is a large overlap in the prey species consumed by *C. crocuta*, lion (*Panthera leo)* and wild dog (*Lycaon pictus*). Buffon's kob (*Kobus kob kob*) is the species most frequently consumed by *C. crocuta* and *P. leo*. This ungulate is also targeted by a further potential competitor, baboons (*Papio* spp., Breuer, 2005). In the Kalahari, southern Africa, *C. crocuta* and *P. leo* both predate most frequently wildebeest (*Connochaetes* spp.) and gemsbok (*Oryx gazella*) (Mills, 1990).

Competition between the large carnivores is also evident through direct interactions, or interference competition. *C. crocuta* has been observed to obtain food from prey killed by other predators including *P. leo*, cheetah (*Acinonyx jubatus*), leopard (*Panthera pardus*), *L. pictus* and jackals (*Canis mesomelas*) (Kruuk, 1972; Mills, 1990; Cooper *et al.*, 1999). The exact dynamics of these competitive interactions vary. In a study in the Kalahari, *C. crocuta* often obtained carcasses after the original predator had departed. In cases of direct interactions, *C. crocuta* were more successful in appropriating carcasses from *P. pardus* and *A. jubatus* than from *P. leo* (Mills, 1990). In the case of the *P. brunnea* (a frequent scavenger), *C. crocuta* is the dominant species and frequently appropriates carcasses from *P. brunnea*. On the other hand, little food is lost to *P. brunnea* (Mills, 1990). *C. crocuta* may also lose food to *P. leo* and *L. pictus* (Kruuk, 1972; Cooper *et al.*, 1999). In the plains area of the Serengeti, 42 % of *P. leo*'s scavenged items were obtained from *C. crocuta* (Schaller, 1972). In the Ngorongoro Crater, Tanzania, *P. leo* were observed to approach 21 % of *C. crocuta* kills, and frequently obtained a substantial amount of food (Kruuk, 1972). Some of these interactions with *P. leo* can be fatal to *C. crocuta* individuals (Périquet *et al.*, 2015, and references therein).

On occasions when *C. crocuta* attempt to scavenge from *P. leo*, success depends upon the numbers of *C. crocuta*, and the absence of an adult *P. leo* male. When *P. leo* attempt to take food from *C. crocuta*, the presence of an adult *P. leo* male will force *C. crocuta* to surrender its carcass (Höner *et al.*, 2002). In observations within the Timbavati Private Nature Reserve, South Africa, by Bearder (1977), *C. crocuta* frequently consumed giraffe that had been killed by *P. leo*,

although they waited until the lions had finished before approaching the carcass. The lions left a great deal of the carcass behind, which the author suggested might be due to the tough skin of the giraffe, which only *C. crocuta* is able to exploit.

In a model assessing the amount of prey exploited by a species, versus the amount gained or lost through competition, Volmer and Hertler (2016) ranked the success of five large carnivore species (*C. crocuta*, *P. leo*, *P. pardus*, *A. jubatus*, *L. pictus*) in the Kruger and Serengeti National Parks. In the Kruger National Park, *P. leo* was the dominant species, followed by *C. crocuta*. In the Serengeti National Park, *C. crocuta* was the dominant species (Volmer and Hertler, 2016).

Competition may be reduced through spatial partitioning. For example, in the Serengeti, *P. leo* occupies the plains but is more frequently found within wooded grassland, *L. pictus* frequents both wooded grassland and plains, *P. pardus* prefers thickets and riparian forests, and *A. jubatus* and *C. crocuta* most frequently occupy the plains and the border of the wooded grassland (Schaller, 1972). By contrast, Périquet *et al.*, (2015) noted that *P. leo* and *C. crocuta* may occupy similar areas, influenced by the abundance of prey. The authors also noted that *P. leo* require some vegetation cover to allow them to ambush their prey. In a study of *C. crocuta* in the Savuti region of the Chobe National Park, Botswana, there appeared to be no relationship between hunting and vegetation cover, as different prey species were hunted in different vegetation (Cooper, 1990).

Some temporal separation also occurs. *C. crocuta*, *P. leo*, *P. pardus*, *P. brunnea* and *H. hyaena* are usually nocturnal or crepuscular hunters. In contrast, *A. jubatus* and *L. pictus* are diurnal (Schaller, 1972; Hofer, 1998; Mills, 1998; Périquet *et al.*, 2015). Indeed, Cooper (1990) found that *C. crocuta* individuals were unable to hunt in temperatures above about 20°C. By contrast, Swanson *et al.* (2016) found *P. leo* to be active throughout most of the day. In the Talek region, Kenya, along with alteration of vegetation preference with increased livestock grazing (Section 2.3.1), *C. crocuta* activity changed from crepuscular to nocturnal, again exhibiting a rapid behavioural response (Boydston *et al.*, 2003).

Despite these examples of spatial and temporal partitioning, Swanson *et al.* (2016) found that in the long-term, *P. leo*, *C. crocuta* and *A. jubatus* did not avoid each other in the Serengeti. The numbers of sightings of each species at a particular spot were positively correlated, although a threshold was reached at the highest numbers of *P. leo*. In the short-term, *A. jubatus* did not avoid *C. crocuta*, and the *C. crocuta* only avoided an area for a short period (12 hours) after *P. leo* was seen. In fact, *C. crocuta* and *P. leo* tracked each other, perhaps due to similar prey preferences (Swanson *et al.*, 2016). Similarly, *C. crocuta* and *P. leo* appeared to track each other during the dry season of 2013 in Ruaha National Park, Tanzania (Cusack *et al.*, 2017).

Separation of predators also occurs through targeting of different prey classes. In the Kalahari, *C. crocuta* will target the calves of *Connochaetes* spp. and *O. gazella*, while *P. leo* targets the adults and subadults (Mills, 1990). Meanwhile, *P. pardus* and *A. jubatus* prey upon smaller species such as springbok (*Antidorcas marsupialis*). Further, Mills (1990) stated that the fact that *C. crocuta* scavenges more than *P. leo* helps in reducing the competition between the two species. Hayward and Kerley (2008) reviewed dietary studies of *C. crocuta*, *P. leo*, *P. pardus*, *A. jubatus* and *L. pictus* to assess potential interspecific competition. The authors suggested that whilst interference competition occurs, it is exploitation competition that exerts the strongest influence upon some carnivore populations when food is the limiting factor. *A. jubatus* and *L. pictus* experienced the greatest overlap in diets with each other, and thus the potential for competition was high. The predator with which *C. crocuta* prey preference overlapped the most was *P. leo*. However, evidence suggested that competition between *C. crocuta* and *P. leo* does little to limit to the abundance of either species (Hayward and Kerley, 2008). A large overlap of diet between *C. crocuta* and *P. leo* was also found by Périquet *et al.* (2015), with both species mostly targeting medium-sized prey. However, some separation occurs with *P. leo* preying upon more large-sized prey than *C. crocuta*, and *C. crocuta* consuming more very large-sized prey and other prey, such as birds, rodents and other predators (Périquet *et al.*, 2015).

Two of the other large predators in Africa, *H. hyaena* and *P. brunnea*, scavenge much of the vertebrate portion of their diet, which is supplemented with small vertebrates they kill themselves, in addition to fruits and insects (Hofer, 1998b; Mills, 1998). The difference between *H. hyaena* and *C. crocuta* is illustrated by observations from Djibouti. *C. crocuta* prey species diversity was higher than that of *H. hyaena*. As *H. hyaena* are mainly scavengers, they are reliant upon carcass availability, whereas *C. crocuta* are able to hunt cooperatively and may thus have a wider choice available to them (Fourvel *et al.*, 2015).

2.3.4 Denning

There are two different types of den used by *C. crocuta*: the natal den and the communal den (East *et al.*, 1989; Holekamp and Smale, 1998; Boydston *et al.*, 2006). The natal den is occupied by one, or occasionally two, female adults and their cubs (Boydston *et al.*, 2006). The majority of cubs are born within natal dens (East *et al.*, 1989; Boydston *et al.*, 2006). The young are moved from the natal to the communal den, which was observed to occur up to four weeks of age in the Talek region (Holekamp and Smale, 1998) and at 11 days old on average in the Serengeti National Park (East *et al.*, 1989). The mother, and occasionally a close female relative of the mother, such as a sibling, may reside within the entrance to the den. The interior of the den is,

however, so narrow that only the cubs can enter, allowing protection from predators (East *et al.*, 1989; Holekamp and Smale, 1998). Many dens are excavated by warthogs (*Phacochoerus africanus*) or aardvarks (*Orycteropus afer*) and dug further by *C. crocuta* cubs (Kruuk, 1972; Boydston *et al.*, 2006).

Like natal dens, the interior of communal dens is usually only accessible to cubs, allowing them to hide from predators and potentially cannibalistic adult *C. crocuta*, since mothers are often away from these dens for long periods when searching for food (Kruuk, 1972; East *et al.*, 1989; Cooper, 1993; Holekamp and Smale, 1998). In contrast to natal dens, the communal dens contain young from many different females, and it is within this environment that *C. crocuta* begin to establish their social rankings (Holekamp and Smale, 1998). In the Talek region, Boydston *et al.* (2006) observed frequent inhabitation and subsequent abandonment of communal dens. The longest continuous period of occupation of a den was 8.1 months. Although the reason for den abandonment was not always known, occasionally the moves were prompted by events such as disturbance by humans, *P. leo* or *C. crocuta* from outside the clan, the death of a cub or flooding (Boydston *et al.*, 2006). Communal dens are visited by both male and female adults, and younger *C. crocuta* that have left the den (Holekamp and Smale, 1998). Males are allowed within a closer proximity to cubs at communal dens whereas they are chased away from natal dens (East *et al.*, 1989). This indicates the importance of dens for the survival of cubs, and thus the importance of Pleistocene *C. crocuta* in finding suitable denning sites.

Adults may also require shelter during the day. For example, the entrance of a large den in Namib-Naukluft Park in Namibia, which was not used by cubs during the period of study, was used as daytime shelter for adults (Henschel *et al.*, 1979). Shallow holes within the Comoé National Park were likely used as shelter during the day, but did not function as an area for raising cubs (Korb, 2000). As mentioned, *C. crocuta* seem to be unable to hunt in high temperatures (Cooper, 1990). The presence of shelters large enough for daytime use of adults avoiding high temperatures may therefore have been important during Pleistocene interglacials.

Dens may be located in caves or other openings in rock, or in burrowed into sediments, as indicated in Table 2.2. The burrows studied by Kruuk (1972) in the Serengeti and Ngorongoro Crater had already been at least partially excavated by a different species. A further consideration is whether vegetation may influence den location. As indicated in Table 2.2, there does not appear to be a consistent type of vegetation for den location. Indeed, Périquet *et al.* (2016) found no influence of vegetation density upon den location in the Hwange National Park, Zimbabwe. A further consideration is proximity to water sources. Some of the dens in Table 2.2 are located near to rivers. Indeed, as mentioned, proximity to water sources is an important factor influencing *C. crocuta* density (Cooper, 1989). On the other hand, Kruuk (1972) observed

that many dens were located up to 30 km from water sources in the Serengeti and the Ngorongoro Crater. Périquet *et al.* (2016) found that *C. crocuta* were able to locate their dens further from water sources, and thus further from concentrations of prey and associated concentrations of *P. leo*, although most dens were still within 3 km of water.

Table 2.2: *C. crocuta* den locations and associated environmental conditions.

Location	Substrate	Proximity to water	Vegetation	Den/occupation type	Reference
Namib-Naukluft Park, Namibia	Under rocky outcrop	Bank and ravine of seasonally dry Kuiseb River	Patches of shrubs, isolated trees	Entrance as daytime shelter by adults	Henschel *et al.* (1979) Tilson *et al.* (1980)
Mashtu Game Reserve, Botswana	Caves			Juveniles and adults present	Kuhn (2012)
Near Kajiado, Kenya	Cracks in lava				Sutcliffe (1970)
Urikaruus den, Gemsbok National Park, South Africa	Calcrete	Auob River bank			Mills and Mills (1977)
Kaspersdraai den, Gemsbok National Park, South Africa		Nassob River bed			Mills and Mills (1977)
Wright's den, Gemsbok National Park, South Africa	Dune	Overlooking Nassob River			Mills and Mills (1977)
Talek Region, Kenya	Soil			Natal and communal dens	Boydston *et al.* (2006)
Queen Elizabeth National Park, Uganda	Alluvial sediments				Sutcliffe (1970)
Serengeti and Ngorongoro Crater, Tanzania	Sediments	Up to 30 km from water	Preferentially in plains, rather than wooded areas		Kruuk (1972)
Ngorongoro Crater, Tanzania		Near lake			Sutcliffe (1970)
Amboseli Airstrip Den, Kenya	Trench in calcrete		Open grassland	Natal and communal den	Faith (2007)
Comoé National Park, Côte d'Ivoire			Forest patches	Raising cubs	Korb (2000)
Comoé National Park, Côte d'Ivoire			Savannah	Shallow holes for shelter	Korb (2000)
Hwange National Park, Zimbabwe	Sand	More dens further from water, up to 3 km	Variable		Périquet *et al.* (2016)

One further consideration regarding den availability is competition. Kruuk (1972) observed that in the Serengeti and Ngorongoro Crater, other users of sediment burrows include *P. africanus*, jackals and spring hares (*Pedetes capensis*). Even burrows excavated by an animal as small as *P. capensis* are large enough for inhabitation by a *C. crocuta* cub (Périquet *et al.*, 2016). However, a literature search revealed little evidence for den competition. One *C. crocuta* den in the Gemsbok National Park, South Africa, was visited by porcupines (*Hystrix africaeaustralis*), yet there was no interaction between the species. Another den was inhabited at separate times by *C. crocuta*, *P. brunnea* and *Hystrix* sp. (Mills and Mills, 1977). Overall, it appears that there are few controlling factors on the location and availability of *C. crocuta* dens, suggesting that during the Pleistocene, so long as there were available caves or soft sediment potentially close to a river, there may not have been any restrictions on den locations. However, as seen in Section 2.4.2, different conditions during the Pleistocene may have had different influences on den availability.

C. crocuta may carry carcasses back to the den to feed themselves; cubs are not provisioned by this food, according to Skinner (2006). Indeed, cubs are not weaned until they are nearly fully grown (Kruuk, 1972). Lansing *et al.* (2009) made observations of females bringing food to dens to provision cubs, and one observation of a male attempting to bring food to a sibling, but these amounted to only 3 % of the prey items brought to the dens. In the Talek region, young hyaenas at communal dens were observed chewing on, among other things, bones, aiding in the development of strong cranial bone and musculature (Holekamp and Smale, 1998). In the Serengeti, an adult female was thrice observed carrying a wildebeest leg for her own consumption to the natal den where her cub was located (East *et al.*, 1989). The reason for taking food to the den for consumption is to avoid inter- and intraspecific competition (Skinner, 2006; Fourvel *et al.*, 2015). Indeed, in comparison to open-air sites with greater interspecific competition, there was a lower degree of breakage of bones found inside a cave in Syokimau Gorge, Kenya. This suggested that decreased competition meant that the individuals did not have to consume the entire carcass to obtain sufficient food (Egeland *et al.*, 2008). This is an important consideration when considering bone consumption by Pleistocene *C. crocuta*, since increased bone consumption may indicate interspecific competition or dietary stress, as observed in *C. lupus* during Marine Oxygen Isotope Stage (MIS) 5a (Flower and Schreve, 2014).

The act of bringing food back to the den leads to accumulation of bones. Bones and teeth, most exhibiting carnivore damage, were found around the vicinity of *C. crocuta* dens in Timbavati Private Nature Reserve, South Africa (Bearder, 1977). Bones of prey were found outside Heraide den in Djibouti (Fourvel *et al.*, 2015), and outside dens within forest patches of Comoé National Park (Korb, 2000). Only 1 % of the prey remains at dens in the Talek region were taken inside

(Lansing *et al.*, 2009). By contrast, the bones of Yangula Ari den in Djibouti, and a den in the Namib-Naukluft Park, were located both outside and inside (Henschel *et al.*, 1979; Fourvel *et al.*, 2015). Many bones were also discovered inside a cave that functioned as a *C. crocuta* den in Syokimau Gorge, Kenya (Egeland *et al.*, 2008).

C. crocuta bone assemblages are smaller and accumulate at a slower rate than those accumulated by *P. brunnea* and *H. hyaena*. This is thought to be because, unlike *C. crocuta*, the other species more frequently provide food for their young at the dens (Skinner and Chimimba, 2005; Lansing *et al.*, 2009).

2.3.5 Mortality

Kruuk (1972) assessed the cause of death for 28 *C. crocuta* in Ngorongoro Crater and the Serengeti. Of those where cause was determined, the greatest mortality was through competition for food: *C. crocuta* were killed by other *C. crocuta* or by *P. leo*. Predation by *P. leo* upon *C. crocuta* cubs has also been observed, and was especially prevalent in the Serengeti in 1997 and 1998. The El Niño conditions of these years meant that rainfall was earlier, greater in volume, and almost continuous. This resulted in a net-like vegetation through which *C. crocuta* had difficulty moving, thus making it difficult to evade predators (Hofer, 2000).

Within the Ngorongoro Crater and Serengeti, starvation or disease constituted 21 % of *C. crocuta* deaths, although this mostly comprised subadults (Kruuk, 1972). Vulnerability of younger individuals is illustrated in a study by Binder and Valkenburgh (2000). Of newly-weaned *C. crocuta*, the bite strength and ability to crunch bone are diminished compared to older individuals. These authors suggested therefore that if food is not plentiful, these younger *C. crocuta* may starve especially if their mothers are low in the social structure of the clan and thus would have access to only the poorer and tougher parts of the carcass (Binder and Van Valkenburgh, 2000). Holekamp and Smale (1998) suggest that in a litter of more than one cub, the siblings quickly develop a dominance hierarchy, with the dominant cub obtaining a greater share of the mother's milk. When food is scarce, a subordinate cub may thus starve. Further evidence of the influence of food on mortality comes from a more recent study of Ngorongoro Crater populations. A reduction in food availability, coupled with increased direct competition with *P. leo* for food likely increased mortality, causing a decline in *C. crocuta* populations from the 1960s to 1990s (Höner *et al.*, 2005).

Lack of food may also influence susceptibility to disease. Between the years 2002 and 2003, there was an outbreak of the bacterium *Streptococcus equi ruminatorum* within the *C. crocuta* population of the Ngorongoro Crater (Höner *et al.*, 2006). This resulted in an increased mortality

rate, and associated population decline, with the hardest hit demographics being those individuals without preferential access to food. The disease also became more prevalent with greater interspecific competition and lower prey density, indicating the importance of food availability in influencing the impact of disease (Höner *et al.*, 2012).

An additional cause of death may be aridity coupled with scarce fresh prey, as discussed above.

Humans are also an important cause of *C. crocuta* mortality, causing 8 % of deaths in the Ngorongoro Crater and Serengeti (Kruuk, 1972). This is most prevalent outside of protected areas but does also occur within. Direct persecution occurs due to livestock predation, the presence of settlements, competition with trophy hunters, recreation, and use of *C. crocuta* body parts for food and medicine. The varied methods include poisoning, trapping, shooting, and through snares set for other species (Hofer and Mills, 1998b, and references therein).

While the impact disease is difficult to determine in Pleistocene populations, the other factors (water and food availability, direct competition) are all important considerations when assessing the causes of the extirpation of *C. crocuta* from Europe.

2.3.6 Summary

Overall, this review indicates that the behavioural plasticity of *C. crocuta* allows them to survive under different environmental conditions, including diverse habitats, varying competition levels, prey species, food availability, and den locations. However, there are indications that if severe enough, several factors may limit *C. crocuta* survival, including competition, food availability, water availability and disease, in addition to human impacts.

From this review, a number of hypotheses can be formed regarding Pleistocene *C. crocuta*.

1. Greater competition and/or lower prey availability led to increased bone consumption. This may have been a factor contributing to the extirpation of *C. crocuta* from Europe. This will be assessed through the predator and prey species diversity from the literature. The level of bone consumption will be indicated through craniodental morphometrics, and tooth breakage levels.
2. Reduced access to water was a factor leading to the extirpation of *C. crocuta* from Europe. This will be assessed through local palaeoenvironmental reconstructions coupled with dated *C. crocuta* records from the literature.

2.4 Pleistocene Crocuta crocuta

2.4.1 Presence in Europe

The first European record of *C. crocuta* is from Trinchera Dolina, Spain, dated to around 850-780 ka (thousand years ago), Marine Oxygen Isotope Stage (MIS) 21-19 (Garcia and Arsuaga, 2001), followed by the occurrence at Casal Selce, Italy, dated to around 800 ka, MIS 19-18 (Sardella and Petrucci, 2012).

After the first arrival in Europe, *C. crocuta* were apparently not present throughout Europe through all climatic periods and environmental conditions. This can be illustrated particularly well in Britain, in light of the good stratigraphical record that allows determination of the species' presence. Its earliest recorded presence is in deposits of approximately MIS 17-age from Pakefield, Corton, West Runton and Palling, all in East Anglia (Stuart and Lister, 2001; Parfitt *et al.*, 2005; Lewis *et al.*, 2010). Later records from the early Middle Pleistocene exist from Westbury and Boxgrove (Bishop, 1982; Parfitt, 1999; Roberts and Parfitt, 1999; Turner, 1999), correlated with MIS 13. During the late Middle Pleistocene, *C. crocuta* was present during MIS 9 and the later part of MIS 7 (Schreve, 2001). There is good evidence, however, that *C. crocuta* were absent from Britain during MIS 11 (Schreve, 2001), and possibly from the rest of Europe too (Stuart and Lister, 2014). During the Late Pleistocene, *C. crocuta* were present during MIS 5e, 5c and 3 (Currant and Jacobi, 2011), and were absent from Britain during MIS 5a (Turner, 2009). Currant and Jacobi (2011) suggested that this may be due to the cold conditions of MIS 5b, and the subsequent prevention of recolonization in MIS 5a due to high sea levels isolating Britain from the rest of Europe.

Extensive dating of *C. crocuta* remains by Stuart and Lister (2014) revealed that the species disappeared from eastern Europe around 40 ka. The final extirpation from Europe was dated to around 31-30 ka. This will be further discussed below.

While *C. crocuta* were spatially widespread across Europe during the Pleistocene, a search of the literature has not revealed any records of the species' presence in northern Europe, specifically Norway, Sweden, Finland, Denmark, Lithuania, Estonia or Latvia.

2.4.2 Denning and cave use

Pleistocene *C. crocuta* are notable for their use of caves in Europe, to the extent that they have been named the cave hyaena, as discussed in Section 2.2.3. This use allowed for the abundant accumulation of *C. crocuta* bones and coprolites, as well as remains of their prey. Indeed, caves such as Tornewton in Britain, and Teufelslucken in Austria have yielded hundreds of *C. crocuta*

bones and teeth (Ehrenberg, 1966a; Currant, 1998). Although few have been found, there is evidence that dens were also dug into sediment, such as in Glaston, Britain (Cooper *et al.*, 2012), and Biedenstag, Germany (Diedrich, 2006).

Diedrich (2011a) suggested that there were two different types of hyaena den in Pleistocene Europe: communal dens and cub-raising dens. A cub-raising den assemblage is characterised by a large proportion of juvenile *C. crocuta*, while a communal den assemblage is comprised mostly of adults with some juveniles (Diedrich, 2011a). This contrasts with present-day *C. crocuta* communal dens, which are used only by juveniles, and are not entered by adults (East *et al.*, 1989; Holekamp and Smale, 1998, see Section 2.3.4). A further use of caves is as a prey 'depot', which was used to hide food from other predators (Diedrich, 2011c). The *C. crocuta* found in prey depots are all adults (Diedrich, 2011a), accompanied by a large number of prey remains (Diedrich, 2011c).

C. crocuta dens are very common in western and southern Europe, especially ones dating to the Late Pleistocene. By contrast, they are much less common in eastern Europe. For example, *C. crocuta* dens in Serbia are represented by a very small number of caves, two of which are the Late Pleistocene (not dated to a particular Marine Oxygen Isotope stage) deposits of Janda Cavity (Dimitrijević *et al.*, 2014) and the MIS 3 aged deposits of Baranica Cave (Dimitrijević, 2011). Some of the other known caves containing Pleistocene deposits had been occupied by humans, and the majority by cave bears (during both the Middle and Late Pleistocene; Dimitrijević, 2011; Cvetković and Dimitrijević, 2014). This may therefore indicate that *C. crocuta* were outcompeted for caves by bears and humans.

Some caves have evidence of use by *C. crocuta* and other predators, further indicating the potential for competition for shelter (see Table 2.3). Discamps *et al.* (2012) stated that it is difficult to assess the temporal gap between cave occupations by *C. crocuta* and humans. However, given the apparent prevalence of both *C. crocuta* and Neanderthals (*Homo neanderthalensis*) in southwestern France, the author suggested that competition for caves was likely. This uncertainty about the time between occupations, and the degree of overlap with *C. crocuta* may also hold for other species listed in Table 2.3.

The above will be an important consideration when assessing the reasons for the extirpation of *C. crocuta* from Europe. In contrast with the evidence from modern dens (Section 2.3.4), Pleistocene *C. crocuta* may have experienced enhanced competition for the use of caves as shelter or food storage.

Table 2.3: Some examples of European caves with evidence of use by *C. crocuta* and other predators.

Site	Country	Age	Other occupants	References
TD8 level, Gran Dolina	Spain	Middle Pleistocene	Temporary shelter by bear (*Ursus* sp.), wolf (*Canis mosbachensis*), fox (*Vulpes* sp.), European jaguar (*Panthera gombaszoegensis*), lynx (*Lynx* sp.), badger (*Meles* sp.)	Blasco *et al.* (2011)
Grotta Paglicci	Italy	Middle/Late Pleistocene	Hominins	Crezzini *et al.* (2015)
Level F, Payre	France	MIS 8-7	Hibernation by cave bear (*Urusus spelaeus*). Occasional use by *C. lupus* and cave lion (*Panthera leo* (*spelaea*)). Repeated, short term use by *H. neanderthalensis*	Daujeard *et al.* (2011)
Bárta's pit III, Prepoštská Cave	Slovakia	Late Pleistocene	Occasional use by *H. neanderthalensis*	Sabol *et al.* (2013)
Camiac	France	Late Pleistocene	Hominins	Discamps *et al.* (2012)
La Chauverie	France	Late Pleistocene	Short term visits by hominins	Discamps *et al.* (2012)
Pešturina Cave	Serbia	MIS 5d and 3	Repeated use by hominins	Blackwell *et al.* (2014)
Baranica I	Serbia	MIS 3	Hominins, wolf (*Canis lupus*), red fox (*Vulpes vulpes*)	Dimitrijević (2011)
Tournal Cave	France	MIS 3	Repeated use by hominins. Hibernation by *U. spelaeus* and brown bear (*Ursus arctos*)	Magniez and Boulbes (2014)
Les Rochers-de-Villeneuve	France	MIS 3	Hominins	Beauval *et al.* (2005)

2.4.3 Diet and competition

Physical evidence of hyaena diet is determined from prey bones and teeth showing marks from *C. crocuta*'s teeth and gastric acid (Stuart 1982; Sutcliffe 1970). Diet may also be inferred from the carbon and nitrogen stable isotope composition of carnivore and herbivore remains (e.g. Bocherens *et al.*, 2011, 2015, 2016) and through prey DNA in coprolites (Bon *et al.*, 2012). Table 2.4 contains a summary of studies using these lines of evidence to reconstruct Pleistocene *C. crocuta* diets. The studies indicate that the prey species largely correspond with the size and type of ungulate prey species targeted by present day *C. crocuta* (see Section 2.3.3), although there may have been a greater reliance on rhinoceros, especially woolly rhinoceros (*Coelodonta antiquitatis*). There is little to no evidence of small prey consumption, contrasting with some of the modern studies. However, this may be partly because smaller prey bones are more easily completely consumed and are therefore not preserved in the fossil records.

In addition, there is evidence that *C. crocuta* preyed or scavenged upon other carnivores. *V. vulpes* of Bukovynka Cave, Ukraine, may have been prey of *C. crocuta* (Bondar and Ridush, 2015). Cooper *et al.* (2012) suggested that *C. crocuta* consumed wolverine (*Gulo gulo*) in Glaston. Gnawed *U. spelaeus* remains were found in *C. crocuta* dens in France from MIS 5e, 5c and 3 (Fourvel *et al.* 2014). *U. spelaeus* found in Bukovynka Cave, may have been the prey of *C. crocuta* (Ridush, 2009). Based on the paucity of the remains of herbivores at sites such as Zoolithen Cave and Rösenbeck Cave, Germany, Diedrich (2011a) and Diedrich (2011b) suggested that cave bears were important food sources for *C. crocuta* (whether through predation or scavenging) in Late Pleistocene boreal forest environments.

Hominins may also have been a food source. The MIS 3 aged deposits of Les Rochers-de-Villeneuve yielded a bone of *H. neanderthalensis* that has been gnawed by *C. crocuta*, although it was unclear whether the individual had been directly preyed upon or its remains scavenged (Beauval *et al.*, 2005).

There is evidence of *C. crocuta* cannibalism from Biedensteg (Diedrich, 2006), Balve Cave (Diedrich, 2011b) and Rösenbeck Cave, Germany (Diedrich, 2011a), Sloup Cave (Diedrich, 2012a) and Koněprusy Caves, Czech Republic (Diedrich 2012b), and Baranica Cave (Dimitrijević, 2011).

In Late Pleistocene Italy, while *C. crocuta* and hominins had similar prey preferences (*C. elaphus* was most important), *C. lupus* preyed on different species (*C. ibex*, *C. capreolus* and smaller species). However, *C. crocuta* and *C. lupus* preyed mostly on the oldest and youngest individuals whereas hominins preyed on prime-aged adults. Collectively, this indicates that the three predators occupied different environmental niches (Stiner, 1992, 2004).

A review of MIS 3 and 4 age deposits in France revealed dietary similarities between *H. neanderthalensis* and *C. crocuta*, but the relative contributions of prey species were different. While both species consumed bovids, equids and cervids, *C. crocuta* consumed more bovids and equids, whereas *H. neanderthalensis* consumed more cervids. Additionally, assemblages accumulated by *C. crocuta* were more species-diverse, due in part to consumption of carnivores (Dusseldorp, 2013a). Similarly, at the site of Saint-Césaire, France, attributed to MIS 3, isotopic results suggested some differences in the preferred prey species of *C. crocuta* and *H. neanderthalensis*. The diet of both species contained approximately the same proportion of bovids, large cervids and horse (*Equus caballus*), but *C. crocuta* consumed more reindeer (*Rangifer tarandus*), while *H. neanderthalensis* consumed more *C. antiquitatis* and woolly mammoth (*Mammuthus primigenius*; Bocherens *et al.* 2005).

Remains from Payre, France (MIS 8/7), indicated spatial partitioning of preferred prey species. *C. crocuta* and *P. leo* (*spelaea*) preyed upon species likely found within the wet, denser vegetation of the valley surrounding the site, including *Stephanorhinus* sp., horse (*Equus mosbachensis*), *M. giganteus* and *C. capreolus*. By contrast, *C. lupus* largely targeted different species that inhabited the drier, more open vegetation of the plateau near the cave, including *C. elaphus* and thar (*Hemitragus bonali*). *H. neanderthalensis* altered its targeted prey species over time, at one point targeting the valley prey, and at another point targeting the plateau prey (Bocherens *et al.*, 2016).

By contrast, other studies indicate some overlap of carnivore diets. *C. crocuta* were likely responsible for the bones of animals such as equids and red deer (*Cervus elaphus*), found within the lower layers in Caldeirão Cave, Portugal. However, the leopard (*Panthera pardus spelaea*) and the bearded vulture (*Gypaetus barbatus*) may also have contributed to the accumulation (Davis *et al.*, 2007). Bones of bison (*Bison* sp.), and horse (*Equus* sp.) in Les Rochers-de-Villeneuve, France exhibited damage caused by both *C. crocuta* and humans, indicating competition between the two predators (Beauval *et al.*, 2005).

Isotopic data has also indicated potential competition. Isotopic values from MIS 3 age assemblages from the Ardennes, Belgium, revealed competition between *C. crocuta*, *P. pardus*, *G. gulo* and *U. arctos* for prey species. There was no overlap of prey species between *C. crocuta* and *P. leo* (*spelaea*). However, after *C. crocuta* disappeared from the area, *P. leo* (*spelaea*) began to consume what had been *C. crocuta*'s preferred prey, suggesting that competition from *C. crocuta* had previously excluded *P. leo* (*spelaea*) from taking that prey species (Bocherens *et al.* 2011).

Table 2.4: Some studies indicating the herbivore species that *C. crocuta* consumed during the Pleistocene of Europe.

Site	Country	Age	Evidence	Prey species	References
Grotta Paglicci	Italy	Middle/Late Pleistocene	Prey remains	Aurochs (*Bos primigenius*) fallow deer (*Dama dama*), *C. elaphus*	Crezzini *et al.* (2015)
Koněprusy Caves	Czech Republic	Late Pleistocene	Prey remains	Predominantly C. antiquitatis. Also Przewalski's horse (*Equus ferus przewalskii*), bison (*Bison priscus*), giant deer (*Megaloceros giganteus*), *C. elaphus*, *R. tarandus*	Diedrich (2012b)
Biedensteg	Germany	Late Pleistocene	Prey remains (in order of most to least abundant)	*C. antiquitatis*, *E. f. przewalskii*, *B. priscus*, *M. giganteus*, *R. tarandus*, *M. primigenius*	Diedrich (2006)
Janda Cavity	Serbia	Late Pleistocene	Prey remains	*M. primigenius*, *C. antiquitatis*, horse (*Equus germanicus*), *M. giganteus*, *B. priscus*	Dimitrijević *et al.* (2014)
Various	Italy	Late Pleistocene	Prey remains	*C. elaphus*, *B. primigenius*, *E. caballus*, roe deer (*Capreolus capreolus*), fallow deer (*Dama dama*), wild boar (*Sus scrofa*), ibex (*Capra ibex*)	Stiner (2004)
Lower layers, Caldeirão Cave	Portugal	Late Pleistocene	Prey remains	Equids, *C. elaphus*	Davis *et al.* (2007)
Cueva del Búho	Spain	MIS 5d-3	Prey remains	*Equus* sp., Bovidae sp., Cervidae sp.	Iñigo *et al.* (1998)
Various	France	MIS 3 and 4	Prey remains	Bovids, equids, cervids	Dusseldorp (2013)
Bois Roche	France	MIS 4	Prey remains	Predominantly bovids and horse *E. caballus*. Some *R. tarandus*	Marra *et al.* (2004), Villa *et al.* (2010)
Baranica Cave	Serbia	MIS 3	Prey remains	*E. caballus*, wild horse (*Equus ferus*), *M. giganteus*, *B. priscus*, *C. ibex*, very young or old *C. antiquitatis* and *M. primigenius*	Dimitrijević (2011)

Coygan Cave	Britain	MIS 3	Prey remains	Damage to many bones. *C. antiquitatis* and *E. ferus* most abundant	Aldhouse-Green *et al.* (1995)
Glaston	Britain	MIS 3	Prey remains	Damage predominantly to *C. antiquitatis* bones, in addition to those of *G. gulo* and *M. primigenius*	Cooper *et al.* (2012)
Goat's Hole Paviland	Britain	MIS 3	Prey remains	*C. antiquitatis, R. tarandus* (including shed antlers)	Turner (2000)
Kents Cavern	Britain	MIS 3	Prey remains	Including *M. primigenius* (predominantly juveniles), *E. ferus*	Pengelly (1872), Lister (2001)
Pin Hole	Britain	MIS 3	Prey remains	Including *C. antiquitatis,* possibly *M. giganteus*	Busk (1875)
Rochers-de-Villeneuve	France	MIS 3	Prey remains	*Bison* sp., *Equus* sp.	Beauval *et al.* (2005)
San Teodoro	Italy	MIS 3	Prey remains	*Palaeoloxodon mnaidriensis* (dwarf elephant) and *Cervus elaphus siciliae* (Sicilian red deer), *Bos primigenius siciliae*/*Bison priscus siciliae* (Sicilian aurochs/Sicilian bison) *S. scrofa, Equus hydruntinus* (stenonid ass)	Mangano (2011)
Tournal Cave	France	MIS 3	Prey remains	*M. giganteus*, *C. elaphus*, Pyrenean ibex (*Capra capra praepyrenaica*), wild boar (*Sus scrofa*), *E. caballus*, bovids. Possibly *R. tarandus* and *C. antiquitatis*	Magniez and Boulbes (2014)
Saint-Césaire	France	MIS 3	Isotopic analysis	*R. tarandus*, bovids, large cervids, *E. caballus*	Bocherens *et al.* (2005)
Payre	France	MIS 8-7	Isotopic analysis	Rhinoceros (*Stehanorhinus* sp.), *C. capreolus*, *M. giganteus*, horse (*Equus mosbachensis*), possibly bovids	Bocherens *et al.* (2016)
Coumere	France	Likely MIS 3	*C. crocuta* coprolite DNA	*C. elaphus*	Bon *et al.* (2012)

The evidence outlined above therefore suggests that *C. crocuta* may have been in competition with some species for food, but that there was scope for niche differentiation, whether that was through the species targeted or the age demographics of prey. Whilst much is known about the diet of *C. crocuta* and competition for food in the Pleistocene, little is known about how food availability has changed with changing environments. An analysis of evidence of nutritional stress is therefore needed to address this issue, and will be presented in this thesis.

2.4.4 Body size and morphometrics

Previous authors have attempted to examine variations in size in Pleistocene *C. crocuta*, and differences in morphology when compared to modern *C. crocuta*, although conclusions are contradictory. Klein and Scott (1989) proposed that measurements of m1 (first lower molar) length indicated that *C. crocuta* from the Devensian (last cold stage) period in Britain were larger than those from the Ipswichian (Last Interglacial), a change that was assumed to be a response to declining temperatures, following Bergmann's rule. However, reconstructions of British *C. crocuta* body masses revealed that whilst there was some difference in the average body masses between MIS 5e, 5c-a and 3, the differences were not significant (Collinge, 2001). Conversely, Turner (1981) measured bones and teeth of British *C. crocuta* and found no overall size difference between those of Ipswichian and those of Devensian age.

Turner (1981) did, however, find that overall Ipswichian and Devensian *C. crocuta* were larger than modern day African *C. crocuta*. However, the radius, tibia, metacarpal III and metatarsal III were all smaller than those of modern *C. crocuta*, making the Ipswichian and Devensian *C. crocuta* more robust and powerful. This was suggested to be due to differences in the size and resistance of prey (Turner, 1981). Additionally, canines from *C. crocuta* of Devensian age were found to be larger than those from the Ipswichian, suggesting that this may be in response to prey having more subcutaneous fat in the colder Devensian climate, thus requiring more powerful dentition to penetrate the surface (Turner, 1981).

The length of the skulls of individuals from central Europe during the last glacial period were also larger than modern African *C. crocuta* (Diedrich, 2011a). According to Diedrich (2011a), the sagittal crests of Late Pleistocene *C. crocuta* from central Europe took three different forms: flat, slightly convex, and highly convex. The author suggested that the highly convex sagittal crest developed as a result of disease or damage to the muscles attached to the sagittal crest during the life of the individual. No explanation was given for the flat and slightly convex forms, other than that they were 'normal', i.e. not pathological (Diedrich, 2011a).

A reassessment of the morphology of British *C. crocuta* will be undertaken in this thesis. This will be supplemented by an assessment of Late Pleistocene *C. crocuta* morphometrics from across Europe.

Diedrich (2011) attempted to determine the sex of *C. crocuta* specimens from central Europe during the last glacial period. Measurements included the skull length, occipital condyle width and the lengths and distal widths of long bones. These measurements were split into males and females by Diedrich (2011) with the assumption that the largest specimens were female and the smallest were male. However, the author acknowledged that there is overlap between the largest (assumed) males and the smallest (assumed) females. There appears to be no indication as to how the decision was made to group certain specimens as female and others as male. Moreover, this was done with no apparent consideration as to whether the measurements are adequate in distinguishing between males and females of present day *C. crocuta*, or even whether females actually are larger than males in all the above measurements.

This thesis will therefore include an analysis of the manifestation of sexual size dimorphism in the bones and teeth of present day *C. crocuta*. This will be used to indicate whether sexual size dimorphism needs to be considered when interpreting Pleistocene morphometrics.

2.4.5 Extirpation from Europe

Stuart and Lister (2014) created a chronology of *C. crocuta* presence in Europe during MIS 3, based on a collation of radiocarbon dates, derived directly from *C. crocuta* remains. Dates were excluded if they were dated before 1980, or if they did not fit the pattern exhibited by the other dates. The results of Stuart and Lister's (2014) model indicated that *C. crocuta* became extirpated from the Urals and central/eastern Europe at around 40 ka. Following this, the species became extirpated from northwestern and southern Europe around 31-30 ka, with the latest dated specimen from Grotta Paglicci, Italy.

A number of dates were re-dated by Stuart and Lister (2014) using a newer pre-treatment method: ultrafiltration. Compared to other methods, ultrafiltration is more successful in removing contaminants from bone samples, and usually results in older dates (Higham *et al.*, 2006; Jacobi *et al.*, 2006). Nevertheless, a number of dated specimens were included in Stuart and Lister's (2014) model that had not been subjected to the ultrafiltration method, presenting a potential problem with the accuracy of the model.

Potential problems with Stuart and Lister's (2014) model were highlighted by Dinnis *et al.* (2016). Dates from Caldey Island, Britain were included in Stuart and Lister's (2014) model. However,

the specimens from Caldey Island may have been conserved with varnish (van Nédervelde and Davies, 1975 cited in Dinnis *et al.*, 2016), leading Dinnis *et al.* (2016) to exclude these dates from their analysis of *C. crocuta* presence in Britain during MIS 3.

The dates from Caldey Island were the youngest dates for *C. crocuta* in Britain in Stuart and Lister's (2014) model. Therefore, excluding the Caldey dates resulted in the latest evidence of *C. crocuta* presence in Britain to be older, at around 35 ka (Dinnis *et al.*, 2016).

Given the issue with some of the dates, the publication of new dates and the publication of a new calibration curve (IntCal 13, Reimer *et al.*, 2013), a new model will be created in Chapter 7.

Several suggestions have been made about the causes of the extirpation of *C. crocuta* from Europe. *C. crocuta* may have been physically intolerant to decreasing temperatures towards the end of MIS 3 (Stuart and Lister, 2014). There may have been reduction in prey availability due to overall reduction in prey biomass and/or increased competition from other predators (Stiner, 2004; Stuart and Lister, 2014). Finally, there may have been increased competition for cave sites with the arrival into Europe of modern humans (Stuart and Lister, 2014).

Varela *et al.* (2010) modelled *C. crocuta* distributions during five time periods (126 ka, 42 ka, 30 ka, 21 ka and the present day) in order to determine whether climate change was the cause of the species' extirpation from Europe. The results indicated that climate was not the sole cause, as there were areas in Europe that were still suitable *C. crocuta* habitation at 21 ka. The author instead suggested the prey availability and competition with humans should be investigated.

Lack of confidence may be placed in the results, however, as the conditions from all five time periods, including 21 ka, were used to determine the climatic requirements of *C. crocuta* (Varela *et al.*, 2010). Many of the samples that had yielded very late dates of *C. crocuta* presence in Europe were subsequently re-dated by Stuart and Lister (2014), revealing that the species was likely present in Europe no later than 30 ka. Thus, Varela *et al.*'s (2010) suggestion that the climatic conditions in part of Europe during MIS 2 were suitable for *C. crocuta* may not have been the case.

In Chapter 7, the cause of *C. crocuta* extirpation will be re-examined, including climate, given that interstadials became shorter, while stadials became longer and more frequent towards the end of MIS 3, as evidenced in the Greenland ice core data. Vegetation cover, food availability and competition and competition for shelter will also be investigated.

2.4.6 Summary

This review has indicated that Pleistocene *C. crocuta* may have differed from present-day *C. crocuta* in the factors that influenced their survival. Particularly, it appears that the use of dens was even more important for all ages of individuals. Additionally, *C. crocuta* may have experienced competition for shelter from other species. This may have been a limiting factor in their survival.

The review indicates that there are still gaps in the knowledge of Pleistocene *C. crocuta*, which will be addressed in this study. Firstly, a thorough morphological assessment over different temporal and geographical scales in warranted. This will demonstrate how *C. crocuta* responded to environmental changes, and whether these changes were sufficient to ensure their survival. Secondly, there has yet to be an assessment on *C. crocuta* food availability and dietary stress during the Pleistocene. This will be addressed through the level of bone consumption. These will be coupled with a review of the literature detailing local environmental conditions, including, where available: potential competitors, prey species, and climatic conditions. Taken together, these may shed further light on the potential causes of *C. crocuta* extirpation from Europe.

3 Body size, craniodental and postcranial morphology review

3.1 Body size

3.1.1 Introduction

Body size can be influenced by a diverse range of factors acting through natural selection of genes and genetic drift, or phenotypic plasticity as a result of the environmental conditions prevalent during the growth of an individual (Gienapp *et al.*, 2008; Merilä and Hendry, 2014). These will be discussed in the following review, with a view to aiding the interpretation of geographical variation in body size of present day and Pleistocene *C. crocuta*.

3.1.2 Influences on body size

One of the most heavily-researched influences on body size is ambient temperature, as in the case of Bergmann's Rule. The rule was originally defined as 'larger species live farther north and the smaller ones farther south' (Bergmann, 1847, p. 648, cited in James, 1970, p. 390), although it was later reinterpreted with a more intraspecific view point (Meiri, 2011); '[r]aces of warm blooded vertebrates from cooler climates tend to be larger than races of the same species from warmer climates' (Mayr, 1956, p. 105).

The traditional explanation behind individuals being of larger body size in colder environments is that the relative surface area of an individual is reduced, thereby facilitating heat conservation (Mayr, 1956). This thermal efficiency should, in theory, mean that mass-specific metabolic rates are relatively lower in the larger animals, thus reducing energetic costs (Steudel *et al.*, 1994). However, some authors such as Scholander (1955), Irving (1957) and Steudel *et al.* (1994) have suggested that other factors are important in temperature conservation, including an insulating pelage and subcutaneous fat, the ability of tissue to withstand cold temperatures, and vascular control regulating heat in the appendages (i.e. a counter-current heat exchange system). Furthermore, Meiri *et al.* (2007) stated that variation of body size with latitude may not be due to temperature, but rather caused by factors such as food availability, which may also vary with latitude. This is in agreement with McNab (1971) who stated that where carnivores conform to Bergmann's Rule, it is likely due to the size of their prey varying with latitude, but see (Ashton *et al.*, 2000), discussed below.

Not all species' body mass distributions follow Bergmann's Rule but a majority of those reviewed in the recent literature do. Meiri and Dayan (2003) found that 65.1 % of the 149 mammal species studied conformed to Bergmann's Rule, whether that be through a relationship with

temperature or with latitude. Meiri *et al.* (2004) found that 50 % of carnivore species conformed to Bergmann's Rule when relationship with latitude was assessed, although 11 % of species showed a significant inverse relationship with latitude, i.e. they were larger in lower latitudes. Of particular relevance here is the observation by Ashton *et al.* (2000), who found that a greater proportion of carnivorans follow Bergmann's Rule. Twenty-six of 33 species of carnivores (79 %), including *C. crocuta* and *P. brunnea*, showed a positive relationship with latitude, so were larger in higher latitudes. Similarly, 11 of 14 species of carnivores (79 %) had a negative relationship with temperature, so were larger in colder temperatures (Ashton *et al.*, 2000).

Specific studies relating to *C. crocuta* include Klein (1986), who used latitude as a proxy for temperature, finding that *C. crocuta* first lower molars are larger further from the equator, thus corresponding with Bergmann's Rule. Roberts (1951) measured *C. crocuta* skulls and found that those from South Africa are larger than those from eastern Africa. This is also reflected in other large carnivores in Africa, such as *P. leo*, which are smaller in Tanzania and Kenya and larger in more southern populations (Smuts *et al.*, 1980). It is anticipated that this pattern will be reflected in the Pleistocene *C. crocuta* record.

The seasonality of environments has been demonstrated to be more important for some species than relative temperature. Highly seasonal environments may result in seasonal fluctuations in food availability, necessitating larger body size through increased fat reserves to endure fasting, as demonstrated in female bobcats (*Lynx rufus*, Wigginton and Dobson, 1999), Tibetan macaque (*Macaca thibetana*) and Japanese macaque (*Macaca fuscata*, Weinstein, 2011). Millar and Hickling (2008) however suggested that larger size through increased fat reserves is only advantageous when food is absent for a period of time or food shortages are unpredictable, as smaller individuals will deplete their reserves first and succumb to starvation. When food is available but is limited for a prolonged period, the authors stated that smaller body size is advantageous as less food is required for the individual to stay alive. In contrast, larger-bodied animals will eventually lose their reserves as they are unable to obtain the required food for their large size over such a long period of low food availability (Millar and Hickling, 1990). This is something to bear in mind in terms of *C. crocuta*, as some areas have seasonal migrations of prey species (such as migrations between the Maasai Mara and Serengeti), so food availability varies (Cooper *et al.*, 1999).

A further influence upon body size is food quality and abundance. These factors are in turn related to climatic conditions such as rainfall, and to competition (McNab, 2010). *U. arctos* in Alaska have larger body size in areas with higher quality foods and the highest population densities of *U. arctos*, although this latter factor is itself influenced by food quality and availability (McDonough and Christ, 2012). Similarly, reduced sea ice and an associated

reduction in prey accessibility was the likely cause of polar bear (*Ursus maritimus*) body size decrease over time (Rode *et al.*, 2010). Body size of female *U. arctos* in Sweden is influenced by population density-controlled food availability; *U. arctos* were smaller in higher population densities as competition was higher. Additionally, geographical differences were observed, with smaller individuals in the north (*contra* Bergmann's Rule). This was because of lower primary productivity and the shorter growing season of berries, in addition to longer hibernation periods in the north (Zedrosser *et al.*, 2006). In view of this, variation in food availability (whether through prey biomass or competition) may have influenced *C. crocuta* body size during the Pleistocene.

The relationship between interspecific competition and size has largely been confined to individual characteristics related to feeding (Dayan and Simberloff, 1998, and references therein). Studies that have focussed upon overall body size include Jones (1997) who found that variation in size with latitude was a more important determinant on carnivorous marsupials than competition. However, McNab (1971) suggested that the presence of competitors of larger body size may constrain a species to a smaller size. An example is the puma (*Felis concolor*), which is smallest when its range overlaps with that of the jaguar (*Panthera onca*), and is larger outside of this range (McNab, 1971). The latter study may have relevance to understanding patterns of size distributions during the Pleistocene where the distribution of large carnivore species vary over time and space. *C. crocuta* may have become bigger after MIS 12 in Britain, when many big carnivores such as the cave bear (*Ursus deningeri*) and the European 'jaguar' (*Panthera gombaszoegensis*) became extinct (Stewart, 2008).

Across species, population density correlates negatively with body size (Damuth, 1981, 1987). Within-species population density variation may also have some influence over an individual's body size. However, as reviewed by Dayan and Simberloff (1998), studies are contradictory. On one hand, some studies suggested that increased population density leads to smaller litters, and increased lifespan, leading to greater body size. Other studies suggested that greater population density leads to smaller body size (see Dayan and Simberloff, 1998). This latter scenario may occur through intraspecific competition limiting food availability (Boucher *et al.*, 2004).

Other variables that have been considered in the literature include whether distance from the species' range edge influences body size because of the potential for suboptimal habitats in these areas (Meiri *et al.*, 2009). Some carnivores were found to be larger at range edges (the percentages of species exhibiting these patterns varied with the statistical test conducted). However, the authors attributed this to corresponding geographic variation in other factors such as temperature or resources (Meiri *et al.*, 2009).

A further consideration is Cope's Rule, whereby a species will evolve towards an optimum body size (Stanley, 1973). This was observed in hypercarnivorous canids, in that they increased in body mass and at the same time, developed more specialised craniodental morphology for predation and meat-eating (Van Valkenburgh *et al.*, 2004), which will be discussed in more detail below.

The Island Rule describes the body size changes in a species after isolation. Studies of carnivores have indicated body size decreases on islands (Foster, 1964; Van Valen, 1973; Meiri *et al.*, 2008). Body sizes of 324 populations of Carnivora populations exhibited significant size changes once isolated, and this change in body size was demonstrated to be rapid. This rapidity was not quantified, but the extant populations were isolated for less than 10 ka (Lomolino *et al.*, 2013).

Carnivores that hunted prey larger than themselves on the mainland exhibited dwarfism when small prey were available on islands (Lyras *et al.*, 2010). This is because the smaller prey consumption cannot sustain the large body size. However, if small prey are not available, the isolated carnivore will not exhibit much reduction in body size (van der Geer *et al.*, 2010).

Reduction in competitors may also drive the Island Rule (Lomolino, 1985; Faurby and Svenning, 2016). If a carnivore had a competitor of larger size than itself on the mainland, the absence of this competitor on the island may allow the isolated carnivore to increase in size. This may be because the isolated carnivore is able to exploit a greater range of resources, including larger prey, from which it was previously out-competed on the mainland (Lomolino, 1985). However, Raia and Meiri (2006) found no significant influence of competition upon the body size of isolated carnivores.

3.1.3 Implications for the Pleistocene

The present research will critically examine the evidence for body mass varying geographically using modern *C. crocuta* across Africa. The changes in body size of European Pleistocene *C. crocuta* spatially and temporally will also be assessed. The following hypotheses will be tested:

1. Pleistocene *C. crocuta* followed Bergmann's Rule and were larger in colder conditions. This will be assessed by reconstructing *C. crocuta* body masses from periods of different palaeoclimatic conditions.
2. Pleistocene *C. crocuta* were constrained to a smaller body size when competitors were present. This will be assessed by comparing body masses of *C crocuta* against those of other carnivores from the literature.

3. Pleistocene *C. crocuta* were smaller when there was less food available. Elevated levels of bone consumption is an indication of food stress, particularly determined from mandibular bending strength and tooth breakage.
4. Pleistocene *C. crocuta* were influenced by the Island Rule, and were therefore smaller on islands. This will be tested by comparing *C. crocuta* on Sicily with those from mainland Europe.

3.2 Sexual size dimorphism

3.2.1 Introduction

Sexual size dimorphism (SSD) is another way in which body size can vary. SSD is not present in all species, nor does it occur in the same direction or degree. In mammals, males are frequently the larger of the two sexes, although female-biased SSD does occur, one example of which is *C. crocuta* (Ralls, 1976). As with body size, there are a number of theories about the causes of SSD, which will be outlined below.

SSD in present-day *C. crocuta* bones and teeth will be assessed in this thesis. Furthermore, geographical variation in the degree of SSD will be assessed across Africa, thus allowing any changes in SSD to be established. It is important to be aware of the degree of SSD when interpreting Pleistocene records, since failure to identify any great differences between males and females may add to variation in Pleistocene morphometric records making it harder to interpret underlying patterns.

3.2.2 Influences on sexual size dimorphism

The root cause of SSD is often thought to be sexual selection. Where males are larger than females in polygynous species, Lindenfors *et al.* (2007) suggested larger size in males evolves because it confers advantages when competing for females.

Ralls (1976) outlined many reasons why sexual selection for female-female competition is unlikely the sole cause for female-biased SSD in mammals. For example, there is no consistent pattern in the degree of parental investment by males over females in species with female-biased SSD, which might be expected to be the case if females were competing for males. Furthermore, while male-male competition exists in polygynous species, there is no evidence in any mammal species of the opposite, i.e. polyandry (Ralls, 1976). Indeed, Frank (1986) stated that *C. crocuta* is a polygynous species.

Rather, Ralls (1976) suggested that selection for smaller males is a likely cause of female-biased SSD, possibly combined with selection for larger females. The author notes that selection for smaller males, or at least a lack of selection for larger males, may occur in some species where there is little competition between males for mates.

The degree of SSD may be influenced by environmental factors, for example, latitude and its accompanying changes in seasonality and resource availability (Isaac, 2005). Seasonality of environmental factors, such as food, may influence whether breeding is seasonal or aseasonal,

with seasonal breeding in polygynous species leading to less male-male competition and thus reduced SSD as there are more females in season at one time (Isaac, 2005, and references therein).

Intra- or interspecific competition may also influence SSD. An increase in the population density of a species may result in a reduction of available food per individual. If males and females respond differently to this food scarcity, e.g. males through size reduction and females through delayed reproduction but no size change, the degree of SSD would decrease (Isaac, 2005, and references therein).

An additional factor to consider is Rensch's Rule, which states that where males are larger than females, the degree of SSD increases with larger body size. On the other hand, where females are larger than males, the degree of SSD decreases with larger body size (Rensch, 1950, cited in Abouheif and Fairbairn, 1997). If SSD does not follow this hyperallometric trend with body size, it may be hypoallometric, or there may be no change in SSD with increased size (Abouheif and Fairbairn, 1997; Fairbairn, 1997). Rensch's Rule is more common in taxa with male-biased SSD than those with female-biased SSD (Abouheif and Fairbairn, 1997). The cause of Rensch's Rule is thought to be sexual selection favouring increase in male size, regardless of whether the species exhibits male-biased or female-biased SSD (Abouheif and Fairbairn, 1997). It is anticipated that Rensch's Rule will not be exhibited in *C. crocuta*, although this will be investigated in this thesis.

Overall, Isaac (2005) stated that SSD is ultimately likely a result of a combination of factors. This is in agreement with Ralls (1976, p.259) who stated that 'the degree of sexual dimorphism in size in a mammalian species is the result of the difference between the sum of all the selective pressures affecting the size of the female and the sum of all those affecting the size of the male.'

As mentioned, *C. crocuta* is one species in which females are larger than males. One of the earliest assessments of variation in size of *C. crocuta* was performed by Matthews (1939). Here, the author measured individuals from the Serengeti, Tanzania, and determined that in terms of the length of the head and body, the tail, the hind foot and the ear, females were larger than males. In the southern Kalahari body mass and heart girth of females were significantly larger than those of males; however, there was no significant difference in body length (Mills, 1990). Of the individuals captured in Aberdare National Park, Kenya, females on average had greater body mass, body length and heart girth, however these differences were not significant (Sillero-Zubiri and Gottelli, 1992). In summary, canines, fourth upper premolar (P4), skull length, moment arm of resistance at the lower canines, and body mass of female *C. crocuta* are on

average larger than those of males. However, width of the first lower molar (m1), and indications of bite force (measurements of the moment arm of the temporalis, and moment arm of the masseter) are all greater in males than in females (Gittleman and Van Valkenburgh, 1997). It is difficult to say whether this means that males possess greater bite force than females, as bite force is based on the relationship between the muscle moment arms and the moment arm of resistance (Kiltie, 1982; Alexander, 1983). This relationship will be discussed in more detail in Section 3.3.6.1. Sexual dimorphism in bite force will also be investigated in this thesis. The length of the m1 was greater in females in Gittleman and Van Valkenburgh's (1997) study, although Klein (1986) found no difference between males and females.

The most robust examination of SSD in *C. crocuta* was carried out by Swanson *et al.* (2013) with measurements on 651 live, wild individuals in the Maasai Mara National Reserve, Kenya. Females were larger than males in most of the measured traits. The authors interpreted the discrepancies between their results and those of previous studies as being due to previously insufficient sample sizes. The measured traits that exhibited dimorphism were body mass, body length, skull length, head circumference, distance from the zygomatic arch to the top of the sagittal crest, distance from the zygomatic arch to the back of the sagittal crest, neck circumference, girth of the torso, shoulder height, scapular length, and upper leg length. Only three traits failed to exhibit dimorphism: lower-leg length, fore-foot length, hind-foot length (Swanson *et al.*, 2013). Some of these results are different to those mentioned above by other authors, which is probably because of the larger sample size used by Swanson *et al.* (2013).

Differential female/male access to food was ruled out as the cause of dimorphism by Swanson *et al.* (2013) as a study of captive *C. crocuta* where both sexes were fed the same food revealed similar SSD to the wild *C. crocuta*. It was thus suggested that the dimorphism is a result of genetic factors. Some traits were found to be more dimorphic than others, with mass and those associated with robustness exhibiting the greatest differences in size between males and females. Differences in the level of dimorphism were associated with the age at which the measured trait stopped growing. It was also found that as females and males cease growing at the same age, SSD is due to females growing faster (Swanson *et al.*, 2013).

Isaac (2005) suggested that the female-biased SSD in *C. crocuta* is due to the control that the females exert over the mating process (East *et al.*, 1993), and that mating success in males is unrelated to size, rather it is determined by the order in which males arrive into a clan (East and Hofer, 1993). Isaac (2005) suggested that the lack of male-male competition related to size would explain the smaller size of the males. In addition, the author suggested that female-female competition for dominance or food may select for larger females.

3.2.3 Summary

As indicated in the review, there is still some uncertainty about the causes of SSD. *C. crocuta* exhibits female-biased SSD is many traits. However, it is as yet unknown whether the majority of bones and teeth of *C. crocuta* exhibit SSD. This will be investigated in the present study by studying body mass, bones and teeth of wild-caught *C. crocuta* across Africa. The impact of environmental conditions upon the degree of SSD will also be assessed. It will highlight how SSD is exhibited in present-day C. crocuta, which may lead to misinterpretations of the Pleistocene.

3.3 Craniodental morphology

3.3.1 Introduction

The cranium is a complex structure associated with numerous processes (Tseng and Binder, 2010): ingestion, mastication (Lucas, 2015), food acquisition (i.e. prey capture; Biknevicius *et al.*, 1996), vision, hearing, olfaction (Nummela *et al.*, 2013) and respiration (Smith and Rossie, 2008; Macrini, 2012), as well as housing the brain (Ewer, 1973). The mandible, on the other hand, is associated exclusively with the processes of feeding (Tseng and Binder, 2010): food acquisition (Rahmat and Koretsky, 2015), ingestion and mastication (Lucas, 2015).

The morphology of the cranium, the mandible and dentition can therefore be adapted to, and constrained by, these processes, in addition to the constraints imposed by phylogeny (Tseng and Binder, 2010; Figueirido *et al.*, 2011). This may occur through evolution or phenotypic plasticity (Gienapp *et al.*, 2008; Whitman and Agrawal, 2009; see Section 3.3.8). In light of the importance of the aforementioned processes for species survival and success, assessment of the morphology of the skull is important in studies of how *C. crocuta* responded to environmental changes during the Pleistocene.

Consequently, when examining both Pleistocene and modern specimens for morphological variation, it is important to acknowledge the potential range of influences on the morphology of the specimens. The following review considers the various influences on the mammalian skull, focussing particularly on the Carnivora, and drawing on studies of *C. crocuta* where available. In addition to features on the outer skull surface, some of which are assessed in the present study, internal skull features and soft tissues are also briefly included in the review. This is because some of the processes that influence external skull morphology (e.g. feeding, vision), may also be controlled by elements that are only evident from the internal structure, or from soft tissues that do not influence the morphology of the cranium. It should therefore be borne in mind that the external morphology of the skull may not present all the relevant information about a process.

Ontogenetic development is briefly reviewed below (see Section 3.3.7). This is an important consideration in light of the potential for continued development of some skull features after adulthood has been reached, which may lead to erroneous interpretation of Pleistocene material if not recognised.

Figure 3.1 to Figure 3.3 illustrate the anatomical terminology of the external skull surface used within this review.

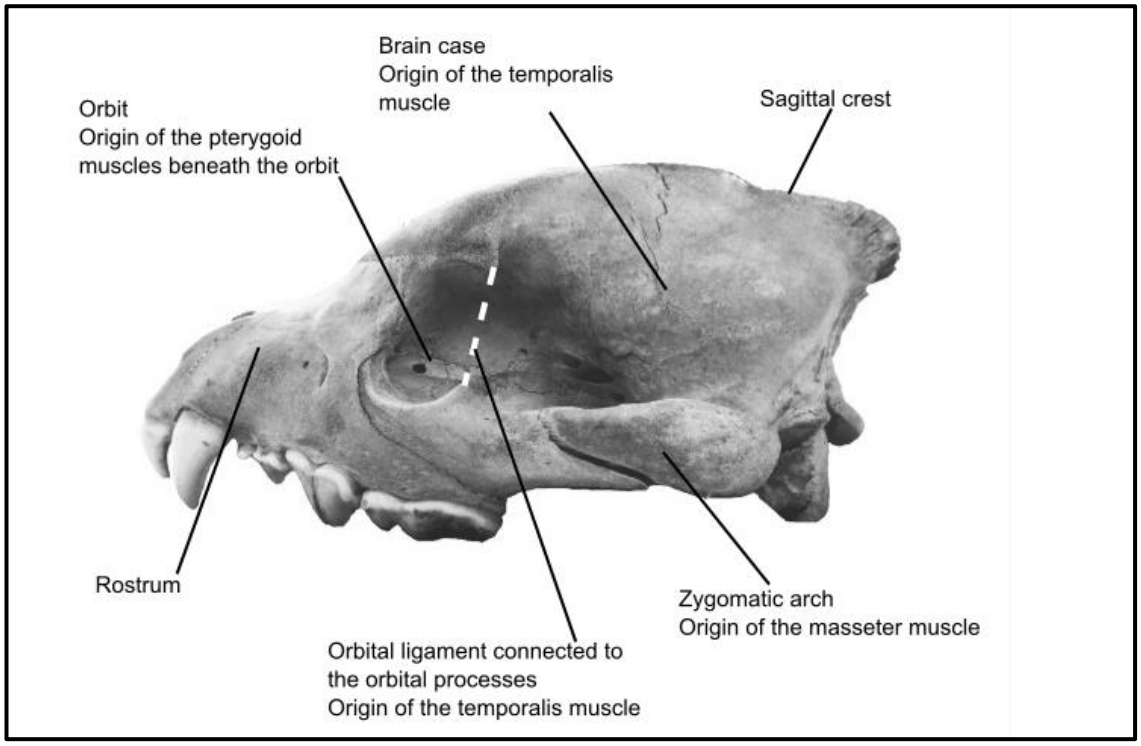

Figure 3.1: Lateral view of *C. crocuta* cranium with labels of anatomical features mentioned in this review. Muscle origin sites from Ewer (1973). See text for more detail.

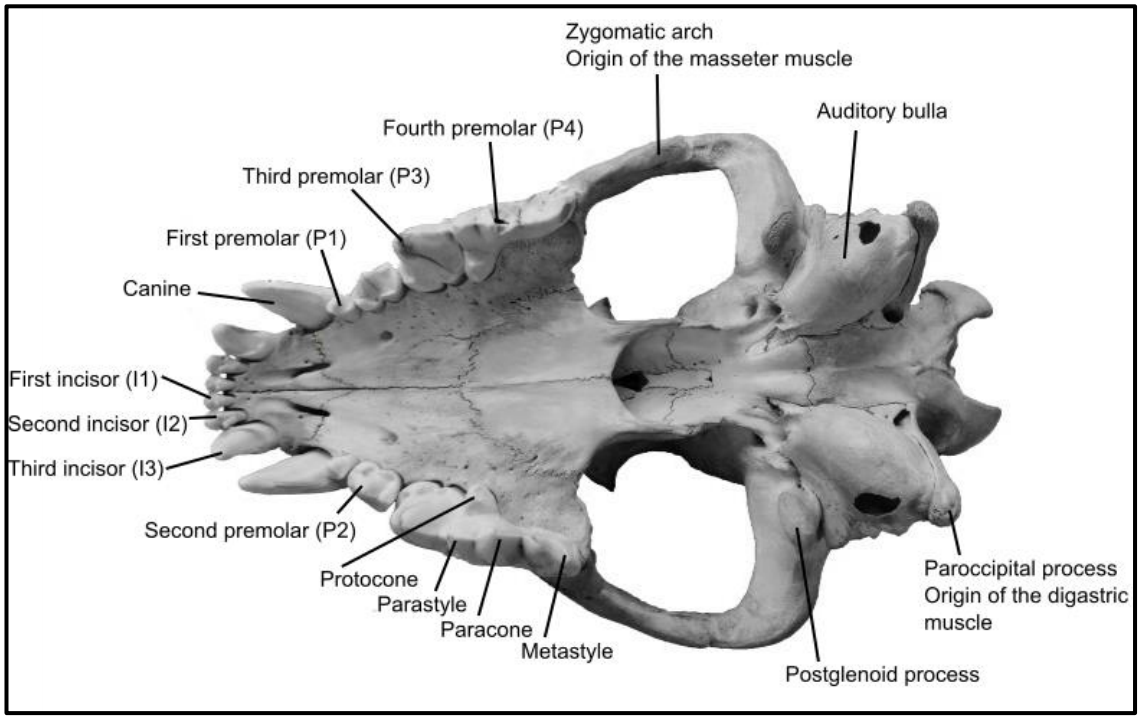

Figure 3.2: Ventral view of *C. crocuta* cranium with labels of anatomical features mentioned in this review. Muscle origin sites from von Toldt (1905), cited in Turnbull (1970), and Ewer (1973). See text for more detail.

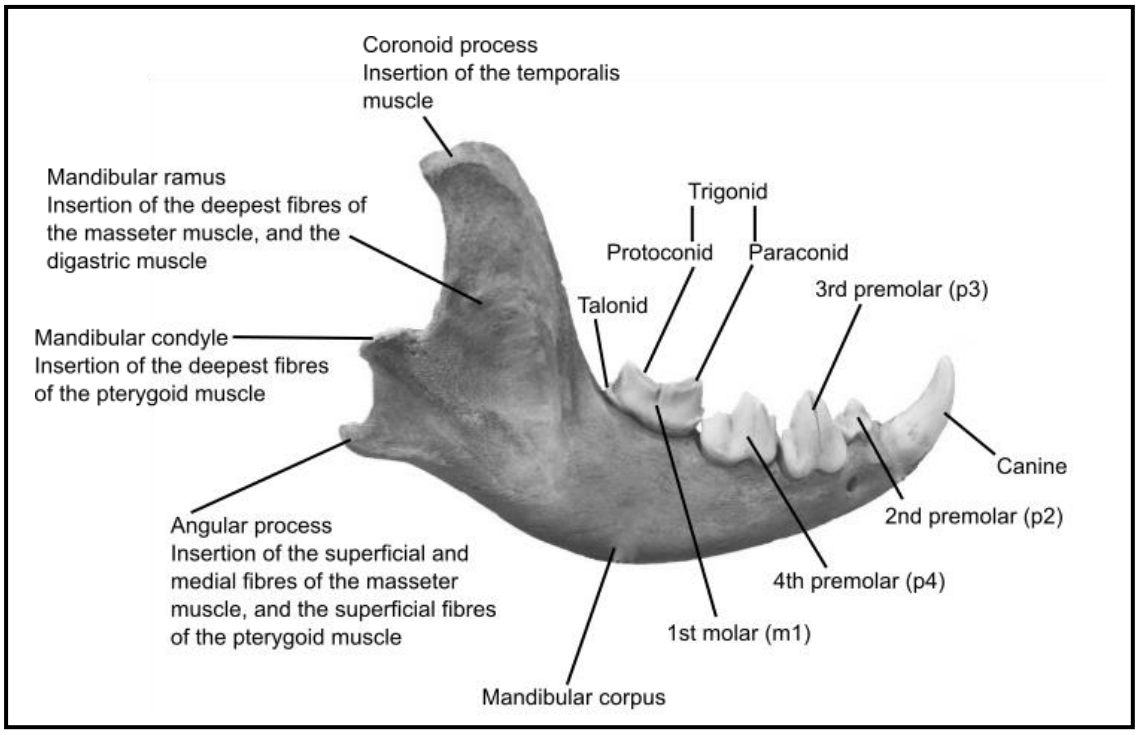

Figure 3.3: *C. crocuta* mandible with labels of anatomical features mentioned in this review. Muscle insertion sites from von Toldt (1905), cited in Turnbull (1970), and Ewer (1973).

3.3.2 The brain

The brain influences cranial shape through the size of the brain case (Ewer, 1973; Thomason, 1991). There is negative allometry between body mass and brain size and thus, larger species have proportionately smaller brains (Ewer, 1973). Brain size develops early in ontogeny and is less responsive than body size in both phenotypic and genetic terms to environmental changes (Dunbar, 1998).

Many theories have been proposed to explain influences upon brain size. One theory is that larger brains occur due to larger overall body size. Another theory is that the brain is larger in species that consume rich diets as surplus energy is available for brain development during gestation (Dunbar 1998, and references therein). However, Dunbar (1998) refuted these theories on the basis that the brain is energetically expensive to maintain, so there must be an advantage to having a large brain to outweigh this cost; the brain will not become larger merely because it is able to do so.

A further theory is the social brain hypothesis, in that a large brain is needed to process the additional information required with greater sociality and more complex relationships (Dunbar, 1998, 2009). Although relative brain size has been suggested to relate to sociality in primates,

ungulates and carnivores (Pérez-Barbería *et al.*, 2007), other studies have failed to demonstrate this relationship among members of the Carnivora (Gittleman, 1986; Finarelli and Flynn, 2009; Swanson *et al.*, 2012).

The size of the brain is also related to problem solving, with species of Carnivora with larger brain volume (relative to body size) more successful at opening boxes containing food (Benson-Amram *et al.*, 2016). In the Carnivora, species with carnivorous diets have larger brains than omnivores and insectivores, potentially due to the more greater challenge and thus cognitive processing involved in predation (Gittleman, 1986; Swanson *et al.*, 2012 and references therein).

It can therefore be hypothesised that periods in the Pleistocene involving more challenging food procurement led to larger brain sizes. This may have involved more frequent hunting than scavenging, and the targeting of larger or behaviourally more complex prey. In the present study, this hypothesis will be assessed through measurements of the width of the brain case.

However, the complication is that the morphology of the brain case is not solely influenced by the size of the brain. Wroe *et al.* (2005) suggested that there is a trade-off between the size of brain and the size of the masticatory muscles, which consequently impacts upon bite force. Indeed, in hypercarnivorous canids, larger masticatory muscles in some large species were positively correlated with brain volume (Damasceno *et al.*, 2013). Conversely, Ewer (1973) stated that when the brain case does not allow sufficient attachment area for a muscle, the sagittal crest provides a further attachment site for the temporalis muscle, thus allowing the muscle to be larger than would otherwise be expected.

3.3.3 Vision

Among the Felidae, Canidae, Mustelidae and Viverridae, Radinsky (1981a) found that the area of the orbits scales negatively with allometry, meaning that larger species have relatively smaller orbits. Radinsky (1981a) suggested that larger eyeballs are indicative of better developed visual ability. In a study of four carnivore families, relative to skull length, felids had the largest orbital area, followed by canids, viverrids and finally mustelids. This led to author to suggest that felids had the greatest visual abilities of the four families (Radinsky, 1981a). A second study increased the number of Viverridae and Mustelidae species, and was extended to include Procyonidae, Ursidae and Hyaenidae. The orbital area relative to skull length was greater for *C. crocuta* than all the other species in this second study. The value was greater than the average for the Canidae family as a whole but still lower than that of the Felidae family: 1.15 for *C. crocuta*, 1.07 for Canidae, 1.45 for Felidae (Radinsky, 1981a, 1981b). Based on this, it could be suggested that *C. crocuta* visual ability is intermediate between Felidae and Canidae. How this impacts

C. crocuta behaviour relative to felids and canids is difficult to determine, as visual ability involves a number of different factors, including vision in different light levels and spatial resolution, as outlined below.

The time of day during which animals are active may be indicated by orbit size. There is evidence from studies of primates that, relative to body size, nocturnal species have larger orbits than diurnal species (Schultz, 1940; Kay and Kirk, 2000). The implications of this in terms of Pleistocene climates are outlined below.

However, the anatomy relating to other variables of visual ability are limited to the eye itself rather than the bone (Ewer, 1973; Savage, 1977). For example, the photoreceptors (cones and rods) of the retina are related with visual ability in low or high light levels. The rods of *C. crocuta* only comprise around 0.9 % of the total number of photoreceptors, indicating strong nocturnal vision (Calderone *et al.* 2003). The density of ganglion cells is associated with spatial resolution. The spatial resolution achieved by the *C. crocuta* eye is similar to other carnivores (Calderone *et al.* 2003, and references therein).

A complicating factor is that the area of the orbits are not only associated with the eye. The temporalis muscle has some fibres that originate in the orbital ligament and the tissue at the back of the orbit. The orbital ligament connects the orbital process on the frontal bone and the orbital process of the zygomatic arch. Therefore, the size of the temporalis muscle, along with the size of the eye influences the size of the postorbital processes. Large eyes and temporalis muscle would lead to large postorbital processes (Ewer, 1973). When considering size changes of the orbits of Pleistocene individuals, the influence of both the eye and of muscles must therefore be considered. The influence of the masticatory muscles upon the orbits is outlined in more depth in Section 3.3.6.1.

3.3.4 Hearing

Important aspects of hearing include the ability to locate sounds, the ability to distinguish between sounds, and hearing sensitivity to sound frequencies. These are important for prey location and communication between group members (Ewer, 1973).

The external cranial morphology related to hearing is represented by the auditory bulla (measured in this thesis) that encloses the middle ear (Hildebrand, 1974). Among the Canidae, Felidae, Viverridae and Mustelidae, the volume of the auditory bulla scales negatively with allometry (Radinsky, 1981a). Many Carnivora, including *C. crocuta* have inflated bullae.

Sensitivity to sound may be achieved through increasingly inflated bullae or expansion of the middle ear; the two do not have to co-occur (Hunt, 1974).

Similar to vision, aspects of hearing may also be influenced by changes in features that are not preserved in the Pleistocene record. One example is the pinna, which does not contain bone but is instead constructed of cartilage, ligaments and muscles (Gray, 2003), which is associated both with hearing and temperature regulation; larger pinnae allow both increased collection of sound waves and increased heat loss (Ewer, 1973; Hildebrand, 1974). Therefore, colder periods in the Pleistocene may have encouraged enlargement of the pinnae, as might any conditions that necessitated improved auditory ability (see below). Similarly, larger auditory bullae may have occurred during periods that necessitated increased sensitivity to sound, explored further below.

3.3.5 Olfaction and respiration

Respiration and olfaction are considered together as some of the same features are important to both functions. The features of the skull that are associated with respiration are the turbinals (Smith and Rossie, 2008; Macrini, 2012), which are also associated with olfaction, as are the cribriform plate (also called the ethmoid bones), and the impression upon the bone of the olfactory bulb of the brain (Bird *et al.*, 2014). These features are internal and there does not appear to be any information in the literature as to how they influence the external structure of the skull, and will therefore not be discussed further.

As would be anticipated, there is cooperation between the senses. Nummela *et al.* (2013) assessed the size of organs relating to vision, hearing and olfaction in 119 mammalian species. The size of the eyeball and the tympanic sulcus (the bony ridge surrounding the tympanic membrane between the outer and middle ear) showed positive correlation with each other. By contrast, the size of the cribriform plate was independent of the sizes of the eyeballs and the tympanic sulcus.

Nummela *et al.*'s (2013) study also differentiated between the sense organs of species with different diets. While there appeared to be a trade-off between olfaction against vision and hearing, this was not the case for the carnivorous species. Relative to overall body size, species with carnivorous diets had medium- to large-size eyeballs, tympanic sulci and cribriform plates. The enhanced-size of these features, despite their high metabolic cost during ontogeny and daily use, indicate the importance of vision, olfaction and hearing to the survival of carnivorous taxa

(Nummela *et al.*, 2013). Indeed, Kruuk (1972) provided evidence for the great olfactory, hearing and nocturnal visual abilities of *C. crocuta* from observations of their reactions to sights, smells and sounds of prey and clan members, many of which were imperceptible to the human observers.

The importance of the senses in food acquisition was demonstrated in the predominantly wooded Timbavati Private Nature Reserve, South Africa. *C. crocuta* were able to locate carrion by following scent trails, even those trails created three days previously. Hearing was also important in that *C. crocuta* responded to simulations of prey calls and sounds of group feedings. They were also able to follow lion calls to locate a *P. leo* kill. Auditory ability was also used to avoid conflict with *P. leo*; if *C. crocuta* were feeding and a *P. leo* call was heard, the *C. crocuta* abandoned the food (Bearder, 1977).

Change in size of the orbital areas of the skull or of the auditory bullae may have occurred in response to changing environments during the Pleistocene. For example, the time of day during which *C. crocuta* were active may have changed. *C. crocuta* have been classed as crepuscular (Kruuk, 1972; Hayward and Hayward, 2007), although activity does continue to occur through the night, albeit decreasing between 02.00 and 05.00 hours (Hayward and Slotow, 2009), behaviour that Hayward and Hayward (2007) suggested may exist in order to avoid high temperatures during the day. Indeed, (Cooper, 1990) observed *C. crocuta* hunting in daylight in temperatures no higher than 20°C. In cooler periods or higher latitudes in Europe during the Pleistocene, *C. crocuta* may have become more diurnal, reducing the need for such enhanced nocturnal vision. Their orbital area of the skull may thus be smaller.

Vegetation may also alter the importance of the senses. In closed vegetation situations, olfaction and hearing may have to be more acute to compensate for the vegetation obscuring vision. The auditory bullae may thus be larger in individuals from periods of wide-spread, closed vegetation. Alternatively, during periods such as MIS 5e in Britain, when there was a combination of closed forest, semi-open forest and more open landscapes (Sandom *et al.*, 2014), *C. crocuta* may have preferentially occupied the semi-open and open areas, such as occurred on river floodplains (Gibbard and Stuart, 1975).

3.3.6 Food acquisition, ingestion, mastication

3.3.6.1 Cranial and mandibular structure

Probably the most studied aspect of the skull is the morphology related to the three key processes of feeding: food acquisition (predation or scavenging in the case of *C. crocuta*), ingestion and mastication. Feeding behaviour, such as prey size and type of food consumed, are determined by skull morphology. This includes cranial and mandibular structure, dental morphology, and musculature, which in turn relate to bite force, the ability to resist stresses and strains, and gape (Thomason, 1991; Meers, 2002; Lucas and Peters, 2007; Lucas, 2015). Figueirido *et al.* (2013) stated that the important morphological features relating to durophagous feeding (including the bone cracking typical of *C. crocuta*) are the ability to exert a powerful bite force, and the ability to resist the loads involved during biting.

Bite force is 'the amount of force that can be exerted by the jaw adductor musculature and realised at the tooth row, as a function of jaw geometry' (Meers 2002, p.1). Across a subset of Carnivora, Crocodilia, Squamata and Chelonia, the larger the predator's body mass, the greater the bite force (Meers, 2002). This is generally because an increase in body size is associated with an increase in the size of the masticatory muscles (Werdelin, 1989; Ferretti, 2007). Therefore, inherent in the production of bite force is both the structure of the cranium and the mandible, and also their role as attachment sites of the masticatory muscles.

There are a number of masticatory muscles attached to the carnivore skull (see Figure 3.1 to Figure 3.3). The temporalis, masseter, and pterygoid are the jaw adductor muscles whereas the digastric opens the jaw (Turnbull 1970; Ewer 1973). The temporalis muscle originates on the side of the brain case and the orbital ligament, and inserts into the coronoid process. The masseter muscle originates in the zygomatic arch. The superficial fibres originate on the anterior part of the arch and insert in the angular process. The medial fibres originate on the central area of the zygomatic arch also insert on the angular process. The deepest fibres originate on the posterior part of the zygomatic arch and insert on the mandibular ramus. Some authors such as von Toldt (1905, cited in Turnbull 1970) and Turnbull (1970) suggest there is an additional muscle, the zygomatic-mandibular, attached to the zygomatic arch and the coronoid process. However, it is difficult to distinguish this from the temporalis and masseter muscles. The pterygoid muscles originate beneath the orbit with the superficial fibres inserting on the angular process and the deeper fibres inserting on the mandibular condyle (Ewer, 1973). The origin of the jaw opening digastric muscle is the paroccipital process, and the insertion is the posterior, lower edge of the mandibular ramus (von Toldt 1905, cited in Turnbull 1970; Ewer 1973).

In the Carnivora, the temporalis muscle is the largest masticatory muscle. Within Turnbull's (1970) 'Specialised Group I' (Carnivora), the jaw opening muscles accounted for between 7.5 and 14 % of total masticatory muscle mass (the averages for the jaw closing muscles were 64 % for temporalis, 28 % for masseter, and 8 % for pterygoid). Based on autopsies of four *C. crocuta*, the average weight of the temporalis was 247 g and the masseter 136 g. From this, it was estimated that the temporalis contributed 50 %, the masseter 32 %, and the pterygoid 18 %, to the total adductor muscle mass (Tanner *et al.*, 2008). The mass of muscles influences the force they can exert during feeding (Tseng and Binder, 2010). Thus, of the jaw closing muscles, the temporalis is dominant, followed by the masseter and then the pterygoid (Turnbull, 1970).

The morphology of the skull may aid in interpretation of musculature when only the bone is present. Two aspects of the mandible led Rahmat and Koretsky (2015) to highlight the powerful musculature of *C. crocuta* and its bone cracking suitability. These features were the deep mandibular fossa and the prominent angular process, which, as mentioned, are areas of insertion of the adductor muscles. Additionally, in comparing the mandibles of *C. crocuta*, *H. hyaena* and *P. brunnea*, Werdelin (1989) noted that the distance between the mandibular condyles of *C. crocuta* was greatest, and that this was due to the greater muscle volume in this species.

Bite force is often assessed by modelling the carnivoran jaw as a lever. These models differ in complexity (Herring, 1993, and references therein). However, all lever models require a pivot, which is the jaw joint, an "in-force", which is the lifting action of the masticatory muscles, and an "out-force", which is the resistance force at the teeth (Moore, 1981).

The in-force and out-force can be measured by the moment arms or lever arms, that is, the distance from the joint to the line of force acting upon the joint (Figure 3.4). The moment arms of the adductor muscles represent in-force and various methods have been applied to measure them, using both distances from the muscle attachment on the cranium to the jaw joint, and distances from the attachment on the mandible to the jaw joint. The moment arm of resistance (MAR) represents the out-force, and is a measure of the distance from the bite point to the jaw joint (e.g. Emerson and Radinsky, 1980; Kiltie, 1982; Van Valkenburgh and Ruff, 1987). These in turn provide information about the mechanical advantage of the muscles. Mechanical advantage is the relationship between the in-force and out-force: the greater the out-force relative to the in-force, the greater the mechanical advantage (Alexander, 1983). Out-force is greater with smaller out-levers or moment arms of resistance, and in-force is greater with longer in-levers or muscle moment arms (Kiltie, 1982). Bite forces are therefore stronger at the carnassials than at the canines (Thomason, 1991; Bourke *et al.*, 2008; Ellis *et al.*, 2009). This is due to the shorter MAR when biting at the carnassials (Bourke *et al.*, 2008; Ellis *et al.*, 2009). An

estimation of the maximum force the muscles are able to generate may be applied to the lever model to provide further information on bite force (e.g. Kiltie 1982; Thomason 1991).

An example of a lever model is one applied to crania of selected Canidae species by Ellis *et al.* (2009). In this model, larger species had a greater bite force at both the canine and molars than smaller species. In these larger species, those with brachycephalic crania (shorter relative facial lengths) had the highest bite force. Bite force was mainly influenced by the shorter out-lever arm, and thus greater MAR, in the brachycephalic species (Ellis *et al.*, 2009).

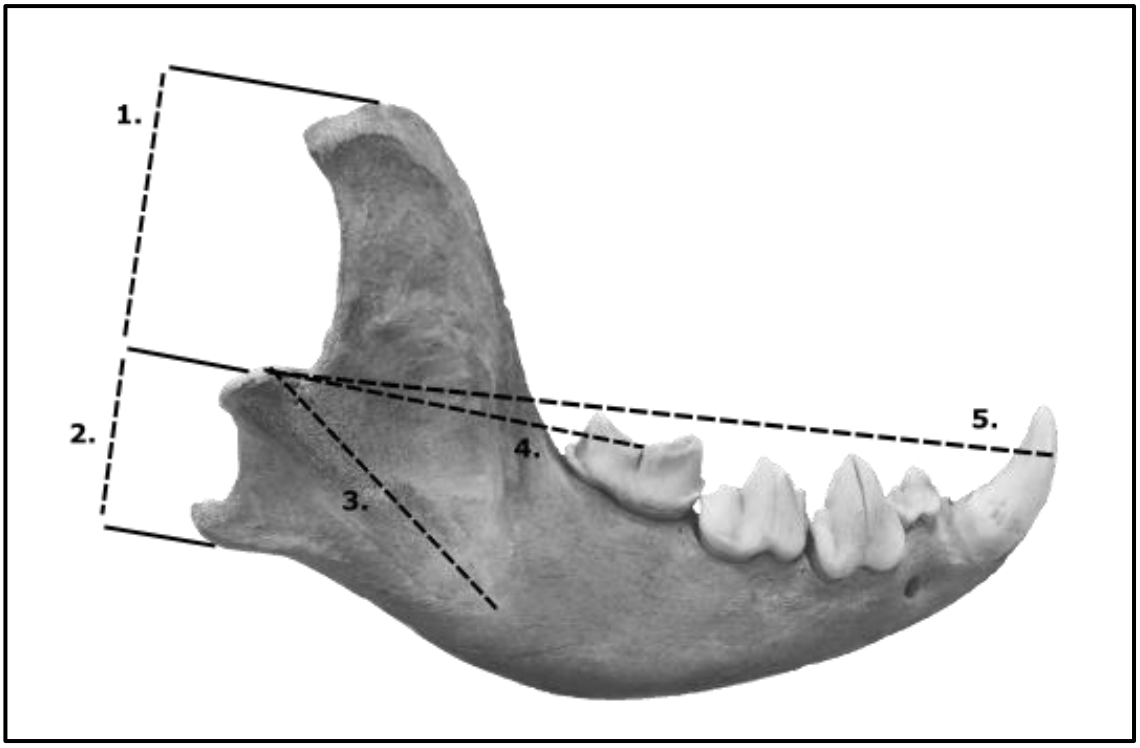

Figure 3.4: Mandible of a jaw of *C. crocuta* with examples of measurements of moment arms of the masticatory muscles and moment arms of resistance at two bite points. 1. Moment arm of the temporalis. 2. Moment arm of the superficial masseter. 3. Moment arm of the deep masseter. 4. Moment arm of resistance at the carnassial (Emerson and Radinsky, 1980). 5. Moment arm of resistance at the canine (Van Valkenburgh and Ruff, 1987).

Van Valkenburgh and Ruff (1987) measured the ratio of the moment arm of the temporalis (MAT) and the MAR at the canines of extant hyaenid, felid and canid species. The length of the MAT relative to the MAR was greater in hyaenids and felids, meaning that the mechanical advantage of the temporalis muscle was greater in the two families. The authors suggested that in light of the importance of the temporalis muscle in jaw closing, a greater mechanical advantage would enable a greater bite force at the canines. Additional evidence for the powerful

bite force of *C. crocuta* was found in a study of 98 species of Carnivora. Of all the species, *C. crocuta* and *P. brunnea* had the smallest MAR when biting at the point of the first lower molar (m1), after controlling for body size (Radinsky, 1981a,b). This therefore indicates the potential for relatively more powerful bites at the carnassial for these two species (Radinsky, 1982).

The mandibular condyle is located roughly level with the teeth in the Carnivora, meaning that the lever arm of the masseter muscle is reduced relative to that in herbivores or rodents where the condyle is usually located above the tooth row (Hildebrand, 1974). This angular notch between the condyle and angular process is particularly narrow in the Hyaenidae, including *C. crocuta*, which Ferretti (2007) suggested may be related to bone cracking. Specifically, the author posited that the reduction in distance between the angular process and the condyle increases the mechanical advantage of the temporalis muscle, rather than the masseter muscle. This would increase bite force, given that the temporalis is larger than the masseter (Turnbull, 1970).

An alternative explanation for the small moment arm of the masseter muscle may be to protect the jaw joint. When using the cheek teeth, if the temporalis acted alone to lift the mandible and so close the jaw, there would be a large force at the condyle and the jaw might become dislocated. However, the small moment arm of the masseter allows effective stabilisation of the mandible. The temporalis lifts the mandible upwards and backwards, whereas the masseter and the pterygoid pull the mandible upwards and forwards. Therefore, there is little reaction force at the jaw joint during closing (Moore, 1981; Alexander, 1983).

In comparisons of extant species of Carnivora and Marsupialia, bite forces at the canines and carnassials were high for *C. crocuta* and were only exceeded by some large felids and ursids (Christiansen and Adolfssen, 2005; Wroe *et al.*, 2005; Christiansen and Wroe, 2007). However, body mass was then taken into account to produce the bite force quotient (BFQ). The BFQ of *C. crocuta* was similar to, or in some cases lower, than that of other species from all eight extant carnivore families and the Dasyuridae (Wroe *et al.*, 2005; Christiansen and Wroe, 2007). This was also the case for bone-cracking predators as a whole, leading Wroe *et al.* (2005) to suggest that craniodental morphology allowing resistance to high stresses is a more important adaptation to bone cracking than bite force.

As mentioned, in addition to bite force, another important property of the cranium and mandible is resistance to loads incurred during feeding (Figueirido *et al.*, 2013). Loads may be intrinsic, extrinsic or a combination of the two. Intrinsic loads are due to the muscle forces acting

on the bone. Extrinsic loads include the forces applied by food items such as struggling prey (Slater and Van Valkenburgh, 2009; Slater *et al.*, 2009). Inherent in the resistance to loads is the resistance to stress and strain. Stress is the transmission of force to an object from a load. Strain is the deformation of an object as a result of the application of a load (Hildebrand, 1974). Strain, when applied perpendicular to an object is measured as the change in length of an object divided by the original length, and thus may be positive (where tension occurs to lengthen the object), or negative (where compression occurs; Hildebrand 1974; Hylander 1979). In addition, shear stress, when a force is applied parallel to an object, causes deformation of one side of an object in the opposite direction to the other side (Hildebrand, 1974). In bending, both compression and tension occur. Torsion may also occur; this is when an object is twisted, and shear, tension and compression occur (Hylander, 1979). Strength is the ability of an object to resist forces without yielding (permanent or plastic deformation) or failure (formation of a crack), and thus return to its original dimensions after removal of a load (a process termed elasticity; Hildebrand 1974).

Mandibles are often modelled as elliptical beams in order to assess their resistance to loads in terms of bending strength. The length of the mandibular corpus as well as the magnitude of the size of the loads applied while biting necessitate development of bending strength (Biknevicius and Ruff, 1992). The height and width of the mandibular corpus, as well as the distance from the mandibular condyle to the point of load application (i.e. tooth position), are involved in calculation of bending strength (Biknevicius and Ruff, 1992; Therrien, 2005; Palmqvist *et al.*, 2011). Deeper beams have a greater bending strength in response to dorsoventral loads, wider beams have a greater bending strength to labiolingual loads, and shorter beams have a greater bending strength than longer beams (Hildebrand, 1974).

Prey killing invokes both dorsoventral stresses due to biting at the canines, and labiolingual stresses due to struggling prey (Biknevicius and Ruff, 1992). During biting, the balancing hemi-mandible (non-biting side) undergoes dorsoventral bending and torsion due to the pull of the adductor muscles, and reaction forces across the mandibular symphysis and jaw joint. On the working side (the side on which biting occurs), the hemi-mandible undergoes bending, torsion and shear strain. These are influenced by the pull of the muscles, reactionary forces, the point along the mandible at which an object is placed, and bite force. Furthermore, strain levels are higher when biting upon tough foods that require larger bite forces (Hylander, 1979).

Studies modelling the mandible of *C. crocuta* as a beam have found that dorsoventral bending strength increased posteriorly along the corpus. Deep mandibles allow resistance to dorsoventral loads occurring during biting, especially bone cracking (Biknevicius and Ruff, 1992; Therrien, 2005; Ferretti, 2007; Meloro *et al.*, 2008; Palmqvist *et al.*, 2011). Dorsoventral bending strength was also greatest posterior to the bone-processing teeth in *C. lupus* (Biknevicius and

Ruff 1992). In addition to the increase in height, the cortical bone of *C. crocuta* and *C. lupus* thickened dorsoventrally (Biknevicius and Ruff, 1992), which increased dorsoventral bending strength (Therrien, 2005). By contrast, this does not occur in felids, which seldom consume bone (Biknevicius and Ruff, 1992).

In support of this, upon comparing species with different diets from the Hyaenidae, Ursidae and Canidae, Raia (2004) found that there were certain similarities in the cranial morphologies of tough food (bone or tough vegetation) consumers. The mandibles were deep among the tough food consumers, necessary to withstand the bending stress induced by this food. Again, the mandibles were found to be deepest posterior to the bone-processing teeth in the Hyaenidae and Canidae. This occurrence of similar mandible structure in different families indicated a functional significance of the feature, rather than a merely phylogenetic signal (Raia, 2004).

Turner (1984) also noted that the mandible of *C. crocuta* is deeper posteriorly than anteriorly but stated that the age of the individuals is relevant, with older individuals having a greater degree of difference in depth between the anterior and posterior regions of the mandible.

At the canines, the corpus of *C. crocuta* has been found to be more rounded, and thus better able to resist labiolingual forces, such as torsion occurring when biting struggling prey (Therrien, 2005; Palmqvist *et al.*, 2011). However, the anterior mandible was more rounded in the Canidae than in the sub-Family Hyaeninae, perhaps due the latter occasionally cracking bone with the canines (Therrien, 2005). Overall bending strength at the canines in both dorsoventral and labiolingual directions was lower for the Hyaeninae than for the Felidae, which Therrien (2005) suggested reflected the differing killing behaviours of rapid bites for Hyaeninae versus a single, powerful bit for the Felidae. This would probably produce more powerful and unpredictable loads for the Felidae.

The morphology of the cranium also provides features to resist stresses. An example lies in the zygomatic arch, which, as mentioned, is the area of origin for the adducting masseter muscle (Ewer, 1973). The morphology of the zygomatic arch is deeper than it is wide, enabling it to have a greater bending strength against the muscles pulling on it (Hildebrand, 1974).

In beam models of the crania of North American opossum (*Didelphis virginiana*) and canid and felid species, Thomason (1991) determined that resistance to bending of the crania was stronger than necessary, given the forces applied to them. The author suggested therefore that resistance to torsion and shear stress may also be important in addition to bending strength. Additionally, the morphology of the cranium was suggested to be influenced by factors such as encasing the brain, masticatory muscles, olfactory system and the eyes. (Thomason, 1991).

The sinuses of *C. crocuta* also aid in resistance to stresses. Instead of a flat forehead, *C. crocuta* has an arching line that almost reaches the sagittal crest (Werdelin, 1989; Werdelin and Solounias, 1991; Joeckel, 1998; Ferretti, 2007). This vaulting is due to the expansion of the anterior frontal sinuses (Joeckel, 1998). The vaulted shape allows the stresses invoked through bone cracking to be transferred throughout the top of the skull, instead of concentrated in one area, and the evolution of an increasingly vaulted forehead through the Hyaenidae lineage indicates an adaptation to increased bone cracking and thus more thorough consumption of a carcass (Werdelin, 1989; Werdelin and Solounias, 1991). The elongated sinuses mean that the sagittal crest is pneumatised (in contrast to the bony plates in other carnivores), which better resits forces imposed during mastication than do the bony plates in other carnivores (Joeckel, 1998). In addition to stress dissipation during biting, the front sinus expansion is a light-weight structure (Curtis and Van Valkenburgh, 2014). Stress dissipation through the pneumatised sagittal crest were also confirmed in Finite Element Analysis models (Tanner *et al.*, 2008; Tseng, 2009).

Alongside bite force and resistances to loads, gape is important in feeding. This has not been measured in the present study, but it is worth briefly mentioning in light of its relationship with bite force. Gape is related to the size of prey targeted, and the size of the food item (such as a bone), that can be ingested (Binder and Van Valkenburgh, 2000). However, there is a trade-off, with wider gapes resulting in reduced bite force (Bourke *et al.*, 2008; Santana, 2016). This may be due to a longer out-lever arm facilitating a wider gape, but lowering the mechanical advantage of the jaw (Slater and Van Valkenburgh, 2009; Santana, 2016). Additionally, excessive stretching of muscles may occur at wider gapes, resulting in reduced bite force (Santana, 2016). However, Slater and Van Valkenburgh (2009) suggested that in the Felidae at least, factors such as overall muscle cross-sectional area or increase in the length of the in-lever arm may compensate for the lower force produced with the longer jaw.

Many studies have assessed multiple aspects of skull morphology in relation to feeding. For example, using a Finite Element Analysis model, Tseng and Binder (2010) found the bite force of a sub-adult *C. crocuta* at p3, p4 or m1 was lower than the corresponding bite points in an adult *C. lupus*. However, the authors also discovered that the stress and strain invoked when biting at the p3, p4 or m1 were fairly consistent at all three points for a sub-adult *C. crocuta*, but much less so for an adult *C. lupus*, which showed much lower values at m1 than at the position of the premolars. This suggests that the mandible of *C. crocuta* is better adapted for using the

premolars for biting than *C. lupus*, and is also adapted for using the m1 more actively. Additionally, *C. crocuta* exhibited overall lower stress and strain levels in the mandible than *C. lupus*, indicating that the *C. crocuta* mandible is better able to resist bending for a given mandible length (Tseng and Binder, 2010).

There are morphological similarities between species that consume similar foods. Some of these have been mentioned, such as the greater dorsoventral bending strength posterior to the bone-processing teeth in the mandibles of the Hyaenidae and Canidae (Biknevicius and Ruff, 1992; Raia, 2004). As mentioned in Section 3.3.3, the morphology of the orbit is influenced by the eye and the temporalis muscle. An in-depth study of 84 species from 19 mammalian Orders by Cox (2008), proposed a strong link between the morphology of the bones that comprise the orbital area, and feeding groups. The four feeding groups were based on those defined by Turnbull (1970): Specialised Group I, carnivore-shear; Specialised Group II, ungulate-grinding; Specialised Group III, rodent-gnawing and a Generalised Group. Group I comprised the Carnivora, and Cox (2008) found that the Chiroptera possessed similar orbital characteristics. Both of these orders have a temporalis-dominated masticatory system. The characteristics of Group I tended towards large orbits set close together, forward-facing and positioned over the tooth row. This positioning was related to the short rostrum and wide face that is characteristic of this group. The Felidae are the most extreme in the shortness of their rostrum and the degree to which their orbits face forwards. There was also a distinction between those species for which the temporalis is the dominant jaw adductor muscle, and those for which the masseter is dominant. Cox (2008) determined that most bones of the orbit were influenced predominantly by the masticatory musculature. The exceptions to these were the orbitosphenoid and the frontal bones. Expansion of these bones corresponded with expansion of the orbits relative to skull size, meaning that it was the upper part of the orbit that expanded, for example as seen in the domestic cat (*Felis catus*).

Figueirido *et al.* (2013) assessed the morphological traits of durophagous members of the Carnivora, specifically focussing on bone crackers and bamboo consumers. The cranial traits shared by the durophagous species included a deep frontal region (due to the expanded sinuses), a large sagittal crest, downward-positioned orbits, a short and deep rostrum, and large postglenoid processes and consequently a deep glenoid fossa. The mandibular traits included a dorsally-positioned condyle, a large coronoid process (resulting in a larger distance between the coronoid and condyloid processes), and a concave and deep corpus. Additional traits specific to bone crackers were well-developed premolars and upper carnassials, front-facing orbits, and a posteriorly positioned occiput. Many of these features aid in enhancing bite force, or resistance to the loads produced whilst biting (Figueirido *et al.*, 2013).

Furthermore, although results of geometric morphometric analyses on extant and extinct carnivores (including the Hyaenidae) revealed that to an extent, mandibular morphology is determined by phylogeny, there were some features that were deemed important for hypercarnivory, regardless of the Family to which the species belonged. These features relate to bite force: in-lever arms of the masticatory muscles, out-lever moment arms at the canines and carnassials, and the mandibular ramus. In addition, the slicing morphology of carnassials characterises hyercarnivores. For the Hyaeninae specifically, great bite force is achieved through developed in-lever arms (high coronoid process), reduced out-lever arms (shortening of the mandible through the loss of post-carnassial molars), and a deep mandibular ramus (Figueirido *et al.*, 2011).

In contrast to the mandible, Figueirido *et al.* (2011) determined that there is a greater phylogenetic signal with relation to the overall shape of the cranium; there is thus no convergent morphology that typifies all the hypercarnivorous species. This is because, in contrast to the mandible, the cranium is involved in sensory process and contains the brain, in addition to feeding functions. This need to provide different functions results in compromises and constraints upon morphology. There are, however, morphological similarities between durophagous species (including the Hyaeninae) in line with the requirement for powerful temporalis muscles and the need to withstand large dorsoventral loads while feeding. These features include a dorsoventrally deep cranium, a large sagittal crest and large premolars. In addition, these species also have fairly small canines (Figueirido *et al.*, 2011).

It is therefore anticipated that the features of the cranium and mandible dedicated to consumption may have changed during the Pleistocene. Any periods that necessitated more frequent bone consumption may have led to enhancements of the above mentioned morphological features associated with durophagy. There may have been changes of features to provide greater resistance to stresses and strains, and to increase bite force. However, the mandible may have responded more readily than the cranium in light of the multiple functions of, and constraints upon, the latter.

3.3.6.2 Dentition

The dental formula of *C. crocuta*, as stated by Hillson (2005) is:

$$\mathrm{i}\frac{3}{3}, \mathrm{c}\frac{1}{1}, \mathrm{p}\frac{4}{3}, \mathrm{m}\frac{0}{1}$$

Although the dental formula does not include first upper molars, they are occasionally present. However, they are very small in size (Mills, 1990; Werdelin and Solounias, 1991). The evolution

of the Hyaenidae records the loss of teeth such as the upper second molar (M2), the lower first premolar (p1), and the lower second molar (m2) (Werdelin and Solounias, 1991).

Biknevicius *et al.* (1996) found that the curvature of the incisor dental arcade, and the robustness of individual teeth in the Hyaenidae were intermediate between those of canid and felid species. The upper incisors of felids were in a linear formation, whereas those of canids were curved. Taking body size into account, the bending strength and shear strength of canid incisors were greater than in felid incisors. There was thus a correlation between the curvature of the incisor arcade and the robustness of the first upper incisor (I1) and second upper incisor (I2), particularly to mediolateral forces. This was assumed to be because in a straight arcade, such as seen in the Felidae, the third upper incisor (I3) would buttress the medial incisors. However, the I1 and I2 of curved arcades are exposed to mediolateral forces and thus need to be more robust (Biknevicius *et al.*, 1996). Additionally, Biknevicius *et al.* (1996) suggested that the work of incisors and canines together in curved arcades allows larger and more damaging bites than the use of canines alone. They noted that the greater importance of the incisors in the Canidae and the Hyaenidae, as opposed to the Felidae, is likely related to the method of killing; the Felidae kill with a single bite, facilitated with their long and robust canines (see below), whereas the Canidae and Hyaenidae kill using multiple bites (Biknevicius *et al.*, 1996).

In terms of ingestion, Van Valkenburgh (1996) observed *C. crocuta* feeding on carcasses, finding that incisors were frequently used to cut skin alone, and were the teeth most often used when cutting skin with attached subcutaneous tissue, and when feeding on muscle. Kruuk (1972) also observed the incisors and canines being used to remove soft meat from a carcass. Ferretti (2007) suggested that the I3 may be implemented in bone cracking, for which its large size is an advantage.

In a comparison of the extant Hyaenidae, Felidae and Canidae, Van Valkenburgh and Ruff (1987) found that the upper canines in all Families were larger in the anteroposterior diameter than in the mediolateral diameter. However, the canines of hyaenids and felids were less compressed in the mediolateral diameter than those of canids. Around both the anteroposterior and mediolateral axes, hyaenid and felid canines had greater bending strengths than canid canines. This facilitates resistance to bending from stresses incurred when biting and ripping flesh. Furthermore, this may provide resistance when contact is made with bone. In the case of the Felidae, this may occur during the deep killing bites. The Hyaenidae will use their anterior teeth to break bone. In contrast, the Canidae have weaker canines, take shallower killing bites and

process bone with their post-carnassial molars, and are thus less likely to make contact with bone with their canines (Van Valkenburgh and Ruff, 1987). Although not the most frequently used tooth, canines were also observed to be employed in consumption of muscle with attached bone (Van Valkenburgh, 1996). Greater bending strength in hyaenid canines compared to those in the Canidae was also found by Christiansen and Adolfssen (2005), even when taking into account the larger bite forces produced by the Hyaenidae.

Based on the above information, a number of scenarios may have influenced changes in canine size during the Pleistocene. Predation upon larger species may have caused greater stresses and thus necessitated more robust canines. More complete consumption of carcasses may also have necessitated more robust canines in order to lessen the chance of accidental breakage through contact with bone. This may also have been the case when feeding competition was high, such as with larger *C. crocuta* group sizes, low prey availability, or large populations of aggressive competitors; rapid feeding may increase the chance of accidental contact with bone as teeth are often used less precisely (Van Valkenburgh 1996, and see below).

The absence of post-carnassial molars in Hyaenidae has brought the canines closer to the condyle. As with canid species, which have reduced post-carnassial molars, this means that the MAR at the canines is reduced. This morphology occurs in four canid species that regularly predate animals larger than themselves, thus requiring greater bite force (Van Valkenburgh and Koepfli, 1993). It may be expected that predation of larger species during the Pleistocene encouraged shorter tooth rows (perhaps through reduction in size of the carnassials and the premolars) to bring the canines closer to the jaw joint and facilitate greater bite forces. However, this is on the assumption that bone consumption did not also increase in this period as this would necessitate large premolars to withstand the stresses incurred in consuming bones more frequently (see below). If this was the case, perhaps larger muscles rather than reduced length of the tooth row would have been sufficient to induce larger bite forces.

The upper first premolar (P1), and upper and lower second premolars (P2 and p2) are reduced in size in *C. crocuta* (Ferretti, 2007). The premolar shape consists of a main, central cusp, with anterior and posterior cusps that are reduced in size (Ewer, 1973). The upper third premolar (P3) and lower third premolar (p3) are especially pyramidal in shape (Werdelin and Solounias, 1991), and the lower fourth premolar (p4) also has a robust cone (Hillson, 2005).

The evolution of bone cracking is associated with large, broad, pyramid-shaped teeth. This is true not only of the P3 and p3 in the Hyaenidae such as *C. crocuta*, but also the P4 and p4 of the canids *Osteoboros* and *Borophagus*, which were inferred to be bone crackers (Werdelin, 1989;

Werdelin and Solounias, 1991). Through the Hyaenidae lineage, the P3 became increasingly wide relative to its length, indicating increased carcass utilisation in these species (Werdelin and Solounias, 1991). Indeed, the species of the Carnivora with the widest premolars relative to body mass are those that consume bone. These wider teeth wear at a slower rate and thus maintain functionality until a greater age than smaller teeth (Van Valkenburgh, 1989). However, while smaller occlusal areas of unworn teeth require less force to crack bone than worn teeth of older individuals, the greater muscle force of these older individuals compensates for this disadvantage (Tseng *et al.*, 2011). Observations of feeding have shown that premolars of *C. crocuta* were the most frequently used teeth when consuming muscle with attached bone. They were also used frequently alone, or in combination with carnassials when consuming solely bone (Van Valkenburgh, 1996).

Larger teeth, especially an increase in width, may occur as a result of prolonged periods of increased bone consumption. Relatively longer than wide premolars may be characteristic of periods with less frequent bone consumption.

The upper fourth premolar (P4) is comprised of two anterior cusps, the protocone and the parastyle, which are pronounced and linearly aligned (Werdelin and Solounias, 1991; Hillson, 2005). The metastyle and the paracone comprise the blade, which is especially long in *C. crocuta*, compared with other Hyaenidae (Werdelin, 1989; Werdelin and Solounias, 1991).

The first lower molar (m1) of *C. crocuta* has a protoconid and a paraconid that make up the trigonid blade. Both of these are tall and stout in shape (Hillson, 2005). The m1 also has a metaconid and a single talonid cusp (Werdelin and Solounias, 1991), both of which are reduced in size (Hillson, 2005). Turner (1984) also stated that the metaconid is sometimes absent.

The length of the m1 trigonid relative to total m1 length is greatest in those Carnivora (including *C. crocuta*) for which meat makes up a large proportion of the diet (Van Valkenburgh, 1989). Werdelin (1989) stated that the length of the P4 blade, and the reduction of the m1 talonid make these teeth ideal for meat slicing. The carnassials of *C. crocuta* were observed to be the teeth most frequently used to remove skin from a carcass. The carnassials were also employed with premolars, or alone when consuming bone (Van Valkenburgh, 1996).

The position of the carnassials in *C. crocuta* is such that they are parallel to the sagittal plane, rather than parallel to the cheek tooth row (Kurtén and Werdelin, 1988; Werdelin and Solounias, 1991). Kurtén and Werdelin (1988) suggested that this allows bone to be cracked by the premolars, including the protocone and parastyle of the P4, without contacting and damaging

the cutting blades of the carnassials, on the assumption that bone most frequently enters the mouth parallel to the premolars.

However, evidence from microwear analysis indicates that microscopic wear features consistent with tooth-on-bone contact are present on the wear facets of the m1 blades (Van Valkenburgh *et al.*, 1990; Goillot *et al.*, 2009; Schubert *et al.*, 2010; Bastl *et al.*, 2012). Nevertheless, the evolution of P3 and p3 as bone-cracking teeth in the Hyaenidae allowed the carnassials to maintain a meat-cutting blade. This is in comparison to borophagine canids that employed the carnassials as bone-cracking teeth, thereby incurring heavy wear from this activity (Werdelin, 1989; Van Valkenburgh, 2007). Werdelin (1989) stated that *C. crocuta* is thus well-suited both for bone and meat consumption.

Differences can also been seen among the Hyaeninae. The carnassials of *C. crocuta* are different from those of *H. hyaena* and *P. brunnea*, in that those of *C. crocuta* maintain a relatively longer cutting trigonid blade, and have less grinding area due to their more hypercarnivorous diet (Van Valkenburgh *et al.*, 2003; Palmqvist *et al.*, 2011). Additionally, a longer carnassial blade, coupled with greater bite force, facilitates rapid ingestion of food, a necessity in situations such as social feeding and thus intraspecific competition (Van Valkenburgh, 2007). This was the case for *C. lupus* during Marine Oxygen Isotope Stage 5a, inferred to be a time of dietary stress for the species (Flower and Schreve, 2014). Indeed, *C. crocuta* clan sizes are large in some areas, with numbers recorded at 50 individuals in the Chobe National Park, Botswana (Cooper, 1990), 55 in the Aberdare National Park, Kenya (Sillero-Zubiri and Gottelli, 1992), and 65 in the Maasai Mara National Reserve, Kenya (Holekamp *et al.*, 1997). Although hunting groups may be small, other members of the clan often converge on a kill, and competition for a share of the carcass thus occurs (Cooper, 1990; Holekamp *et al.*, 1997).

Longer carnassial blades in Pleistocene *C. crocuta* may have occurred in response to low prey availability or large feeding groups due to high *C. crocuta* abundances, thus encouraging rapid consumption of a carcass. Larger P4 cusps may have occurred in response to dietary stress and thus the need to more thoroughly consume carcasses and so process more bone.

Enamel structure is not assessed in the present study. However, it is worth noting as it may provide further adaptations to resist breakage of teeth (Ferretti, 2007). Microscopic enamel structures, Hunter-Schreger Bands (HSB), are of zigzag formation in *C. crocuta* teeth. Based on the presence of zigzag HSB in extant and extinct bone-cracking hyaenids, and durophagous species from other families, it was suggested that the formation of zigzag HSB is an adaptation to consumption of hard foods (Stefen and Rensberger, 1999). In species of the Hyaenidae,

Ferretti (2007) found a correlation between the intensity of HSB folding, and the robustness of P3. Zigzag HSB provide the enamel with resistance to the tensile stresses that occur upon biting hard foods, in addition to resistance to propagation of any cracks that have formed in the enamel (Rensberger and Wang, 2005).

Despite the above adaptations to bone consumption, Van Valkenburgh (2009) found that durophagous species had greater incidences of tooth breakage than omnivores, insectivores, or those that consume mostly meat. In *C. crocuta*, those teeth most frequently broken were canines and premolars, followed by incisors, then the carnassials. As noted above, all these teeth are used to some extent in bone cracking. In a similar study, Van Valkenburgh (1988) suggested that canines were frequently broken in part due to the unpredictability of the movements of struggling prey; it is difficult to have a tooth sufficiently adapted to these stresses. Additionally, species exhibiting greater intraspecific aggression had greater canine breakage incidences (*C. crocuta* was classified as exhibiting a high level of aggression), suggesting breakage during fights (Van Valkenburgh, 2009). Although teeth could be made larger or the enamel made stronger, this is not selected for because of the metabolic costs involved, the size of the jaw, and the constraints imposed by the material properties of the teeth. Additionally, canine teeth must remain long rather than stout to enable successful predation (Van Valkenburgh, 1988). Furthermore, Van Valkenburgh (1996) suggested that while some teeth may be better suited to consuming certain tissue types, the use of other teeth may be due to the rapid speed at which food must be consumed, especially in competitive circumstances. This may thus cause breakage of teeth that are less suitable for consuming foods that impart high loads.

The reasons for the effectiveness of different teeth for breaking up different foods lie in the physical properties of the foods: the stress required to produce initial failure in the food, the resistance to cracks propagating and eventually splitting the food after the initial failure, and the degree to which the food will deform at low strain levels (Lucas and Peters, 2007).

Meat is a tough food, meaning that after the initial failure of the meat, and thus crack formation, there is high resistance to the crack propagating. A long blade, such as those of the P4 and m1, is needed to accomplish this; a pointed tooth will merely pierce the meat (Lucas and Peters, 2007). This contrasts with the observations by Van Valkenburgh (1996) that incisors were used most frequently in consuming muscle, and skin with attached subcutaneous tissue. However, in this study, movements of the neck were important in removing these tissues from the carcass, aiding the work of the teeth. Additionally, Van Valkenburgh (1996) focussed more on the initial removal of food from the carcass, and ingestion, rather than subsequent mastication. Mammal

skin is another tough material that requires the scissoring motion of blades (such as occurs between carnassials) to break through it (Lucas and Peters, 2007).

By contrast Lucas and Peters (2007) suggested that cusps rather than blades are suited to breaking bone. Additionally, blunted cusps are better as sharp teeth will likely fracture under the high stress levels required to crack the bone (Lucas and Peters, 2007). This explains why the robust, conical shaped premolars of *C. crocuta* are ideally suited to bone cracking. However, as mentioned, Van Valkenburgh (1996) noted that carnassials were also used to crack bone, suggesting that the anterior cusps of the P4 (which occlude with the posterior region of the p4) are used rather than the carnassials' blades. Additionally, Van Valkenburgh (1996) suggested that the enamel microstructure may aid in preventing tooth breakage when teeth other than premolars are used for cracking bones.

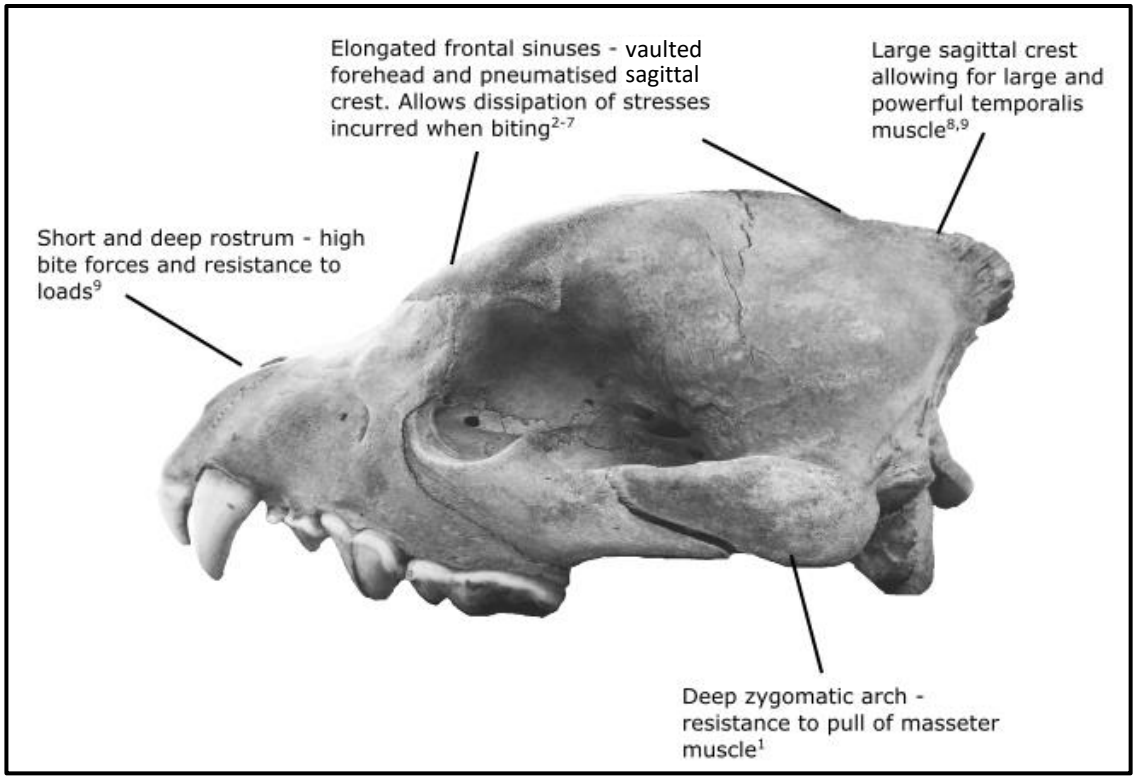

Figure 3.5: Summary of cranial features related to feeding. See text for details. [1]Hildebrand (1974); [2]Werdelin (1989); [3]Werdelin and Solounias (1991); [4]Joeckel (1998); [5]Tanner *et al.* (2008); [6]Tseng (2009); [7]Curtis and Van Valkenburgh (2014); [8]Figueirido *et al.* (2011); [9]Figueirido *et al.* (2013).

Many of the above points are summarised in Figure 3.5 to Figure 3.7. Overall, the craniodental morphology of *C. crocuta* seems well-suited to hypercarnivory, bone cracking and competitive feeding. The above has concentrated largely upon adult *C. crocuta*. Ontogenetic development of these features will be discussed below, a consideration that is important when interpreting the modern and Pleistocene material.

3.3.7 Ontogeny

A study of captive *C. crocuta* by Binder and Van Valkenburgh (2000) documented some aspects of craniodental ontogenetic development. Permanent dentition was attained by around 12 to 14 months of age, with replacement first of the deciduous incisors, then the carnassials, premolars and canines. The skull finished growing at around 20 months of age. Bite strength, as measured through live individuals biting on a force transducer, continued to increase up to four years of age. Binder and Van Valkenburgh (2000) suggested that either this may indicate that muscle growth continued after skull growth had stopped, or that their measures of skull size were not sufficient to reveal the entirety of muscle growth. The authors pointed to a study by Gay and Best (1996), which found that skulls of the puma (*Puma concolor*) continued growing well into adulthood (individuals older than two years of age were considered as adult) and ceased growing at five to six years of age for females, and seven to nine years for males. Hartová-Nentvichová *et al.* (2010) also found that certain measurements of red fox (*Vulpes vulpes*), crania continued growing through life. These included measurements of width (zygomatic breadth, interorbital breadth and rostrum breadth for both sexes, in addition to jugular breadth for males). Conversely, the same study found that the smallest distance behind the supraorbital processes decreased after six months of age (the age at which maximum skull length was reached), although it later stabilised in size (Hartová-Nentvichová *et al.*, 2010). This width behind the supraorbital processes decreases with the development of masticatory muscles (Ansorge 1994, cited in Hartová-Nentvichová *et al.* 2010).

A further study by Tanner *et al.* (2010) of *C. crocuta* osteological specimens from a wild, studied population indicated that prior to weaning (14 months of age), the rostrum lengthened in line with replacement of deciduous with permanent teeth. The mechanical advantage of the masseter muscle remained constant through ontogeny, suggesting that the in-lever and out-lever arms grew isometrically. By contrast, the mechanical advantage of the temporalis increased with age, reaching its full-grown state at 22 months of age. However, bite force likely continued to increase after full mechanical advantage of the adductor muscles was reached. This was indicated by the continued growth of the zygomatic arches and the sagittal crests, both

important attachment sites for the temporalis and masseter muscles, which thus suggests that the muscles continued growing as well. The skull reached full growth at 35 months of age, well after both weaning and reproductive maturity (24 months) (Tanner *et al.*, 2010). This is supported by Arsznov *et al.*'s (2011) study of skulls of the same population, where 85 % of skull length of endocranial volume was reached by 14 months of age, and 95 % by 34 months. The timings of full development of skull features in adults is important when interpreting measurements of both Pleistocene and modern specimens.

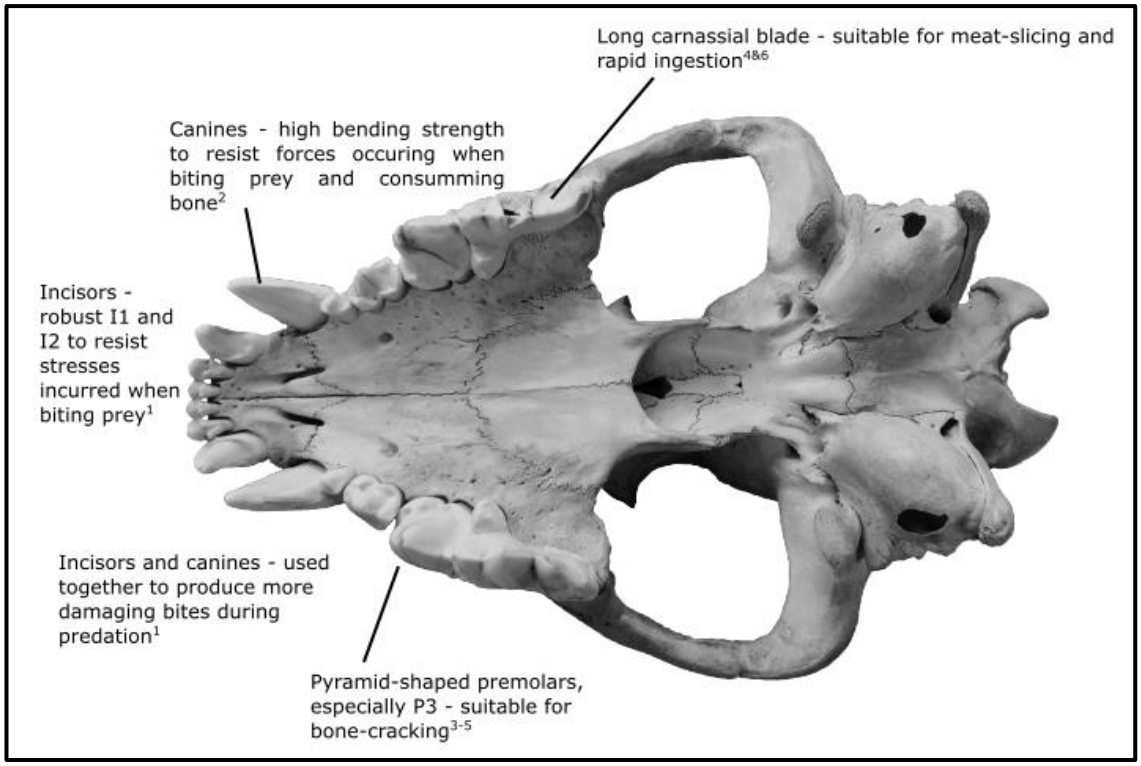

Figure 3.6: Summary of the features of the upper dentition relating to feeding. See text for details. [1]Biknevicius *et al.* (1996); [2]Van Valkenburgh and Ruff (1987); [3]Van Valkenburgh (1989); [4]Werdelin (1989); [5]Werdelin and Solounias (1991); [6]Van Valkenburgh (2007).

Younger, captive individuals varied the teeth they used to bite bone. As they grew older, however, the time spent biting on bone with the incisors and anterior premolars decreased, and the time spent using the posterior premolars increased. It was suggested that this may be due to the reduced gape of smaller jaws, thus limiting how posterior the bone may be positioned, and also due to the need to limit damage to the blade of the deciduous carnassials (Binder and Van Valkenburgh, 2000). While juveniles have a disadvantage relative to adults when feeding, due to lower masticatory muscle mass and thus lower bite force, they have an additional

disadvantage due to the position of their teeth in the jaw. The deciduous teeth are located anteriorly in the jaw, relative to the permanent dentition, meaning that the position of the deciduous teeth further reduces the bite force relative to adults. Additionally, teeth are weaker once they are first erupted, which may limit the bite force of younger individuals (Binder and Van Valkenburgh, 2000). With the mandible of juvenile *C. crocuta* modelled as a beam, Therrien (2005) found that aside from absolute strength, there was little difference in the profiles between adults and juveniles. However, the post-m1 position of the juvenile was not as strong in resistance to dorsoventral loads as in the adults, indicating a disadvantage in bone cracking at posterior teeth relative to the adults (Therrien, 2005). Together, this indicates the disadvantage that juvenile *C. crocuta* have when compared with adults in competing for food at a carcass. This may hold implications for survival when food is scarce and food competition is high; juvenile mortality may be high. Pervasive food stress may lead to population declines and is an important consideration when assessing the ultimate extirpation of *C. crocuta* from Europe.

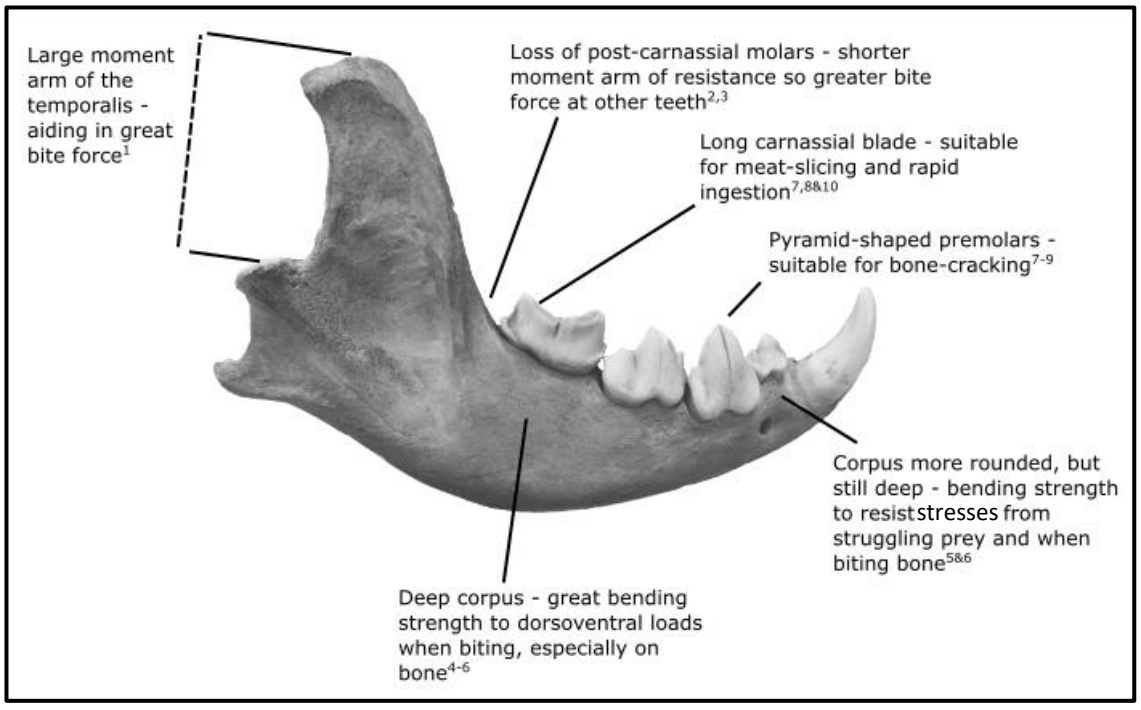

Figure 3.7: Summary of the mandibular and dental morphological features associated with feeding. See text for details. [1]Van Valkenburgh and Ruff (1987); [2]Van Valkenburgh and Koepfli (1993); [3]Figueirido *et al.* (2013); [4]Biknevicius and Ruff (1992); [5]Therrien (2005); [6]Palmqvist *et al.* (2011); [7]Van Valkenburgh (1989); [8]Werdelin (1989); [9]Werdelin and Solounias (1991); [10]Van Valkenburgh (2007).

3.3.8 Phenotypic plasticity of craniodental morphology

The phenotype is determined by an interaction between the environment, and the genotype, which sets limits on the range of possible morphologies (Hillson, 2005; Whitman and Agrawal, 2009). Morphological differences may therefore occur as a result of phenotypic plasticity or genetic change, or both (Gienapp *et al.*, 2008; Whitman and Agrawal, 2009).

In most cases it is difficult to assess whether phenotypic change is a result of genetic change or plasticity (Gienapp *et al.*, 2008; Merilä and Hendry, 2014). When plasticity has been determined as the cause of morphological change, it has mainly been in studies where specific environmental variables were controlled. For example, prairie deer mice (*Peromyscus maniculatus bairdii*) fed either soft or hard diets exhibited differences in position of the upper incisors. In addition the zygomatic arches and the masseteric tubercles, both points of origin of the masseter muscle, were larger in the mice fed hard diets (Myers *et al.*, 1996). Another study on mice also involved feeding them soft or hard foods. The mandibles of those fed hard foods had greater mechanical advantages of both the masseter and the temporalis muscles when biting at the incisor and the m1 (Anderson *et al.*, 2014).

In contrast to bone, tooth morphologies are influenced much less by plasticity. Teeth grow within the mandible and are fully developed by the time of eruption. Other than through wear and breakage, the enamel cannot be altered after deposition (Caumul and Polly, 2005). Thus, using feeding as an example, when teeth are employed in mastication, they cannot alter their shape in response to any prevalent food type. Caumul and Polly (2005) found that diet had a greater influence upon cranial and mandibular morphology than upon tooth morphology in marmots (*Marmota*). The authors stated that this was due to the lack of phenotypic plastic response in the teeth. Similarly, in a study of the Mediterranean and the Eurasian water shrews (*Neomys anomalus* and *Neomys fodiens*) in Poland, Rychlik *et al.* (2006) found that the cranial and mandibular shapes were both correlated with the same geographical and climatic variables. By contrast, molar shape was correlated with fewer variables. The authors suggested that this difference was due to the greater potential for the cranium and the mandible to respond phenotypically to the environment during the life of an individual. Change in morphology of teeth to foods and the environment thus most often occurs as an adaptive genetic response (Caumul and Polly, 2005).

The above information is important for the interpretation of the Pleistocene material. Firstly, lacking phenotypic plasticity to external conditions such as food type, the teeth of *C. crocuta* may lack the immediate response of the cranium and the mandible. If the change in the

environmental condition is short-term, or if it is in its early stages, the bones of skull may show a response, while the teeth remain unaffected.

While teeth are less plastically adaptive to environmental conditions, stress occurring during tooth development may result in plastic responses. This stress may be induced by disease or other health conditions, as has been demonstrated in the development of teeth during gestation in humans (Garn *et al.*, 1979). However, it is anticipated that while health of the mother and young may have affected Pleistocene *C. crocuta*, this is likely to make up a small proportion of assemblages.

Luke *et al.* (1979) conducted studies on three groups of pigs. The control group was allowed unlimited food, another group had unlimited fats and carbohydrates but limited protein, and the final group had limited calories. Food was controlled after the individual pigs were 10 days old, by which age the M1 and m1 teeth had finished growing, the crowns of the upper and lower second molars (M2 and m2) were partially formed, and the development of the crowns of the upper and lower third molars (M3 and m3) had not yet commenced. The M1 and m1 were similar in size across all three groups of pigs. The calorie and protein restricted groups exhibited slightly smaller M2 and m2 than the control group, while the M3 and m3 were much smaller than those of the control group. Furthermore, the mandible was smaller in the protein and calorie limited group than in the control group (Luke *et al.*, 1979). This indicates that prevalence of small tooth size in a Pleistocene sample may indicate long-term food deficiency. It is anticipated that the longer the period of stress, the more features of an individual, and the more individuals in a population, will show this change in size.

3.3.9 Summary

Overall, the cranium, mandible and dentition of *C. crocuta* are well-suited to resist many of the loads experienced with a hypercarnivorous and durophagous diet, and when targeting large prey. Spotted hyaenas are thus able to consume a carcass fully and the adults at least are able to ingest food rapidly, a necessary attribute when intraspecific competition is high. Additional pressures influencing the morphology of the cranium are related to the brain, respiration, olfaction, vision and hearing. The post-cranial morphology, such as neck musculature and limbs, provides further influences upon feeding behaviour (Kruuk, 1972; Van Valkenburgh, 1996; Meers, 2002) and will be considered later.

From the review, a number of hypotheses can be formed regarding Pleistocene *C. crocuta*.

1. Due to increased cognitive demands, when predation was the most important method of food procurement, and when larger prey were targeted, the size of the brain increased, as evidenced by the width of the brain case.
2. During periods of closed vegetation, where vision may have been compromised by obscuring vegetation, hearing was enhanced in order to locate prey, clan members and competitors. This will be demonstrated by enlarged auditory bullae.
3. In times of increased bone consumption, *C. crocuta* exhibited changes in cranial and mandibular features to better resist stress and strain, and increase bite force. Changes may have occurred in features such as the depth of the mandibular corpus, size of the muscle attachment sites, and length of the dentary.
4. In times of increased bone consumption, gape increased to facilitate ingestion of larger bones, while the reduction in bite force incurred by the longer jaw offset by other features of the skull.
5. In times of increased bone consumption, the teeth have developed a greater resistance to fracture, though the response was be less rapid than in the more plastic cranium and mandible. This will be exhibited in the overall robustness of the premolars in terms of breadth relative to length.

.

3.4 Post-cranial morphology

3.4.1 Introduction

The functions of the post-cranial bones are related to weight-bearing, locomotion and prey capture (Hildebrand, 1974; Van Valkenburgh, 1985). *C. crocuta*'s locomotion is classed as terrestrial, defined by Van Valkenburgh (1985, p.408) as a species that '[r]arely or never climbs, may dig to modify burrow but not regularly for food.' The Hyaenidae are cursorial, capable of prolonged trotting (Taylor, 1989). *C. crocuta* is a pursuit hunter, as classified by Van Valkenburgh (1985), which involves a long distance chase, without grappling with prey, and rarely involves stalking. Indeed, the distance recorded by Holekamp *et al.* (1997) of *C. crocuta* chasing prey is 4 km. The response of *C. crocuta* to predator encounters is to run (with the potential retreat to a burrow) or to fight (Van Valkenburgh, 1985).

The above processes are important for the survival of an individual and of the species as a whole, justifying investigation into the morphological changes of post-crania of *C. crocuta* during the Pleistocene. With a focus on the Carnivora, and *C. crocuta* where possible, this review will outline the morphological features of the post-crania that are intrinsic in locomotion, weight-bearing and prey capture, in addition to their environmental correlates.

3.4.2 Limb bones

As will be outlined below, limb morphology is associated with weight-bearing, locomotion and object manipulation. Furthermore, factors associated with locomotion include speed, stabilisation, endurance, and resistance to stresses and loads. Factors associated with object manipulation (i.e. grappling prey, handling food, digging holes) are dexterity, and resistance to stresses and loads.

The length of the entire limb influences locomotion. The longer the limb, relative to body size, the longer the stride. Most important is the effective limb length, i.e. the length of the leg that contributes to stride length. Hyaenids are digitigrades (Hildebrand, 1974), a posture that involves an individual's weight resting on the distal ends of the metapodials. This is opposed to plantigrady where the carpals and tarsals are in contact with the ground (Polly, 2010). Digitigrady therefore increases the effective leg length by including the metapodials in the length (Hildebrand, 1974). As will be outlined below, the length of the limb as a whole, and the morphology of individual bones, can be related to stride length and speed, and to different locomotor styles, hunting behaviours, and habitats.

When limb lengths are increased, this is produced through lengthening of the distal long bones and the metapodials (Hildebrand, 1974). Coupled with shorter but thicker proximal limb bones, this allows for endurance of locomotion at high speeds (Hildebrand and Hurley, 1985). For example, an association was found between speed, and the relative metatarsal and femur lengths in mammals. Slower species had relatively shorter metatarsals. However, among the faster species (including *C. crocuta*), there was only a weak relationship between relative bone lengths and speed (Van Valkenburgh, 1987). Indeed, Christiansen (2002) found that across mammals, a combination of limb measurements are better predictors of maximum running speed than single measurements. However, there was still much variation in the data, unexplained by the limb measurements. The author suggested that limbs might be adapted to minimise energy expenditure during all forms of locomotion, not just to enable fast running.

In another study of the metatarsal and femur lengths, Van Valkenburgh (1985) found that ambush (stalking followed by short distance rush), pounce/pursuit (searching ending in pounce or chase) and pursuit hunters (long distance chase, typical of *C. crocuta*) had long metatarsals relative to femoral length. This was associated with the high speed (even for a short distance) associated with these predatory behaviours (Van Valkenburgh, 1985). Harris and Steudel (1997) also found a relationship between limb morphology and hunting methods of carnivorans. Hindlimb length (combined lengths of femur, tibia, and longest metatarsal) was not significantly related to home-range area, daily movement distance or prey size, and was only related to hunting methods. Of relevance to *C. crocuta*, species that chased prey over long distances and species that scavenged, had neither longer nor shorter hindlimbs relative to body size (Harris and Steudel, 1997).

Cursorial carnivorans (such as *C. crocuta*) are characterised by having greater brachial (radius/humerus lengths) and crural (tibia/femur lengths) indices. This, again, indicates that the distal bones (radius and tibia) are long relative to the proximal limb bones (Meachen *et al.*, 2016).

The calcaneum is also associated with locomotion behaviours. The calcaneum can be modelled as a lever in parasagittal (anteroposterior) limb movement (see Section 3.3.6.1 for an explanation of levers). In this mechanism, the pivot is located at the astragalus. The muscles associated with anteroposterior movement are the gastrocnemius and soleus muscles, which attach to the Achilles tendon. This tendon then attaches at the proximal tuber of the calcaneum, forming the in-lever. The out-lever is the distal calcaneum, metatarsals and phalanges. Greater calcaneum tuber length (from the proximal area of the calcaneum to either one of the articulating points of the astragalus) results in a longer in-lever, a greater in-force, and thus

greater forward thrust (Polly, 2010; Panciroli *et al.*, 2017). This scenario is associated with terrestrial and cursorial locomotion amongst carnivorans (Panciroli *et al.*, 2017).

The breadth of the limb bones is also associated with carnivoran behaviours. The main direction of limb movement of pursuit predators (such as *C. crocuta*) is anteroposteriorly. As such, the humeral shaft is shaped so as to resist loads placed on the bone during locomotion; it is broader anteroposteriorly and narrow mediolaterally. By contrast, occasional predators (such as *P. brunnea*) have a rounded shaft to facilitate grappling prey or handling food. Occasional predators and ambush predators also have a more robust radius and ulna for the same reason (Martín-Serra *et al.*, 2016).

Morphological features of the joints are also associated with locomotion and predation behaviours. One example is the distal articulation of the humerus. The distal humerus morphology of hyaenids is similar to that of other cursors: large canids and *A. jubatus*. The morphology of these species favours anteroposterior movement, instead of resistance against lateral forces such as in species that handle food with their forelimbs. As such, in comparison with food-handlers, the humerus morphology of cursors includes a narrower humero-ulnar area, a smaller trochlear flange, and a deeper mid-trochlea furrow (Andersson, 2004). A study by Martín-Serra *et al.* (2016) also found that the morphology of the humerus is associated with predation behaviours. The humerus of pursuit predators has a deep and narrow trochlea, restricting lateral movement, and favouring anteroposterior movement, important for such predation behaviours. By contrast, occasional predators (such as *P. brunnea*) have a greater ability to rotate the humerus laterally (Martín-Serra *et al.*, 2016).

Further differentiation between pursuit and occasional predators lies in the morphology of the proximal humerus. The greater tuberosity is larger in pursuit predators, allowing for greater mechanical advantage of the supraspinatus muscle when protracting the humerus. This facilitates locomotion over long time periods or at high speeds (Martín-Serra *et al.*, 2016).

Limb morphology and associated locomotion behaviours are also associated with environmental conditions. For example, digitigrade and cursorial carnivorans are largely found in open habitats. Plantigrade species are commonly found in forested environments (Polly, 2010). Furthermore, Van Valkenburgh (1985) found that cursorial carnivorans, and those predominantly inhabiting open environments (*C. crocuta* was classed as such) had long third metacarpals relative to their phalanges. The opposite was true of forest-dwelling species. This was also related to hunting type, as open-habitat carnivores are predominantly pursuit or pounce hunters (Van Valkenburgh, 1985). A relatively longer calcaneum tuber is associated with increasing digitigrady and open habitats in North American carnivorans. The opposite scenario is associated with

forested habitats. Heterogeneous vegetation is associated with greater diversity of relative tuber lengths (Polly, 2010).

Meachen *et al.* (2016) investigated the relationship between climate and post-cranial morphology. Brachial index was greater in carnivorans inhabiting warmer and drier climates. The shoulder moment index (humerus delopectoral crest length/humerus length) was smaller in warmer and drier climates. The greater trochanter height index (femoral greater trochanter height/femur length) was smaller in drier climates. The authors stated that these features might have developed in response to habitat features that are determined by climate, such as vegetation openness, which, as mentioned is linked to cursoriality.

Weight-bearing also influences the morphology of limbs. In order to allow for increased speed endurance, the mass of some bones is reduced. The fibula and distal area of the ulna are slender in cursorial species, reducing the load on the locomotor system (Hildebrand, 1974). Pursuit predators (such as *C. crocuta*) were found to have a slender humerus, radius and ulna. By contrast, occasional hunters (such as *P. brunnea*) have more robust forelimb long bones. This is to prioritise stress resistance over energy efficiency as bending stresses occur during frequent acceleration and deceleration (Martín-Serra *et al.*, 2016). In *P. leo*, the loading of the hindlimb likely passes through the third metatarsal and the ectocuneiform, suggested by the greater length of the former compared to other metatarsals, and the overall large size of the latter (Argot, 2010).

Finally, not all postcranial bones are functionally important; vestigial features are exhibited in *C. crocuta*. In the forelimb, the first distal phalanx is lost, and the first proximal phalanx and metacarpal are reduced. In the hindlimb, the first metatarsal and a first phalanx are reduced, while the other first phalanx is lost (Senter and Moch, 2015).

The clavicle is reduced in many species of Carnivora, and is lost in the Hyaenidae (Senter and Moch, 2015). This allows the scapula to move, increasing the stride length of the forelimb (Hildebrand, 1974).

Despite the morphological features discussed above, injuries may still arise from predation and locomotion. Dire wolves (*Canis dirus*) from the La Brea Tar Pits (California, USA), exhibit a great number of injuries at muscle and tendon attachment sites on limb bones. This was assumed to be due to pursuit hunting (Brown *et al.*, 2017).

Overall, the above studies indicate that *C. crocuta* (classed as cursorial, open-habitat dwelling, pursuit hunter) has limbs modified to enable long durations and high speeds of locomotion, predominantly in order to catch prey, but also potentially to avoid interactions with other predators.

3.4.3 Vertebrae

In comparison with the limbs, the functional morphology of the vertebrae has received less attention. The vertebrae included in the present study are the atlas, axis and sacrum. The other vertebrae will be discussed briefly in the following overview, as their function and relation to the studied vertebrae should be born in mind when later discussing the morphological results.

The vertebral column itself is formed so as to allow support and movement (Hildebrand, 1974; Randau *et al.*, 2016). However, there is some evidence that the morphology of individual vertebrae may also reflect these functions.

Van Valkenburgh (1996) noted that the neck was often used in feeding, through pulling and twisting movements, and suggested that this use may be reflected in the cervical vertebrae. Indeed, it is the connection between the atlas vertebra and the occipital condyles of the skull that allows the up and down motion of the head. The connection between the atlas and the axis vertebrae allows side-to-side and rotational motions (Hildebrand, 1974). In *C. crocuta*, twisting was observed more frequently when bone, or bone and muscle were consumed. Pulling was more frequent when skin alone, muscle alone, or skin with connective tissue and muscle were consumed. This led Van Valkenburgh (1996) to suggest that these pulling and twisting movements might be reflected in the cervical vertebrae, although no published studies could be found to support or refute this theory.

As mentioned in Section 3.3.6, hyaenids and large canids have similar methods of killing prey. Frequent injuries of the first three cervical vertebrae of *C. dirus* from the La Brea Tar Pits have been observed. This may be due to the strains imposed on the vertebrae by the neck muscles when biting large prey (Brown *et al.*, 2017).

Vertebrae may also be adapted to body mass. In felids, the centrum height in many of the cervical (including the axis) and thoracic vertebrae is relatively larger in larger species, providing greater stability with greater body mass (Randau *et al.*, 2016).

Overall, some of the axis and atlas measurements may reflect changes in diet of *C. crocuta*, in light of the different neck movements used. However, in light of the lack of studies, it would be difficult to assess.

3.4.4 Phenotypic plasticity in post-crania

The relationship outlined in Section 3.1 between temperature and body size is complicated in that proportions may be influenced, rather than body size as a whole. This is the case with Allen's Rule whereby 'certain parts of the organism vary more than does general size, there being a

marked tendency to enlargement of peripheral parts under high temperature, or toward the tropics' (Allen, 1877, p. 116). Harris and Steudel (1997) found no significant relationship between hindlimb length (femur, tibia and longest metatarsal lengths combined) and latitude in species of Carnivora, after body size influences had been taken into account.

By contrast, a study of mice under controlled temperatures has shown that limbs are smaller in mice growing in colder temperatures. This is controlled by the temperature influence upon the growth of cartilage at the epiphyseal plates (Serrat *et al.*, 2008). A further study found that the difference between warm and cold temperatures was greatest in the radius. The effect of temperature is modulated by exercise; limb lengths were similar between mice that exercised, regardless of temperature (Serrat *et al.*, 2010).

3.4.5 Summary

Overall, this review indicates that *C. crocuta* are well-suited for chasing prey over long distances. Coupled with the information about the craniodental morphology (Section 3.3), *C. crocuta* seem able to target a number of food sources, including the morphology necessary for taking down fast-running ungulates, and the morphology needed to consume most of the carcass, including bone.

Based on this review, a number of hypothesis can be constructed about Pleistocene *C. crocuta*.

1. *C. crocuta* had a greater effective leg length when they inhabited open landscapes during the Pleistocene, than during periods of closed vegetation.
2. If *C. crocuta* subsisted more on scavenged items, rather than hunting, the post-cranial bones resembled more closely those of occasional hunters. This may include more robust long bones.
3. *C. crocuta* conformed to Allen's Rule by having shorter and stockier limb bones in colder periods.

4 Materials and methods

4.1 Introduction

This chapter outlines the materials and site details used in the studies of population biomass, present-day body mass, SSD, morphometrics and diet, and Pleistocene body mass reconstruction, morphometrics and palaeodiet. Methods used to obtain the primary data are presented and finally, the statistical analyses are discussed.

4.2 Material and site details

4.2.1 Modern biomass sites

The influences of environmental variables upon *C. crocuta* and *P. leo* biomass were investigated from 14 sites across Africa (Figure 4.1), requiring the following data to be obtained from each site:

- Biomass of *P. leo* (for the *C. crocuta* model) or *C. crocuta* (for the *P. leo* model), and other predators (*P. pardus, A. jubatus, L. pictus, P. brunnea*), to assess competition
- Biomass of very small-, small-, medium-, large-, and very large-body size prey, to assess the influence of food availability, and of different prey size classes
- Minimum temperature of the coolest month, maximum temperature of the warmest month, and temperature seasonality, to assess the influence of temperature, especially temperature extremes
- Precipitation of the driest month, precipitation of the wettest month and precipitation seasonality, to assess the influence of water availability, and precipitation extremes
- Closed vegetation cover, semi-open vegetation cover, and open vegetation cover, to assess the influence of vegetation density

The predator and prey population biomass data were obtained from a database in Hatton *et al.* (2015), who collated animal abundance data from the literature for locations across Africa. Sites were excluded from the present study if *C. crocuta* were absent, if the abundance of a species was uncertain, if *C. crocuta* abundance was combined with that of another hyaenid, or if the boundary of the site could not be determined. In total, 30 datasets were included in the biomass analyses from different years spanning 1962 to 2009 (Table 4.1 and Figure 4.1).

Large predators are here regarded as those with an adult body mass of over 20 kg. In Africa, there are seven large mammalian predators: *C. crocuta*, *P. brunnea, H. hyaena, P. leo, P. pardus, A. jubatus* and *L. pictus*. However, *H. hyaena* was not included as data for this species are scarce. This is with the exception of the Tarangire National Park, Tanzania, where *H. hyaena* abundance data were provided in lieu of *P. brunnea* abundance (Hatton *et al.*, 2015, and references therein). *H. hyaena* is solitary and occurs at low densities (Hofer and Mills, 1998b) so its exclusion from the present study should not greatly influence the results.

Figure 4.1: Location of sites used in the biomass analyses. Base map from Esri (2006).

Hatton *et al.*'s (2015) database includes biomasses of potential prey species over 5 kg in weight. Prey were split into five body size classes, following the distinctions of Périquet *et al.* (2015): very small (<20 kg), small (20-120 kg), medium (120-400 kg), large (400-600 kg), very large (>600 kg).

Unless otherwise stated in the original publications or by Hatton *et al.* (2015), the boundaries of the sites were taken to be the entire area, i.e. the entire national park, national reserve, game reserve, or district. The Serengeti ecosystem datasets in Hatton *et al.* (2015) were derived from a number of different publications, therefore, the boundaries of this site were taken from the map of the Serengeti ecosystem by Hopcraft (2008). Latitudes and longitudes were obtained from Image Landsat, Google Earth Pro (2013).

Table 4.1: Sites from Hatton *et al.*'s (2015) database included in the *C. crocuta* and *P. leo* biomass analyses.

Site	**Year (season)**
Amboseli National Park, Kenya	2007
Hluhluwe iMfolozi National Park, South Africa	1982, 2000
Hwange National Park, Zimbabwe	1973
Kalahari Gemsbok National Park, South Africa	1979
Kidepo Valley National Park, Uganda	2009
Kruger National Park, South Africa	1975, 1984, 1997, 2009
Lake Manyara National Park, Tanzania	1970
Maasai Mara National Reserve, Kenya	1992, 2003
Mkomazi Game Reserve, Tanzania	1970 (dry), 1970 (wet)
Nairobi National Park, Kenya	1966, 1976, 2002
Ngorongoro Crater, Tanzania	1965, 1978, 1988, 1997, 2004
Queen Elizabeth National Park, Uganda	2009
Serengeti ecosystem, Tanzania	1971, 1977, 1986, 2003
Tarangire National Park, Tanzania	1962 (dry), 1962 (wet)

The climate variables used were as follows: maximum temperature of the warmest month, minimum temperature of the coolest month, temperature seasonality (as standard deviation), precipitation of the wettest month, precipitation of the driest month, precipitation seasonality (as the coefficient of variation). All data are from WorldClim (Hijmans *et al.*, 2005), and was derived from interpolated records of climate data recorded between the years 1950 to 2000. The variables were taken from the bioclimatic dataset at a resolution of 2.5 minutes. Each temperature and precipitation value was taken from the centre of each site. The centre point of each site was the point where the median latitude and longitude intersected. Median latitude was calculated from the most northerly and southerly latitudes of each location. The same was performed for longitude.

The vegetation data are from the University of Maryland Global Land Cover Classification at 1 km resolution (Hansen *et al.*, 1998, 2000) and obtained by the Advanced Very High Resolution Radiometer satellites between 1981 and 1994. For each site, the type of vegetation in each pixel (each 1 km^2) was recorded along two transects with widths of 1 km. The north-south transect ran through the centre point of the site, to the most northern and southern boundaries. The equivalent procedure was conducted for the east-west transect. The counts for both transects were then combined.

Vegetation types were split into three categories: (1) open vegetation (grassland), (2) semi-open vegetation (wooded grassland, open shrubland) and (3) closed vegetation (evergreen broadleaf forest, deciduous broadleaf forest, woodland, closed shrubland) (see Table 4.2). The percentage cover of each classification was calculated. Some transects fell over pixels classed as water, cropland or bare ground. These were excluded from the percentage calculations as it was assumed that *C. crocuta* and *P. leo* would not be regularly inhabiting these areas.

Full details of the biomass, climate and vegetation data for each site are included in Spreadsheet 1.

Table 4.2: Vegetation classes and descriptions from the University of Maryland Global Land Cover Classification at 1 km resolution (Hansen *et al.*, 1998, 2000), and classes used in the present study.

Vegetation class	**Description**	**Vegetation class in present study**
Evergreen broadleaf forest	Dominated by trees Tree canopy cover > 60 % Tree height > 5 m Most trees remain green all year Canopy never without green foliage	Closed vegetation
Deciduous broadleaf forest	Dominated by trees Tree canopy cover > 60 % Tree height > 5 m Trees shed their leaves simultaneously in response to dry or cold seasons	
Woodland	Herbaceous or woody understories Tree canopy cover > 40 % and < 60 % Tree height > 5 m Trees evergreen or deciduous	
Closed shrubland	Dominated by shrubs Shrub canopy cover > 40 % Tree canopy cover < 10 % Shrub height < 5 m Shrubs evergreen or deciduous Remaining cover barren or herbaceous	
Wooded grassland	Herbaceous or woody understories Tree canopy cover > 10 % and < 40 % Tree height > 5 m Trees evergreen or deciduous	Semi-open vegetation
Open shrubland	Dominated by shrubs Shrub canopy cover > 10 % and < 40 % Shrub height < 2 m Shrubs evergreen or deciduous Remaining cover barren or annual herbaceous cover	
Grassland	Continuous herbaceous cover Tree or shrub canopy cover < 10 %	Open vegetation

4.2.2 Modern African body mass sites

Body mass records of *C. crocuta* were sourced from the literature (see Figure 4.2 for site locations) in order to assess the environmental influences upon body mass (see Appendix 10.5, Table 10.10). SSD was calculated (see Section 4.4.1.4) from these body mass data in order to assess the degree of SSD and any environmental correlations with variation in SSD. Body masses

of *P. leo*, *P. pardus, A. jubatus*, *L. pictus, P. brunnea* and *H. hyaena* were also sourced from the literature (see Appendix 10.5, Table 10.11 to Table 10.15) for comparison with *C. crocuta* SSD. Data were rejected when bias was obvious (such as selective shooting of largest individuals), when pregnant females were included in the average weight without the raw data available to recalculate the mean, or when weights were estimated instead of measured. However, where methods or bias were not stated, the otherwise small datasets justify their inclusion in the present analyses.

The variables included in the body mass and SSD analyses were:

- *C. crocuta* and *P. leo* density, to assess competition (as biomass includes a measure of body mass in its calculation, it was felt that density would be more appropriate)
- Prey biomass, to assess the influence of food availability (this excluded prey species that weigh more than 600 kg)
- Minimum temperature of the coolest month, and maximum temperature of the warmest month, to test Bergmann's Rule
- Precipitation of the driest month, and precipitation of the wettest month, to assess water availability and extremes of precipitation levels
- Closed vegetation cover, semi-open vegetation cover, and open vegetation cover, to assess the influence of vegetation density
- Distance from the equator, to test Bergmann's Rule, in body mass analysis only

Biomass data of other large predators (*P. pardus*, *A. jubatus*, *L. pictus* and *P. brunnea*) were not included as this information was not available for one of the sites (the Salient area of the Aberdare National Park, Kenya, see below). In light of the small sample size, it was deemed more appropriate to include this site and exclude the variable.

The density data were taken from Hatton *et al.* (2015), apart from the Salient area (of the Aberdare National Park), for which abundance data were obtained from Sillero-Zubiri and Gottelli (1992) and Kibanya, (1996), as this was not included in Hatton *et al.*'s (2015) database. All other environmental data were sourced in the same way as outlined in Section 4.2.1. The boundaries of the study area in the Salient area of the Aberdare National Park were taken as accurately as possible from the map in the original publication by Sillero-Zubiri and Gottelli (1992), however, some estimation was involved when translating this into Image Landsat, Google Earth Pro (2013).

Only body mass estimates with specific locality information (rather than just the country) were included in the analyses, in order to ensure that vegetation and climate data were as representative as possible, given the potential for major variation across an entire country. As far as possible, the body mass data were paired with the population metrics based on site locality. Some locations have multiple density/biomass estimates from different years. When this was the case the closest corresponding date of the population and body mass studies was chosen. In total, eight sites were included in the analyses (Figure 4.2). Full details of the population density, biomass, climate, vegetation and latitude data of each site are included in Spreadsheet 2.

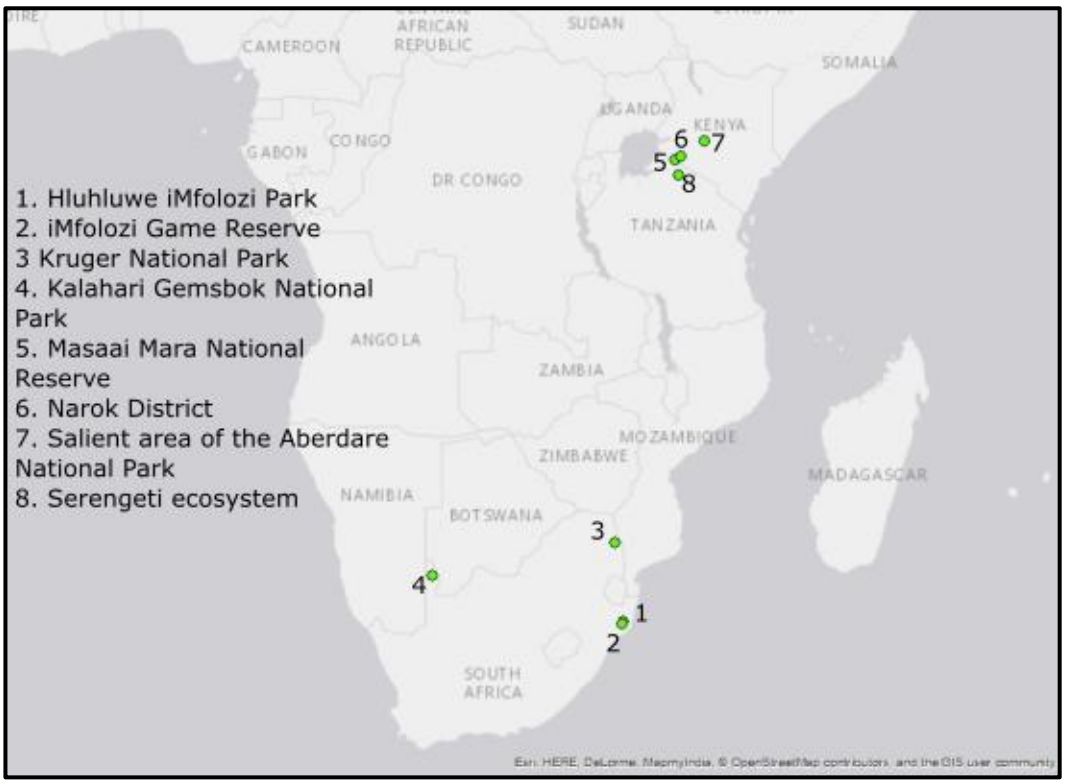

Figure 4.2: Location of sites used in the modern *C. crocuta* body mass and SSD analyses. Base map from Esri (2006).

4.2.3 Modern African specimen sites

The cranial and post-cranial specimens used for morphometric and dietary analyses were located at the following museums:

- American Museum of Natural History (Department of Mammalogy), New York
- Museum für Naturkunde (Recent Mammals), Berlin
- Natural History Museum (Mammal Section), London
- National Museum of Wales (Natural Sciences), Cardiff
- Royal Belgian Institute of Natural Sciences (Recent Vertebrates), Brussels
- Royal Museum for Central Africa, Tervuren
- Smithsonian Institution National Museum of Natural History (Division of Mammals), Washington DC
- South West Heritage Trust, Taunton
- University Museum of Zoology, Cambridge

Captive individuals were not measured. The specimens analysed from each museum are detailed in Spreadsheets 4-6

Where specific locality details were given in the museum records, the locality was expanded to include the province, region, etc. This was for two reasons. Firstly, many localities were listed as towns or villages, where the animals were likely not themselves inhabitants. Expanding the location to a wider region more likely encompassed the habitats of the individuals. Secondly, expanding localities allowed more specimens to be grouped together, thus strengthening the statistical analyses. In some cases, the location detailed on the museum label could not be found, so these specimens were classified by country. Table 4.3 includes the locations as listed on the museum records, together with the expanded and grouped site locations used in this study. The sites are mapped in Figure 4.3.

For each site, climatic and vegetation data were derived, following the procedure outlined in Section 4.2.1. Full details of this data are found in Spreadsheet 3. Predator and prey biomass data were not obtained due to the lack of correspondence between the localities in Hatton *et al.* (2015) biomass database and the localities of the cranial and post-cranial specimens.

Table 4.3: Site details of present-day African *C. crocuta* specimens. DRC = Democratic Republic of the Congo.

Country	**Location (from museum records)**	**Location (expanded to region, district, province, etc. where possible)**	**Locality no.**
Angola	Ngemba	Zaire Province	1.1
Benin	Parakou	Borgou	2.1
Botswana	Joverega	Chobe National Park, Savuti Chobe National Park, Mababe Zokotsama Community Concession	3.1
	Mababe Flats		
	Mababe Flats, Bechuanaland Protectorate		
	Tsane, 25 mi east northeast	Kgalagadi District	3.2
Burundi	Rumonge	Rumonge Province	4.1
Cameroon	Babessi	North West Region	5.1
	Tibati	Adamawa Region	5.2
	Yoko	Centre Region	5.3
DRC	.	Democratic Republic of the Congo	6
	Vele		
	Ubangi, Liki River, Liki-Bembe Savannah, Poshe River Post road		
	Lubumbashi River		
	Ngaye S.Katanga		
	Bosobolo Region	Nord Ubangi District,	6.1
	Gaia of Bili where the Bondo Gufuru road cuts the way	Bas Uele District	6.2
	Poko		
	Gwane Region		
	Faradje	Haut Uele District	6.3
	Uélé, Parc National de la Garamba	Parc National de la Garamba and surrounding hunting grounds (Domaine de Chasse de Azande, Domaine de Chasse de Gangala Na Bodio, Domaine de Chasse Mondo Missa)	6.4
	Stanleyville (now Kisangani), Province Orientale	Tshopo District	6.5

	Boga	Ituri District	6.6
	Geti		
	Lac Albert, Kasenye		
	Nioka		
	Kilo Region		
	Kivu, Semliki River plain	Ituri and North Kivu Districts (combined)	6.7
	Semliki plain		
	Semliki Plain, south of Lac Albert		
	Road Goma to Rutshuru	North Kivu District	6.8
	Rwindi	Parc National des Virunga	6.9
	Kivu, Parc National Albert (now Parc National des Virunga), Rwindi River plain		
	Kivu, Parc National Albert (now Parc National des Virunga), Ganjo		
	Kivu, Parc National Albert (now Parc National des Virunga), Kasindi		
	Kivu, Parc National Albert (now Parc National des Virunga), Kasindi, port on Lac Édouard		
	Kivu, Parc National Albert (now Parc National des Virunga), Katanda, north of Rutshuru		
	Parc National Albert (now Parc National des Virunga), Masuku		
	Vitshumbi		
	Kafubu	Haut Katanga District	6.10
	Katanga, Parc National de l'Upemba, Kaswabilenga, Lufira River, Lusinga-Mabwe trail	Parc National de l'Upemba	6.11
	Katanga, Parc National de l'Upemba, Lusinga		
	Kasiki, Marungu	Tanganyika District	6.12
	South of Kabinda	Lomami Province	6.13
	Kisantu	Lukaya District	6.14

	Kwango, Kindongo	Kwilu and Kwango Districts (combined)	6.15
Eritrea	Senafe	Debub (Southern) Region	7.1
Ethiopia	Argobba, south Harrar	Ethiopia	9
	Diré Daoua	Dire Dawa chartered city	9.1
	Ghimbi, Wollega, 09°10'N 35°50'E, Alt. 2150 m	West Welega Zone	9.2
Kenya	2 mi south of Merti, Baraquoi District	Kenya	10
	Baraquoi District		
	Guaso Nyiro		
	Lakiundu River, Merele Water		
	Marsabit Road		
	Marsabit Road, Merele Water		
	Masi Sand River		
	Merti, Baragoi District		
	Guaso Ngishu Plateau		
	Guaso Ngishu Plateau, Nzoia River		
	Archers Post	Samburu County	10.1
	Sotik, Kabalolot Hill	Narok County and Bomet County	10.2
	Sotik, Loita Plains		
	Sotik, Telek River		
	Guaso Nyiro, Sotik		
	1 mi west of Galma Galla, Garissa District	Garissa County	10.3
	0.5 mi northeast of Masabubu, Garissa District		
	5 mi west of Galma Galla, Garissa District		
	Ziwani	Taita-Taveta County	10.4
	Mount Kenya	Mount Kenya National Park	10.5
	Mount Kenya, south west slope		
	Mount Kenya, west slope		
	Kitanga Farm	Nairobi National Park	10.6
Mozambique	8km south west of Chioco, Tete District	Tete Province	11.1
Namibia	Malindi Pan, Caprivi Strip	Caprivi Strip	12.1

	Near Malindi, Caprivi Strip		
	Windhuk (Windhoek)	Khomas Region	12.2
Rwanda	Mutara-Gabiro hunting area	Akagera National Park	13.1
	Parc nat. Kagera, Gabiro		
	Nya-katare (Nyagatare)	Nyagatare District	13.2
Senegal	Tiliboubakar (Thille Boubacar)	Podor Department	14.1
Sierra Leone	Near. Gberia, Koindagu District	Koinadugu District	15.1
Somalia	British Somaliland	Somalia	16
	Hargeisa, Somaliland	Woqooyi Galbeed Region	16.1
	Heleschid	Jubbada Dhexe (Middle Jubbada) Region	16.2
South Africa	East Transvaal	Mpumalanga Province	17.1
	Pongola R. Zululand	Zululand District	17.2
South Sudan	Near Kaka, White Nile	Upper Nile State	18.1
Sudan	Northern Darfur	North (Shamal) Darfur State	19.1
	South Dafur	South (Janub) Darfur State	19.2
	Kulme, Wadi Aribo, Darfur	West (Gharb) Darfur State	19.3
Swaziland	.	Swaziland	20.1
Tanzania	Near Mara Rio	Mara Region	21.1
	Surroundings of Schirati on Lake Victoria		
	Quihara at Tabora	Tabora Region	21.2
	Tabora		
	Near Moshi	Kilimanjaro Region	21.3
	Kondoa	Dodoma Region	21.4
	Kondoa Irangi		
	Kwa Mtoro at Ussandani		
	Mpapua (Mpwapwa)		
	Iringa	Iringa Region	21.5
	Msamwia camp at the Msamwia, adjacent to the river Mtembwa, before leaving the mountains, near Bismarkburg	Rukwa Region	21.6

	Msamwia		
	Msamwialager (Msamwia Camp)		
	Rukwa-Steppe		
	Mgera	Tanga Region	21.7
	Pangani		
	Kilossa	Morogoro Region	21.8
	Mkalinso (Mkalinju)	Pwani Region	21.9
	Mroweka	Lindi Region	21.10
	Tendaguru		
	Songea	Ruvuma Region	21.11
	Balbal, Tanganyika Territory	Ngorongoro Conservation Area	21.12
Togo	Bismarckburg	Centrale Region	22.1
	Bismarckburg, Station		
	Sansanne, Mangu	Savanes Region	22.2
Uganda	Ngetta Lira Lango, Alt. 2700'	Lira District	23.1
	River Cheki, Gulu District	Gulu District	23.2
	Kasawere, north east Mount Elgon	Mount Elgon	23.3
Kenya - Uganda	Mount. Elgon		
Zambia	13 mi north east of. Lusangazi Game Camp, east Bank Luangwa River, Fort Jameson District	Eastern Province	24.1
	Camp II, 0.5 mi south of Chibembe Pontoon, east Bank Luangwa River, Lundazi District		
	In camp, east Bank Luangwa River, Fort Jameson District		
	Kabompo District	Northwestern Province	24.2
Zimbabwe	Between Bulawayo and Victoria Falls, Malindi	Matabeleland North Province	25.1

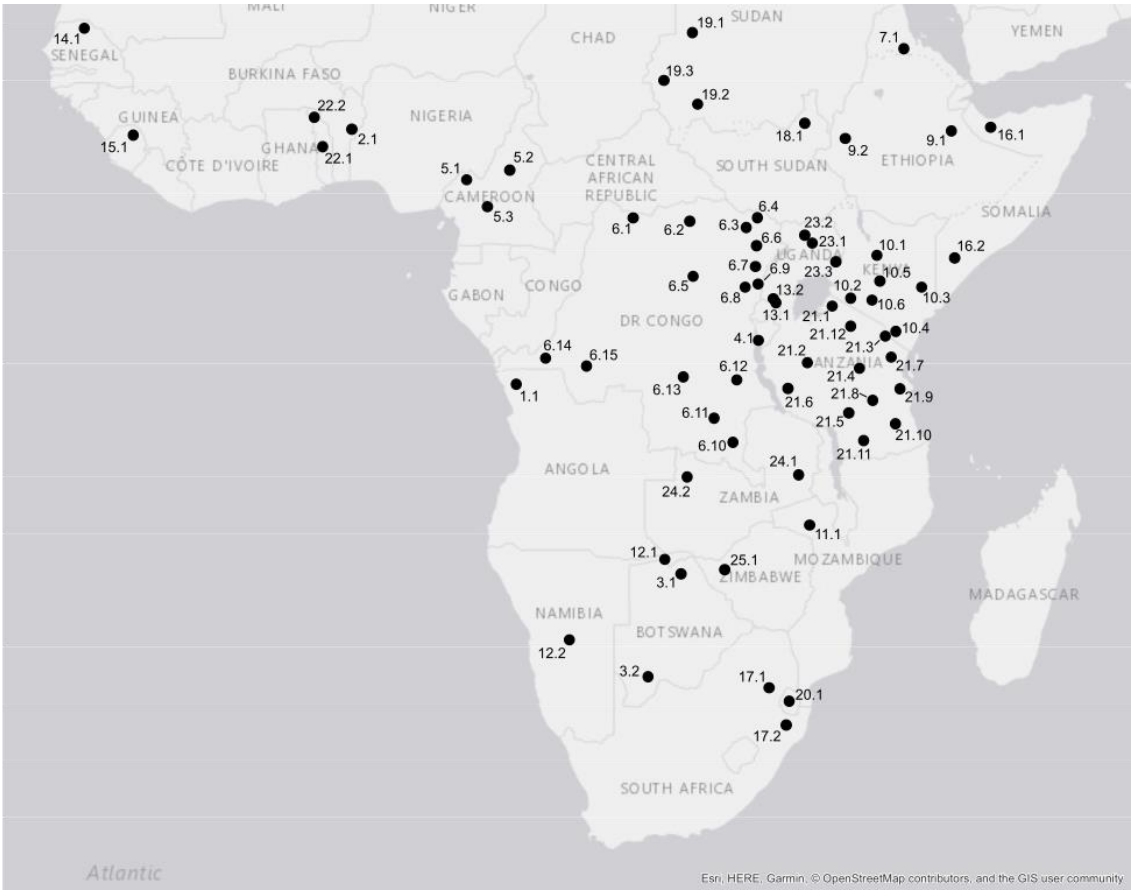

Figure 4.3: African sites included in the modern morphometric and dietary analyses. 1.1 Zaire Province. 2.1 Borgou. 3.1 Chobe National Park, Savuti Chobe National Park, Mababe Zokotsama Community Concession. 3.2 Kgalagadi District. 4.1 Rumonge Province. 5.1 North West Region. 5.2 Adamawa Region. 5.3 Centre Region. 6.1 Nord Ubangi District. 6.2 Bas Uele District. 6.3 Haut Uele District. 6.4 Parc National de la Garamba and surrounding hunting grounds. 6.5 Tshopo District. 6.6 Ituri District. 6.7 Ituri and North Kivu Districts (combined). 6.8 North Kivu District. 6.9 Parc National des Virunga. 6.10 Haut Katanga District. 6.11 Parc National de l'Upemba. 6.12 Tanganyika District. 6.13 Lomami Province. 6.14 Lukaya District. 6.15 Kwilu and Kwango Districts (combined). 7.1 Debub (Southern) Region. 9.1 Dire Dawa chartered city. 9.2 West Welega Zone. 10.1 Samburu County. 10.2 Narok County and Bomet County. 10.3 Garissa County. 10.4 Taita-Taveta County. 10.5 Mount Kenya National Park. 10.6 Nairobi National Park. 11.1 Tete Province. 12.1 Caprivi Strip. 12.2 Khomas Region. 13.1 Akagera National Park. 13.2 Nyagatare District. 14.1 Podor Department. 15.1 Koinadugu District. 16.1 Woqooyi Galbeed Region. 16.2 Jubbada Dhexe (Middle Jubbada) Region. 17.1 Mpumalanga Province. 17.2 Zululand District. 18.1 Upper Nile State. 19.1 North (Shamal) Darfur State. 19.2 South (Janub) Darfur State. 19.3 West (Gharb) Darfur State. 20.1 Swaziland. 21.1 Mara Region. 21.2 Tabora Region. 21.3 Kilimanjaro Region. 21.4 Dodoma Region. 21.5 Iringa Region. 21.6 Rukwa Region. 21.7 Tanga Region. 21.8 Morogoro

Region. 21.9 Pwani Region. 21.10 Lindi Region. 21.11 Ruvuma Region. 21.12 Ngorongoro Conservation Area. 22.1 Centrale Region. 22.2 Savanes Region. 23.1 Lira District. 23.2 Gulu District. 23.3 Mount Elgon. 24.1 Eastern Province. 24.2 Northwestern Province. 25.1 Matabeleland North Province. Base map from Esri (2006).

The m1 lengths from the modern African specimens were paired with the body mass data (Section 4.2.2) in the model to calculate Pleistocene body masses (Section 4.4.2.1). The m1 data included in the model were from specimens with provenance locations as close as possible to where the body masses were recorded (Table 4.4 and Figure 4.4). In total there were six body mass locations paired with eight m1 length locations, to provide a total of 11 data points when split into male and female body masses. The small number of body mass values necessitated the inclusion of body masses for which only country of provenance was known. The sites ranged in median latitude from 9.151° to -22.364°, providing a large latitudinal range and encompassing much of the present-day latitudinal extent of *C. crocuta*. Climate and vegetation details of each m1 length site and body mass site (except where only country is known) can be found in Spreadsheets 2 and 3.

Table 4.4: Body mass sites and m1 length sites of recent *C. crocuta* used in the model to reconstruct Pleistocene *C. crocuta* body masses.

Body mass location	**m1 length location**	**Sex**
Botswana	3.1 Chobe, Savuti Chobe, Mababe Zokotsama; 3.2 Kgalagadi District, Botswana (Joverega; Tsane)	F
Botswana	3.1 Chobe, Savuti Chobe, Mababe Zokotsama, Botswana (Mababe Flats)	M
Ethiopia	9 Ethiopia (Argobba)	F
Masai Mara National Reserve, Kenya	10.2 Narok Country and Bomet County, Kenya (Sotik)	F
Masai Mara National Reserve, Kenya	10.2 Narok Country and Bomet County, Kenya (Sotik)	M
Salient area of the Aberdare National Park, Kenya	10.5 Mount Kenya National Park, Kenya (Mount Kenya)	F
Salient area of the Aberdare National Park, Kenya	10.5 Mount Kenya National Park, Kenya (Mount Kenya)	M
Serengeti, Tanzania	21.12 Ngorongoro Conservation Area, Tanzania	F
Serengeti, Tanzania	21.12 Ngorongoro Conservation Area, Tanzania	M
Zambia	24.1 Eastern Province, Zambia (Lundazi District)	F
Zambia	24.1 Eastern Province; 24.2 Northwestern Province, Zambia (Fort Jameson District; Kabompo District)	M

Figure 4.4: African sites from which body mass (BM) and m1 lengths were derived, and included in the model to reconstruct Pleistocene body masses. 1. Ethiopia (BM) and Argobba (m1). 2. Salient area of the Aberdare National Park (BM) and Mount Kenya National Park (m1). 3. Masai Mara National Reserve (BM) and Narok Country and Bomet County (m1). 4. Serengeti (BM) and Ngorongoro Conservation Area (m1). 5. Zambia (BM) and Eastern Province, Northwestern Province (m1). 6. Botswana (BM) and Chobe, Savuti Chobe, Mababe Zokotsama, Kgalagadi District (m1).

4.2.4 Pleistocene European specimen sites

The cranial and post-cranial specimens used for morphometric and dietary analyses were located at the following museums:

- Bristol Museum and Art Gallery (Geology), Bristol
- British Geological Survey (Palaeontology), Keyworth
- Creswell Crags Museum and Heritage Centre, Worksop
- Krahuletz-Museum, Eggenburg
- Laboratorija za bioarheologiju, Univerzitet u Beogradu, Belgrade
- Leeds Discovery Centre, Leeds
- Lower Winskill, Settle
- Manchester Museum (Earth Science Collections), Manchester
- Museo della Fauna, Università degli Studi di Messina, Messina
- Museo Nacional de Ciencias Naturales (Colección de Paleontología de Vertebrados y de Prehistoria), Madrid
- Museu de Geologia, Museu de Ciències Naturals de Barcelona, Barcelona
- National Museum of Ireland (Natural History), Dublin
- National Museum of Wales (Palaeolithic and Mesolithic Archaeology), Cardiff
- Natural History Museum (Fossil Mammals), London
- Naturhistorisches Museum Wien (Vertebrate Palaeontology), Vienna
- Nottingham Natural History Museum, Wollaton Hall, Nottingham
- Oxford University Museum of Natural History, Oxford
- Plymouth City Museum and Art Gallery, Plymouth
- Royal Belgian Institute of Natural Sciences (Palaeontology), Brussels
- Sedgwick Museum of Earth Sciences, Cambridge
- South West Heritage Trust, Taunton
- Torquay Museum, Torquay
- University of Bristol Spelaeological Society museum, Bristol

- University Museum of Zoology, Cambridge
- Wells and Mendip Museum, Wells
- Yorkshire Museum, York

The specimens analysed from each museum are detailed in Spreadsheets 7, 8 and 10.

In total, Pleistocene *C. crocuta* were measured from 65 assemblages in Austria, Belgium, Britain, the Czech Republic, Ireland, Italy, Serbia and Spain. Figure 4.5 and Figure 4.6 show the locations of these sites. Table 4.5 details the ages of these assemblages. Further information about these sites, including palaeoenvironmental conditions, mammalian species and references can be found in Appendix 10.1 Table 10.1 to Table 10.3.

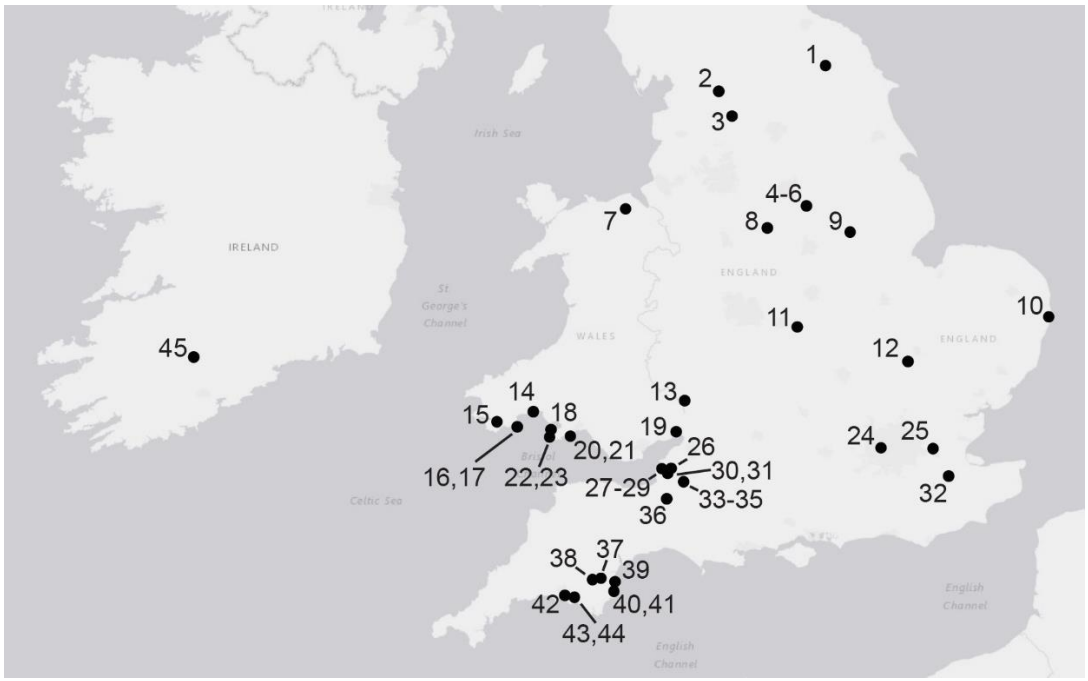

Figure 4.5: British and Irish Pleistocene sites included in the morphometric and palaeodietary analyses. 1. Kirkdale Cave. 2. Victoria Cave. 3. Raygill Fissure. 4. Church Hole. 5. Pin Hole. 6. Robin Hood Cave. 7. Ffynnon Beuno Cave. 8. Hoe Grange. 9.Little Syke. 10. Pakefield. 11. Lawford. 12. Barrington. 13. King Arthur's Cave. 14. Coygan Cave. 15. Priory Farm Cave. 16. Nanna's Cave. 17. Daylight Rock Fissure. 18. Prissen's Tor Cave. 19. Caerwent Quarry. 20. Caswell Bay. 21. Minchin Hole. 22. Lewes Castle Cave. 23. Goat's Hole Paviland. 24. Brentford. 25. Grays. 26. Sandford Hill. 27. Hutton Cavern. 28. Uphill Caves 7 or8. 29. Bleadon. 30. Picken's Hole. 31. Soldier's Hole. 32. Boughton Mount. 33. Badger Hole. 34. Hyaena Den. 35. Milton Hill. 36. The Burtle Beds. 37. Tornewton Cave. 38. Joint Mitnor Cave. 39. Kents Cavern. 40. Bench Cavern. 41. Brixham Cave/Windmill Hill. 42. Oreston Cave. 43. Eastern Torrs Quarry. 44. Yealm Bridge. 45. Castlepook Cave. Base map from Esri (2006).

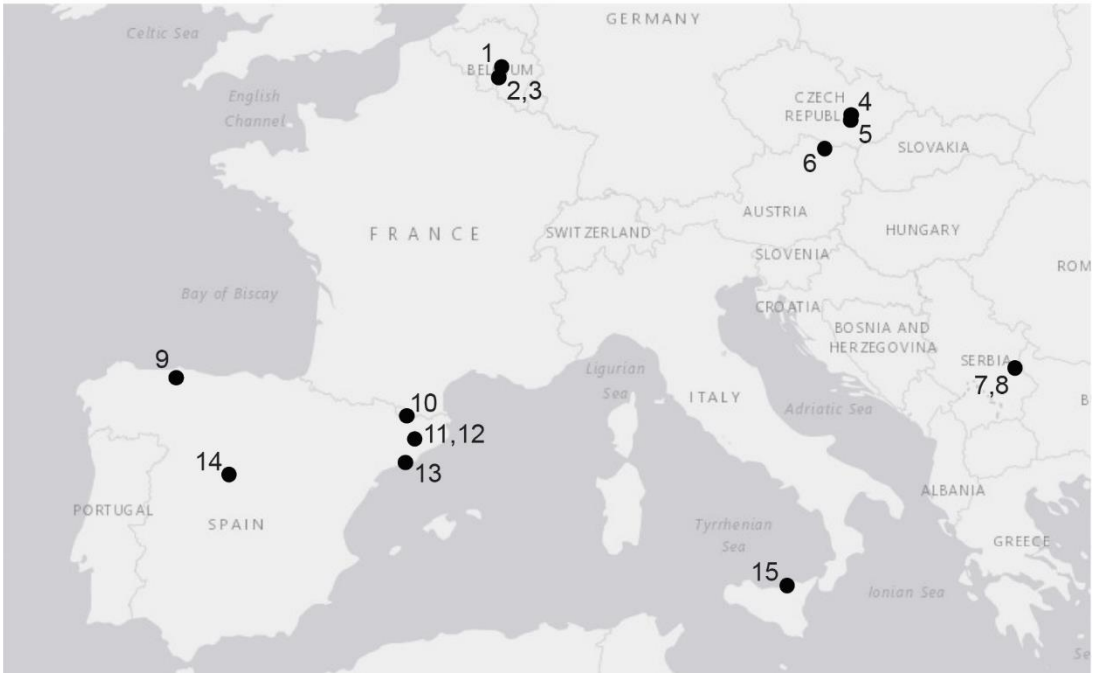

Figure 4.6: Austrian, Belgian, Czech, Italian, Serbian and Spanish Pleistocene sites included in the morphometric and palaeodietary analyses. 1. Goyet Caves. 2. Trou Magrite. 3. Caverne Marie-Jeanne. 4. Slouper Höhle. 5. Höhle Výpustek. 6. Teufelslucke. 7. Baranica I. 8. Baranica II. 9. Cueva de las Hienas. 10. Cova B d'Olopte. 11. Cova de les Toixoneres. 12. Cova del Toll. 13. Cova del Gegant. 15. Cueva del Búho. 16. San Teodoro. Base map from Esri (2006).

Figure 4.7 illustrates the direct dates on the assemblages from MIS 3 alongside the replotted NGRIP oxygen isotope ($\delta\ ^{18}O$) record. Where possible, only dates that are not associated with human presence (e.g. dates on humans or human-modified bones) are included. This is to attempt to capture the potential occupation of *C. crocuta* at each of the sites, as *C. crocuta* likely would not have been occupying the caves at the same time as humans. The only exception is the inclusion of the *Homo neanderthalensis* (Neanderthal) date from Cova del Gegant as this was the only species dated from this assemblage. Further details and dates are outlined in Appendix 10.1 Table 10.4.

Table 4.5: Ages of assemblages included in the Pleistocene morphological studies. See Appendix 10.1 Table 10.1 to Table 10.3 for details and references.

Site	Age
Britain	
Pakefield, Suffolk	Early Middle Pleistocene
Grays, Essex	MIS 9
Bleadon, Somerset	Later MIS 7
Hutton Cavern, Somerset	Later MIS 7
Lawford, Warwickshire	Possibly later MIS 7
Oreston Cave, Plymouth	Later MIS 7
Prissen's Tor Cave = Spritsail Tor, Swansea	Possibly Later MIS 7
Barrington, Cambridgeshire	MIS 5e
Brentford, London	MIS 5e
Burtle Beds, Somerset	MIS 5e
Eastern Torrs Quarry, Devon	MIS 5e
Hoe Grange, Derbyshire	MIS 5
Joint Mitnor Cave, Devon	MIS 5e
Kirkdale Cave, Yorkshire	MIS 5e
Little Syke, Lincolnshire	MIS 5e
Milton Hill, Somerset	MIS 5e
Minchin Hole, Outer Beach, Glamorgan	MIS 5
Raygill Fissure, Yorkshire	MIS 5e
Tornewton Cave, Devon (Lower Hyaena Stratum)	MIS 5c
Tornewton Cave, Devon (Upper Hyaena Stratum)	MIS 5c
Victoria Cave, Yorkshire	MIS 5e
Badger Hole, Wookey Hole, Somerset	MIS 3
Bench Cavern, Devon	MIS 3
Boughton Mount, Kent	MIS 3

Brixham Cave/ Windmill Hill, Devon	MIS 3
Cae Gwyn Cave, Clywd	MIS 3
Caerwent Quarry, Monmouthshire	MIS 3
Caswell Bay, Swansea	MIS 3
Church Hole, Creswell Crags, Nottinghamshire	MIS 3
Coygan Cave, Carmarthenshire	MIS 3
Daylight Rock Fissure, Pembrokeshire	MIS 3
Ffynnon Beuno Cave, Denbighshire	MIS 3
Goat's Hole Paviland, Swansea	MIS 3
Hyaena Den, Wookey Hole, Somerset	MIS 3
Kents Cavern, Devon	MIS 3
King Arthur's Cave, Herefordshire (Unit 3)	MIS 3
Lewes Castle Cave, Swansea	MIS 3
Nanna's Cave, Caldey Island, Pembrokeshire	MIS 3
Picken's Hole, Somerset (Layer 3)	MIS 3
Pin Hole, Creswell Crags, Derbyshire	MIS 3
Priory Farm Cave, Pembrokeshire	MIS 3
Robin Hood Cave, Creswell Crags, Derbyshire (1969 and 1981 excavations)	MIS 3
Sandford Hill, Somerset	MIS 3
Soldier's Hole, Somerset	MIS 3
Tornewton Cave, Devon (Elk Stratum)	MIS 3
Uphill Caves 7 or 8, Somerset	MIS 3
Yealm Bridge, Devon	MIS 3
Austria	
Teufelslucke, Eggenburgh	MIS 3
Belgium	
Goyet caves, Namur Province (3eme Caverne, Chamber A, 4eme Niveau Ossifère, Galleries Voisines de l'Entrée)	MIS 3
Goyet caves, Namur Province (3eme Caverne, Chamber A, 3eme Niveau)	MIS 3
Goyet caves, Namur Province (3eme Caverne, Chamber A, 1er Niveau Ossifère)	MIS 3

Caverne Marie-Jeanne, Hastière (4eme Niveau)	MIS 3
Trou Magrite, Pont-à-Lesse, Namur	Probably MIS 5b to 3
Czech Republic	
Höhle Výpustek	MIS 3
Slouper Höhle	Late Pleistocene
Ireland	
Castlepook Cave, County Cork	MIS 3
Italy	
San Teodoro, Acquedolci, Sicily	MIS 3-2
Serbia	
Baranica I	MIS 3-2
Baranica II	MIS 3
Spain	
Cova de les Toixoneres = Cova de les Teixoneres, Barcelona	MIS 3
Cova del Toll, Barcelona	Late Pleistocene
Cova del Gegant, Barcelona	MIS 4-3
Cova B d'Olopte	MIS 3
Cueva de las Hienas = Las Caldas, Asturias	MIS 5b-3
Cueva del Búho, Segovia	MIS 5d-3

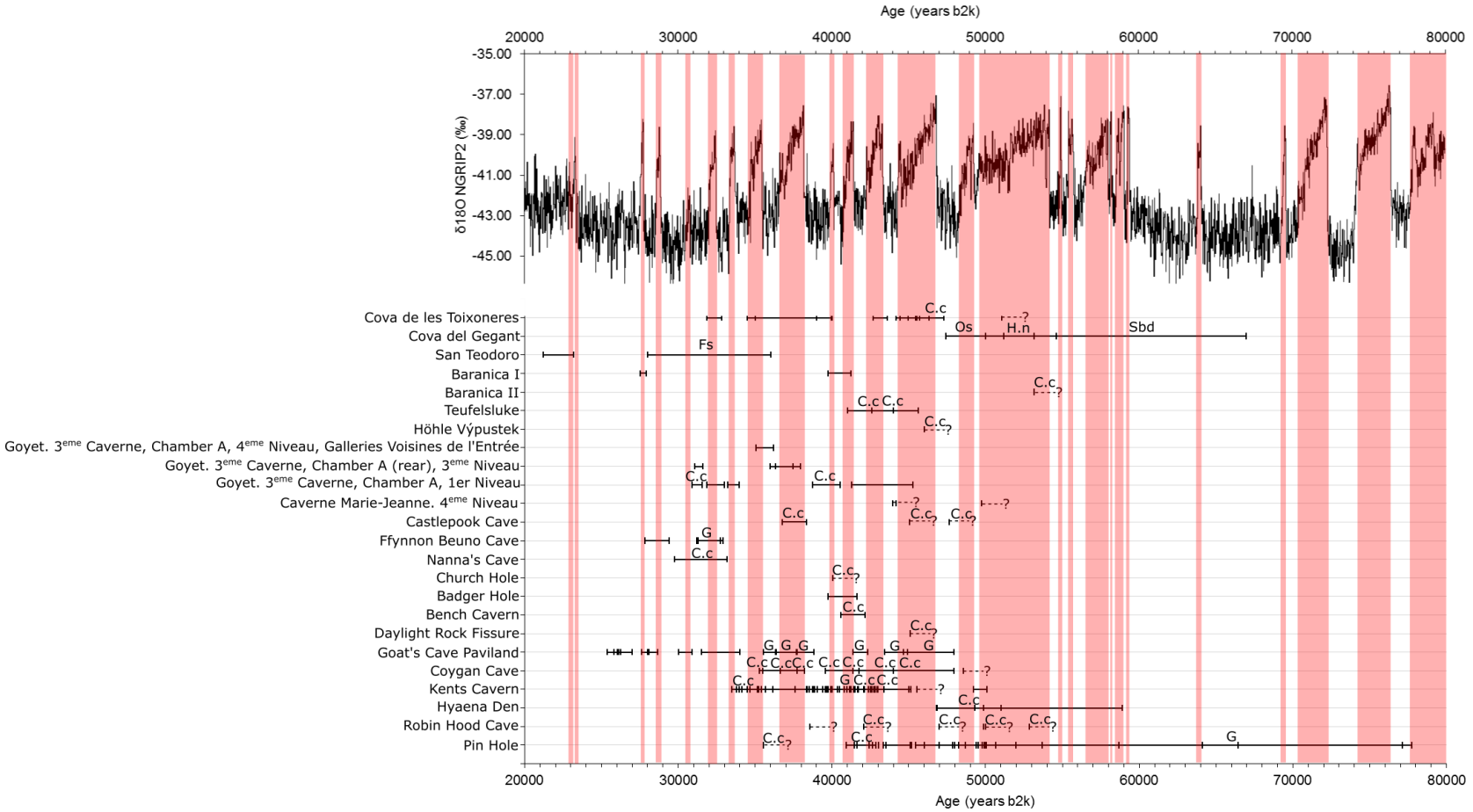

Figure 4.7: Dates on Pleistocene assemblages. $\delta^{18}O$ NGRIP2 20 year mean data, chronology and events from (Andersen *et al.*, 2004; Rasmussen *et al.*, 2014; Seierstad *et al.*, 2014). Radiocarbon dates were calibrated using OxCal 4.3 and IntCal13, with 95.4 % confidence range (Bronk Ramsey, 2009; Reimer *et al.*, 2013). C.c = *C. crocuta*. G = gnawed bone. Fs = flowstone. Os = overlying sequence. H.n = *H. neanderthalensis*). Sbd = speleothem at base of deposits. b2k = years before A.D. 2000. Pink shaded bands indicate interstadials. See Appendix 10.1 Table 10.1 to Table 10.4 for details and references.

4.2.5 Dates for radiocarbon models

Stuart and Lister (2014) collated radiocarbon dates of *C. crocuta* specimens and created a chronological model of *C. crocuta* extirpation from Eurasia. Since then, a new calibration model (IntCal13, Reimer *et al.*, 2013) and new radiocarbon dates on *C. crocuta* have been published, necessitating a rerun of the model. Additionally, the dates included in the model in the present study were subjected to stricter selection criteria.

In addition to the *C. crocuta* model, a model was run of dates on *P. leo* (*spelaea*), in order to facilitate a comparison between the two potential competitors. Models were also run on three of *C. crocuta*'s potential prey species: *C. antiquitatis*, *C. elaphus* and *R. tarandus* to assess where and when these species may have been available to *C. crocuta*. As *C. elaphus* and *R. tarandus* still live in Europe today, dates were only included up until 18,000 ^{14}C BP. This post-dates the youngest *C. crocuta* date, thereby fully demonstrating the relationship between the prey species and *C. crocuta* occupation of Europe during MIS 3.

Databases of dates on *C. crocuta* (Stuart and Lister, 2014), *P. leo* (*spelaea*) (Stuart and Lister, 2011) and *C. antiquitatis* (Stuart and Lister, 2012) were used, and further dates for all five species were sourced from the literature.

Dates were included in the models if they followed the following selection criteria:

- The dates were on specimens of the five species of interest without any uncertain species identification
- The specimens had undergone ultrafiltration pre-treatment, which has been shown to remove more contaminants than other pre-treatment methods (Higham *et al.*, 2006). Where publications did not mention whether the specimen had been subject to ultrafiltration, the Oxford Radiocarbon Accelerator Unit (ORAU) database (ORAU, no date) was used to check for information about ORAU dates
- Dates from contaminated specimens were excluded. Following Dinnis *et al.* (2016), dates from Caldey Island sites (previously included in Stuart and Lister, 2014) were excluded as they may have been conserved with varnish (van Nédervelde and Davies, 1975 cited in Dinnis *et al.*, 2016). There is only one exception for this selection criterion. Some of the earlier specimens that were subjected to ultrafiltration at ORAU were contaminated by the equipment (Bronk Ramsey *et al.*, 2004), which affected a number of dates from the five species of interest in the present study. However, there are two reasons for including these dates in the models. Firstly, the dates most affected were those of less than two ^{14}C half-lives (Higham *et al.*, 2006), which is younger than the

youngest dates included in the models. Moreover, the error is only about 100-300 years (Bronk Ramsey *et al.*, 2004). There is therefore little concern that the contamination will affect the conclusions of this study

- Burnt or heated bones were excluded as this condition may result in ages that are erroneously young (Higham *et al.*, 2011a)
- Dates on specimens with uncertain provenance were excluded
- Dates were only from European sites. Dates on other species from European Russia were excluded as the sites were far from the *C. crocuta* sites. Dates on other species were also excluded from countries where there have been no records of *C. crocuta* occupation
- Where the information is specified in the publications, dates were included if the collagen yield was equal to or greater than 1 %, and the atomic C:N (carbon:nitrogen) ratio was between 2.9 and 3.5 (following Higham *et al.*, 2011b)
- ORAU dates with a prefix 'OxA-X' were excluded as this indicates either analytical values that are outside of the acceptable range or specimens that had undergone an experimental pre-treatment method (Higham *et al.*, 2011b)

The sites from which the dated specimens originated are shown in Figure 4.8 to Figure 4.12. For the purpose of the radiocarbon models, the sites were grouped into regions, which are also shown in the figures.

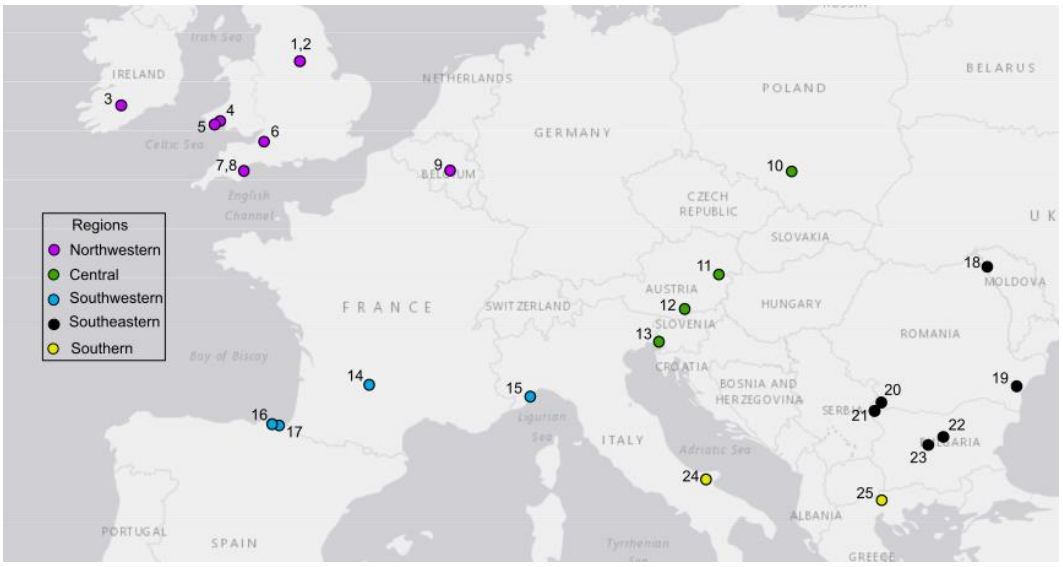

Figure 4.8: Sites of the dated *C. crocuta* specimens that are included in the new radiocarbon model. 1. Pin Hole. 2. Robin Hood Cave. 3. Castlepook Cave. 4. Coygan Cave. 5. Cefn Cave. 6. Hyaena Den. 7. Kents Cavern. 8. Bench Cavern. 9. Scladina Cave. 10. Komarowa Cave. 11. Melwurmhöhle. 12. Griffen Cave. 13. Grotta Pocala. 14. Igue du Gral. 15. Arene Candide. 16. Grotte de Canacaude. 17. Amalda. 18. Duruitoarea Veche. 19. La Adam Cave. 20. Desnisukhi Peck Cave. 21. Magura Cave. 22. Bacho Kiro Cave. 23. Balkan Range. 24. Grotta Paglicci. 25. Agios Georgios Cave. Base map from Esri (2006).

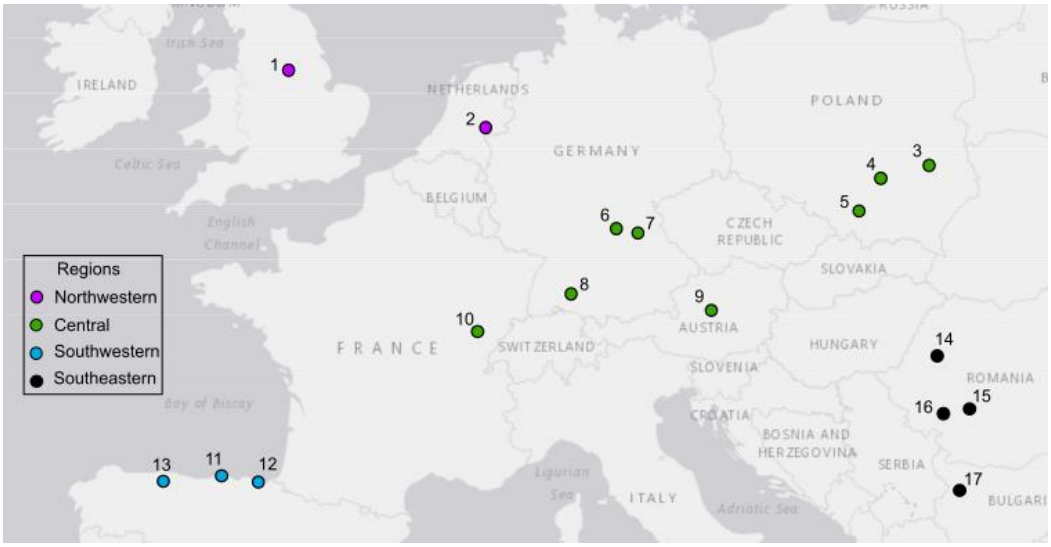

Figure 4.9: Sites of the dated *P. leo* (*spelaea*) specimens that are included in the new radiocarbon model. 1. Pin Hole. 2. Lathum. 3. Wierchowska Górna. 4. Jaskinia Raj. 5. Zawalona Cave. 6. Gremsdorf. 7. Zoolithenhöhle. 8. Zigeunerfels Cave. 9. Gamssulzen Höhle. 10. Abri des Cabones. 11. La Garma. 12. Uritaga Cave. 13. Jou'l Llobu. 14. Peştera Urşilor. 15. Peştera Muierii. 16. Peştera Cloşani. 17. Lakatnik Cave. Base map from Esri (2006).

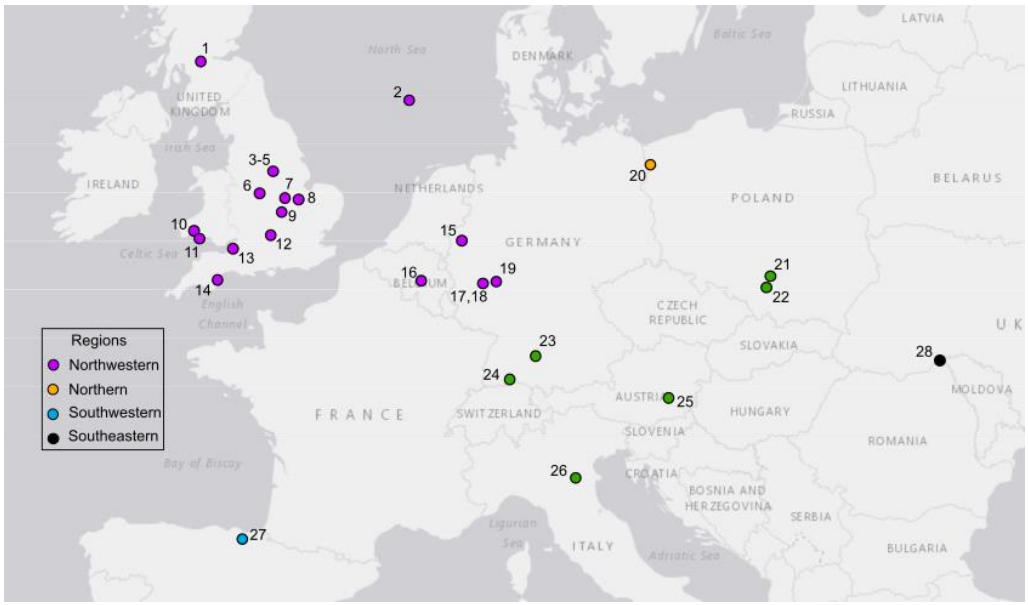

Figure 4.10: Sites of the dated *C. antiquitatis* specimens that are included in the new radiocarbon model. 1. Wilderness Pit. 2. North Sea. 3. Ash Tree Cave. 4. Pin Hole. 5. Robin Hood Cave. 6. Whitemoor Haye Quarry. 7. Grange Farm. 8. Bradley Fen. 9. Clifton Hill. 10. Coygan Cave. 11. Goat's Hole Paviland. 12. Sutton Courtenay. 13. Picken's Hole. 14. Kents Cavern. 15. Herne West. 16. Goyet Caves. 17. Gönnersdorf. 18. Koblenz-Metternich. 19. Wildscheuer Cave. 20. Szczecin. 21. Deszczowa Cave. 22. Jasna Cave. 23. Geißenklösterle. 24. Kesslerloch Cave. 25. Tropfsteinhöhl Kugelstein. 26. Settepolesini. 27. Labeko Koba Cave. 28.Duruitoarea Veche. Base map from Esri (2006).

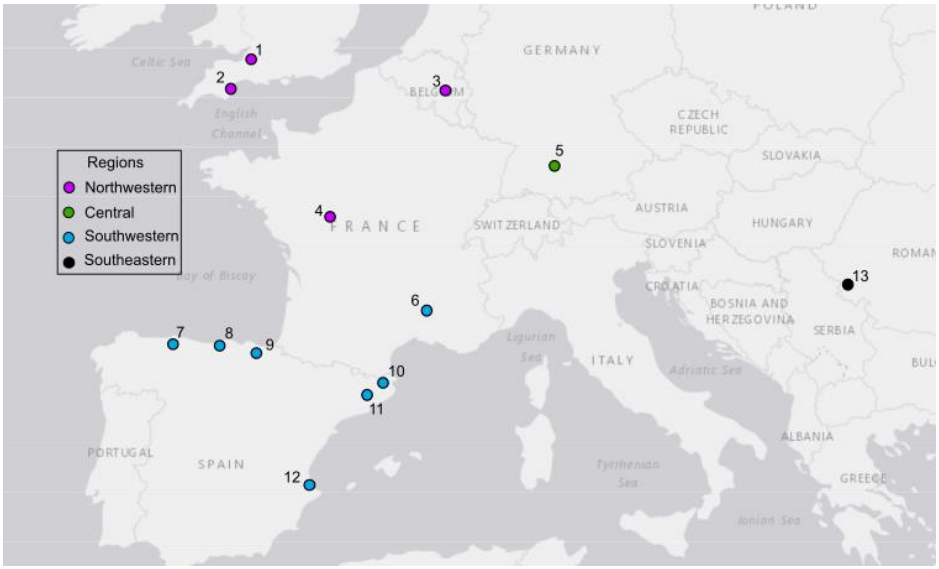

Figure 4.11: Sites of dated *C. elaphus* specimens that are included in the new radiocarbon model. 1. Hyaena Den. 2. Kents Cavern. 3. Trou Al'Wesse. 4. Bordes-Fitte Rockshelter. 5. Geißenklösterle. 6. Saint-Marcel. 7. La Viña. 8. El Castillo. 9. Labeko Koba Cave. 10. L'Arbreda. 11. Cova de les Toixoneres. 12. Cova del Papalló. 13. Peştera cu Oase. Base map from Esri (2006).

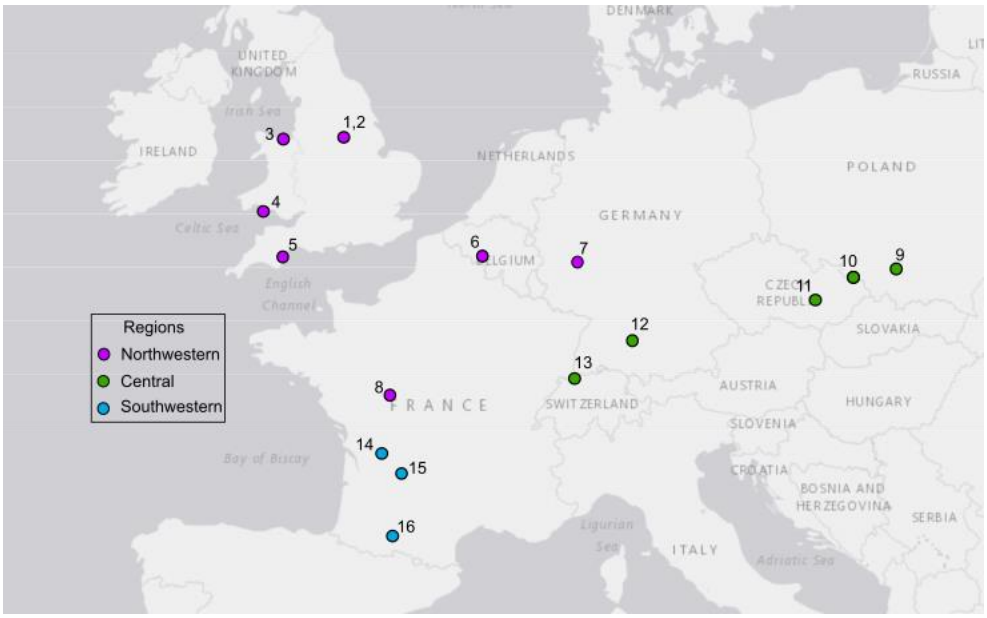

Figure 4.12: Sites of dated *R. tarandus* specimens that are included in the new radiocarbon model. 1. Pin Hole. 2. Robin Hood Cave. 3. Pontnewydd. 4. Goat's Hole Paviland. 5. Kents Cavern. 6. Champ de Fouilles. 7. Gönnersdorf. 8. Bordes-Fitte Rockshelter. 9. Jaskini Mamutowa. 10. Čertova díra. 11. Kůlna Cave. 12. Geißenklösterle. 13. Kastelhöhle. 14. La Chauverie. 15. Abri Pataud. 16. Les Harpons.

4.3 Methods

4.3.1 Linear morphometrics

4.3.1.1 Measurements

Linear measurements were taken on the modern and Pleistocene *C. crocuta* specimens. These measurements were taken using digital callipers, with a resolution of 0.01 mm and accuracy of 0.03 mm. The linear measurements of the bones and teeth along with references are detailed in Table 4.6 and Table 4.7. Figure 4.13 to Figure 4.16 illustrate how the measurements were taken.

Table 4.6: Linear measurements of each craniodental element. [1]Van Valkenburgh and Ruff (1987), [2]Werdelin (1989), [3]von den Driesch (1976), [4]Emerson and Radinsky (1980), [5]Therrien (2005), [6]Palmqvist et al. (2011).

Element	**Measurement**
Canine (upper and lower)	Anteroposterior diameter[1]
	Mediolateral diameter[1]
Premolars (P1, P2, P3, p2, p3, p4)	Length[2]
	Width[2]
P4	Length[3]
	Greatest width[3]
	Width[3]
m1	Length[3]
	Width[3]
Cranium	Total length[3]
	Condylobasal length[3]
	Basal length[3]
	Basicranial axis[3]
	Basifacial axis[3]
	Upper neurocranium length[3]
	Viscerocranium length[3]
	Facial length[3]
	Greatest length of the nasals[3]
	Snout length[3]
	Median palatal length[3]
	Length of the horizontal part of the palatine[3]
	Length of the cheektooth row, P1-P4[3]
	Length of the cheektooth row, P1-P3[3]
	Greatest diameter of the auditory bulla[3]
	Greatest mastoid breadth[3]
	Breadth dorsal to the external auditory meatus[3]
	Greatest breadth of the occipital condyles[3]
	Greatest breadth of the paraoccipital processes[3]

Cranium	Greatest breadth of the foramen magnum[3]
	Height of the foramen magnum[3]
	Greatest neurocranium breadth[3]
	Zygomatic breadth[3]
	Least breadth of the skull[3]
	Frontal breadth[3]
	Least breadth between the orbits[3]
	Greatest palatal breadth[3]
	Least palatal breadth[3]
	Greatest height of the orbit[3]
	Skull height[3]
	Height of the occipital triangle[3]
	Temporal fossa length[4]
Mandible	Condyle to symphysis length[3]
	Angular process to symphysis length[3]
	Condyle/angular process indentation to symphysis length[3]
	Condyle to posterior edge of c alveolus length[3]
	Angular process to posterior edge of c alveolus length[3]
	Condyle/angular process indentation to posterior edge of c alveolus length[3]
	c alveolus to m1 alveolus length[3]
	Length of the cheektooth row, p2-m1[3]
	Length of the cheektooth row, p3-m1[3]
	Length of the premolar row, p2-p4[3]
	Height of the vertical ramus[3]
	Mandibular depth at p2/p3[5,6]
	Mandibular width at p2/p3[5,6]
	Mandibular depth at p3/p4[5,6]
	Mandibular width at p3/p4[5,6]
	Mandibular depth at p4/m1[5,6]
	Mandibular width at p4/m1[5,6]
	Mandibular depth at post-m1[5,6]
	Mandibular width at post-m1[5,6]
	Distance from the p2/p3 to the middle of the articular condyle[5,6]
	Distance from the p3/p4 to the middle of the articular condyle[5,6]
	Distance from the p4/m1 to the middle of the articular condyle[5,6]
	Distance from the post-m1 to the middle of the articular condyle[5]
	Distance from the dorsal surface of the condyle to the ventral border of the angular process[4]
	Distance from the condyle to the apex of the coronoid process[4]
	Distance from the back of the condyle to the anterior rim of the masseteric fossa[4]
	Distance from the glenoid to the anterior side of c[1]
	Distance from the back of the condyle to the m1 notch[4]

Table 4.7: Linear measurements taken on each post-cranial element. All measurements follow von den Driesch (1976).

Element	**Measurement**
Atlas	Greatest length
	Greatest breadth of the cranial articular surface
	Greatest breadth of the caudal articular surface
	Greatest length from the cranial to caudal articular surfaces
	Length of the dorsal arch
	Height
Axis	Greatest length in the region of the corpus
	Greatest length of the arch
	Greatest breadth of the cranial articular surface
	Greatest breadth across the caudal articular process
	Greatest breadth across the transverse process
	Smallest breadth
	Greatest breadth of the caudal articular surface
	Height
Sacrum	Physiological length
	Greatest breadth of the cranial articular surface
	Greatest height of the cranial articular surface
Scapula	Smallest length of the neck
	Greatest length of the glenoid process
	Length of the glenoid cavity
	Breadth of the glenoid cavity
Pelvis	Length of the acetabulum on the rim
Humerus	Greatest length
	Greatest length from the caput
	Greatest depth of the proximal end
	Smallest breadth of the diaphysis
	Greatest breadth of the distal end
Radius	Greatest length
	Greatest breadth of the proximal end
	Smallest breadth of the diaphysis
	Greatest breadth of the distal end
Ulna	Greatest length
	Depth across the anconeal process
	Smallest depth of the olecranon
	Greatest breadth across the proximal articular surface
Femur	Greatest length
	Greatest breadth of the proximal end
	Greatest depth of the femoral head
	Smallest breadth of the diaphysis
	Greatest breadth of the distal end
Tibia	Greatest length
	Greatest breadth of the proximal end
	Smallest breadth of the diaphysis
	Greatest breadth of the distal end
Fibula	Greatest length
Patella	Greatest length

	Greatest breadth
Scapho-lunar	Greatest breadth
Navicular	Greatest breadth
Astragalus	Greatest length
Calcaneum	Greatest length
	Greatest breadth
Metapodials	Greatest length
	Greatest breadth of the distal end

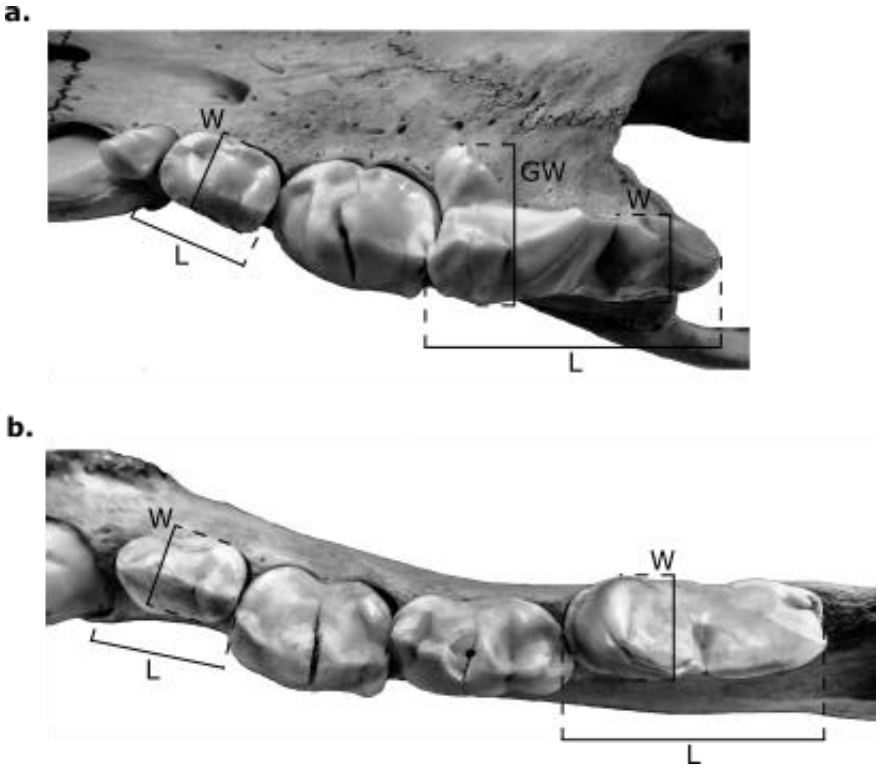

Figure 4.13: Diagrams of dentition measurements, following von den Driesch (1976) and Werdelin (1989). a. Upper dentition, showing the length (L) and width (W) of the premolars, illustrated on the P2. L, W and greatest width (GW) of the P4. b. Lower dentition, showing L and W of the premolars, illustrated on the p2. L and W of the m1.

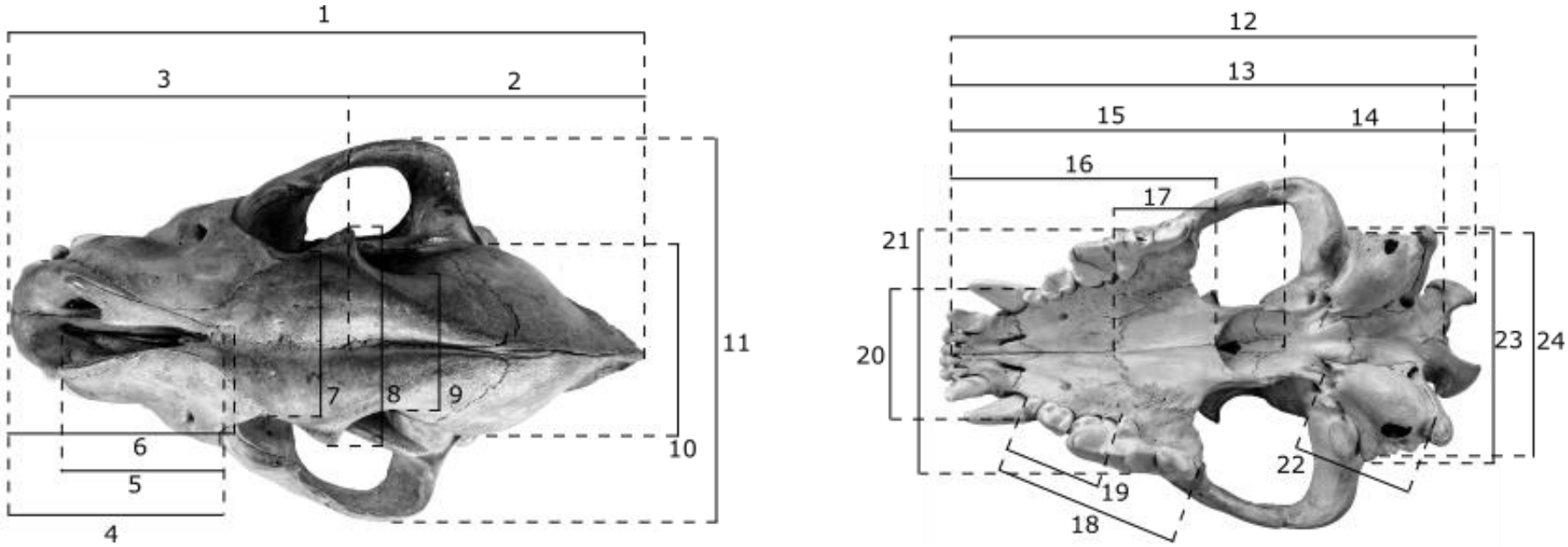

Figure 4.14: Diagrams of cranial measurements, following von den Driesch (1976) and Emerson and Radinsky (1980). 1. Total length. 2. Upper neurocranium length. 3. Facial length. 4. Viscerocranium length. 5. Greatest length of the nasals. 6. Snout length. 7. Least breadth between the orbits. 8. Frontal breadth. 9. Least breadth of the skull. 10. Greatest neurocranium breadth. 11. Zygomatic breadth. 12. Condylobasal length. 13. Basal length. 14. Basicranial axis. 15. Basifacial axis. 16. Median palatal breadth. 17. Length of the horizontal breadth of the palatine. 18. Length of the cheektooth row, P1-P4. 19. Length of the cheektooth row, P1-P3. 20. Least palatal breadth. 21. Greatest palatal breadth. 22. Greatest diameter of the auditory bulla. 23. Breadth dorsal to the external auditory meatus. 24. Greatest mastoid breadth. 25. Greatest breadth of the paraoccipital process. 26. Greatest breadth of the occipital condyles. 27. Greatest breadth of the foramen magnum. 28. Height of the foramen magnum. 29. Skull height. 30. Height of the occipital triangle. 31. Greatest height of the orbit. 32. Temporal fossa length.

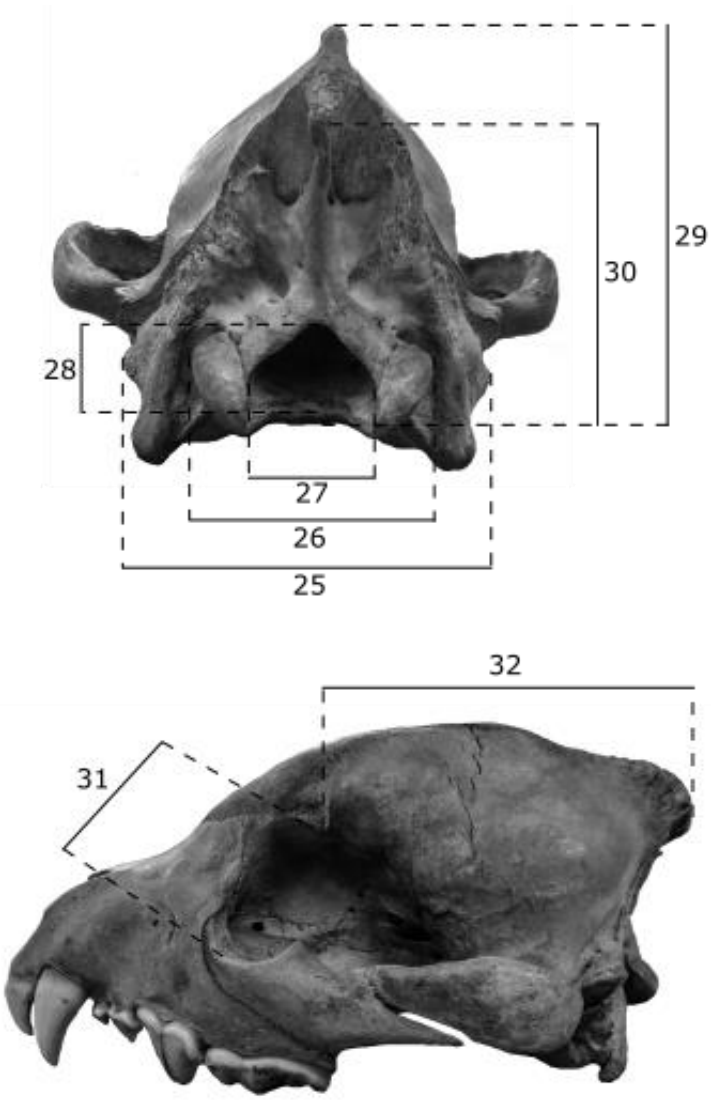

Figure 4.14 continued.

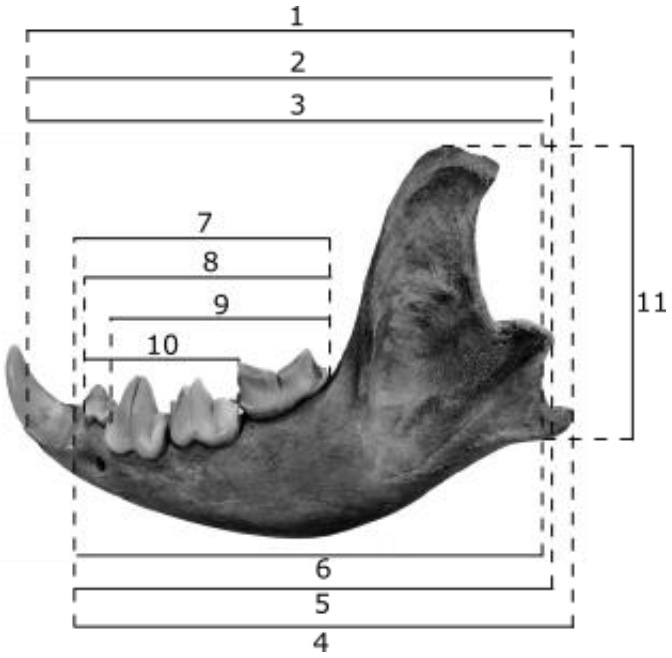

Figure 4.15: Diagrams of mandibular measurements, following von den Driesch (1976), Emerson and Radinsky (1980), Van Valkenburgh and Ruff (1987), Therrien (2005) and Palmqvist et al. (2011). 1. Angular process to symphysis length. 2. Condyle to symphysis length. 3. Condyle/angular process indentation to symphysis length. 4. Angular process to posterior edge of c alveolus length. 5. Condyle to posterior edge of c alveolus length. 6. Condyle/angular process indentation to posterior edge of c alveolus length. 7. c alveolus to m1 alveolus length. 8. Length of the cheektooth row, p2-m1. 9. Length of the cheektooth row, p3-m1. 10. Length of the premolar row, p2-p4. 11. Height of the vertical ramus. 12. Distance from the glenoid to the anterior side of c. 13. Distance from p2/p3 to the middle of the articular condyle. 14. Distance from p3/p4 to the middle of the articular condyle. 15. Distance from p4/m1 to the middle of the articular condyle. 16. Distance from the back of the condyle to the m1 notch. 17. Distance from post-m1 to the middle of the articular condyle. 18. Distance from the condyle to the apex of the coronoid process. 19. Distance from the dorsal surface of the condyle to the ventral border of the angular process. 20. Distance from the back of the condyle to the anterior rim of the masseteric fossa. 21. Mandibular depth at p2/p3. 22. Mandibular depth of p3/p4. 23. Mandibular depth at p4/m1. 24. Mandibular depth at post-m1. 25. Mandibular width at p2/p3. 26. Mandibular width at p3/p4. 27. Mandibular width at p4/m1. 28. Mandibular width at post-m1.

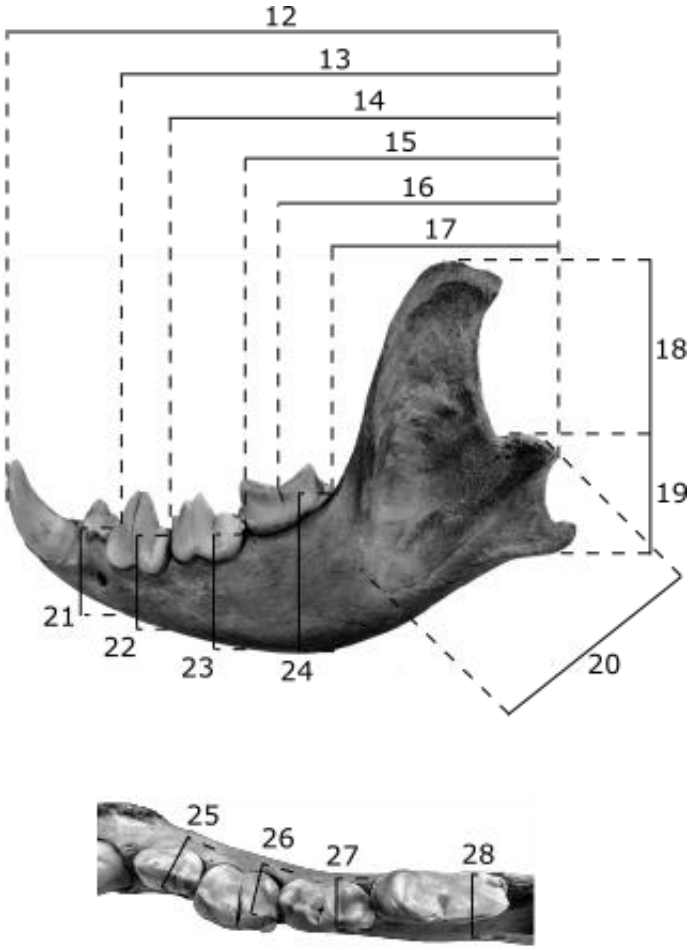

Figure 4.15 continued.

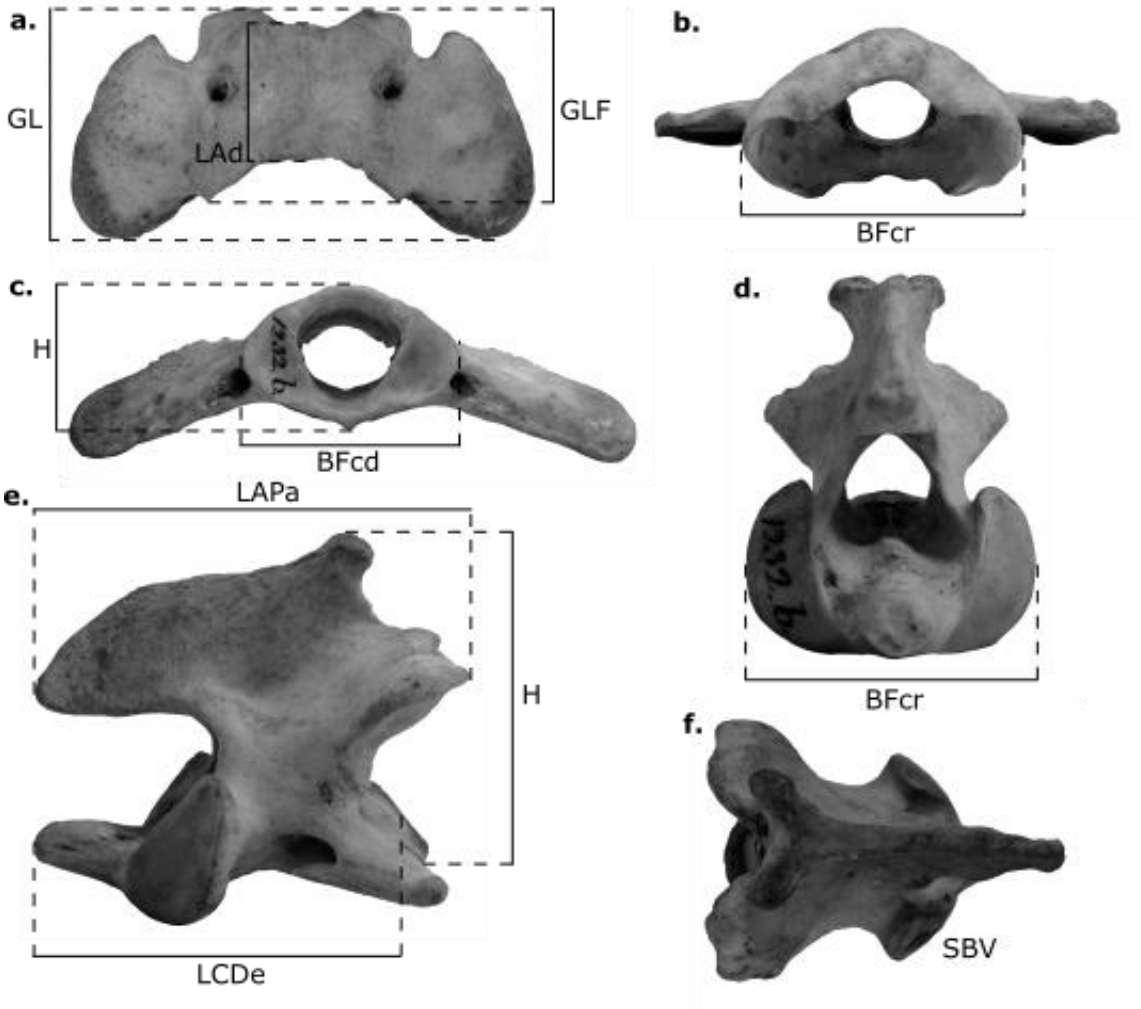

Figure 4.16: Diagrams of post-cranial measurements with corresponding abbreviations, following von den Driesch (1976). a-c. Atlas. d-f. Axis. g-h. Sacrum. i-j. Scapula. k. Pelvis. l-m. Humerus. n-o. Ulna. p. Radius. q-r. Femur. s. Fibula. t. Tibia. u. Patella. v. Scapho-lunar. w. Navicular. x. Astragalus. y. Calcaneum. z. Metapodial. GL = greatest length. GLF = greatest length from the cranial to caudal articular surfaces. LAd = length of the dorsal arch BFcr = greatest breadth of the cranial articular surface. BFcd = greatest breadth of the caudal articular surface. H = height. LAPa = greatest length of the arch. LCDe = greatest length in the region of the corpus. SBV = smallest breadth of the vertebra. BFacd = greatest breadth across the caudal articular process. BPtr = greatest breadth across the transverse process. PL = physiological length. HFcr = greatest height of the cranial articular surface. SLC = smallest length of the neck of the scapula. GLP = greatest length of the glenoid process. LG = length of the glenoid cavity. BG = breadth of the glenoid cavity. LAR = length of the acetabulum on the rim. GL = greatest length. GLC = greatest length from the caput. SD = smallest breadth of the diaphysis. Dp = depth of the proximal end. Bp = greatest breadth of the proximal end. Bd = greatest breadth of the distal end. BPC = greatest breadth across the proximal articular surface. SDO = smallest depth of the olecranon. DPA = depth across the anconeal process. DC = greatest depth of the femoral head. GB = greatest breadth.

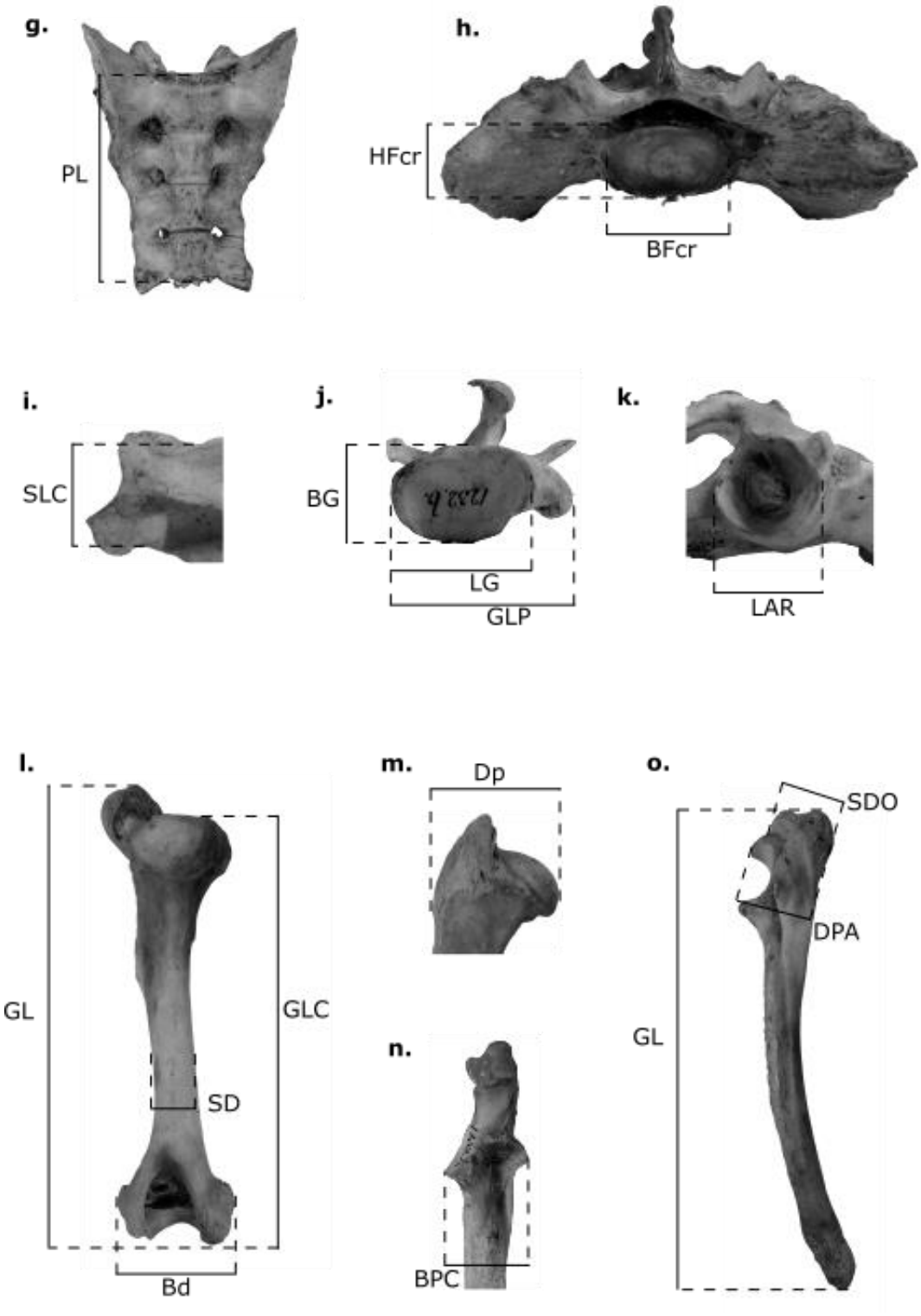

Figure 4.16 continued.

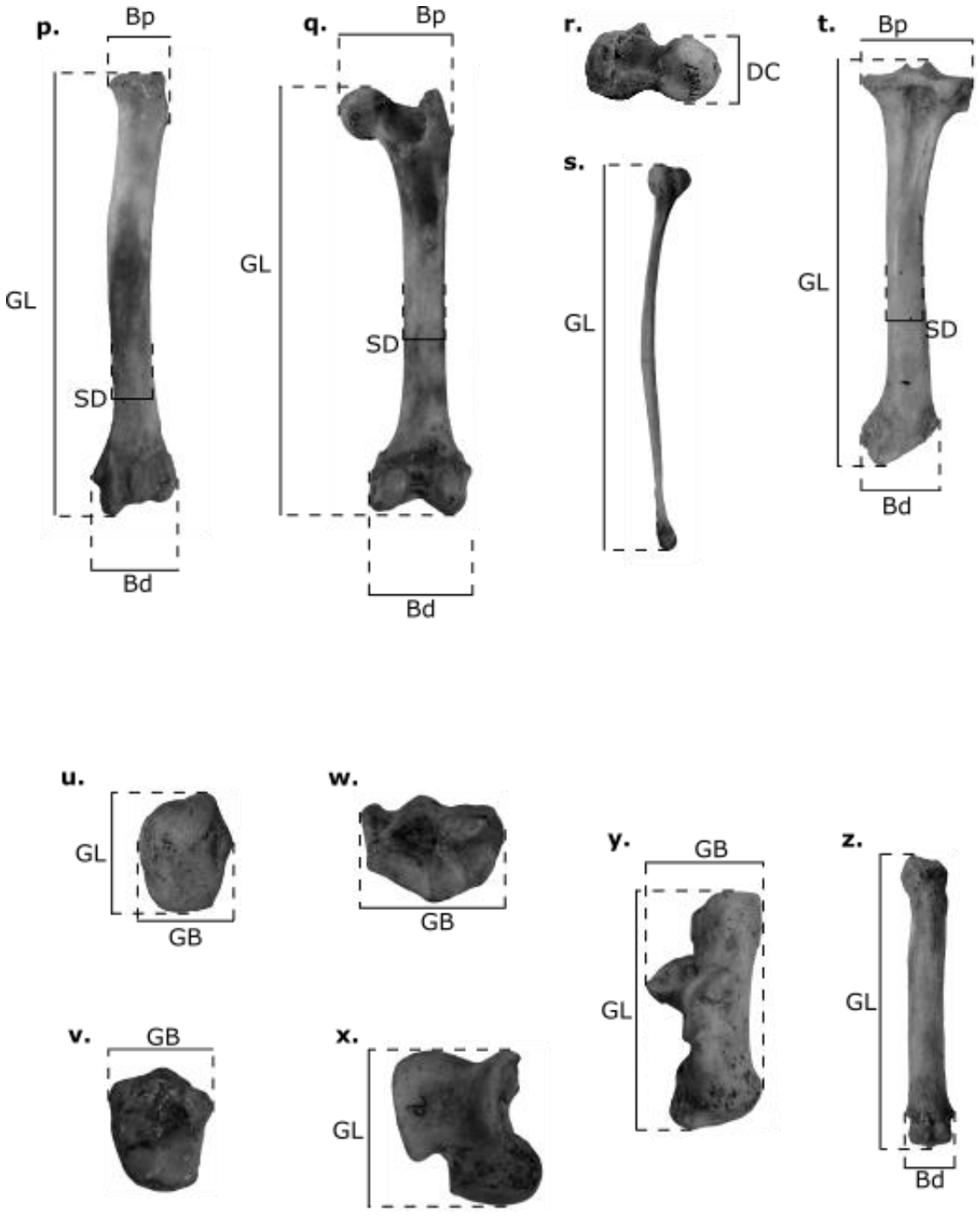

Figure 4.16 continued.

4.3.1.2 Mandibular bending strength

Following Therrien (2005) and Palmqvist *et al.* (2011), the measurements used to calculate mandibular bending strength were the depths and widths of the mandibular corpus at the p2/p3, p3/p4, p4/m1 and post-m1 interdental gaps, in addition to the distances from the mandibular condyle to each of these interdental gaps (see Table 4.6). This followed the principle of modelling the mandible as an elliptical beam. The depth and width measurements, when converted into radius values, allowed calculation of the distribution of bone around the dorsoventral and labiolingual planes (Figure 4.17). The mandibular condyle acted as the hinge or fulcrum in the lever model. The distance from the condyle to each interdental gap, coupled with the radius values of the corpus, allows calculation of bending strength along the mandible (Therrien, 2005; Palmqvist *et al.*, 2011).

Figure 4.17: From Therrien (2005). Cross-sectional view through the mandibular corpus. Ix = the distribution of bone in the dorsoventral plane or around the x axis. Iy = the distribution of bone in the labiolingual plane or around the y-axis. zx = the mandibular bending strength in the dorsoventral plane or around the x-axis. zy = the mandibular bending strength in the labiolingual plane or around the y=axis.

Following Therrien (2005) and Palmqvist *et al.* (2011), three indices were calculated (zx/L, zy/L and zx/zy) at each interdental gap, using the following equations:

Equation 4.1:

$$Ix = \frac{\pi b a^3}{4}$$

and

Equation 4.2:

$$Iy = \frac{\pi a b^3}{4}$$

where Ix is the is the distribution of bone in the dorsoventral plane, and Iy is the distribution of bone in the labiolingual plane, of the mandibular corpus. a is the dorsoventral radius, or half the depth of the mandibular corpus. b is the labiolingual radius, or half the width.

Next, the following equations were used:

Equation 4.3:

$$zx = Ix/a$$

and

Equation 4.4:

$$zy = Iy/b$$

where zx is the mandibular bending strength in the dorsoventral plane, and zy is the mandibular bending strength in the labiolingual plane.

The cross-sectional area or relative bending strength of the mandibular corpus (zx/zy index) was calculated by dividing zx by zy. Where the value is greater than one, the mandible is deeper than wide, and has greater resistance to dorsoventral bending than labiolingual bending (Therrien, 2005; Palmqvist *et al.*, 2011).

Finally, zx/L and zy/L indices were calculated by dividing zx and zy by the distance from the condyle to the corresponding interdental point. For example, if zx and zy were calculated from the depths and widths of the mandible at the p2/p3 interdental point, the resulting values for zx and zy would be divided by the distance from the condyle to p2/p3. The zx/L and zy/L values indicate the bending strength at each interdental point. Greater values have a greater bending strength (Therrien, 2005; Palmqvist *et al.*, 2011).

4.3.1.3 Bite force

The mandible was measured as a lever to calculate the mechanical advantage of the jaw-closing muscles, providing an indication of bite force. The pivot was the mandibular condyle, the in-force was the lifting action of the masticatory muscles, and the out-force was the resistance force at each bite point along the mandible, following (Moore, 1981).

In-levers and out-levers (or moment arms) are represented by some of the measurements in Table 4.6 and Figure 4.15, following Emerson and Radinsky (1980) and Van Valkenburgh and Ruff (1987). The measurements and their corresponding levers are outlined in Table 4.8. Except for the canine and the m1, moment arms were measured at interdental gaps (p2/p3, p3/p4, p4/m1), following the measurements used by Therrien (2005) and Palmqvist *et al.* (2011) in bending strength calculations. Measurements from the condyle to the interdental gaps were used instead of the teeth themselves, in order to prevent the measurements being influenced by the height and wear stage of the premolars. The moment arm of resistance at the canine was measured to the anterior edge of the canine, rather than the cusp (following Van Valkenburgh and Ruff, 1987), so that tooth wear would not influence the measurement. The same is true of the moment arm of resistance at the m1, which was measured at the notch between the two blades (following Emerson and Radinsky, 1980).

In order to calculate the mechanical advantage of the muscle at each point along the mandible, the in-lever was divided by the out-lever, following Van Valkenburgh and Ruff (1987). The greater the out-lever or out-force relative to the in-lever or in-force, the greater the mechanical advantage (Alexander, 1983).

Table 4.8: Measurements of moment arms (in-levers and out-levers) of the mandible. [1]Emerson and Radinsky (1980), [2]Van Valkenburgh and Ruff (1987), [3]Therrien (2005) and [4]Palmqvist et al. (2011).

Measurement	**Moment arm and lever**
From the condyle to the dorsal-most part of the coronoid process[1]	Moment arm of the temporalis (in-lever)
From the ventral part of the angular process to the dorsal surface of the condyle[1]	Moment arm of the superficial masseter (in-lever)
From the condyle to the anterior rim of the masseteric fossa[1]	Moment arm of the deep masseter (in-lever)
From the condyle to the anterior side of the canine[2]	Moment arm of resistance at the canine (out-lever)
From the condyle to the p2/p3 interdental gap[3,4]	Moment arm of resistance at p2/p3 (out-lever)
From the condyle to the p3/p4 interdental gap[3,4]	Moment arm of resistance at p3/p4 (out-lever)
From the condyle to the p4/m1 interdental gap[3,4]	Moment arm of resistance at p4/m1 (out-lever)
From the condyle to the notch between the paraconid and protoconid[1]	Moment arm of resistance at the m1 (out-lever)

4.3.1.4 Post-cranial indices

A number of indices were calculated from some of the post-cranial measurements (Table 4.7 and Figure 4.16) to analyse further aspects of locomotion. The brachial index (radius length/humerus length) and crural index (tibia length/femur length) values are greater in cursorial carnivorans (Meachen *et al.*, 2016). Hindlimb proportion (femur length/metatarsal IV length) values are lower with greater speed (Van Valkenburgh, 1985). Forelimb length (humerus length + radius length + Metacarpal III length) and hindlimb length (femur length + tibia length + Metatarsal IV length) were calculated following Christiansen (2002). The forelimb length and hindlimb length are an indication of effective limb length, which is related to stride length (Hildebrand, 1974).

4.3.2 Dental macrowear

Dental macrowear was used to provide an estimate of the relative age at death of each individual. This is not an absolute, numerical age; it merely allows splitting of the individuals into a number of wear categories, which can then be used as a proxy for age classes. The wear of the P3 and p3 were recorded following a classification scheme by Stiner (2004), see Figure 4.18. This

scheme includes eight categories (the first category, deciduous tooth, was not used) from stage II (the tooth is unworn and still erupting) to IX (the tooth is much worn).

Additionally, the wear of all teeth was categorised, following Van Valkenburgh (1988), into 'slight', 'moderate' and 'heavy'. Slight is classified as having slightly worn shear facets and cusps. Moderate is classified as having shear facets present and cusps blunted and heavy is described as when the carnassial shear facets are pronounced, and the other teeth are well-rounded with blunted cusps. An additional category of 'unworn' was also used.

Figure 4.18: From Stiner (2004). The categories of P3/p3 wear stages. d = deciduous. ↑ = erupting.

4.3.3 Tooth breakage

Teeth were further classified as broken or unbroken. They were classified as broken if there was obvious wear after breakage occurred, following Van Valkenburgh (1988), in order to exclude teeth that had been broken *post mortem*. Breakage was generally identified when the tooth did not follow the usual wear pattern. Additional indications were apparent when the tooth was still *in situ* in the jaw; it may initially have appeared to be heavily worn, yet the teeth around it exhibited considerably less wear. This tooth was therefore likely broken. Examples of broken teeth are shown in Figure 4.19 and Figure 4.20.

Figure 4.19: Broken right m1. Specimen RBINS 2419-9 from Trou Magrite, Belgium. Held at the Royal Belgian Institute of Natural Sciences, Brussels.

Figure 4.20: Broken right p2 and p3. Specimen MGB V778 from Cova del Toll, Spain. Held at Museu de Geologia, Museu de Ciències Naturals de Barcelona.

The alveoli were also inspected when a tooth was absent. Records were made when the alveolus was fully or partially healed, which indicated loss of a tooth during life. Teeth may be lost through infection of the alveolus, either through bacteria entering the exposed pulp of a broken tooth (Losey *et al.*, 2014), or through inflammation and subsequent infection of the gum (Pekelharing, 1974). It is acknowledged that a missing tooth with apparently healed bone may actually be due to congenital absence of the tooth (Losey *et al.*, 2014). An example is shown in Figure 4.21.

Figure 4.21: Partially healed alveoli of left i1, healed alveoli of right i1. Specimen AMNH 187780 from 10.3 Garissa County, Kenya. Held at the American Museum of Natural History, New York.

4.4 Data analyses

4.4.1 Modern African Crocuta crocuta

4.4.1.1 Modern *Crocuta crocuta* and *Panthera leo* biomass

An assessment was made to discover whether the population biomass distribution of each African predator (*C. crocuta*, *P. brunnea*, *P. leo*, *P. pardus*, *A. jubatus*) differed from each other. A histogram was produced to allow visual assessment of the relative abundance of each species. Kolmogorov-Smirnov tests were also performed. The null hypothesis of each test was that the distribution of populations from each dataset were the same.

Prior to the assessment of the influence of environmental conditions upon *C. crocuta* and *P. leo* biomass, the biomass, temperature and precipitation datasets were base-10 logarithmically transformed to reduce skew and to avoid autocorrelation. Some datasets contained values of zero that could not be log transformed. Where this was the case, the value of zero was converted to a value a unit of magnitude lower than the lowest non-zero value in the dataset. For example, if the lowest value was one, the zero was converted to 0.1, and then base-10 logarithmically transformed.

The vegetation cover data are expressed as percentages and therefore could not simply be logarithmically transformed. Percentage data suffer from the auto-sum problem whereby the value of one variable is dependent on the value of the other variables that are used to calculate the percentage (Pollard *et al.*, 2006). To avoid this, the vegetation data were transformed by the centred log-ratio, following Kucera and Malmgren (1998) and Pollard *et al.* (2006), with the equation:

Equation 4.5:

$$g(x) = (x_1 \dots x_d)^{1/d}$$

where g is the geometric mean of the vegetation category counts for each site, x is the count value of each vegetation category, and d is the number of vegetation categories. The ratio of a vegetation category count and the geometric mean was then calculated and base-10 logarithmic transformed:

Equation 4.6:

$$clr(x) = log10(\frac{x}{g(x)})$$

where clr is the centred log-ratio, and $log10$ is the base-10 logarithmic transformation.

Multiple regression is a common statistical tool used to determine the relationship between independent and dependent variables, either to explain or predict the dependent variables. However, one major disadvantage of multiple regression is its inability to deal with multicollinearity in independent variables, which may mean that the causal independent variable is excluded from the final model, at the expense of other independent variables with which it is correlated (Mac Nally, 1996, 2000; Carrascal *et al.*, 2009). Spearman Rank Order correlations revealed significant correlations between many of the independent environmental variables (Appendix 10.2, Table 10.5), so this is a particular problem in the present study.

An alternative method to circumvent the above problems, proposed by Mac Nally (1996, 2000), is hierarchical partitioning. However, Olea *et al.* (2010) assessed the hierarchical partitioning package for R (R Core Team, 2016), hier.part package (Walsh and Mac Nally, 2004, 2005, 2007). The documentation for the current version, hier.part version 1.0-4 (Walsh and Mac Nally, 2013), and earlier versions, includes a caution that rounding of analyses may occur when more than nine independent variables are included in the model (Walsh and Mac Nally, 2005b, 2007b, both cited in Olea *et al.*, 2010; Walsh and Mac Nally, 2015). When more than nine independent variables were included in a model, Olea *et al.* (2010) found that on more than 90 % of runs, the order in which the variables were input into the model affected the resulting order of importance of the variables. In the present study, there are 16 independent variables, so hierarchical partitioning is unsuitable.

A further alternative is partial least squares (PLS) regression, whereby associations are assessed between the independent variables to produce a smaller number of latent variables, or components, in a way that maximises the explained variance in the dependent variable (Carrascal *et al.*, 2009). In a comparison of three statistical tests (multiple regression, principal components analysis followed by multiple regression, and PLS), Carrascal *et al.* (2009) found that PLS performed better under multicollinearity. Additionally, PLS performed well even under low sample sizes. The combination of these points makes PLS the best method for the present study.

For each PLS, leave-one-out cross-validation was performed in order to select the appropriate number of components. The number of components selected was based on the highest r^2–predicted value. Each PLS model had a p-value. The strength of association of each independent variable with the dependent variable was indicated by the standardised coefficients.

The results were assessed for outliers and leverage points. A site was classed as an outlier if its standardised residual had a value greater or less than two. A site was deemed as a leverage point if its value fell beyond the vertical leverage reference line (LRL), which was calculated by:

Equation 4.7:

$$LRL = \frac{2m}{n}$$

where m is the number of components in the PLS, and n is the number of observations (Minitab Inc., 2010).

To assess the validity of the PLS models, each model was re-run, excluding one site each time. This indicated whether some sites were disproportionately influencing the results, and also whether *C. crocuta* and *P. leo* biomasses varied consistently with environmental conditions across all sites. The standardised coefficients were displayed in boxplots to highlight the variables with consistently positive or negative values, which would indicate that there was a consistent relationship between the dependent and independent variable, regardless of which sites were included in the model.

4.4.1.2 Repeated linear measurements

In order to assess precision of the linear measurements, the following six measurements were repeated 30 times on a *C. crocuta* specimen held in the Department of Geography, Royal Holloway University of London (see Section 4.3.1 for full details of measurements):

- Total length of the cranium
- Length of the m1
- Width of the m1
- Mandibular depth at the p2/p3 interdental gap
- Mandibular width at the p2/p3 interdental gap
- Distance from the mandibular articular condyle to the p2/p3 interdental gap

Each set of measurements was then randomly sub-sampled into two groups of 15 observations. Anderson-Darling tests were used to assess normal distribution. Depending on normal distribution, t-tests or Mann Whitney tests were performed to assess significant differences between the sub-samples. Absence of significant differences would indicate consistency in taking the linear measurements.

4.4.1.3 Ontogenetic size change

The crania and post-crania of modern *C. crocuta* from Africa were used to assess the change in values of skeletal measurements during ontogeny. Male and female *C. crocuta* were treated

separately in case of different ontogenetic changes. The specimens were split into P3/p3 wear stages, to indicate different age categories. The absolute values of each measurement were not used as these would have been related to the final, adult size of each individual. Instead, a ratio was calculated against the length of the m1. As teeth stop growing once they have erupted, the m1 was fully grown in each specimen. Furthermore, this tooth varies predictably with body mass (Van Valkenburgh, 1990). The ontogeny ratio therefore allows comparison of measurement size with age, taking into account variation in overall size unrelated to ontogeny. The ratio was calculated using the following equation:

Equation 4.8:

$$Ontogeny\ ratio = Log10\left(\frac{S}{m1}\right)$$

where S is the skeletal measurement, and $m1$ is the length of the m1. This ratio is a variation of one preferred by Smith (1999) in assessing sexual size dimorphism (see Section 4.4.1.4 for a full discussion).

For each ontogeny ratio, box plots were constructed to visually compare the data for each P3/p3 wear stage. An analysis of variance (ANOVA) with post-hoc Tukey's test was conducted on three or more datasets with a sample size of ten or more, in order to determine any significant differences between ontogeny ratios of individuals with different P3/p3 stages. Tukey's test was chosen as it reduces the chance of a Type 1 error, that the null hypothesis will be incorrectly rejected (Hancock and Klockars, 1996). Levene's test was conducted to check that the data conformed to the assumption of normal variance, prior to conducting the ANOVA tests. Where there were only two datasets, t-tests were conducted. Anderson-Darling tests for normality and tests for equal variances were conducted in order to confirm that the datasets met the requirements of the ANOVA or t-tests. Where this was not the case, the non-parametric Mann Whitney test was performed instead.

4.4.1.4 Sexual size dimorphism

SSD of present-day *C. crocuta* was calculated using the mean female and male body masses or morphometric measurements from each site. There are various methods to calculate SSD, including numerous ratios, many of which were assessed by Smith (1999). However, the author advocates the use of only two ratios. The first ratio involves one of two equations:

Equation 4.9:

$$SSD\ =\ Log(\frac{F}{M})$$

or

Equation 4.10:

$$SSD = Log(\frac{M}{F})$$

where F is the female measurement, and M is the male measurement. Equation 4.9 is used for species in which females are more frequently larger than males, and Equation 4.10 is used when males are more frequently larger than females.

The second ratio is a variation of the method proposed by Lovich & Gibbons (1992) and adapted by Smith (1999). For a species in which females are more frequently larger than males, two equations would be used:

Equation 4.11:

$$SSD = \frac{F}{M}$$

and

Equation 4.12:

$$SSD = 2 - \frac{M}{F}$$

Equation 4.11 is used when females are larger, and Equation 4.12 is used when males are larger. The equations would be reversed in species where males are more frequently larger than females:

Equation 4.13:

$$SSD = \frac{M}{F}$$

and

Equation 4.14:

$$SSD = 2 - \frac{F}{M}$$

Equation 4.13 would be used when males are larger, and Equation 4.14 would be used when females are larger.

The reason Smith (1999) prefers these equations over others is partly in light of occasions when, for example, a species has mostly female-biased SSD, but there are some populations where males are larger. Other equations would truncate the ratios where the males were larger to values between 0 and 1, whereas where females were larger, the values could extend from 1 upwards (Smith, 1999). In the present study, to calculate SSD of *C. crocuta* populations, Equation

4.9 was used. Equation 4.10 was used to calculate the SSD of *P. leo*, *P. pardus*, *A. jubatus*, *P. brunnea* and *L. pictus*. The logarithmic transformation was base-10.

A box plot was constructed to compare the body mass SSD values of the aforementioned large carnivores, to put into context the degree of SSD seen in *C. crocuta*. For craniodental linear measurement SSD, individual value plots were constructed to allow visual assessment of whether any measurements were consistently larger in males or females, and to compare the degree of SSD between measurements. Small sample sizes of post-crania did not permit construction of boxplots, so the SSD values were instead displayed in a table.

For the craniodental linear measurements, tests were performed to assess significant differences between base-10 logarithmically transformed males and female measurements from Site 21.12 (Ngorongoro Conservation Area, Tanzania). This site was chosen as it has the largest sample size. The significant difference tests were performed when there were at least ten values for females and ten for males. Tests were not performed on the post-crania due to small sample sizes. Anderson Darling tests were performed to assess whether the data were normally distributed. Subsequently, t-tests were performed on normally distributed data, and Mann-Whitney tests were performed on non-normally distributed data.

Additionally, the body mass data and craniodental measurements were assessed for Rensch's Rule, i.e. whether the degree of SSD decreases with larger body size or linear measurements, following Rensch (1950, cited in Abouheif and Fairbairn, 1997). The linear morphometrics included in the analyses were those that appeared to exhibit SSD, in addition to the condylobasal and m1 length as these measurements scale closely with overall body size (Van Valkenburgh, 1990). Postcranial sample sizes were too small to test for Rensch's Rule.

Many studies test for Rensch's Rule through regression of male or female body mass against the SSD ratio, and while Smith (1999) agrees with this method, other authors (e.g. Fairbairn 1997) refute this on the basis that the SSD ratios are calculated with the body mass data against which they are being regressed. An alternative method is to regress male body mass or morphometrics against female body mass or morphometrics. According to Fairbairn (1997), the problem with this is that in ordinary least squares regression analyses, the x-axis variable should be measured without error. That male and female body mass and linear morphometrics are both measured in the same way confounds this. Fairbairn (1997) proposes major axis regression or reduced major axis regression as alternatives. Smith (2009) states that it is the relative error between the x- and y-axis that is important, advocating the reduced major axis regression as an alternative to least squares regression when the x-axis error is not relatively small. Again, this is the case in the current study whereby both x- and y-axis variables (female and male body masses and

morphometrics) contain similar errors. Additionally, Smith (2009) advocates the use of reduced major axis regressions as opposed to ordinary least squares regressions in situations where neither the x- and y-axis variables are dependent on each other, as is the case with male against female body mass data.

Accordingly, in the present study, reduced major axis regressions compared base-10 logarithmically transformed mean female body mass or morphometrics on the x-axis against base-10 logarithmically transformed mean male body mass or morphometrics on the y-axis. When the value of the regression slope is greater than 1, SSD is associated with hyperallometric growth (male size increases more than female size), and thus Rensch's Rule is followed. In the case of female-biased SSD, the degree of SSD therefore decreases. When the slope is less than 1, SSD is associated with hypoallometric growth (male size increases less than female size). The degree of SSD increases in species with female-biased SSD. When the slope is 1, there is no variation between degree of SSD and body mass (Fairbairn 1997).

Tests were also run to assess the association of degree of SSD with environmental variables. The linear SSD measurements upon which correlations were performed were again those that had a sample size of at least six sites, and appeared to exhibit SSD, in addition to condylobasal length and m1 length due to their relationship with body size (Van Valkenburgh, 1990). Eight sites were included in the body mass SSD tests. Due to small sample sizes of *C. crocuta* body mass and craniodental linear measurement SSD, PLS regressions were not run. Instead, Spearman Rank Order correlations were performed. This test was chosen to avoid the elevated chance of Type I errors associated with individual regression models. Post-cranial SSD sample sizes were too small to undertake the tests.

To further avoid the elevated chance of Type I errors when performing multiple correlations, Bonferroni corrections were performed to calculate a stricter critical p-value (Armstrong, 2014). This was calculated using the following equation:

Equation 4.15:

$$\alpha 1 = \frac{\alpha}{T}$$

where α is the critical p-value (0.05 in this thesis), T is the number of Spearman Rank correlations performed, and $\alpha 1$ is the adjusted p-value.

The Spearman Rank Order tests assessed the correlation of *C. crocuta* SSD with the minimum temperature of the coolest month, maximum temperature of the warmest month, precipitation of the driest month, precipitation of the wettest month, closed vegetation cover, semi-open vegetation cover and open vegetation cover. For *C. crocuta* body mass SSD only, correlations

were also performed against *C. crocuta* density, *P. leo* density, prey biomass (without very large-sized prey biomass). The density and biomass data were not available for the locations of the craniodental sites. Population density data were base-10 logarithmically transformed, and the other variables were transformed as outlined in Section 4.4.1.1.

4.4.1.5 Modern *Crocuta crocuta* body mass, craniodental and post-cranial geographic variation

In order to assess the relationship between present-day *C. crocuta* body mass and environmental variables, Spearman Rank Order correlations were performed. Due to small sample sizes (eight sites), a PLS was not performed. Additionally, Spearman Rank Order correlations were chosen instead of linear regressions due to the risk of Type 1 errors in the latter test. Male and female *C. crocuta* body masses were treated as separate variables.

The association between linear measurements and environmental variables were also assessed. Where no SSD was apparent in the linear measurements, male and female data were combined, and specimens of unknown sex were also included. With sample sizes ranging from 26 to 62 sites, the craniodental variables had large enough sample sizes to allow PLS regressions to be performed. The justification for PLS regression is the same as for the biomass analyses (Section 4.4.1.1); there were a large number of independent variables, many of which were significantly correlated with each other (Appendix 10.6, Table 10.16). The PLS regressions were also performed as set out in Section 4.4.1.1.

Sample sizes of post-cranial measurements were too small to permit the use of PLS regressions. Spearman Rank Order correlations were therefore performed, with the same justification as discussed above for body mass. Where no SSD was apparent, male and female data were combined, and specimens of unknown sex were included. The correlations were performed on measurements with at least six data points.

The correlations and PLS regressions assessed the relationships between *C. crocuta* body mass and linear measurements with *C. crocuta* density, *P. leo* density, prey biomass, minimum temperature of the coolest month, maximum temperature of the warmest month, precipitation of the driest month, precipitation of the wettest month, closed vegetation cover, semi-open vegetation cover, open vegetation cover. Correlations were also performed to assess the relationship between *C. crocuta* male and female body masses and distance from the equator.

For the correlations and PLS regressions, body masses, linear measurements, distance from the equator and population density data were base-10 logarithmically transformed. All other

variables were treated as in Section 4.4.1.1. PLS regressions were also performed as discussed in Section 4.4.1.1, with the PLS regressions that exhibited the highest r2 values assessed for robustness.

Where linear measurements exhibited similar PLS results, tests were conducted to assess allometry between the two variables. RMA regressions were performed to assess this allometry, with the same approach and justification discussed in assessing Rensch's Rule (Section 4.4.1.4).

4.4.1.6 Tooth breakage

The frequency of tooth breakage with sex and age was assessed. Firstly, two split bar graphs, one of females and one of males, were produced from the data of specimens from Site 21.12 (Ngorongoro Conservation Area, Tanzania). This graph showed the number of individuals in each age class without broken teeth or partially or fully healed alveoli on one side, and on the other side showed the number of individuals with broken teeth, with (partially) healed alveoli, or with broken teeth and (partially) healed alveoli. The graph therefore illustrated whether there were relatively more individuals without broken or lost teeth in younger or older *C. crocuta*. The graph was repeated, combining data of males and females from all sites. It is acknowledged that there may have been some geographical variation in tooth breakage, however, the method was warranted in order to increase the sample size, particularly of the older age classes that were underrepresented in the data from Site 21.12.

The percentage of teeth of known condition were calculated for each age class of males and females separately from Site 21.12. The calculated percentages were of three categories: unbroken, broken, partially or fully healed alveoli. The percentage of teeth of known condition was chosen rather than the percentage of all teeth as some teeth were lost or broken *post-mortem* so the original condition was unknown. The percentages were plotted into a bar graph to assess the proportion of broken and (partially) healed alveoli in each age category.

Finally, differences in tooth breakage between males and females were assessed. The data were first split into age categories, and sites were included if there were data from both males and females of the same age within a site. Individual graphs were plotted for each age category, and comprised of two separate calculations. The first was the proportion of individuals with no broken teeth, broken teeth, (partially) healed alveoli, or broken teeth and (partially) healed alveoli. The second was the proportion of teeth of known condition: unbroken, broken or (partially) healed alveoli. These graphs were then repeated, but were further split into tooth types: incisors (I1-I3, i1-i3), canines (C, c), premolars (P1-P3, p2-p4) and carnassials (P4, m1). The

graphs were only produced for wear stages IV, V and VI due to insufficient data from the other age classes.

4.4.2 Pleistocene Crocuta crocuta

4.4.2.1 Body mass reconstruction

Body mass reconstruction of fossil individuals commonly involves regressing body mass against linear or area measurements of a skeletal or dental element from extant species, which produces an equation into which the equivalent fossil measurement can be inserted (Martin, 1990). For carnivores, skeletal elements have included: skull length, occiput-to-orbit length (Van Valkenburgh, 1990), measurements of post-cranial elements such as lengths, circumferences and cross-sectional areas (Anyonge, 1993), in addition to the head-body length (Van Valkenburgh, 1990).

An additional element that is commonly used to reconstruct carnivore body masses is the first lower molar (m1) area (Legendre and Roth, 1988) or length (Van Valkenburgh, 1990; Thackeray and Kieser, 1992; Flower, 2016). The theory behind this is that the m1 has low variability in form (Legendre and Roth, 1988), is well-developed in carnivores (Van Valkenburgh, 1990), is an important meat-slicing tooth (Van Valkenburgh, 1989), and thus varies predictably with body mass (Van Valkenburgh, 1990). The use of the m1 of *C. crocuta* also has a practical advantage of being generally well-preserved and abundant in the Pleistocene record.

Regression models using m1s to predict body masses have included: models with species from multiple carnivore families combined (Legendre and Roth, 1988; Van Valkenburgh, 1990; Thackeray and Kieser, 1992), models with species split into groups according to body size (Van Valkenburgh, 1990), and models of species from a single family (Legendre and Roth, 1988; Van Valkenburgh, 1990; Thackeray and Kieser, 1992; Flower, 2016). Models of species from individual families have a higher correlation coefficient (Legendre and Roth, 1988), or have a greater predictive ability (Van Valkenburgh, 1990), than models that combine species from many carnivore families. However, this interspecific approach is unsuitable for the Hyaenidae as the family has only four living species. Collinge (2001) recognised this, and used the following equation to reconstruct Pleistocene *C. crocuta* body masses using mean data instead:

Equation 4.16:

$$Pleistocene\ Mass = Modern\ Mass * (\frac{PM}{MM})^3$$

where MM is the mean measurement of a skeletal or dental element in modern specimens, and PM is the mean measurement of the same element in Pleistocene specimens. $Modern\ Mass$ is

the average mass of the modern species. However, this is again not ideal for *C. crocuta*, given that the recorded body masses of this species range widely from 35.83 kg to 80.06 kg (Table 5.23). The equation thus masks much of the geographic diversity in *C. crocuta* body size.

Given the unsuitability of both the interspecific approach and Collinge's (2001) equation for use in reconstructing Pleistocene *C crocuta* body masses, a new interspecific method is proposed here explicitly to address this issue. This method involves a collation of body masses and m1 lengths of *C. crocuta* from across a wider part of *C. crocuta*'s range in Africa (Table 4.4), thereby accounting for the first time more fully for natural variation.

All body mass and m1 length measurements were base-10 logarithmically transformed. Logarithmic transformation is a common statistical practice studies of body mass reconstruction (e.g. Legendre and Roth, 1988; Van Valkenburgh, 1990; Thackeray and Kieser, 1992). Although the data in the present study were already normally distributed, logarithmic transformation has other benefits such as reducing the influence of outliers. The transformation of values with different units of measurements also allows assessment of proportional change between the two variables (Smith, 1984).

There are many debates, summarised by Smith (2009), about the use of ordinary least squares (OLS) regression versus reduced major axis (RMA) regression. Generally, OLS assumes lack of error in the x-axis variable, and assumes that there is a causal relationship between the x- and y-axis variables. However, the error issue is not as important as the causal relationship, given that much of the error in this case is likely due to natural variation. Generally, OLS is advocated over RMA when the model is used for prediction, although extrapolated values should be used with caution (Smith, 2009). Moreover, most of the correction factors for detransformation bias (see below) have been formulated for least squares regression (Smith, 1993). In light of this, it was therefore deemed suitable to use OLS regression in the present study.

In order to assess the strength of the model, a number of statistical analyses were employed. As is standard, the p-value and r^2 values were assessed. However, the r^2 value is not necessarily a good indicator of the predictive ability of the model, due to the influence of the range of the x- and y- axis values, and the slope of the regression line (Smith, 1984). Therefore, the percent prediction error (%PE) was calculated, following Smith (1984) and Van Valkenburgh (1990):

Equation 4.17:

$$\%PE = \frac{y - ((antilog\ z) * CF)}{(antilog\ z) * CF} * 100$$

where y is the original untransformed y value, and z is the predicted y value, prior to detransformation. CF is the correction factor for detransformation bias (see below). All the individual %PE values are then averaged to produce a mean %PE value.

The percent standard error of the estimate (%SEE) values were also used to assess the model, following Brody (1945), cited in Smith (1984), Smith (1984) and Van Valkenburgh (1990):

Equation 4.18:

$$\%SEE = antilog(SEE + 2) - 100$$

where SEE is the standard error of the estimate, prior to detransformation. The lower the %PE and %SEE, the stronger the predictive ability of the model.

To assess whether there were any outlying data points, the residuals and leverage values (h_i) were considered. The leverage values indicate the distance of an x value to the mean x values. The leverage values were considered large if they exceeded a threshold, calculated with the equation (Helsel and Hirsch, 2002):

Equation 4.19:

$$h_i\ threshold = 3 * p/n$$

where p is the number of coefficients in the model, and n is the number of observations.

The residual values indicate outliers in the y direction. Standardised residuals with a value greater than 3 are extreme outliers, and those greater than 2 are considered outliers, following Helsel and Hirsch (2002).

Cook's Distance values (D_i) were also assessed. These values take into account the residuals and the leverage values, so they can indicate any influential points in both the x and y directions (Cook, 1977; Cook and Weisberg, 1980). Helsel and Hirsch (2002) suggested that D_i is considered influential if it is greater than the F statistic at 0.1 significance, with degrees of freedom at $p + 1$ and $n - p$, where n is the numer of observations, and p is the number of coefficients. Bollen and Jackman (1990, cited in Flower, 2016) proposed a threshold of $4/n$. The smaller of the two values will be used as the threshold.

The next step was to calculate the Pleistocene body mass values. The Pleistocene m1 length values were base-10 logarithmically transformed so that they could be entered into the OSL equation to calculate a corresponding body mass value.

In a model in which the x- and y-value axes have been log transformed, the predicted values suffer from detransformation bias. That is, statistical manipulation of logarithmically transformed values results in logarithmic values that are not equivalent to the arithmetic (detransformed) values. For example, the arithmetic mean of logarithmic values is actually the geometric mean when detransformed. Therefore, when a value of y is derived from a regression model with logarithmically transformed x- and y-axis values, detransformation of this value results in the geometric mean as the estimate of the y value. Correction factors must therefore be applied to the detransformed, predicted y values (Smith, 1993).

One correction factor is the quasi-maximum likelihood estimator (QMLE). For a regression in which the x- and y-axis values were base-10 logarithmically transformed, the equation follows Smith (1993):

Equation 4.20:

$$QMLE = antilog\ (RMS * 1.1513)$$

where RMS is the residual mean square (mean square error) prior to detransformation. The antilog taken here is the base-10 antilog (Smith, 1993).

A second correction factor is the smearing estimate (SE), which is the mean of the detransformed residuals (Duan, 1983; Smith, 1993):

Equation 4.21:

$$SE = \frac{1}{n}\sum(antilog\ r_i)$$

where r_i is the residual prior to detransformation.

A third correction factor is the ratio estimator (RE) (Snowdon, 1991, cited in Smith, 1993; Smith, 1993):

Equation 4.22:

$$RE = \frac{\bar{y}}{antilog\ \bar{z}}$$

where $\bar{y}$ is the mean of the observed y values prior to transformation, and $\bar{z}$ is the mean of the predicted y values prior to detransformation.

These correction factors are simply multiplied by the detransformed y value to produce the corrected y value (Smith, 1993), for example:

Equation 4.23:

$$Corrected\ y = QMLE * (antilog\ z)$$

where z is the predicted y value prior to detransformation. QMLE can be substituted for SE or RE.

As the correction factors potentially result in over-correction (Smith, 1993), all correction factors were calculated for the model and assessed for suitability.

Prediction intervals (PI) were calculated for each predicted Pleistocene body mass value. This is because the predicted value has uncertainties surrounding it (Smith, 1996). The following equation was used (Helsel and Hirsch, 2002):

Equation 4.24:

$$PI = t * SEE * \sqrt{1 + \left(\frac{1}{n}\right) + \frac{(x_0 - \bar{x})^2}{SSx}}$$

where t is the t-distribution value. In this study, the t-distribution value is for 95 % with degrees of freedom of n – 2. SEE is the standard error of the estimate. n is the sample size. x_0 is x-axis value used to predict a new y value. $\bar{x}$ is the mean value of the x values in the model. SSx is the sum of squares for the x-axis, calculated by (Helsel and Hirsch, 2002):

Equation 4.25:

$$SSx = \sum (x_i - \bar{x})^2$$

where x_i is the ith x value in the model.

The further the x value is from the mean x value, the greater the prediction interval (Helsel and Hirsch, 2002). The resulting prediction interval, once detransformed, was multiplied by the correction factor, as in Equation 8.

The body mass reconstructions are detailed in Spreadsheet 9.

4.4.2.2 Body mass variation

Predicted Pleistocene *C. crocuta* body masses and their corresponding prediction intervals were plotted to visually compare body masses between assemblages. An ANOVA with post-hoc Tukey's test was conducted on datasets with a sample size of ten or more, in order to determine any significant differences between assemblages. Prior to the test, Levene's test was conducted to check that the data conformed to the assumption of normal variance. Where datasets were

not normally distributed (indicated by Anderson Darling tests), Mann Whitney tests were also used to assess significant differences. It is acknowledged that the ANOVA and Mann Whitney tests were unable to take into account the prediction intervals of each data point.

Further analyses were undertaken on the body masses from Late Pleistocene British assemblages. Data were combined from all assemblages from MIS 5e, all assemblages from MIS 5c, and all assemblages from MIS 3. Tests were run to assess whether body masses from each marine oxygen isotope stage were significantly different to each other. In the case of normally distributed data, t-tests were performed. Mann Whitney tests were performed on non-normally distributed data.

Where possible, the body masses from MIS 3, British assemblages were also plotted in date order, according to direct dating of the specimens from the same assemblage. Assemblages with a broad range of dates such as Pin Hole (Figure 4.7) were excluded. Preferred dates were those derived from *C. crocuta* specimens, or bones of other species assumed to be gnawed by *C. crocuta*. The purpose of plotting the body masses chronologically was firstly to assess whether there was a consistent direction of body mass change over time. Secondly, the plot enabled an assessment of whether body masses changed subsequent to two potentially important events. The first of these events was the earliest arrival of modern humans in Britain, dated to 42,350−40,760 cal BP (Higham *et al.*, 2011c; Proctor *et al.*, 2017). The second event was the point after which interstadials became shorter and less frequent, around 36.5 b2k (years before A.D. 2000), as evidenced by the Greenland ice core $\delta^{18}O$ data (Andersen *et al.*, 2004; Rasmussen *et al.*, 2014; Seierstad *et al.*, 2014).

The influence of vegetation was assessed by colour coding the body mass data according to the dominant vegetation type in the vicinity of each site. The vegetation classifications were grassland, forested or mixed. Only those deposits from which vegetation was directly reconstructed were included (see Appendix 10.1, Table 10.1 and Table 10.2 for details and references).

C. crocuta body mass reconstructions were plotted against those from other predators and potential prey species to assess whether there was covariation in body mass between the species in Britain. The body mass data for *C. lupus*, derived from the m1, are from Flower (2016). The other species included are *P. leo* (*spelaea*)*, U. arctos,* Rhinocerotidae (both *S. hemitoechus* and *C. antiquitatis* plotted the in same graph)*, M. giganteus, R. tarandus, C. elaphus, C. capreolus, D. dama, E. ferus, B. primigenius* and *B. priscus*. These were all reconstructed using the post-crania (deemed to be the most accurate) by Collinge (2001).

The mean and standard deviations of the *C. crocuta* body mass reconstructions were used in the comparisons with Collinge's (2001) data. It is acknowledged that this means that the prediction intervals for *C. crocuta* body masses could not be included. The sample size was insufficient to run tests for significant correlation.

4.4.2.3 Morphometrics

The craniodental and post-cranial morphometric data were displayed in box and whisker plots and individual value plots to allow visual comparison of the data from each assemblage. Where there were fewer than four values, data were plotted in a table. This was also the case for the post-cranial indices.

For measurements with sample sizes greater than ten, statistical tests were conducted to assess significant differences between assemblages. ANOVA with post-hoc Tukey's tests were conducted on three or more datasets that were normally distributed and exhibited normal variance, as indicated by Anderson Darling and Levene's tests. In the case of non-normal variance but normal distributions, individual t-tests were conducted. Where data were not normally distributed, Mann Whitney tests were performed.

Data of mandibular bending strength and mechanical advantage of the masticatory muscle were displayed in line graphs. These graphs displayed the profiles of each mandible, and thus showed the bending strength of mechanical advantage values at each position along each mandible.

Where the significant difference tests indicated that the morphometrics exhibited different trends, allometric relationships were assessed. The reason for this was to understand whether some elements were relatively larger or smaller than others with overall size. To test for allometry, RMA regressions were performed, following the reasoning outlined in Section 4.4.1.4.

RMA regressions were also performed to assess the allometric relationships between the length and width of each premolar, e.g. P2 length and P2 width. The purpose of this was to assess whether the relationship between length and width of each premolar was constant with changes in tooth size. Hyperallometric or hypoallometric relationships between length and width may indicate a change in robustness with overall tooth size.

Premolar robustness was further investigated in *C. crocuta* from Britain. Scatterplots were made for each premolar with length and width on each axis, and data split into age (early Middle Pleistocene, MIS 9, later 7, 5e, 5c and 3). The purpose of constructing these graphs was to assess whether premolars were more or less robust through time.

4.4.2.4 Age profiles of assemblages

Prior to assessing tooth breakage, the age profiles of each assemblage were assessed in order to determine whether there was a dominance of young or old individuals, or a relatively even split of age classes. The percentage of P3s and p3s within each wear stage (III to IX) was calculated for each assemblage and plotted into a bar graph. For assemblages with fewer than ten P3/p3 data points, the wear stage of all teeth were used to calculate the percentage of teeth that exhibited the following wear: slight, slight/medium, medium, medium/heavy, heavy. Unworn teeth were excluded in case they had not been fully erupted from the jaw.

4.4.2.5 Tooth breakage

The percentage of teeth of known condition that were broken or had (partially) healed alveoli was calculated for each assemblage with a sample size of at least ten. This was firstly conducted for all teeth combined, then split into individual tooth types (incisors, canines, premolars and carnassials). These percentages were then plotted in bar graphs to allow visual comparison of the percentages of broken and (partially) healed alveoli between assemblages.

All the aforementioned statistical analyses were performed in Microsoft Excel, Minitab® Statistical Software 17.3.1, Minitab® Statistical Software 18.1 and PAST 3.12 (Hammer *et al.*, 2001).

4.4.3 Extirpation of Crocuta crocuta from Europe

Radiocarbon dates of *C. crocuta*, *P. leo* (*spelaea*), *C. antiquitatis*, *C. elaphus* and *R. tarandus* were used in five models to assess the chronology of these species in Europe during the Late Pleistocene. Additionally, the models were used to determine the timing of the extirpation of *C. crocuta* from Europe (excluding Russia). For *P. leo* (*spelaea*) and *C. antiquitatis* the models were used to determine the end date of each species' occupation of areas that *C. crocuta* also inhabited.

The models were produced using OxCal 4.3 (Bronk Ramsey, 2009). For *C. crocuta*, *P. leo* (*spelaea*) and *C. antiquitatis*, dates from each region were input using overlapping phases in the model, which created end boundaries for each region (following Blockley and Pinhasi, 2011).

As *C. elaphus* and *R. tarandus* still live in Europe today, it was not appropriate to create end dates for these species. Therefore, the dates of these species were split into their appropriate regions using phases without boundaries.

The R_combine function in OxCal was used to combine either repeated radiocarbon dates on the same specimen, or radiocarbon dates on multiple bones from the same individual (such as in the case of an articulated skeleton). The calibration curve used for all models was IntCal13 (Reimer *et al.*, 2013). The modelled, calibrated dates were plotted against the NGRIP ice core $\delta^{18}O$ record (Andersen *et al.*, 2004).

5 Modern *Crocuta crocuta*

5.1 Population biomass

5.1.1 Introduction

C. crocuta is one of the most abundant large predators in Africa. Records of *C. crocuta* population biomass range from 0.47 kg/km^2 in the Kalahari Gemsbok National Park, South Africa, to 76.93 kg/km^2 in the Ngorongoro Crater, Tanzania (Hatton *et al.* 2015, and references therein). As explored in Section 2.3.2, there have been localised studies upon some aspects of *C. crocuta* population dynamics. However, few studies have focussed upon larger scale geographic patterns, environmental correlates and population variation of this species in relation to their major competitor, *P. leo*. The habitats of the two species overlap considerably, with 94.5 % of *P. leo*'s range overlapping with that of *C. crocuta* (Périquet *et al.*, 2015). Despite this and the fact that the two species frequently compete for food (Section 2.3.3), the densities of both species are often correlated (Périquet *et al.*, 2015). An analysis of the available data on *C. crocuta* populations in the literature is thus justified to shed further light on the effect of the environment and possible competition on this species' population ecology.

An understanding of the influences upon *C. crocuta* biomass may provide insights into potentially larger scale changes in size observed across the Pleistocene, particularly regarding its ultimate extirpation from Europe.

The research questions posed are threefold:

- How far are *C. crocuta* and *P. leo* abundances mediated by competition with each other, and other large predators?
- Do other environmental variables influence *C. crocuta* and *P. leo* abundance?
- Is there evidence of environmental partitioning between *C. crocuta* and *P. leo*?

5.1.2 Results

5.1.2.1 African predator biomasses

As illustrated in Figure 5.1, alongside *P. leo*, *C. crocuta* is frequently the most abundant predator in the African sites, and both predators occur at the highest population biomass. Despite this, the Kolmogorov-Smirnov tests (Table 5.1) indicate that the biomass distributions of *P. leo* and *C. crocuta* are significantly different, although the lower test statistic indicates that the

distributions are more similar than when compared with any other species. *P. pardus* and *A. jubatus* are intermediate, frequently occurring at lower biomasses. *P. brunnea* and *L. pictus* occur most infrequently and at the lowest biomasses. Differences between the species are also shown in Figure 5.2, which shows the relative proportions of each predator in each site, in terms of their biomass. The sites with the greatest proportion of *C. crocuta* are Amboseli National Park in Kenya with *C. crocuta* making up 79.14 % of the total predator biomass, and the Ngorongoro Crater in Tanzania, from the year 1965, with 76.89 %. Together, *C. crocuta* and *P. leo* make up the largest proportion of predator biomass in most sites. A notable site with smaller biomasses of *C. crocuta* and *P. leo* is the Kalahari National Park in South Africa where *P. pardus*, *A. jubatus* and *P. brunnea* together make up 36.22 % of the predator biomass.

There is some evidence of temporal change in the relative abundance of each species, most notable in the Ngorongoro Crater, and in the Serengeti, Tanzania. The raw biomass values for both species are presented in Table 5.2. In the Ngorongoro Crater, both species show biomass decreases in the years 1988 and 1997. Additionally, the earliest record of *P. leo* biomass, from 1965, is the lowest of all years. In the Serengeti, Table 5.2 illustrates that the change in proportion between the two species is primarily driven by an increase in *C. crocuta* biomass.

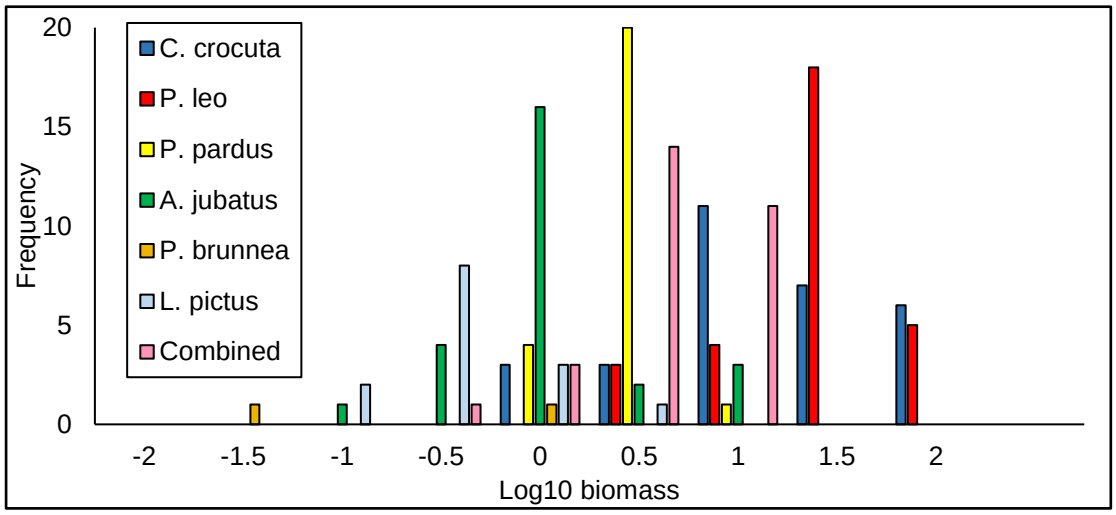

Figure 5.1: Histogram of base-10 logarithmically transformed biomass (originally in kg/km^2) of the large African predators across 30 datasets . 'Combined' is the combined biomass of *P. pardus*, *A. jubatus*, *P. brunnea* and *L. pictus*.

Table 5.1: Results of Kolmogorov-Smirnov tests of distribution similarity for the biomass data across 30 datasets. 'Combined' is the combined biomass of *P. pardus*, *A. jubatus*, *P. brunnea* and *L. pictus*. The top figure in each box is the test statistic, and the bottom figure is the p-value. Where the p-value is stated as '<0.05', the value was so low that a meaningful reading was not given. All tests are therefore significant at 95 % confidence.

	C. crocuta	***P. leo***	***P. pardus***	***A. jubatus***	***L. pictus***	**Combined**
C. crocuta		0.367 0.025	0.767 <0.05	0.733 <0.05	0.929 <0.05	0.663 <0.05
P. leo			0.893 <0.05	0.83 <0.05	0.967 <0.05	0.8 <0.05
P. pardus				0.655 <0.05	0.889 <0.05	
A. jubatus					0.706 <0.05	
L. pictus						
Combined						

Table 5.2: Biomass values for *C. crocuta* and *P. leo* in the Ngorongoro Crater and the Serengeti ecosystem, from Hatton *et al.* (2015) and references therein. The figures illustrate temporal changes in biomass. Note that the years are those stated by Hatton *et al.* (2015), and may not be exact as some datasets are comprised of data from a number of years.

Site	**Year**	***C. crocuta* biomass (kg/km^2)**	***P. leo* biomass (kg/km^2)**
Ngorongoro Crater	1965	60.577	14.538
Ngorongoro Crater	1978	62.515	45.165
Ngorongoro Crater	1988	45.962	43.941
Ngorongoro Crater	1997	34.323	26.155
Ngorongoro Crater	2004	76.923	29.077
Serengeti ecosystem	1971	6	12.096
Serengeti ecosystem	1977	8.586	11.501
Serengeti ecosystem	1986	10.322	11.768
Serengeti ecosystem	2003	16.4	15.12

Figure 5.2: Proportions of large predator biomasses within each African site.

5.1.2.2 *Crocuta crocuta* population biomass

Partial least squares (PLS) regressions were performed in order to address the research questions. These are summarised in Table 5.3. PLS 1 assessed influences upon *C. crocuta* biomass and is significant with a p-value of <0.05 and an r^2 value of 0.837. The plot of the residuals versus the order of sites (Figure 5.3) was assessed. This shows that there are some clusters of observations that have residuals increasing or decreasing together, rather than fluctuating. This may mean that the results are influenced by the order in which the sites are entered into the PLS. In order to assess this, four further PLS regressions were run (PLS 1b – e), with the sites entered in random orders. The resulting standardised coefficients (Table 5.4) are the same for each PLS run, indicating that the site order does not affect the results.

Table 5.3: Details of the Partial Least Squares Regressions run on *C. crocuta* and *P. leo* biomass.

PLS regression	**Dependent variable**	**p-value**	**r^2 value**
PLS 1	*C. crocuta* biomass	<0.05	0.837
PLS 2	*C. crocuta* biomass (without Kalahari)	<0.05	0.957
PLS 3	*P. leo* biomass	<0.05	0.608
PLS 4	*P. leo* biomass (without Kalahari)	<0.05	0.967

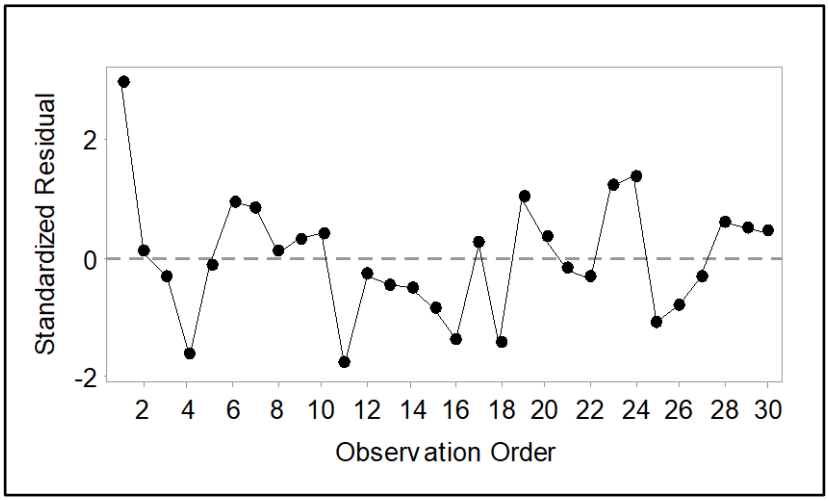

Figure 5.3: The observation order (the order in which the sites were input to PLS 1), against the standardised residuals.

Table 5.4: The standardised coefficients for each PLS 1 model run (PLS 1a-1e), with sites input to the model in random orders.

Variable	Standardised coefficient
***P. leo* biomass**	0.13
Other predator biomass	0.109
Very small prey biomass	0.175
Small prey biomass	0.146
Medium prey biomass	0.24
Large prey biomass	0.093
Very large prey biomass	0.025
Min. temperature of coolest month	0.009
Max. temperature of warmest month	-0.108
Temperature seasonality	-0.003
Precipitation of driest month	0.053
Precipitation of wettest month	0.093
Precipitation seasonality	0.019
Closed vegetation cover	0.075
Semi-open vegetation cover	0.034
Open vegetation cover	-0.092

The plot of standardised residuals against leverages (Figure 5.4) was assessed for outliers and leverage points. Points were classed as outliers if the residuals had a value greater or less than two. Only one site is an outlier: Amboseli National Park, Kenya. In the case of PLS 1, the LRL value (see Section 4.4.1.1) is 0.133. Four sites fall just beyond the LRL. A fifth site, Kalahari Gemsbok National Park in South Africa, has an extreme leverage value of 0.685. As leverage points may have a strong influence upon the coefficients, the PLS was run again without Kalahari Gemsbok National Park.

The new PLS (PLS 2) with *C. crocuta* biomass as the dependent variable is again significant with a p-value of < 0.05 and a greater r^2 value of 0.957. Analysis of the chart of standardised residuals versus leverages for PLS 2 (Figure 5.5) reveals that Nairobi National Park (Kenya from 2002) and the Serengeti ecosystem (Tanzania from 2003) are both outliers, although they do not fall far beyond the outlier reference line. Five sites are classed as leverage points: Amboseli National Park in Kenya, Hwange National Park in Zimbabwe, Lake Manyara National Park in Tanzania, Nairobi National Park in Kenya from 1966, and Queen Elizabeth National Park in Uganda. However, with leverage values ranging from 0.572 to 0.69, these sites are not far beyond the LRL value of 0.552.

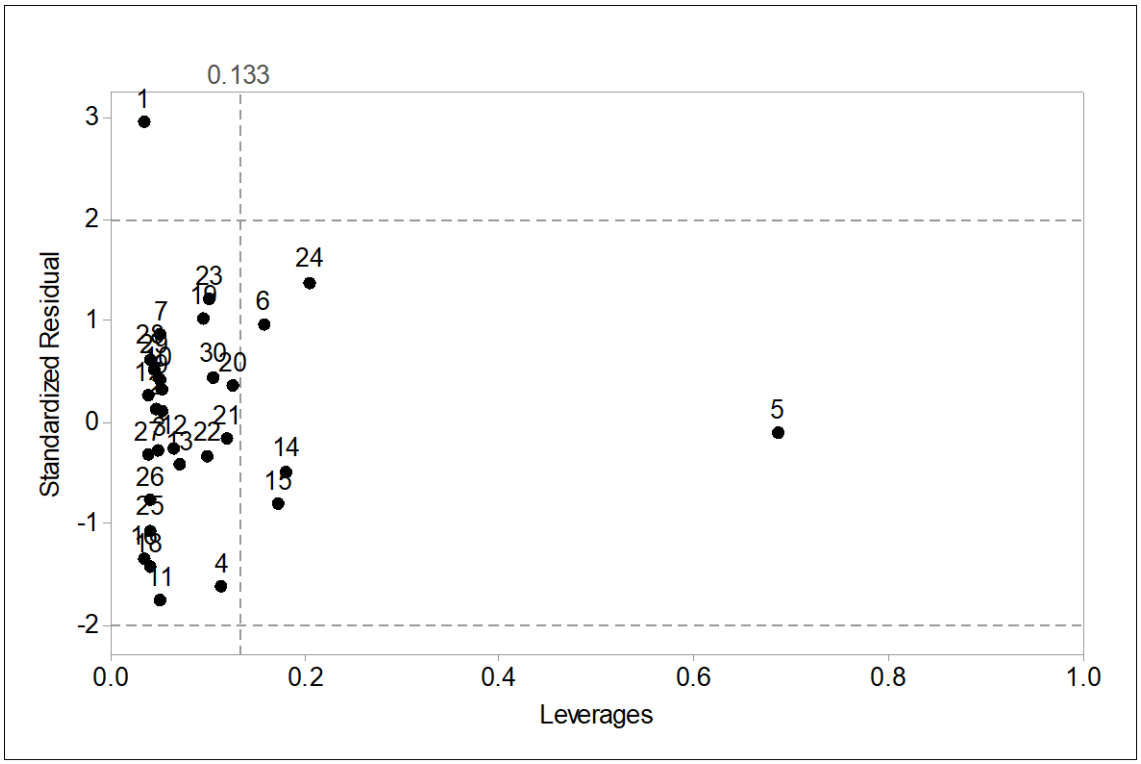

Figure 5.4: Standardised residuals against leverage values for each site in PLS 1, with *C. crocuta* biomass as the dependent variable. The horizontal lines indicate the outlier boundaries. The vertical line represents the leverage reference line boundary. The numbers on the points correspond to sites as follows: 1. Amboseli National Park, 2007, 2. Hluhluwe iMfolozi National Park, 1982, 3. Hluhluwe iMfolozi National Park, 2000, 4. Hwange National Park, 1973, 5. Kalahari Gemsbok National Park, 1979, 6. Kidepo Valley National Park, 2009, 7. Kruger National Park, 1975, 8. Kruger National Park, 1984, 9. Kruger National Park, 1997, 10. Kruger National Park, 2009, 11. Lake Manyara National Park, 1970, 12. Maasai Mara National Reserve, 1992. 13. Maasai Mara National Reserve, 2003, 14. Mkomazi Game Reserve, 1970 (dry), 15. Mkomazi Game Reserve, 1970 (wet), 16. Nairobi National Park, 1966, 17. Nairobi National Park, 1976, 18. Nairobi National Park, 2002, 19. Ngorongoro Crater, 1965, 20. Ngorongoro Crater, 1978, 21. Ngorongoro Crater, 1988, 22. Ngorongoro Crater, 1997, 23. Ngorongoro Crater, 2004, 24. Queen Elizabeth National Park, 2009, 25. Serengeti ecosystem, 1971, 26. Serengeti ecosystem, 1977, 27. Serengeti ecosystem, 1986, 28. Serengeti ecosystem, 2003, 29. Tarangire National Park, 1962 (dry), 30. Tarangire National Park, 1962 (wet).

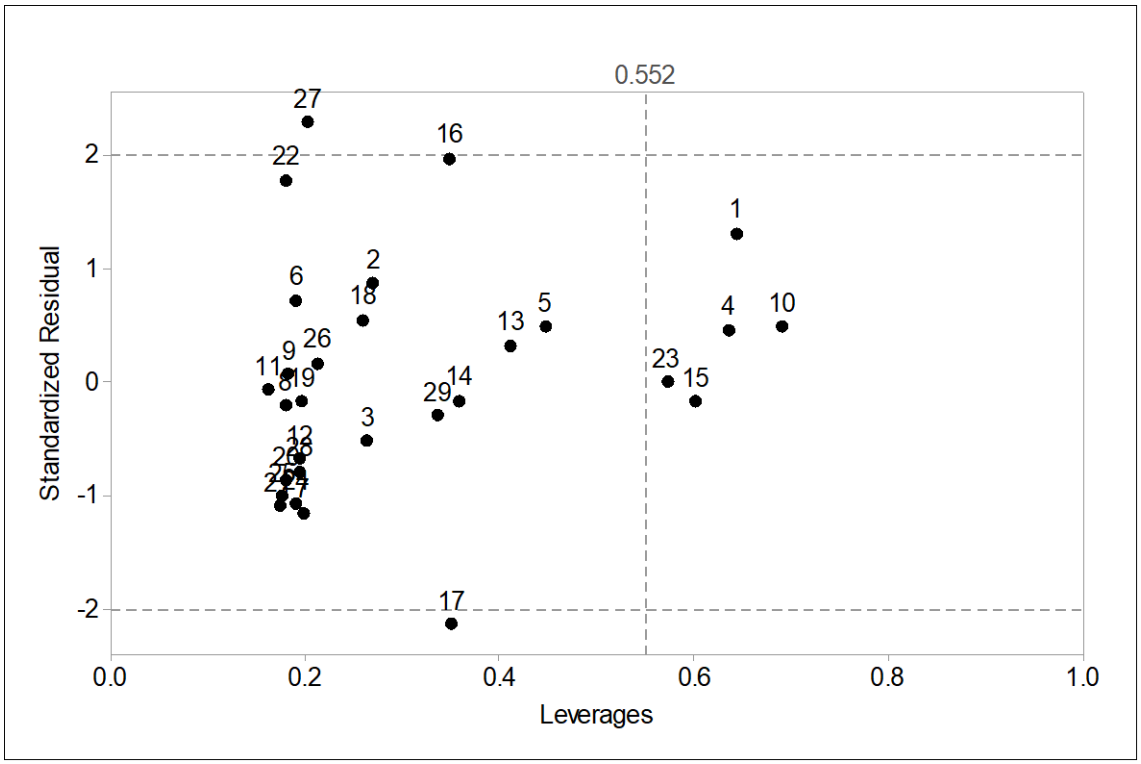

Figure 5.5: Standardised residuals against leverage values for each site in PLS 2, with *C. crocuta* biomass as the dependent variable. The horizontal lines indicate the outlier boundaries. The vertical line represents the leverage reference line boundary. The numbers on the points correspond to sites as follows: 1. Amboseli National Park, 2007, 2. Hluhluwe iMfolozi National Park, 1982, 3. Hluhluwe iMfolozi National Park, 2000, 4. Hwange National Park, 1973, 5. Kidepo Valley National Park, 2009, 6. Kruger National Park, 1975, 7. Kruger National Park, 1984, 8. Kruger National Park, 1997, 9. Kruger National Park, 2009, 10. Lake Manyara National Park, 1970, 11. Maasai Mara National Reserve, 1992. 12. Maasai Mara National Reserve, 2003, 13. Mkomazi Game Reserve, 1970 (dry), 14. Mkomazi Game Reserve, 1970 (wet), 15. Nairobi National Park, 1966, 16. Nairobi National Park, 1976, 17. Nairobi National Park, 2002, 18. Ngorongoro Crater, 1965, 19. Ngorongoro Crater, 1978, 20. Ngorongoro Crater, 1988, 21. Ngorongoro Crater, 1997, 22. Ngorongoro Crater, 2004, 23. Queen Elizabeth National Park, 2009, 24. Serengeti ecosystem, 1971, 25. Serengeti ecosystem, 1977, 26. Serengeti ecosystem, 1986, 27. Serengeti ecosystem, 2003, 28. Tarangire National Park, 1962 (dry), 29. Tarangire National Park, 1962 (wet).

The standardised coefficients of the PLS 2 (Figure 5.6) show some differences when compared to PLS 1. Notably, minimum temperature of the coolest month and semi-open vegetation cover are more important in PLS 2. PLS 1 shows that *P. leo* biomass, other predator biomass, and precipitation of the wettest month have positive influences upon *C. crocuta* biomass. However, removal of the Kalahari suggests that these three variables have only a small, negative influence.

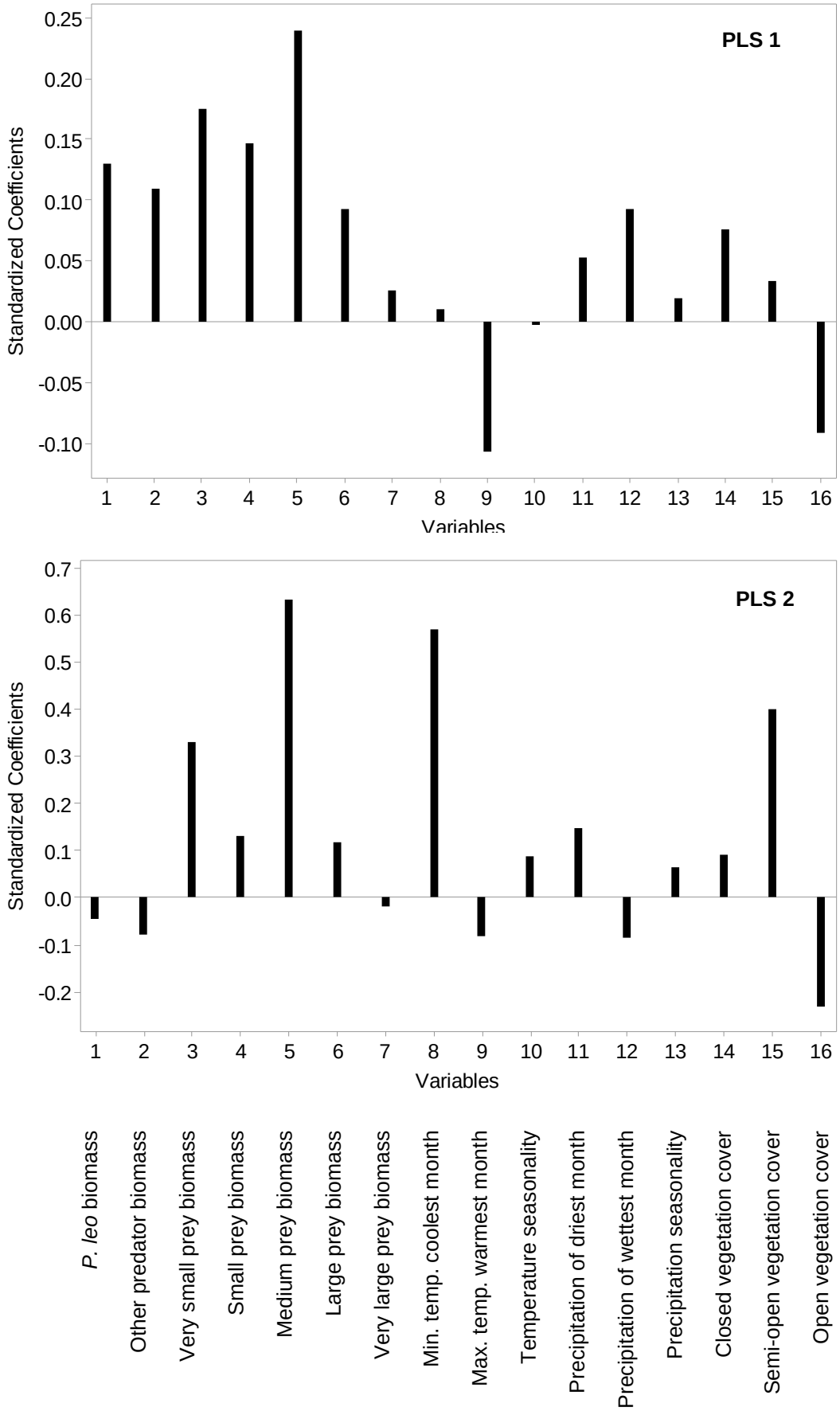

Figure 5.6: Standardised coefficients from PLS 1 (with Kalahari) and PLS 2 (without Kalahari) with *C. crocuta* biomass as the dependent variable.

Table 5.5: r^2 values and p-values of repeated runs of PLS 2, with *C. crocuta* biomass as the dependent variable. Each run removed one site at a time.

Run no.	Removed site	r^2 value	p-value
1	Amboseli National Park, Kenya, 2007	0.961	<0.05
2	Hluhluwe iMfolozi National Park, South Africa, 1982	0.96	<0.05
3	Hluhluwe iMfolozi National Park, South Africa, 2000	0.958	<0.05
4	Hwange National Park, Zimbabwe, 1973	0.951	<0.05
5	Kidepo Valley National Park, Uganda, 2009	0.961	<0.05
6	Kruger National Park, South Africa, 1975	0.958	<0.05
7	Kruger National Park, South Africa, 1984	0.96	<0.05
8	Kruger National Park, South Africa, 1997	0.957	<0.05
9	Kruger National Park, South Africa, 2009	0.957	<0.05
10	Lake Manyara National Park, Tanzania, 1970	0.955	<0.05
11	Maasai Mara National Reserve, Kenya, 1992	0.956	<0.05
12	Maasai Mara National Reserve, Kenya, 2003	0.956	<0.05
13	Mkomazi Game Reserve, Tanzania, 1970 (dry)	0.95	<0.05
14	Mkomazi Game Reserve, Tanzania, 1970 (wet)	0.95	<0.05
15	Nairobi National Park, Kenya, 1966	0.959	<0.05
16	Nairobi National Park, Kenya, 1976	0.968	<0.05
17	Nairobi National Park, Kenya, 2002	0.967	<0.05
18	Ngorongoro Crater, Tanzania, 1965	0.954	<0.05
19	Ngorongoro Crater, Tanzania, 1978	0.953	<0.05
20	Ngorongoro Crater, Tanzania, 1988	0.956	<0.05
21	Ngorongoro Crater, Tanzania, 1997	0.959	<0.05
22	Ngorongoro Crater, Tanzania, 2004	0.958	<0.05
23	Queen Elizabeth National Park, Uganda, 2009	0.957	<0.05
24	Serengeti ecosystem, Tanzania, 1971	0.959	<0.05
25	Serengeti ecosystem, Tanzania, 1977	0.96	<0.05
26	Serengeti ecosystem, Tanzania, 1986	0.957	<0.05
27	Serengeti ecosystem, Tanzania, 2003	0.969	<0.05
28	Tarangire National Park, Tanzania, 1962 (dry)	0.96	<0.05
29	Tarangire National Park, Tanzania, 1962 (wet)	0.954	<0.05

In order to assess the validity of the results, PLS 2 was re-run 29 times, removing one site each time. All runs were significant with p-values of <0.05. The r^2 values ranged from 0.95 to 0.969 (Table 5.5), indicating that most of the variation in *C. crocuta* biomass was explained by each PLS run, regardless of the site that was removed. The confidence intervals of the standardised coefficients are low, ranging from 0.008 for closed vegetation cover, to 0.021 for minimum temperature of the coolest month (Table 5.6) This indicates that confidence can be placed in the results, as no one site alters the results. This can also be seen in the plot of the standardised coefficients for each run (Figure 5.7). The coefficients of some variables (*P. leo* and other predator biomasses, large and very large prey biomasses, precipitation seasonality) cluster around zero, suggesting that these hold little importance in explaining the variation in *C. crocuta*

biomass. However, other variables consistently plot far from zero, indicating importance in explaining *C. crocuta* biomass variation. These include very small prey biomass and semi-open vegetation on the positive side, and open vegetation on the negative side. The largest standardised coefficients are medium prey biomass and minimum temperature of the coolest month, both of which are positively associated with *C. crocuta* biomass. This pattern reflects that seen in the original PLS 2 (Figure 5.6).

Table 5.6: Standardised coefficient means and confidence intervals (CI) for repeated runs of PLS 2, with *C. crocuta* biomass as the dependent variable.

Independent variable	Standardised coefficient mean	Standardised coefficient CI	Standardised coefficient minimum CI	Standardised coefficient maximum CI
***P. leo* biomass**	-0.035	0.011	-0.047	-0.024
Other predator biomass	-0.065	0.014	-0.079	-0.050
Total biomass very small prey	0.306	0.019	0.287	0.325
Total biomass small prey	0.136	0.018	0.118	0.154
Total biomass medium prey	0.635	0.011	0.624	0.647
Total biomass large prey	0.111	0.013	0.098	0.124
Total biomass very large prey	-0.012	0.011	-0.023	-0.001
Minimum temperature coolest month	0.577	0.021	0.555	0.598
Maximum temperature warmest month	-0.096	0.015	-0.111	-0.081
Temperature seasonality	0.082	0.009	0.074	0.091
Precipitation driest month	0.136	0.012	0.123	0.148
Precipitation wettest month	-0.102	0.019	-0.121	-0.084
Precipitation seasonality	0.073	0.016	0.058	0.089
Closed vegetation	0.094	0.008	0.087	0.102
Semi-open vegetation	0.395	0.012	0.383	0.406
Open vegetation	-0.234	0.009	-0.243	-0.225

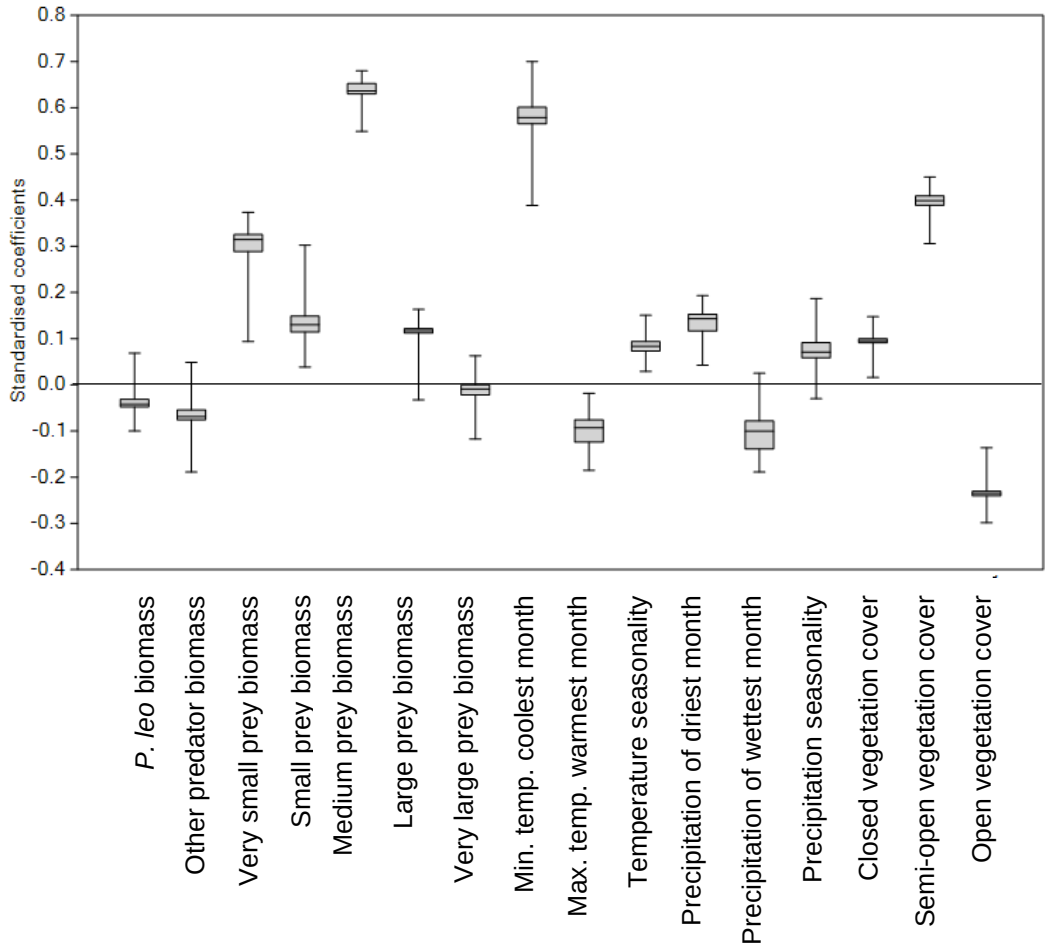

Figure 5.7: Standardised coefficients from repeated runs of PLS 2, with *C. crocuta* biomass as the dependent variable.

5.1.2.3 *Panthera leo* population biomass

A further PLS regression (PLS 3) was performed with *P. leo* biomass as the dependent variable. This was in order to determine any differences in the influences upon the biomasses of *P. leo* compared with *C. crocuta*. PLS 3 is significant with a p-value of <0.05, although the r^2 value is only 0.608. Only one site shows as an outlier in Figure 5.8: Tarangire National Park, wet season. The LRL value is 0.067 and a number of sites fall beyond this line. Only Kalahari Gemsbok National Park has an extreme leverage value (0.471), warranting a re-run of the PLS.

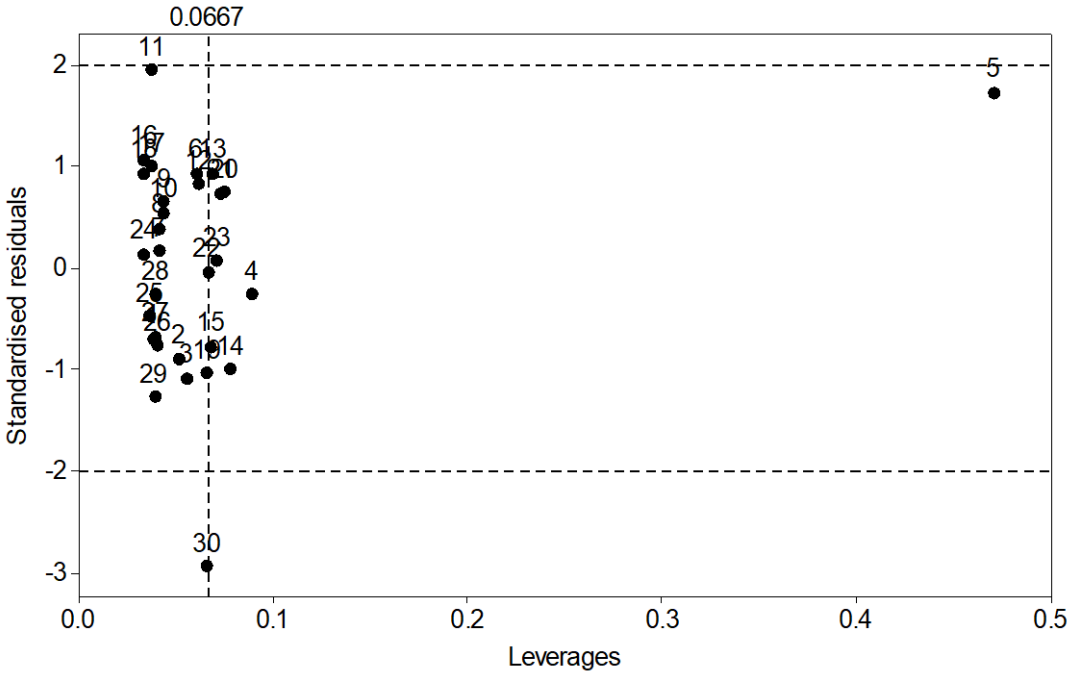

Figure 5.8: Standardised residuals against leverage values for each site in PLS 3, with *P. leo* biomass as the dependent variable. The horizontal lines indicate the outlier boundaries. The vertical line represents the leverage reference line boundary. The numbers on the points correspond to sites as follows: 1. Amboseli National Park, 2007, 2. Hluhluwe iMfolozi National Park, 1982, 3. Hluhluwe iMfolozi National Park, 2000, 4. Hwange National Park, 1973, 5. Kalahari Gemsbok National Park, 1979, 6. Kidepo Valley National Park, 2009, 7. Kruger National Park, 1975, 8. Kruger National Park, 1984, 9. Kruger National Park, 1997, 10. Kruger National Park, 2009, 11. Lake Manyara National Park, 1970, 12. Maasai Mara National Reserve, 1992. 13. Maasai Mara National Reserve, 2003, 14. Mkomazi Game Reserve, 1970 (dry), 15. Mkomazi Game Reserve, 1970 (wet), 16. Nairobi National Park, 1966, 17. Nairobi National Park, 1976, 18. Nairobi National Park, 2002, 19. Ngorongoro Crater, 1965, 20. Ngorongoro Crater, 1978, 21. Ngorongoro Crater, 1988, 22. Ngorongoro Crater, 1997, 23. Ngorongoro Crater, 2004, 24. Queen Elizabeth National Park, 2009, 25. Serengeti ecosystem, 1971, 26. Serengeti ecosystem, 1977, 27. Serengeti ecosystem, 1986, 28. Serengeti ecosystem, 2003, 29. Tarangire National Park, 1962 (dry), 30. Tarangire National Park, 1962 (wet).

The PLS of *P. leo* biomass without Kalahari National Park (PLS 4) is again significant with a p-value of <0.05. The r^2 value greater at 0.967. Nairobi National Park (Kenya from 1966) and Ngorongoro Crater (Tanzania from 1965) were identified as outliers, although they do not fall far beyond the boundaries in Figure 5.9. Furthermore, five sites were identified as leverage points. However, with values ranging from 0.833 to 0.937, and relative to the LRL of 0.828, they are not extreme values.

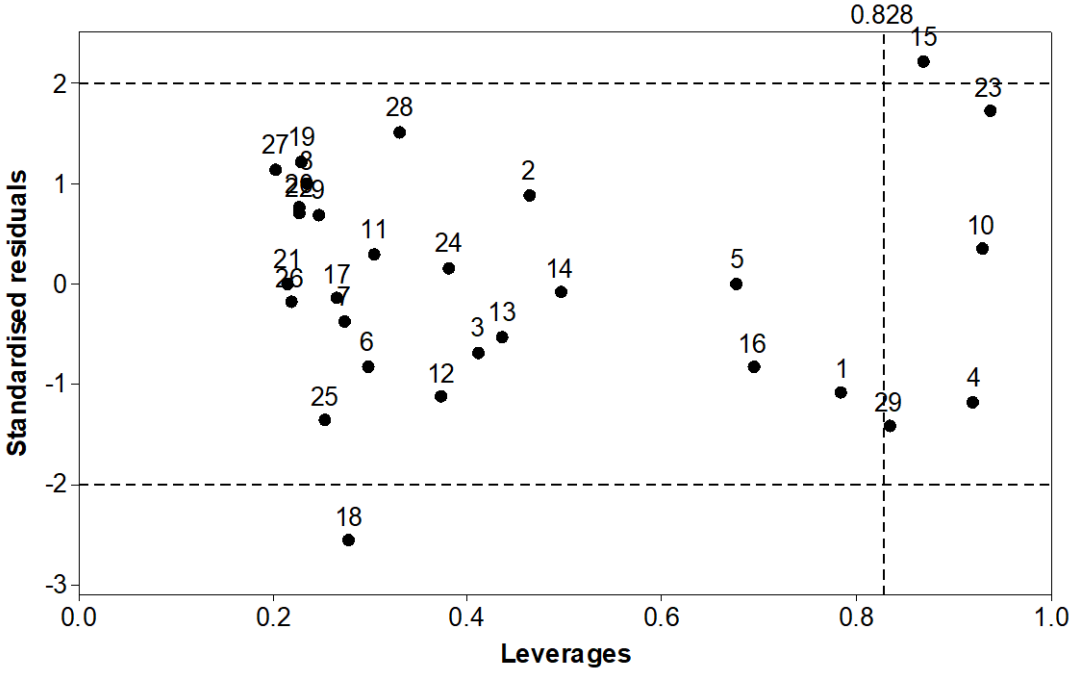

Figure 5.9: Standardised residuals against leverage values for each site in PLS 4, with *P. leo* biomass as the dependent variable. The horizontal lines indicate the outlier boundaries. The vertical line represents the leverage reference line boundary. The numbers on the points correspond to sites as follows: 1. Amboseli National Park, 2007, 2. Hluhluwe iMfolozi National Park, 1982, 3. Hluhluwe iMfolozi National Park, 2000, 4. Hwange National Park, 1973, 5. Kidepo Valley National Park, 2009, 6. Kruger National Park, 1975, 7. Kruger National Park, 1984, 8. Kruger National Park, 1997, 9. Kruger National Park, 2009, 10. Lake Manyara National Park, 1970, 11. Maasai Mara National Reserve, 1992. 12. Maasai Mara National Reserve, 2003, 13. Mkomazi Game Reserve, 1970 (dry), 14. Mkomazi Game Reserve, 1970 (wet), 15. Nairobi National Park, 1966, 16. Nairobi National Park, 1976, 17. Nairobi National Park, 2002, 18. Ngorongoro Crater, 1965, 19. Ngorongoro Crater, 1978, 20. Ngorongoro Crater, 1988, 21. Ngorongoro Crater, 1997, 22. Ngorongoro Crater, 2004, 23. Queen Elizabeth National Park, 2009, 24. Serengeti ecosystem, 1971, 25. Serengeti ecosystem, 1977, 26. Serengeti ecosystem, 1986, 27. Serengeti ecosystem, 2003, 28. Tarangire National Park, 1962 (dry), 29. Tarangire National Park, 1962 (wet).

Comparison of the standardised coefficients from the two PLS runs indicates that removal of the Kalahari National Park has resulted in large changes in the magnitude of the relationship between many of the variables and *P. leo* biomass (Figure 5.10). In PLS 4, the strongest positive associations with *P. leo* biomass are very small prey biomass and the maximum temperature of the warmest month, followed by precipitation seasonality. The main negative associations are temperature seasonality and semi-open vegetation cover, followed by precipitation of the wettest month and the minimum temperature of the coolest month.

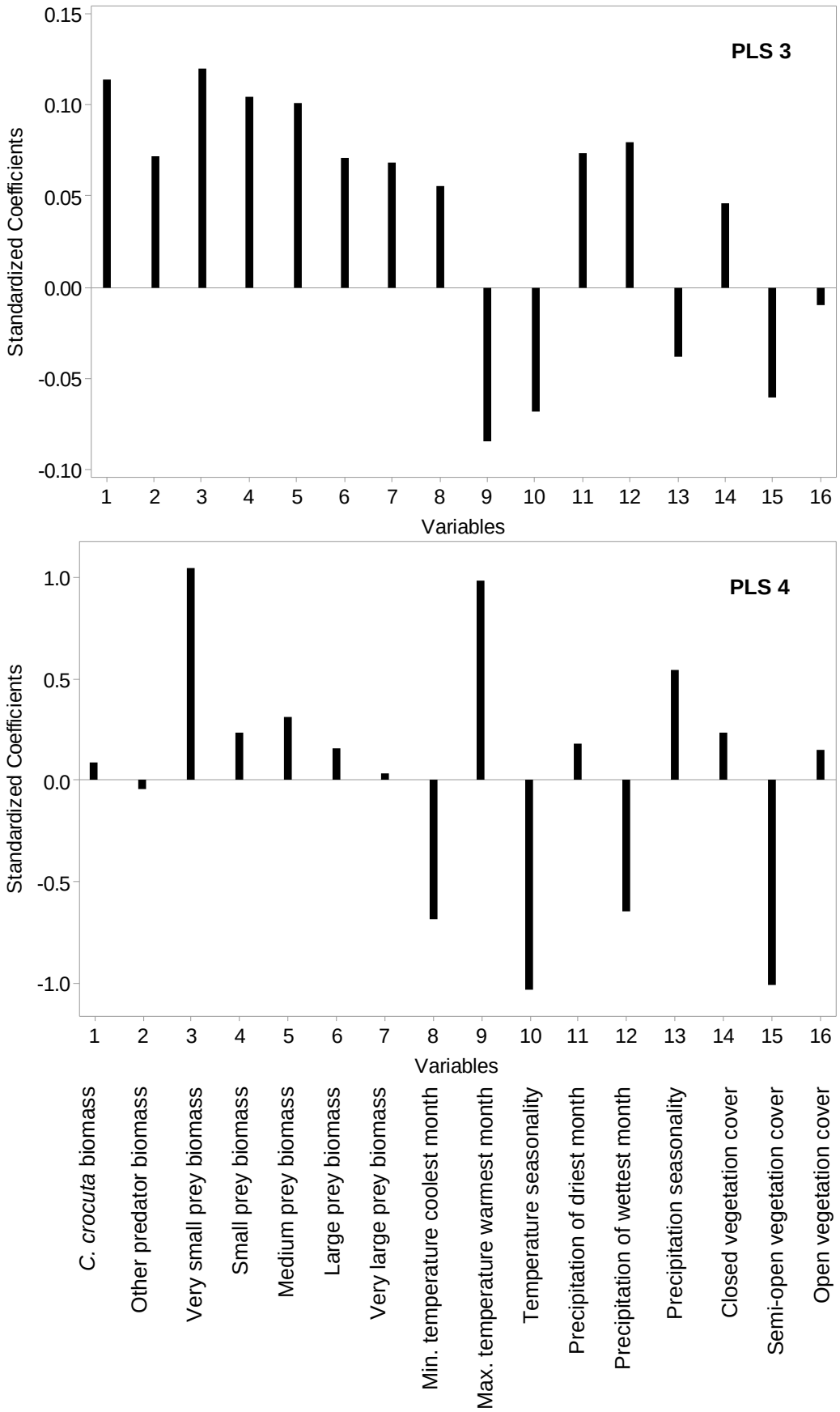

Figure 5.10: Standardised coefficients from PLS 3 and PLS 4 with *P. leo* biomass as the dependent variable.

PLS 4 with *P. leo* biomass as the dependent variable was re-run 29 times, removing one site each time. Unlike the repeated *C. crocuta* PLS, the results for PLS 4 indicate that there was considerable variation in the results when some sites were removed. The p-values are <0.05 for each run, indicating that the regressions are significant. However, the r^2 values range from 0.983 to 0.555 (Table 5.7), indicating that there is much variation in *P. leo* biomass that is unexplained by the variables. The PLS regressions without the following sites have the lowest r^2 values: Kidepo Valley National Park, Lake Manyara National Park, Mkomazi Game Reserve (dry), Mkomazi Game Reserve (wet), Nairobi National Park (1976), Nairobi National Park (2002), Serengeti ecosystem (1971), Serengeti ecosystem (2003). Of these, only Lake Manyara was originally identified as a leverage point for PLS 4 (Figure 5.9).

Table 5.7: r^2 values and p-values of repeated runs of PLS 4, with *P. leo* biomass as the dependent variable. Each run removed one site at a time.

Run no.	Removed site	r^2 value	p-value
1	Amboseli National Park, Kenya, 2007	0.971	<0.05
2	Hluhluwe iMfolozi National Park, South Africa, 1982	0.969	<0.05
3	Hluhluwe iMfolozi National Park, South Africa, 2000	0.968	<0.05
4	Hwange National Park, Zimbabwe, 1973	0.969	<0.05
5	Kidepo Valley National Park, Uganda, 2009	0.631	<0.05
6	Kruger National Park, South Africa, 1975	0.969	<0.05
7	Kruger National Park, South Africa, 1984	0.968	<0.05
8	Kruger National Park, South Africa, 1997	0.967	<0.05
9	Kruger National Park, South Africa, 2009	0.969	<0.05
10	Lake Manyara National Park, Tanzania, 1970	0.639	<0.05
11	Maasai Mara National Reserve, Kenya, 1992	0.966	<0.05
12	Maasai Mara National Reserve, Kenya, 2003	0.968	<0.05
13	Mkomazi Game Reserve, Tanzania, 1970 (dry)	0.555	<0.05
14	Mkomazi Game Reserve, Tanzania, 1970 (wet)	0.574	<0.05
15	Nairobi National Park, Kenya, 1966	0.979	<0.05
16	Nairobi National Park, Kenya, 1976	0.605	<0.05
17	Nairobi National Park, Kenya, 2002	0.608	<0.05
18	Ngorongoro Crater, Tanzania, 1965	0.983	<0.05
19	Ngorongoro Crater, Tanzania, 1978	0.967	<0.05
20	Ngorongoro Crater, Tanzania, 1988	0.964	<0.05
21	Ngorongoro Crater, Tanzania, 1997	0.967	<0.05
22	Ngorongoro Crater, Tanzania, 2004	0.966	<0.05
23	Queen Elizabeth National Park, Uganda, 2009	0.977	<0.05
24	Serengeti ecosystem, Tanzania, 1971	0.596	<0.05
25	Serengeti ecosystem, Tanzania, 1977	0.972	<0.05
26	Serengeti ecosystem, Tanzania, 1986	0.965	<0.05
27	Serengeti ecosystem, Tanzania, 2003	0.595	<0.05
28	Tarangire National Park, Tanzania, 1962 (dry)	0.972	<0.05
29	Tarangire National Park, Tanzania, 1962 (wet)	0.965	<0.05

The confidence intervals of the standardised coefficients are larger than for the *C. crocuta* repeated PLS. For PLS 4, the confidence intervals ranged from 0.008 for very large prey biomass, to 0.186 for temperature of the warmest month (Table 5.8). The graph of standardised coefficients (Figure 5.11) also indicates that the removal of individual sites has a large influence on the PLS results. Most of the variables have coefficient values that are both positive and negative. Only two variables have coefficients that are consistently negative: temperature seasonality and semi-open vegetation cover. Three variables have coefficients that are consistently positive: very small prey biomass, large prey biomass, and closed vegetation cover. Despite this, all these variables have coefficients from some runs that are close to zero. There is therefore no indication that any variables are consistently and strongly related to *P. leo* biomass.

Table 5.8: Standardised coefficient means and confidence intervals (CI) for repeated runs of PLS 4, with *P. leo* biomass as the dependent variable.

Independent variable	Standardised coefficient mean	Standardised coefficient CI	Standardised coefficient minimum CI	Standardised coefficient maximum CI
***C. crocuta* biomass**	0.104	0.082	0.031	0.073
Other predator biomass	-0.005	0.155	0.059	-0.064
Total biomass very small prey	0.812	0.426	0.162	0.650
Total biomass small prey	0.187	0.098	0.037	0.150
Total biomass medium prey	0.230	0.142	0.054	0.176
Total biomass large prey	0.123	0.058	0.022	0.101
Total biomass very large prey	0.044	0.027	0.010	0.034
Minimum temperature coolest month	-0.474	0.306	0.116	-0.590
Maximum temperature warmest month	0.674	0.488	0.186	0.488
Temperature seasonality	-0.736	0.431	0.164	-0.900
Precipitation driest month	0.194	0.130	0.049	0.145
Precipitation wettest month	-0.398	0.327	0.124	-0.523
Precipitation seasonality	0.390	0.282	0.107	0.283
Closed vegetation	0.180	0.086	0.033	0.147
Semi-open vegetation	-0.703	0.429	0.163	-0.866
Open vegetation	0.087	0.082	0.031	0.056

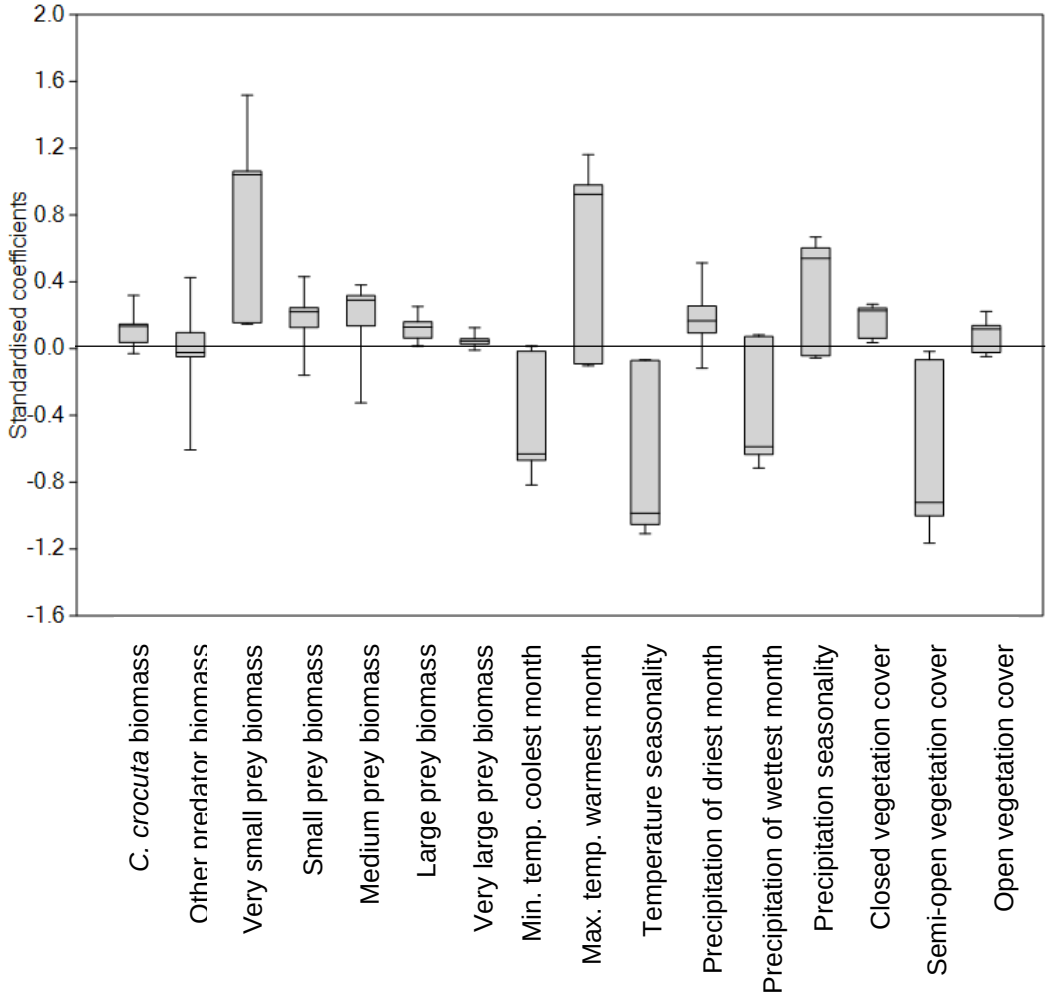

Figure 5.11: Standardised coefficients for repeated runs of PLS 4, with *P. leo* biomass as the dependent variable.

5.1.3 Discussion

5.1.3.1 African predator biomasses

Along with *P. leo*, *C. crocuta* is the most abundant species of large carnivore in many areas of Africa. Temporal changes in the abundance of both *P. leo* and *C. crocuta* are apparent in the Ngorongoro Crater and the Serengeti ecosystem. In the Ngorongoro Crater, the initial low biomass of *P. leo* reflects the reduction in population due to an outbreak of stable flies (*Stomoxys calcitrans*) in 1962 (Fosbrooke, 1963, cited in Kissui and Packer, 2004), and subsequent population recovery. The *P. leo* population was hit by an unknown disease in 1994 and 1997, and in 2001 by a tick-borne disease and the canine distemper virus (Kissui and Packer, 2004), reflected by the lower biomass values in 1997 and 2004 (Table 5.2). The cause of the lower *C. crocuta* biomass in the years 1988 and 1997 may have been due to lower populations of their

preferred prey, and more frequent competitive interactions with *P. leo* (Höner *et al.*, 2005). Conversely, in the Serengeti, the increase in migratory prey populations may have facilitated the *C. crocuta* population increase seen in Table 3.2 (Hofer and East, 1995).

5.1.3.2 *Crocuta crocuta* population biomass

When assessing the potential factors determining *C. crocuta* biomass, a decision needs to be made as to which PLS model is most appropriate. The Kalahari Gemsbok National Park in South Africa was identified as an extreme leverage point, meaning that it likely had a strong influence on the PLS results. Indeed, removing this site and rerunning the PLS revealed different values in many of the standardised coefficients.

The Kalahari Gemsbok National Park differs from other sites as it has the lowest abundance of *C. crocuta* with a biomass of 0.47 kg/km^2. The next highest biomass is Mkomazi Nature Reserve in Tanzania with a value of 0.92 kg/km^2. Additionally, Hatton *et al.*, (2015) noted that the prey abundances recorded from the Kalahari were higher than previous estimates, so there were fewer predators than may have been expected given the prey biomass. This variation in prey abundance may be due to the correlation between prey and rainfall, the latter of which is unpredictable in the area (Mills, 1990). This potential lag of predator abundance behind prey abundance means that it is more appropriate to proceed with the PLS without the Kalahari (PLS 2) in the interpretation of *C. crocuta* biomass.

The repeated runs of PLS 2, removing one site each time, provided further justification for excluding the Kalahari. Despite the removal of each site in turn, all runs reveal similar results to the original PLS 2. By contrast, all maintain different results than PLS 1, with the Kalahari. The similarity of all PLS 2 runs allows confidence to be placed in the assumption that the results are representative of *C. crocuta* populations.

The r^2 values of all PLS 2 runs are 0.95 or higher, indicating that most of the variation of *C. crocuta* biomass is explained by the model. The standardised coefficients indicate that five variables are important: very small prey biomass, medium prey biomass, minimum temperature of the coolest month, open vegetation cover, and semi-open vegetation cover.

Biomass of medium-sized prey has the strongest overall influence on *C. crocuta* biomass. Despite *C. crocuta* being adaptable in the prey it targets (Mills, 1990; Hayward, 2006), this result is to be expected given that its preferred prey weighs 56-182 kg (Hayward and Kerley, 2008), equivalent to small- to medium-sized prey in this study.

Very small prey biomass also has a positive relationship with *C. crocuta* biomass, although not as strong as medium prey biomass. Very small prey here are classed as weighing <20 kg, including *E. thomsonii* and duiker species (*Cephalophus* spp.). Prey such as these can provide an important food source, especially when larger prey are migratory. This is the case in the Serengeti where *E. thomsonii* is the most abundant ungulate, and the most commonly targeted species prior to the arrival of *C. taurinus* (Cooper *et al.*, 1999).

The relationship between prey biomass and *C. crocuta* biomass agrees with Hatton *et al.* (2015) in that predator density and biomass are positively correlated. It also agrees with Cooper's (1989) observation that higher *C. crocuta* densities occur in areas with large biomasses of resident prey populations. However, the PLS suggest that there are other strong influences upon *C. crocuta* abundance.

The minimum temperature of the coolest month has a strong positive relationship, suggesting that *C. crocuta* is averse to the very coldest temperatures, i.e. *C. crocuta* populations are greater when winter temperatures are warmer. The maximum temperature of the warmest month has a negative relationship, although the potential influence is lower than winter temperatures. This is supported by Cooper (1990) who found that *C. crocuta* individuals were unable to hunt in temperatures above about 20°C. Indeed, the summer temperatures of sites included in the present study range from 25.1 to 33.7°C. *C. crocuta* may circumvent this to an extent through crepuscular or nocturnal activities (Cooper, 1990; Hayward and Hayward, 2007). As *C. crocuta* were able to hunt successfully on moonlit nights, and during the day when temperatures were cooler, Cooper (1990) concluded that it is temperature, rather than a need for darkness, that prompts this switch to nocturnal hunting. Very hot temperatures also lead to more rapid decomposition of carrion, thus limiting the period during which carcasses are available as a food source (DeVault *et al.*, 2003). However, avoidance of high temperatures through nocturnal activity may be the reason why high temperatures have only a small influence on. *C. crocuta* biomass.

Precipitation has some influence upon *C. crocuta*, with adverse effects of very dry conditions. Very dry conditions may be limiting due to a lack of available water bodies. Indeed, Cooper (1989) noted that higher *C. crocuta* densities are associated with reliable water resources. In addition, hot and dry conditions may lead to more rapid desiccation of carcasses, which themselves are important sources of water for *C. crocuta*, especially in periods of drought (Cooper, 1990; Cooper *et al.*, 1999). This ability to source water from carcasses may be one of the reasons for the limited influence of precipitation.

Another strong influence is vegetation. Perhaps unexpectedly, open vegetation cover has a strong negative relationship with *C. crocuta* abundance. *C. crocuta* often hunts by pursuing its prey (Kruuk, 1972; Mills, 1990), so it would seem logical that open grassland should provide the ideal vegetation. However, Mills (1990) observed *C. crocuta* chasing its prey in areas of open shrubland or open woodland in the Kalahari, which is similar to the semi-open vegetation category in the present study (open shrubland and wooded grassland; Table 4.2). This explains the positive influence of semi-open vegetation cover on *C. crocuta* biomass, yet fails to explain the negative influence of open vegetation cover. Moreover, there appears to be no consistent vegetation preference for den location (Section 2.3.4). The preference for semi-open vegetation over open vegetation is therefore difficult to explain. An alternative explanation may lie in the limitations of the dataset. The data was collected between the years 1981 and 1994 (Hansen *et al.*, 1998, 2000), and so record any change in vegetation before or after this time period, potentially leading to misclassification of vegetation cover in some sites.

The final point to consider is the influence of other predators. Both *P. leo* and the other predators (*P. brunnea, A. jubatus, P. pardus, L. pictus*) have negligible influences on *C. crocuta* abundance. This might be due to the nature of competitive interactions. Although *C. crocuta* are frequently successful in obtaining food from other predators, the reverse can be true, with the success of direct interactions depending upon the persistence of the challenger, the number of individuals present, and the presence of males in the case of *P. leo* (Kruuk, 1972; Mills, 1990; Cooper *et al.*, 1999; Höner *et al.*, 2002). Therefore, any negative influence of other predators may be largely cancelled out by *C. crocuta* succeeding in competitive interactions. Furthermore, as suggested by other studies (Section 2.3.3), environmental partitioning may limit the negative impact of other predators upon *C. crocuta* abundance.

5.1.3.3 *Panthera leo* population biomass

The influences upon *P. leo* biomass were also investigated. As with the investigation of *C. crocuta*, biomass, the Kalahari Gemsbok National Park was rejected from the analyses, with the same justification: the lag between prey and predator abundance (Hatton *et al.*, 2015). Therefore, the following discussion focusses on the results from PLS 4 only.

While the original PLS 4 points to some variables that have a strong association with *P. leo* biomass, the re-runs of PLS 4 dispute this. Most variables have standardised coefficients that are both positive and negative, depending upon the site removed. The exceptions are temperature seasonality and semi-open vegetation cover, which are consistently negative. Very small prey biomass, large prey biomass, and closed vegetation cover are consistently positive.

Some tentative suggestions may be made about the reasons for these results. *P. leo* most commonly target prey weighing 190-550 kg (Hayward and Kerley, 2008), equivalent to medium- to large-sized prey species in this study. Further, large prey provide more energy intake for large predators, which is necessary to offset energy expended, including that expended while hunting (which is particularly high for predators of large body mass such as *P. leo*, Carbone *et al.*, 2007). This is therefore in support of the positive association between *P. leo* biomass and large-sized prey biomass. However, the positive association with very small-size prey biomass is thus unexpected.

The areas with the highest biomass of very small-sized prey species are the Maasai Mara and the Ngorongoro Crater. In these localities, it is *E. thomsonii* that make up the majority of the very small-sized prey biomass (Hatton *et al.*, 2015, and references therein). In the Seronera area of the Serengeti, although *P. leo* predate on small- to large-sized prey species, during periods when these species are unavailable, *P. leo* will survive on very small-sized prey, namely *E. thomsonii* (Schaller, 1972). The great importance of very small-sized prey species may therefore reflect the importance of these species in allowing the survival of *P. leo* when preferred (larger) prey are unavailable. Further research is required to better understand within-species carnivore abundance patterns in relation to the size and abundance of their prey base (following Carbone *et al.*, 2011; Hatton *et al.*, 2015).

The negative association between *P. leo* biomass and temperature seasonality suggest that *P. leo* abundance is greatest in areas that have either predominantly year-round high temperatures, or predominantly year-round low temperatures, but not great seasonal temperature fluctuations.

The final consideration is vegetation. In contrast to *C. crocuta*, semi-open vegetation cover is negatively associated with *P. leo* biomass. Indeed, even in individual sites, spatial partitioning has been observed between *C. crocuta* and *P. leo*. For example, in the Serengeti, *C. crocuta* occupy the plains and woodland borders while *P. leo* occupy the plains, but are most frequently within wooded grassland (Schaller, 1972). However, this in itself presents a problem as wooded grassland is classed as semi-open vegetation in the present study. Additionally, Périquet *et al.* (2015) suggested that some vegetation cover is needed to allow *P. leo* to ambush its prey. As with *C. crocuta*, it is difficult to explain the influence of vegetation upon *P. leo* biomass, unless the explanation lies within the limitations of the dataset, as discussed previously.

The biomass of *C. crocuta* and of the other large African predators has a negligible influence upon *P. leo* biomass, perhaps due to the influence of environmental partitioning discussed in Section 2.3.3.

However, although the five variables discussed above are the only ones that have a consistent positive or negative association with *P. leo* biomass, many of the coefficients are close to zero, depending upon the site removed from the PLS run. The overall lack of consistency between runs suggests that the conditions influencing *P. leo* biomass are site-specific, or that there are additional influences that were not considered in the analyses. This is backed up by the low r^2 values on some of the PLS runs, which suggest that a large proportion of the variation in *P. leo* biomass is not explained by the model.

The results of the *P. leo* PLS are partly supported by a study by Celesia *et al.* (2010) that found *P. leo* density was positively influenced by herbivore biomass. However, in contrast to the present study, Celesia *et al.* (2010) found that mean annual rainfall and mean annual temperature, in addition to soil nutrients were positively correlated with *P. leo* density. It is difficult to explain the difference between the two studies, apart from the fact that different climate metrics were used.

5.1.3.4 Implications for the Pleistocene

The results suggest that *C. crocuta* biomass is more sensitive to environmental conditions than *P. leo* biomass. This will be explored further in Section 7. The environmental variables that appear to influence *C. crocuta* biomass may be important when considering the responses of the species to Pleistocene environmental changes, particularly its extirpation from Europe. As *C. crocuta* appear to be negatively influenced by colder winters, the shorter and cooler interstadials towards the end of MIS 3 (Davies and Gollop, 2003) are an important consideration. Similarly, vegetation may have changed in such a way as to negatively impact *C. crocuta*, such as a reduction in semi-open vegetation and expansion of open vegetation. These need to be considered alongside potential adaptations to changing conditions such as morphology and diet.

5.2 Ontogenetic size change

5.2.1 Introduction

Prior to other undertaking analyses of bones of *C. crocuta*, it is important to assess how individual elements change in size through life. Failure to recognise this may lead to erroneous interpretation of Pleistocene morphometrics, such as identifying an environmental response, when the signal actually indicates ontogenetic variation. Using fully erupted dentition as an indication of a fully-grown skull is likely invalid. Indeed, while *C. crocuta* permanent dentition is fully erupted by 12-14 months of age (Binder and Van Valkenburgh, 2000), measurements of the skull continue increasing in size after this point (Binder and Van Valkenburgh, 2000; Tanner *et al.*, 2010; Arsznov *et al.*, 2011). The analyses in this section will expand upon the areas of the skull and mandible studied by the aforementioned authors. Feeding ability with age, specifically the ability to consume bone, will also be assessed. This may hold important implications for the Pleistocene if bone consumption constituted an increasingly important food source.

Ontogeny of the post-crania will also be assessed, first to determine whether there are any changes with age that may influence the interpretation of the morphometric analyses. Second, any change in size of post-crania will be assessed with regards its functional significance, such as the relationship between functional limb length and locomotion (Hildebrand, 1974; Section 3.4.2).

The research questions are therefore as follows:

- Do measurements of the skull, mandible and post-crania continue changing through life of *C. crocuta*?
- Do bending strength and bite force change with age in *C. crocuta*?
- Does the effective limb length change with age in *C. crocuta*?

5.2.2 Results

5.2.2.1 Repeated linear measurements

Before ontogenetic change can be analysed, the precision of the linear measurements must be assessed. The statistics from the randomly sampled repeated measurements are shown in Table 5.9. While these indicate that some of the samples are not normally distributed, the standard deviations are low for all measurements. Moreover, in no case are the measurements in Sample 1 significantly different at 95 % confidence than the measurements in Sample 2. Therefore, there is little concern that measurement precision will influence the morphometric results.

Table 5.9: Statistical results of the randomly sub-sampled repeated linear measurements (each sub-sample is comprised of 15 values). A = total length of the cranium. B = length of the m1. C = Breadth of the m1. D = mandibular depth at p2/p3. E = Mandibular width of p2/p3. F = Distance from p2/p3 to the middle of the articular condyle. See Appendix 10.3, Table 10.6 and Table 10.7 for the raw data.

Measurement	**A**		**B**		**C**		**D**		**E**		**F**	
Sub-sample	**1**	**2**	**1**	**2**	**1**	**2**	**1**	**2**	**1**	**2**	**1**	**2**
Standard Deviation	0.07	0.06	0.021	0.028	0.074	0.075	0.128	0.13	0.193	0.189	0.4	0.4
Anderson-Darling statistic	0.13	0.4	1.35	0.82	0.44	0.47	0.24	0.69	0.51	0.41	0.74	0.44
Anderson Darling p-value	0.972	0.327	<0.005	0.026	0.255	0.209	0.735	0.056	0.163	0.302	0.042	0.259
t-test t-value	0.05				0.78		0.04		0.36			
t-test p-value	0.957				0.441		0.966		0.719			
Mann-Whitney statistic			235.5								251	
Mann-Whitney p-value			0.384								0.455	

5.2.2.2 Ontogeny of the cranium and mandible

In order to facilitate analysis of ontogeny of *C. crocuta* skull measurements, the P3/p3 wear stages were used as an indication of the age of each specimen, following Stiner (2004), with the youngest individuals classed as wear stage III (see Section 4.3.2). The analyses are two-fold. The box plots are useful for visualising any changes in size, particularly for the wear stages with sample sizes too small for further statistical analysis. Secondly, where sample sizes included at least ten specimens, tests for significant differences were conducted. This enabled comparison of P3/p3 wear stage IV and stage V in females. In males, sample sizes were sufficient to allow statistical comparison of stages III, IV and V. The data used in the analyses are the ratios of each cranial or mandibular measurement against length of the m1, as discussed in Section 4.4.1.3.

Both males and females show similar patterns in size variation with age of most cranial and mandibular measurements, as displayed in the boxplots (Figure 5.12 and Figure 5.13, and Appendix 10.4, Figure 10.1 and Figure 10.2). In most cases, the single stage III female specimen exhibits smaller morphometrics than those of later wear stages. The sample size for stage III males is larger, and there is overlap with the older individuals. However, the median values, lower quartile, and smallest values for stage III *C. crocuta* are smaller than older individuals in most cases.

Exceptions include some of the cranial measurements that exhibit little difference in size between stage III and older stages, (maxillary cheektooth row lengths in males, breadth and height of the foramen magnum in males, greatest palatal breath in males, and least breadth of the skull in both males and females). Some of the mandibular width measurements also show little difference between stage III and older *C. crocuta*, especially at p3/p4 in males, p4/m1 in females, and post-m1 in both males and females.

In both males and females, there is generally little change in size from stage IV onwards. A few measurements show a different pattern. The breadth of the skull dorsal to the external auditory meatus, and the breadth of the occipital condyles appear to decrease in size in males. This pattern is not apparent in females, where there is little change in size from stage IV.

Finally, several graphs indicate increase in size through life, at least up until stage VIII (there is no data for later stages). These include the frontal breadth and measurements of mandible depth, particularly at the p2/p3 and p4/m1 in males.

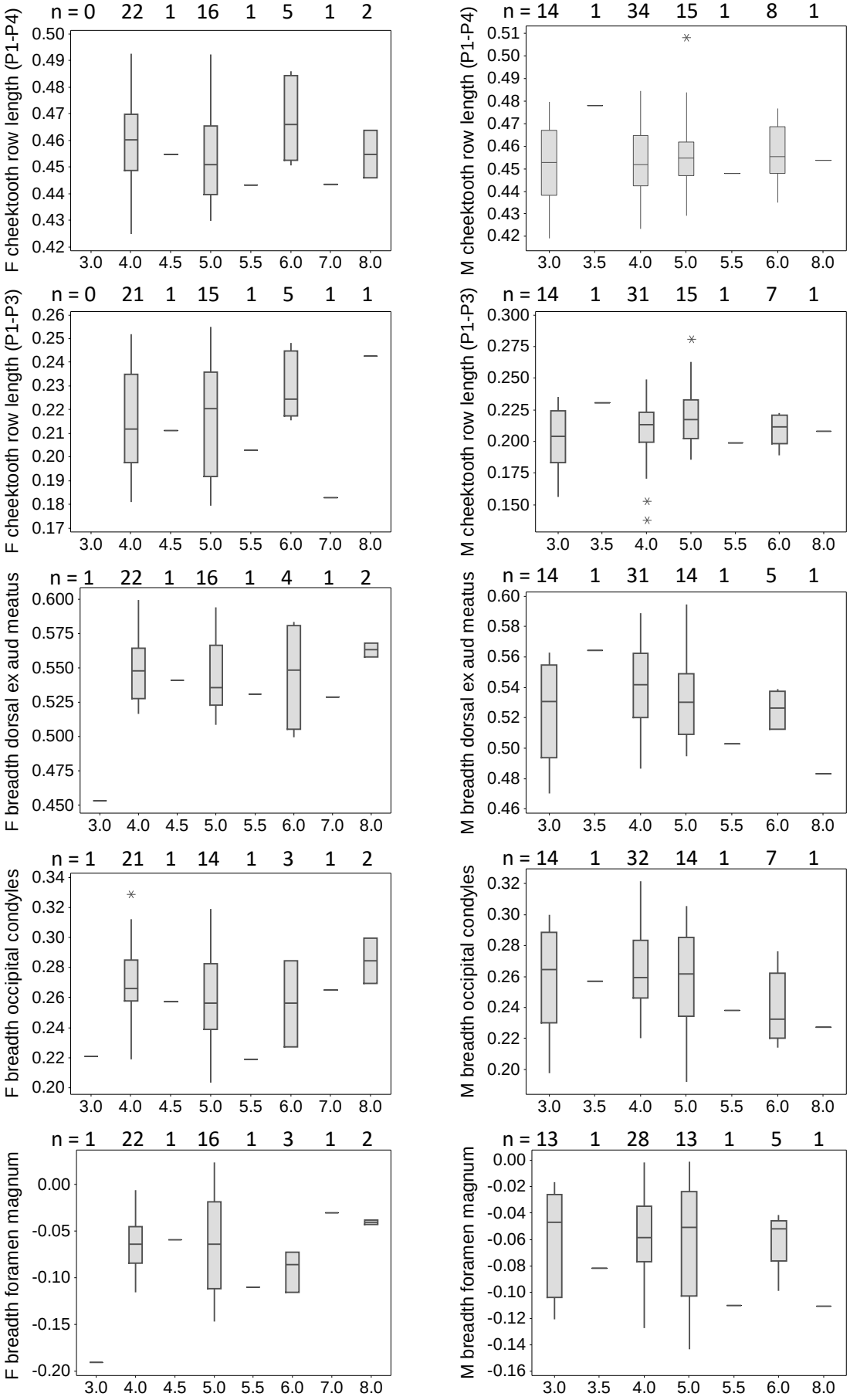

Figure 5.12: Boxplots of female (F) and male (M) *C. crocuta* cranial measurements divided by m1 length, base-10 logarithmically transformed. x-axis numbers are P3/p3 wear stages.

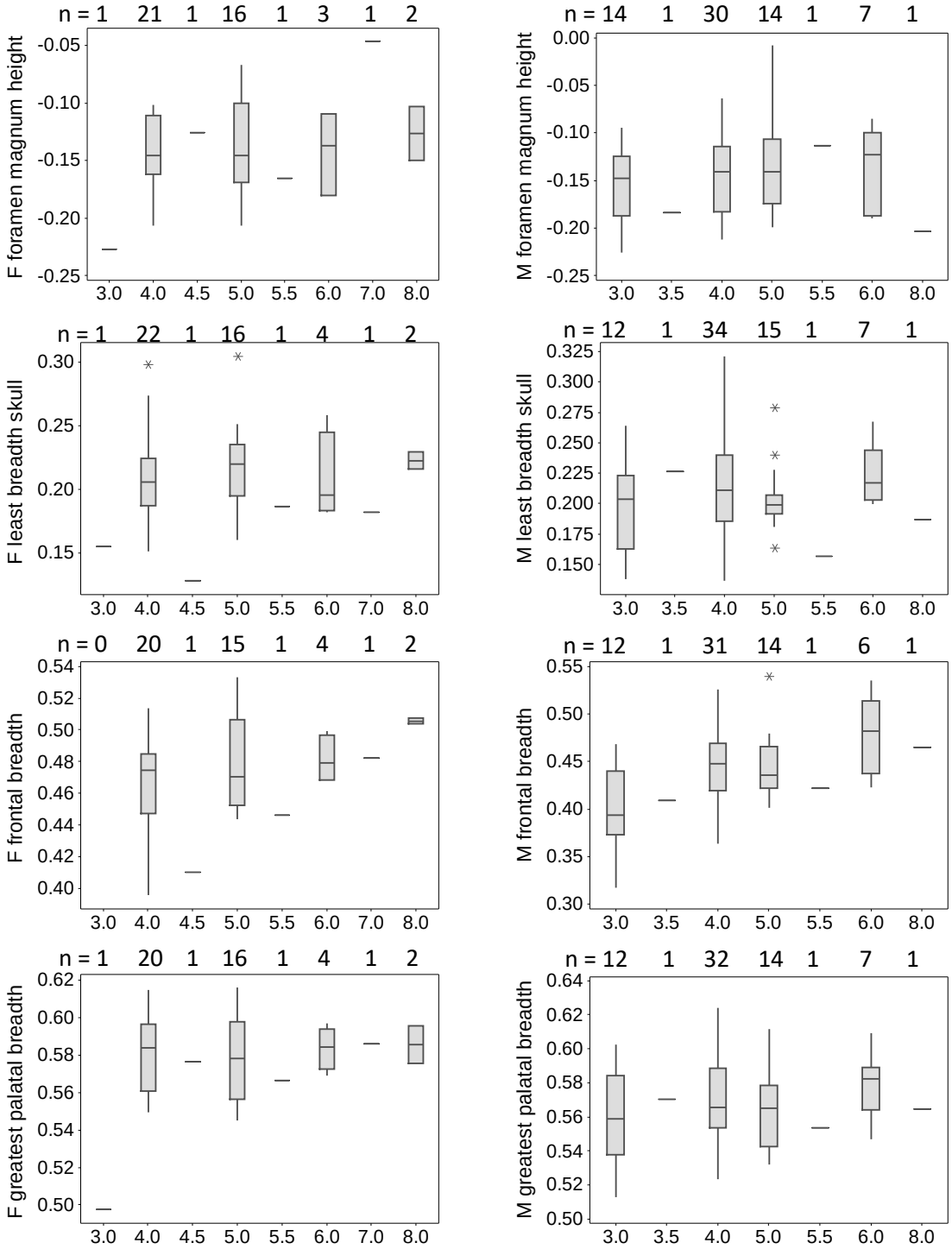

Figure 5.12 continued.

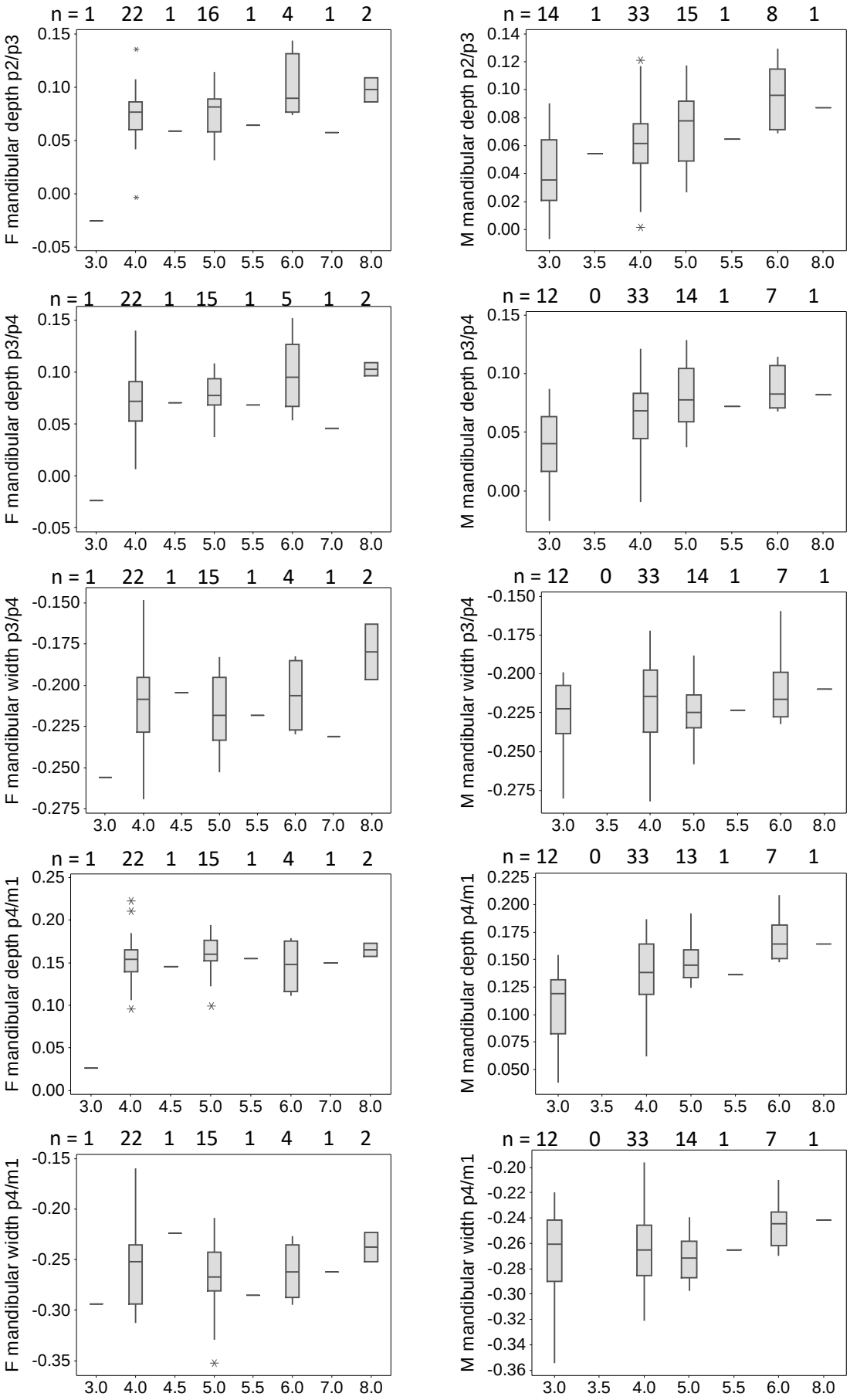

Figure 5.13: Boxplots of female (F) and male (M) *C. crocuta* mandibular measurements divided by m1 length, base-10 logarithmically transformed. x-axis numbers are P3/p3 wear stages.

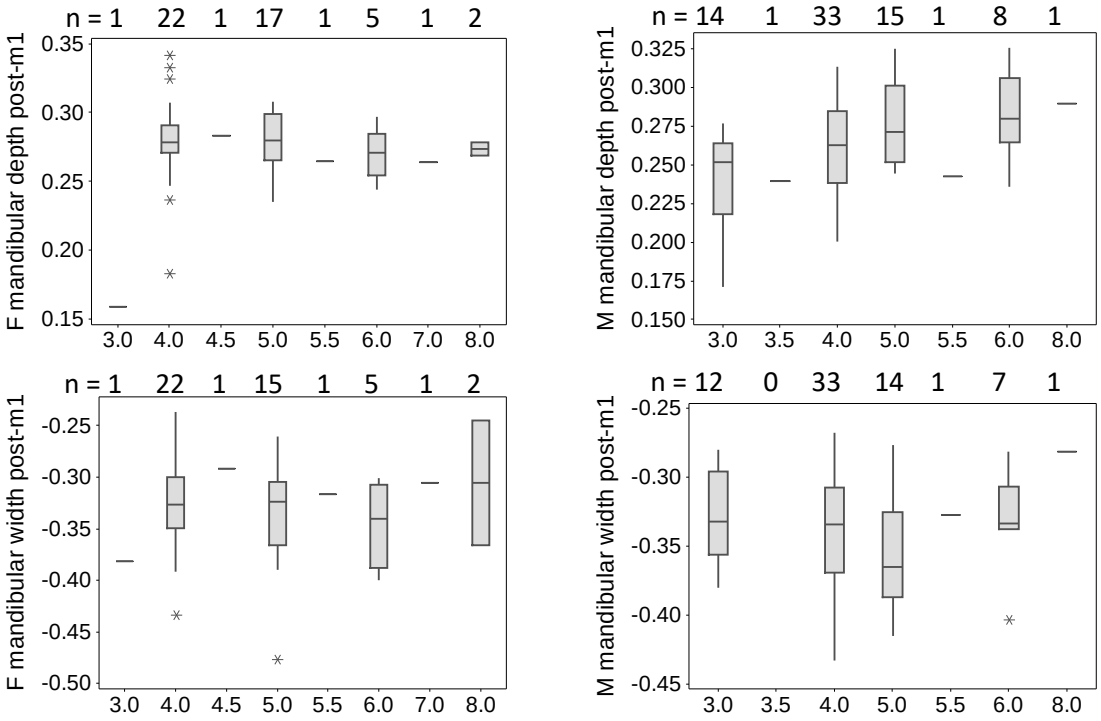

Figure 5.13 continued.

The tests for significant difference largely support the observations from the boxplots (Table 5.12 and Table 5.13). However, the measurements that are indicated as larger (post-stage IV in the box plots) are not significantly so. In fact, no cranial or mandibular measurements are significantly different at 95 % confidence between stages IV and V.

A number of tests, however, indicate that cranial measurements of wear stage III are significantly smaller at 95 % confidence than stages IV and V (length of the cranium, neurocranium length, facial length, zygomatic breadth, frontal breadth, least breadth between the orbits, and temporal fossa length). The length of the snout and skull height of stage III individuals are significantly smaller than only stage V individuals. Of the mandible, only measurements of mandibular depth exhibit significant differences. The depths at p2/p3, p3/p4 and p4/m1 of stage III individuals are significantly smaller than stage IV and V individuals. Stage III measurements of post-m1 depth are also significantly smaller than stage V measurements.

Table 5.10: Tests for significant differences of female *C. crocuta* cranial measurements between different ages. Measurements used in the tests were ratios with m1 lengths and base-10 logarithmically transformed.

P3/p3 wear stage	Test	Total length of cranium	Condylobasal length	Basal length	Basicranial axis	Basifacial axis	Upper neurocranium length	Viscerocranium length	Facial length	Greatest length of the nasals	Snout length	Median palatal length	Length of the horizontal part of the palatine	Length of the cheektooth row (P1-P4)	Length of the cheektooth row (P1-P3)	Greatest diameter of the auditory bulla	Greatest mastoid breadth
	t-test																
IV vs V	*t-value*	0.61	0.91	1.26			0.3	0.03	0.59	0.18		0		1.04	0.03	0.51	0.58
	p-value	0.548	0.368	0.217			0.767	0.975	0.557	0.856		0.997		0.306	0.977	0.616	0.567

Table 5.10 continued.

P3 wear stage	Test	Breadth dorsal to the external auditory meatus	Greatest breadth of the occipital condyles	Greatest breadth of the bases of the paraoccipital processes	Greatest breadth of the foramen magnum	Height of the foramen magnum	Greatest neurocranium breadth	Zygomatic breadth	Least breadth of the skull	Frontal breadth	Least breadth between the orbits	Greatest palatal breadth	Least palatal breadth	Greatest height of the orbit	Skull height	Height of the occipital triangle	Temporal fossa length
	t-test																
IV vs V	*t-value*	0.73	0.96	0.76	0.07	0	0.93	0.19	0.9	1.27	0.99	0.38	0.38	0.09	0.05	0.43	0.73
	p-value	0.473	0.347	0.435	0.947	0.999	0.36	0.848	0.377	0.214	0.33	0.71	0.703	0.93	0.961	0.669	0.473

Table 5.11: Tests for significant differences of male *C. crocuta* cranial measurements between different ages. Measurements used in the tests were ratios with m1 lengths and base-10 logarithmically transformed. Shaded boxes indicate significant difference at 95 % confidence.

P3 wear stage	Test	Total length of cranium	Condylobasal length	Basal length	Basicranial axis	Basifacial axis	Upper neurocranium length	Viscerocranium length	Facial length	Greatest length of the nasals	Snout length	Median palatal length	Length of the horizontal part of the palatine	Length of the cheektooth row (P1-P4)	Length of the cheektooth row (P1-P3)	Greatest diameter of the auditory bulla	Greatest mastoid breadth
	ANOVA																
III	*Category*		A				B		B		B		A	A		A	A
IV	*Category*		A				A		A		A & B		A	A		A	A
V	*Category*		A				A		A		A		A	A		A	A
	p-value		0.087				0.005		0.025		0.043		0.137	0.496		0.408	0.25
	t-test																
III vs IV	*t-value*				1.2												
	p-value				0.245												
	Mann Whitney																
III vs IV	*W-value*	143		175		148						163			291		
	p-value	0.044		0.165		0.197						0.078			0.455		
III vs V	*W-value*	89		120		85						107			176		
	p-value	0.038		0.218		0.14						0.082			0.144		
IV vs V	*W-value*	671		584		454						579			681		
	p-value	0.309		0.641		0.349						0.812			0.271		

Table 5.11 continued.

P3 wear stage	Test	Breadth dorsal to the external auditory meatus	Greatest breadth of the occipital condyles	Greatest breadth of the bases of the paraoccipital processes	Greatest breadth of the foramen magnum	Height of the foramen magnum	Greatest neurocranium breadth	Zygomatic breadth	Least breadth of the skull	Frontal breadth	Least breadth between the orbits	Greatest palatal breadth	Least palatal breadth	Greatest height of the orbit	Skull height	Height of the occipital triangle	Temporal fossa length
	ANOVA																
III	*Category*	A	A	A		A	A	B		B	B	A		A	B		B
IV	*Category*	A	A	A		A	A	A		A	A	A		A	A & B		A
V	*Category*	A	A	A		A	A	A		A	A	A		A	A		A
	p-value	0.184	0.74	0.159		0.497	0.059	0.031		0.005	0.003	0.515		0.238	0.034		0.008
	t-test																
III vs IV	*t-value*																
	p-value																
	Mann Whitney																
III vs IV	*W-value*				283				243				237			213	
	p-value				0.79				0.335				0.051			0.172	
III vs V	*W-value*				180				171				186			123	
	p-value				0.837				0.903				0.448			0.048	
IV vs V	*W-value*				599				908				708			673	
	p-value				0.769				0.212				0.413			0.333	

Table 5.12: Tests for significant differences of female *C. crocuta* mandibular measurements between different ages. Measurements used in the tests were ratios with m1 lengths and base-10 logarithmically transformed.

P3 wear stage	Test	Condyle to symphysis length	Angular process to infradentlale length	Condyle/angular indentation to symphysis length	Condyle to c alveolus length	Condyle/angular indentation to c alveolus length	Angular process to c alveolus length	c alveolus to m1 alveolus length	Length of cheektooth row (p2 – m1)	Length of cheektooth row (p3 – m1)	Length of premolar row (p2 – p4)	Height of the vertical ramus	Mandibular depth at p2/p3	Mandibular width at p2/p3	Mandibular depth at p3/p4
	t-test														
IV vs V	*t-value*	0.52	0.52	0.45	0.94	0.45	0.75	0.55	0.02	0.24	0.47	0.05	0.45	1.05	0.59
	p-value	0.64	0.608	0.654	0.356	0.656	0.456	0.586	0.984	0.808	0.643	0.964	0.654	0.303	0.558
P3 wear stage	**Test**	**Mandibular width at p3/p4**	**Mandibular depth at p4/m1**	**Mandibular width at p4/m1**	**Mandibular depth at post-m1**	**Mandibular width at post-m1**	**Distance from p2/p3 to middle of articular condyle**	**Distance from p3/p4 to middle of articular condyle**	**Distance from p4/m1 to middle of articular condyle**	**Distance from post-m1 to middle of articular condyle**	**Moment arm of the masseter**	**Moment arm of the temporalis**	**Masseteric fossa length**	**Moment arm of resistance at m1**	**Moment arm of resistance at c**
	t-test														
IV vs V	*t-value*	0.98	0.55	0.84		0.52	0.52	0.64	0.39	0.15	0.85	0.25	0.21	0.87	1.23
	p-value	0.335	0.583	0.409		0.605	0.608	0.524	0.696	0.88	0.399	0.806	0.831	0.389	0.23
	Mann Whitney														
IV vs V	*W-value*				440										
	p-value				1										

Table 5.13: Tests for significant differences of male *C. crocuta* mandibular measurements between different ages. Measurements used in the tests were ratios with m1 lengths and base-10 logarithmically transformed. Shaded boxes indicate significant difference at 95 % confidence. Where measurements belong to different ANOVA categories, there is a significant difference.

P3 wear stage	Test	Condyle to symphysis length	Angular process to infradentlale length	Condyle/angular indentation to symphysis length	Condyle to c alveolus length	Condyle/angular indentation to c alveolus length	Angular process to c alveolus length	c alveolus to m1 alveolus length	Length of cheektooth row (p2 – m1)	Length of cheektooth row (p3 – m1)	Length of premolar row (p2 – p4)	Height of the vertical ramus	Mandibular depth at p2/p3	Mandibular width at p2/p3	Mandibular depth at p3/p4	Mandibular width at p3/p4
	ANOVA															
III	*Category*		A	A		A	A	B	A	A	A	A	B	A	B	A
IV	*Category*		A	A		A	A	A & B	A	A	A	A	A	A	A	A
V	*Category*		A	A		A	A	A	A	A	A	A	A	A	A	A
	p-value		0.078	0.246		0.213	0.509	0.051	0.76	0.52	0.657	0.057	0.007	0.339	0.003	0.552
	Mann Whitney															
III vs IV	*W-value*	201			255											
	p-value	0.796			0.42											
III vs V	*W-value*	105			157											
	p-value	0.531			0.153											
IV vs V	*W-value*	662			648											
	p-value	0.598			0.318											

Table 5.13 continued.

P3 wear stage	Test	Mandibular depth at p4/m1	Mandibular width at p4/m1	Mandibular depth at post-m1	Mandibular width at post-m1	Distance from p2/p3 to middle of articular condyle	Distance from p3/p4 to middle of articular condyle	Distance from p4/m1 to middle of articular condyle	Distance from post-m1 to middle of articular condyle	Moment arm of the masseter	Moment arm of the temporalis	Masseteric fossa length	Moment arm of resistance at m1	Moment arm of resistance at c
	ANOVA													
III	*Category*	B	A		A	A	A			A				
IV	*Category*	A	A		A	A	A			A				
V	*Category*	A	A		A	A	A			A				
	p-value	0.002	0.85		0.197	0.152	0.143			0.108				
	Mann Whitney													
III vs IV	*W-value*			262				221	219		227	230	244	221
	p-value			0.087				0.162	0.147		0.073	0.067	0.137	0.382
III vs V	*W-value*			159				140	134		153	148	165	121
	p-value			0.028				0.269	0.157		0.167	0.065	0.289	0.1
IV vs V	*W-value*			753				812	780		776	780	805	554
	p-value			0.221				0.65	0.789		0.575	0.533	0.947	0.118

As explained in Section 4.4.1.3, only *C. crocuta* from Balbal, Tanzania are used to assess ontogenetic change of mandibular bending strength and bite force. Sample sizes were too small to allow tests for significant difference, so only box plots were produced.

The plots of bending strength (Figure 5.14 and Figure 5.15) indicate that the zx/L indices (showing resistance to dorsoventral bending) increase with age, which is particularly apparent in males. This occurs at least until wear stage VI (sample sizes are one or zero for later stages). The zy/L indices (indicating resistance to labiolingual bending) also increase with age, again particularly in males to at least wear stage VI. All zx/zy indices (showing the mandibular cross-sectional shape) are greater than one. The values increase with age at the post-m1 position, at least until wear stage VI. There is little change with age at the other interdental points.

Again, as explained in Section 4.4.1.3, ontogenetic change of bite force, as measured in the mandible, was conducted with only the *C. crocuta* specimens from Balbal. Sample sizes were too small to allow tests for significant differences, so only boxplots were constructed.

The boxplots (Figure 5.16 and Figure 5.17) indicate that differences of bite force with ontogeny are less clear than for bending strength. There is little change in the mechanical advantage of the temporalis in females. By contrast, this appears to decrease in males, although the small sample size of the later wear stages make this difficult to assess. There is little change with age in both males and females of the mechanical advantage of the superficial masseter. Finally, the mechanical advantage of the deep masseter appears to increase with age in males, although the small sample sizes of the later wear stages make this difficult to assess. Females show some decrease in the mechanical advantage of the deep masseter with age.

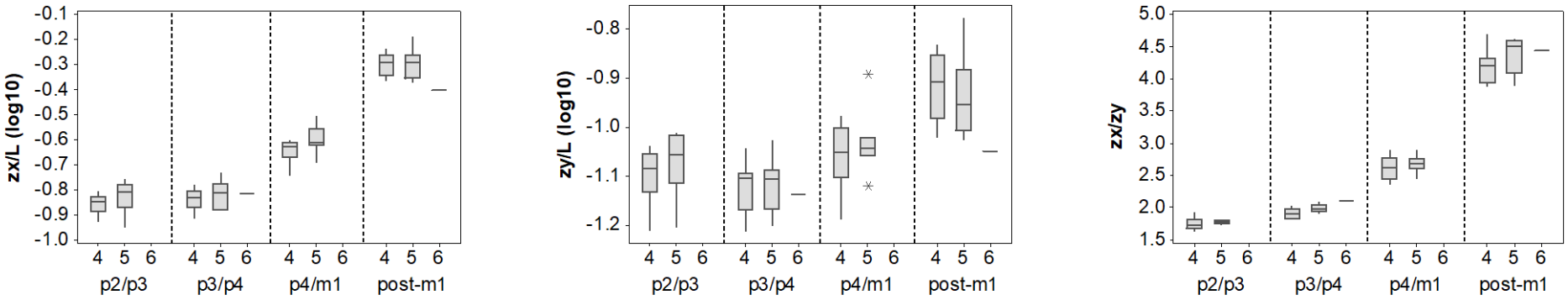

Figure 5.14: Mandibular bending strengths of female *C. crocuta* from Balbal, Tanzania. The upper x-axis values (4 - 6) are P3/p3 wear stages. The lower x-axis labels are the interdental gaps. zx/L indicates strength in dorsoventral bending. zy/L indicates strength in labiolingual bending. zx/zy is mandibular cross-sectional shape. Sample sizes for p2/p3: stage 4 (n = 12), stage 5 (n = 7), stage 6 (n = 0). Sample sizes for p3/p4: stage 4 (n = 11), stage 5 (n = 7), stage 6 (n = 1). Sample sizes for p4/m1: stage 4 (n = 12), stage 5 (n = 7), stage 6 (n = 0). Sample sizes for post-m1: stage 4 (n = 11), stage 5 (n = 7), stage 6 (n = 1).

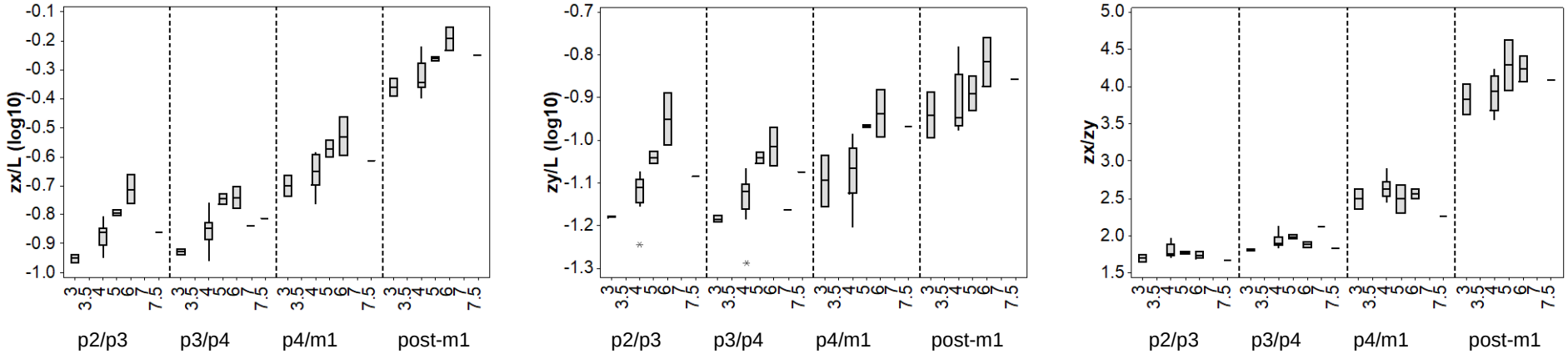

Figure 5.15: Mandibular bending strengths of male *C. crocuta* from Balbal, Tanzania. The upper x-axis values (3 - 7.5) are P3/p3 wear stages. The lower x-axis labels are the interdental gaps. zx/L indicates strength in dorsoventral bending. zy/L indicates strength in labiolingual bending. zx/zy is mandibular cross-sectional shape. Sample sizes for p2/p3: stage 3 (n = 2), stage 3.5 (n = 0), stage 4 (n = 9), stage 5 (n = 2), stage 6 (n = 2), stage 7 (n = 0), stage 7.5 (n = 1). Sample sizes for p3/p4: stage 3 (n = 2), stage 3.5 (n = 0), stage 4 (n = 9), stage 5 (n = 2), stage 6 (n = 2), stage 7 (n = 1), stage 7.5 (n = 1). Sample sizes for p4/m1: stage 3 (n = 2), stage 3.5 (n = 0), stage 4 (n = 9), stage 5 (n = 2), stage 6 (n = 2), stage 7 (n = 0), stage 7.5 (n = 1). Sample sizes for post-m1: stage 3 (n = 2), stage 3.5 (n = 0), stage 4 (n = 9), stage 5 (n = 2), stage 6 (n = 2), stage 7 (n = 0), stage 7.5 (n = 1).

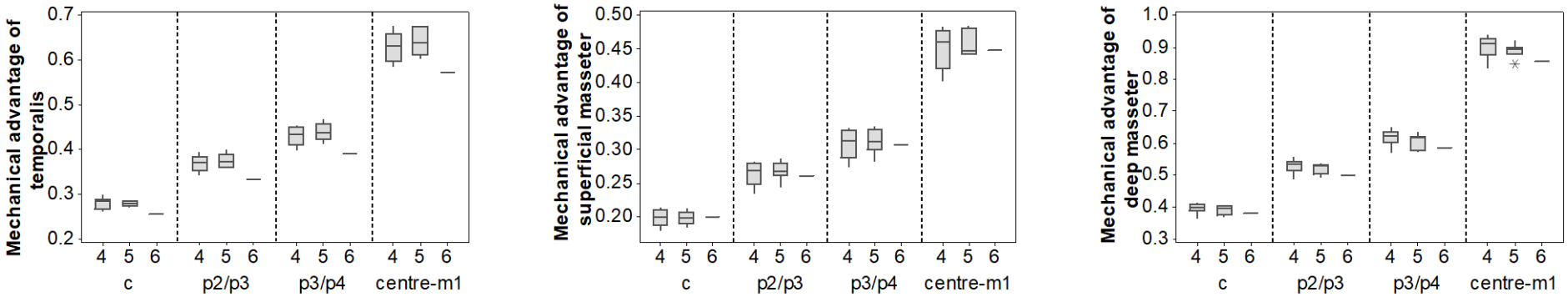

Figure 5.16: Bite forces of female *C. crocuta* from Balbal, Tanzania. The upper x-axis values (4 - 6) are P3/p3 wear stages. The lower x-axis labels are the positions along the mandible. Sample sizes for mechanical advantage of the temporalis at c: stage 4 (n = 11), stage 5 (n = 5), stage 6 (n = 1). Sample sizes for mechanical advantage of the temporalis at p2/p3: stage 4 (n = 11), stage 5 (n = 7), stage 6 (n = 1). Sample sizes for mechanical advantage of the temporalis at p3/p4: stage 4 (n = 11), stage 5 (n = 7), stage 6 (n = 1). Sample sizes for mechanical advantage of the temporalis centre of m1: stage 4 (n = 11), stage 5 (n = 7), stage 6 (n = 1). Sample sizes for mechanical advantage of the superficial masseter at c: stage 4 (n = 12), stage 5 (n = 5), stage 6 (n = 1). Sample sizes for mechanical advantage of the superficial masseter at p2/p3: stage 4 (n = 12), stage 5 (n = 7), stage 6 (n = 1). Sample sizes for mechanical advantage of the superficial masseter at p3/p4: stage 4 (n = 12), stage 5 (n = 7), stage 6 (n = 1). Sample sizes for mechanical advantage of the superficial masseter at centre of m1: stage 4 (n = 12), stage 5 (n = 7), stage 6 (n = 1). Sample sizes for mechanical advantage of the deep masseter at c: stage 4 (n = 12), stage 5 (n = 5), stage 6 (n = 1). Sample sizes for mechanical advantage of the deep masseter at p2/p3: stage 4 (n = 12), stage 5 (n = 7), stage 6 (n = 1). Sample sizes for mechanical advantage of the deep masseter at p3/p4: stage 4 (n = 12), stage 5 (n = 7), stage 6 (n = 1). Sample sizes for mechanical advantage of the deep masseter at centre of m1: stage 4 (n = 12), stage 5 (n = 7), stage 6 (n = 1).

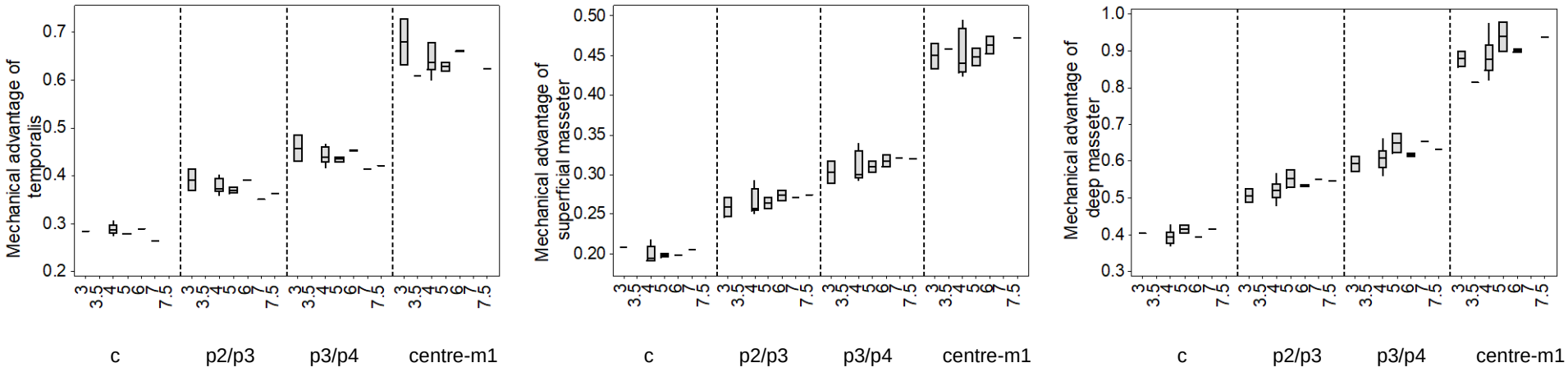

Figure 5.17: Bite forces of male *C. crocuta* from Balbal, Tanzania. The upper x-axis values (3 – 7.5) are P3/p3 wear stages. The lower x-axis labels are the positions along the mandible. Sample sizes for c: stage 3 (n = 1), stage 3.5 (n = 0), stage 4 (n = 8), stage 5 (n = 2), stage 6 (n = 1), stage 7 (n = 1), stage 7.5 (n = 0). Sample sizes for p2/p3: stage 3 (n = 2), stage 3.5 (n = 0), stage 4 (n = 9), stage 5 (n = 2), stage 6 (n = 2), stage 7 (n = 1), stage 7.5 (n = 1). Sample sizes for p3/p4: stage 3 (n = 2), stage 3.5 (n = 0), stage 4 (n = 9), stage 5 (n = 2), stage 6 (n = 2), stage 7 (n = 1), stage 7.5 (n = 1). Sample sizes for centre of m1: stage 3 (n = 2), stage 3.5 (n = 1), stage 4 (n = 9), stage 5 (n = 2), stage 6 (n = 2), stage 7 (n = 0), stage 7.5 (n = 1).

5.2.2.3 Ontogeny of the post-crania

To test ontogenetic size change of the post-crania, measurements were again divided by m1 lengths and base-10 logarithmically transformed. Only bones with completely fused epiphyses were used. Due to the relative scarcity of *C. crocuta* post-crania in museum collections, tests for statistical significance could not be conducted. The small sample sizes also mean that data are displayed as individual value plots rather than box plots. Data were sufficient to allow this to be conducted for the following elements: humerus, radius, ulna, femur, tibia, fibula, patella, scapho-lunar, navicular, astragalus, and calcaneum. Additionally, the brachial index (radial length/humeral length) and the crural index (tibial length/femoral length) were calculated.

The individual value plots indicate size (relative to the m1 length) at each wear stage (Figure 5.18). The sample sizes are very small, however, most measurements either show no consistent pattern with age, or show differences in patterns between males and females.

The exceptions are the greatest breadth of the distal end of the radius, the greatest breadth of the articular surface of the ulna, and the greatest breadth of the scapho-lunar. These suggest an increase in size with age, although this is based on a small number of female specimens. There are insufficient specimens to distinguish a pattern in male *C. crocuta*.

The depth of the femoral caput appears to decrease in size with age in both males and females. The brachial index also appears to decrease with age in females, although this is based on a small number of specimens (n=6).

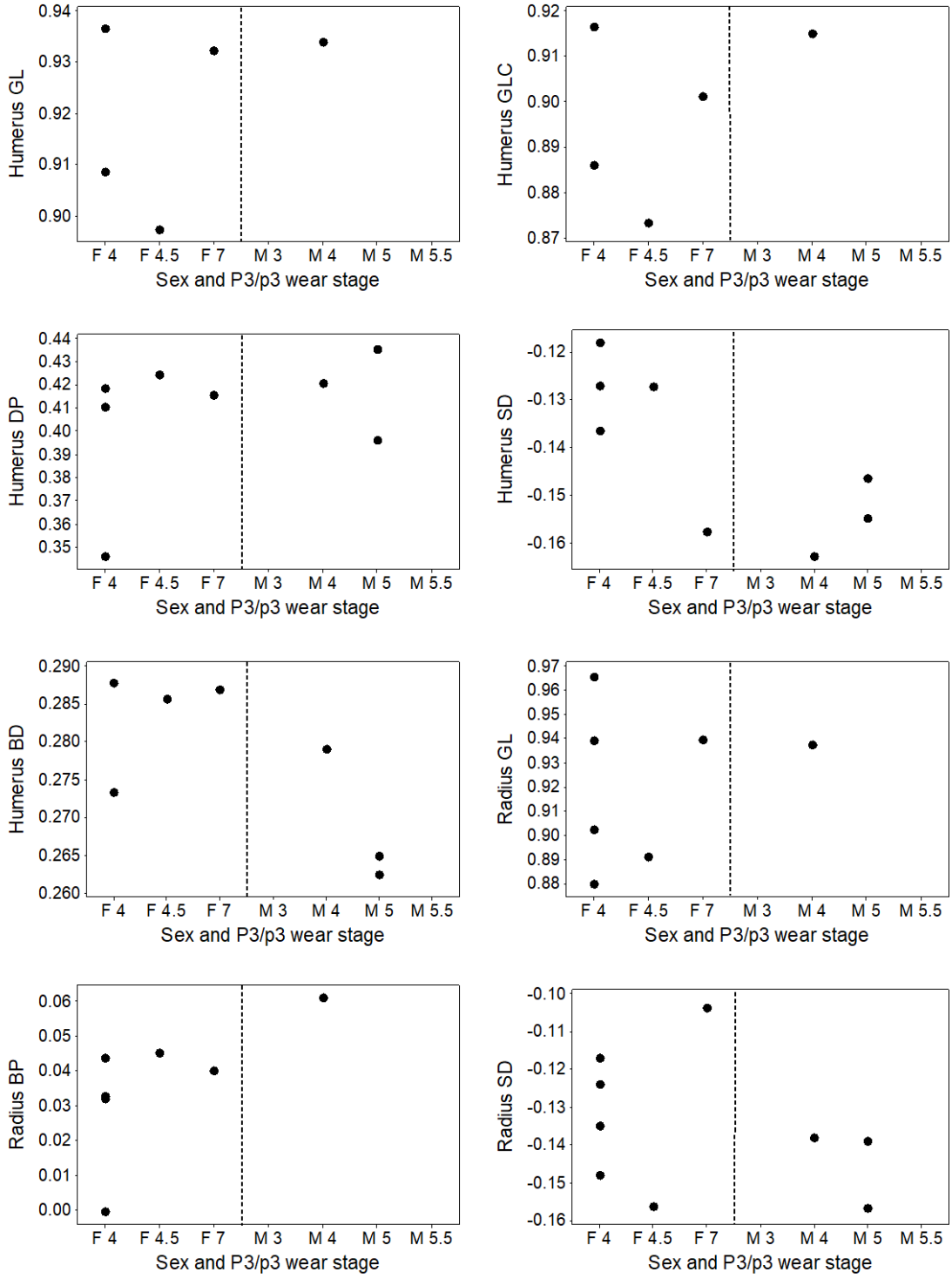

Figure 5.18: Present-day C. crocuta post-cranial measurements divided by m1 length, and base-10 logarithmically transformed. F = female. M = male. GL = greatest length. GLC = greatest length from the caput. DP = greatest depth of the proximal end. SD = smallest breadth of the diaphysis. BD = greatest breadth of the distal end. DPA = depth across the anconeal process. SDO = smallest depth of the olecranon. BPC = greatest breadth across the proximal articular surface. DC = greatest depth of femoral head. GB = greatest breadth.

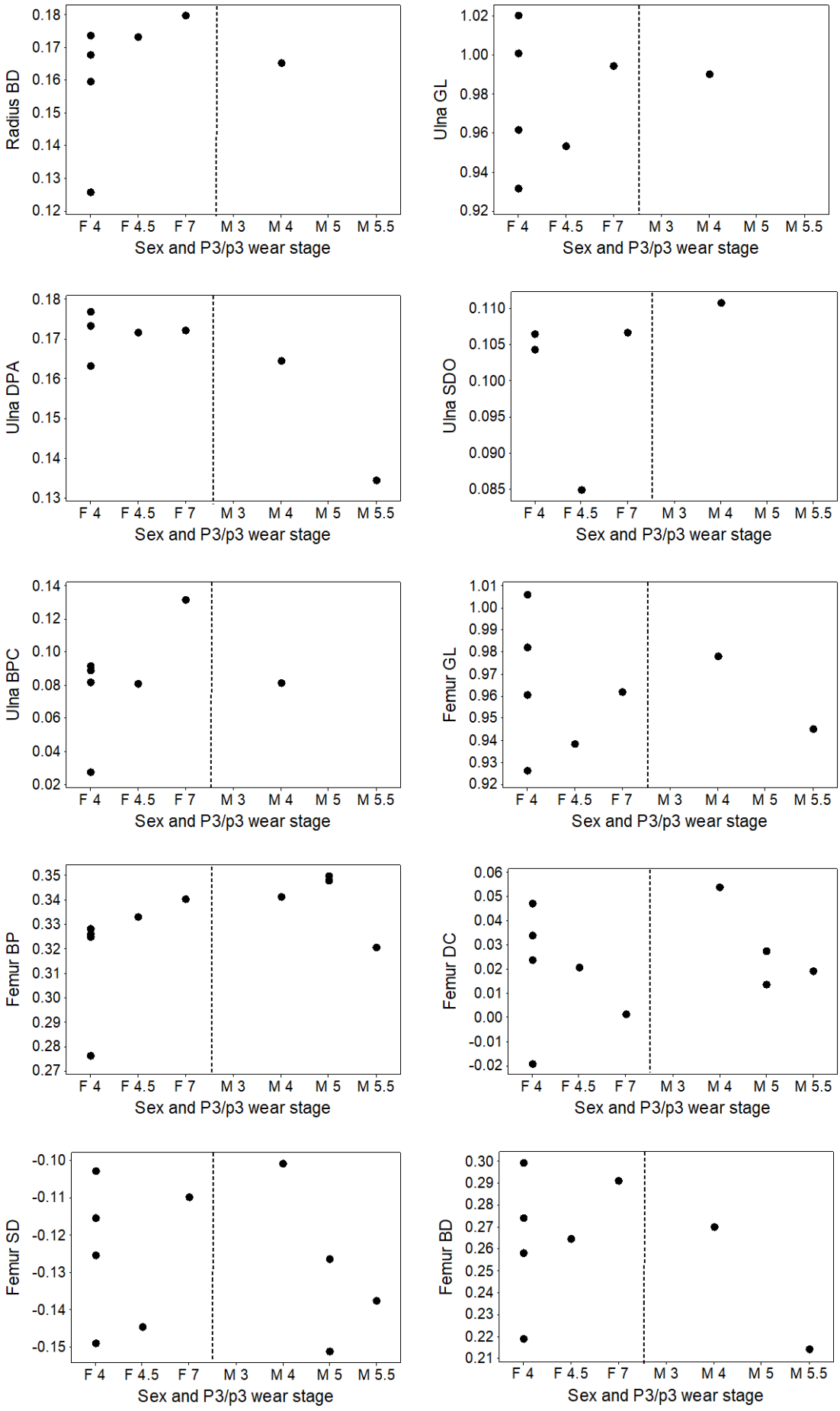

Figure 5.18 continued.

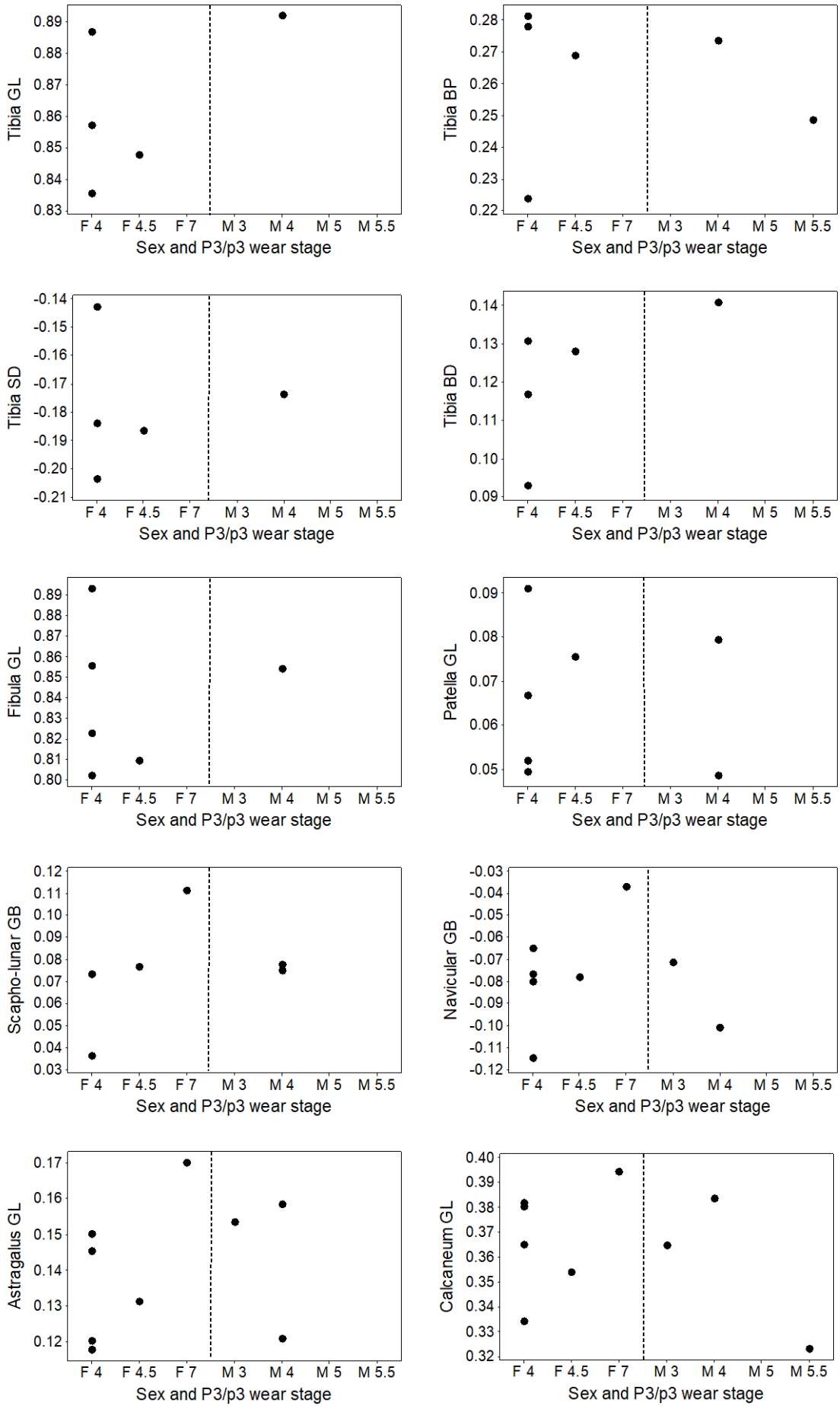

Figure 5.18 continued.

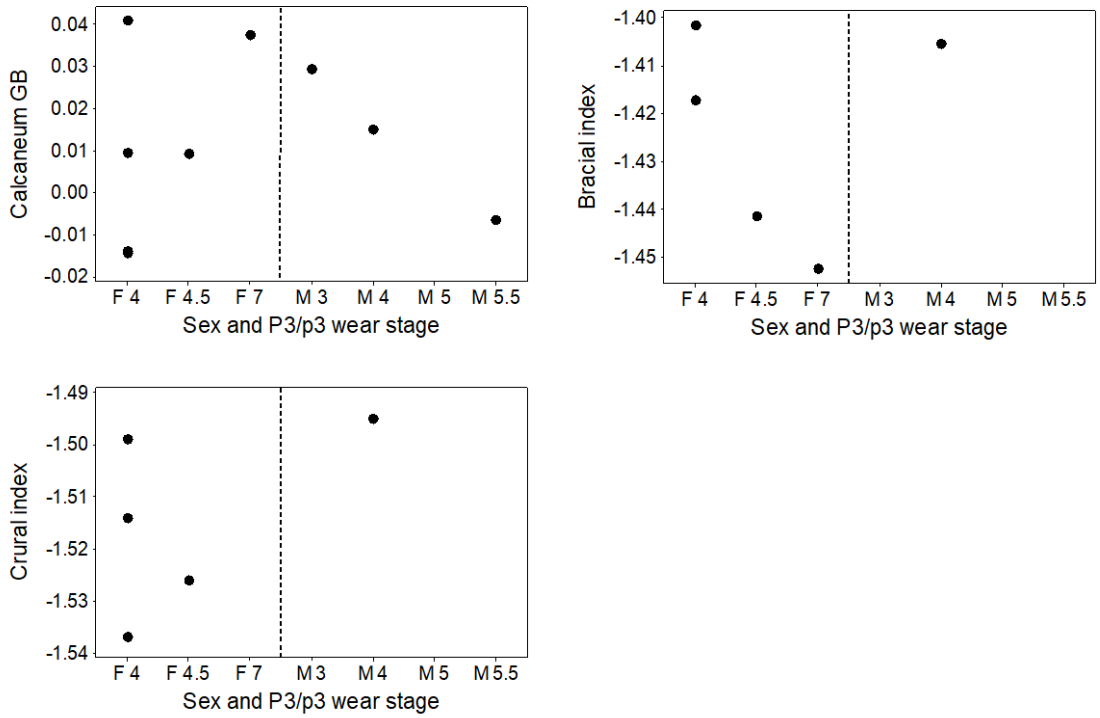

Figure 5.18 continued.

5.2.3 Discussion

5.2.3.1 Repeated linear measurements

The results of the repeated linear measurements of a *C. crocuta* skull indicate that there are no statistically significant differences between two random samples of each measurement. There is therefore no concern that the precision of the measurements will influence the results of morphological analyses.

5.2.3.2 Ontogeny of the cranium and mandible

The results indicate that many measurements of the skull are not fully-grown in *C. crocuta* individuals with stage III P3/p3 wear. Of functional significance to feeding is the breadth of the zygomatic arches, which is significantly smaller at stage III than stages IV and V. As the zygomatic arches are attachment sites for the masseter muscle (von Toldt, 1905 cited in Turnbull, 1970; Ewer, 1973), the breadth is an indication of the size of the masseter muscle and thus of bite strength (Radinsky, 1981a; Tanner *et al.*, 2010). Therefore, the younger stage III individuals likely had smaller masseter muscles, and therefore reduced bite strength when compared to older individuals.

Conversely, there are measurements that show no difference between stages III and IV. These may have reached full size earlier than other measurements.

There are also measurements that appear to increase in size through life, at least until stage VIII (frontal breadth, and measurements of mandibular depth, particularly at p2/3 and p4/m1 in males). Different skull measurements of *V. vulpes* also have different patterns of ontogenetic size change, with some measurements increasing through life (Hartová-Nentvichová *et al.*, 2010).

In addition, in males two measurements decrease in size through life (the breadth of the occipital condyles, and the breadth external to the auditory meatus). Although the measurements are different, the smallest distance behind the supraorbital processes (least breadth of skull in the present study) decreased after six months of age in *V. vulpes* (Hartová-Nentvichová *et al.*, 2010).

As mentioned, measurements of mandibular depth increase with age up to at least stage VIII. Additionally, the zx/L indices increase with age up until at least wear stage VI. These are particularly apparent in males. Both measurements indicate resistance to dorsoventral bending (Hildebrand, 1974; Biknevicius and Ruff, 1992; Therrien, 2005; Palmqvist *et al.*, 2011). The zx/zy indices, giving an indication of mandibular shape, have values greater than one along the mandible for all wear stages, suggesting that the mandible is better suited to resist dorsoventral stresses. The zx/zy indices increase with age at the post-m1 position. Together, these measurements and indices indicate that *C. crocuta* mandibles (particularly males) become increasingly more suited to resist dorsoventral stresses through life. The mandible incurs dorsoventral stresses during biting, particularly during bone-cracking (Biknevicius and Ruff, 1992; Therrien, 2005; Ferretti, 2007; Meloro *et al.*, 2008; Palmqvist *et al.*, 2011). This indicates that mandibles of older *C. crocuta* are better suited for bone-cracking.

The zy/L indices, an indication of resistance to labiolingual stresses (Hildebrand, 1974; Biknevicius and Ruff, 1992; Therrien, 2005; Palmqvist *et al.*, 2011), also increase until at least stage VI. This is particularly apparent in males. Struggling prey may exert labiolingual stresses upon the mandible (Biknevicius and Ruff, 1992). This indicates that individuals are increasingly able to successfully target larger prey as they grow older. Although it must be borne in mind that successful hunts are dependent upon other factors, such as hunting group size (Holekamp *et al.*, 1997).

The measurements of bite strength, as measured through mechanical advantage of the muscles, have less clear patterns. The mechanical advantage of the superficial masseter exhibits little change through life, at all bite points. This was also found in a study of individuals of known ages

(Tanner *et al.*, 2010). By contrast, in the present study, the mechanical advantage of the deep masseter increases in males, yet decreases in females.

In the aforementioned studied population, mechanical advantage of the temporalis muscles increased until 22 months of age (Tanner *et al.*, 2010), which is after permanent dentition is attained at 12-14 months of age (Binder and Van Valkenburgh, 2000). However, in the present study, this changes little in females, and decreases with age in males.

Where there is no change in mechanical advantage with age, there is an isometric relationship between the in-lever and out-lever (Tanner *et al.*, 2010), and thus bite force remains constant. A decrease in mechanical advantage suggests that the out-lever grows hyperallometrically when compared to the in-lever, and vice versa when there is an increase in bite strength. There is thus a decrease in bite strength with lower mechanical advantage, and an increase in bite force with greater mechanical advantage.

Taking the mechanical advantages of each muscle together, it is unclear whether *C. crocuta* bite force increases, decreases or remains constant through life. Evidence is seen through the smaller masseter in stage III individuals (as measured through zygomatic breadth) in the present study. This was also seen in Tanner *et al.*'s (2010) study, where zygomatic arch width increased until 33 months of age. In a study using a force transducer on live individuals, Binder and Van Valkenburgh (2000) discovered that bite force increased until four years of age. Unfortunately, the P3/p3 wear stage cannot be translated into years of age, so the results cannot be directly compared with those of the present study.

This change in bending strength and potentially bite strength through life indicates that younger *C. crocuta*, particularly males, may be less able to consume tough food such as bone. This may be a disadvantage when competition is high as younger *C. crocuta*, particularly those of lower ranking mothers, may be left with the less preferential parts of carcasses (Frank *et al.*, 1989; Egeland *et al.*, 2008). Reduced ability to consume bone may limit survival of younger *C. crocuta* if food scarcity is prolonged. This is an important consideration for the Pleistocene as prolonged conditions resulting in food scarcity may have factored into the reduction in populations of *C. crocuta*, and eventually led to their extirpation.

In light of the results, cranial and mandibular measurements of wear stage III *C. crocuta* will be excluded from future analyses. Additionally, those measurements that increase or decrease with age through life will be analysed within separate wear stages in further analyses. Apart from these measurements, the results indicate that amalgamating the other measurements from different wear stages (IV onwards) will not influence results of the morphological analyses.

5.2.3.3 Ontogeny of the post-crania

Post-cranial sample sizes are small, so only tentative observations can be made. Moreover, material was only sufficient for analysis of the long bones, patella, carpals and tarsals. Most measurements appear to change little with age from P3/p3 wear stage IV. This suggests that after fusion of the epiphyses, the elements do not noticeably change in size. However, no P3/p3 wear stage III specimens were included in the analyses due to lack of data.

Three measurements appear to increase in size with age: the greatest breadth of the distal end of the radius, greatest breadth of the articular surface of the ulna, and greatest breadth of the scapho-lunar.

Change with ontogeny was also assessed in the brachial and crural indices. There is insufficient data to confidently determine whether the crural index changes with age as the value from the wear stage IV individual overlaps with those of the stage IV individuals. However, the brachial index appears to decrease in age in females. This means that the humerus is relatively longer when compared with the radius in older individuals. However, sample sizes are small, so this cannot be confidently concluded.

As there are few Pleistocene specimens with associated cranial material with which the P3/p3 wear stage can be determined, the post-cranial elements that potentially exhibit change with ontogeny will be treated with caution in the analysis of Pleistocene morphometrics.

5.3 Sexual size dimorphism

5.3.1 Introduction

C. crocuta exhibit reverse SSD (i.e. the females are larger than the males), which is uncommon in mammal species (Ralls, 1976; Swanson *et al.*, 2013). This has been observed in body mass (Sillero-Zubiri and Gottelli, 1992; Swanson *et al.*, 2013) and morphological traits measured externally on live individuals: body length, skull length, head circumference, distance from the zygomatic arch to the top of the sagittal crest, distance from the zygomatic arch to the back of the sagittal crest, neck circumference, girth of the torso, shoulder height, scapular length, and upper leg length (Swanson *et al.*, 2013). Female-biased SSD in *C. crocuta* has only been determined in a small number of craniodental elements: canines, carnassials and skull length. Male biased SSD has been observed in the moment arms of the temporalis and superficial masseter, and the moment arm of resistance at the canines (Gittleman and Van Valkenburgh, 1997). Apart from this, there has been little research on SSD in skeletal and dental elements of *C. crocuta*. This study will attempt to address this, through an analysis of SSD of a large population of recent *C. crocuta* from Balbal, Tanzania. Additionally, SSD will be calculated for body mass, bones and teeth from other localities across Africa, in order to assess whether there is any geographical variation in SSD, and if so, whether there are any environment correlates. The SSD values of other African predators have also been calculated so that *C. crocuta* SSD values can be put into context.

The research questions are as follows:

- In which morphological features does *C. crocuta* exhibit SSD?
- Does SSD vary between populations across Africa?
- If so, do these variations follow Rensch's Rule?
- Do temperature, precipitation and vegetation correlate with variations in the degree of SSD?

5.3.2 Results

5.3.2.1 Body mass

The degree of SSD in *C. crocuta* body mass is not constant (Table 5.14). Calculated values range from 0.003 in South Africa to 0.086 in the Kruger National Park, South Africa, with females larger than males. Furthermore, there is one location, Botswana, where males were recorded as being heavier than females with an SSD value of -0.052.

To put the *C. crocuta* values into context, SSD values have been calculated for other large African predators (Figure 5.19 and Appendix 10.5, Table 10.11 to Table 10.15). All species exhibit predominantly male-biased SSD, except for *L. pictus* for which there is only a single data point with a very low value of 0.009 indicating little difference between males and females. With values between 0.097 and 0.277, *P. pardus* exhibits greater SSD than *C. crocuta*. The SSD values of *P. leo*, *A. jubatus*, and *P. brunnea* all overlap the upper range of *C. crocuta* values, yet these species have greater SSD than *C. crocuta* at some sites.

Table 5.14: Recent *C. crocuta* calculations of sexual size dimorphism SSD. Positive values indicate that females are larger.

Country	Location	SSD
Botswana		-0.052
Kenya	Aberdare National Park	0.039
Kenya	Maasai Mara National Reserve	0.044
Kenya	Narok District	0.066
South Africa		0.036
South Africa	Hluhluwe-iMfolozi Park	0.022
South Africa	iMfolozi Game Reserve	0.085
South Africa	Kalahari Gemsbok National Park	0.08
South Africa	Kruger National Park	0.086
South Africa	Kruger National Park	0.038
South Africa and Zimbabwe	Transvaal and Zimbabwe	0.05
Southern Africa		0.003
Tanzania	Serengeti	0.055
Zambia		0.003

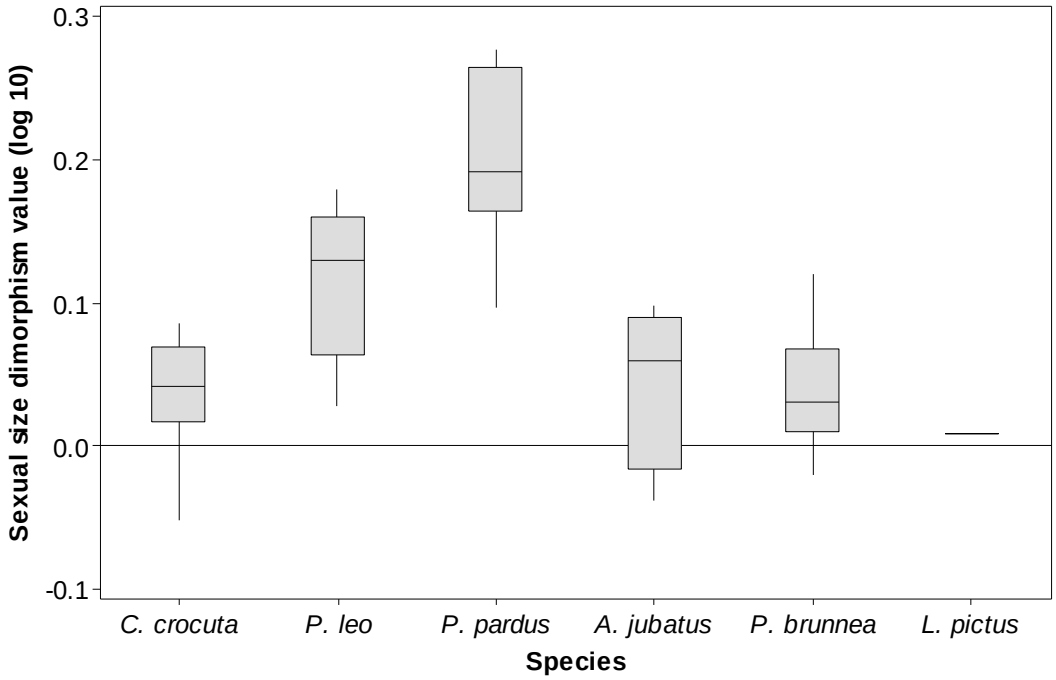

Figure 5.19: Box plot of sexual size dimorphism values of recent large carnivore body masses from sites in Africa. Positive values for *C. crocuta* indicate that females are larger. Positive values for *P. leo*, *P. pardus*, *A. jubatus*, *P. brunnea* and *L. pictus* indicate that males are larger. *C. crocuta* n = 14. *P. leo* n = 11. *P. pardus* n = 7. *A. jubatus* n = 4. *P. brunnea* n = 6. *L. pictus* n = 1.

In order to assess whether SSD varies with body size, a reduced major axis regression was performed on base-10 logarithmically transformed female body mass against base-10 logarithmically transformed male body mass (Figure 5.20). The Pearson's r correlation value is high at 0.929, and is significant at 95 % with a p-value of 0.0003. The slope is 1.057. The 95 % bootstrapped confidence intervals are 0.759-1.345, which span the regression slope value of 1.

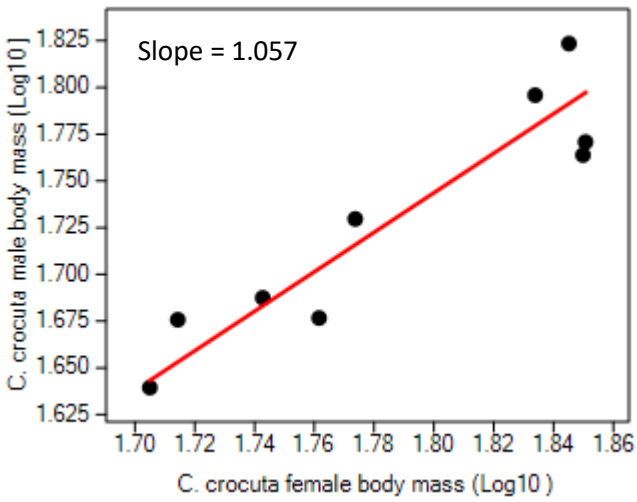

Figure 5.20: Reduced major axis regression of base-10 logarithmically transformed *C. crocuta* female body mass and base-10 logarithmically transformed *C. crocuta* male body mass (n = 9).

Sample sizes are too small to run a PLS regression with *C. crocuta* body mass SSD as the dependent variable. As running individual regression increases the likelihood of Type I errors, individual Spearman Rank Order correlations were performed. These assessed the correlation between *C. crocuta* body mass SSD and *C. crocuta* density, *P. leo* density, prey biomass, minimum temperature of the coolest month, maximum temperature of the warmest month, precipitation of the driest month, precipitation of the wettest month, closed vegetation cover, semi-open vegetation cover and open vegetation cover.

All correlations are insignificant at 95 % confidence (Table 5.15). The strongest correlation is against semi-open vegetation cover with an r_s value of 0.544.

Table 5.15: Spearman Rank Order statistics of *C. crocuta* body mass SSD against each variable (n = 9).

Variable	r_s	p-value
***C. crocuta* density**	-0.259	0.5
***P. leo* density**	-0.326	0.391
Prey biomass	-0.243	0.529
Min. temp. coolest month	-0.168	0.666
Max. temp. warmest month	0.37	0.327
Precipitation driest month	-0.37	0.327
Precipitation wettest month	-0.343	0.366
Closed vegetation cover	-0.293	0.444
Semi-open vegetation cover	0.544	0.13
Open vegetation cover	-0.326	0.391

5.3.2.2 Crania and dentition

The degree of SSD was calculated for cranial and dental measurements from localities across Africa. In light of the results in Section 5.2, specimens with P3/p3 wear stages of III were excluded from the cranial and mandibular analyses. Additionally, SSD of the breadth of the occiput condyles, breadth of the auditory meatus, mandible depths, and mandibular bending strength indices at each wear stage were assessed separately.

With values between -0.059 and 0.063 (Figure 5.21), the SSD of teeth is small. None of the dental measurements show consistent positive (females are larger) or negative (males are larger) SSD values. The SSD values of cranial measurements (Figure 5.22) similarly do not show consistent positive or negative values. The values have a larger range from -0.066 to 0.077, but are still low.

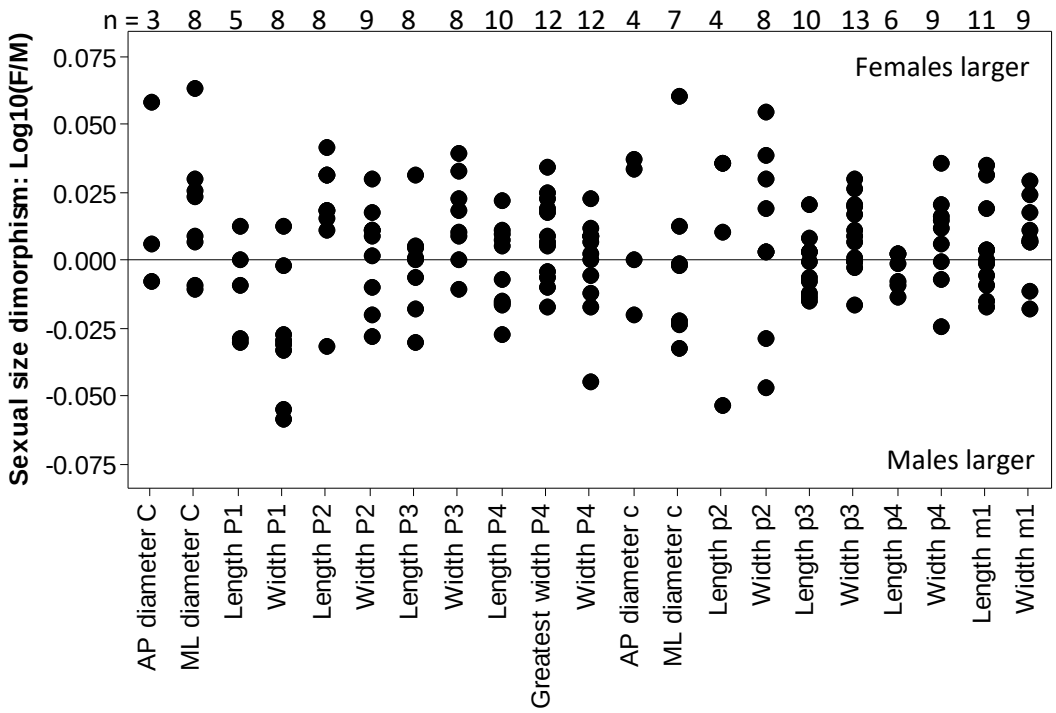

Figure 5.21: SSD values of *C. crocuta* dental measurements from localities across Africa. Positive values indicate females are larger, negative values indicate males are larger. AP = anteroposterior. ML = mediolateral.

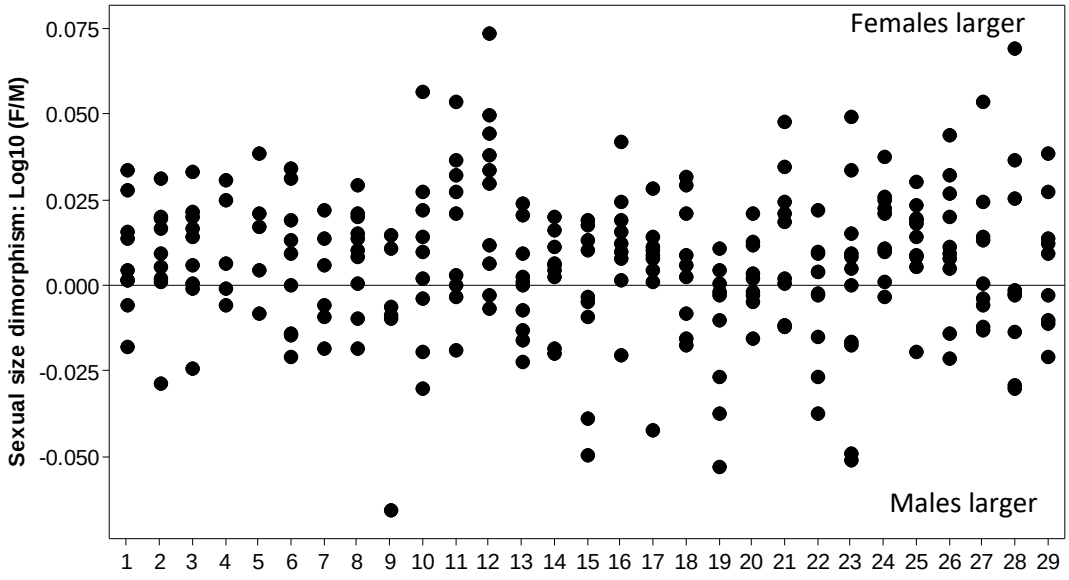

Figure 5.22: SSD values of *C. crocuta* cranial measurements from localities across Africa. Positive values indicate females are larger, negative values indicate males are larger. 1. Total length of cranium (9). 2. Condylobasal length (9). 3. Basal length (9). 4. Basicranial axis (5). 5. Basifacial axis (5). 6. Upper neurocranium length (9). 7. Viscerocranium length (6). 8. Facial length (10). 9. Greatest length of the nasals (6). 10. Snout length (9). 11. Median palatal length (9). 12. Length of the horizontal part of the palatine (10). 13. Length of the cheektooth row (P1-P4) (10). 14. Length of the cheektooth row (P1-P3) (9). 15. Greatest diameter of the auditory bulla (9). 16. Greatest mastoid breadth (9). 17. Greatest breadth of the bases of the paraoccipital processes (9). 18. Greatest breadth of the foramen magnum (9). 19. Height of the foramen magnum (9). 20. Greatest neurocranium breadth (9). 21. Zygomatic breadth (9). 22. Least breadth of the skull (10). 23. Least breadth between the orbits (11). 24. Greatest palatal breadth (9). 25. Least palatal breadth (10). 26. Greatest height of the orbit (10). 27. Skull height (9). 28. Height of the occipital triangle (9). 29. Temporal fossa length (9). Numbers in brackets indicate sample sizes.

The SSD values of the mandibular linear measurements show a different pattern (Figure 5.23). Again, none of the measurements have values that are consistently positive or negative. However, many of the measurements have only one negative SSD value. These measurements are the lengths of the condyle to the symphysis, canine, and p2/p3; lengths of the angular process to the symphysis and canine; lengths of the notch between the condyle and angular processes to the symphysis and canine; height of the ramus; width at p2/p3; moment arm of resistance at the canine. This negative SSD value derives from the same locality for all these

measurements: Parc National de l'Upemba, from which there is only one female and one male specimen. Nevertheless, the positive SSD values are still low for these measurements, with a maximum of 0.05. Across all measurements, the SSD values range from -0.054 to 0.105. This range is greater than that for the dental and cranial SSD values, although one measurement (mandibular width behind the m1) accounts for much of this variation.

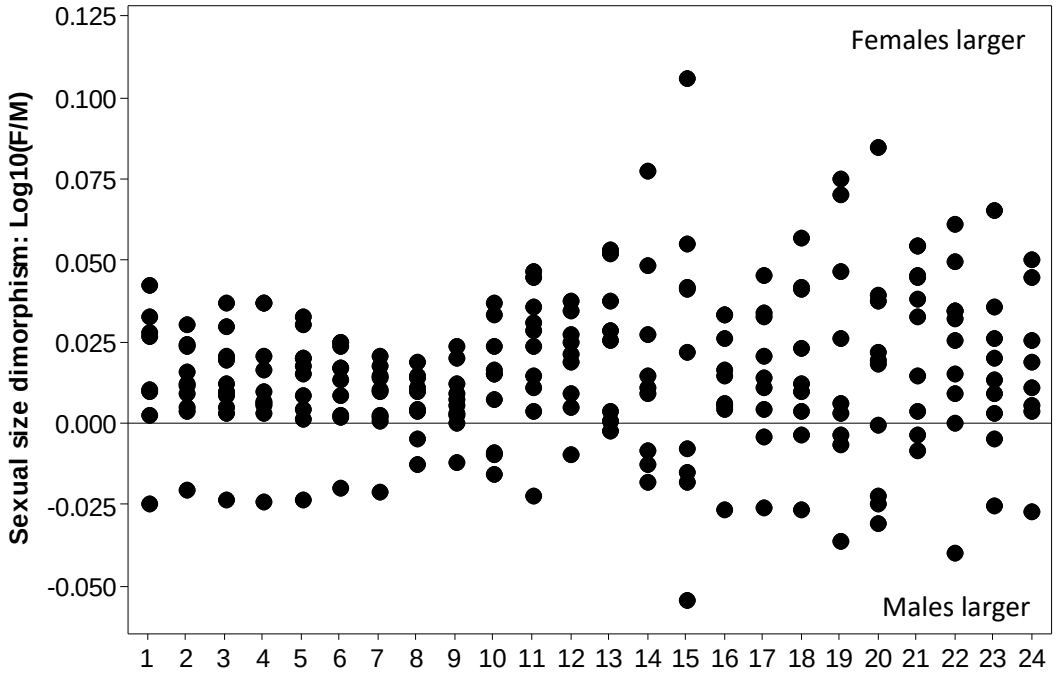

Figure 5.23: SSD values of *C. crocuta* mandibular measurements from localities across Africa. Positive values indicate females are larger, negative values indicate males are larger. 1. Condyle to symphysis length (8). 2. Angular process to symphysis length (10). 3. Condyle/angular indentation to symphysis length (10). 4. Condyle to c alveolus length (10). 5. Condyle/angular indentation to c alveolus length (10). 6. Angular process to c alveolus length (10). 7. c alveolus to m1 alveolus length (10). 8. Length of cheektooth row (p2 – m1) (9). 9. Length of cheektooth row (p3 – m1) (10). 10. Length of premolar row (p2 – p4) (10). 11. Height of the vertical ramus (10). 12. Mandibular width at p2/p3 (9). 13. Mandibular width at p3/p4 (9). 14. Mandibular width at p4/m1 (9). 15. Mandibular width at post-m1 (9). 16. Distance from p2/p3 to middle of articular condyle (9). 17. Distance from p3/p4 to middle of articular condyle (9). 18. Distance from p4/m1 to middle of articular condyle (9). 19. Distance from post-m1 to middle of articular condyle (9). 20. Moment arm of the superficial masseter (10). 21. Moment arm of the temporalis (10). 22. Masseteric fossa length (10). 23. Moment arm of resistance at m1 (9). 24. Moment arm of resistance at c (8). Numbers in brackets indicate sample sizes.

In light of the results from Section 5.2 that the frontal breadth, breadth of the occipital condyles, breadth external to the auditory meatus, mandibular depth and mandibular bending strength change in size through the life of an individual, SSD of these features was calculated once data were split into different wear stages. The SSD values of frontal breadth, breadth of the occipital condyles, and breadth external to the auditory meatus (Figure 5.26) are both positive and negative for wear stages V and VI. The SSD values at wear stage IV are positive, however, this result is comprised of data from only two sites. The SSD values are low, ranging from -0.03 to 007 for frontal breadth, -0.014 to 0.028 for the breadth of the occipital condyles, and -0.034 to 0.039 for the breadth external to the auditory meatus.

The SSD values of mandibular depths show some pattern with wear stage (Figure 5.27). All SSD values are positive at all interdental gaps at wear stage IV. At wear stage V, values are positive and negative for all interdental gaps. There are only two samples at wear stage VI. Both are negative, although the value for the p3/p4 interdental gap is close to zero at -0.002. Overall, the SSD values are low for all measurements, ranging from -0.054 to 0.051.

The SSD values for bending strength (Figure 5.28 and Figure 5.29) indicate that at wear stage IV, SSD values are positive at all interdental positions in the dorsoventral plane (zx/L), and at all points in the labiolingual plane (zy/L) except for the post-m1 position. At wear stage V, some sites have positive SSD values and some have negative values. At wear stage VI, the SSD values are negative. However, this is based on only one site. Some SSD values are high, ranging from -0.212 to 0.211 for zx/L, and from -0.235 to 0.265 for zy/L.

As shown in Figure 5.30, there are few measurements with consistently positive or negative SSD values of the relative mandibular bending strengths in the labiolingual and dorsoventral planes (zx/zy). This is except for the wear stage IV p4/m1 position with negative values, the wear stage IV post-m1 position with positive values, and both VI positions with positive values. However, sample sizes are again low. SSD values are also low, ranging from -0.091 to 0.047.

In contrast to the linear mandibular measurements, the mechanical advantage of the temporalis and masseter exhibit no consistent positive or negative SSD values (Figure 5.31). All SSD values are low, ranging between -0.087 and 0.076.

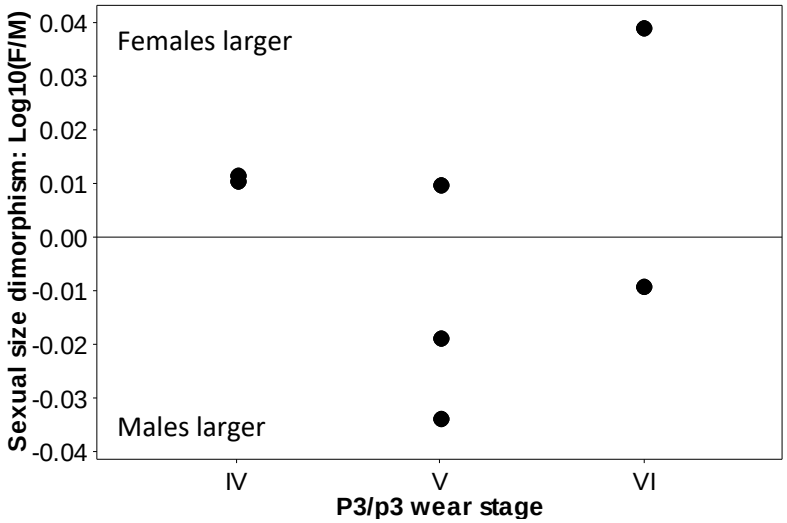

Figure 5.24: SSD values of *C. crocuta* breadth dorsal to the external meatus. From localities in Africa.

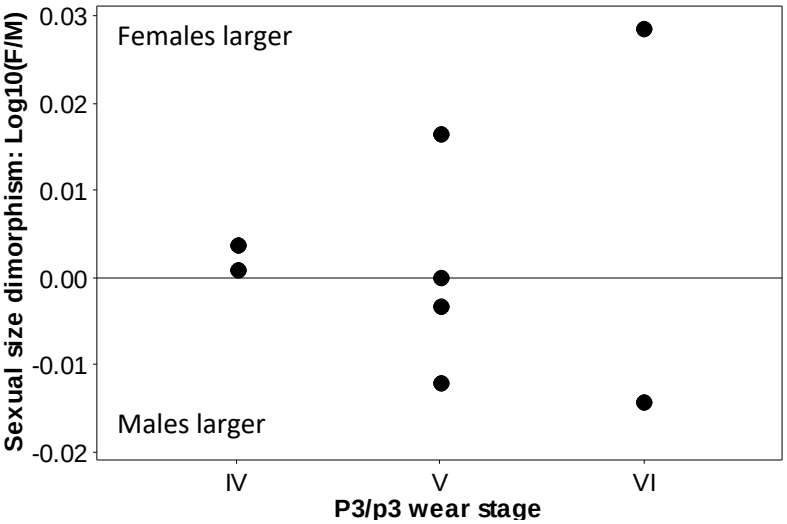

Figure 5.25: SSD values of *C. crocuta* breadth of the occipital condyles, from localities in Africa.

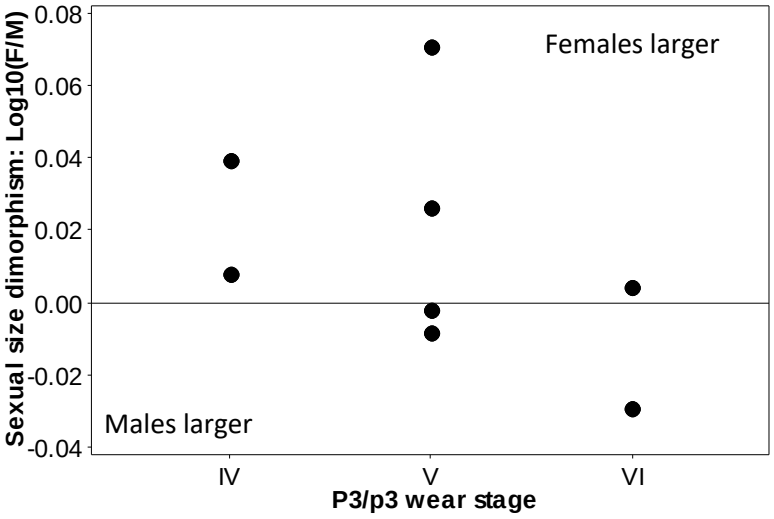

Figure 5.26: SSD values of *C. crocuta* frontal breadth, from localities in Africa.

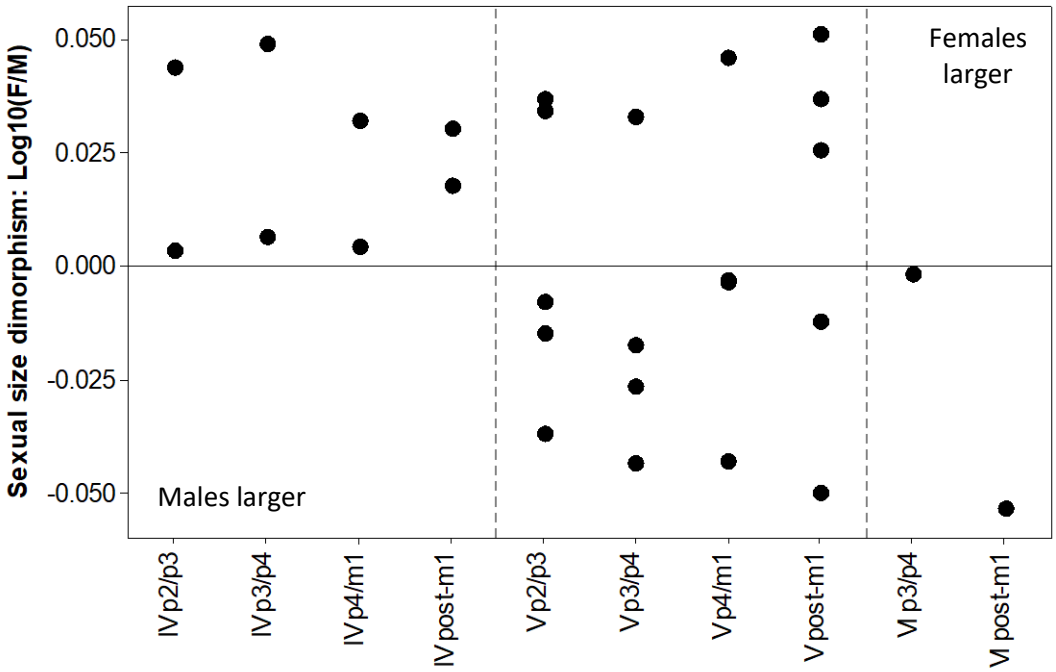

Figure 5.27: SSD values of *C. crocuta* mandibular depths at each interdental gap, from localities in Africa. IV, V and VI indicate P3/p3 wear stages.

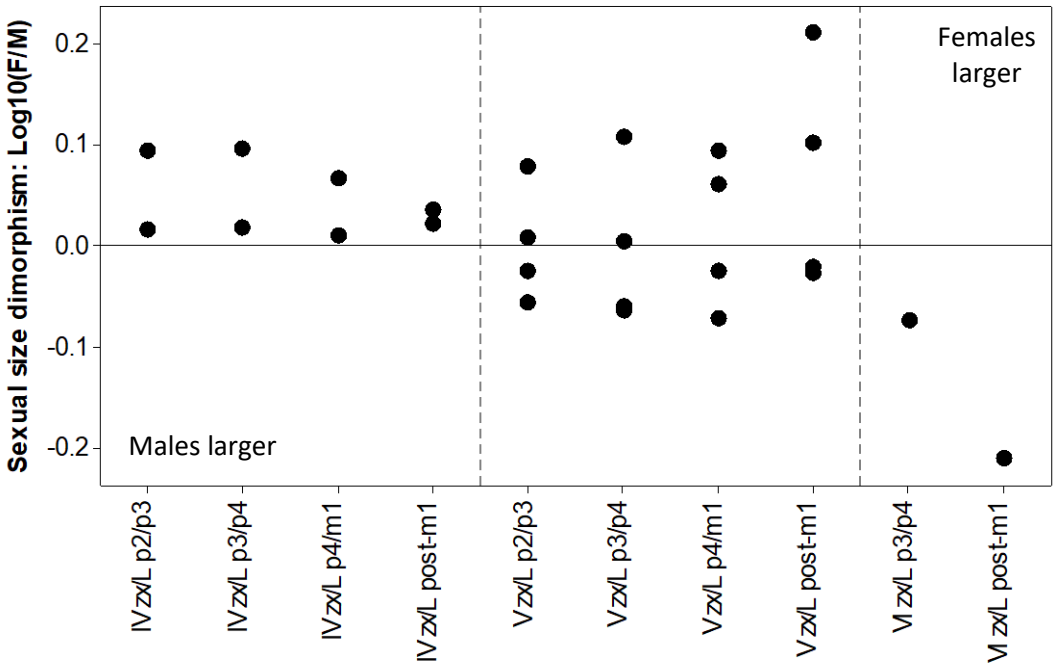

Figure 5.28: SSD values of *C. crocuta* mandibular bending strength in the dorsoventral plane (zx/L) at each interdental gap, from locations in Africa.

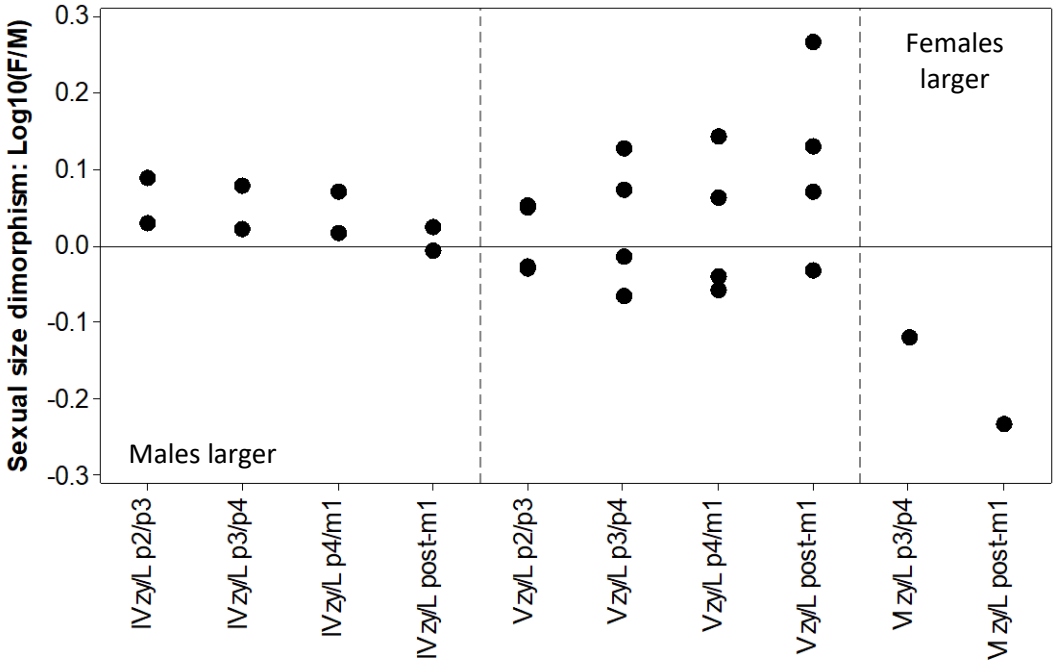

Figure 5.29: SSD values of *C. crocuta* mandibular bending strength in the labiolingual plane (zy/L) at each interdental gap, from locations in Africa.

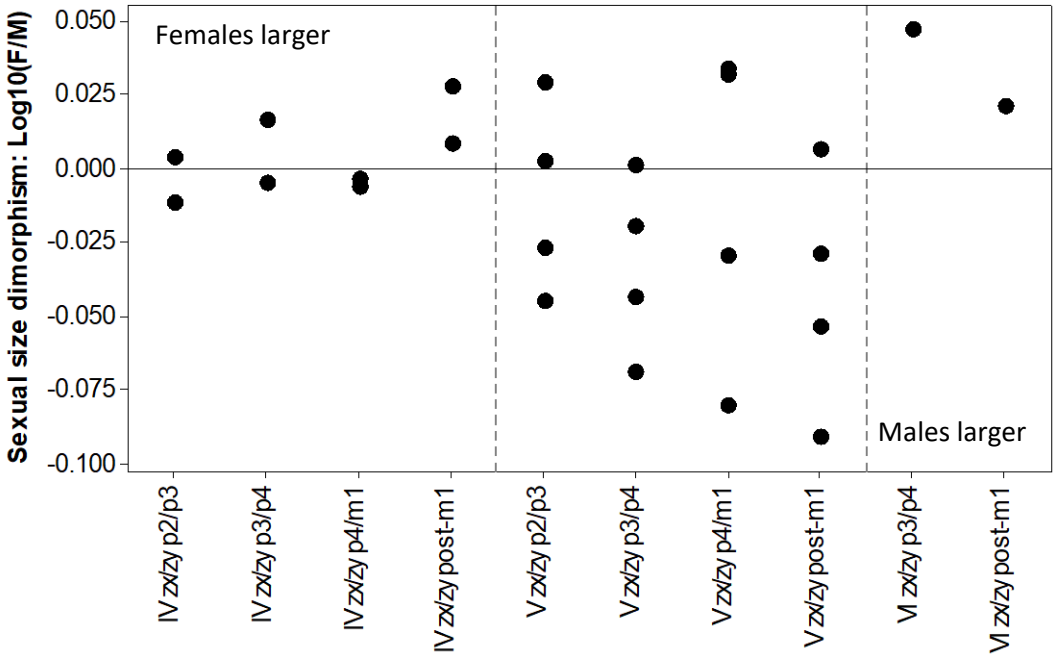

Figure 5.30: Figure 5.28: SSD values of *C. crocuta* relative mandibular bending strength in the dorsoventral and labiolingual planes (zx/zy) at each interdental gap, from locations in Africa.

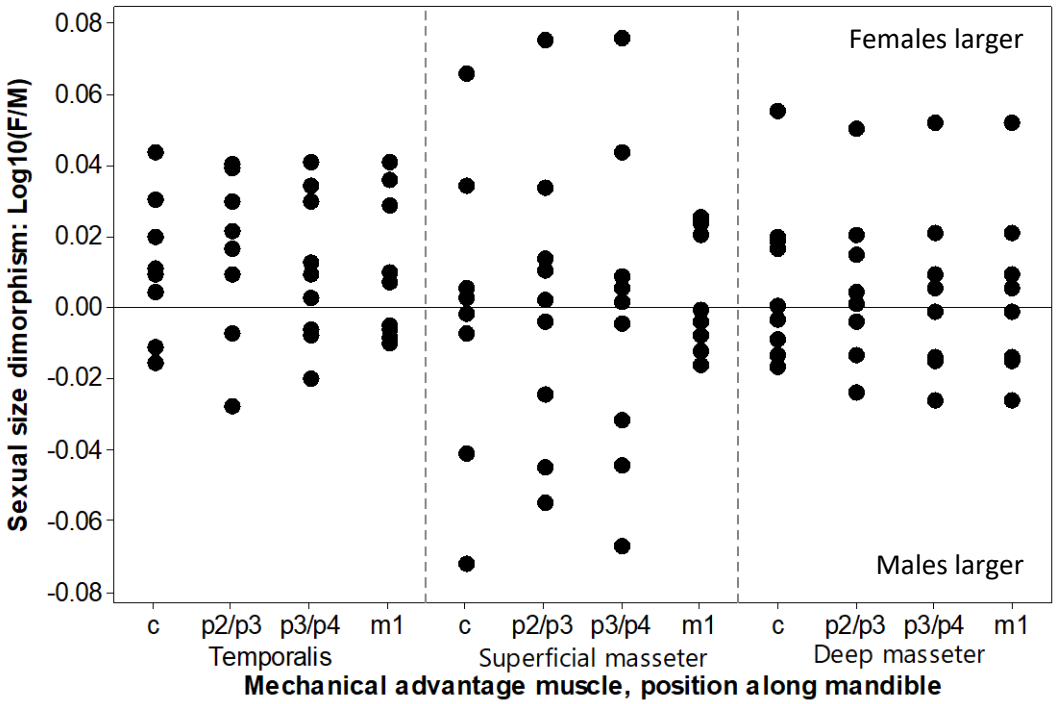

Figure 5.31: SSD values of *C. crocuta* indices of mechanical advantage of the masticatory muscles from localities in Africa. Positive values indicate females are larger, negative values indicate males are larger. Sample sizes for mechanical advantage: at the canines (n = 8), at p2/p3 (n = 9), at p3/p4 (n = 9), at m1 (n = 9).

To further assess the extent to which SSD is reflected in *C. crocuta* cranial, mandibular and dental measurements, tests for statistical significance were conducted. The t-tests and Mann Whitney tests (in the case of non-normally distributed data) compared male and females measurements of specimens from Balbal, Tanzania. Due to small sample sizes, these tests were not performed on the anteroposterior lengths of the upper and lower canines, the basicranial axis, basifacial axis and viscerocranium length. Additionally, these tests were not performed on those measurements that change in size through life, again due to small sample sizes in each P3/p3 wear category.

The results show that there are no significant differences at 95 % confidence between males and females in any measurement (Table 5.16 – Table 5.19). This is also true for the mandibular measurements that appear to be larger in females, as shown in Figure 5.23. Additionally, there are no significant differences between males and females of mechanical advantages of the masticatory muscles at any bite point along the mandible.

Table 5.16: Results of t-tests and Mann Whitney tests comparing male and female *C. crocuta* dental measurements of specimens from Balbal, Tanzania.

Test	Mediolateral diameter of C	Length of P1	Width of P1	Length of P2	Width of P2	Length of P3	Width of P3	Length of P4	Greatest width of P4	Width of P4
t-test										
t-value	1.28		1.16	1.77		0.56		1.04	0.94	1.21
p-value	0.217		0.256	0.09		0.581		0.307	0.355	0.237
Mann Whitney										
W-value		294.5			415.5		336			
p-value		0.857			0.152		0.479			

Test	Mediolateral diameter of c	Length of p2	Width of p2	Length of p3	Width of p3	Length of p4	Width of p4	Length of m1	Width of m1
t-test									
t-value	0.24		0.26		1.31	0.3	1.71	0.65	0.99
p-value	0.815		0.799		0.198	0.765	0.096	0.522	0.333
Mann Whitney									
W-value		420.5		384					
p-value		0.223		0.494					

Table 5.17: Results of t-tests and Mann Whitney tests comparing male and female *C. crocuta* cranial measurements of specimens from Balbal, Tanzania.

Test	Total length of cranium	Condylobasal length	Basal length	Upper neurocranium length	Facial length	Greatest length of the nasals	Snout length	Median palatal length	Length of the horizontal part of the palatine	Length of the cheektooth row (P1-P4)	Length of the cheektooth row (P1-P3)	Greatest diameter of the auditory bulla	Greatest mastoid breadth	Greatest breadth of bases of paraoccipital processes
t-test														
t-value	0.76		0.11	0.01	1.18	1.09	0.23	0.38	0.25		0.38	0.62	0.28	0.12
p-value	0.453		0.917	0.988	0.254	0.29	0.817	0.707	0.808		0.71	0.541	0.784	0.908
Mann Whitney														
W-value		228								351				
p-value		0.645								0.316				

Test	Greatest breadth of the foramen magnum	Height of the foramen magnum	Greatest neurocranium breadth	Zygomatic breadth	Least breadth of the skull	Frontal breadth	Least breath between the orbits	Greatest palatal breadth	Least palatal breadth	Greatest height of the orbit	Skull height	Height of the occipital triangle	Temporal fossa length
t-test													
t-value	0.15	0.94	0.3	0.1	0.22	0.27	0.01	0.19		1.79	0.12	0.2	0.56
p-value	0.879	0.352	0.766	0.921	0.827	0.793	0.993	0.854		0.085	0.903	0.847	0.581
Mann Whitney													
W-value									280				
p-value									0.278				

Table 5.18: Results of t-tests and Mann Whitney tests comparing male and female *C. crocuta* mandibular measurements of specimens from Balbal, Tanzania.

Test	Condyle to symphysis length	Angular process to infradentlale length	Condyle/angular indentation to symphysis length	Condyle to c alveolus length	Condyle/angular indentation to c alveolus length	Angular process to c alveolus length	c alveolus to m1 alveolus length	Length of cheektooth row (p2 – m1)	Length of cheektooth row (p3 – m1)	Length of premolar row (p2 – p4)	Height of the vertical ramus	Mandibular width at p2/p3	Mandibular width at p3/p4	Mandibular width at p4/m1	Mandibular width at post-m1
t-test															
t-value	0.46		0.55	0.58	0.21	0.3	0.29	0.68	0.57	1.29	0.52	0.46	0.26	0.75	1.57
p-value	0.651		0.589	0.566	0.838	0.763	0.776	0.503	0.57	0.209	0.608	0.649	0.798	0.458	0.125
Mann Whitney															
W-value		292													
p-value		0.439													

Test	Distance from p2/p3 to middle of articular condyle	Distance from p3/p4 to middle of articular condyle	Distance from p4/m1 to middle of articular condyle	Distance from post-m1 to middle of articular condyle	Moment arm of the temporalis	Moment arm of the superficial masseter	Moment arm of the deep masseter	Moment arm of resistance at c	Moment arm of resistance at m1
t-test									
t-value	0.76	0.89	0.61	0.39	0.55	0.15	0.01	0.59	0.45
p-value	0.454	0.379	0.545	0.698	0.587	0.879	0.994	0.561	0.655

Table 5.19: Results of t-tests comparing male and female *C. crocuta* masticatory muscle mechanical advantage calculations of specimens from Balbal, Tanzania.

t-test statistic	**Moment arm temporalis/ moment arm resistance c**	**Moment arm temporalis/ moment arm resistance p2-p3**	**Moment arm temporalis/ moment arm resistance p3-p4**	**Moment arm temporalis/ moment arm resistance centre m1**	**Moment arm superficial masseter/ moment arm resistance c**	**Moment arm superficial masseter/ moment arm resistance p2-p3**	**Moment arm superficial masseter/ moment arm resistance p3-p4**	**Moment arm superficial masseter/ moment arm resistance centre m1**	**Moment arm deep masseter/ moment arm resistance c**	**Moment arm deep masseter/ moment arm resistance p2-p3**	**Moment arm deep masseter/ moment arm resistance p3-p4**	**Moment arm deep masseter/ moment arm resistance centre m1**
t-value	1.68	1.14	1.24	1.27	0.29	0.59	0.64	0.41	0.6	0.54	0.59	0.2
p-value	0.106	0.264	0.226	0.212	0.773	0.561	0.528	0.687	0.556	0.595	0.563	0.846

Conformity to Rensch's Rule was assessed through reduced major axis regressions and accompanying Pearson correlation on the mandibular measurements that appear to exhibit SSD (Table 5.20 and Figure 5.32). Condylobasal and m1 lengths were also included because these measurements scale closely with overall body size (Van Valkenburgh, 1990).

Only three of the 12 measurements have significant linear correlations between males and females at 95 % confidence (m1 length, mandibular ramus height, width of the mandible at p2/p3). The associated Pearson's r correlation value is highest for these measurements. Moment arm of resistance at the canine has a very low Pearson's r value of 0.031. This statistic and Figure 5.32 show that there is very little correlation between male and female sizes. Except for mandibular ramus height, all measurements have slope values that are greater than one. However, the 95 % bootstrapped confidence intervals of the slope all span one for every measurement.

Table 5.20: Results of reduced major axis regressions, with base-10 logarithmically transformed *C. crocuta* female measurements on the x-axis, and base-10 logarithmically transformed *C. crocuta* male measurements on the y-axis. Statistics include Pearson's r correlation and associated p-value. Also shown are the regression slope values, with associated 95 % bootstrapped confidence intervals of the slope.

Statistic	Condylobasal length	m1 length	Mandibular condyle to symphysis	Angular process to symphysis	Condyle/angular indentation to symphysis	Mandibular condyle to c
Pearson's r	0.553	0.816	0.295	0.557	0.45	0.443
p-value	0.123	0.002	0.478	0.094	0.192	0.199
Slope	1.664	1.078	1.494	1.459	1.681	1.376
Min. CI	0.373	0.452	0.296	0.217	-0.315	0.406
Max. CI	2.566	1.424	5.983	2.179	6.7	4.768

Statistic	Angular process to c	Condyle/angular indentation to c	Mandibular ramus height	Mandibular width at p2/p3	Mandibular condyle to p2/p3	Moment arm of resistance at c
Pearson's r	0.601	0.461	0.638	0.859	0.331	0.031
p-value	0.066	0.179	0.047	0.003	0.384	0.942
Slope	1.314	1.443	0.966	1.117	1.505	1.976
Min. CI	0.578	0.195	0.547	-0.102	0.405	0.972
Max. CI	1.967	5.152	1.451	1.42	5.766	9.804

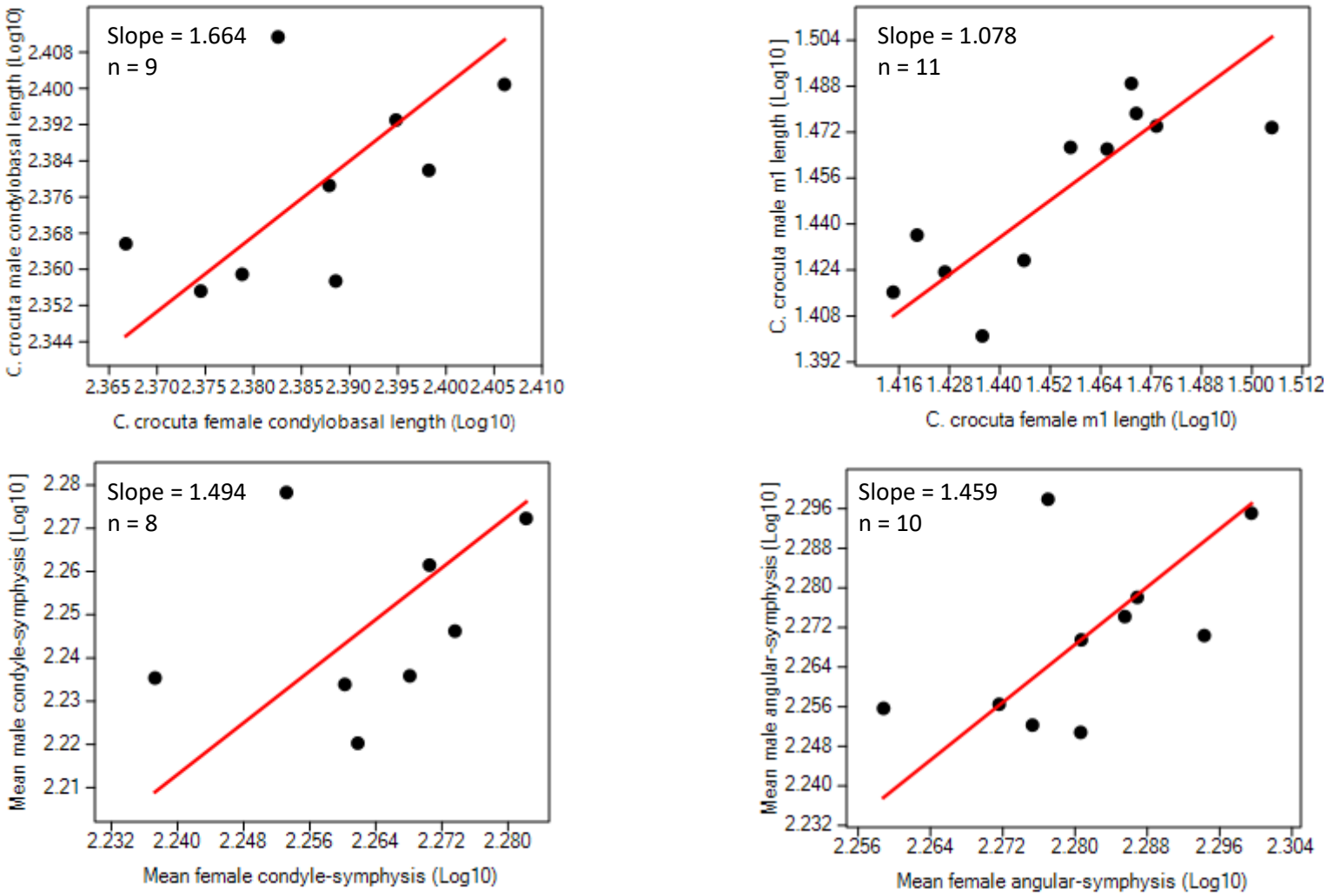

Figure 5.32: Reduced major axis regression of Log10 male *C. crocuta* measurements against Log10 female *C. crocuta* measurements.

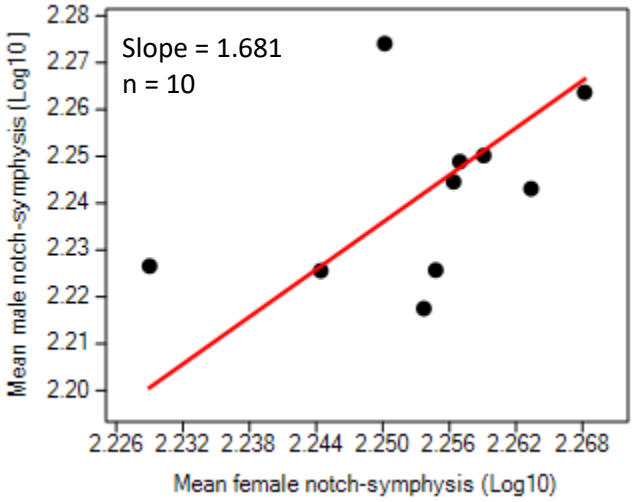

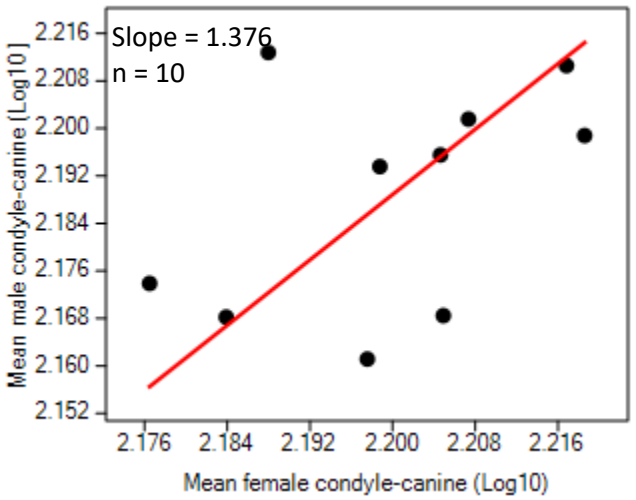

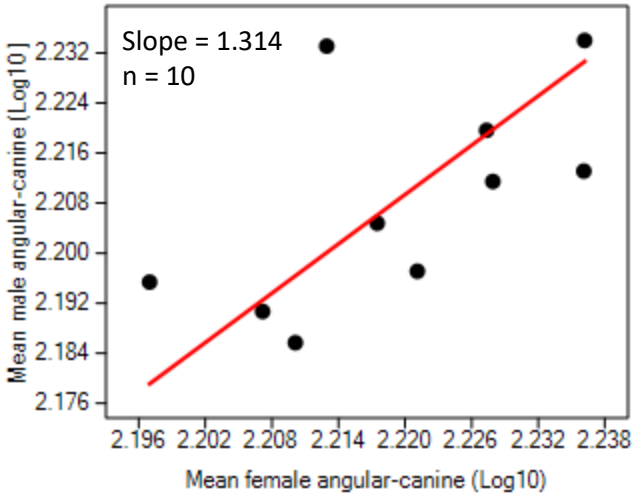

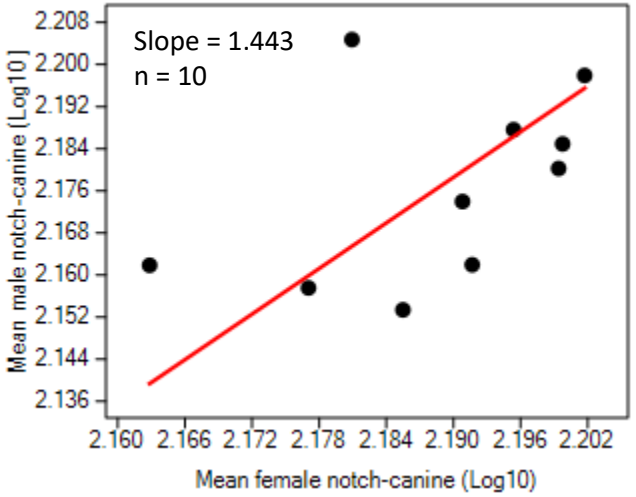

Figure 5.32 continued.

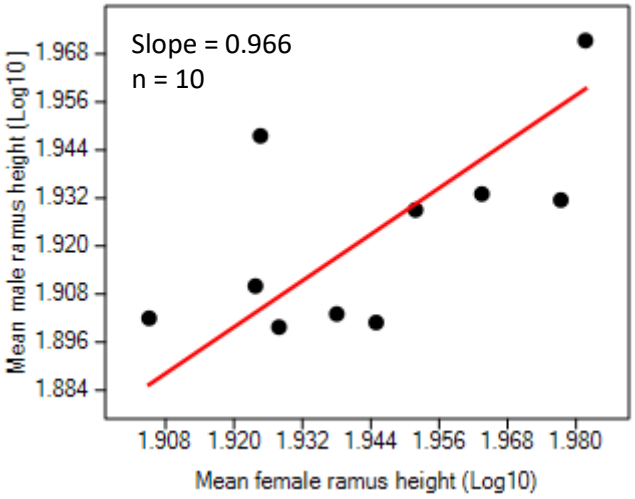

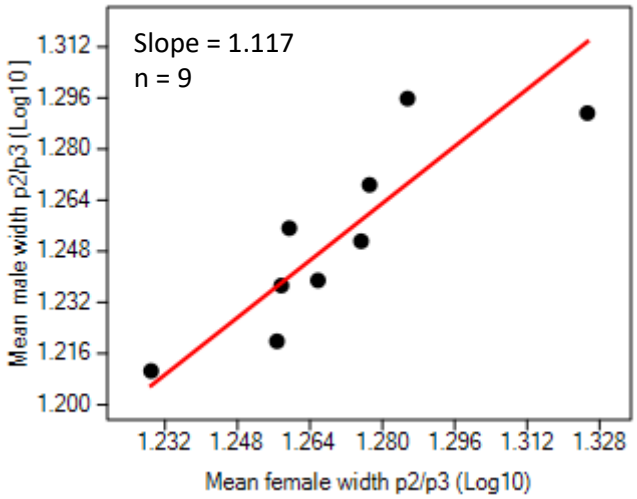

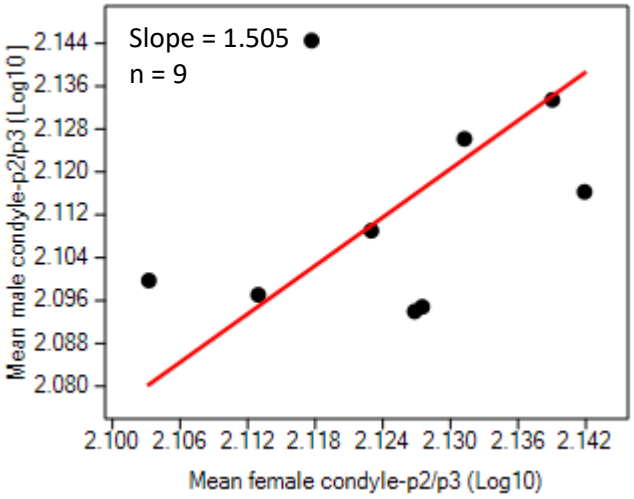

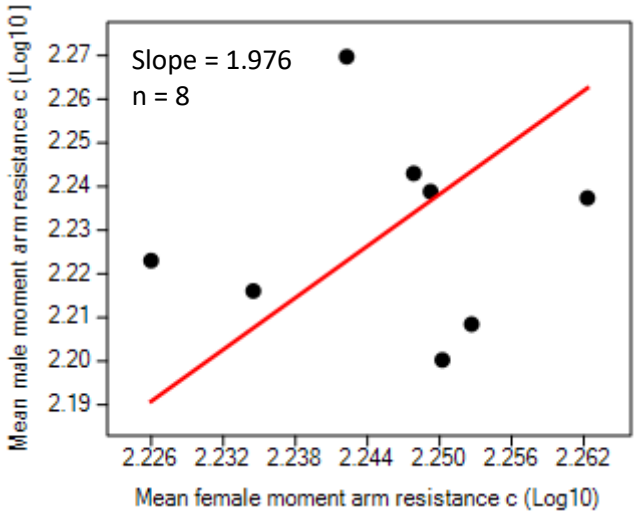

Figure 5.32 continued.

Craniodental SSD sample sizes are too small to run PLS regressions. Spearman Rank Order correlations were performed in order to avoid the elevated chance of Type I errors associated with individual regression models. The mandibular measurements that potentially exhibit SSD were included. Condylobasal length and m1 length were also included as these scale closely with body mass (Van Valkenburgh, 1990). The tests assessed the correlation of these craniodental variables against the following environmental variables: minimum temperature of the coolest month, maximum temperature of the warmest month, precipitation of the driest month, precipitation of the wettest month, close vegetation cover, semi-open vegetation cover and open vegetation cover.

The results are insignificant at 95 % confidence (Table 5.21). The exception is the negative correlation between the mandibular condyle to symphysis length and closed vegetation cover (r_s = -0.886, p-value = 0.019). However, this value is insignificant when the Bonferroni correction is applied, which means the p-value is only significant if less than 0.071. While the correlations between closed vegetation cover and the other mandibular measurements are all insignificant, they are also all negative. Correlations of the mandibular measurements with precipitation of the driest month and open vegetation cover are also all consistently positive.

Table 5.21: Spearman Rank Order statistics of *C. crocuta* craniodental SSD values against environmental variables. The top number is the rs value. The bottom number is the p-value. All variables except vegetation were base-10 logarithmically transformed prior to the analyses. The vegetation variables were centred log ratio transformed. Bonferroni corrected p-value = 0.0071. Shaded section is significant at 95 % uncorrected confidence (p<0.05).

	Condylobasal length	m1 length	Mandibular condyle to symphysis	Angular process to symphysis	Condyle/angular indentation to symphysis	Mandibular condyle to c	Angular process to c	Condyle/angular indentation to c	Mandibular ramus height	Mandibular width at p2/p3	Mandibular condyle to p2/p3	Moment arm of resistance at c
No. sites	7	9	6	8	8	8	8	8	8	7	7	6
Min. temp. coolest month	0.321 0.482	-0.217 0.576	0.143 0.787	0.381 0.352	0.405 0.32	-0.048 0.911	0.381 0.352	0.405 0.32	0.545 0.16	0 1	0.321 0.482	0.257 0.623
Max. temp. warmest month	0 1	-0.383 0.308	0.143 0.787	0.262 0.531	0.143 0.736	0.262 0.531	0.262 0.531	0.143 0.736	0.5 0.207	-0.107 0.819	0 1	0.143 0.787
Precipitation driest month	0.667 0.102	-0.131 0.738	0.638 0.173	0.61 0.108	0.708 0.05	0.22 0.601	0.61 0.108	0.708 0.05	0.512 0.194	0.523 0.229	0.667 0.102	0.667 0.148
Precipitation wettest month	-0.286 0.535	-0.017 0.966	-0.257 0.623	-0.048 0.911	-0.143 0.736	0.048 0.911	-0.048 0.911	-0.143 0.736	0.048 0.911	-0.107 0.819	-0.286 0.535	-0.257 0.623
Closed vegetation cover	-0.75 0.052	0.383 0.308	-0.886 0.019	-0.452 0.26	-0.476 0.233	-0.5 0.207	-0.452 0.26	-0.476 0.233	-0.214 0.61	-0.464 0.294	-0.75 0.052	-0.714 0.111
Semi-open vegetation cover	-0.429 0.337	-0.633 0.067	-0.314 0.544	-0.333 0.42	-0.405 0.32	-0.19 0.651	-0.071 0.867	-0.405 0.32	-0.071 0.867	0.143 0.76	-0.429 0.337	-0.543 0.266
Open vegetation cover	0.643 0.119	0.35 0.356	0.6 0.208	0.619 0.102	0.643 0.086	0.333 0.42	0.405 0.32	0.643 0.086	0.405 0.32	0.036 0.939	0.643 0.119	0.714 0.111

5.3.2.3 Post-crania

To assess further the difference in size between male and female *C. crocuta*, SSD values were calculated for measurements of the post-crania. Unfortunately, due to the relative scarcity of post-cranial specimens, SSD values could be calculated from only two sites: Site 6.11. (Parc National de l'Upemba, Democratic Republic of Congo), and Site 10.5 (Mount Kenya National Park, Kenya). Due to lack of data, SSD values were only calculated for some of the post-cranial bones: axis, scapula, pelvis, humerus, radius, ulna, femur, fibula, astragalus and calcaneum. Additionally, due to small sample sizes, the brachial and crural indices could not be calculated. As the results of the ontogenetic size change assessment suggested little change with age in most measurements (Section 5.2.2.3), data from individuals for all wear stages were combined. This is except for the greatest breadth of the distal articular surface of the radius and the greatest breadth of across the proximal articular surface of the ulna, which potentially exhibited change through ontogeny and were thus excluded. The greatest depth of the femoral head was included, but was only calculated using two individuals from Site 6.11, both of which are wear stage V.

The SSD values are not consistently positive or negative. However, where there are two samples for the femoral measurements, the SSD values have the same sign. The smallest breadth of the radial diaphysis is larger in females in Site 6.11, yet is larger in males in Site 10.5. The values range from -0.073 to 0.038. These are low compared with the more sexually dimorphic species (*P. leo* and *P. pardus*) in Figure 5.19.

Table 5.22: Sexual size dimorphism values of present-day *C. crocuta*. Positive values indicate females are larger. Negative values indicate males are larger. A = Site 6.11, Parc National de l'Upemba, Democratic Republic of Congo. B = Site 10.5,Mount Kenya National Park, Kenya.

	Atlas			**Scapula**				**Pelvis**					
Site	Greatest breadth over the wings	Greatest length	Greatest breadth of the cranial articular surface	Smallest length of the neck	Greatest length of the glenoid process	Length of the glenoid cavity	Breadth of the glenoid cavity	Greatest length of one half	Length of the acetabulum on the rim	Smallest height of the ilium shaft	Smallest breadth of the ilium shaft	Inner length of the obturator foramen	Greatest breadth across the coxal tuberosity
A	-0.041	-0.025	0.0003	-0.009	-0.027	-0.008	-0.052	-0.011	0.035	-0.013	-0.029	-0.058	-0.073

	Pelvis			**Humerus**			**Radius**			**Ulna**		
Site	Greatest breadth across the acetabulum	Greatest breadth across the ischial tuberosity	Length of the symphysis	Greatest depth of the proximal end	Smallest breadth of the diaphysis	Greatest breadth of the distal end	Greatest length	Greatest breadth of the proximal end	Smallest breadth of the diaphysis	Greatest length	Depth across the anconeus process	Smallest depth of the olecranon
A	-0.049	-0.053	-0.131	-0.022	-0.023	-0.007			-0.024			
B							0.018	0.0001	0.004	0.017	0.038	0.023

	Femur						**Fibula**	**Astragalus**	**Calcaneus**	
Site	Greatest length	Greatest length from the caput	Greatest breadth of the proximal end	Greatest depth of the femoral head	Smallest breadth of the diaphysis	Greatest breadth of the distal end	Greatest length	Greatest length	Greatest length	Greatest breadth
A			-0.008	0.0001	0.005					
B	0.033	0.033	-0.023		0.007	0.024	0.035	0.019	0.025	0.017

5.3.3 Discussion

5.3.3.1 Body mass

As opposed to the other large African predators, *C. crocuta* exhibits female-biased SSD, as found in other studies (Matthews, 1939; Mills, 1990; Swanson *et al.*, 2013). There is variation in the degree of SSD across the study sites. First, the data was assessed for conformity to Rensch's Rule. To test this, female body masses were regressed against male body masses. The theory is that if the regression slope is >1 in species in which females are larger than males, SSD decreases with size, and thus Rensch's Rule is followed (Fairbairn, 1997, see Section 3.2). The regression produced a slope with a value of 1.024, suggesting a hyperallometric relationship of male body mass to female body mass. However, the confidence interval (0.759-1.345) of this slope spans the value of one. This, coupled with the strong significant relationship between male and female body mass, suggests that male and female body mass has an isometric relationship. SSD does not increase or decrease with greater body mass, and therefore Rensch's Rule is not followed (following Abouheif and Fairbairn, 1997; Fairbairn, 1997). SSD may, therefore, be due to other factors.

Spearman Rank Order correlations were run to assess correlations between body mass SSD and environmental variables (predator density, prey biomass, temperature, precipitation, vegetation cover). None of the correlations are significant, although the sample size is low, with only nine sites included. The strongest correlation is a positive relationship of SSD with semi-open vegetation cover, however, there appears to no indication in the literature as to why there may be a relationship between the two variables.

Most investigations into variations of SSD have been explained by food availability or competition (e.g. Ralls and Harvey, 1985; Isaac, 2005; McDonough and Christ, 2012). In the present study, however, the results of the correlations suggest that intraspecific competition, competition with *P. leo*, and prey biomass have very little association with *C. crocuta* body mass SSD.

Overall, the lack of significance and small r_s values suggest that the variables have only weak associations with *C. crocuta* body mass SSD. This may be a real signal, or may be due to the small sample size. The geographical coverage is also poor (Figure 4.2). A further factor to consider is the degree of SSD compared to other species. *P. leo*, and *P. pardus* exhibit stronger SSD than *C. crocuta*. The concern is therefore whether the geographical variation in the degree of SSD is actually large enough to warrant attribution to any environmental variables.

Furthermore, the variations in SSD in *C. crocuta* may merely be due to problems with using body mass as an indicator of SSD. Body mass is highly variable and may be affected by how much an individual has recently eaten (East and Hofer, 1993). This may be especially important in *C. crocuta* as adult males are often outcompeted by higher ranking females at a carcass (Frank *et al*., 1989). Therefore, the degree of SSD after feeding may be greater as females may have consumed more. This, therefore, raises questions about the validity of using body mass as a means of determining levels of SSD, and supports the use of alternative elements such as measurement of bones and teeth.

5.3.3.2 Crania and dentition

The results show that there is little consistent direction of sexual size dimorphism in most cranial, mandibular and dental measurements. The SSD values indicate that females are larger in some sites, whereas males are larger in other sites. Moreover, a comparison with the SSD values of other carnivores such as *P. leo* and *P. pardus* (Figure 5.19) suggests that *C. crocuta* SSD values are low. This suggests that the positive or negative SSD values for each site are merely an indication of a factor such as sample size, or small, local variations. Potential exceptions to this are some of the mandibular measurements. For these measurements, only one site has a negative SSD value, and this was calculated with only one male and one female. Despite this, the t-tests and Mann Whitney tests on the Balbal specimens revealed no significant differences at 95 % between males and females in any cranial, mandibular or dental traits.

This means that going forward, the males, females, and specimens of unknown sex can be combined in analyses. However, the mandibular measurements that potentially exhibit SSD will be treated so that males and females are assessed separately. Similarly, the results mean that, aside from the few mandibular measurements, sex will not be a consideration when interpreting the Pleistocene data.

Measurements of mandible length potentially exhibit female-biased SSD, as do measurements from the condyle to the p2/p3 and the canine. These measurements are included in the calculations of mechanical advantage of the masticatory muscles and of bending strength. Potential female-biased SSD is also observed in the width of the mandible at p2/p3, which is also included in bending strength calculations. There is no indication of SSD in mechanical advantage. By contrast, there appears to be variation in SSD of dorsoventral and labiolingual bending strength with age. Younger *C. crocuta* exhibit female-biased SSD in these indices. As age increases, the indices exhibit male-biased SSD, although sample sizes are small. However, as the mandible incurs stresses during biting hard food and struggling prey (Biknevicius and Ruff, 1992;

Therrien, 2005; Ferretti, 2007; Meloro *et al.*, 2008; Palmqvist *et al.*, 2011) this suggests that older males have greater bending strengths and are thus better suited to consume bone and target larger prey. However, males are disadvantaged relative to females when they are younger. It is difficult to determine whether this may have a noticeable impact on the feeding ability of males and females as the calculations of bending strength were not subject to tests for significant difference due to small sample sizes. Moreover, the SSD values are variable. Many of the values are less than 0.1, however, some of the values are large, and equal the higher SSD values of the more sexually dimorphic carnivore species such as *P. leo* and *P. pardus* (Figure 5.19).

The measurements that potentially exhibit SSD, in addition to indicators of body size (cranium length and m1 length) were assessed for Rensch's Rule. Except for mandibular ramus height, all measurements have a slope greater than one, suggesting that males increase in size hyperallometrically to females. However, in all cases, the confidence intervals span one. The measurements with the largest confidence intervals are those for which there is weak correlation between male and female sizes. Other measurements (cranium and m1 lengths, mandibular ramus height, and mandibular width at p2/p3) have significant correlations between males and females, and small slope confidence intervals. For these measurements, there is likely an isometric relationship, so that neither males nor females increase in size more than the other. This also means that degree of SSD does not increase or decrease with larger size, and therefore do not follow Rensch's Rule.

Spearman Rank Order correlations were run to assess the relationship between craniodental SSD and environmental variables. Most tests show that there are only weak and insignificant correlations between the SSD values and environmental variables. The exception is the length between the mandibular condyle and symphysis, which has a negative correlation with closed vegetation cover. The other mandibular measurements exhibit the same relationship, although these are weaker and insignificant. In terms of the Pleistocene, this suggests that during periods of greater vegetation cover, the mandible exhibited reduced SSD. However, the relationship between the length of the mandibular condyle-symphysis and closed vegetation cover is insignificant when the Bonferroni correction is applied, meaning that the uncorrected significance may have been a Type I error.

Other than this one example, the environmental variables included in this analysis do not have strong associations with degree of SSD. There are a number of potential explanations for this. Firstly, the environmental influences upon SSD as outlined in Section 3.2 are mostly comprised of body mass studies. Therefore, there may not be direct environmental influences upon craniodental elements. Secondly, the sample sizes of the tests were small, and therefore may have been insufficient to highlight any relationships between SSD and environmental variables.

Lastly, there may be influences that were not included in the model. For example, abundance of *C. crocuta*, other large predators and prey were not included due to lack of data for most sites. Competition for food was suggested to be a driver of SSD (Isaac, 2005, and references therein). Food availability influences degree of SSD of body size in *U. arctos* (McDonough and Christ, 2012) and *Mustela* spp.(Ralls and Harvey, 1985). Seasonality in food may also drive body size SSD (Isaac, 2005, and references therein), which may explain the potential influence of cold winters and warm summers on greater SSD of the least breadth of the skull.

Overall, the results of this section differ from other studies of SSD in *C. crocuta*. Notably, Swanson *et al.* (2013) and Matthews (1939) observed female-biased SSD in skull length. However, these measurements were made on live individuals, and thus comprised not only the size of the skull, but also other tissues such as muscle. One explanation for the disparity may be that muscles continue growing after the skull has stopped growing. Indeed, in a study by Binder and Van Valkenburgh (2000), bite strength measured on live *C. crocuta* continued to increase until four years of age, long after skull had finished growing at 20 months of age. This led the authors to suggest that the muscles continued growing after the skull stopped growing. Indeed, Swanson *et al.* (2013) stated that the most dimorphic features are those that stop growing later in life.

The results also contrast with a study by Gittleman and Van Valkenburgh (1997) who observed female-biased SSD in canines, P4, m1 length, skull length, and moment arm of resistance at the lower canines of *C. crocuta*, and male-biased SSD in width of the m1, moment arm of the temporalis, and moment arm of the superficial masseter. Except for moment arm of resistance at the canines, all of these measurements revealed no consistent direction in SSD in the present study. The disparity between the two studies is because Gittleman and Van Valkenburgh's (1997) studied specimens from only one geographical area. The results do support Klein's (1986) finding that *C. crocuta* 4.5° south of the equator exhibit no SSD in m1 length.

5.3.3.3 Post-crania

The sample size used to calculate SSD is small, due to the paucity of post-cranial specimens in museums when compared with the abundance of crania. However, where femoral SSD was calculated from two sites, the direction of SSD is consistent, lending support to the results. This was not the case for the smallest breadth of the radial diaphysis, where female measurements are on average smaller in Site 6.11, yet larger in Site 10.6. Some measurements show positive SSD (larger in females), and some measurements show negative SSD (larger in males). The SSD values are low, especially when compared with the other large carnivores (Figure 5.19). This

suggests that there is little size difference in post-cranial bones between male and female *C. crocuta*.

Swanson *et al.* (2013) observed that lower fore-limb length was not sexually dimorphic in *C. crocuta*. The radius and the ulna lengths in the present study both exhibit female-biased SSD, yet similarly to Swanson *et al.* (2013), the degree of SSD is low.

Overall, in light of the small SSD values, male and female post-cranial measurements will be combined in further analyses. Additionally, the results suggest that SSD will not influence morphometric analyses of Pleistocene post-crania. Finally, the small SSD values suggest that there are no functional differences in the post-crania of males and females.

5.4 Geographical variation in body size and morphology

5.4.1 Introduction

Body mass and the size of individual skeletal and dental elements hold important functional implications. For example, body mass may influence hunting ability (Biewener, 1989), targeted prey size (Carbone *et al.*, 2007), and temperature conservation to a limited extent (Steudel *et al.*, 1994). Craniodental morphology is associated with the size of the brain, vision, hearing, olfaction, respiration and feeding (Ewer, 1973; Biknevicius, 1996; Smith and Rossie, 2008; Tseng and Binder, 2010; Macrini, 2012; Nummela *et al.*, 2013; Lucas, 2015; Rahmat and Koretsky, 2015; and see Section 3.3). The post-crania are related to weight bearing, prey capture and locomotion (Hildebrand, 1974; Van Valkenburgh, 1985; and see Section 3.4). Gaining insights into the morphological variation of these elements may therefore provide valuable information about the responses to *C. crocuta* to different environmental conditions.

Average body mass of *C. crocuta* has been recorded as varying from 35.83 kg in Ethiopia (Powell-Cotton n.d., cited in Shortridge 1934) to 80.06 in Botswana (Smithers 1971). Skeletal and dental elements have also been record as varied, with m1 lengths greater further from the equator (Klein, 1986), and skulls larger in South Africa than eastern Africa (Roberts, 1951). These studies indicate that *C. crocuta* are larger at higher latitudes, and therefore conform to Bergmann's Rule. However, conformity to Bergmann's Rule has not been investigated in body mass in *C. crocuta*. Moreover, the range of geographical localities used to assess the influence of Bergmann's Rule are few, and other factors have not been considered. Barring the above studies, there have been no investigations of geographical variation of craniodental or post-cranial elements in present-day *C. crocuta*.

This study will assess the geographical variation and associated environmental influences upon body mass, and skeletal and dental elements of present-day *C. crocuta* in Africa. It is hoped that this may provide some insight into the possible drivers of any changes in *C. crocuta* body size and morphology during the Pleistocene, by confirming whether environmental factors are sufficient to explain variation in present-day *C. crocuta*.

The research questions are as follows:

- Is there geographical variation in *C. crocuta* body mass and skeletal and dental elements?
- Does *C. crocuta* conform to Bergmann's Rule?
- Are there other environmental variables that may explain variation in *C. crocuta* body size and morphology?

5.4.2 Results

5.4.2.1 Body mass

C. crocuta female body mass values (Table 5.23) range from 35.83 kg in Ethiopia (Powell-Cotton, n.d., cited in Shortridge, 1934) to 78.25 kg in Malawi (Wood, n.d., cited in Shortridge 1934), with a range of 42.42 kg. Male body mass ranges from 43.6 kg in the Narok District of Kenya (Neaves *et al*., 1980) to 80.6 kg in Botswana (Smithers, 1971), with a range of 37 kg.

Spearman Rank Order correlations were performed to assess the relationship of male and female body masses with environmental variables (*C. crocuta* density, *P. leo* density, prey biomass, minimum temperature of the coolest month, maximum temperature of the warmest month, precipitation of the driest month, precipitation of the wettest month, closed vegetation cover, semi-open vegetation cover, open vegetation cover). The correlation of male and female body mass with distance from the equator was also assessed.

At 95 % confidence, female body mass is significantly negatively correlated with precipitation of the wettest month (r_s = -0.854, p-value = 0.003) and *P. leo* density (r_s = -0.711, p-value = 0.032, Table 5.24). It is also significantly, positively correlated with maximum temperature of the warmest month (r_s = 0.005, p-value = 0.005). Male body mass is also positively correlated with maximum temperature of the warmest month (r_s = 0.622) and negatively correlated with *P. leo* density (r_s = -0.552), yet these are insignificant (p-value = 0.074 and 0.123, respectively). The only significant correlation with male body mass is precipitation of the wettest month (r_s = -0.686, p-value = 0.041).

The Bonferroni correction value for all tests in Table 5.24 is 0.0045. Only the correlation between female body mass and precipitation of the wettest month is significant under this corrected 95 % confidence p-value.

Distance from the equator is insignificantly and positively correlated with both female (r_s = 0.636, p-value = 0.066) and male (r_s = 0.586, p-value = 0.097) body mass.

Table 5.23: Mean female and male body mass (BM) data of present-day *C. crocuta*. [1]Mean value calculated from the minimum and maximum values (78.02 and 78.47 kg; Wood, n.d., cited in Shortridge 1934).

Country	Location	Mean female BM (kg)	Mean male BM (kg)	Reference
Botswana		70.99	80.06	Smithers (1971)
Ethiopia		35.83		Powell-Cotton (n.d., cited in Shortridge 1934)
Kenya		58.51		Meinertzhagen (1938)
Kenya			55.79	Talbot and Talbot (1962)
Kenya	Aberdare National Park	51.8	47.4	Sillero-Zubiri and Gottelli (1992)
Kenya	Maasai Mara National Reserve	59.39	53.67	Swanson *et al*. (2013)
Kenya	Narok District	50.7	43.6	Neaves *et al*. (1980)
Malawi		78.25[1]		Wood (n.d., cited in Shortridge 1934)
South Africa		61.1	56.2	Skinner (1976)
South Africa	Hluhluwe-iMfolozi Park	70	66.6	Whateley (1980)
South Africa	iMfolozi Game Reserve	57.75	47.5	Green *et al*. (1984)
South Africa	Kalahari Gemsbok National Park	70.9	59	Mills (1990)
South Africa	Kruger National Park	70.76	58.06	Stevenson-Hamilton (1947)
South Africa	Kruger National Park	68.2	62.5	Henschel (1986, cited in Skinner and Chimimba 2005)
South Africa	Kruger National Park	67.92		Lindeque (1981, cited in Smithers 1983)
South Africa	Transvaal		53.6	Rautenbach (1982, cited in Silva and Downing 1995)
South Africa and Zimbabwe	Transvaal and Zimbabwe	64.8	57.8	Rautenbach (1978, cited in Smithers 1983); Smithers (1983)
Southern Africa		47.18	46.87	Thackeray and Kieser (1992)
Tanzania	Serengeti	55.3	48.7	Kruuk (1972)
Zambia	Eastern Province	68		Wilson (1968, cited in Silva and Downing 1995)
Zambia		68.2	67.7	Wilson (1975, cited in Silva and Downing 1995)
	Minimum	35.83	43.6	
	Maximum	78.25	80.6	
	Range	42.42	37	

Table 5.24: Spearman Rank Correlation statistics of female *C. crocuta* body mass and male *C. crocuta* body mass against environmental variables (n = 9). All variables, except for vegetation cover, were base-10 logarithmically transformed prior to analyses. Vegetation cover variables were centred log ratio transformed. Bonferroni corrected p-value = 0.0045. Grey shaded sections are significant at 95 % uncorrected confidence ($p<0.05$). Orange shaded sections are also significant at 95 % corrected confidence ($p<0.0045$).

	Female body mass		**Male body mass**	
Variable	**r_s value**	**p-value**	**r_s value**	**p-value**
***C. crocuta* density**	-0.577	0.104	-0.519	0.152
***P. leo* density**	-0.711	0.032	-0.552	0.123
Prey biomass	-0.661	0.053	-0.485	0.185
Min. temp. coolest month	-0.21	0.587	-0.017	0.966
Max. temp. warmest month	0.84	0.005	0.622	0.074
Precipitation driest month	-0.563	0.114	-0.403	0.282
Precipitation wettest month	-0.854	0.003	-0.686	0.041
Closed vegetation cover	-0.452	0.222	-0.351	0.354
Semi-open vegetation cover	0.653	0.057	0.402	0.284
Open vegetation cover	-0.368	0.33	-0.084	0.831
Distance from equator	0.636	0.066	0.586	0.097

5.4.2.2 Crania and dentition

As with *C. crocuta* body mass, the cranial, mandibular and dental measurements exhibit considerable geographic variation. For example, of individuals with P3/p3 wear stage IV or greater, the mean total length of the cranium ranges from 243.17 mm in Site 7.1 (Debub Region, Eritrea), to 294.21 mm in Site 25.1 (Matabeleland North Province, Zimbabwe).

To assess the environmental influences upon the measurements, PLS regressions were performed (PLS 5-82). Measurements that potentially exhibit SSD (Section 5.3) and those that change in size through life (Section 5.2) were not included. Independent variables included in the models were minimum temperature of the coolest month, maximum temperature of the warmest month, precipitation of the driest month, precipitation of the wettest month, closed vegetation cover, semi-open vegetation cover, and open vegetation cover.

The r^2 and p-values of the PLS regressions are shown in Table 5.25-Table 5.27. All models are significant at 95 %. However, the r^2 values are all low, with the highest value at only 0.447 for the condylobasal length of the cranium (PLS 31). Most PLS models have many sites that are classed as leverages. In light of the number of leverages, only extreme values (classed as having a leverage value greater than two above the leverage reference line) were removed from subsequent PLS reruns (see Appendices Table 10.17-Table 10.19).

Reruns without the extreme leverage points resulted in reduced r^2 values in most cases, although the PLS regressions are still significant. One exception is the greatest neurocranium breadth, with an r^2 value that increased from 0.256 (PLS 52) to 0.29 (PLS 53) after removal of Site 17.1, Mpumalanga Province, South Africa. The other exception is the moment arm of the superficial masseter, with an r^2 value that increased from 0.272 (PLS 79) to 0.285 (PLS 80) after removal of Site 17.1. Nevertheless, these r^2 values are still low.

In most cases, the most extreme leverage value removed from the PLS reruns was Site 17.1. This is except for the leverage site of PLS 17 (anteroposterior diameter of the lower canine), which was Site 10.6, Nairobi National Park, Kenya.

The only models that will be further assessed are the ones with the greatest r^2 values. These are the condylobasal length (PLS 31, $r^2 = 0.447$) and the length from canine alveolus to the m1 alveolus of the mandible (PLS 64, $r^2 = 0.441$).

Table 5.25: r^2 values and p-values for PLS regressions run with each of the *C. crocuta* dental measurements as dependent variables. [1]Rerun without Site 17.1, Mpumalanga Province, South Africa. [2]Rerun without Site 10.6, Nairobi National Park, Kenya.

Statistic	Anteroposterior diameter of C	Mediolateral diameter of C	Length of P1	Width of P1	Length of P2	Width of P2	Length of P3	Width of P3	Length of P4	Greatest width of P4	Width of P4
PLS no.	5	6	7	8	9	10	11	13	14	15	16
r^2 value	0.325	0.26	0.142	0.095	0.177	0.166	0.301	0.138	0.156	0.284	0.228
p-value	0.002	<0.05	0.018	0.029	0.003	0.002	0.001	0.007	0.003	<0.05	<0.05
No. leverages	10	16	13	50	19	19	5	17	21	17	20
PLS no.							12[1]				
r^2 value							0.176				
p-value							0.004				
No. leverages							18				

Table 5.25 continued.

Statistic	Anteroposterior diameter of c	Mediolateral diameter of c	Length of p2	Width of p2	Length of p3	Width of p3	Length of p4	Width of p4	Length of m1	Width of m1
PLS no.	17	19	20	22	24	25	26	27	28	29
r^2 value	0.276	0.202	0.267	0.222	0.177	0.12	0.198	0.153	0.211	0.227
p-value	0.005	0.007	0.004	0.002	0.002	0.012	0.003	0.002	<0.05	<0.05
No. leverages	9	12	8	11	23	18	16	23	18	16
PLS no.	18[2]		21[1]	23[1]						
r^2 value	0.228		0.163	0.178						
p-value	0.014		0.006	0.002						
No. leverages	8		18	15						

Table 5.26: r^2 values and p-values of PLS regressions run with *C. crocuta* cranial measurements as dependent variables. [1]Rerun without Site 17.1, Mpumalanga Province, South Africa.

Statistic	Total length of cranium	Condylobasal length	Basal length	Basicranial axis	Basifacial axis	Upper neurocranium length	Viscerocranium length	Facial length	Greatest length of the nasals	Snout length	Median palatal length	Length of the horizontal part of the palatine	Length of the cheektooth row (P1-P4)	Length of the cheektooth row (P1-P3)	Greatest diameter of the auditory bulla
PLS no.	30	31	32	33	34	35	36	37	38	39	40	41	42	44	46
r^2 value	0.289	0.447	0.415	0.291	0.292	0.258	0.416	0.205	0.313	0.124	0.244	0.199	0.348	0.327	0.254
p-value	<0.05	<0.05	<0.05	0.001	0.001	<0.05	<0.05	0.001	<0.05	0.012	<0.05	0.002	<0.05	0.009	<0.05
No. leverages	25	23	20	19	17	24	22	24	19	25	19	20	15	55	21
PLS no.													43[1]	45[1]	
r^2 value													0.3	0.325	
p-value													<0.05	0.011	
No. leverages													17	5	

Table 5.26 continued.

Statistic	Greatest mastoid breadth	Greatest breadth of bases of paraoccipital processes	Greatest breadth of the foramen magnum	Height of the foramen magnum	Greatest neurocranium breadth	Zygomatic breadth	Least breadth of the skull	Least breath between the orbits	Greatest palatal breadth	Least palatal breadth	Greatest height of the orbit	Skull height	Height of the occipital triangle	Temporal fossa length
PLS no.	47	48	49	50	52	54	55	57	58	59	60	61	62	63
r^2 value	0.34	0.246	0.294	0.325	0.256	0.222	0.332	0.289	0.2	0.373	0.224	0.171	0.173	0.242
p-value	<0.05	<0.05	<0.05	0.016	<0.05	0.001	<0.05	<0.05	0.001	<0.05	<0.05	0.004	0.03	<0.05
No. leverages	27	23	22	9	15	22	34	23	24	20	17	22	24	25
PLS no.				51[1]	53[1]		56[1]							
r^2 value				0.165	0.29		0.293							
p-value				0.006	0.005		<0.05							
No. leverages				14	8		21							

Table 5.27: r^2 values and p-values of PLS regressions, run with *C. crocuta* mandibular measurements as the dependent variables. [1]Rerun without Site 17.1, Mpumalanga Province, South Africa.

Statistic	c alveolus to m1 alveolus length	Length of cheektooth row (p2 – m1)	Length of cheektooth row (p3 – m1)	Length of premolar row (p2 – p4)	Mandibular width at p3/p4	Mandibular width at p4/m1	Mandibular width at post-m1	Distance from p3/p4 to middle of articular condyle	Distance from p4/m1 to middle of articular condyle	Distance from post-m1 to middle of articular condyle	Moment arm of the temporalis	Moment arm of the superficial masseter	Moment arm of the deep masseter	Moment arm of resistance at m1
PLS no.	64	65	67	69	70	72	73	74	75	76	77	79	81	82
r^2 value	0.441	0.322	0.35	0.217	0.36	0.264	0.125	0.334	0.324	0.253	0.28	0.272	0.164	0.188
p-value	<0.05	0.006	0.001	<0.05	<0.05	<0.05	0.012	<0.05	<0.05	<0.05	<0.05	0.01	0.003	0.01
No. leverages	16	3	5	19	9	17	15	15	16	14	9	4	15	18
PLS no.		66[1]	68[1]		71[1]						78[1]	80[1]		
r^2 value		0.267	0.298		0.309						0.225	0.285		
p-value		<0.05	<0.05		<0.05						<0.05	0.017		
No. leverages		18	19		16						16	6		

PLS 31 (condylobasal length of the cranium) has 23 leverage values. However, none of the leverage sites are extreme, as indicated in Figure 5.33. The standardised coefficient with the greatest value is open vegetation cover at -0.268 (Figure 5.34). With lower values are maximum temperature of the warmest month, closed vegetation cover and semi-open vegetation cover, which have positive coefficients, while precipitation of the driest month has a negative coefficient. Minimum temperature of the coolest month and precipitation of the wettest month both have small negative coefficients.

The robustness of PLS 31 was tested by rerunning the model and removing one site each time, resulting in 47 runs (Table 5.28). All runs are significant at 95 % with p-values <0.05 (too low for the software to give a meaningful value). The r^2 values for all runs are very similar, ranging from 0.411 (removal of Site 14.1, Podor Department, Senegal) to 0.552 (removal of Site 12.1, Caprivi Strip, Namibia).

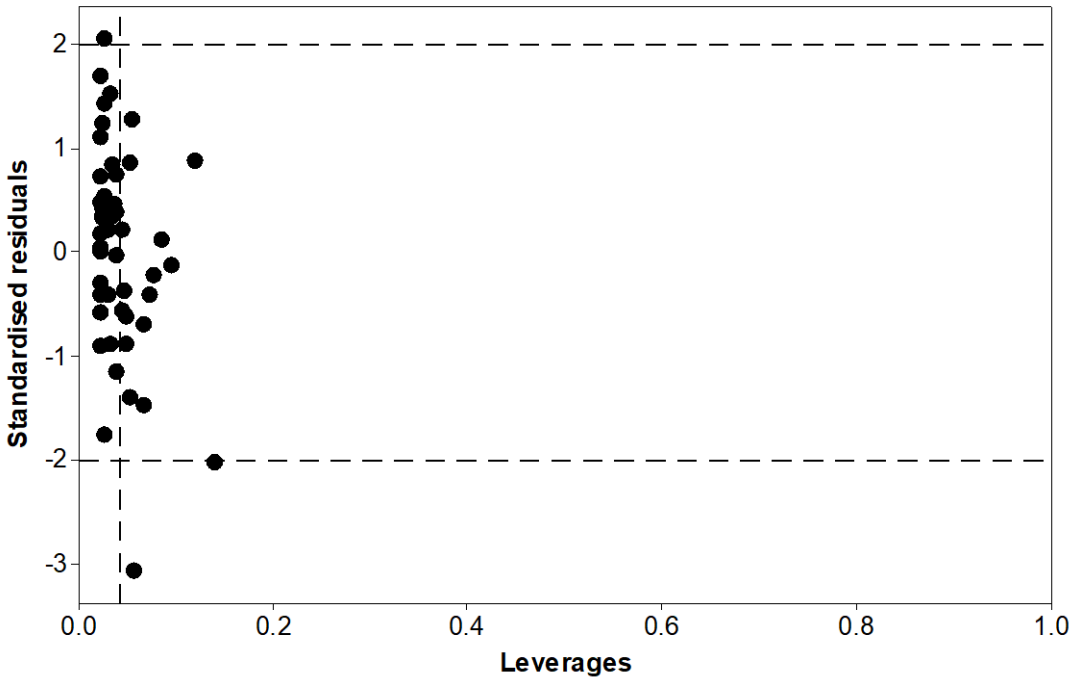

Figure 5.33: Standardised residuals against leverage values for each site in PLS 31, with *C. crocuta* condylobasal length of the skull as the dependent variable. See Appendix 10.6, Table 10.18 for site numbers corresponding to each leverage point.

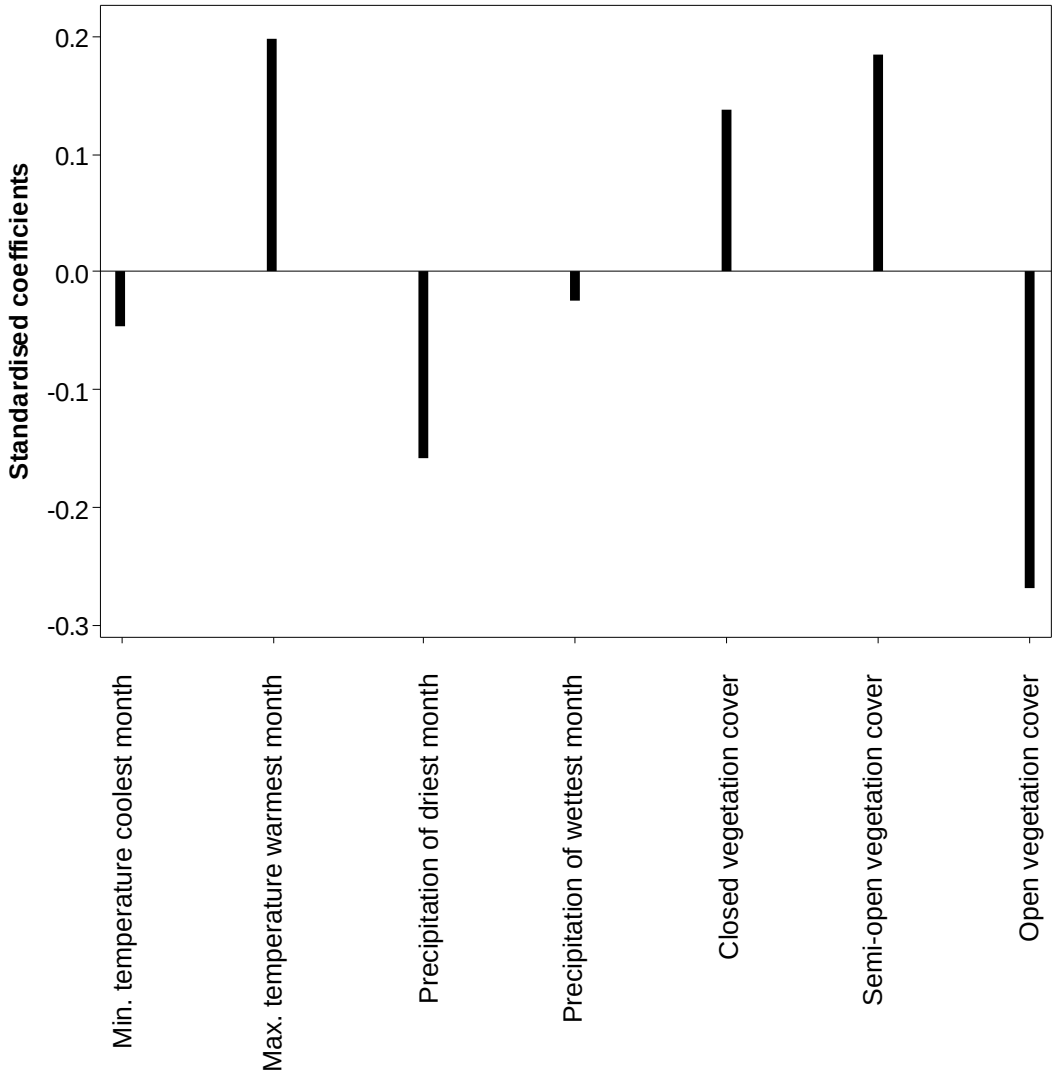

Figure 5.34: Standardised coefficients from PLS 31 with *C. crocuta* condylobasal length as the dependent variable. All variables had been base-10 logarithmically transformed.

CI values of the standardised coefficients from PLS 31 reruns were calculated (Table 5.29). The CI values are low, ranging from 0.002 for maximum temperature of the warmest month to 0.1 for minimum temperature of the coolest month. The signs are also constant so that no confidence interval crosses zero. This is also illustrated in Figure 5.35, showing that most of the coefficients are clustered together, with the exception of runs that excluded Site 6.13 (Lomami Province, Democratic Republic of the Congo) and Site 12.1 (Caprivi Strip, Namibia). Nevertheless, only precipitation of the wettest month has coefficients that are both positive and negative. Otherwise, the coefficients reflect the results of the original model with all sites (Figure 5.34).

Table 5.28: r^2 values of repeated runs of PLS 31, with *C. crocuta* condylobasal length as the dependent variable. Each run removed one site at a time. All runs have a p-value of <0.05.

Run no.	Removed site	r^2 value
1	1.1 Zaire Province, Angola	0.448
2	3.1 Chobe, Savuti Chobe, and Mababe Zokotsama, Botswana	0.431
3	3.2 Kgalagadi District, Botswana	0.449
4	5.3 Centre Region, Cameroon	0.467
5	6.2 Bas Uele District, Democratic Republic of the Congo	0.447
6	6.3 Haut Uele District, Democratic Republic of the Congo	0.443
7	6.4 Parc National de la Garamba, Democratic Republic of the Congo	0.445
8	6.6 Ituri District, Democratic Republic of the Congo	0.448
9	6.7 Ituri and North Kivu Districts, Democratic Republic of the Congo	0.448
10	6.9 Parc National des Virunga, Democratic Republic of the Congo	0.449
11	6.10 Haut Katanga District, Democratic Republic of the Congo	0.446
12	6.11 Parc National de l'Upemba, Democratic Republic of the Congo	0.44
13	6.12 Tanganyika District, Democratic Republic of the Congo	0.449
14	6.13 Lomami Province, Democratic Republic of the Congo	0.532
15	6.14 Lukaya District, Democratic Republic of the Congo	0.447
16	6.15 Kwilu and Kwango Districts, Democratic Republic of the Congo	0.453
17	7.1 Debub Region, Eritrea	0.446
18	9.1 Dire Dawa Region, Ethiopia	0.427
19	10.1 Samburu County, Kenya	0.441
20	10.2 Narok and Bomet Counties, Kenya	0.429
21	10.3 Garissa County, Kenya	0.434
22	10.4 Taita-Taveta County, Kenya	0.426
23	11.1 Tete Province, Mozambique	0.444
24	12.1 Caprivi Strip, Namibia	0.552
25	12.2 Khomas Region, Namibia	0.454
26	13.1 Akagera National Park, Rwanda	0.443
27	13.2 Nyagatare District, Rwanda	0.441
28	14.1 Podor Department, Senegal	0.411
29	16.1 Woqooyi Galbeed Region, Somalia	0.448
30	17.1 Mpumalanga Province, South Africa	0.46
31	17.2 Zululand District, South Africa	0.466
32	18.1 Upper Nile State, South Sudan	0.472
33	19.1 Shamal Darfur State, Sudan	0.44
34	19.2 Janub Darfur State, Sudan	0.429
35	21.1 Mara Region, Tanzania	0.436
36	21.2 Tabora Region, Tanzania	0.473
37	21.3 Kilimanjaro Region, Tanzania	0.448
38	21.4 Dodoma Region, Tanzania	0.449
39	21.6 Rukwa Region, Tanzania	0.444
40	21.8 Morogoro Region, Tanzania	0.447
41	21.11 Ruvuma Region, Tanzania	0.447
42	21.12 Ngorongoro Conservation Area, Tanzania	0.435
43	22.1 Centrale Region, Togo	0.457
44	23.1 Lira District, Uganda	0.462
45	23.2 Gulu District, Uganda	0.45
46	24.1 Eastern Province, Zambia	0.457
47	25.1 Matabeleland North Province, Zimbabwe	0.444

Table 5.29: Standardised coefficient means and confidence intervals (CI) for repeated runs of PLS 31, with *C. crocuta* condylobasal length as the dependent variable.

Independent variable	Standardised coefficient mean	Standardised coefficient CI	Standardised coefficient mean - CI	Standardised coefficient mean + CI
Minimum temperature coolest month	-0.053	0.01	-0.064	-0.043
Maximum temperature warmest month	0.196	0.002	0.194	0.198
Precipitation driest month	-0.155	0.003	-0.158	-0.151
Precipitation wettest month	-0.027	0.004	-0.031	-0.023
Closed vegetation	0.142	0.008	0.134	0.151
Semi-open vegetation	0.182	0.003	0.179	0.185
Open vegetation	-0.27	0.006	-0.276	-0.265

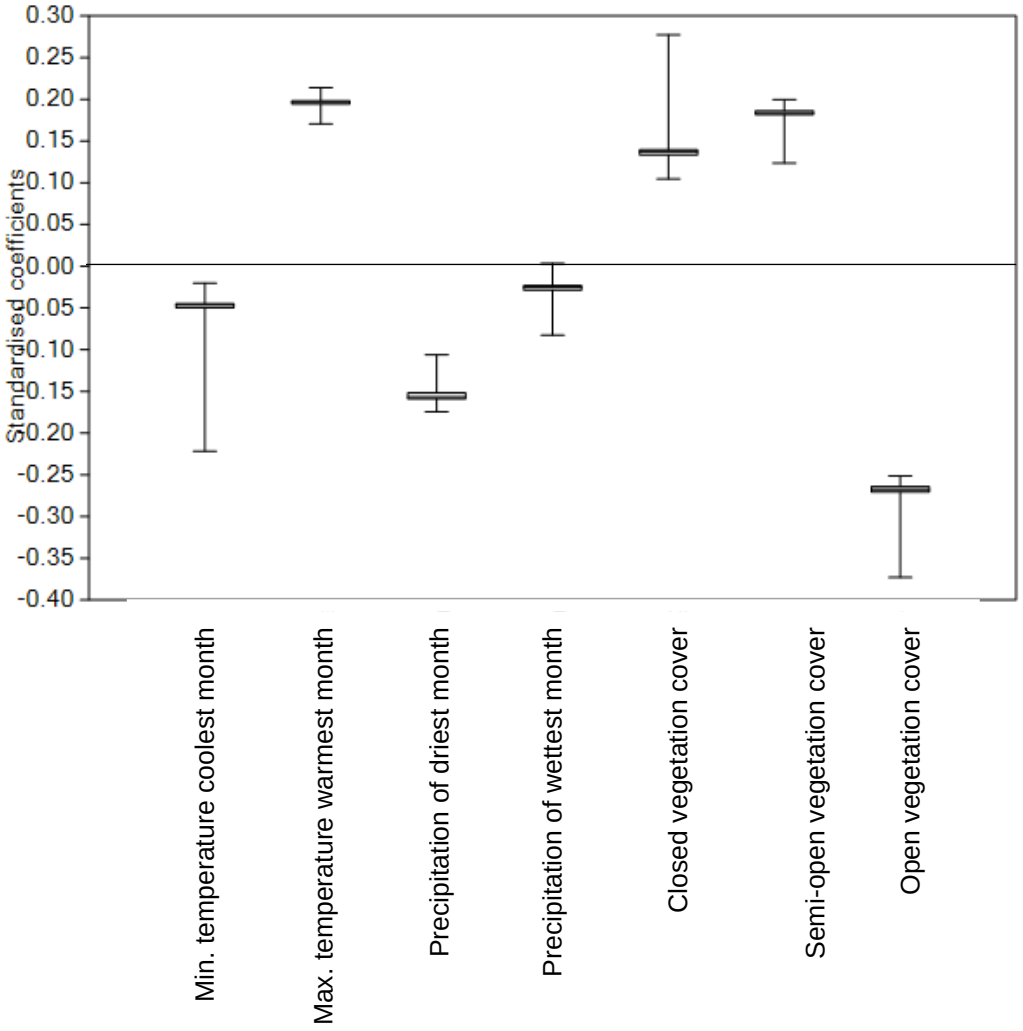

Figure 5.35: Standardised coefficients from reruns of PLS 31, with *C. crocuta* condylobasal length as the dependent variable.

None of the 16 leverage values from PLS 64 (length from c alveolus to m1 alveolus) are extreme (Figure 5.36). The independent variable with the greatest standardised coefficient is open vegetation cover with a negative coefficient (Figure 5.37). Next is precipitation of the driest month, which also has a negative coefficient, and semi-open vegetation cover, closed vegetation and maximum temperature of the warmest month, which all have positive associations with the dependent variable. Minimum temperature of the coolest month has a small, negative association, and precipitation of the warmest month, which has a small, positive association.

In order to test the robustness of PLS 64, this was rerun 50 times, removing one site each time. All reruns are significant at 95 % confidence with all p-values <0.05 (Table 5.30). The r^2 values are similar to the original regression (r^2 = 0441), and have a small range from 0.414 to 0.484.

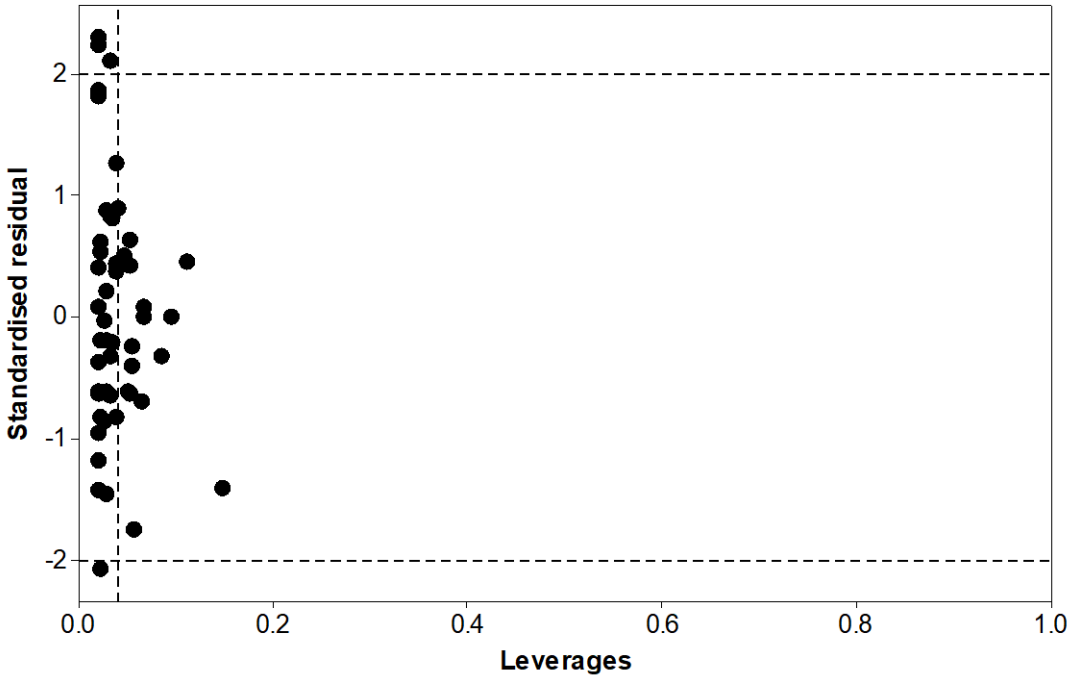

Figure 5.36: Standardised residuals against leverage values for each site in PLS 64, with *C. crocuta* length between the c and m1 alveoli as the dependent variable. See Appendix 10.6, Table 10.19 for site numbers corresponding to each leverage point.

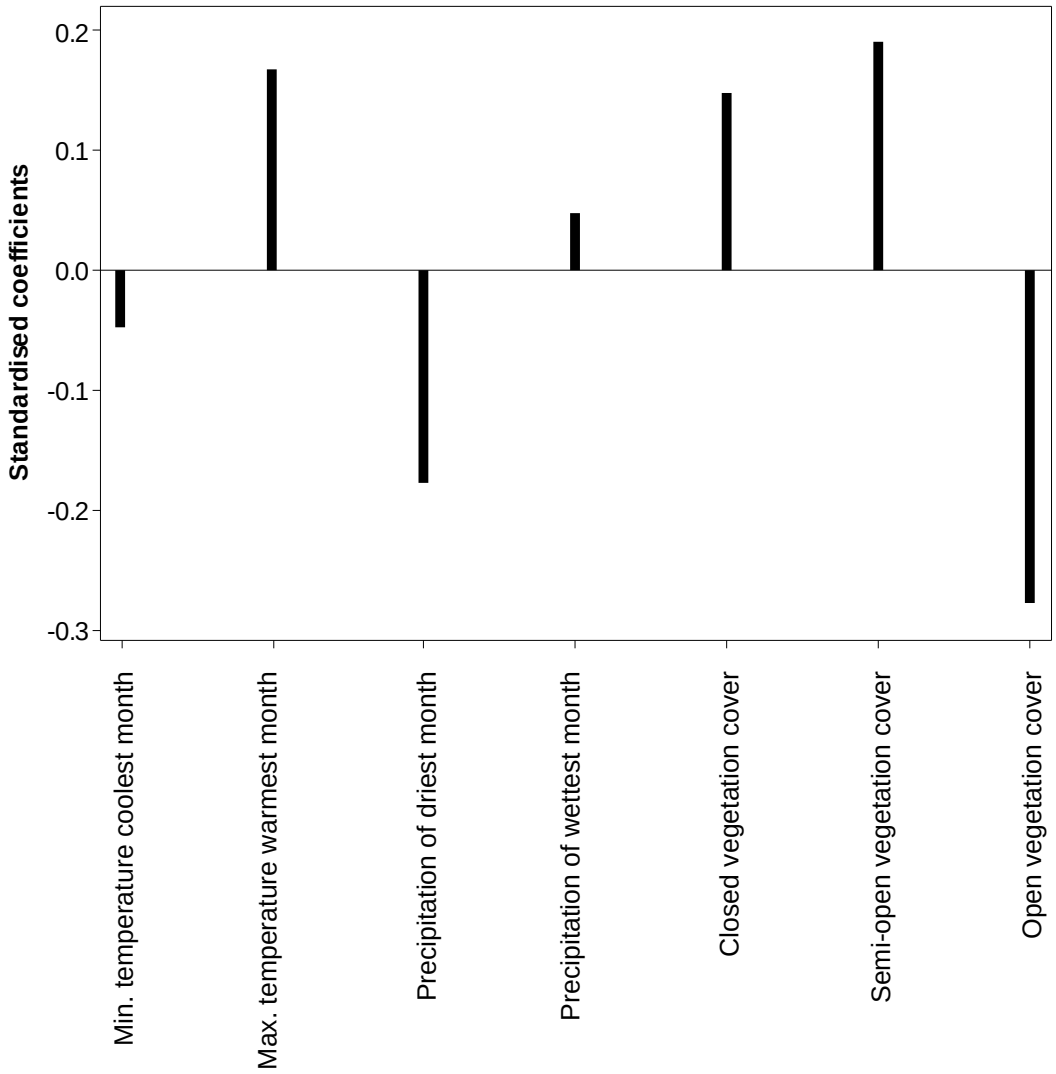

Figure 5.37: Standardised coefficients from PLS 64 with *C. crocuta* length between the c and m1 alveoli as the dependent variable. All variables had been base-10 logarithmically transformed.

The CI of the standardised coefficients from repeated runs of PLS 64 are small, ranging from 0.002 to 0.003 (Table 5.30). The means +/- CI do not cross zero. This is supported by Figure 5.38, in which none of the independent variables have standardised coefficients that cross zero. Maximum temperature of the warmest month, precipitation of the wettest month, closed vegetation cover, and semi-open vegetation cover are all consistently positive. Temperature of the coolest month, precipitation of the driest month, and open vegetation cover are all consistently negative.

The results of PLS 64 (Figure 5.38) are similar to PLS 31 (Figure 5.35).The only difference is that in PLS 31, precipitation of the wettest month has standardised coefficients that are positive and negative.

Table 5.30: r^2 values of repeated runs of PLS 64, with *C. crocuta* length between the c and m1 alveoli as the dependent variable. Each run removed one site at a time. All runs have a p-value of <0.05.

Run no.	Removed site	r^2 value	Run no.	Removed site	r^2 value
1	1.1 Zaire Province, Angola	0.44	**26**	12.2 Khomas Region, Namibia	0.478
2	2.1 Borgou, Benin	0.452	**27**	13.1 Akagera National Park, Rwanda	0.458
3	3.1 Chobe, Savuti Chobe, and Mababe Zokotsama, Botswana	0.422	**28**	13.2 Nyagatare District, Rwanda	0.435
4	3.2 Kgalagadi District, Botswana	0.444	**29**	14.1 Podor Department, Senegal	0.414
5	5.2 Adamawa Region, Cameroon	0.453	**30**	15.1 Koinadugu District, Sierra Leone	0.471
6	6.2 Bas Uele District, Democratic Republic of the Congo	0.437	**31**	16.1 Woqooyi Galbeed Region, Somalia	0.435
7	6.3 Haut Uele District, Democratic Republic of the Congo	0.437	**32**	16.2 Jubbada Dhexe Region, Somalia	0.427
8	6.4 Parc National de la Garamba, Democratic Republic of the Congo	0.439	**33**	17.1 Mpumalanga Province, South Africa	0.449
9	6.6 Ituri District, Democratic Republic of the Congo	0.444	**34**	17.2 Zululand District, South Africa	0.444
10	6.7 Ituri and North Kivu Districts, Democratic Republic of the Congo	0.442	**35**	19.1 Shamal Darfur State, Sudan	0.445
11	6.9 Parc National des Virunga, Democratic Republic of the Congo	0.441	**36**	19.2 Janub Darfur State, Sudan	0.433
12	6.10 Haut Katanga District, Democratic Republic of the Congo	0.438	**37**	21.1 Mara Region, Tanzania	0.435
13	6.11 Parc National de l'Upemba, Democratic Republic of the Congo	0.432	**38**	21.2 Tabora Region, Tanzania	0.44
14	6.12 Tanganyika District, Democratic Republic of the Congo	0.427	**39**	21.4 Dodoma Region, Tanzania	0.44
15	6.13 Lomami Province, Democratic Republic of the Congo	0.445	**40**	21.6 Rukwa Region, Tanzania	0.44
16	6.14 Lukaya District, Democratic Republic of the Congo	0.448	**41**	21.7 Tanga Region, Tanzania	0.439
17	6.15 Kwilu and Kwango Districts, Democratic Republic of the Congo	0.448	**42**	21.8 Morogoro Region, Tanzania	0.441
18	7.1 Debub Region, Eritrea	0.422	**43**	21.10 Lindi Region, Tanzania	0.462
19	9.1 Dire Dawa Region, Ethiopia	0.428	**44**	21.11 Ruvuma Region, Tanzania	0.476
20	10.1 Samburu County, Kenya	0.434	**45**	21.12 Ngorongoro Conservation Area, Tanzania	0.426
21	10.2 Narok and Bomet Counties, Kenya	0.431	**46**	22.1 Centrale Region, Togo	0.484
22	10.3 Garissa County, Kenya	0.422	**47**	23.1 Lira District, Uganda	0.455
23	10.4 Taita-Taveta County, Kenya	0.425	**48**	23.2 Gulu District, Uganda	0.444
24	11.1 Tete Province, Mozambique	0.43	**49**	24.1 Eastern Province, Zambia	0.435
25	12.1 Caprivi Strip, Namibia	0.459	**50**	25.1 Matabeleland North Province, Zimbabwe	0.432

Table 5.31: Standardised coefficient means and confidence intervals (CI) for repeated runs of PLS 64, with *C. crocuta* length between the c and m1 alveoli as the dependent variable.

Independent variable	Standardised coefficient mean	Standardised coefficient CI	Standardised coefficient mean - CI	Standardised coefficient mean + CI
Minimum temperature coolest month	-0.047	0.003	-0.050	-0.045
Maximum temperature warmest month	0.169	0.002	0.167	0.171
Precipitation driest month	-0.178	0.002	-0.180	-0.176
Precipitation wettest month	0.047	0.003	0.044	0.05
Closed vegetation	0.148	0.002	0.145	0.15
Semi-open vegetation	0.192	0.002	0.19	0.193
Open vegetation	-0.277	0.002	-0.279	-0.275

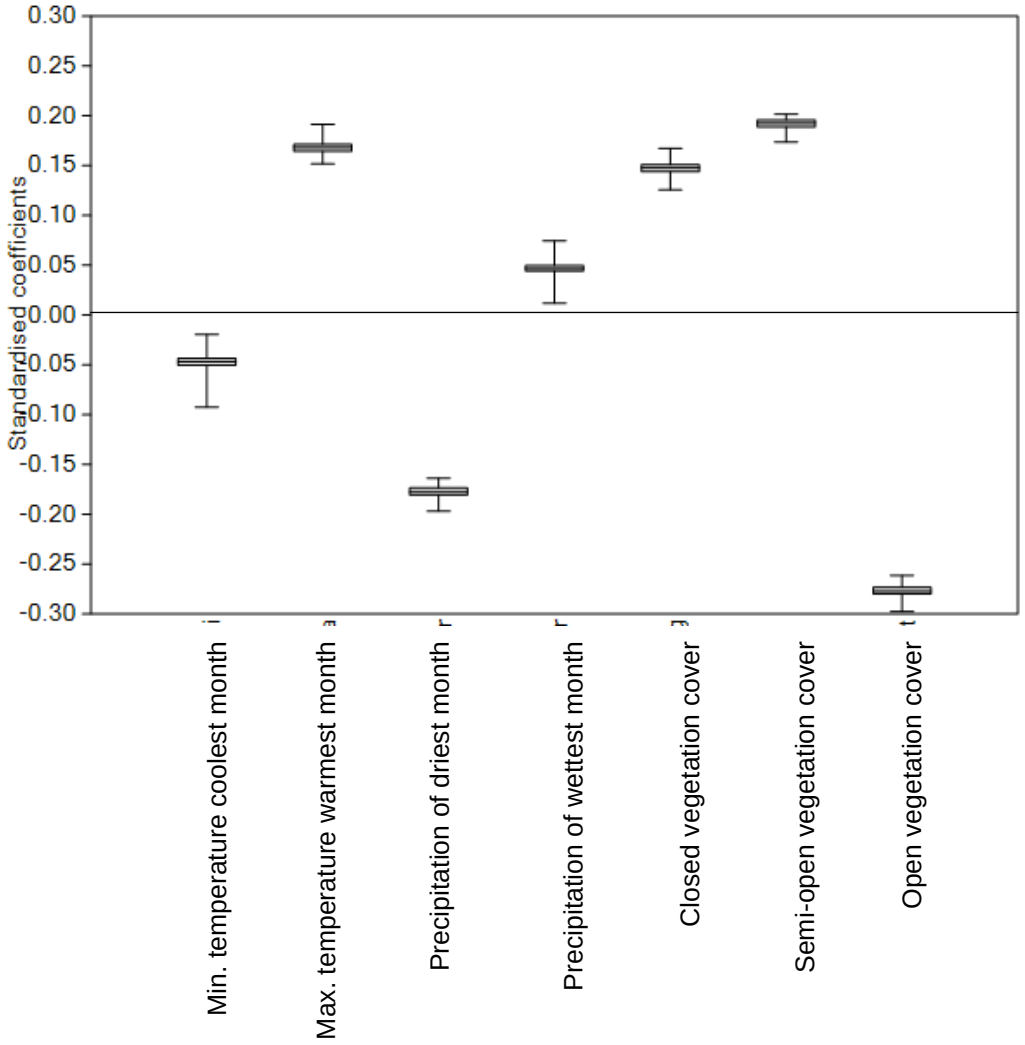

Figure 5.38: Standardised coefficients from reruns of PLS 64, with *C. crocuta* length c to m1 alveoli as the dependent variable.

In light of the similarities between PLS 31 and PLS 64, RMA regression was performed to assess the allometric relationship between the condylobasal length and the length between the c and m1 alveoli (Figure 5.39). The data here are individual specimens, rather than averages for each site. The Pearson's r correlation is strongly positive (r = 0.85) and is significant at 95 % confidence (p-value = <0.05). The RMA slope is 0.954, with the 95 % bootstrapped CI ranging from 0.874 to 1.028. These CI values therefore cross a slope with a value of one.

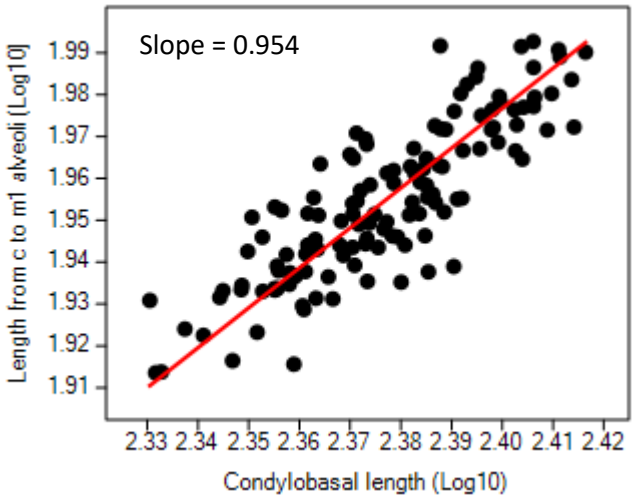

Figure 5.39: Reduced major axis regression of *C. crocuta* Log10 condylobasal length against the log10 length between the c and m1 alveoli.

In summary, PLS 31 (condylobasal length) and PLS 64 (length from the c-m1 alveoli) have the greatest r2 values of all the craniodental PLS regressions. Minimum temperature of the coolest month, precipitation of the driest month and open vegetation cover are negatively associated with both condylobasal length and length from the c-m1 alveoli. Maximum temperature of the warmest month, closed vegetation cover and semi-open vegetation cover are positively associated with both measurements. The only difference is that precipitation of the wettest month is positively associated with length from c-m1 alveoli, yet this variable is not consistently positively or negatively associated with condylobasal length. The RMA regression of condylobasal length against length from c-m1 alveoli is significant and positive, with a minimum slope CI below one and a maximum slope CI above one.

5.4.2.3 Post-crania

Spearman Rank Order correlations have been performed to assess association between post-cranial measurements and environmental variables. In light of the small sample sizes, PLS regressions have not been used.

At 95 % confidence, 19 of the Spearman Rank Order correlations are significant at 95 % uncorrected confidence (Table 5.32). Using the Bonferroni correction, tests are only significant if $p<0.0071$. Using the corrected p-value, only six tests are significant: atlas greatest breadth of the cranial articular surface (BFcr) with precipitation of the wettest month, scapula greatest length of the glenoid process (GLP) with maximum temperature of the warmest month and open vegetation cover, scapula length of the glenoid cavity (LG) with maximum temperature of the warmest month and open vegetation cover, and scapula breadth of the glenoid cavity (BG) with open vegetation cover.

Overall, most of the measurements show similar results. The strongest correlations are generally with maximum temperature of the warmest month, precipitation of the wettest month, closed vegetation cover and open vegetation cover. These are the only variables for which there are significant correlations at 95 % confidence. Most of the correlations, except the greatest breadth across the transverse process (BPtr) of the axis have positive correlations with maximum temperature. Except for axis smallest breadth (SBV) and greatest length of the arch (LAPa) of the axis, all variables have positive correlations with precipitation of the wettest month and closed vegetation cover. Except for axis SBV, all measurements have negative correlations with open vegetation cover.

Table 5.32: Spearman Rank Order correlations of C. crocuta post-cranial measurements with environmental variables. Top figure = Spearman Rank Order statistic (r_s). Bottom figure = p-value. GL = greatest length. BFcr = greatest breadth of the cranial articular surface. LAPa = greatest length of the arch. BPtr = greatest breadth across the transverse process. SBV = smallest breadth. SLC = smallest length of the neck. GLP = greatest length of the glenoid process. LG = length of the glenoid cavity. BG = breadth of the glenoid cavity. Dp = greatest depth of the proximal end. SD = smallest breadth of the diaphysis. Bd = greatest breadth of the distal end. Bp = greatest breadth of the proximal end. Bonferroni corrected p-value = 0.0071. Grey shaded sections are significant at 95 % uncorrected confidence (p<0.05). Orange shaded sections are also significant at 95 % corrected confidence (p<0.0071).

	Atlas GL	Atlas BFcr	Axis LAPa	Axis BPtr	Axis SBV	Scapula SLC	Scapula GLP	Scapula LG	Scapula BG	Humerus Dp	Humerus SD	Humerus Bd	Femur Bp	Femur SD
No. sites	6	6	6	6	6	6	6	6	6	6	6	6	7	7
Min. temp. coolest month (°C)	-0.086 0.872	0.086 0.872	0.257 0.623	0.486 0.329	0.1 0.873	-0.086 0.872	0.143 0.787	-0.029 0.957	0.257 0.623	0.6 0.208	-0.086 0.872	0.029 0.957	0.321 0.482	0.179 0.702
Max. temp. warmest month (°C)	0.899 0.015	0.58 0.228	0.551 0.257	0.493 0.321	-0.41 0.493	0.899 0.015	0.928 0.008	0.986 <0.05	0.783 0.066	0.638 0.173	0.899 0.015	0.812 0.05	0.667 0.102	0.811 0.027
Precipitation driest month (mm)	-0.203 0.7	0 1	-0.029 0.957	0.087 0.87	0.205 0.741	-0.203 0.7	-0.116 0.827	-0.29 0.577	0.145 0.784	0.406 0.425	-0.203 0.7	-0.348 0.499	-0.09 0.848	-0.595 0.159
Precipitation wettest month (mm)	0.6 0.208	0.943 0.005	0.771 0.072	-0.086 0.872	-0.9 0.037	0.6 0.208	0.886 0.019	0.771 0.072	0.829 0.042	0.543 0.266	0.6 0.208	0.771 0.072	0.5 0.253	0.464 0.294
Closed vegetation cover (%)	0.429 0.397	0.829 0.042	0.6 0.208	-0.143 0.787	-0.9 0.037	0.429 0.397	0.771 0.072	0.657 0.156	0.657 0.156	0.429 0.397	0.429 0.397	0.657 0.156	0.679 0.094	0.607 0.148
Semi-open vegetation cover (%)	0.314 0.544	-0.486 0.329	-0.371 0.468	0.771 0.072	0.7 0.188	0.314 0.544	0.029 0.957	0.2 0.704	-0.029 0.957	0.257 0.623	0.314 0.544	-0.086 0.872	0.286 0.535	0.143 0.76
Open vegetation cover (%)	-0.829 0.042	-0.829 0.042	-0.657 0.156	-0.257 0.623	0.8 0.104	-0.829 0.042	-1 <0.05	-0.943 0.005	-0.943 0.005	-0.771 0.072	-0.829 0.042	-0.771 0.072	-0.714 0.071	-0.714 0.071

5.4.3 Discussion

5.4.3.1 Body mass

There is much geographical variation in both male and female body masses of *C. crocuta*. Overall, the results from the Spearman Rank Order correlations suggest that both male and female body masses vary similarly with environmental conditions. However, only precipitation of the wettest month is significantly correlated with male and female body mass, while maximum temperature of the warmest month and *P. leo* density are also correlated with female body mass. This may be due in part to the small sample sizes. Furthermore, the geographical coverage of Africa is very poor (Figure 4.2), so there may be environmental conditions that *C. crocuta* currently inhabit that were not covered in the analyses.

That increasing distance from the equator (in this case towards southern Africa) is associated with larger body mass (although insignificant), which supports Bergmann's Rule, whereby individuals of a species occurring in higher latitudes and colder conditions are larger than their lower latitude counterparts, in order to reduce body size and conserve heat. This is supported by Ashton *et al.* (2000) who found that 79 % of carnivorans (including some canids, ursids and felids) were found to be larger in higher latitudes. Additionally, first lower molars of *C. crocuta* were found to be larger further from the equator (Klein, 1986) and *C. crocuta* skulls from South Africa were larger than those from eastern Africa (Roberts, 1951). However, there is also a new, positive association noted here between the temperature of the warmest month and *C. crocuta* body size (significant at 95 % uncorrected confidence, and approaching significance with the Bonferroni corrected critical p-value). This is contrary to Ashton *et al.*'s (2000) study in which 79 % of carnivorans were larger in colder temperatures. This cautions against substituting temperature for latitude as previous researchers have done when investigating the influence of Bergmann's Rule (e.g. McNab, 1971; Klein, 1986). The difference between *C. crocuta* and the other carnivorans in Ashton *et al.*'s (2000) may be because the relationship between body mass and temperature is not direct; temperature influences other environmental factors, which may in turn be affecting body mass change (see Section 3.1 for examples).

Why higher temperatures may induce a larger body mass in *C. crocuta* is unclear as there appears to be little indication in the literature of biological reasons for increased body mass at higher temperatures. One possibility is that *C. crocuta* in higher temperatures have a greater body mass due to larger appendages to facilitate heat loss, rather than a larger overall body size, as per Allen's Rule (Allen, 1877). This links back to the finding that hotter temperatures appear to be negatively associated with *C. crocuta* population biomass (Section 5.1). However, in controlled experiments with mice, although individuals in warmer conditions developed longer

limbs, ears and tails, their body masses were similar to individuals that inhabited colder conditions (Serrat *et al*., 2008). Similarly, domestic pigs (*Sus scrofa domesticus*), when raised in warmer conditions had longer limbs and tails and larger ears, however, their body mass was similar to that of their siblings raised in colder conditions (Weaver and Ingram, 1969). Unfortunately, as the post-cranial specimens measured in this study did not have associated body mass information, this cannot be further investigated at present.

P. leo density has a negative association with *C. crocuta* body mass, although this is not significant under Bonferroni's correction and so may be a Type 1 error. If the relationship is true, this suggests that the presence of a competitor may constrain body size, such as occurs when the range of the puma (*Felis concolor*) overlaps with the jaguar (*Panthera onca*, McNab, 1971).

The reason for the correlation between body mass and the other significant variable, precipitation of the wettest month, is unclear. Overall, the greater number of significant correlations, and the higher r_s values suggest that female body mass is more strongly associated with environmental variables than is male body mass, although this may be a due to low sample sizes.

However, once the Bonferroni corrected p-value was taken into account, only the relationship between female body mass and precipitation of the wettest month is significant. Although the relationship between female body mass and maximum temperature of the warmest month approaches significance.

5.4.3.2 Crania and dentition

The measurements of the cranium, mandible and dentition vary across Africa. However, the PLS regressions reveal that variation in most of the measurements is poorly explained by temperature, precipitation or vegetation cover.

The PLS regression with the greatest r^2 values are condylobasal length and length from the c to m1 alveoli. The strongest associations with these measurements are positive correlations with temperature of the warmest month, closed vegetation cover, and semi-open vegetation cover. Negative associations are with open vegetation cover, and to a lesser extent with precipitation of the driest month and temperature of the coolest month. Precipitation of the wettest month has a weaker and less consistent association with condylobasal length, however it has a weak, positive association with length between the c and m1 alveoli.

Condylobasal length and c to m1 length are therefore larger in areas with warmer summers, more arid periods, with closed or semi-open vegetation cover, and potentially with cooler

winters. Along with drier conditions in the driest month of the year, the length from the c to m1 may also be greater in areas that experience increased precipitation in wetter months.

Condylobasal length scales well with body mass (Van Valkenburgh, 1990). In light of this, and in light of the similar PLS results, the allometric relationship between the condylobasal length and distance between c to m1 was investigated. There is a strong positive correlation between the two measurements, and the slope value suggests an isometric relationship. Therefore, the two measurements are increasing in line with each other, suggesting that they both reflect actual body size of individuals, rather than variation independent of overall body size. The environmental influences upon these measurements can therefore be interpreted as impacting upon *C. crocuta* body size.

The results suggest that there is no clear relationship between *C. crocuta* and Bergmann's Rule. While they are larger in regions with cooler winters, it is the positive association with summer temperature that has the greater influence. This is supported by the positive association between body mass and temperature of the warmest month (Section 5.4.3.1).

The two measurements and body mass are also positively associated with semi-open vegetation cover. By contrast, body mass is negatively associated with closed vegetation cover (although insignificantly), yet this variable is positively associated with the length measurements. Additionally, c to m1 length is associated positively with precipitation of the wettest month, albeit weakly, yet this variable has a strong negative association with body mass. If the length measurements correlate well with overall body size, the disparity in results between the lengths and body mass may be due to the small sample size in the latter study (47 and 50 sites versus 8 sites).

Despite the significance of the PLS regression, only about 45 % of the variation in condylobasal length, and 44 % of the variation in c to m1 length, is explained by the environmental variables. This value is even lower for other measurements. This may be because there are other variables that are not included in the study. Indeed, *P. leo* density is significantly and negatively correlated with *C. crocuta* female body mass (Section 5.4.2.1) and food quality and abundance have positively been associated with body size in *U. arctos* (Zedrosser *et al.*, 2006; McDonough and Christ, 2012) and *U. maritimus* (Rode *et al.*, 2010). Furthermore, craniodental morphology is associated with feeding, such as acquiring and eating different food types (Biknevicius *et al.*, 1996; Lucas, 2015; Rahmat and Koretsky, 2015). This includes consumption of bone, an act that is associated with low food availability (Kruuk, 1972; Egeland *et al.*, 2008). The associations shown here between the two length measurements and environmental variables may therefore

be a secondary association because food quality and abundance are influenced by climate (McNab, 2010).

The lack of correlation between measurements and environmental variables may also be due to the complexity of elements, particularly the cranium (see Section 3.3), and thus morphology may be constrained by these processes (Tseng and Binder, 2010; Figueirido *et al.*, 2011).

5.4.3.3 Post-crania

The results from the post-cranial measurements suggest that assessed measurements of the atlas, scapula, humerus and femur, and one of the axis measurements, are greater in areas experiencing warmer summers, greater rainfall in the wettest month, with closed vegetation cover. Open vegetation cover has a negative association with these measurements. These associations are the same as those found in the analysis of condylobasal length and c to m1 alveoli length (Section 5.4.3.2). If these length measurements are indeed an indication of overall body size, this suggests that this variation in post-cranial morphology is due to change in overall body size, rather than adaptations of individual elements to the environmental conditions.

Proximal limb bone breadths are associated with ability to endure high speed locomotion (Hildebrand and Hurley, 1985).and with hunting methods in carnivorans, including hyaenids, canids, felids, ursids and procyonids (Martín-Serra *et al.*, 2016). However, as mentioned, the associations between environmental variables and the humerus and femur breadth measurements are likely a signal of overall body size, and therefore do not reflect environmental influences upon locomotion. High speed locomotion (Hildebrand, 1974; Hildebrand and Hurley, 1985), cursoriality (Meachen *et al.*, 2016) and hunting methods (Van Valkenburgh, 1985; Harris and Steudel, 1997) are also associated with length of the limbs, yet these measurements could not be assessed due to small sample sizes.

For the measurements assessed that appear to change with body size, the predictions for their size in the Pleistocene are the same as outlined in Section 5.4.3.2.

5.4.3.4 Implications for the Pleistocene

In light of the body mass and morphometric results, it is predicted that *C. crocuta* (and individual measurements that have an allometric relationship with body mass) were larger in periods with warmer summers, arid periods during the Pleistocene and low predator competition. They may also have been larger when closed or semi-open vegetation was more prevalent, although the disparity between the cranium and body mass results makes this prediction more uncertain.

5.5 Tooth breakage

5.5.1 Introduction

The frequency of tooth breakage has been used in studies of Pleistocene carnivores to aid reconstruction of palaeodiets (Van Valkenburgh and Hertel, 1993; Van Valkenburgh, 2009; Flower and Schreve, 2014). Indeed, teeth may be broken due to bone consumption, although canines in particular may be broken by struggling prey and fighting (Van Valkenburgh, 1988, 2009). In the case of *C. crocuta*, increased bone consumption occurs during periods of low food availability (Kruuk, 1972; Egeland *et al.*, 2008).

A further pathological feature of the maxilla and mandible is the loss of a tooth, resulting in a partially or wholly healed alveolus. This may equally be associated with bone consumption as broken teeth may allow bacteria to enter the alveolus through the exposed pulp, leading to infection and loss of the tooth (Losey *et al.*, 2014). Alternatively, the gum may become inflamed and then infected, leading to infection of the alveolus and loss of teeth. After tooth loss, the alveolus begins to heal (Pekelharing, 1974). Partially and wholly healed alveoli were counted separately to broken teeth in this section because tooth loss may not be due to initial breakage of the tooth.

This section will first assess variation in tooth breakage and loss with age. Next, the differences in tooth breakage and loss between males and females will be examined, namely whether one experiences more frequent tooth breakage and loss, and whether this manifests differently in each tooth type. This is important as tooth loss or breakage may lead to loss or reduction in tooth function, which may make it difficult to survive, particularly when there is prolonged food stress. If older individuals have more lost or broken teeth than younger *C. crocuta*, this may indicate that loss of function need not necessarily lead to death. Finally, this section will highlight whether age or sex need to be considered when interpreting Pleistocene results.

The research questions are:

- Do tooth loss and breakage become more prevalent in older *C. crocuta*?
- Are there differences in the frequency of tooth loss or breakage in female and male *C. crocuta*?
- Does the manifestation of tooth loss and breakage differ between the tooth types?

5.5.2 Results

5.5.2.1 Tooth breakage and loss with age

The large number of specimens from Site 21.12 (Balbal, Ngorongoro Conservation Area, Tanzania) were used to assess the degree of tooth breakage with age. The number of individuals with broken teeth generally increases in line with age (as represented by P3/p3 wear stage) in both female and male *C. crocuta* (Figure 5.40). There is no pattern in the number of individuals with partially or fully healed alveoli.

Breakage with age was repeated for all specimens to allow assessment of the later wear stages not represented in Site 21.12, although it is acknowledged that there may be differences between males and females and between sites. This reflects the trend in Site 21.12, with only three wear stage III specimens exhibiting broken teeth (Figure 5.41). The number of individuals with broken teeth compared to those with no broken or lost teeth increases with age, with all individuals of wear stages VII/VIII, VIII and IX exhibiting lost or broken teeth. The number of individuals that have lost teeth generally increases with age, but numbers are smaller than those with only broken teeth, except for wear stage IX.

The amount of broken and lost teeth as a proportion of teeth of known condition was calculated from Site 21.12 (Figure 5.42). The percentage of broken teeth generally increases with age, although this trend is clearer in female *C. crocuta*. The proportion of lost teeth is greatest at wear stage VI in female *C. crocuta*. Of the male *C. crocuta*, only individuals with wear stage V exhibit lost teeth.

The increase in tooth breakage, and to an extent tooth loss, with older age in *C. crocuta* warrants separation of data in future analyses into individual P3/p3 wear stages.

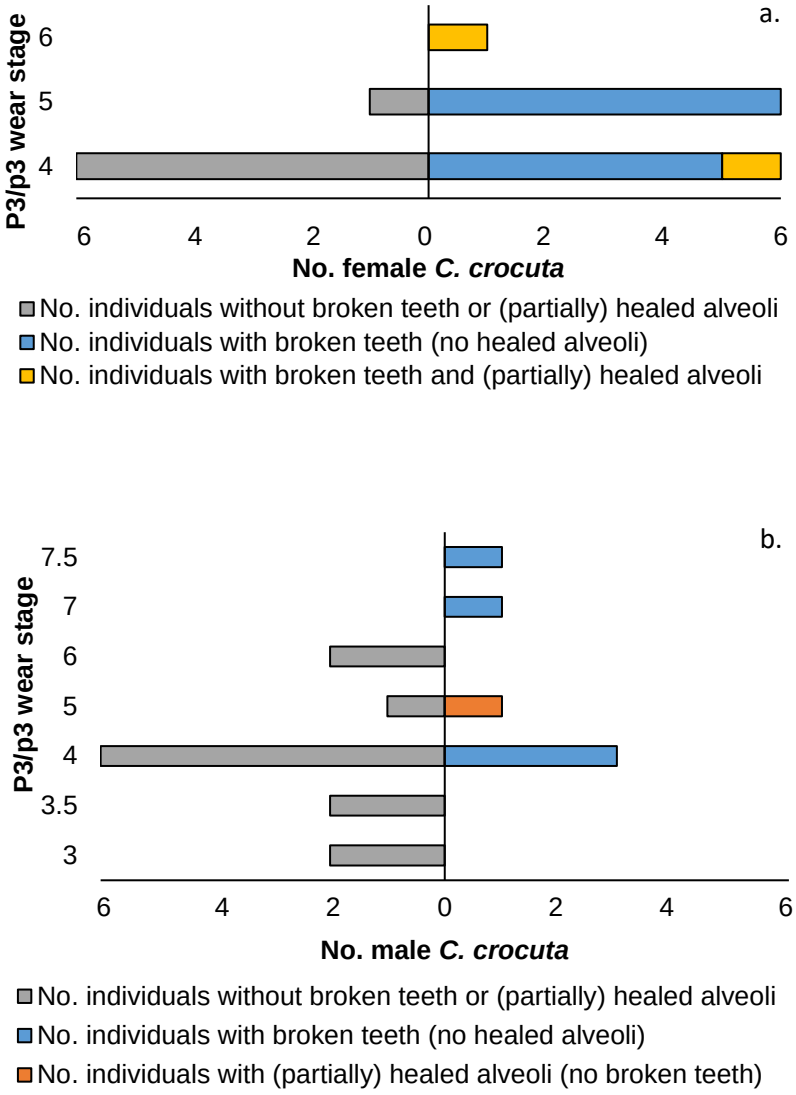

Figure 5.40: Number of a) female or b) male present-day *C. crocuta* with either: no broken teeth, broken teeth without lost teeth, partially or fully healed alveoli without broken teeth, broken teeth and partially or fully healed alveoli. Specimens from Site 21.12, Ngorongoro Conservation Area, Tanzania.

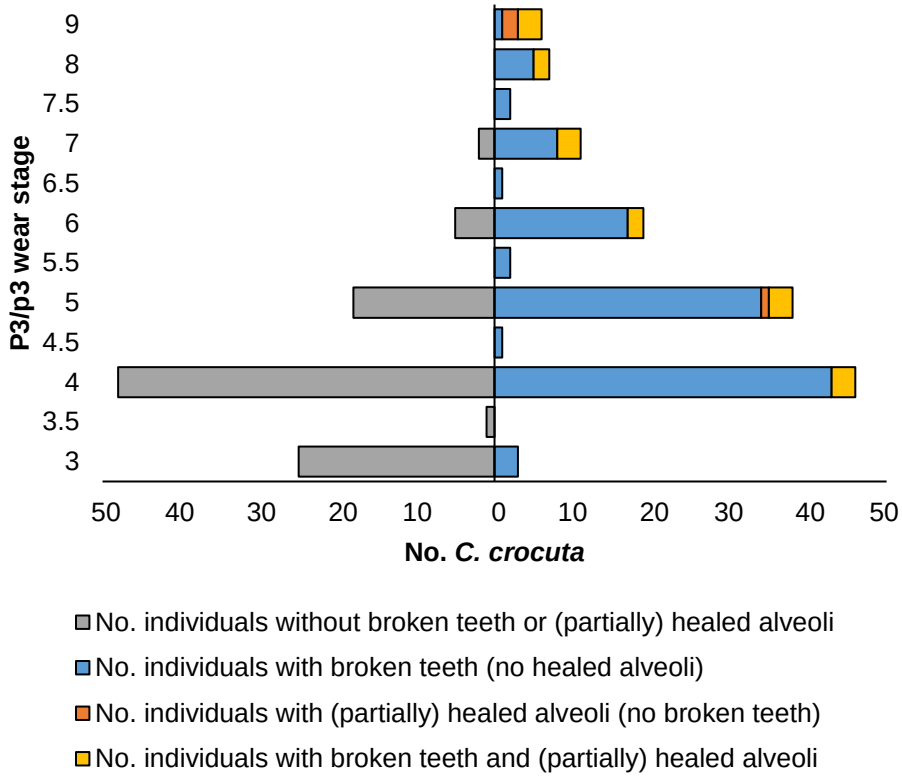

Figure 5.41: Number of present-day *C. crocuta* with either: no broken teeth, broken teeth without lost teeth, partially or fully healed alveoli without broken teeth, broken teeth and partially or fully healed alveoli. Data from all sites in Africa.

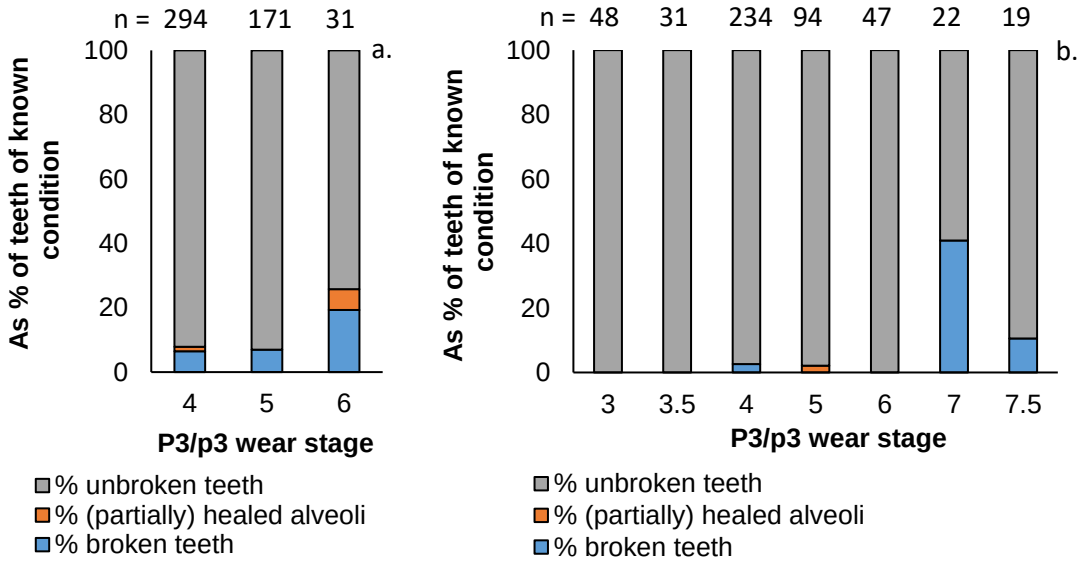

Figure 5.42: Condition of teeth as a percentage of teeth of known condition. a) female *C. crocuta* and b) male *C. crocuta* from Site 21.12, Ngorongoro Conservation Area, Tanzania.

5.5.2.2 Male and female tooth breakage and loss

The quantity of broken, lost and unbroken teeth was calculated as a percentage of teeth of known condition. These proportions are presented for sites from which there were data for both males and females at each P3/p3 wear stage. Wear stage III was excluded from the analysis as none of the sites analysed included individuals with lost or broken teeth. Wear stages greater than VI were also excluded as there were no sites with both males and females.

Combining all tooth types indicates that for each site at each wear stage, there are at least as many, or in some cases more, females than males with broken teeth (Figure 5.43). As a percentage of all teeth of known condition, females have a greater proportion of broken teeth at all sites and all wear stages. Of the sites included, lost teeth are only observed in Site 21.12. At wear stages IV and VI, only females have evidence of fully or partially healed alveoli. At stage V, only males exhibit tooth loss.

After splitting the data into tooth types, the results of stage IV (Figure 5.44) indicate that a greater proportion of individuals have broken premolars than other teeth, and a greater proportion of premolars are broken. The smallest proportion of individuals have broken carnassials. In Site 10.2 (Narok and Bomet Counties, Kenya) a greater proportion of females have broken incisors, canines and premolars, although a greater proportion of males have broken carnassials. Conversely, in Site 21.12, a greater proportion of males have broken incisors and premolars. In both sites, a greater proportion of incisors, canines and premolars are broken in females than males. In Site 21.12, the lost teeth occur at the position of the incisors and premolars in females.

At stage V (Figure 5.45), a smaller proportion of individuals have broken carnassials than other teeth. They were only observed to be broken in females from Site 6.9 (Parc National des Virunga, Democratic Republic of the Congo) and Site 21.12. Canines are less frequently broken than incisors and premolars, with observations from females in Site 6.11 (Parc National de l'Upemba, Democratic Republic of the Congo) and Site 21.12, and from males in Site 11.1 (Tete Province, Mozambique). However, 100 % of canines of known condition are broken from Site 11.1.

Females from four of the five sites exhibit broken incisors, while males from two sites exhibit broken incisors. Site 11.1 is the only site where both males and females have broken incisors. In this site, a greater proportion of female incisors (12.5 %) are broken than males incisors (9.09 %).

In four of the five sites, only females have broken premolars. Of individuals from Site 21.12, 42.86 % of females have broken premolars, while 50 % of males have lost teeth. 5.19 % of premolars of known condition from females are broken, while 11.11 % of premolar alveoli from males are partially or fully healed. In Site 6.9, a large proportion of premolars are broken (90 %).

There are only two sites from which there is data of both females and males at wear stage VI (Figure 5.46). No males have broken teeth. All females from both sites have broken incisors and canines. Only females from Site 21.12 have broken premolars and carnassials. 25 % of premolars and carnassials of known condition are broken, while there is a higher proportion of partially or fully healed carnassial alveoli (25 %) than premolar alveoli (8.33 %). The highest proportion of broken teeth is 66.67 % of canines from Site 3.1 (Chobe National Park, Savuti Chobe National Park and Mababe Zokotsama Community Concession, Botswana).

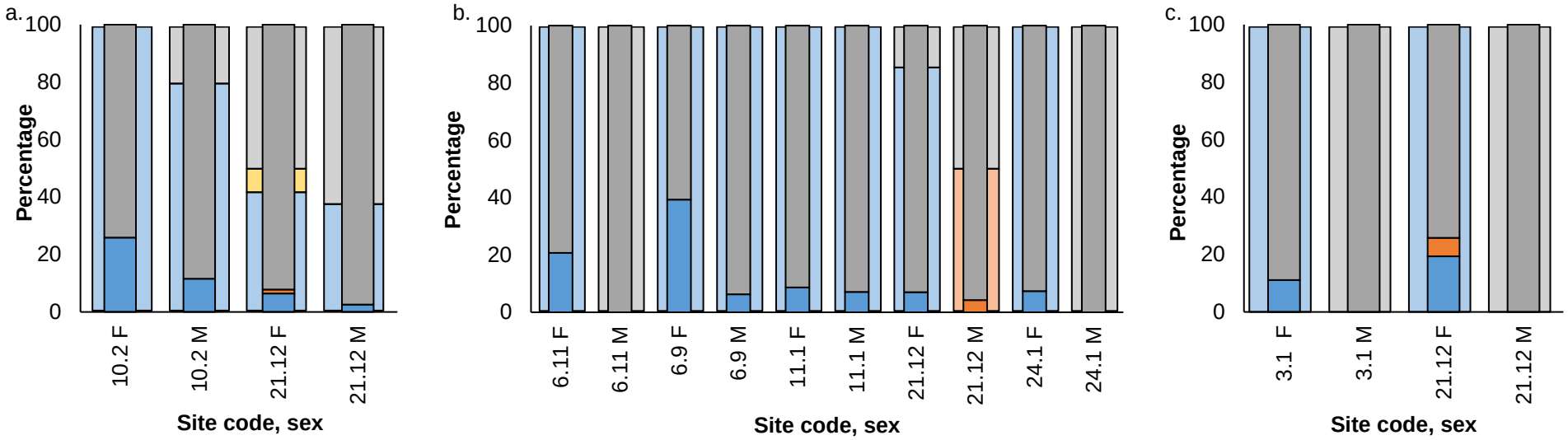

Figure 5.43: The proportion of present-day *C. crocuta* individuals with either no broken teeth, only broken teeth, only partially of fully healed alveoli, or both broken teeth and partially or fully healed alveoli. The proportion of unbroken, broken and partially or fully healed alveoli as a proportion of all teeth of known condition. a) Individuals with wear stage IV. b) Individuals with wear stage V. c) Individuals with wear stage VI. Site 3.1 = Chobe National Park, Savuti Chobe National Park, Botswana. Site 6.9 = Parc National des Virunga, Democratic Republic of the Congo. Site 6.11 = Parc National de l'Upemba, Democratic Republic of the Congo. Site 10.2 = Narok and Bomet County, Kenya. Site 11.1 = Tete Province, Mozambique. Site 21.12 = Balbal, Ngorongoro Conservation Area, Tanzania. Site 24.1 = Eastern Province, Zambia. See Table 5.33 for sample sizes.

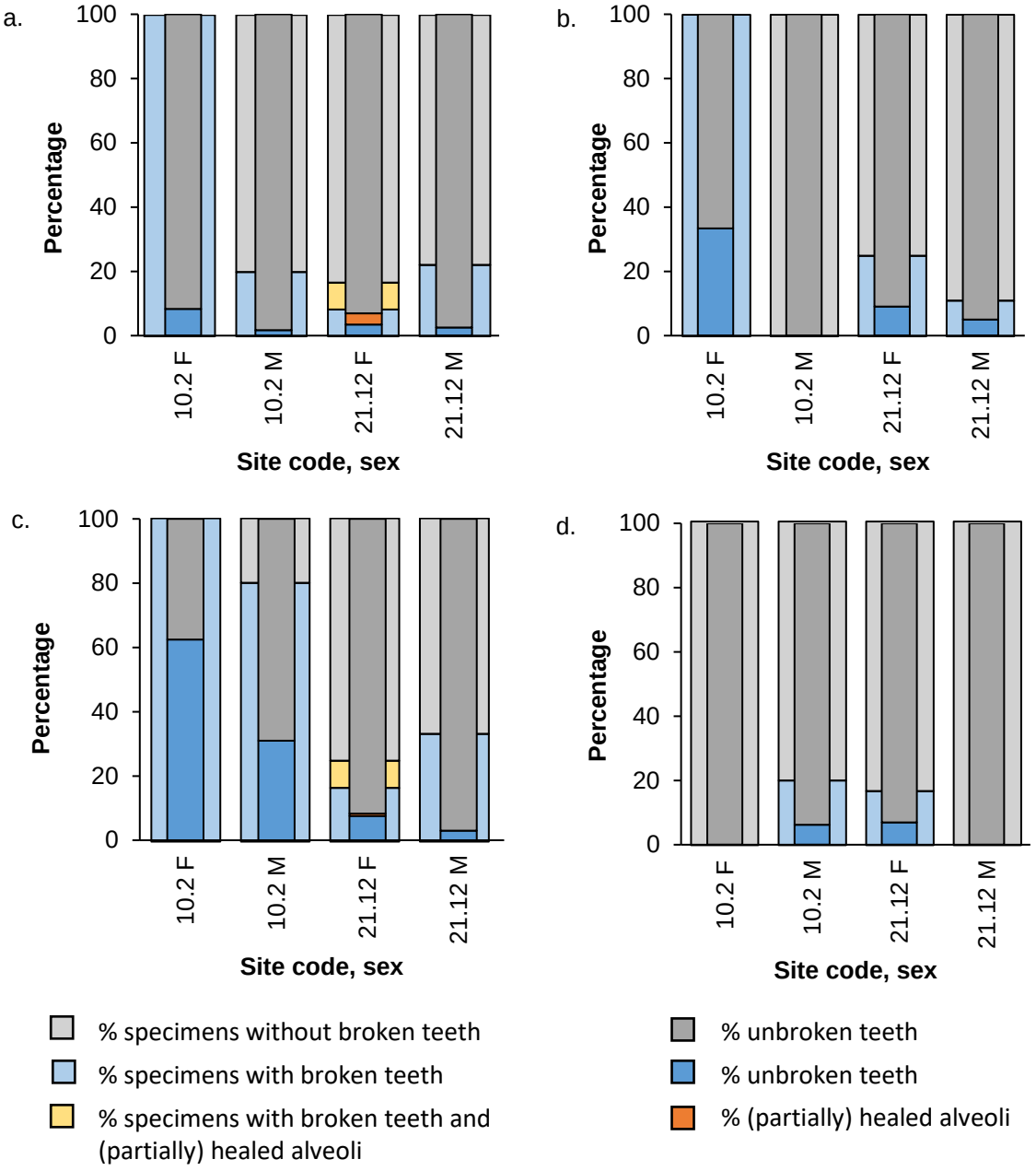

Figure 5.44: Condition of teeth as a percentage of all teeth of known condition for each group. Data are of *C. crocuta* with P3/p3 wear stage IV. F = female. M = male. Site 10.2 = Narok and Bomet County, Kenya, 21.12 = Ngorongoro Conservation Area, Tanzania. a) incisors, b) canines, c) premolars, d) molars. See Table 5.33 for sample sizes.

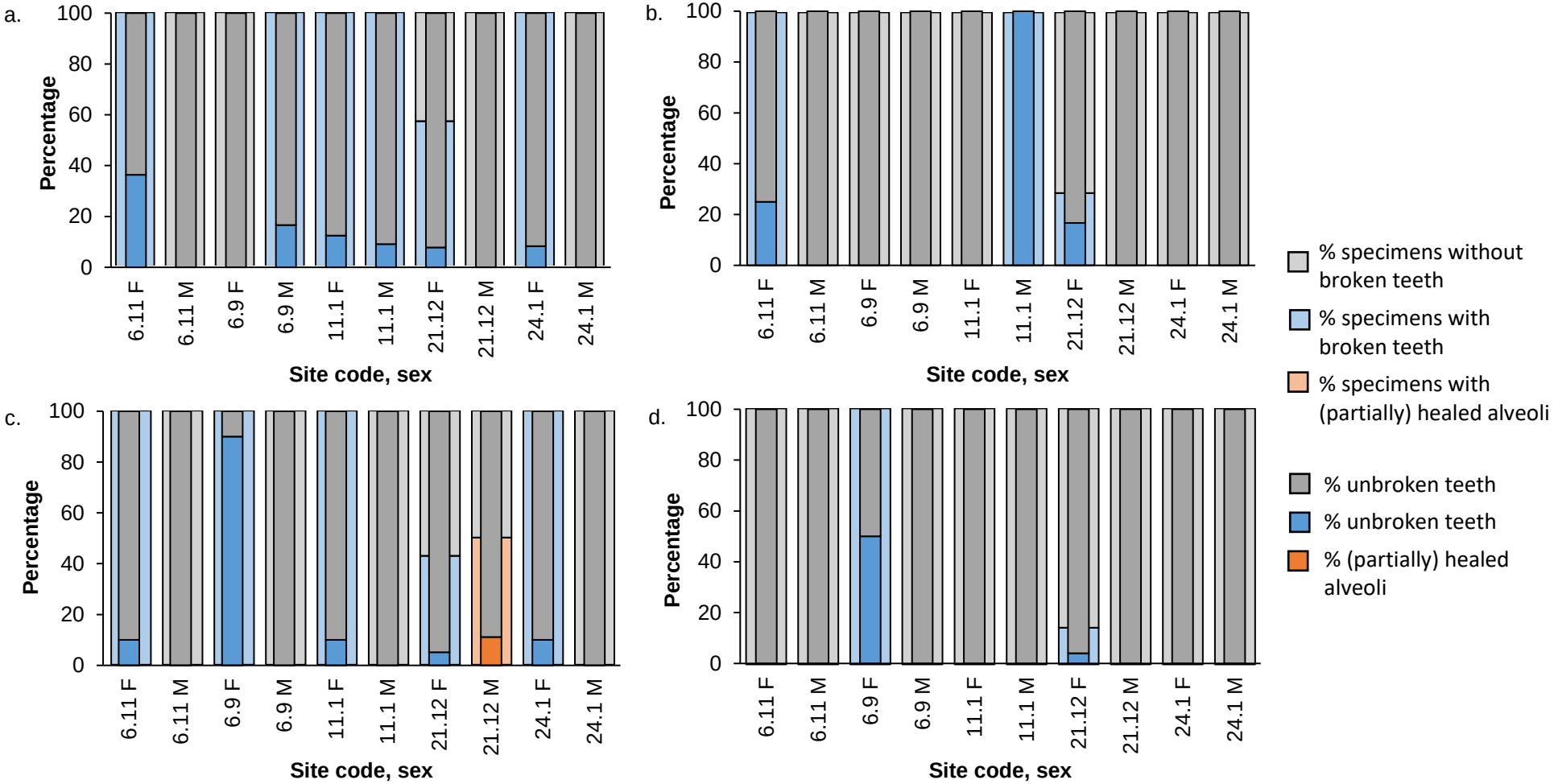

Figure 5.45: Condition of teeth as a percentage of all teeth of known condition for each group. Data are of *C. crocuta* with P3/p3 wear stage V. F = female. M = male. See caption for Figure 5.44 for full site details. a) incisors, b) canines, c) premolars, d) molars. See Table 5.33 for sample sizes.

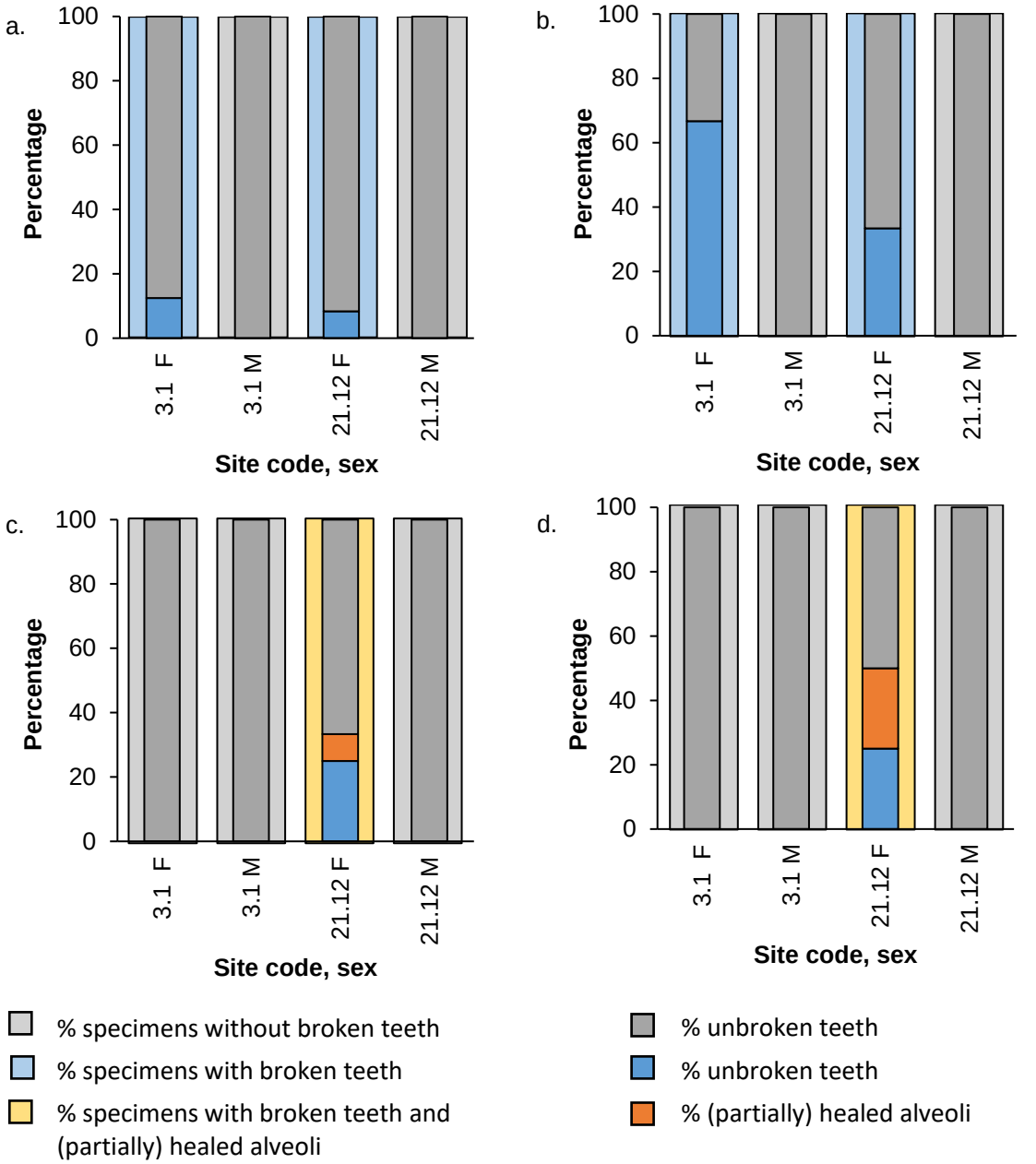

Figure 5.46: Condition of teeth as a percentage of all teeth of known condition for each group. Data are of *C. crocuta* with P3/p3 wear stage IV. F = female. M = male. Site 3.1 = Chobe National Park, Savuti Chobe National Park and Mababe Zokotsama Community Concession, Botswana, 21.12 = Ngorongoro Conservation Area, Tanzania. a) incisors, b) canines, c) premolars, d) molars. See Table 5.33 for sample sizes.

Table 5.33: Sample sizes included in the percentage calculations in Figure 5.43 to Figure 5.46.

Figure	Site/sex	No. C. crocuta individuals	No. teeth
Figure 5.43a (wear stage IV)	10.2 F	1	27
	10.2 M	5	130
	21.12 F	12	294
	21.12 M	9	234
Figure 5.43b (wear stage V)	6.11 F	1	29
	6.11 M	1	31
	6.9 F	1	28
	6.9 M	1	32
	11.1 F	1	23
	11.1 M	1	28
	21.12 F	7	171
	21.12 M	2	47
	24.1 F	1	27
	24.1 M	1	30
Figure 5.43c (wear stage VI)	3.1 F	1	27
	3.1 M	1	18
	21.12 F	1	31
	21.12 M	2	47
Figure 5.44a (incisors)	10.2 F	1	12
	10.2 M	5	59
	21.12 F	12	86
	21.12 M	9	78
Figure 5.44b (canines)	10.2 F	1	3
	10.2 M	5	13
	21.12 F	12	33
	21.12 M	9	20
Figure 5.44c (premolars)	10.2 F	1	8
	10.2 M	5	36
	21.12 F	12	132
	21.12 M	9	100
Figure 5.44d (carnassials)	10.2 F	1	4
	10.2 M	5	16
	21.12 F	12	43
	21.12 M	9	36
Figure 5.45a (incisors)	6.11 F	1	11
	6.11 M	1	12
	6.9 F	1	11
	6.9 M	1	12
	11.1 F	1	8
	11.1 M	1	11
	21.12 F	7	51
	21.12 M	2	17
	24.1 F	1	12
	24.1 M	1	12
Figure 5.45b (canines)	6.11 F	1	4
	6.11 M	1	3
	6.9 F	1	3
	6.9 M	1	4

	11.1 F	1	2
	11.1 M	1	1
	21.12 F	7	18
	21.12 M	2	5
	24.1 F	1	3
	24.1 M	1	3
Figure 5.45c (premolars)	6.11 F	1	10
	6.11 M	1	12
	6.9 F	1	10
	6.9 M	1	12
	11.1 F	1	10
	11.1 M	1	12
	21.12 F	7	77
	21.12 M	2	18
	24.1 F	1	10
	24.1 M	1	12
Figure 5.45d (carnassials)	6.11 F	1	4
	6.11 M	1	4
	6.9 F	1	4
	6.9 M	1	4
	11.1 F	1	3
	11.1 M	1	4
	21.12 F	7	25
	21.12 M	2	7
	24.1 F	1	2
	24.1 M	1	3
Figure 5.46a (incisors)	3.1 F	1	8
	3.1 M	1	1
	21.12 F	1	12
	21.12 M	2	16
Figure 5.46b (canines)	3.1 F	1	3
	3.1 M	1	1
	21.12 F	1	3
	21.12 M	2	3
Figure 5.46c (premolars)	3.1 F	1	12
	3.1 M	1	12
	21.12 F	1	12
	21.12 M	2	21
Figure 5.46d (carnassials)	3.1 F	1	4
	3.1 M	1	4
	21.12 F	1	4
	21.12 M	2	7

5.5.3 Discussion

5.5.3.1 Tooth breakage and loss with age

The proportion of *C. crocuta* individuals with broken teeth increases with age in the specimens from Site 21.12. None of the specimens with wear stage III from Site 21.12 have broken teeth. In fact, out of 29 stage III individuals across all sites, only three have broken teeth. Across all sites, at wear stage VII/VIII and older, all individuals have broken and/or lost teeth. Although the pattern is less clear, the proportion of broken teeth (as a percentage of teeth of known wear) increases with age. This suggests that at least some individuals are able to survive breakage of teeth, despite the loss of function in many cases. Similarly, Van Valkenburgh (2009) found that tooth fracture frequency increases with wear stage in a combined analysis of six carnivore families (Hyaenidae, Mustelidae, Canidae, Mephitidae and Procyonidae).

The number of individuals with partially or fully healed alveoli is low, although in females a greater proportion of stage VI individuals have evidence of lost teeth, and there is a greater proportion of lost teeth at this stage. In males, only stage V individuals exhibit tooth loss. Across specimens from all sites, there are no lost teeth in stage III individuals. When data from all sites are combined, there is some indication that the very oldest individuals are more likely to have lost teeth. Increased tooth loss in *R. rupicapra* was suggestive of increased susceptibility with age, and that individuals of this species also survived the loss of teeth (Pekelharing, 1974). In the present study it can therefore be suggested that older individuals may be are more susceptible to tooth loss. As data are limited, this conclusion is only tentative. The fact that there are individuals with healed alveoli suggest that the associated loss of function is survivable in some individuals.

The incisors and the canines are both used to kill prey (Biknevicius *et al.*, 1996). Incisors are also used to cut skin, subcutaneous tissue and muscle, while canines are used to consume muscle with attached bone (Van Valkenburgh, 1996). They may also be employed to crack bone (Van Valkenburgh and Ruff, 1987). Survival of the loss or breakage of these teeth may be explained by the nature of *C. crocuta* groups. Kruuk (1972) observed that there were some *C. crocuta*, particularly older females that did not participate in hunts. *C. crocuta* will converge on a kill, even if they did not participate in taking down the prey (Kruuk, 1972).

While other teeth may be utilised, the premolars are most frequently used when cracking bone (Van Valkenburgh, 1996). Survival after the loss or breakage of premolars may therefore be more difficult if there are periods of food stress during which consumption of bone is required to gain adequate food. Tooth breakage may also have been greater during the Pleistocene when other hard foods are consumed, notably frozen carcasses during cold periods. Prolonged cold

periods necessitating reliance of frozen carcasses may also limit the survival of individuals with broken teeth.

Overall, this reinforces the method proposed by Binder and Van Valkenburgh (2010) that tooth wear should be taken into account when assessing tooth breakage in Pleistocene deposits. For example, a deposit of predominantly wear stage IV teeth compared with a deposit of predominantly stage VI teeth may elicit a signal reflecting age rather than different ecological conditions.

5.5.3.2 Male and female tooth breakage

Van Valkenburgh (1988) found that in *C. crocuta*, a greater proportion of females had broken teeth. This was also found in the present study, which differed from Van Valkenburgh's (1988) study in that sites were considered separately, in case of geographical variation in tooth breakage. In all sites and all wear stages assessed (IV, V, VI), a greater proportion of females have broken teeth. Additionally, females have a greater proportion of broken teeth. This disparity between females and males is also apparent in most sites when split into the individual tooth types, as explored below.

At wear stages IV and V, a greater proportion of individuals have broken premolars. This is followed by incisors and then canines. The smallest proportion of individuals have broken carnassials, and carnassials are the teeth with the lowest percentage of breakage. At wear stage V, a greater proportion of females have broken incisors and canines, followed by premolars and carnassials. Canines are the tooth most frequently broken. A similar proportion of premolars and carnassials are broken, although more carnassials have been lost.

The prevalence of broken premolars and canines compared to carnassials is similar to other published studies. As a percentage of broken teeth, Van Valkenburgh (1988) found that canines had the greatest proportion, followed by premolars, incisors then carnassials. Similarly, as a percentage of all teeth observed, canines and premolars had the greatest proportion of breakage, followed by incisors and then carnassials (Van Valkenburgh, 2009).

Van Valkenburgh (2009) suggested that increased tooth breakage can be caused by more complete consumption of carcasses, especially consumption of bones. An additional consideration is that more rapid consumption of a carcass may lead to tooth breakage as teeth less suited to breaking bone may come into accidental contact with bone (Van Valkenburgh, 1996, 2009). The greater tooth breakage is therefore unexpected given that females often have preferential access to a carcass, unless a male's mother is a high-ranking female (Frank *et al.*,

1989), and are therefore expected to consume less bone than males. One explanation may be that many males will leave the clan (Hofer, 1998a), and it sometimes takes months until a new clan will accept the immigrant male (Kruuk, 1972). If the males often feed alone during this time, they would avoid the frenzied group feeding that may lead to accidental tooth breakage.

Canines may also be broken by struggling prey (Van Valkenburgh, 1988). However, there is no association between prey size and frequency of tooth breakage between species (Van Valkenburgh, 2009). It is difficult to assess whether tooth breakage many vary with prey size intraspecifically as there is insufficient data available to allow comparisons between sites.

Breakage of canines may also be associated with greater intraspecific aggression such as fighting (Van Valkenburgh, 2009). While there is high intraspecific competition at carcasses, Kruuk (1972) seldom observed fighting, even in the Ngorongoro Crater where there was a high population density of *C. crocuta* relative to prey. *C. crocuta* may be aggressive towards intruding individuals (Boydston *et al.*, 2001). This rarely involves direct physical contact, yet when it does, biting can lead to severe injuries (Kruuk, 1972). Physical contact is rare in defence of dens (Kruuk, 1972). 'Baiting', so called by Kruuk (1972), involves a number of males surrounding a female and occasionally biting her. Individual males may also target and bite a female (East and Hofer, 1993). Conversely, aggression, which may include biting, may be directed by females towards males (East and Hofer, 1993). There does not appear to be any information about the relative proportions of male versus female aggression involving physical contact, so it is unclear at present whether difference in aggression may cause the elevated level of canine breakage observed in females.

The overall less frequent breakage of carnassials compared with other teeth in males and females may be explained by their position in the jaw meaning that the blades are less likely to come into contact with bone (Kurtén and Werdelin, 1988). Bone does come into contact with carnassial blades as observed in dental microwear analyses (Van Valkenburgh *et al.*, 1990; Goillot *et al.*, 2009; Schubert *et al.*, 2010; Bastl *et al.*, 2012), and the protocone and parastyle of the P4 are involved in cracking bone (Kurtén and Werdelin, 1988), explaining why some observed carnassials are broken.

This difference between males and females is a further factor to be borne in mind when interpreting Pleistocene fossil material.

5.6 Conclusion

This chapter first analysed the influences upon *C. crocuta* biomass, and that of its competitor, *P. leo*. The results indicate that *C. crocuta* biomass is more sensitive to environmental conditions. *C. crocuta* are more abundant when prey biomass is greater (particularly very small- to medium-sized prey) and in areas with less extreme temperatures, particularly where winter temperatures are warmer. They are more abundant in areas where the driest month has more precipitation. There appears to be some spatial partitioning, with *C. crocuta* more abundant with greater semi-open vegetation cover, which appears to correspond with lower *P. leo* biomass. Together, this is important in interpreting the changing abundance of fossil C. crocuta in different Pleistocene environments in Europe and in assessing the potential causes of its extirpation.

Ontogenetic change in *C. crocuta* crania, mandibles and post-crania was assessed. This indicates that individuals with P3/p3 wear stage III are not fully grown in many cranial and mandibular measurements. This warrants exclusion of wear stage III individuals from further analysis, except for when assessing the dentition. Post-cranial sample sizes are small, yet most bones appear to be fully grown upon fusion of the epiphyses, regardless of P3/p3 wear stage.

Further, some measurements appear to increase in size through life. These measurements have been treated in separate wear stage groups in this chapter, and will be done so in the Chapter 6. There are measurements of mandibular strength and bite strength that are reduced in younger individuals, indicating that younger individuals may be disadvantaged, particularly when competition is high and consumption of tough foods (e.g. bone) is necessary. This is an important consideration when assessing the Pleistocene measurements, in addition to considering the causes for the extirpation of *C. crocuta* from Europe.

The analysis of SSD indicates that while body mass of *C. crocuta* is largely female-biased, the SSD values are lower than other carnivores such as *P. leo* and *P. pardus*. Most craniodental measurements have no consistent SSD direction, indicating that neither males nor females are consistently larger. This indicates that the representation of males and females in Pleistocene deposits will not influence the morphometric results. The exceptions are some of the mandibular measurements, the results of which indicate that females are larger. None of the SSD values correlated with any of the environmental variables, indicating that degree of SSD does not vary with changes in environmental conditions. Therefore, it is unlikely that the proportion of males and females in the Pleistocene assemblages would influence the morphometric results.

While sample sizes of post-crania were unfortunately insufficient to assess consistency in SSD, the SSD values are low. It is therefore anticipated that for Pleistocene assemblages, sex of the individuals will not influence the morphometric results.

The analysis of environmental influences upon body mass, craniodental and post-cranial measurements show some consistent results. The cranial and mandibular measurements that have the strongest statistical results (condylobasal length, and length between the c and m1 alveoli) appear to increase isometrically with overall body size. Most of the post-cranial measurements have associations with environmental conditions that are similar to the two cranial and mandibular measurements, suggesting that they also increase in size with body size.

The cranial measurement, mandible measurement, post-cranial measurements and body mass are all positively associated with warm summer temperatures. Many of the morphometric measurements are positively associated with semi-open and closed vegetation cover, while they are negatively associated with open vegetation cover. The c-m1 length measurement appears to be weakly but positively influenced by precipitation of the wettest month, as are most of the post-cranial measurements. However, female body masses are significantly and negatively correlated with precipitation of the wettest month. This disparity may be due to the small sample sizes of the body mass tests.

A further influence on female body mass is *P. leo* density, which has a negative correlation. This was not included in the craniodental and post-cranial analyses because of lack of data. However, the absence of such variables may explain why the craniodental models with the strongest statistics still only explain around 45 % of the variance in these measurements.

It is therefore predicted that during the Pleistocene, *C. crocuta* were larger in periods of warmer summers, in areas of semi-open and closed vegetation cover and reduced areas of open vegetation cover. *C. crocuta* may also have been larger during periods with reduced interspecific competition.

Finally, tooth loss and breakage were assessed. Loss of teeth is uncommon, relative to the frequency of broken teeth in *C. crocuta*. There is some indication that tooth loss is more common in older individuals, suggesting that older individuals are more susceptible to tooth loss, or that the associated loss of function is survivable in some cases. Tooth breakage increases with age, warranting assessment of the age profile of the Pleistocene assemblages before interpreting the breakage results. Tooth breakage is also more prevalent in females than males, which will need to be taken into account when interpreting Pleistocene tooth breakage. Carnassials are the tooth that is least frequently broken. In light of this, the Pleistocene breakage results will be split into tooth types prior to interpretation.

6 Pleistocene *Crocuta crocuta*

6.1 Body mass reconstruction

6.1.1 Introduction

Body mass is related to a number of life history and ecological factors, including the size of prey targeted (Carbone *et al.*, 2007) and hunting ability (Biewener, 1989); these may have implications for the persistence or extirpation of an individual from an area. As outlined in Section 5.4, body mass may be influenced by a number of environmental conditions such as temperature (Mayr, 1956), presence of competitors (McNab, 1971) and food quality and abundance (McNab, 2010) , all of which changed through the Pleistocene and may have impacted upon *C. crocuta* body masses.

A new intraspecific method for reconstructing *C. crocuta* body mass is proposed in the current work (Section 4.4.2.1), which will here be used to assess variation in the Pleistocene study sample.

The research questions are as follows:

- Is the model suitable for reconstruction of Pleistocene *C. crocuta* body masses?
- Were there changes in *C. crocuta* body size through time?
- What might be the reasons for these changes?

6.1.2 Results

6.1.2.1 The model

The m1 lengths and body masses included in the OLS regression models can be found in Appendix 10.7, Table 10.20. The results of the OLS regression of *C. crocuta* body mass against m1 length (called OLS1) are shown in Figure 6.1a and b. The test is significant (p-value <0.05) with a high r^2 value (75.87 %). The %PE (7.73 %) and %SEE (12.68 %) are low, indicating good predictive power of the model. The standardised residuals, leverage values, and Cook's distance are shown in Figure 6.1c and d. None of the leverage values exceed the leverage threshold of 0.55. However, the dataset from Ethiopia has a standardised residual value exceeding the threshold value of 2 and a Cook's distance value exceeding the threshold of 0.36. The body mass value from Ethiopia is 35.83 kg (Powell-Cotton, n.d., cited in Shortridge, 1934), more than 10 kg smaller than the next smallest body mass. As the original publication could not be accessed,

there was no way to determine whether the Ethiopian individual was an adult or a juvenile. It was therefore decided to re-run the model without the Ethiopian data.

The results of the model excluding Ethiopia (OLS2) are shown in Figure 6.2. As before, the test is significant with a p-value <0.05. The r^2 value is high at 81.13 %. The %PE (5.79 %) and %SEE (8.7 %) are lower than in OLS1, indicating even better predictive power of the model. None of the leverage or Cook's values exceed the respective thresholds. The female *C. crocuta* dataset from Botswana is a potential outlier with standardised residual value of 2.346. However, there are two reasons for keeping this sample within the model. Firstly, the sample does not exceed the Cook's or leverage thresholds, and only exceeds the residual threshold by 0.346. Secondly, the %PE and %SEE are very low, indicating strong predictive power of the model, even with the inclusion of female *C. crocuta* from Botswana.

The correction factors for detransformation bias were calculated for OLS2 (Figure 6.2a). The range of values is very small with offsets of between 0.29 and 0.35 %, indicating that the choice of factor will have little impact upon the body mass values. The RE factor value was chosen as it is the intermediate value.

a

OLS1 model equation			
Log10 Body mass = -2.688 + (3.083 * Log10 m1 length)			
Model statistics			
r^2	***p-value***	***%PE mean***	***%SEE***
75.87	<0.05	7.73	12.68
Statistical thresholds			
Leverages	***Cook's D F stat***	***Cook's D 4/n***	
0.55	2.81	0.36	
Correction factors			
SE	***RE***	***QMLE***	
1.0058	1.0033	1.0071	

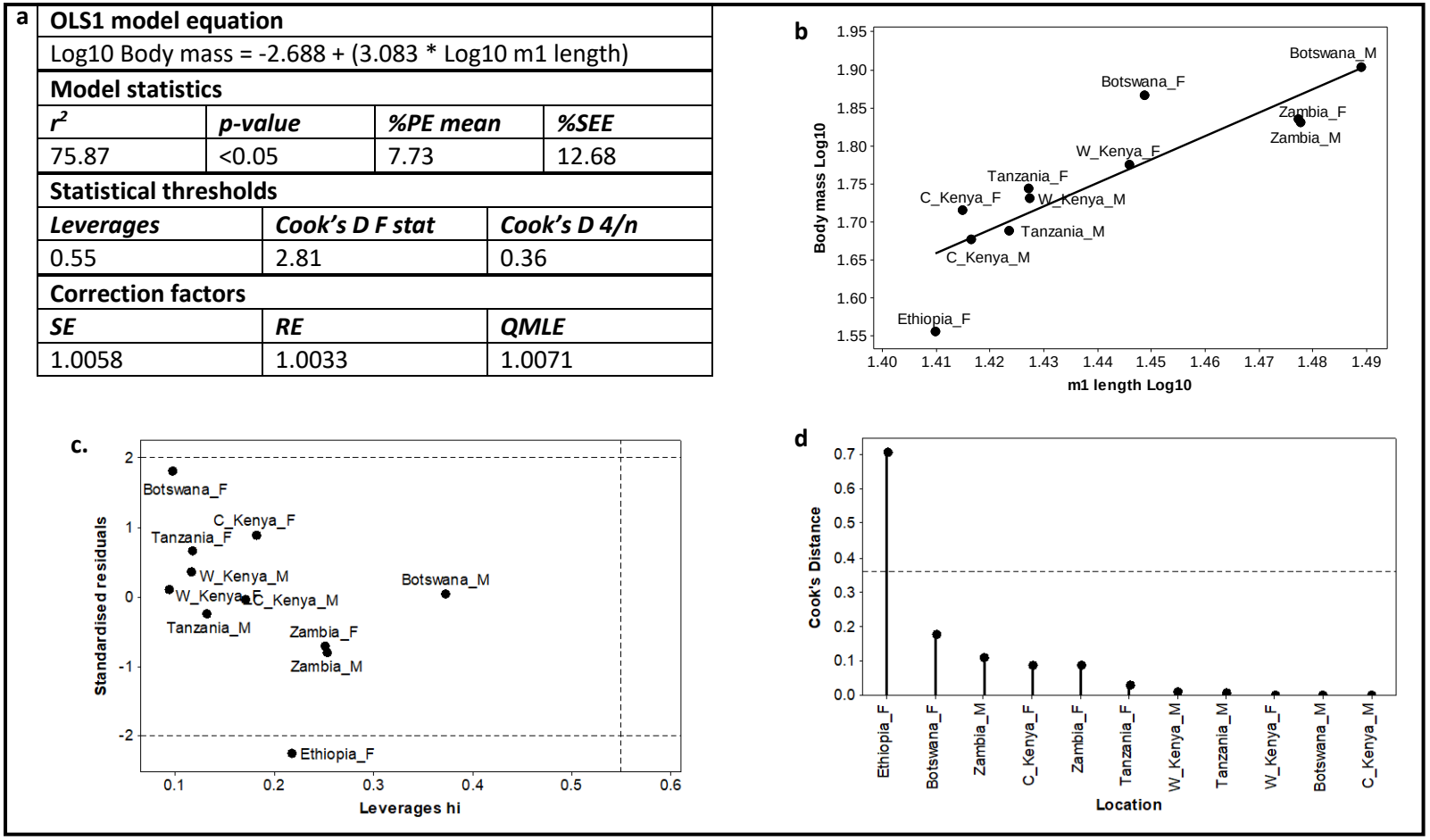

Figure 6.1: Regression model and outliers for OLS1. Dashed lines indicate the outlier threshold values. W_Kenya refers to the Sotik and Masai Mara locations. C_Kenya refers to the Aberdare, Archers Post and Mount Kenya locations. In calculation of the %PE (see Equation 4.17) the detransformed predicted body mass values were multiplied by the SE correction factor, as this factor is larger than the RE but smaller than the QMLE.

a.

OLS2 model equation			
Log10 body mass = -1.92 + (2.558 * Log10 m1 length)			
Model statistics			
r^2	***p-value***	***%PE mean***	***%SEE***
81.13	<0.05	5.78	8.7
Statistical thresholds			
Leverages	***Cook's D F stat***	***Cook's D 4/n***	
0.6	2.92	0.4	
Correction factors			
SE	***RE***	***QMLE***	
1.0029	1.0034	1.0035	

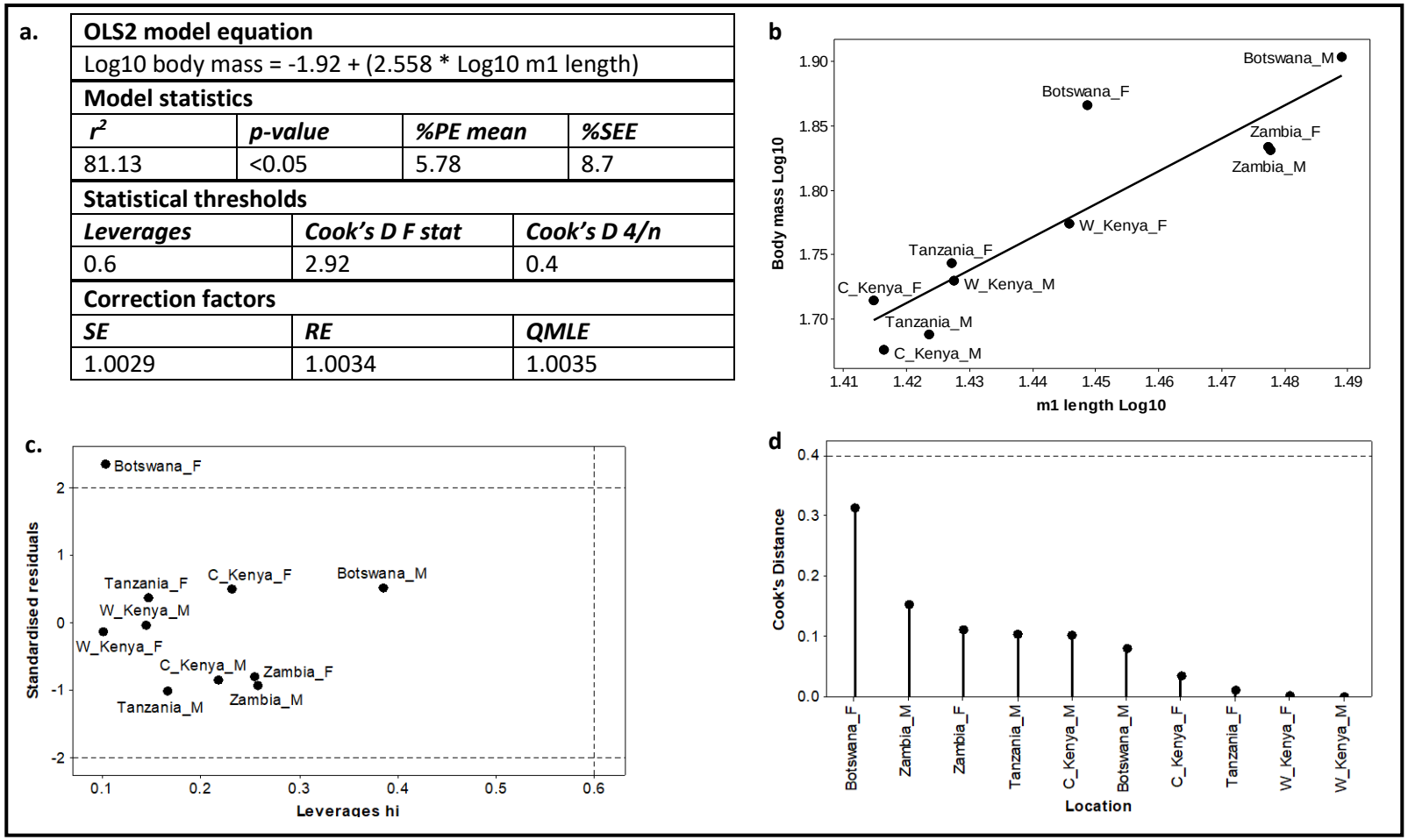

Figure 6.2: Regression model and outliers for OLS2. Dashed lines indicate the outlier threshold values. W_Kenya refers to the Sotik and Masai Mara locations. C_Kenya refers to the Aberdare, Archers Post and Mount Kenya locations. In calculation of the %PE (see Equation 4.17) the detransformed predicted body mass values were multiplied by the RE correction factor, as this factor is larger than the SE but smaller than the QMLE.

6.1.2.2 Body mass reconstruction

The body masses of Pleistocene *C. crocuta* were reconstructed from m1 lengths using the equation from OLS2, and are shown in Figure 6.3. In Britain, *C. crocuta* were small during MIS 9, and large during the later part of MIS 7, although these body mass predictions are based on one individual from each stage, and they overlap with the very largest and smallest values from other stages. While there is variation in the body masses of *C. crocuta* from the Late Pleistocene, there is considerable overlap, with no clear distinctions between MIS 5e, 5c or 3.

Considering the rest of Europe, there is again considerable overlap in the body mass estimates from different countries. The estimates from Castlepook Cave (Ireland) and San Teodoro (Italy) are notably consistently small, while the body masses from other countries range from similarly low values up to higher values. The lowest values from Castlepook Cave (71.08±1.24 kg) and San Teodoro (72.31±1.24 kg) are still larger than the single value from Grays (64.56±1.23 kg). Overall, the very smallest values are from Joint Mitnor Cave (63.81±1.23 and 64.04± 1.23 kg) and Kents Cavern (64.38±1.23 kg).

Across Europe, the largest calculation is from Uphill Cave 7 or 8 at 122.49±1.42 kg, which is around 49 kg larger than the smallest body mass observed. The next largest body masses are from Kents Cavern (116.21±1.4 kg) and Teufelslucke (114.9±1.39 kg), although the former (as noted) spans both the largest and smallest values recorded.

To assess further differences between the reconstructed Pleistocene body masses, an ANOVA with post-hoc Tukey Pairwise Comparisons was run (Table 6.2). Only datasets with sample sizes of ten or greater were included. Data from Joint Mitnor Cave and Kents Cavern are non-normally distributed, so the non-parametric Mann-Whitney tests were performed on these data (Table 6.3).

The p-value of the ANOVA test is <0.05, indicating that there is a significant difference between at least two of the assemblages. The post-hoc Tukey Pairwise Comparisons indicate that *C. crocuta* body masses from the Austrian MIS 3 site of Teufelslucke are significantly larger than those from sites of both Late Interglacial (Tornewton Lower Hyaena Stratum, Tornewton Upper Hyaena Stratum, Kirkdale Cave) and MIS 3 (Sandford Hill) age in Britain. *C. crocuta* body masses from other sites are not significantly different, reflecting the overlapping body mass values in Figure 6.3.

The Mann-Whitney tests (Table 6.3) indicate that body masses from Last Interglacial Joint Mitnor Cave are significantly smaller than those from the Last Cold Stage sites of Coygan Cave, Pin Hole, Uphill Caves 7 or 8, Caverne Marie Jeanne 4eme Niveau, Teufelslucke and Kents Cavern. *C. crocuta* from Kents Cavern are significantly larger than those from Last Interglacial Joint

Mitnor Cave, Kirkdale Cave, Tornewton Upper and Lower Hyaena Stratum, and MIS 3 Sandford Hill, but significantly smaller than those from MIS 3 Teufelslucke. Overall, where there are significant differences, *C. crocuta* from Last Interglacial sites are significantly smaller than those from MIS 3 sites in Britain.

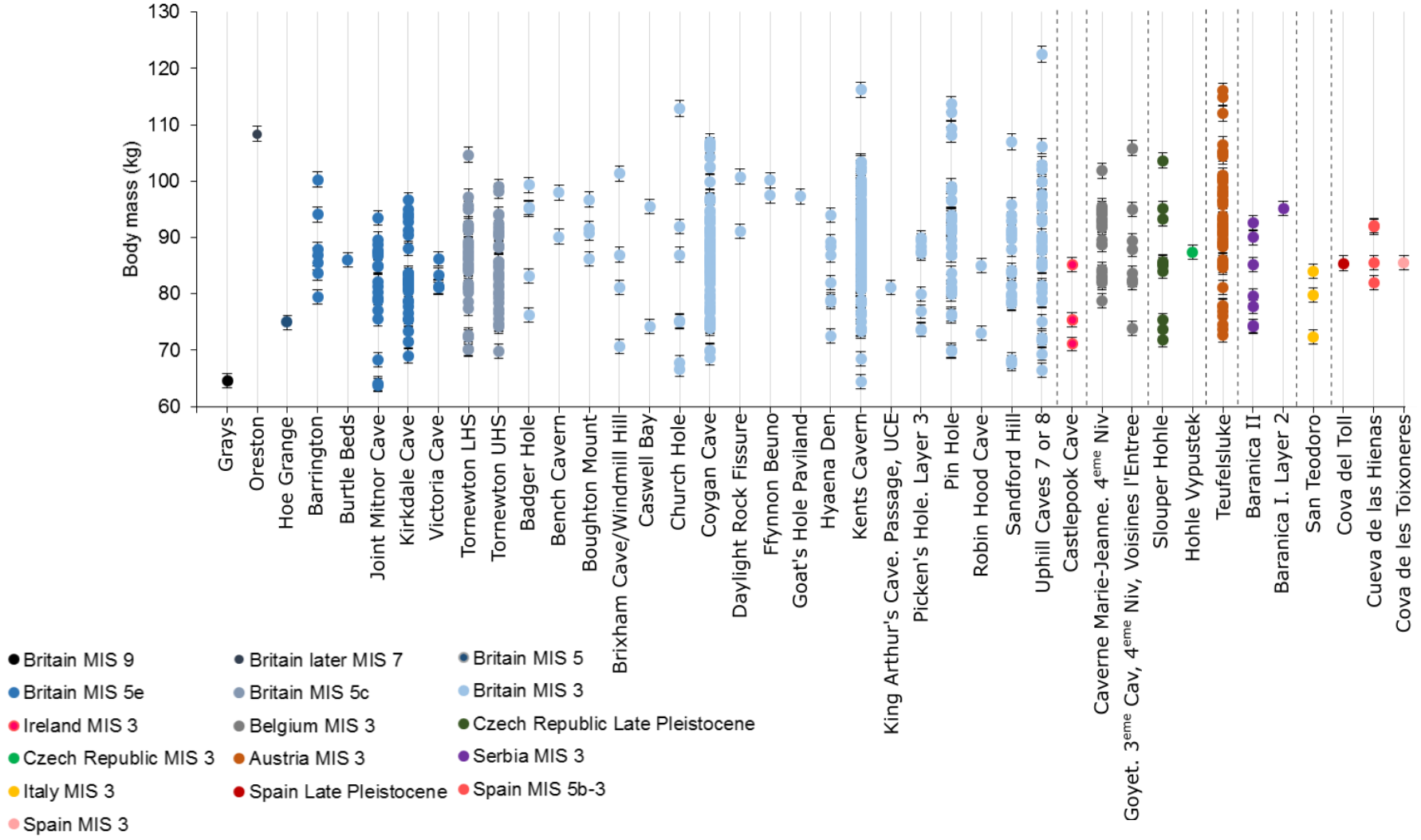

Figure 6.3: Body mass reconstructions and prediction interval of each estimate of Pleistocene *C. crocuta* from Europe. See Table 6.1 for sample sizes.

Table 6.1: Number of body mass reconstructions for each site in Figure 6.3.

Country	Site	No. body mass reconstructions
Britain	Grays	1
	Oreston	1
	Hoe Grange	1
	Barrington	7
	Burtle Beds	1
	Joint Mitnor Cave	19
	Kirkdale Cave	31
	Victoria Cave	4
	Tornewton Lower Hyaena Stratum	33
	Tornewton Upper Hyaena Stratum	34
	Badger Hole	5
	Bench Cavern	2
	Boughton Mount	4
	Brixham Cave/Windmill Hill	4
	Caswell Bay	2
	Church Hole	7
	Coygan Cave	74
	Daylight Rock Fissure	2
	Ffynnon Beuno	2
	Goat's Hole Paviland	1
	Hyaena Den	8
	Kents Cavern	109
	King Arthur's Cave. The Passage, Upper Cave Earth	1
	Picken's Hole. Layer 3	9
	Pin Hole	34
	Robin Hood Cave	2
	Sandford Hill	22
	Uphill Caves 7 or 8	35
Ireland	Castlepook Cave	4
Belgium	Caverne Marie-Jeanne. 4eme Niveau	21
	Goyet. 3eme Caverne, 4eme Niveau Ossifère, Galleries Voisines de l'Entrée	8
Czech Republic	Slouper Höhle	10
	Höhle Výpustek	1
Austria	Teufelslucke	47
Serbia	Baranica II	7
	Baranica I. Layer 2	1
Italy	San Teodoro	3
Spain	Cova del Toll	1
	Cueva de las Hienas	4
	Cova de les Toixoneres	1

Table 6.2: Results of the Tukey Pairwise Comparisons, run after the ANOVA test, on predicted Pleistocene *C. crocuta* Log10 body masses. Sites that do not share a grouping letter are significantly different at 95 % confidence. p-value = <0.05.

Site	n	Mean body mass (Log10)	Grouping
Teufelslucke	47	1.963	A
Caverne Marie Jeanne. 4eme Niveau	21	1.95	A B
Pin Hole	34	1.947	A B
Uphill Caves 7 or 8	35	1.939	A B
Coygan Cave	74	1.936	A B
Slouper Höhle	10	1.927	A B
Tornewton LHS	33	1.926	B
Tornewton UHS	34	1.924	B
Sandford Hill	22	1.92	B
Kirkdale Cave	31	1.915	B

Table 6.3: Results of Mann-Whitney tests for significant differences on Log10 body masses of Pleistocene *C. crocuta*. Top figures are W-values, bottom figures are p-values. Shaded boxes indicate significant differences at 95 % confidence. See Table 6.1 for sample sizes.

Site and median body mass (log10)	Joint Mitnor Cave 1.913	Kents Cavern 1.947
Joint Mitnor Cave 1.913	-	689.5 <0.05
Kirkdale Cave 1.913	469.5 0.772	8439 <0.05
Tornewton LHS 1.929	434 0.19	8326.5 0.01
Tornewton UHS 1.924	450.5 0.25	8429.5 0.006
Coygan Cave 1.937	657 0.025	10573.5 0.121
Kents Cavern 1.947	689.5 <0.05	-
Pin Hole 1.948	370 0.008	7867.5 0.928
Sandford Hill 1.915	363.5 0.36	7561.5 0.024
Uphill Caves 7 or 8 1.941	412.5 0.047	8088.5 0.388
Caverne Marie Jeanne. 4eme Niveau 1.961	270.5 0.001	7030.5 0.492
Slouper Höhle 1.929	269.5 0.491	6679.5 0.183
Teufelslucke 1.964	359 <0.05	7888.5 0.01

Body masses were combined from all sites in Britain dating to MIS 5e, to MIS 5c and to MIS 3. Tests for significant difference were then performed on these combined datasets (Table 6.4). The t-test reveals no significance difference at 95 % confidence in body masses between MIS 5e and 5c. By contrast, the Mann-Whitney tests indicate that *C. crocuta* from the Middle Devensian, MIS 3, are significantly larger than those from the early Devensian, MIS 5e and 5c, in Britain.

Table 6.4: Tests for significant difference of reconstructed *C. crocuta* Pleistocene body masses from different British sites combined for MIS 5e (n = 62), 5c (n = 67) and 3 (n = 323). Shaded boxes indicate significant difference at 95 % confidence.

Comparison	**Mean/Median**	**Test**	
	Mean (log10)	***t-test***	
MIS 5c vs	1.925	*t-value*	-1.29
MIS 5e	1.916	*p-value*	0.198
	Median (log10)	***Mann Whitney***	
MIS 3 vs	1.944	*W-value*	65208.5
MIS 5c	1.928	*p-value*	0.014
MIS 3 vs	1.944	*W-value*	65393
MIS 5e	1.915	*p-value*	<0.05

In order to examine the possible impacts of modern human arrival in Britain and the progressive intensification of abrupt climate change during MIS 3 on *C. crocuta* body mass, body mass values were plotted in chronological order, based on available radiocarbon dates from each assemblage (Figure 6.4). Where possible, dates derived from *C. crocuta* specimens were used. From Ffynnon Beuno, a date was derived from a *M. primigenius* bone that had been gnawed by *C. crocuta*. The only date available from Badger Hole was from an *E. ferus* specimen. See Appendix 10.1, Table 10.1 and Table 10.4 for full details and references.

The results indicate no consistent increase or decrease in body mass through MIS 3 in response to either of the variables of interest.

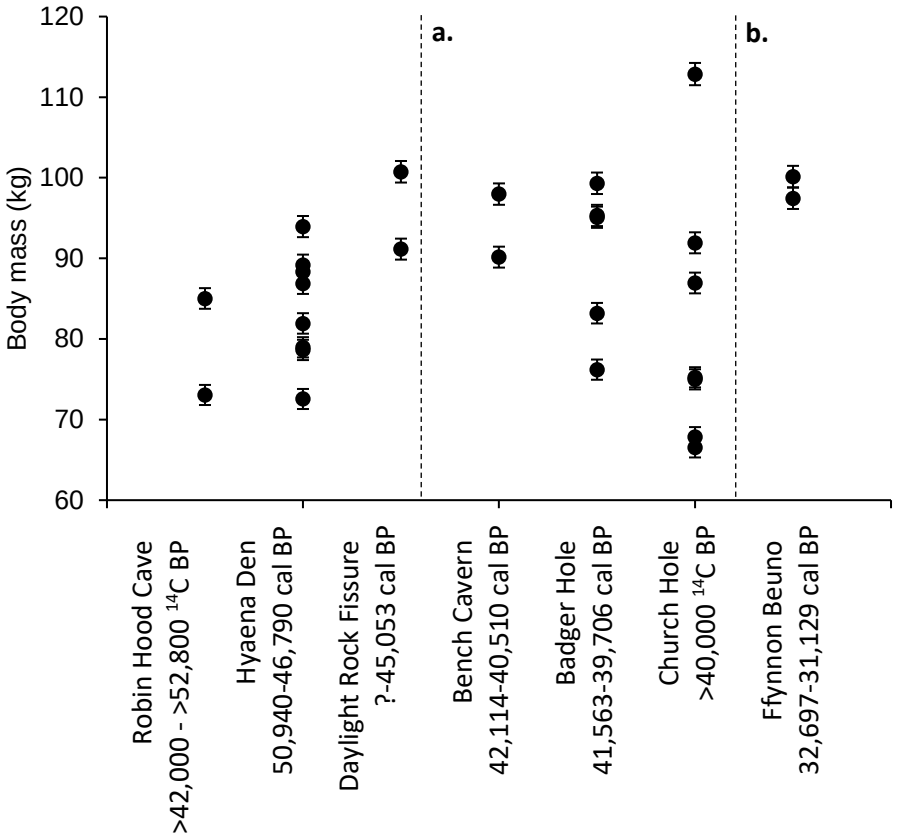

Figure 6.4: Body mass estimates with prediction intervals of Pleistocene *C. crocuta* from Britain, placed in chronological order. See Appendix 10.1, Table 10.1 and Table 10.4 for full details and references, and Table 6.1 for sample sizes. Dashed line (a.) indicates the assemblages dated prior to the earliest arrival of modern humans in Britain (42,350 – 40,760 cal BP; Higham *et al.*, 2011; Proctor *et al.*, 2017). Dashed line (b.) indicates the assemblages dated prior to 36.5 b2k, a point after which interstadials become shorter and less frequent, as evidenced by the Greenland ice core $\delta^{18}O$ data (Andersen *et al.*, 2004; Rasmussen *et al.*, 2014; Seierstad *et al.*, 2014).

Figure 6.5 shows the *C. crocuta* body mass values, categorised by dominant vegetation type (grassland, mixed, forested). The deposits included are only those from which vegetation could be directly reconstructed. See Appendix 10.1, Table 10.1 and Table 10.2 for further details and references.

The largest body masses are from Pin Hole, where open grassland was the dominant vegetation type but there is considerable overlap in the body mass values from areas with grassland and with mixed vegetation. The smallest body mass value is from Grays, characterised by closed woodland vegetation. However, the other body mass reconstruction from a deposit with forested vegetation (Cova de les Toixoneres) has a value that plots within the range of the mixed and grassland deposits. Overall there is no coherent pattern of body mass with vegetation.

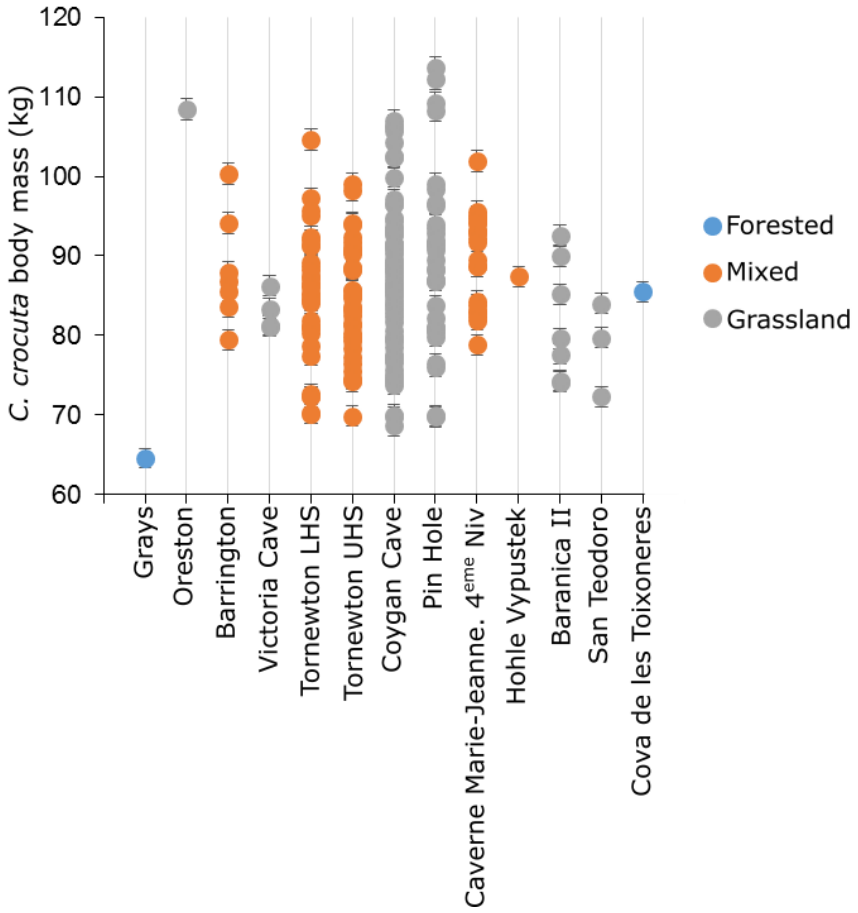

Figure 6.5: *C. crocuta* body mass reconstructions, categorised by dominant vegetation cover. See Appendix 10.1 Table 10.1 and Table 10.2 for further details and references. See Table 6.1 for sample sizes.

C. crocuta body mass estimates were then plotted against those from other predators and potential prey species (Figure 6.6 to Figure 6.11) to assess whether there was covariation between the species in Britain. The body mass data for *C. lupus* were reconstructed by Flower (2016), those for other species by Collinge (2001).

The largest *C. crocuta* body masses occurred during MIS 7 and MIS 3, during which time *C. lupus* were at their smallest, at 35.4 kg and 34.03 kg, respectively (Figure 6.6). It is furthermore interesting to note the absence of *C. crocuta* from Britain during MIS 5a (when wolves reached their maximum body mass, Flower, 2016). While the initial observation might suggest that the presence of hyaenas acted as a control on wolf body mass (and concomitant access to resources) during the relatively open conditions of MIS 7 and MIS 3, the large range of *C. crocuta* body mass variation within each stage and the small datasets across which to compare the species make it difficult to see a definitive pattern.

Other carnivores

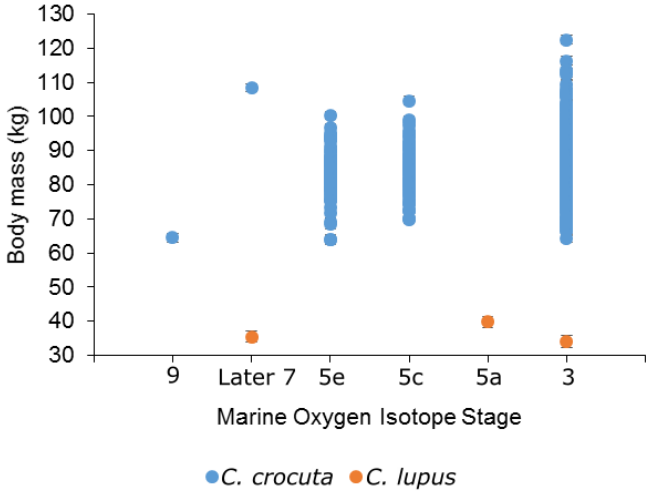

Figure 6.6: Pleistocene *C. crocuta* body masses and *C. lupus* mean body masses with associated prediction intervals (from Flower, 2016). Sample sizes for *C. crocuta*: MIS 9 (n = 1), later MIS 7 (n = 1), MIS 5e (n = 62), MIS 5c (n = 67), MIS 3 (n = 323).

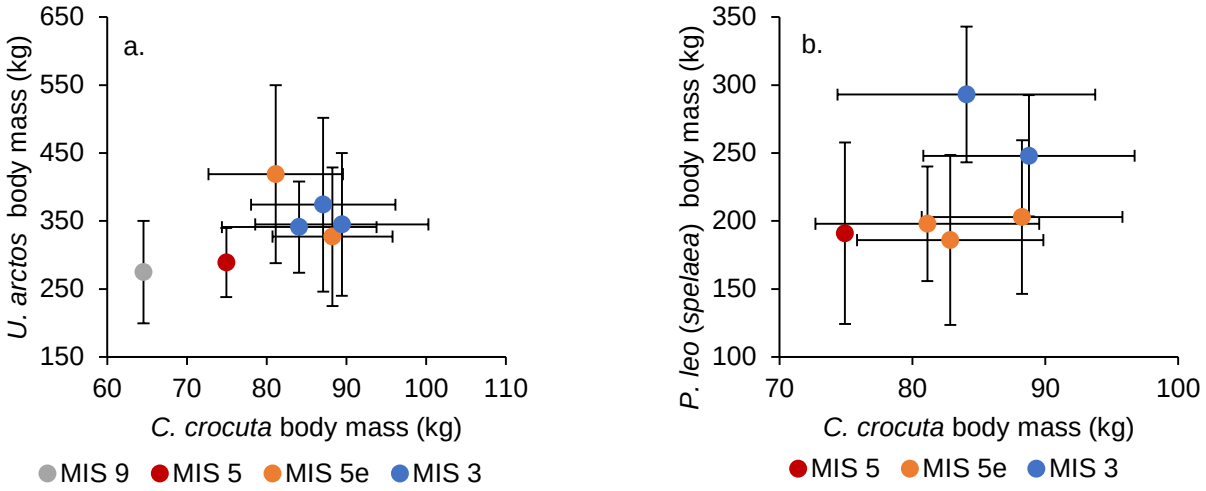

Figure 6.7: Pleistocene *C. crocuta* and other carnivore mean body masses with standard deviations (from Collinge, 2001). a. *U. arctos*. b. *P. leo* (*spelaea*). MIS 5 = undifferentiated.

Cervidae

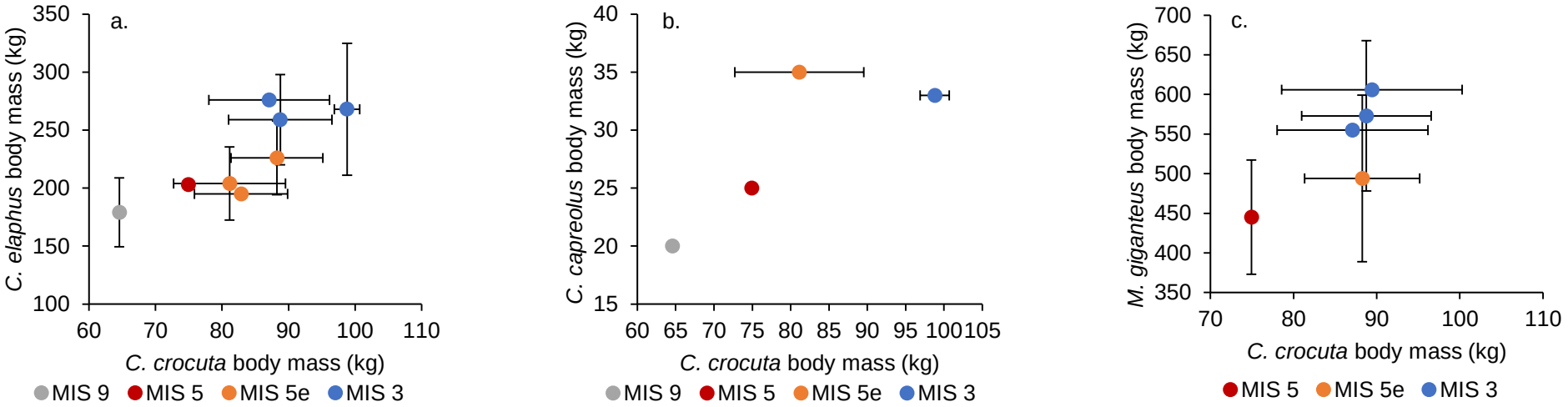

Figure 6.8: *C. crocuta* and Cervidae species mean body masses with standard deviations (from Collinge, 2001). a. *C. elaphus*. b. *C. capreolus*. c. *M. giganteus*. d. *R. tarandus*. e. *D. dama*. MIS 5 = undifferentiated.

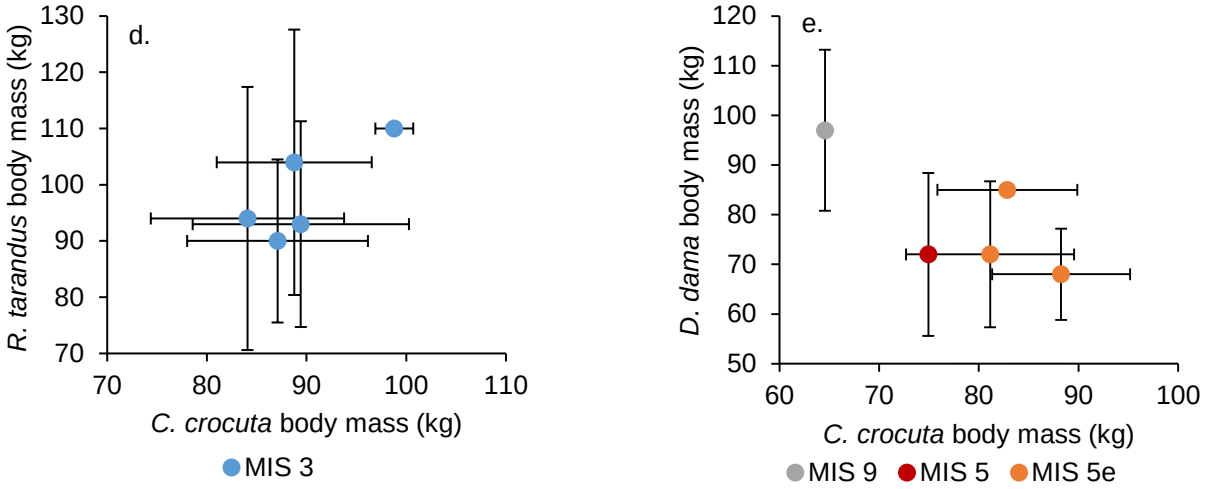

Figure 6.8 continued.

Bovidae

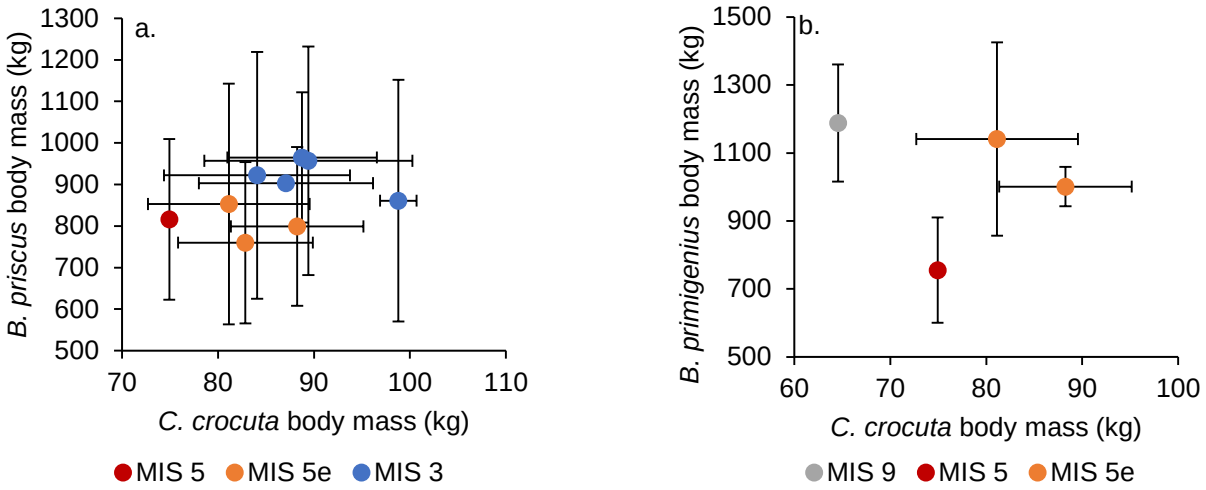

Figure 6.9: *C. crocuta* and Bovidae mean body masses with standard deviations (from Collinge, 2001). a. *B. priscus*. b. *B. primigenius*. MIS 5 = undifferentiated.

Rhinocerotidae

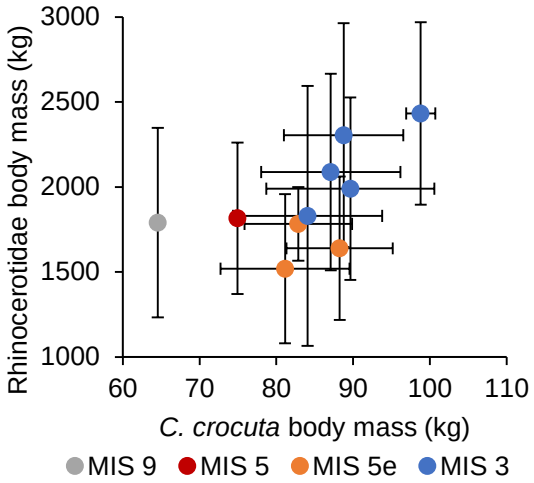

Figure 6.10: *C. crocuta* and Rhinocerotidae species mean body masses with standard deviations (from Collinge, 2001). MIS 9, 5 and 5e = *S. hemitoechus*. MIS 3 = *C. antiquitatis* MIS 5 = undifferentiated.

Equidae

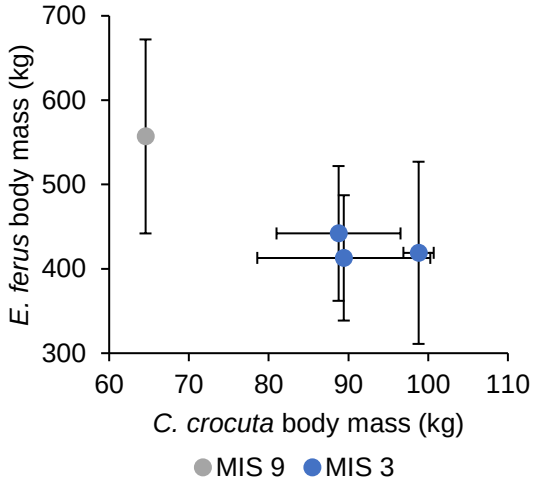

Figure 6.11: *C. crocuta* and potential *E. ferus* mean body masses with standard deviations (from Collinge, 2001). MIS 5 = undifferentiated.

There is some evidence that *C. crocuta* increased in size with a decrease in *U. arctos* body mass during MIS 5e and MIS 3 (Figure 6.7a). However, this pattern does not hold when including Hoe Grange Cavern (MIS 5) and Grays (MIS 9). Figure 6.7b shows that there is no obvious relationship between the body masses of *C. crocuta* and *P. leo* (*spelaea*).

Of the potential prey species, there is a positive correlation between the Rhinocerotidae (*S. hemitoechus* and *C. antiquitatis*) and *C. crocuta* body masses (Figure 6.10). This is especially clear in MIS 5, 5e and 3, although *C. crocuta* are smaller than expected given *S. hemitoechus* body mass during MIS 9. There is also a positive correlation between *C. crocuta* and *C. elaphus* body masses (Figure 6.8a). There is some evidence of a positive correlation between *C. crocuta* and *C. capreolus* body masses (Figure 6.8b) although this is based on only four data points.

C. crocuta body masses do not scale with those of all potential prey species, notably some of the other cervids. During MIS 5e and 3, *M. giganteus* body masses increase while *C. crocuta* body masses remain largely unchanged (Figure 6.8c). There is also little obvious relationship between *C. crocuta* and *R. tarandus* body masses during MIS 3 (Figure 6.8d).

C. crocuta and *D. dama* body masses do not appear to correlate during MIS 5 and 5e (Figure 6.8e), although *C. crocuta* are smaller than expected, given *D. dama* body mass during MIS 9. This is very similar to the relationship between *C. crocuta* and *E. ferus* body masses (Figure 6.11).

There is no relationship between *C. crocuta* and *B. priscus* body masses (Figure 6.9a) and with only four data points to illustrate *C. crocuta* and *B. primigenius* body masses (Figure 6.9b), no obvious relationship with aurochs can be detected either.

6.1.3 Discussion

6.1.3.1 The model

Both OLS1 and OLS2 indicate that there is a significant, positive correlation between body mass and m1 length of modern *C. crocuta*. As mentioned, OLS2 was chosen because of the outlier in OLS1. At 5.78 % and 8.7 %, the %PE and %SEE values for OLS2 are low, indicating that the models have a strong power to predict *C. crocuta* body masses from m1 lengths. This power is especially striking when compared against the values from Van Valkenburgh's (1990) models, where the lowest %PE value was 29 %, and the lowest %SEE was 18 % (both in a model of head-body length against body mass for carnivores weighing more than 100 kg). This indicates that confidence can be placed in reconstructions of Pleistocene *C. crocuta* body masses in the present study. However, it is acknowledged that OLS2 has a small sample size (ten data points).

6.1.3.2 Body mass reconstruction

Body masses of Pleistocene *C. crocuta* were reconstructed using OLS2. They were compared with previous estimates from Thackeray and Kieser (1992) and Collinge (2001) in Table 6.5. Thackeray and Kieser (1992) produced a regression model using the logarithmically transformed m1 lengths and body masses (from the same individuals) of *C. crocuta*, *P. brunnea*, *C. mesomelas* and Cape fox (*Vulpes chama*). The Pleistocene m1 lengths were then put into this regression equation. No correction factor was used after the predicted body masses were detransformed from logarithms by Thackeray and Kieser (1992). The body masses in the present study are around 15 to 20 kg greater than those predicted by Thackeray and Kieser (1992), and may in part be explained by the aforementioned lack of correction factor by those authors. Further variation may be due to differences in the relationship between m1 length and body mass in the different canid and hyaenid species.

As mentioned in Section 4.4.2.1, Collinge (2001) reconstructed Pleistocene *C. crocuta* body masses using an equation with a single, average body mass of modern *C. crocuta*. As Table 6.5 shows, the body masses reconstructed in the present study are greater than those reconstructed by Collinge (2001) using the post-crania. The reconstructions using m1 lengths are more similar between the two studies for *C. crocuta* from MIS 9, 5e (except Barrington) and 5c. Disparity occurs in body masses reconstructed using m1s from Barrington and from MIS 3, with the present study around 5 to 7 kg greater, although the standard deviations overlap. The greatest difference is from Ffynnon Beuno, with Collinge (2001) predicting 81 kg, compared with 98.8 kg (96.9 – 100.7 kg) in the present study. The differences between the two studies may stem from the use of a single average body mass in calculations by Collinge (2001), whereas the present study has taken into account some of the geographic variation in *C. crocuta* body masses.

Collinge (2001) noted that the post-crania may be more representative of body masses in light of their phenotypic responses to environmental conditions. This may also account for some of the greater difference observed between Collinge's (2001) body masses reconstructed from post-crania, and the body mass estimates in the present study. Data were unfortunately insufficient to construct further regression models from *C. crocuta* post-crania. However, the high r^2 value, and low %PE and %SEE values of OLS2 suggest that the body mass reconstructions presented here are a good approximation of the actual values of the Pleistocene individuals.

Table 6.5: Comparison of Pleistocene *C. crocuta* body mass reconstructions from the present study and previous studies. LHS = Lower Hyaena Stratum. UHS = Upper Hyaena Stratum

Site	Mean body mass values and SD (kg) from m1 lengths (this study)	Mean body mass values (kg) from m1 lengths (Thackeray and Kieser, 1992)	Mean body mass values and SD (kg) from post-crania (PC) and m1 length (Collinge, 2001)
Grays	64.56		61 (51.55 – 70.45, PC) 67 (m1)
Barrington	88.25 (81.34 – 95.17)	64.1	68 (62.6 – 73.4, PC) 83 (76.34 – 89.66, m1)
Joint Mitnor Cave	81.13 (72.71 – 89.55)	61.2	65 (58.26 – 71.74, PC) 79 (75.56 – 82.44, m1)
Kirkdale Cave	82.86 (75.85 – 89.86)	62.3	69 (65.12 – 72.88, PC) 79 (75.82 – 82.18, m1)
Tornewton LHS	84.92 (76.85 – 92.99)	62.9 (as 'Tornewton')	68 (63.9 – 72.1, PC) 86 (78.59 – 93.41, m1)
Tornewton UHS	84.56 (77.29 – 91.83)		
Badger Hole	89.83 (80.12 – 99.55)	71.2	
Brixham Cave/ Windmill Hill	85 (72.19 – 97.81)	67.4 (as 'Brixhan Cave')	
Coygan Cave	87.09 (78.02 – 96.15)	66.7	70 (67.84 – 72.16, PC) 80 (75.32 – 84.68, m1)
Ffynnon Beuno	98.8 (96.9 – 100.7)		81 (m1)
Hyaena Den	83.8 (76.81- 90.79)	67.9	
Kents Cavern	88.76 (80.99 – 96.54)	69.2	71 (66.91 – 75.09, PC) 82 (79.33 – 84.67, m1) (as 'Kents Cavern Cave Earth')
Picken's Hole	82.93 (76.07 – 89.79)	67.7	
Pin Hole	89.64 (78.7 – 100.58)	71.2	65 (54.7 – 75.3, PC) 82 (78.12 – 85.88, m1) (as 'Pin Hole Lower Fauna')
Sandford Hill	84.07 (74.37 – 93.76)		68 (63.69 – 72.31, PC) 79 (76.19 – 81.81, m1)

The Pleistocene body mass reconstructions results indicate that *C. crocuta* were consistently small during MIS 9 in Britain (Grays), MIS 3 in Ireland (Castlepook Cave) and MIS 3 on Sicily (San Teodoro). They were notably large during MIS 7 in Britain (Oreston). It is acknowledged that there was only one MIS 9-aged specimen, and one MIS 7-aged specimen, meaning that it is possible that these values may not be representative of the average body mass of the

populations. The *C. crocuta* from other countries and time periods overlap considerably and, in many cases, span a larger range of body sizes.

Pleistocene *C. crocuta* body masses range from 66.81 to 122.49 kg. These lower estimates overlap with body mass records from Africa today, which range from 35.85 to 80.06 kg (Powell-Cotton, n.d., cited in Shortridge, 1934; Smithers, 1971).

As demonstrated in Section 5.4.2.1, present-day *C. crocuta* are significantly negatively correlated with *P. leo* density and precipitation of the wettest month, and positively correlated with temperature of the warmest month. The analysis of Late Pleistocene *C. crocuta* in Britain suggests that they were significantly larger during the generally colder climatic conditions of MIS 3 than during the more temperate MIS 5e and 5c, contradicting the pattern seen in modern *C. crocuta*. This suggests that fossil *C. crocuta* follow Bergmann's Rule (with cold-climate being taken as a proxy for increased latitude). This is supported by some of the data from wider Europe. For example, *C. crocuta* from the mid last cold stage MIS 3 site of Teufelslucke are significantly larger than those from the temperate MIS 5c assemblages of Tornewton Upper and Lower Hyaena Strata, and the MIS 5e Last Interglacial sites of Kirkdale and Joint Mitnor Cave. *C. crocuta* from the MIS 3 site of Caverne Marie Jeanne (4^{eme} Niveau), where mean annual temperature has been reconstructed as 3.35°C (López-García *et al.*, 2017), are also significantly larger than those from Joint Mitnor Cave.

However, when assessing all assemblages of all ages, the overlap in measurements indicates that any size difference is not consistent. This may be because *C. crocuta* responded to shorter term environmental changes that cannot be detected because of a lack of resolution. For example, the variation of body masses during MIS 5e may be explained by temperature variation within this period; although all temperature reconstructions of MIS 5e in Britain exceeded today's summer temperatures, peak warmth occurred for only a short period (less than 1,200 years) of MIS 5e (Candy *et al.*, 2016). Unfortunately, no temperature records have been reconstructed directly form the MIS 5e deposits included in the present study, so this cannot be resolved further.

Multiple abrupt environmental changes also occurred during MIS 3, as evidenced through the Greenland ice core $\delta^{18}O$ data (Andersen *et al.*, 2004; Rasmussen *et al.*, 2014; Seierstad *et al.*, 2014). The graph of direct dates from MIS 3 *C. crocuta* (Figure 4.7) plotted against the Greenland data shows that it is not possible to attribute each deposit to a particular stadial or interstadial. This is because the errors on the dates, in addition to the existence of multiple dates from some deposits, span across climatic transitions.

The Greenland ice core $\delta^{18}O$ data indicates that interstadials became shorter and less frequent after around 36.5 b2k (Andersen *et al.*, 2004; Rasmussen *et al.*, 2014; Seierstad *et al.*, 2014). The graph of chronologically-ordered British MIS 3 body mass reconstructions (Figure 6.4) shows that there is no consistent pattern of body mass change over time. There is also no change to larger or smaller body masses after 36.5 b2k. This may be a true signal. Alternatively, this may be due to the limited available radiocarbon dates, and the fact that many dates were towards the limit of the radiocarbon dating method. To resolve this issue, more extensive radiocarbon dating of specimens is needed to help constrain the timespan over which *C. crocuta* occupied each site. It would be particularly beneficial to directly date the m1s from which body masses were reconstructed. A further improvement would be to reconstruct palaeotemperatures directly from the deposits in which *C. crocuta* were found. This is because temperatures across Europe may diverge from the Greenland signal. For example, the continental temperatures may have lagged behind the signal from Greenland, or they may represent different magnitudes of change.

Overall, there is some evidence that contrary to present-day *C. crocuta*, Pleistocene *C. crocuta* followed Bergmann's Rule. However, this is not consistent nor ubiquitous. As mentioned, present-day *C. crocuta* do not appear to follow Bergmann's Rule. This difference may be a consequence of the small sample size of present-day body masses so that the full climatic range of *C. crocuta* habitats was not covered (see Table 5.23). Alternatively, present-day *C. crocuta* may exhibit true morphological responses to temperature that are different to those of Pleistocene *C. crocuta*.

Klein and Scott (1989) concluded that *C. crocuta* from Britain followed Bergmann's Rule, based on the length of the m1s from Late Pleistocene sites, although there was overlap in values from deposits of different ages. Studies by Turner (1981) and Collinge (2001) both found a lack of consistent relationship with Bergmann's Rule in the Pleistocene, supporting the findings in the present study.

As mentioned, present-day *C. crocuta* body masses are negatively correlated with precipitation of the wettest month. Records of precipitation are lacking in the Pleistocene, with estimations only available from three sites. Annual precipitation from Caverne Marie Jeanne (4^{eme} Niveau) were estimated at 1018 mm, which is wetter than today (López-García *et al.*, 2017). Although quantifiable palaeoclimatic reconstructions are unfortunately unavailable, the deposits from Levels D, E, F and H in Cova del Toll are indicative of wet conditions (Allué *et al.*, 2013). Cova de les Toixoneres Level III is indicative of a humid climate, while Level II is indicative of drier conditions (López-García *et al.*, 2012). The body masses from Caverne Marie Jeanne, Cova del

Toll and Cova de les Toixoneres all overlap. The limited evidence thus suggests no influence of precipitation on Pleistocene body masses.

Vegetation cover was assessed for those deposits from which vegetation had been directly reconstructed. There is evidence that body size does not vary with vegetation. The sample size upon which this is based is small, especially the forested vegetation category, which is represented only by two deposits. However, these results are supported by findings that present-day *C. crocuta* body mass is not correlated with vegetation cover (Section 5.4.2.1).

As mentioned, present-day *C. crocuta* body masses are negatively correlated with *P. leo* density (Section 5.4.2.1). This is a difficult variable to measure in the Pleistocene. However, the response to the presence and absence of potential competitors can be assessed, in addition to an investigation into the covariation in body size between predator species.

Other large predators that occurred in Europe alongside *C. crocuta* included *C. lupus*, *P. leo* (*spelaea*), *P. pardus*, *U. arctos, U. spelaeus* and hominins (Currant and Jacobi, 2011; Dimitrijević, 2011). These species may have competed with *C. crocuta* for food. Indeed, there is evidence of overlapping prey preferences, such as the consumption of bovids, equids and cervids by *C. crocuta* and *H. neanderthalensis* during MIS 4 and 3 in France (Dusseldorp, 2013b). In Payre, France during MIS 7/8, *C. crocuta* and *P. leo* (*spelaea*), and sometimes *H. neanderthalensis*, targeted species such as *Dicerorhinus* (=*Stephanorhinus*) sp., *C. capreolus*, *M. giganteus* and *E. mosbachensis* (Bocherens *et al.*, 2016).

A species' body mass may be constrained if it inhabits the same area as a larger competitor (McNab, 1971). Thus, while *C. lupus* were larger during MIS 5a in Britain, in part due to the absence of *C. crocuta* (Flower, 2016), the reverse was not true. *C. lupus*, *P. leo* (*spelaea*) and *U. arctos* were present in Britain during MIS 9, later 7, 5e, 5c and 3 (Sutcliffe and Zeuner, 1962, cited in Currant, 1998; Schreve, 1997, 2001; Currant and Jacobi, 2011) and so there was no opportunity for competitive release. Additionally, there is little evidence that Pleistocene *C. crocuta* body mass varied alongside *C. lupus* or *P. leo* (*spelaea*) body size. There is some evidence of an increase in *C. crocuta* size alongside reduced *U. arctos* size, during MIS 5e and 3, although this is not the case for MIS 9.

Neanderthals were present in Britain during MIS 9, 7 and 3 (Schreve, 2001; Currant and Jacobi, 2011), but were very likely absent during MIS 5e (Lewis *et al.*, 2011), and there is no evidence of their presence in MIS 5c-aged deposits (Sutcliffe and Zeuner, 1962, cited in Currant, 1998; Currant and Jacobi, 2011). The overlap in body masses in MIS 5e and 5c compared to MIS 3 suggests that the absence of Neanderthals in Britain did not influence *C. crocuta* body mass.

An additional potential factor is the arrival of modern humans in Britain. The earliest evidence of this is a mandible from Kents Cavern, dated to 42,350 to 40,760 cal BP, based on associated fauna (T. Higham, Compton, *et al.*, 2011; Proctor *et al.*, 2017). The body mass estimates placed in chronological order (Figure 6.4) do not show any evidence that *C. crocuta* body masses changed in response to the arrival of modern humans in Britain, although the limitations of the chronology have been discussed above.

Collinge (2001) suggested that the larger size in species such as *C. elaphus* during MIS 3 was due to a greater vegetation productivity. The positive relationship between body masses of *C. crocuta* and *C. elaphus* may therefore indicate an indirect relationship between *C. crocuta* body mass and vegetation productivity, rather than vegetation openness, as discussed above.

Even if the covariation between *C. crocuta* body mass and that of their prey is not causal, the relationship can provide some information about *C. crocuta*'s diet. That *C. crocuta* body mass increased in line with those of Rhinocerotidae and *C. elaphus* suggests that *C. crocuta* were able to continue targeting these species even when they were of large size.

Evidence of *C. crocuta* consumption of *C. elaphus* in Britain comes from Ffynnon Beuno (Aldhouse-Green *et al.*, 2015) and Kents Cavern (Wilson, 2010). Additionally, *C. elaphus* remains are present in many assemblages that were likely accumulated by *C. crocuta* (see Appendix 10.1 Table 10.1).

There is also abundant evidence for the consumption of *C. antiquitatis* in Britain, including damage to bones in MIS 3 deposits of Bench Cavern/Windmill Hill (Prestwich, 1873), Coygan Cave (Aldhouse-Green *et al.*, 1995), Goat's Hole Paviland (Turner, 2000), Pin Hole (Busk, 1875) and Lynford (Schreve, 2012). The importance of *C. antiquitatis* in the diet of Pleistocene *C. crocuta* is interesting given the large size of the individuals (maximum recorded size of 2433±537 kg, Collinge, 2001). There is limited evidence of *C. crocuta* preying upon white rhinoceros (*Ceratotherium simum*), or black rhinoceros (*Diceros bicornis*) today. Kruuk (1972) and Sillero-Zubiri and Gottelli (1991) noted limited hunting attempts by *C. crocuta* upon rhinoceros calves, which were all unsuccessful. Despite this, sites such as Kents Cavern yielded abundant, gnawed remains of juvenile *C. antiquitatis* (Wilson, 2010). This may have been due to successful predation by *C. crocuta*, scavenging by *C. crocuta*, or collection bias from early excavations.

During MIS 9 *C. crocuta* are smaller than expected, given the size of Rhinocerotidae, *D. dama* and *E. ferus*. This may indicate that *C. crocuta* were less able to target these prey species during this period. At 64.56±1.23 kg, the Grays individual is similar in size to *C. crocuta* in some areas in southern Africa, including some records from Kruger National Park and Hluhluwe-iMfolozi Park

(Whateley, 1980; Lindeque, 1981, cited in Smithers, 1983; Henschel, 1986, cited in Skinner and Chimimba, 2005; and see Table 5.23).

Of the large mammals in Kruger National Park, the species most frequently targeted by *C. crocuta* were steenbok (*Raphicerus campestris*), the greater kudu (*Tragelaphus strepsiceros*) and impala (*Aepyceros melampus*; Henschel and Skinner, 1990). *R. campestris* weighs 9-13.2 kg, *A. melampus* weighs 40-76 kg and *T. strepsiceros* weighs 120−315 kg (Estes, 1991, and references therein). Larger species killed by *C. crocuta* included *S. caffer* (Henschel and Skinner, 1990), which weighs 425−870 kg (Estes, 1991, and references therein).

From Grays, *D. dama* was estimated to weigh 97±16.2 kg, *E. ferus* weighed 557±115 kg, and *S. hemitoechus* weighed 1790±557 kg (Collinge, 2001). *D. dama* and *E. ferus* are within the range of species predated by *C. crocuta* in Kruger National Park. *S. hemitoechus* is larger, suggesting that at least the adults would have been too large for *C. crocuta* to predate successfully.

Body masses of individuals from Castlepook Cave are also notably small. However, this does not hold when considering the craniodental morphometrics (see Section 6.2).

Finally, small *C. crocuta* were also found in San Teodoro. Weighing 72.31±1.24 to 84.01±1.28 kg from San Teodoro, the smaller of these individuals are similar to some records of present-day *C. crocuta* from Hluhluwe-iMfolozi Park, Kruger National Park, Kalahari National Park and Botswana (Stevenson-Hamilton, 1947; Smithers, 1971; Whateley, 1980; Mills, 1990). The larger of the *C. crocuta* from San Teodoro exceed the maximum recorded body masses of present-day *C. crocuta*, which are 78.25 kg from Malawi (Wood n.d., cited in Shortridge 1934) and 80.06 kg from Botswana (Smithers, 1971).

In the deposits of San Teodoro, there is *C. crocuta* damage to bones of *Palaeoloxodon mnaidriensis* (dwarf elephant), *Cervus elaphus siciliae* (Sicilian red deer), *Bos primigenius siciliae*/*Bison priscus siciliae* (Sicilian aurochs/Sicilian bison) *S. scrofa* and *E. hydruntinus* (Mangano, 2011). *P. mnaidriensis*, *C. e. siciliae, B. primigenius siciliae and B. priscus siciliae* were all smaller than their mainland ancestors (Raia and Meiri, 2006; Lomolino *et al.*, 2013). *C. crocuta* would therefore likely have been able to prey upon these species (rather than only scavenging the remains), despite *C. crocuta's* relatively small size.

The small size of the *C. crocuta* from San Teodoro is interesting as the Island Rule may have influenced these populations. The premise of the Island Rule is that mammals of large body size, such as *C. crocuta*, will become smaller once isolated (Lomolino, 1985). Reconstructions of relative sea level at the Strait of Messina showed that the land bridge between Sicily and mainland Italy was absent between 40 and 27 ka (Antonioli *et al.*, 2015). The available dates from San Teodoro are younger than 40 ka (32±4 ka on flowstone and 18,330±400 ^{14}C BP =

23,125-21,149 cal BP on *E. hydruntinus*, Bonfiglio *et al.*, 2008), indicating that the San Teodoro fauna were part of populations isolated from the mainland. This is further illustrated in San Teodoro by the presence of dwarf endemic species, which were smaller than their mainland counterparts (Mangano, 2011), and by species diversity that is a subset of the mainland species (Marra, 2009).

There are many theories behind the causes for the Island Rule (see Section 3.1). Raia and Meiri (2006) suggested that the prey biomass or the size of prey on islands influences body size change of insular carnivores. For San Teodoro, the presence of dwarf species (Mangano, 2011) conforms to this theory.

As mentioned, *C. lupus* exhibited variation in body mass during the Pleistocene, with the largest individuals found during MIS 5a, perhaps because of cold conditions and competitive release due to the absence of *C. crocuta* (Flower, 2016). *P. leo* (*spelaea*) were smaller during MIS 5e than during MIS 3, and Collinge (2001) suggested that this was because of the more forested environment during MIS 5e, leading to sub-optimal foraging and concentration on smaller prey. *P. leo* (*spelaea*) therefore conformed to Bergmann's Rule, but the cause of body size change was not a direct relationship with temperature.

U. arctos were largest during MIS 4 according to Collinge (2001). However, assemblages attributed to this period, assigned to the Banwell Bone Cave Mammal Assemblage Zone by (Currant and Jacobi, 2001, 2011), including Windy Knoll, Wretton and the type-site of Banwell Bone Cave, have since been reassigned to MIS 5a (Currant and Jacobi, 2011). Further body mass reconstructions indicated that medium sized *U. arctos* occurred during MIS 6, 5e, 5c and 3, while the smallest individuals occurred during MIS 7 and 9. Collinge (2001) suggested this may have been due to a reduction in plant biomass during MIS 6, 5a, and 3, causing them to switch to a more carnivorous diet. No explanation was given for the medium-sized individuals during MIS 5e and 5c.

Based on the above responses of other large predators, it seems that *C. crocuta* is unusual in that its body size did not consistently change in response to Pleistocene environmental conditions. This may be due to the behavioural plasticity of the species. For example, *C. crocuta* have been observed to move from open to closed vegetation, and change from crepuscular to nocturnal activity in response to the presence of humans (Boydston *et al.*, 2003). They obtain food from both predation and scavenging (Henschel and Skinner, 1990; Gasaway *et al.*, 1991), and feed upon a wide range of species (Mills, 1990; Holekamp *et al.*, 1997; Hayward, 2006). They can also alter the prey species that they target in response to seasonal fluctuations in prey

abundance (e.g. Cooper *et al.*, 1999). However, *C. lupus* also exhibit some behavioural plasticity, yet, as mentioned, they showed body size changes through the Pleistocene (Flower and Schreve, 2014; Flower, 2016).

One thing that *C. crocuta* does differently is that they are able to consume the entirety of a carcass, including bones, in periods of low food availability (Kruuk, 1972; Egeland *et al.*, 2008). While there is competition between *C. crocuta* and *P. leo* today, the two species often show spatial and temporal partitioning (e.g. Mills, 1990; Périquet *et al.*, 2015, and Section 5.1). Indeed, isotopic analysis of MIS 3-aged assemblages from the Ardennes, Belgium indicated that *C. crocuta* consumed most of the prey species present, while *P. leo* (*spelaea*) was forced to subsist on *R. tarandus* and *Ursus* sp. cubs (Bocherens *et al.*, 2011). They may also have been able to out-compete other species. For example, after MIS 5a (when both *C. crocuta* and *P. leo* (*spelaea*) were conspicuously absent from Britain), *C. lupus* reduced its body size during MIS 3 apparently in response to competition from the two larger predators, now returned to Britain, which forced them to target smaller prey species (Flower and Schreve, 2014; Flower, 2016).

It is anticipated that some of this behaviour will be reflected in the craniodental and post-cranial morphological record. This behavioural plasticity may mean that *C. crocuta* responded to environmental changes through behaviour, in particular bone consumption and out-competing other species, thus limiting the necessity for body size changes. This may have had implications for their extirpation from Europe, as will be discussed in Section 7.

6.2 Pleistocene morphometrics

6.2.1 Introduction

As discussed in Section 3.3, craniodental morphology is associated with the size of the brain, vision, hearing, olfaction, respiration and feeding (Ewer, 1973; Biknevicius, 1996; Smith and Rossie, 2008; Tseng and Binder, 2010; Macrini, 2012; Nummela *et al.*, 2013; Lucas, 2015; Rahmat and Koretsky, 2015). Post-cranial morphology also has important functional implications including weight bearing, prey capture and locomotion (Hildebrand, 1974; Van Valkenburgh, 1985; and see Section 3.4). The results from Section 5.4 indicate that these features may be influenced by temperature, precipitation, vegetation cover. Given that these conditions changed during the Pleistocene, this section will assess the variation in morphometrics of *C. crocuta*, and whether this variation can be attributed to environmental variation both temporally and spatially.

The research questions are as follows:

- How did *C. crocuta* morphometrics vary spatially across Europe and temporally through the Pleistocene?
- Can this variation be attributed to any environmental conditions?

6.2.2 Results

6.2.2.1 Crania and dentition

The dental measurements for all Pleistocene assemblages are displayed in Figure 6.12 to Figure 6.29, and see also Appendix 10.8, Figure 10.3. Sample sizes are included in Table 6.6. Where sample sizes were at least ten, tests for significant difference were performed. ANOVA with post-hoc Tukey were performed on normally distributed data, and Mann Whitney tests were performed on non-normally distributed data. In the case of the mediolateral diameter of C, t-tests were performed on normally distributed data as a Levene's test indicated unequal variances in the data ($p-value = 0.016$). The results of the tests for significant difference are displayed in Appendix 10.8, Table 10.22 to Table 10.50.

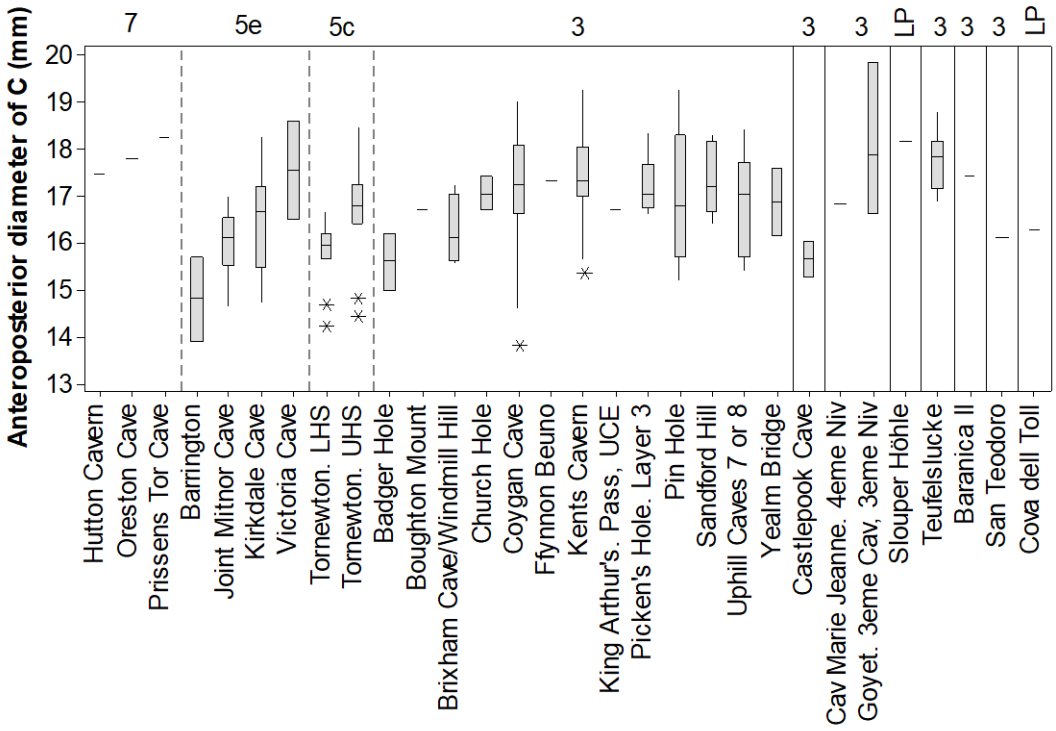

Figure 6.12: Boxplot of Pleistocene *C. crocuta* C anteroposterior diameter measurements. Numbers on top of the graph indicate Marine Oxygen Isotope Stages. LP = Late Pleistocene.

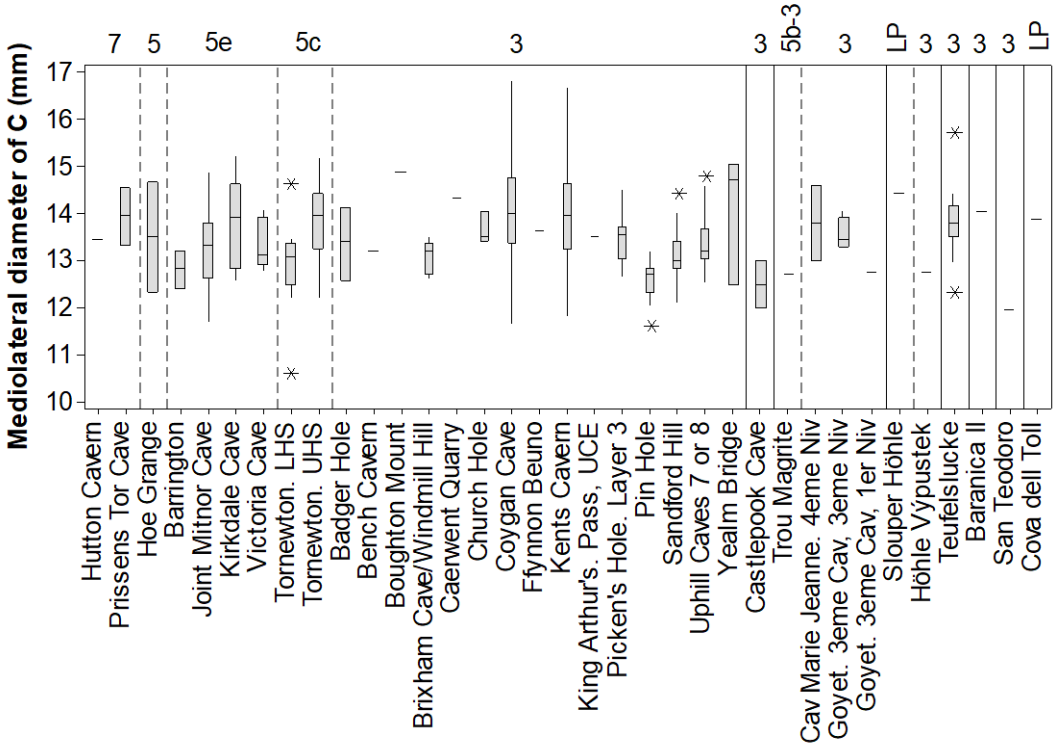

Figure 6.13: Boxplot of Pleistocene *C. crocuta* C mediolateral diameter measurements. Numbers on top of the graph indicate Marine Oxygen Isotope Stages. LP = Late Pleistocene.

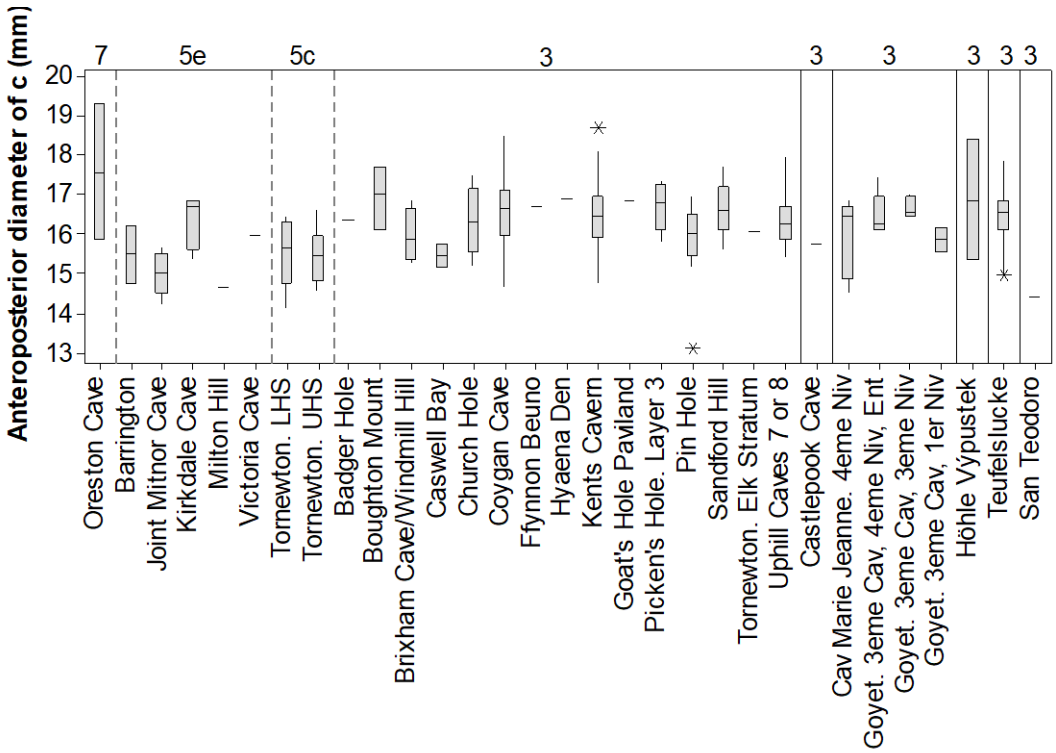

Figure 6.14: Boxplot of Pleistocene *C. crocuta* c anteroposterior diameter measurements. Numbers on top of the graph indicate Marine Oxygen Isotope Stages.

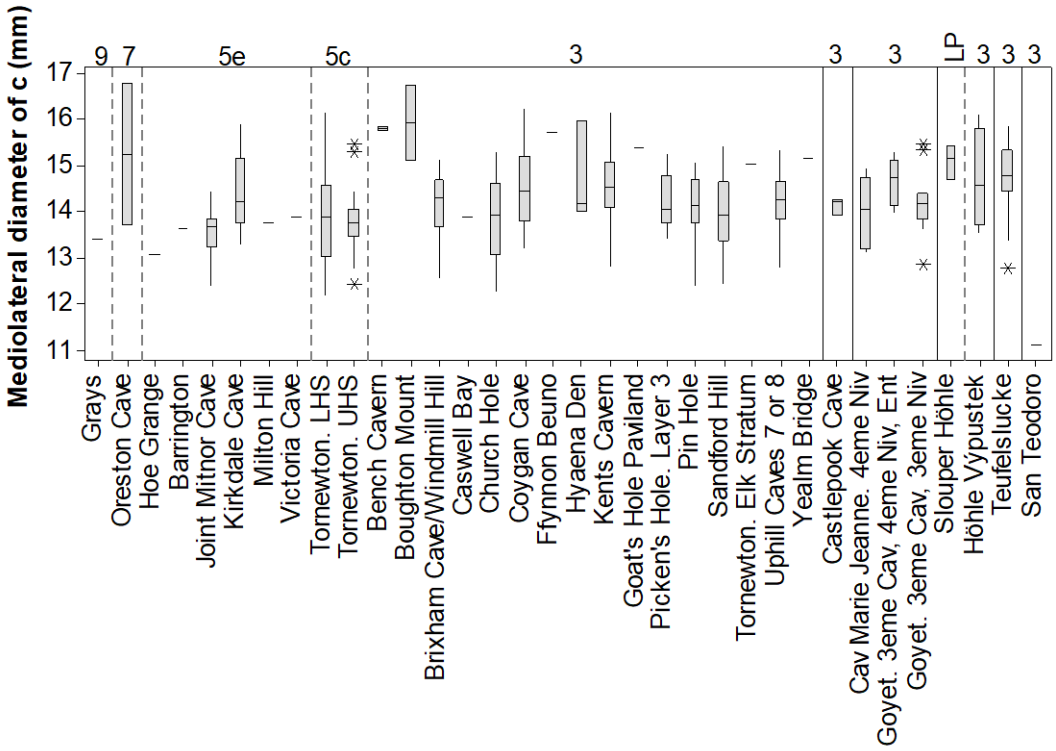

Figure 6.15: Boxplot of Pleistocene *C. crocuta* c mediolateral diameter measurements. Numbers on top of the graph indicate Marine Oxygen Isotope Stages. LP = Late Pleistocene.

For all dental measurements, there is much overlap in the recorded sizes between assemblages. This is the case both within and between different palaeoclimatic episodes and geographic areas. However, some differences are apparent.

The measurements from the early Middle Pleistocene specimen from Pakefield all plot in the mid-range of measurements from all sites. Data from MIS 9 was only available from four measurements from Grays (width of p3, width of p4, and length and width of m1). These consistently plot in the lower range of values from all sites. For most measurements, the teeth from MIS 7 are towards the upper range of sizes, although a notable exception is the length of the p2.

Of assemblages from the Late Pleistocene, Castlepook Cave and San Teodoro stand out. Except for measurements of P2 and p2, mediolateral diameter of c, and length of p3, the measurements from Castlepook Cave plot towards the lower range of values. The measurements from San Teodoro consistently plot in the lower range of values.

Differences between sites are more apparent when the tests for significant differences are considered alongside the boxplots. Where there are significant differences, these tend to show that teeth from MIS 3-aged sites are larger than those from MIS 5e and 5c. In particular, teeth from Teufelslucke, tend to be significantly larger. There are exceptions, however. The length of P1, length of P4 and width of p2 do not exhibit significant differences.

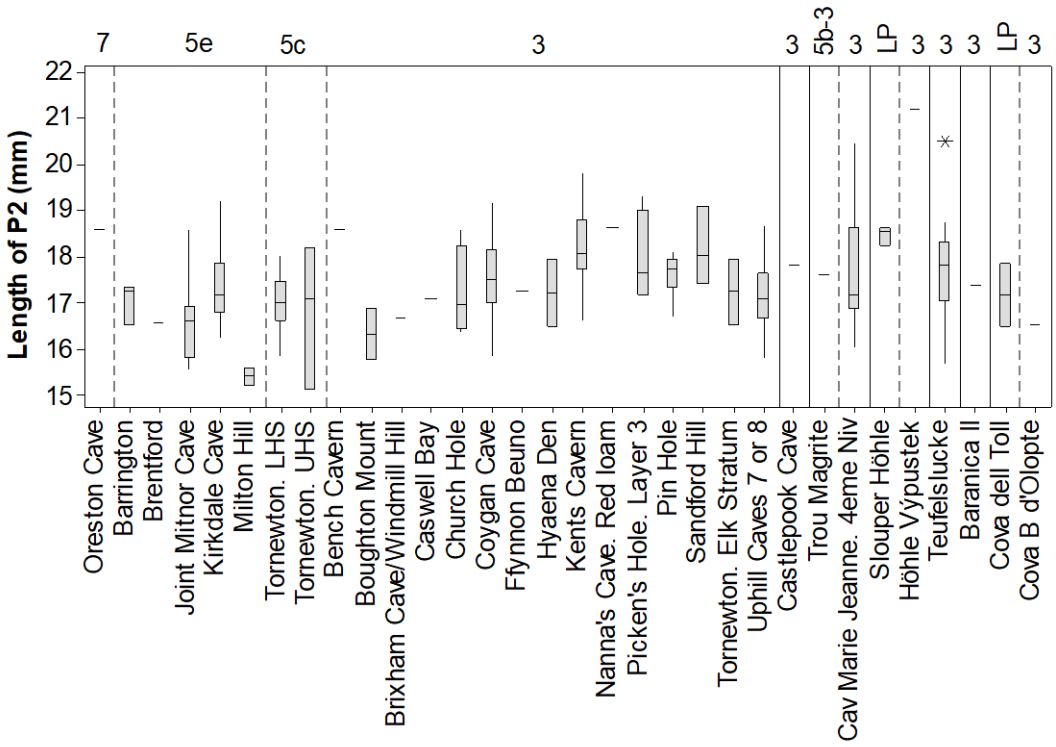

Figure 6.16: Boxplot of Pleistocene *C. crocuta* P2 length measurements. Numbers on top of the graph indicate Marine Oxygen Isotope Stages. LP = Late Pleistocene.

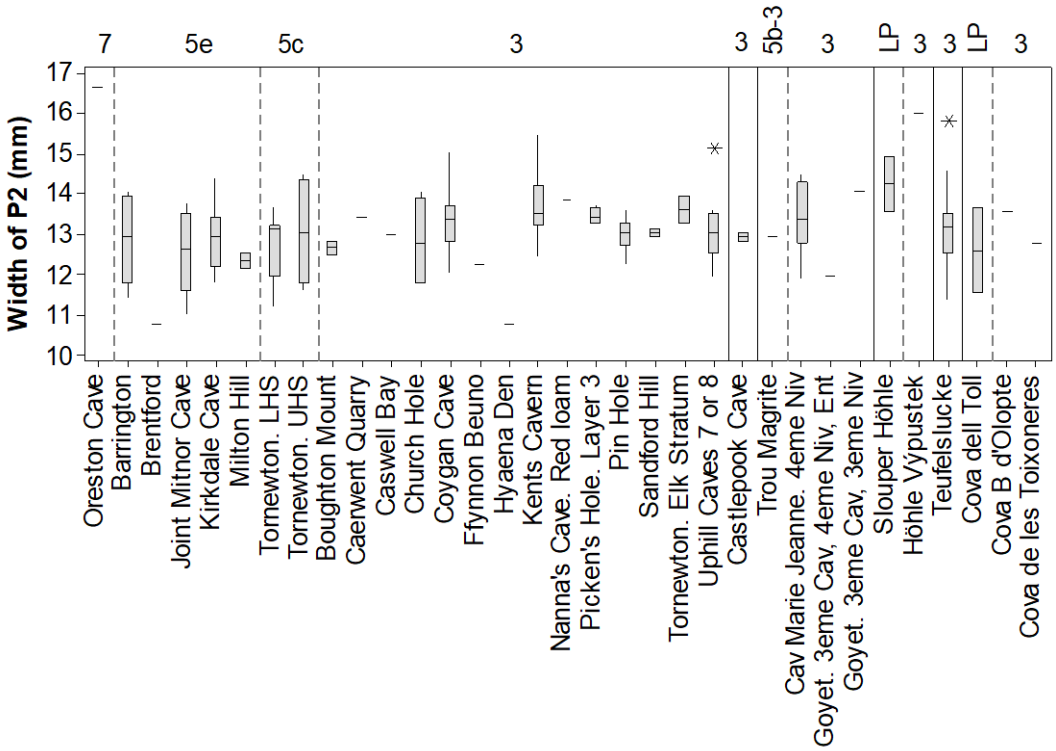

Figure 6.17: Boxplot of Pleistocene *C. crocuta* P2 width measurements. Numbers on top of the graph indicate Marine Oxygen Isotope Stages. LP = Late Pleistocene.

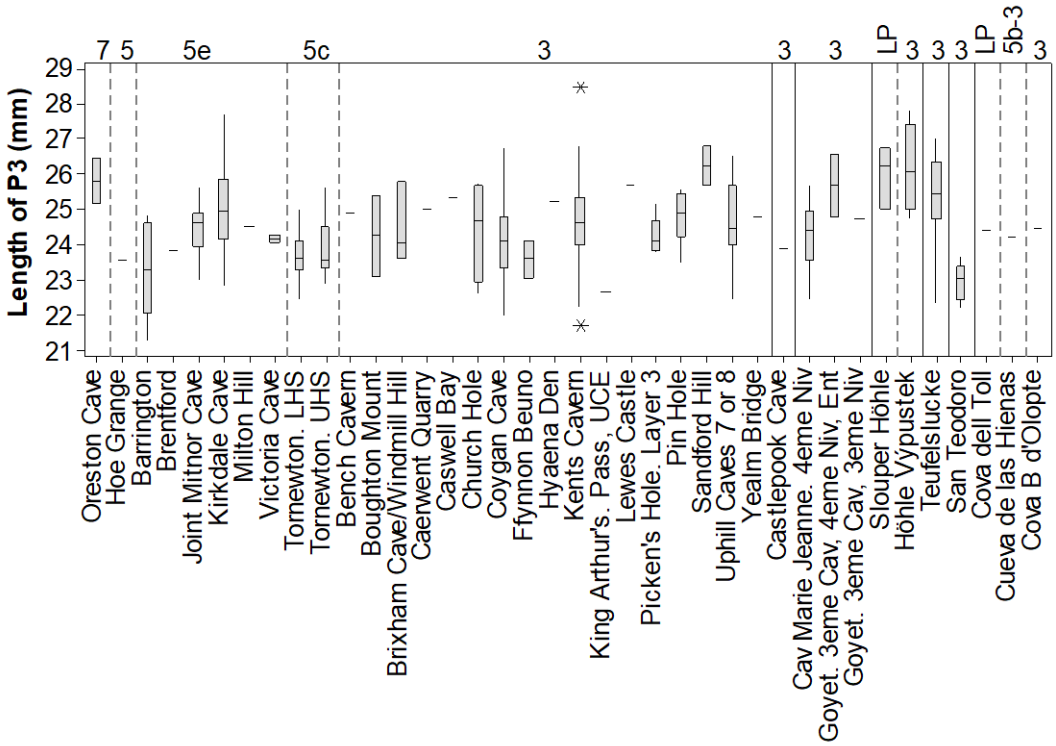

Figure 6.18: Boxplot of Pleistocene *C. crocuta* P3 length measurements. Numbers on top of the graph indicate Marine Oxygen Isotope Stages. LP = Late Pleistocene.

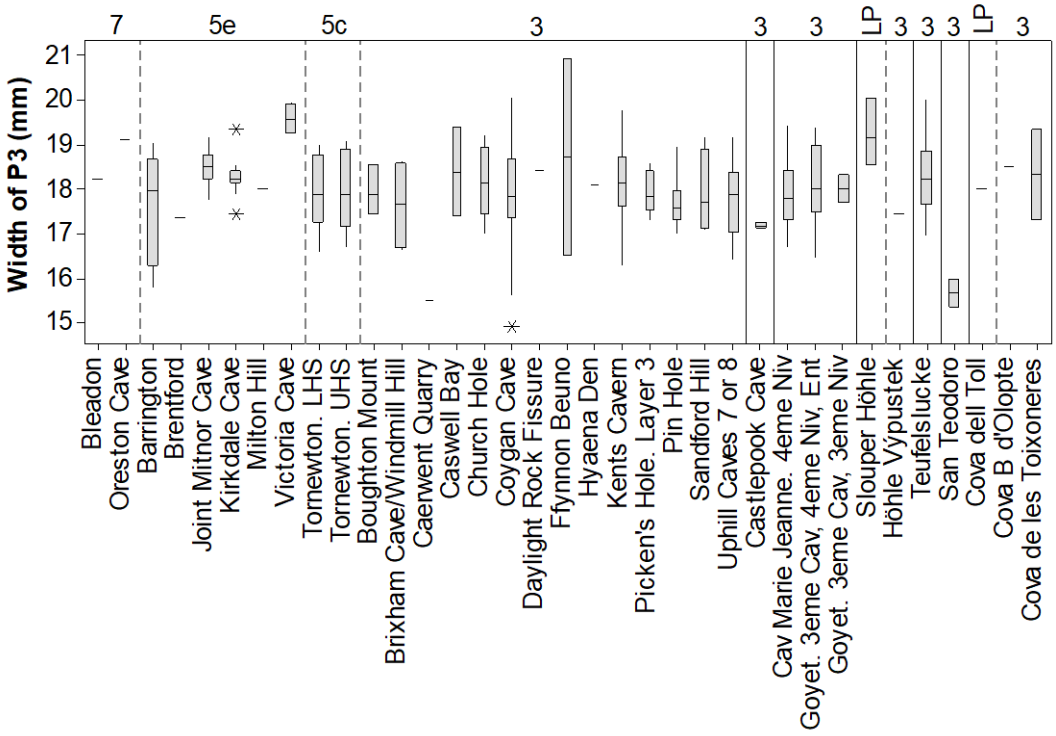

Figure 6.19: Boxplot of Pleistocene *C. crocuta* P3 width measurements. Numbers on top of the graph indicate Marine Oxygen Isotope Stages. LP = Late Pleistocene.

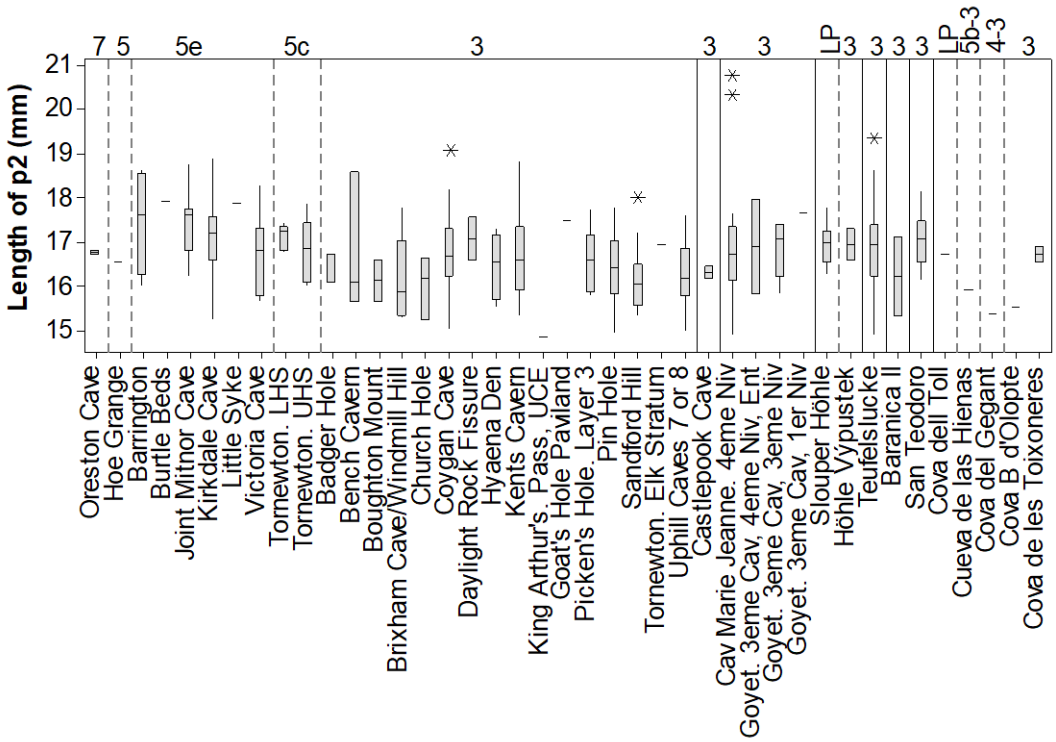

Figure 6.20: Boxplot of Pleistocene *C. crocuta* p2 length measurements. Numbers on top of the graph indicate Marine Oxygen Isotope Stages. LP = Late Pleistocene.

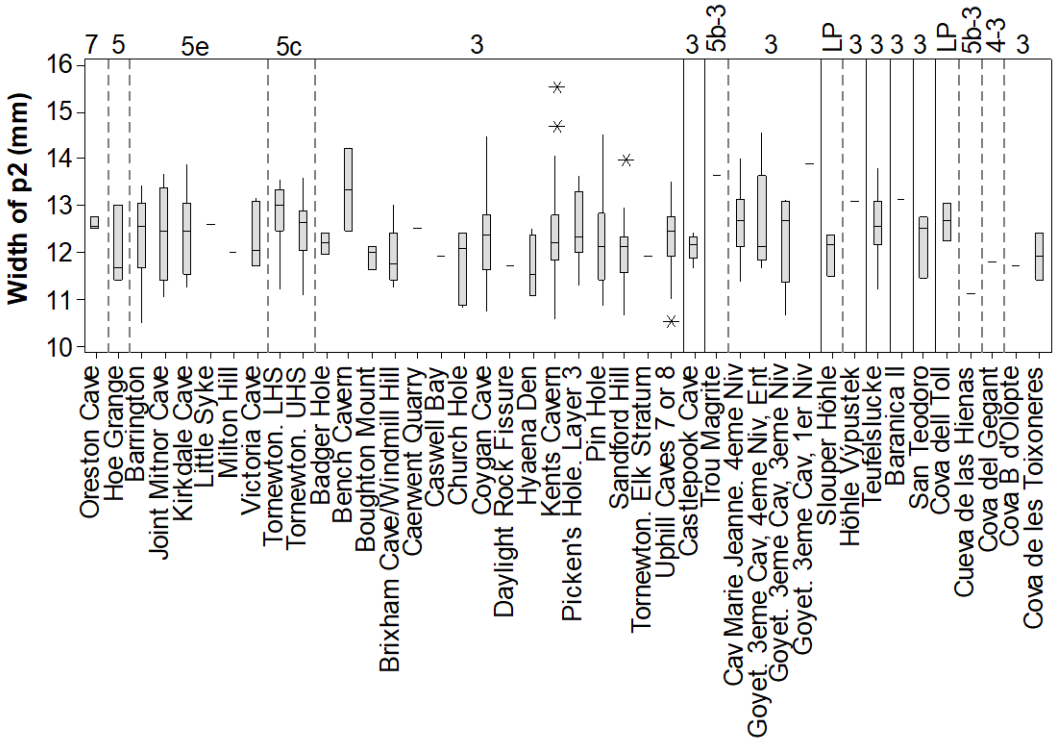

Figure 6.21: Boxplot of Pleistocene *C. crocuta* p2 width measurements. Numbers on top of the graph indicate Marine Oxygen Isotope Stages. LP = Late Pleistocene.

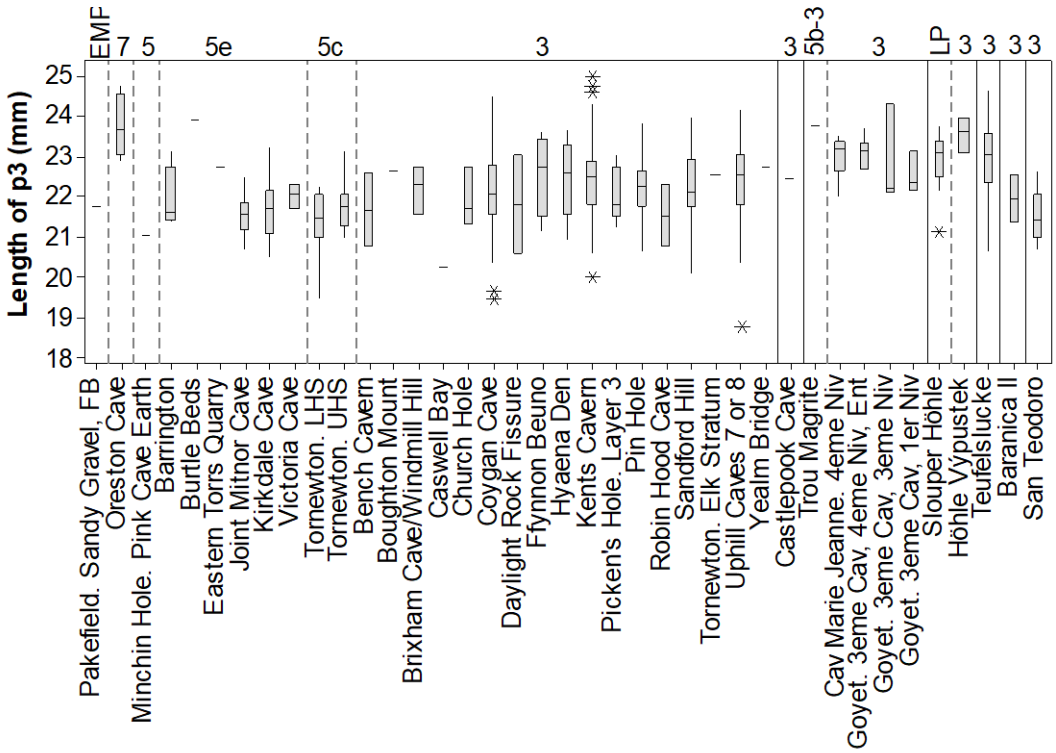

Figure 6.22: Boxplot of Pleistocene *C. crocuta* p3 length measurements. Numbers on top of the graph indicate Marine Oxygen Isotope Stages. LP = Late Pleistocene. EMP = early Middle Pleistocene.

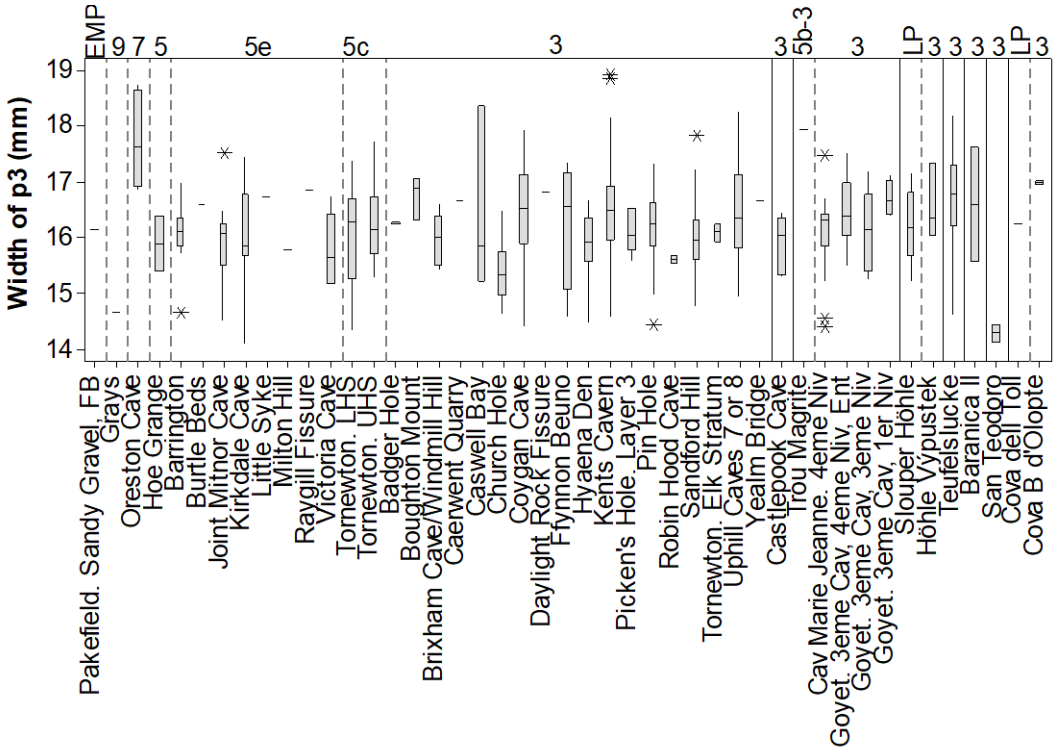

Figure 6.23: Boxplot of Pleistocene *C. crocuta* p3 width measurements. Numbers on top of the graph indicate Marine Oxygen Isotope Stages. LP = Late Pleistocene. EMP = early Middle Pleistocene.

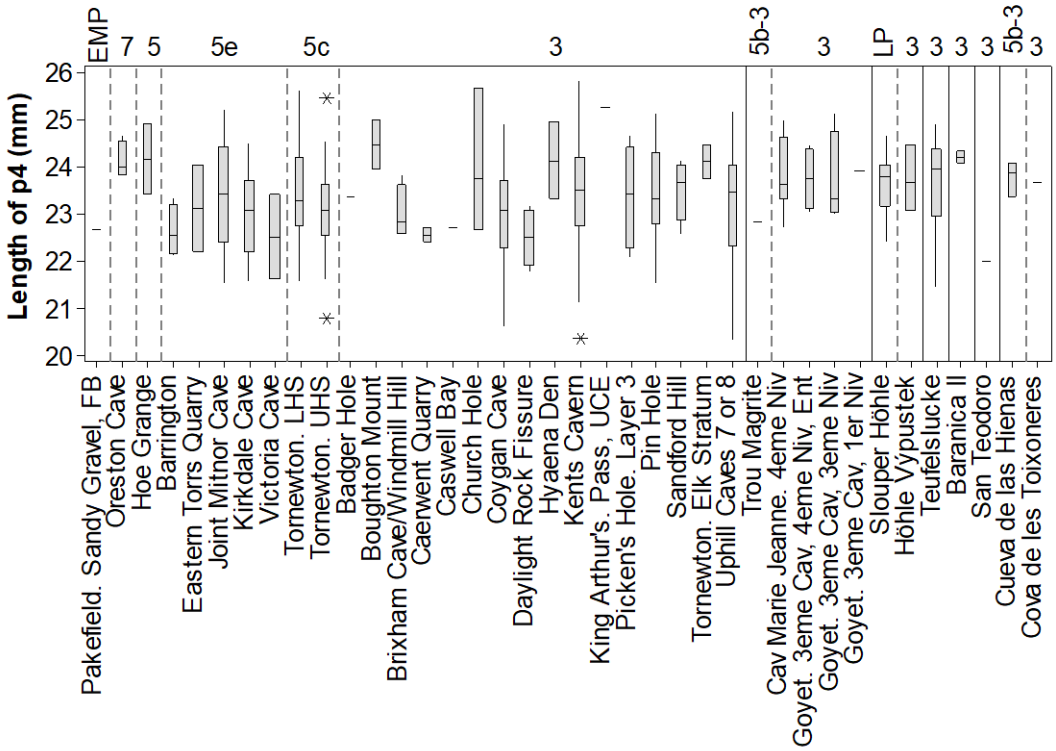

Figure 6.24: Boxplot of Pleistocene *C. crocuta* p4 length measurements. Numbers on top of the graph indicate Marine Oxygen Isotope Stages. LP = Late Pleistocene. EMP = early Middle Pleistocene.

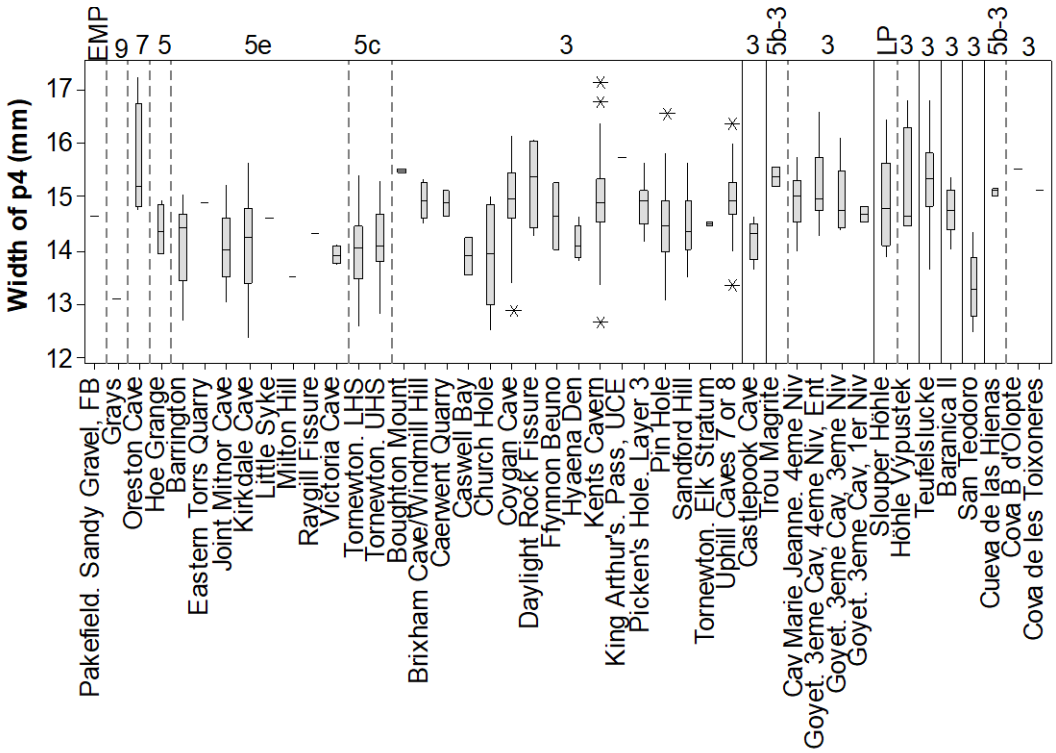

Figure 6.25: Boxplot of Pleistocene *C. crocuta* p4 width measurements. Numbers on top of the graph indicate Marine Oxygen Isotope Stages. LP = Late Pleistocene. EMP = early Middle Pleistocene.

There is also variation within MIS 5; the lengths of P3s from Kirkdale Cave (MIS 5e) are significantly larger than those from Tornewton UHS (MIS 5c). Additionally, there are some significant differences between assemblages from MIS 3. These are the mediolateral diameters of C, the greatest widths of P4, the lengths and widths of p3, the widths of p4 and the lengths of m1. Most often, these significant differences indicate that measurements from Teufelslucke and Cavern Marie Jeanne are larger than those from other sites such as Uphill Caves and Sandford Hill.

The width of the m1 is the most complicated in terms of significant differences. There are no significant differences between m1 widths from MIS 5e and 5c. Widths of m1s from some MIS 3–aged assemblages are larger than those from MIS 5e and 5c. There some significant differences within MIS 3, with m1 widths from Coygan Cave larger than those from Sandford Hill. Widths from Uphill Caves and Teufelslucke are both larger than Coygan Cave and Sandford Hill.

The most obvious exception is the length of p2. As mentioned, for most teeth, those from MIS 3 are significantly larger than those from MIS 5e and 5c. By contrast, the p2s from MIS 5e-aged Joint Mitnor Cave and Kirkdale Cave are significantly longer than those from MIS 3-aged Kents Cavern, Sandford Hill and Uphill Caves.

The other dental measurements with some measurements larger from MIS 5e or 5c are the mediolateral diameters of the upper and lower canines, and the length of the P3.

Tornewton LHS and UHS (both MIS 5c age) measurements do not differ significantly from each other for any teeth except for the anteroposterior and mediolateral diameters of C. For both measurements, those from Tornewton UHS are larger.

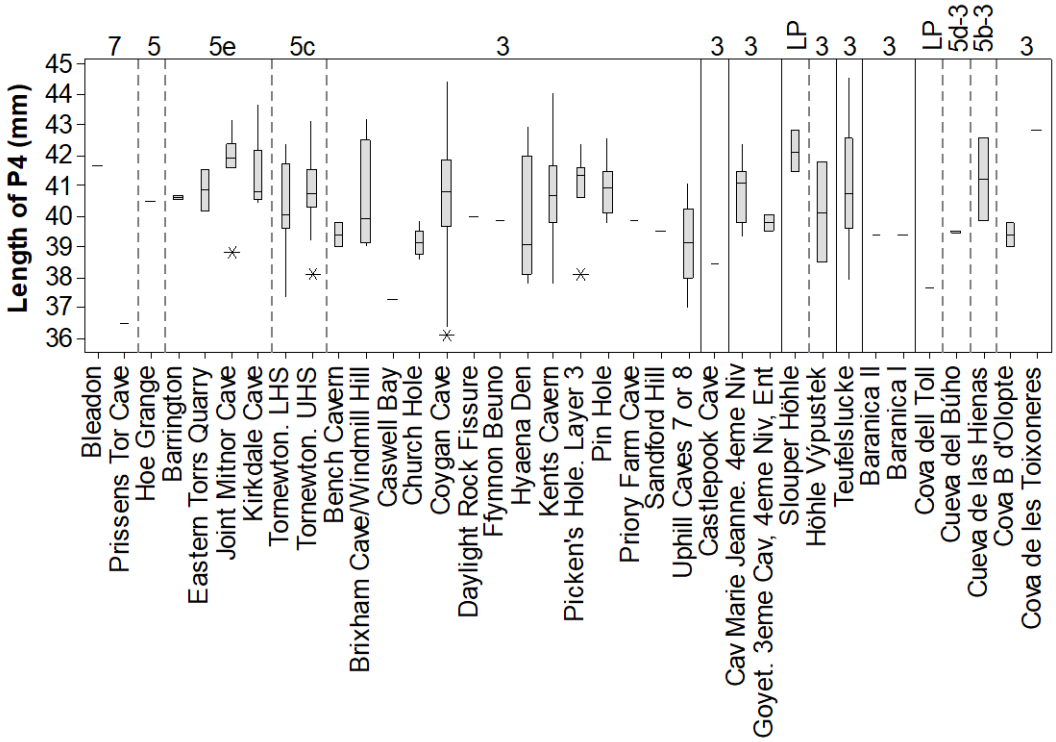

Figure 6.26: Boxplot of Pleistocene *C. crocuta* P4 length measurements. Numbers on top of the graph indicate Marine Oxygen Isotope Stages. LP = Late Pleistocene.

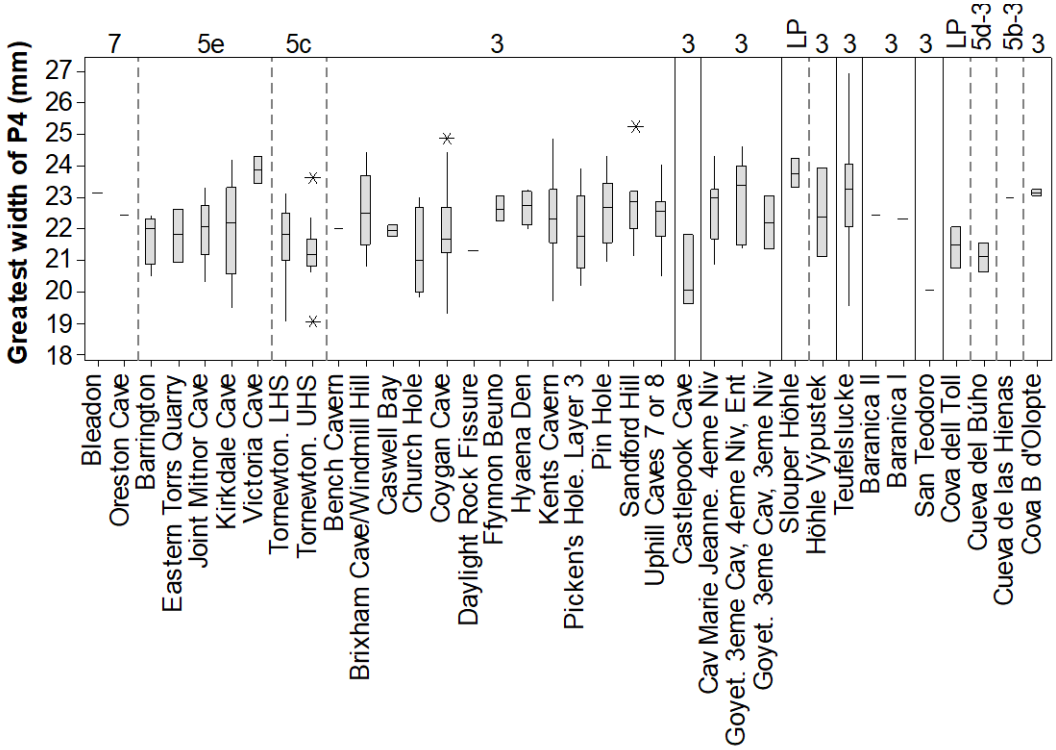

Figure 6.27: Boxplot of Pleistocene *C. crocuta* P4 greatest width measurements. Numbers on top of the graph indicate Marine Oxygen Isotope Stages. LP = Late Pleistocene.

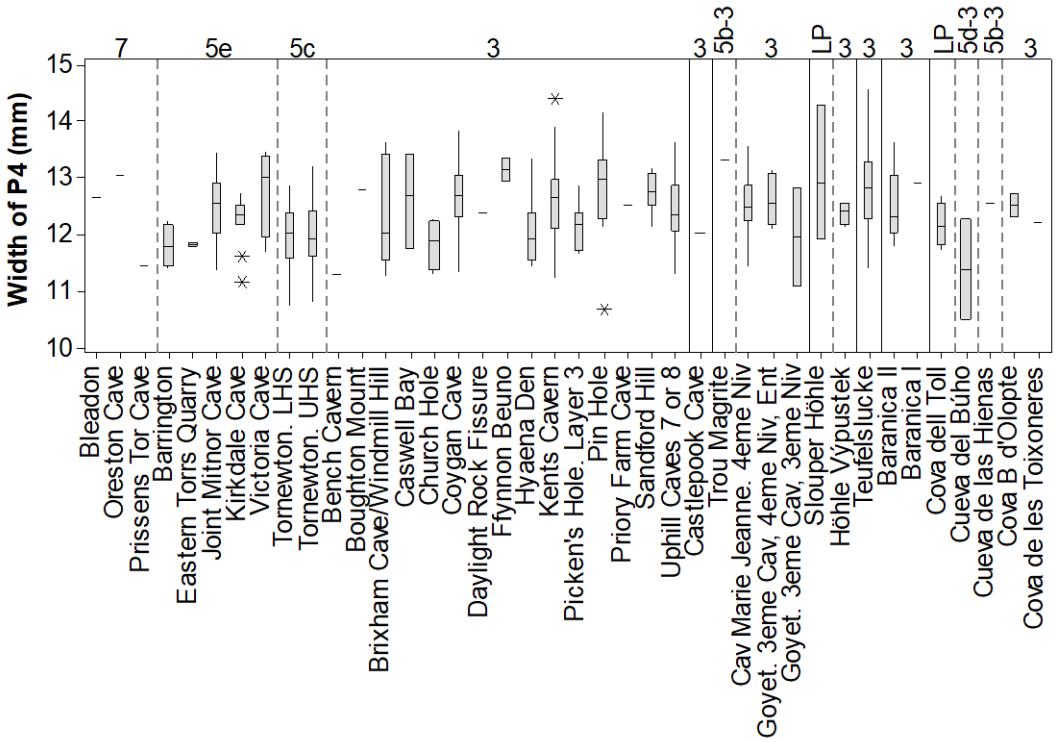

Figure 6.28: Boxplot of Pleistocene *C. crocuta* P4 width measurements. Numbers on top of the graph indicate Marine Oxygen Isotope Stages. LP = Late Pleistocene.

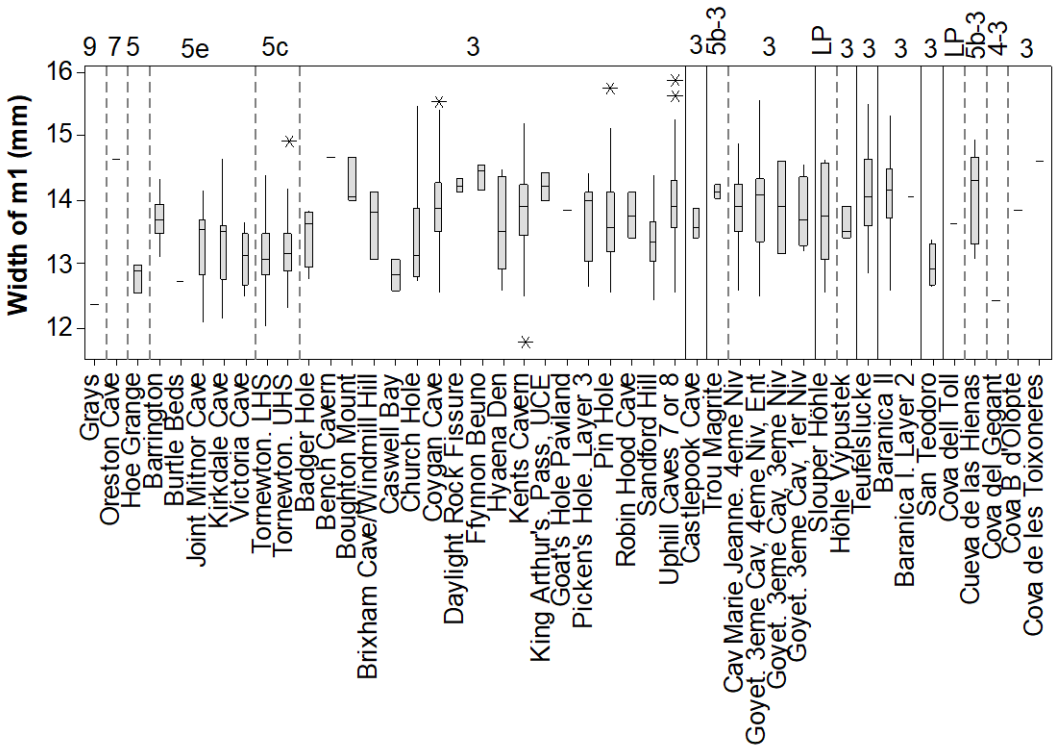

Figure 6.29: Boxplot of Pleistocene *C. crocuta* m1 width measurements. Numbers on top of the graph indicate Marine Oxygen Isotope Stages. LP = Late Pleistocene.

Table 6.6: Sample sizes of dental measurements in Figure 6.12 to Figure 6.29.

Site	C APD	C MLD	c APD	c MLD	P2 L	P2 W	P3 L	P3 W	p2 L	p2 W	p3 L	p3 W	p4 L	p4 W	P4 L	P4 GW	P4 W	m1 W
Pakefield. Sandy Gravel, Forest Bed											1	1	1	1				
Grays				1								1		1				1
Bleadon								1							1		1	
Hutton Cavern		1																
Oreston	1		2	2	1	1	2	2	2	3	4	4	4	4		1	1	1
Prissens Tor Cave	1	2													1		1	
Hoe Grange		2		1			1		1	3		3	2	4	1			3
Barrington	2	2	2	1	3	5	5	6	4	8	4	12	4	6	2	4	4	8
Brentford					1	1	1											
Burtle Beds									1		1	1						1
Eastern Torrs Quarry											1		2	1	2	2	2	
Joint Mitnor Cave	13	13	8	13	13	6	21	14	10	8	16	15	16	22	7	16	15	17
Kirkdale Cave	6	5	5	6	13	13	16	12	19	14	18	17	23	24	7	10	11	19
Little Syke									1	1		1		1				
Milton Hill			1	1	2	2	1	1		1	1	1		1				
Raygill Fissure												1		1				
Victoria Cave	2	5	1	1			2	4	6	7	5	5	4	4		2	4	5
Tornewton. LHS	12	16	11	15	9	11	24	19	5	9	12	18	28	37	23	28	29	34
Tornewton. UHS	13	19	12	18	3	4	13	8	10	12	14	17	35	39	13	13	17	34
Badger Hole	2	3	1						3	2		2	1					4
Bench Cavern		1		2	1		1		3	2	2				2	1	1	1
Boughton Mount	1	1	3	2	2	2	2		2	3	1	3	2	2			1	3
Brixham Cave/Windmill Hill	4	6	7	13	1		3	4	5	6	3	5	4	5	4	5	5	3
Caerwent Quarry		1				1	1	1		1		1	2	2				
Caswell Bay			2	1	1	1	1	2		1	1	3	1	2	1	2	3	2
Church Hole	2	3	7	10	4	6	4	7	3	7	3	8	3	7	5	9	7	7

Site	C APD	C MLD	c APD	c MLD	P2 L	P2 W	P3 L	P3 W	p2 L	p2 W	p3 L	p3 W	p4 L	p4 W	P4 L	P4 GW	P4 W	m1 W
Coygan Cave	40	50	42	57	21	20	50	52	33	43	54	64	66	77	43	50	52	73
Daylight Rock Fissure								1	2	1	2	1	4	4	1	1	1	2
Ffynnon Beuno	1	1	1	1	1	1	2	2			4	4		2	1	2	2	3
Goat's Hole Paviland			1	1					1									1
Hyaena Den			1	3	2	1	1	1	4	4	6	7	2	6	4	4	7	7
Kents Cavern	31	48	58	93	20	20	65	57	54	76	92	155	109	144	60	77	76	115
King Arthur's Cave. The Passage, Upper Cave Earth	1	1					1		1				1	1				2
Lewes Castle							1											
Nanna's Cave. Red loam					1	1												
Picken's Hole. Layer 3	8	9	9	10	4	4	6	7	10	9	6	11	6	11	7	7	7	10
Pin Hole	8	13	9	17	9	12	6	10	18	27	17	26	19	35	12	18	16	34
Priory Farm Cave															1		1	
Robin Hood Cave											2	2						2
Sandford Hill	11	18	6	12	3	2	2	4	11	18	18	31	6	25	1	7	6	22
Tornewton. Elk Stratum			1	1	2	2			1	1	1	2	2	2				
Uphill Caves 7 or 8	6	14	17	24	9	14	20	20	26	22	40	38	25	40	9	16	27	37
Yealm Bridge	2	3		1			1				1	1						
Castlepook Cave	2	2	1	3	2	2	1	3	2	5	1	5		7	1	3	1	3
Trou Magrite		1			1	1				1	1	1	1	2			1	2
Caverne Marie-Jeanne. 4eme Niveau	1	2	6	6	15	14	8	14	18	16	13	19	15	24	9	23	16	26
Goyet. 3eme Caverne, 4eme Niveau Ossifère, Galleries Voisines de l'Entrée			5	8		1	3	7	2	5	6	13	4	7	2	5	5	11
Goyet. 3eme Caverne, 3eme Niveau	3	4	4	11		1	1	2	6	5	3	7	5	12		2	2	2
Goyet. 3eme Caverne, 1er Niveau Ossifère		1	2						1	1	3	4	1	2				4
Slouper Höhle	1	1		3	3	2	3	3	8	3	9	5	7	11	2	2	3	10
Höhle Výpustek		1	2	4	1	1	4	1	2	1	3	3	3	4	3	3	4	3

Site	C APD	C MLD	c APD	c MLD	P2 L	P2 W	P3 L	P3 W	p2 L	p2 W	p3 L	p3 W	p4 L	p4 W	P4 L	P4 GW	P4 W	m1 W
Teufelslucke	10	19	22	28	29	28	43	33	54	43	45	50	32	60	28	42	55	53
Baranica II	1	1			1				2	1	2	2	2	6	2	1	6	10
Baranica I															1	1	1	1
San Teodoro	1	1	1	1			5	2	8	3	7	5	1	6		1		4
Cova del Toll	1	1			2	2	1	1	1	2		1			1	3	4	1
Cueva del Búho															2	2	2	
Cueva de las Hienas							1		1	1			3	3	2	1	1	5
Cova del Gegant									1	1								1
Cova B d'Olopte					1	1	1	1	1	1		2		1	2	2	2	1
Cova de les Toixoneres						1		2	2	2			1	1	1		1	1

As outlined above, the length of the p2 appears to show different patterns to the lengths and widths of the p3 and p4. In order to further investigate this difference, RMA regressions were performed to assess the allometric relationships between these dental measurements (Table 6.7 and Figure 6.30). The results show that the weakest relationship is between p2 and p3 lengths as indicated by the insignificant relationship (p = 0.074), low Pearson's r value (0.219) and the large confidence intervals around the slope (0.543 to 2.596).

The RMA between the other lower premolar lengths and widths are all significant at 95 % confidence. For p3 length against p4 length, and p3 width against p4 width, the confidence interval for the slopes both span one. By contrast, for p2 length against p3 length, p2 width against p3 width, and p2 width against p4 width, with confidence intervals are all less than one.

Table 6.7: Results of reduced major axis regressions, with base-10 logarithmically transformed *C. crocuta* lower premolar measurements. For each pair of measurements, the first named is on the x-axis and the second named is on the y-axis. Statistics include the Pearson's r correlation and associated p-value. Also shown are the regression slope values with associated 95 % bootstrapped confidence intervals of the slope.

Statistic	**p2 length & p3 length**	**p2 length & p4 length**	**p3 length & p4 length**	**p2 width & p3 width**	**p2 width & p4 width**	**p3 width & p4 width**
n	68	29	29	211	154	220
Pearson's r	0.219	0.573	0.511	0.508	0.442	0.768
p-value	0.074	0.001	0.005	<0.05	<0.05	<0.05
Slope	0.909	0.672	1.059	0.807	0.88	1.07
Min. CI	0.543	0.423	0.592	0.705	0.738	0.984
Max. CI	2.596	0.861	1.367	0.901	0.991	1.158

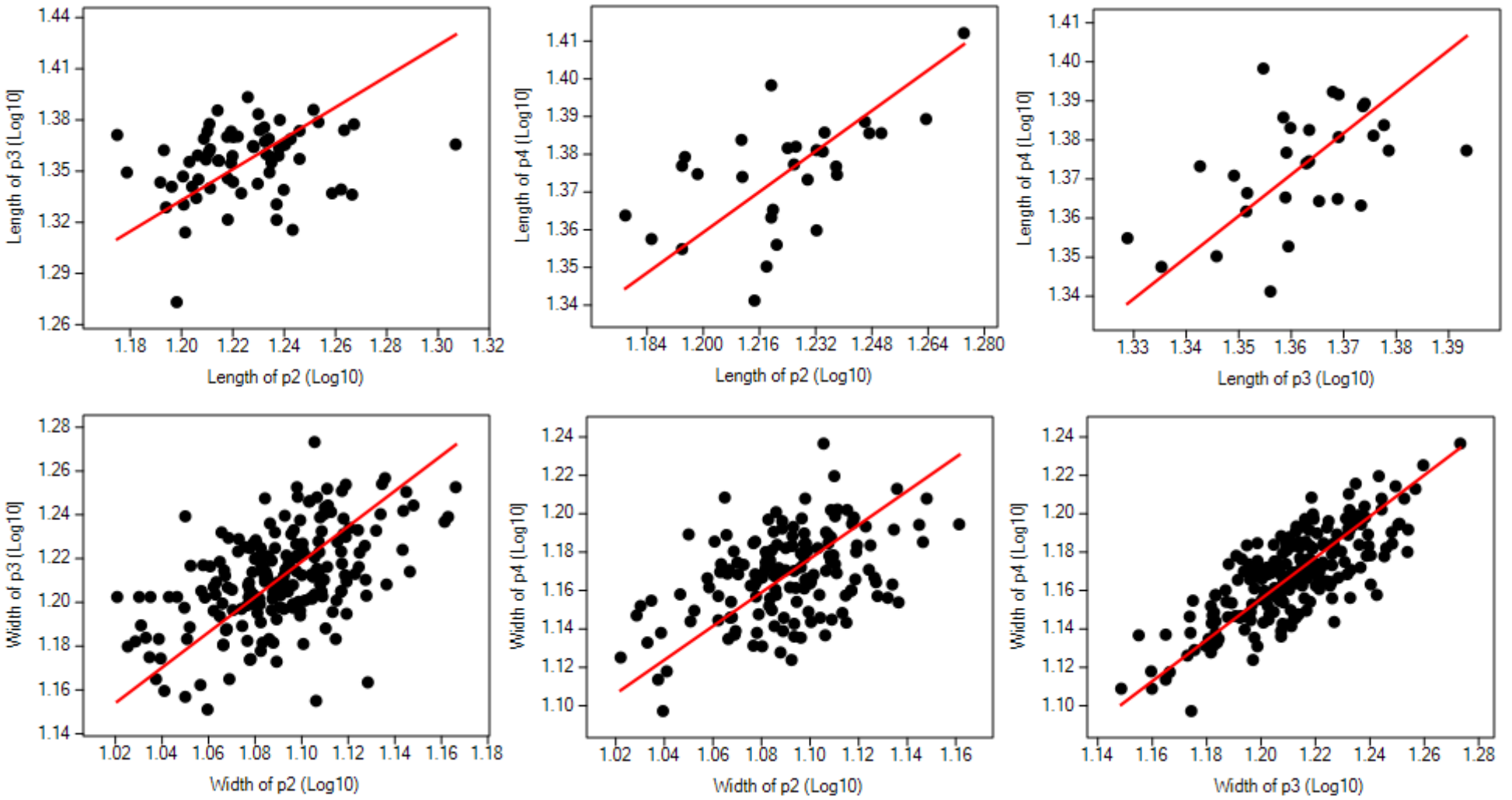

Figure 6.30: Reduced major axis regressions of base-10 logarithmically transformed *C. crocuta* lower premolar measurements.

The robustness of the premolars was assessed. First, in order to investigate the allometric relationships between the lengths and widths of each premolar, RMA regressions were carried out (Table 6.8 and Figure 6.31). All regressions are significant at 95 %. The confidence intervals for the slopes of P3 length against width, and p2 length against width both span one. By contrast, the confidence intervals of the slopes for P2 length against width, p3 length again width, and p4 length against width are all greater than one.

Table 6.8: Results of reduced major axis regressions, with base-10 logarithmically transformed *C. crocuta* premolar measurements. For each pair of measurements, the first named is on the x-axis and the second named is on the y-axis. Statistics include the Pearson's r correlation and associated p-value. Also shown are the regression slope values with associated 95 % bootstrapped confidence intervals of the slope.

Statistic	**P2 length & P2 width**	**P3 length & P3 width**	**p2 length & p2 width**	**p3 length & p3 width**	**p4 length & p4 width**
n	139	204	238	323	374
Pearson's r	0.745	0.601	0.675	0.491	0.452
p-value	<0.05	<0.05	<0.05	<0.05	<0.05
Slope	1.242	1.077	1.06	1.127	1.254
Min. CI	1.053	0.943	0.945	1.009	1.137
Max. CI	1.397	1.198	1.158	1.229	1.369

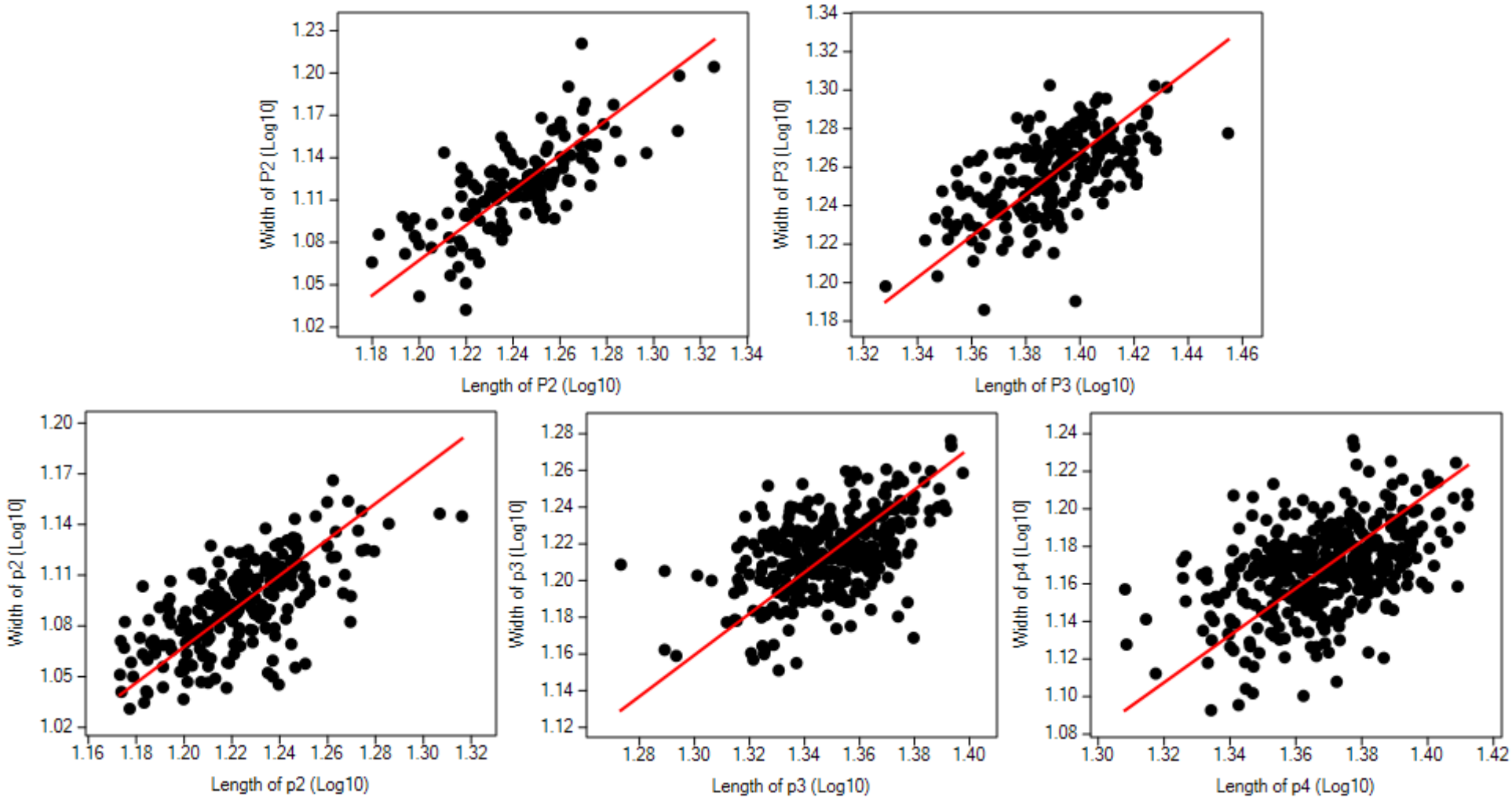

Figure 6.31: Reduced major axis regressions of base-10 logarithmically transformed C. crocuta premolar measurements.

The next assessment of robustness was to plot the length against width of each premolar from British sites (Figure 6.32). The data were split in to palaeoclimatic stages (correlated with Marine Oxygen Isotope Stages), with the addition of the early Middle Pleistocene. There is considerable overlap in teeth from MIS 5e, 5c and 3. This is particularly the case for the P3. Values from MIS 3 span much of the range of values. Within this range, those from MIS 5e tend to be greater in length and width than those from MIS 5c, although there is much overlap.

For the P2, p3 and p4, the MIS 5e and 5c values cluster towards the bottom left of the graphs, i.e. teeth are smaller in both length and width. For the p4, this is particularly the case for the width. This opposite trend is shown for the p2. Additionally, the p2s from MIS 5e tend to be longer relative to their widths than teeth from MIS 3.

There are few data points from MIS 7 and the early Middle Pleistocene. The values from MIS 7 are among the greatest in length and width for the P2 and P3. One of the MIS 7 p4 values is much greater in width than all but one from MIS 3. By contrast, the other MIS 7 points plot within the range of other data, which is also the case for all p2 values. Length and width values for the early Middle Pleistocene are only available for the p3 and p4. In both cases, the early Middle Pleistocene values plot towards the centre of the ranges of the other data.

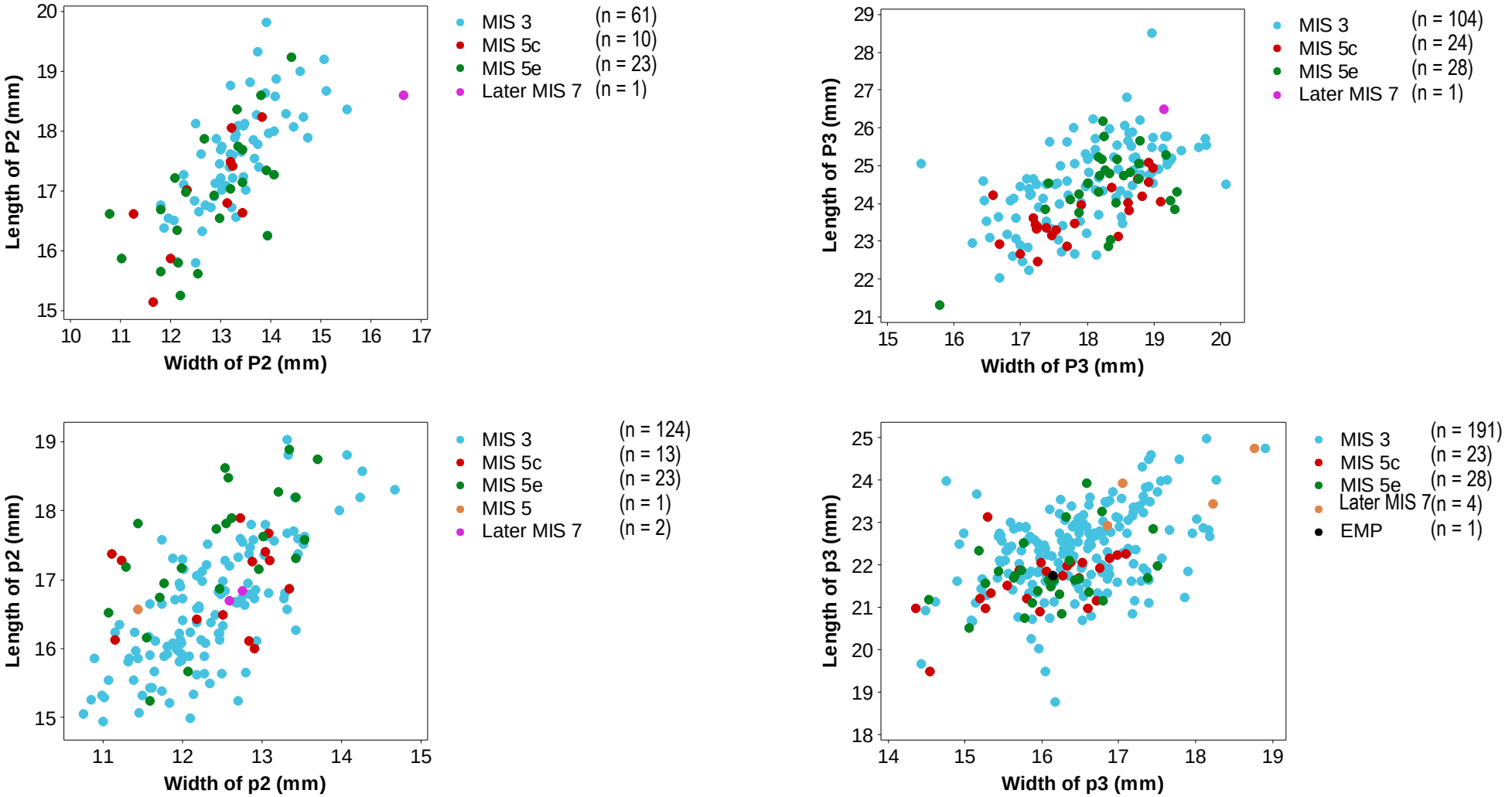

Figure 6.32: Correlations of *C. crocuta* premolar length and width measurements from Pleistocene deposits in Britain.

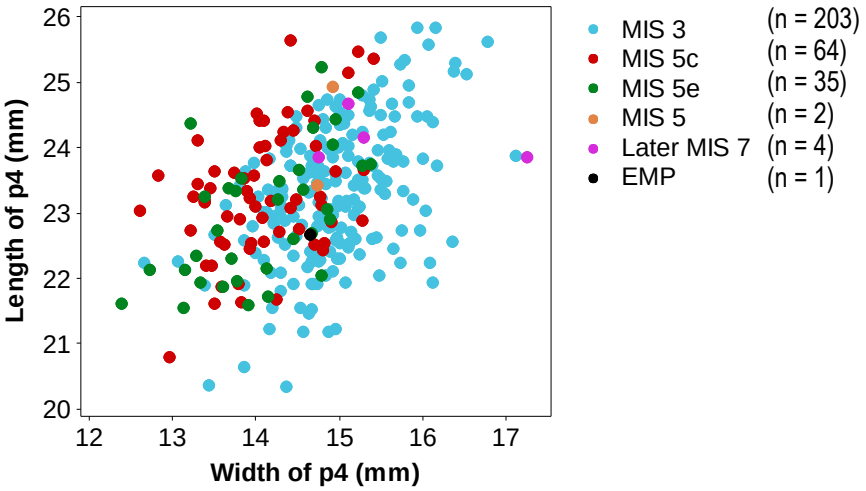

Figure 6.32 continued.

Measurements of the cranium with few data points are displayed in Table 6.9 and Appendix 10.8, Table 10.51. For measurements with four or more data points, these are shown in individual value plots and boxplots (Figure 6.33, and Appendix 10.8, Figure 10.4).

The measurements of skull length from Slouper Höhle are greater than those from other sites. This pattern breaks down for measurements of the viscerocranium length, facial length and snout length, whereby one Slouper Höhle specimen plots among the smallest of the specimens from all sites. The specimens from Britain plot variably in these graphs, including some of the largest and smallest measurements.

Table 6.9: Cranial measurements of Pleistocene *C. crocuta* from Europe. Measurements included are those with fewer than four data values.

Site	Total length of the cranium (mm)	Basicranial axis (mm)	Basifacial axis (mm)	Upper neurocranium length (mm)	Temporal fossa length (mm)
Kents Cavern				156.77	
Sandford Hill		75.63	173.66		
Slouper Höhle	307.61		170.1	170.4	169.49
Slouper Höhle		74.43			
Höhle Výpustek	290.44			160.89	160.41

The greatest diameter of the auditory bulla show close similarities in size between three specimens between 49.47 and 49.95 mm (from Sandford Hill, Slouper Höhle and Höhle Výpustek), yet one specimen from Slouper Höhle measures 5.95 mm larger.

The greatest height of the orbit is smallest in the Barrington specimen and largest in the Höhle Výpustek specimen, with a 12.55 mm difference.

There is some variation in measurements of the neurocranium breadth, although both Slouper Höhle specimens plot towards the centre and larger ranges of measurements, while the Barrington and Sandford Hill specimens plot towards the centre and lower ranges of measurements. There is also a measurement from Castlepook Cave, which plots in the centre of the measurements.

Overall, many of the measurements indicate that specimens from Slouper Höhle and Höhle Výpustek are larger. However, this is not constant for all measurements, and some measurements indicate disparity between specimens from the same site. Moreover, only a small number of sites are represented in these plots.

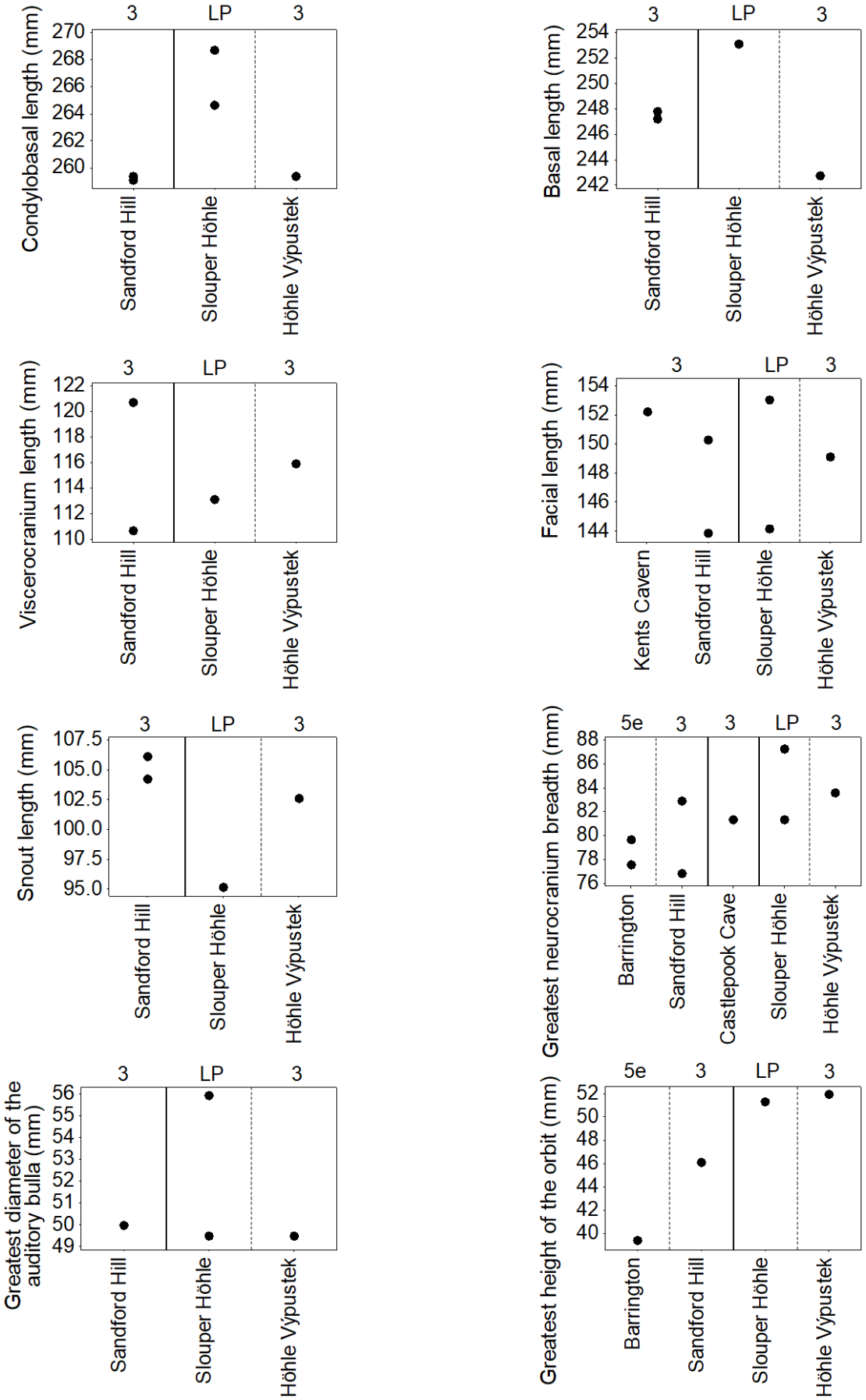

Figure 6.33: Individual value plots of *C. crocuta* cranial measurements from Pleistocene deposits in Europe. Numbers along the top are Marine Oxygen Isotope Stages. LP = Late Pleistocene.

A greater number of sites are represented in the graphs of mandibular measurements, except for the height of the vertical ramus, for which there are specimens from only two sites (Figure 6.34 to Figure 6.43, Appendix 10.8, Table 10.52 and Figure 10.5).

The measurements of mandibular length (from the condyle, the angular process, or the notch between the condyle and angular process) are all consistently large in the specimen from Trou Magrite. One specimen from Teufelslucke is also similar in length to this Trou Magrite specimen. The smallest lengths are from Castlepook Cave specimens, although not all measurements could be recorded from this specimen. The specimen from Barrington is slightly larger than that from Castlepook Cave. Kents Cavern, Pin Hole, Slouper Höhle and one Teufelslucke specimen tend to plot in an intermediate position between the aforementioned largest and smallest measurements.

More measurements were recorded of tooth row lengths. Again, there is much overlap in the range of measurements from each site. The Slouper Höhle mandibles are among the largest in the distances of c – m1, although this is less clear for the distance from and p2 – p4. Some specimens from Kents Cavern are among the largest for c – m1 and p2 – p4, yet the spread of data also includes some of the smaller specimens. Other large specimens are the upper ranges of Pin Hole and Sandford Hill measurements. The c – m1 length is also larger in the Trou Magrite specimens, but these specimens are not notably larger for p2 – p4 length. Of note are the Oreston specimens, which are particularly large across all tooth row measurements.

For c – m1 length, the smallest measurements are from Church Hole, the lower range of Sandford Hill, Uphill Caves (all MIS 3 deposits from Britain), and San Teodoro (MIS 3 in Italy). For p2 – p4 length, the smallest specimens are the lower ranges of measurements from British MIS 3-aged assemblages (Coygan Cave, Pin Hole, Sandford Hill and Uphill Caves).

The specimens from deposits dated to MIS 5e and 5c generally plot within the centre of the graphs for tooth row length measurements.

The p2-p4 length is the only mandibular measurement to allow tests for statistical significance. ANOVA with post-hoc Tukey Pairwise Comparisons test revealed no significant difference between the measurements from Kents Cavern, Pin Hole, Sandford Hill and Teufelslucke at 95 % confidence (Table 6.11).

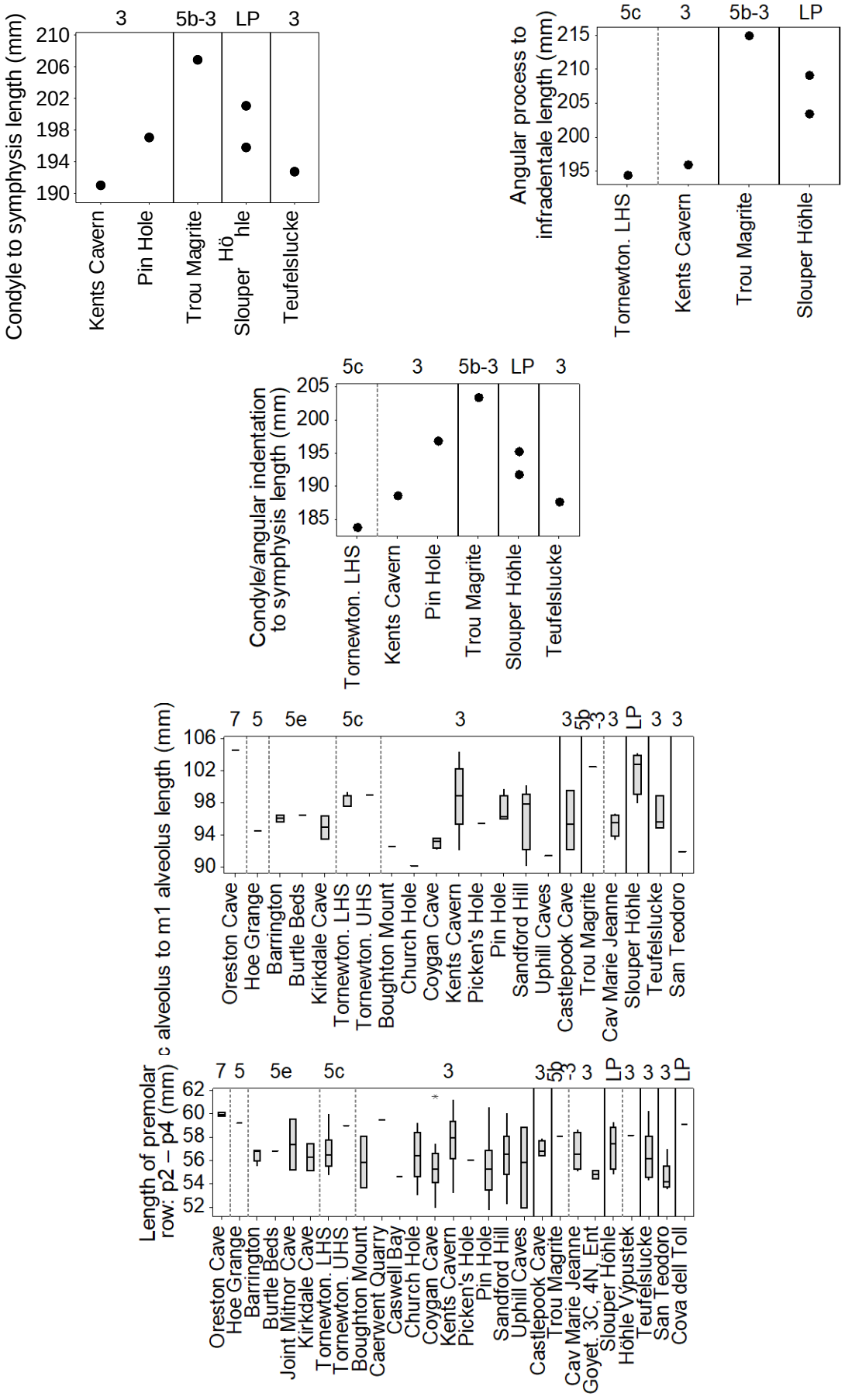

Figure 6.34: Individual value plots and boxplots of *C. crocuta* Pleistocene mandible lengths. Top numbers are Marine Oxygen Isotope Stages. LP = Late Pleistocene. Sample sizes in Table 6.10..

Table 6.10: Sample sizes of each site included in the boxplots in Figure 6.34.

Site	c alveolus to m1 length	Length of premolar row (p2-p4)
Oreston	1	2
Hoe Grange	1	1
Barrington	2	5
Burtle Beds	1	1
Joint Mitnor Cave		2
Kirkdale Cave	2	2
Tornewton. LHS	4	6
Tornewton. UHS	1	1
Boughton Mount	1	2
Caerwent Quarry		1
Caswell Bay		1
Church Hole	1	7
Coygan Cave	4	11
Kents Cavern	12	27
Picken's Hole. Layer 3	1	1
Pin Hole	4	11
Sandford Hill	7	17
Uphill Caves 7 or 8	1	3
Castlepook Cave	3	1
Trou Magrite	1	1
Caverne Marie-Jeanne. 4eme Niveau	7	11
Goyet. 3eme Caverne, 4eme Niveau Ossifère, Galleries Voisines de l'Entrée		2
Slouper Höhle	4	8
Höhle Výpustek		1
Teufelslucke	4	18
San Teodoro	1	6
Cova del Toll		1

Table 6.11: ANOVA with post-hoc Tukey Pairwise Comparisons on base-10 logarithmically transformed measurements of the length of the premolar row (p2-p4). p-value = 0.102.

Site	Mean (Log10)	Category
Kents Cavern	1.76	A
Pin Hole	1.744	A
Sandford Hill	1.752	A
Teufelslucke	1.752	A

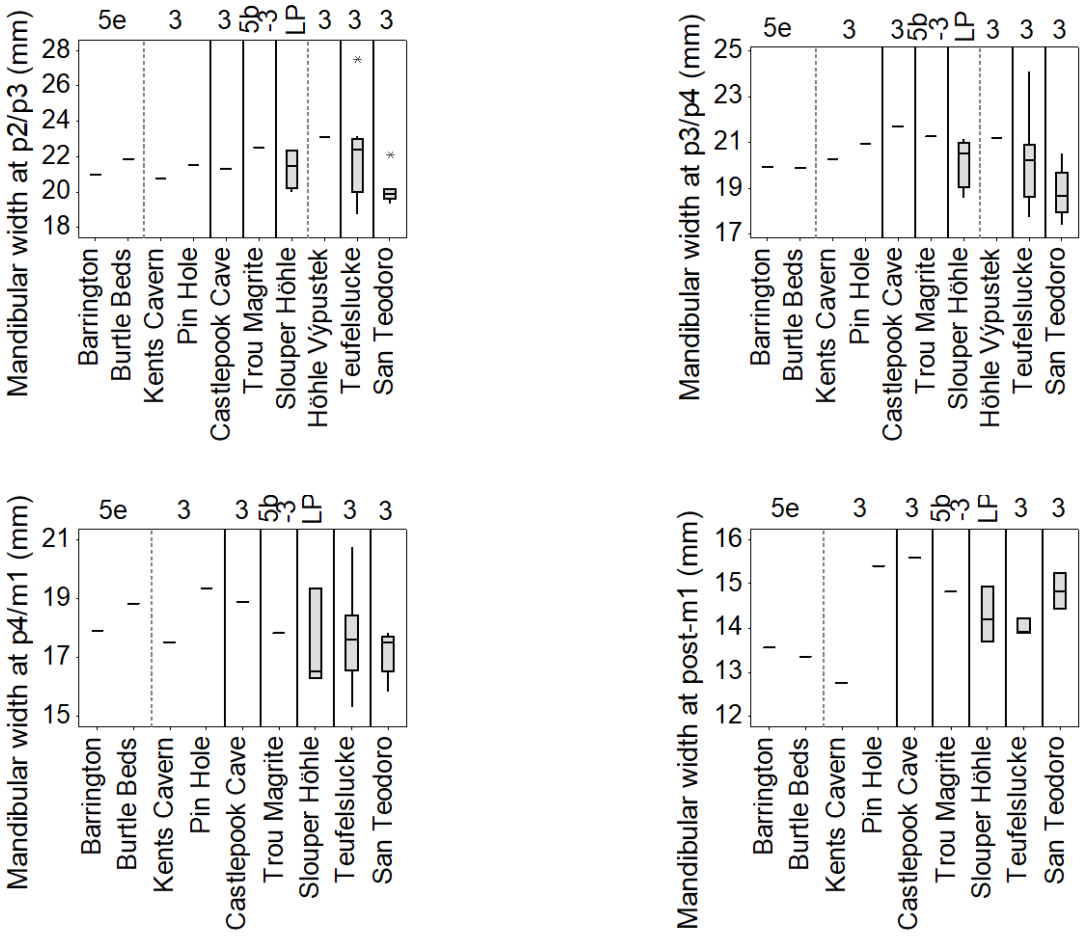

Figure 6.35: Boxplots of *C. crocuta* Pleistocene mandibular width measurements. Numbers along the top of the graphs indicate Marine Oxygen Isotope Stages. LP = Late Pleistocene. See Table 6.12 for sample sizes of the boxplots.

Table 6.12: Sample sizes of each site included in the boxplots in Figure 6.35.

Site	Mandibular width at p2/p3	Mandibular width at p3/p4	Mandibular width at p4/m1	Mandibular width at post-m1
Barrington	1	1	1	1
Burtle Beds	1	1	1	1
Kents Cavern	1	1	1	1
Pin Hole	1	1	1	1
Castlepook Cave	1	1	1	1
Trou Magrite	1	1	1	1
Slouper Höhle	4	4	3	3
Höhle Výpustek	1	1		
Teufelslucke	15	12	9	4
San Teodoro	7	6	6	2

For the mandibular width measurements (Figure 6.35), the specimens from Teufelslucke have the greatest range, spanning the largest and smallest measurements, except for the post-m1 position. Again, except for the post-m1 position, the San Teodoro specimens plot towards the lower range of the graphs. The single specimens from British localities and Trou Magrite plot within the range of measurements from Slouper Höhle, Teufelslucke and San Teodoro. This is except for the post−m1 position where specimens from Barrington, Burtle Beds and Kents Cavern are smaller.

The mandibular depth measurements (Figure 6.36) were split into individual tooth wear stages, in light of the evidence from Section 5.2 that these measurements increase in size through life. For the depth at p2/p3, there are three specimens from San Teodoro. Despite being from older individuals (wear stages VI, VIII and IX), they are consistently small. Other notably small specimens include a number of MIS 3-age from Britain, in addition to some from Castlepook Cave, Slouper Höhle and Teufelslucke, all of which are from younger individuals (wear stage IV). From older individuals, only a specimen from Tornewton Lower Hyaena Stratum (wear stage VIII) is notably small, while the two other specimens of the same age category (from Kents

Cavern and Pin Hole) are among the largest of all specimens. The only specimen from MIS 7 is from Oreston, which plots among the smallest of the specimens from the same age category (wear stage V).

There are fewer specimens from which depths at p3/p4 and p4/1 were recorded. Those from San Teodoro again plot consistently small. Those from Teufelslucke plot are mostly among the largest.

The smallest depths at the post-m1 position are mostly of the younger specimens (wear stage IV) along with one from Kents Cavern (wear stage V) and one from Burtle Beds (VII). This specimen from Burtle Beds is smaller than specimens from younger wear stages, including some from MIS 5e-aged Barrington.

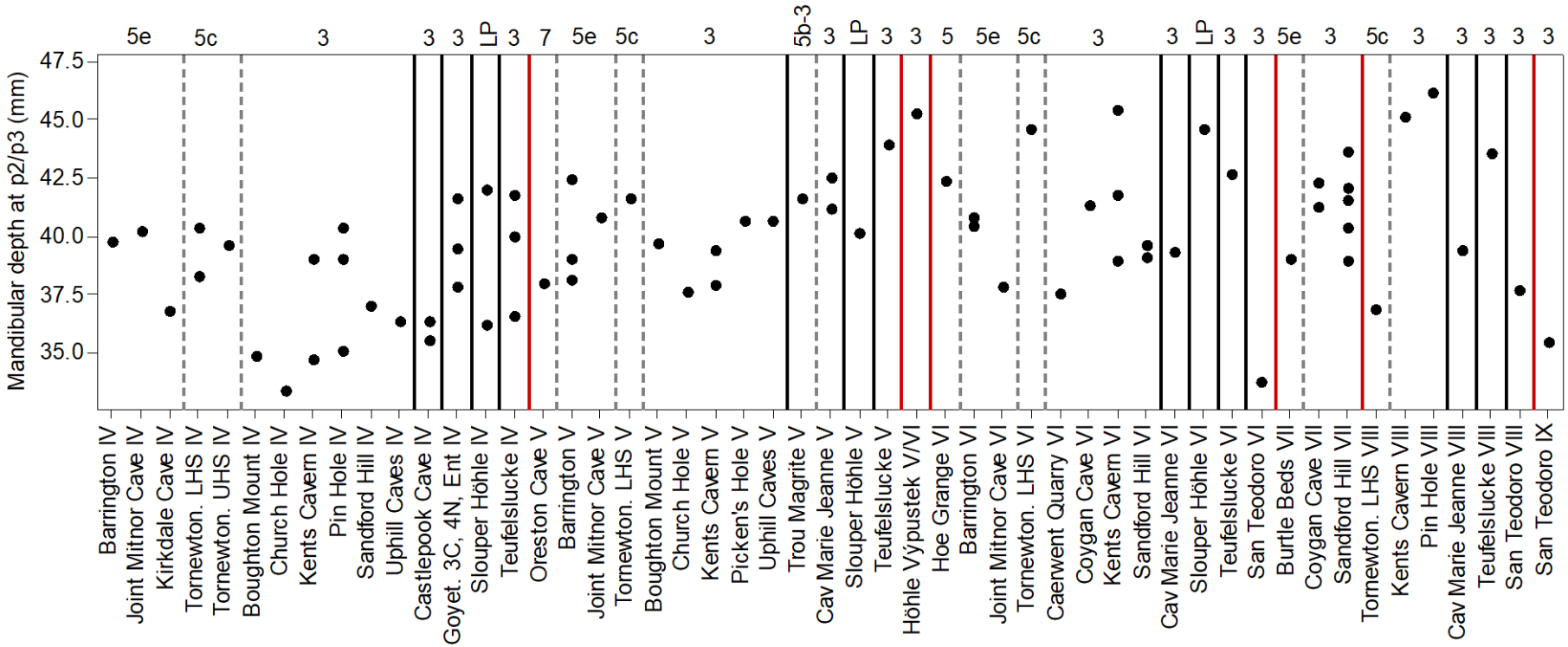

Figure 6.36: Individual value plots of *C. crocuta* Pleistocene mandibular depth measurements. Numbers along the top of the graphs indicate Marine Oxygen Isotope Stages. LP = Late Pleistocene. Dashed lines group sites of the same age. Solid black lines group sites from the same country. Solid red lines group data from with the same P3/p3 wear stage (IV, V, etc.).

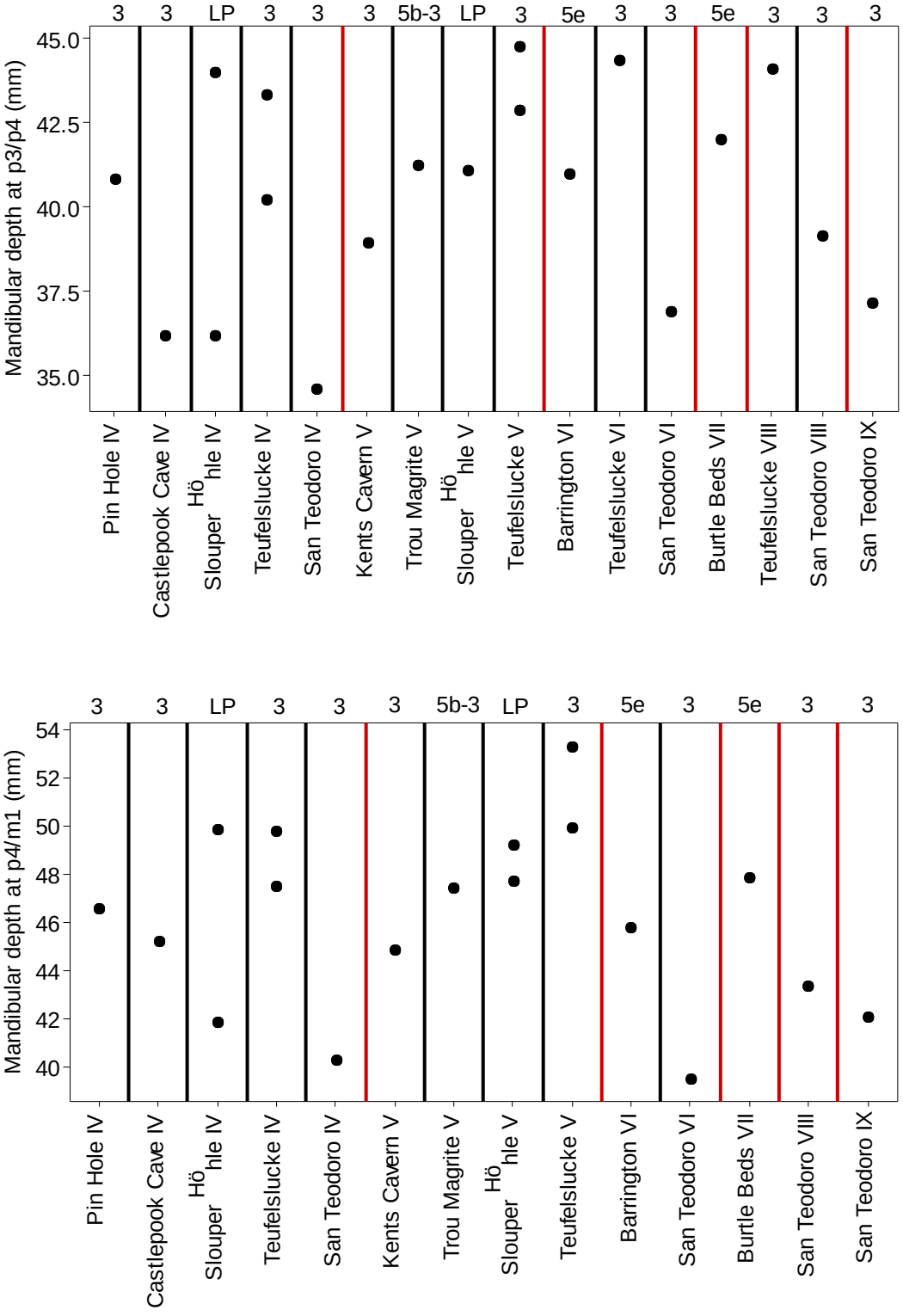

Figure 6.36 continued.

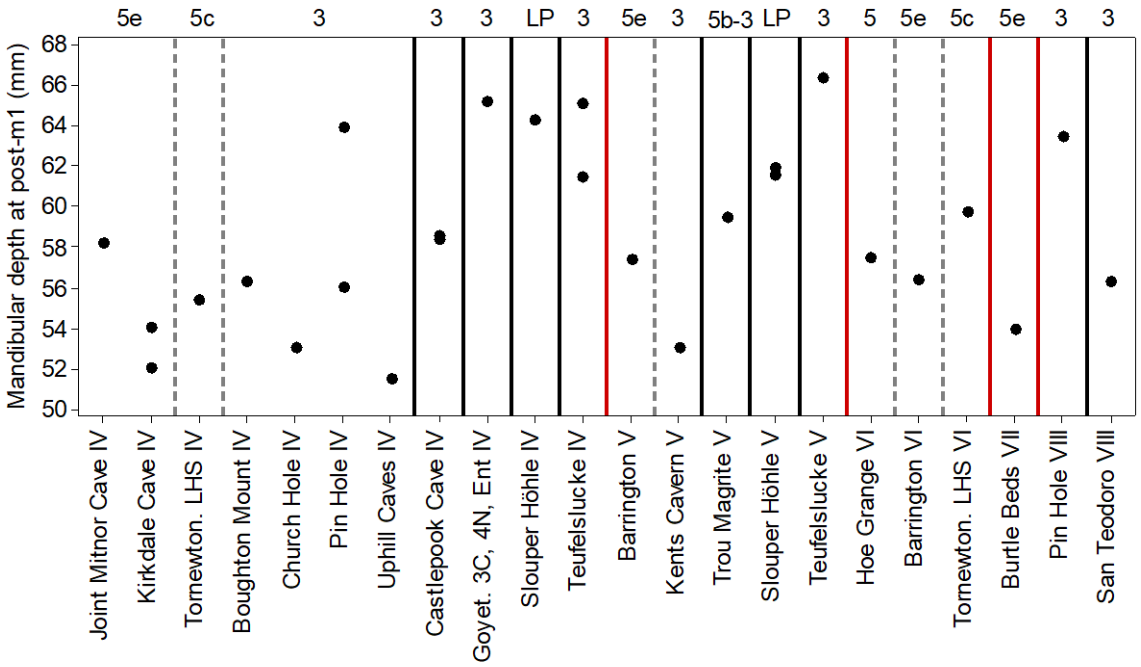

Figure 6.36 continued.

The bending strength profiles were again split into wear stage categories in light of the evidence from Section 5.2. For the zx/L indices (measuring resistance to dorsoventral bending), all values increase with more posterior positions along the mandible (Figure 6.37). At wear stage IV, the four mandibles show similar indices at the p4/m1 and post-m1 positions. However, there are differences anteriorly, with that from Slouper Höhle exhibiting greater indices, and the smallest indices from Castlepook Cave. There are greater differences in the profiles of wear stage V individuals. The specimen from Kents Cavern has lower values at each point along the mandible. The specimen from Trou Magrite has the greatest value at p2/3. At the p4/m1 and post-m1 positions, the greatest values are from Slouper Höhle and Teufelslucke. The profile from Barrington (wear stage VI) is similar to those from the younger wear stages. However, the indices are lower than most specimens of younger age categories from other sites, particularly at the post-m1 position. The specimen from the Burtle Beds (wear stage VII) shows a different profile; the increase in zx/L value is not as pronounced from the p4/m1 to post-m1 positions. In light of this, the indices at the post-m1 position are lower in the Burtle Beds specimen than seen in all specimens of younger age categories, except for the Kents Cavern specimen.

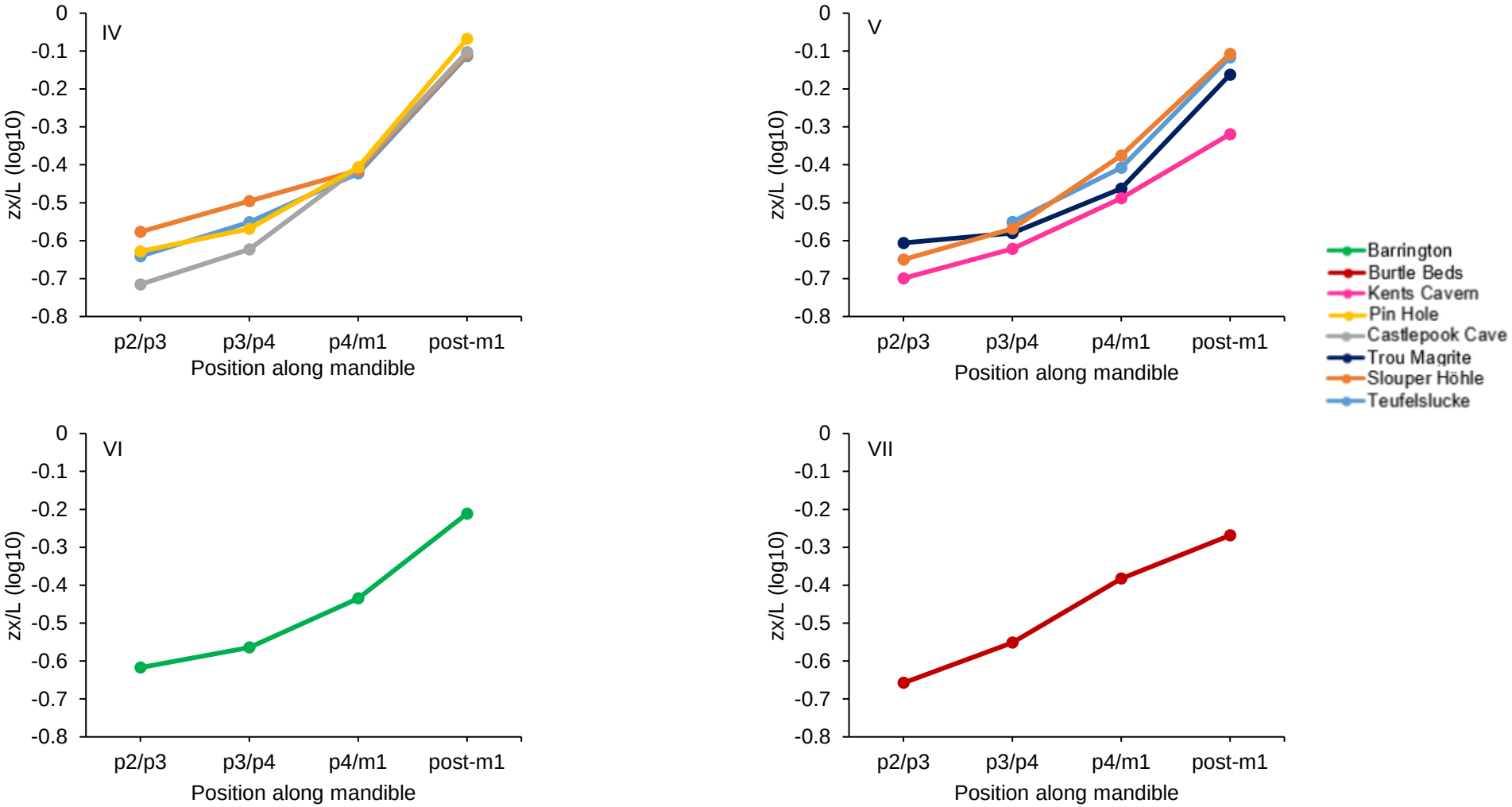

Figure 6.37: Mandibular profiles of zx/L values of *C. crocuta* from Pleistocene deposits in Europe.

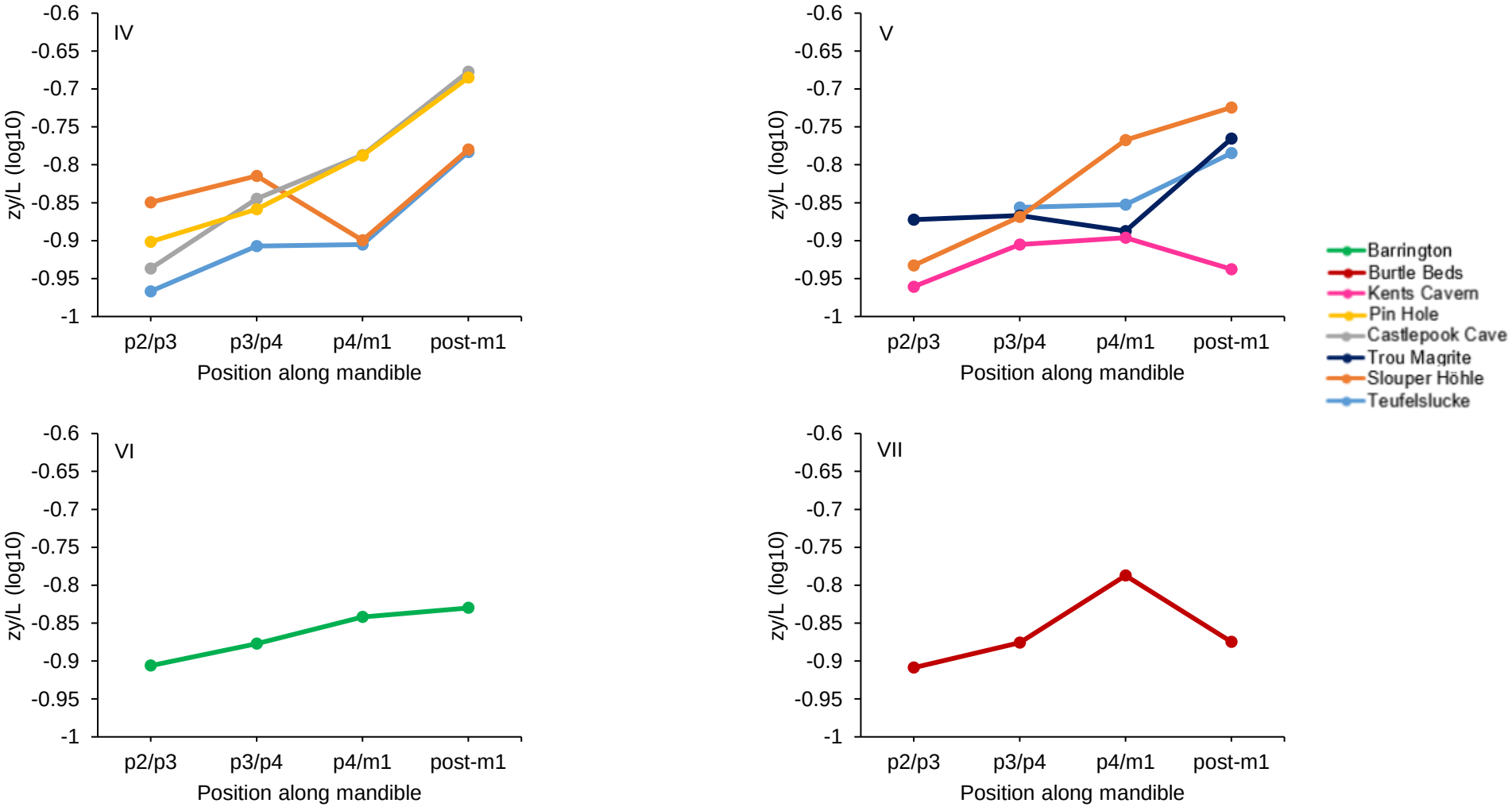

Figure 6.38: Mandibular profiles of zy/L values of *C. crocuta* from Pleistocene deposits in Europe.

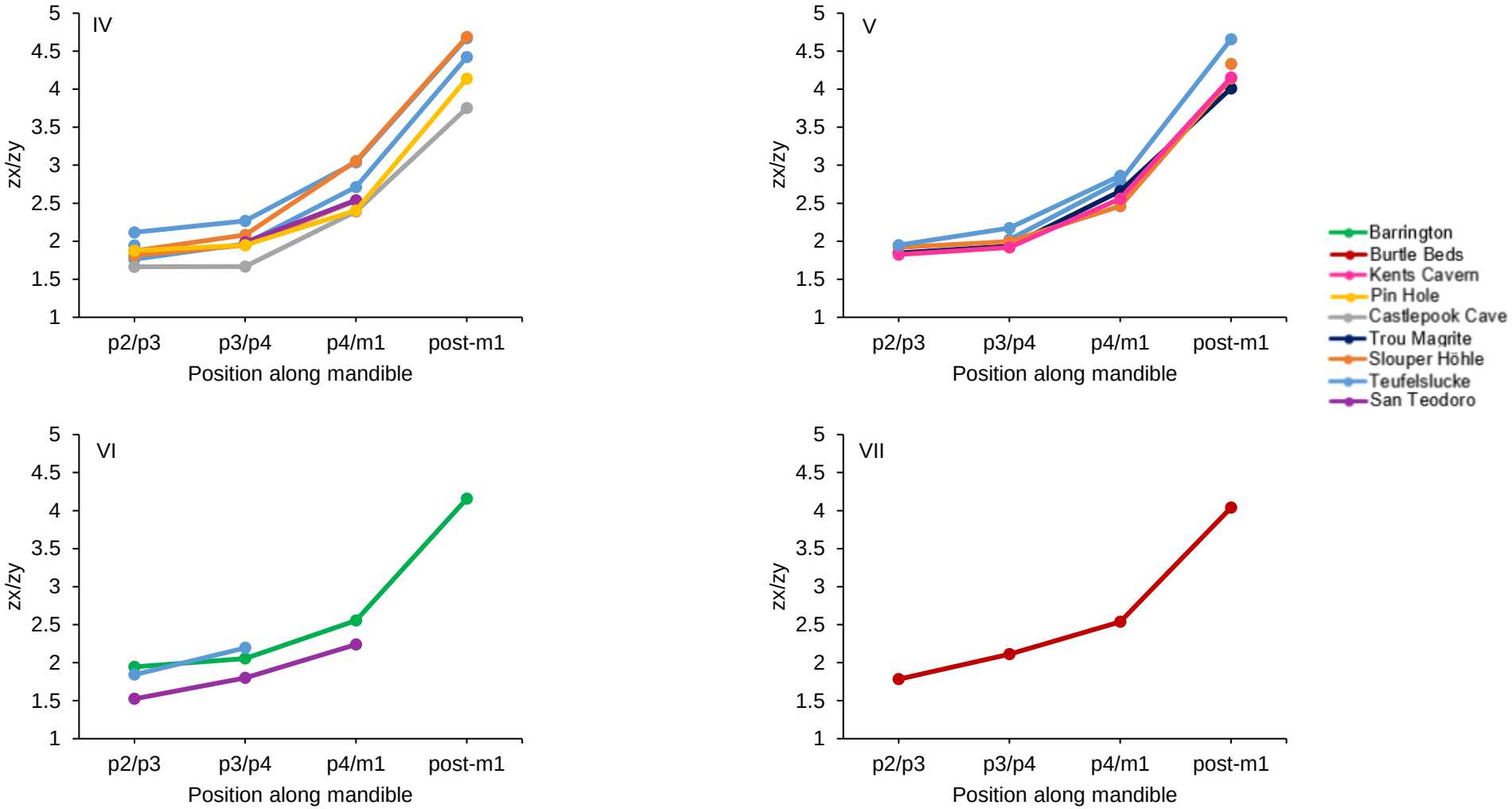

Figure 6.39: Mandibular profiles of zx/zy values of C. crocuta from Pleistocene deposits in Europe.

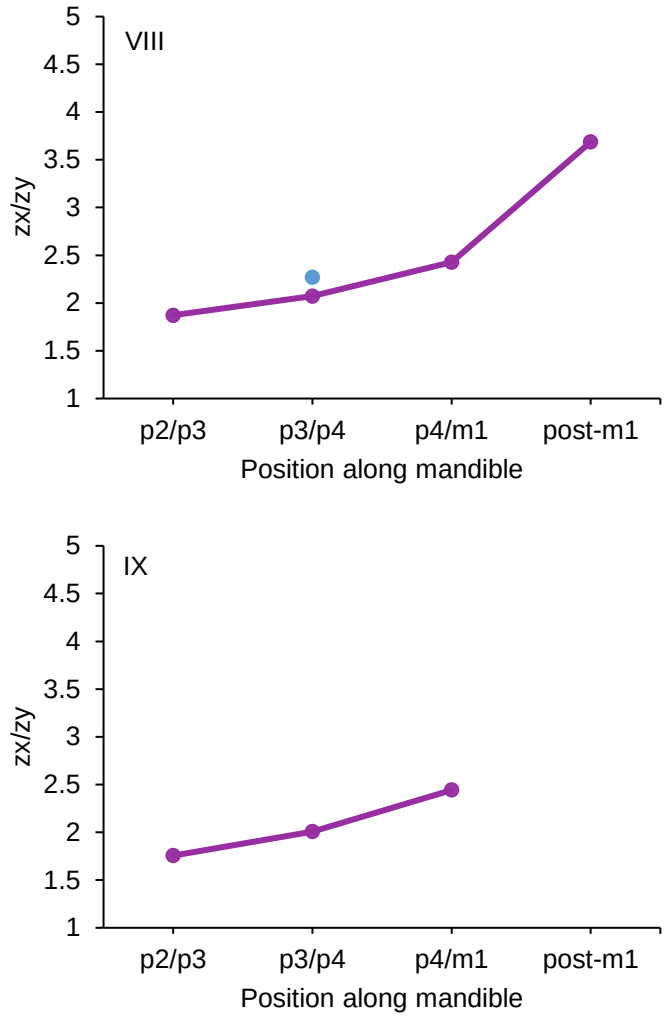

Figure 6.39 continued.

The zy/L indices (measuring resistance to labiolingual bending) show different patterns (Figure 6.38) to the zx/L indices. Some specimens show a decrease in indices along the mandible, such as Slouper Höhle at p4/m1, and Kents Cavern and Burtle Beds at post-m1.

At wear stage IV, the greatest bending strength at p2/p3 and p3/p4 is the Slouper Höhle specimen, whereas at p4/m1 and post-m1 the Pin Hole and Castlepook Cave specimens have greater indices.

At wear stage V, the Kents Cavern specimen has consistently lower values, while the Trou Magrite specimen has the greatest zy/L value at p2/p3 and the Slouper Höhle specimen has the greatest values at p4/m1 and post-m1.

Compared to the other specimens, the profile of the Barrington individual (wear stage VI) shows relatively little change in zy/L values along the mandible. It has the lowest zy/L values at the post-m1 position except for specimens from Burtle Beds and Kents Cavern.

The specimen from Burtle Beds (wear stage VII) has one of the greatest zy/L values at p4/m1, with only slightly higher values from Castlepook Cave (wear stage IV) and Slouper Höhle (wear stage V) specimens. By contrast, at the post-m1 position, its zy/L value is only larger than that from Kents Cavern. Its zy/L value at p2/p3 is similar to the Barrington specimen.

The zx/zy values (showing mandibular cross-sectional shape) are greater than one for all positions along all mandibles (Figure 6.39). The profiles for all specimens show an increase in zx/zy values posteriorly along the mandible.

Of the younger specimens (wear stage IV), the individual from Castlepook Cave has the lowest values. One specimen from Teufelslucke has the large values at each position along the mandible, and the Slouper Höhle specimen has similarly large values at the p4/m1 and post-m1 positions.

At wear stage V, the specimens from Kents Cavern, Trou Magrite and Slouper Höhle have similar values, whereas those from Teufelslucke are larger. At wear stage VI, the values for Barrington and Teufelslucke are similar, whereas the specimen from San Teodoro has smaller values. This specimen has smaller zx/zy values than all other specimens at the p2/p3, p3/p4 and p4/m1 positions.

The Burtle Beds specimen is the only example at wear stage VII. Its zx/zy values are not notably larger or smaller than the other mandibles. At wear stage VIII, there is a single zx/zy measurement at the p3/p4 position from Teufelslucke, which is larger than the one from San Teodoro. Except for the wear stage VI San Teodoro specimen, the San Teodoro mandibles at stage VIII and IX have the lowest zx/zy values at p4/m1 of all mandibles. The wear stage VIII San Teodoro specimen also has the lowest zx/zy value at the post-m1 position.

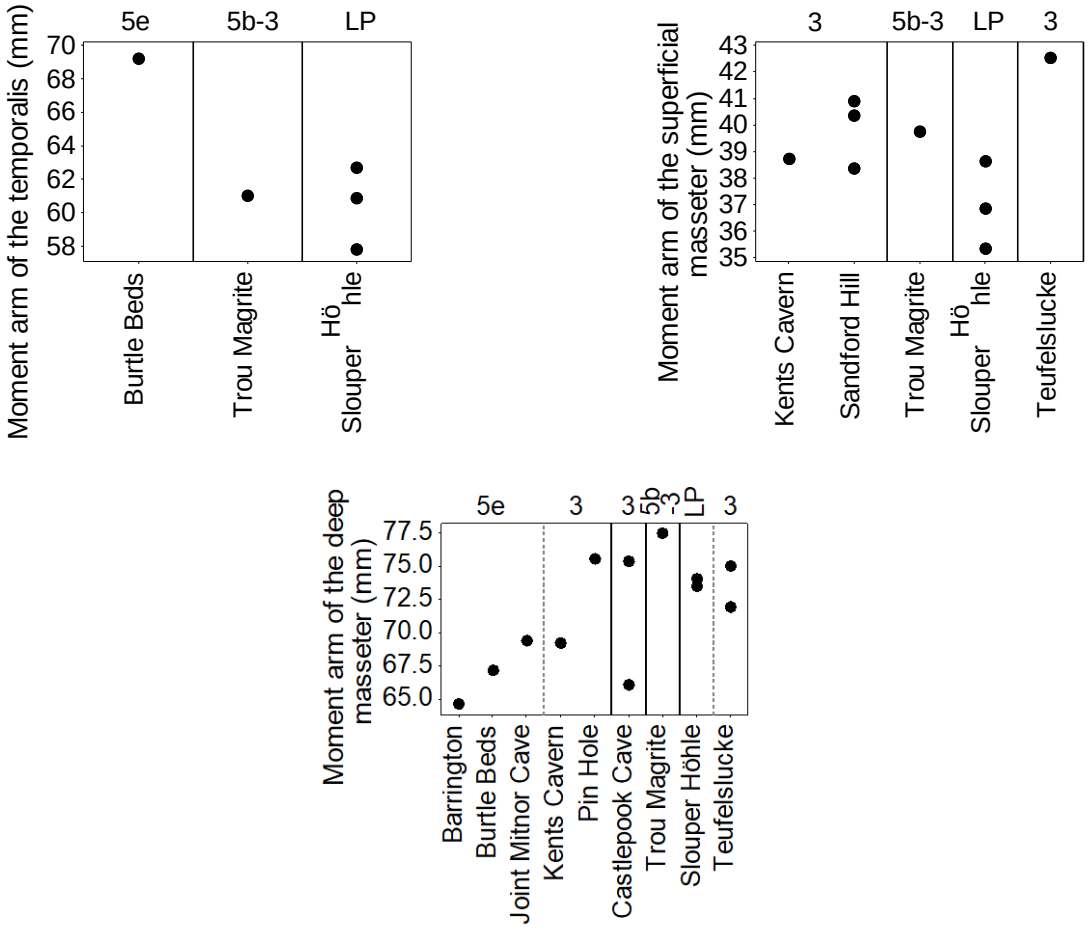

Figure 6.40: Individual value plots of *C. crocuta* Pleistocene muscle moment arms. Numbers along the top of the graphs indicate Marine Oxygen Isotope Stages. LP = Late Pleistocene.

The moment arm of the temporalis (Figure 6.40) is greatest in the Burtle Beds specimen. The moment arm of the superficial masseter is greatest from Teufelslucke, and smallest in two of the three Slouper Höhle specimens. There is a clear divide between the specimens with the largest and smallest moment arm of the deep masseter. The smallest are from Barrington, Burtle Beds, Joint Mitnor Cave, Kents Cavern, and one specimen from Castlepook Cave. The largest are the other specimen from Castlepook Cave, and specimens from Pin Hole, Trou Magrite, Slouper Höhle and Teufelslucke.

The mechanical advantage of the superficial masseter shows an increase in values posteriorly along the mandible for all specimens (Figure 6.41). The specimen from Teufelslucke has the greatest values at each position along the mandible.

In light of the results from Section 5.2, the mechanical advantage of the deep masseter and the temporalis were split into individual wear stage classes (Figure 6.42). At wear stage IV, the mechanical advantage of the deep masseter is greater in mandibles from Slouper Höhle and Pin

Hole, and lower in specimens from Castlepook Cave and Teufelslucke, with the difference becoming more pronounced posteriorly along the mandible. At wear stage V, mandibles from Kents Cavern and Teufelslucke have lower values, with mandibles from Trou Magrite and Slouper Höhle exhibiting greater values. Again, the difference between the Slouper Höhle and the other specimens is more pronounced posteriorly. There is only one specimen at wear stage VI (from Barrington) and at stage VII (from Burtle Beds). At the p3/p4, p4/m1 and m1 position, the specimen from Barrington has the lowest mechanical advantage of the deep masseter value of all mandibles. The values of the Burtle Beds specimen are not notably larger or smaller than those of other mandibles.

Mechanical advantage of the temporalis data are only available for four mandibles (Figure 6.43). At wear stage V, the mandible from Trou Magrite has consistently lower values for positions at c, p2/p3, p3/p4 and p4/m1 (there are no data at the m1 position). The largest values are from the Burtle Beds specimen (wear stage VII) at p2/p3, p3/p4, p4/m1 and m1 positions (there are no data from the c position). Both specimens from Slouper Höhle (wear stages IV and V) have values that are intermediate between the Trou Magrite and Burtle Beds specimens.

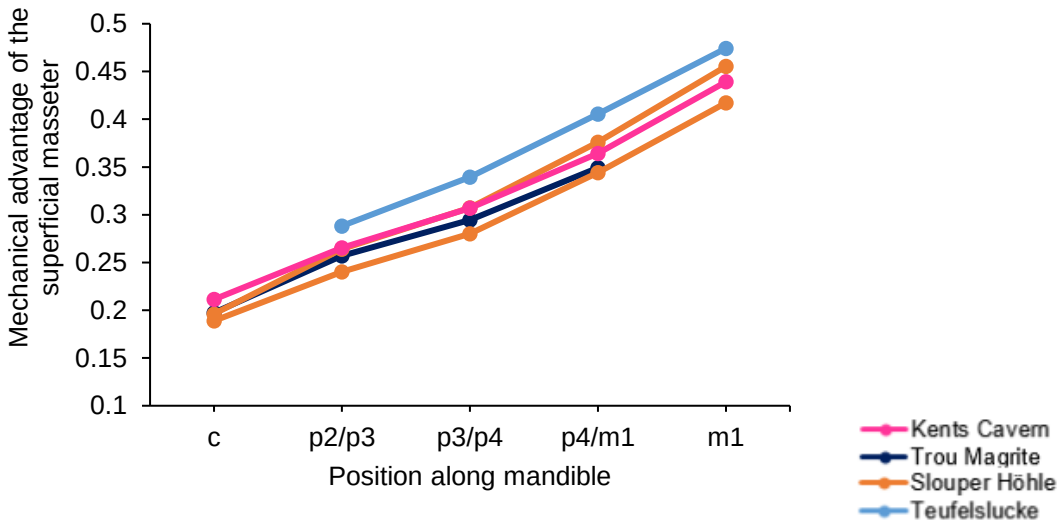

Figure 6.41: Mandibular profiles of the mechanical advantage of the superficial masseter of *C. crocuta* from Pleistocene deposits in Europe.

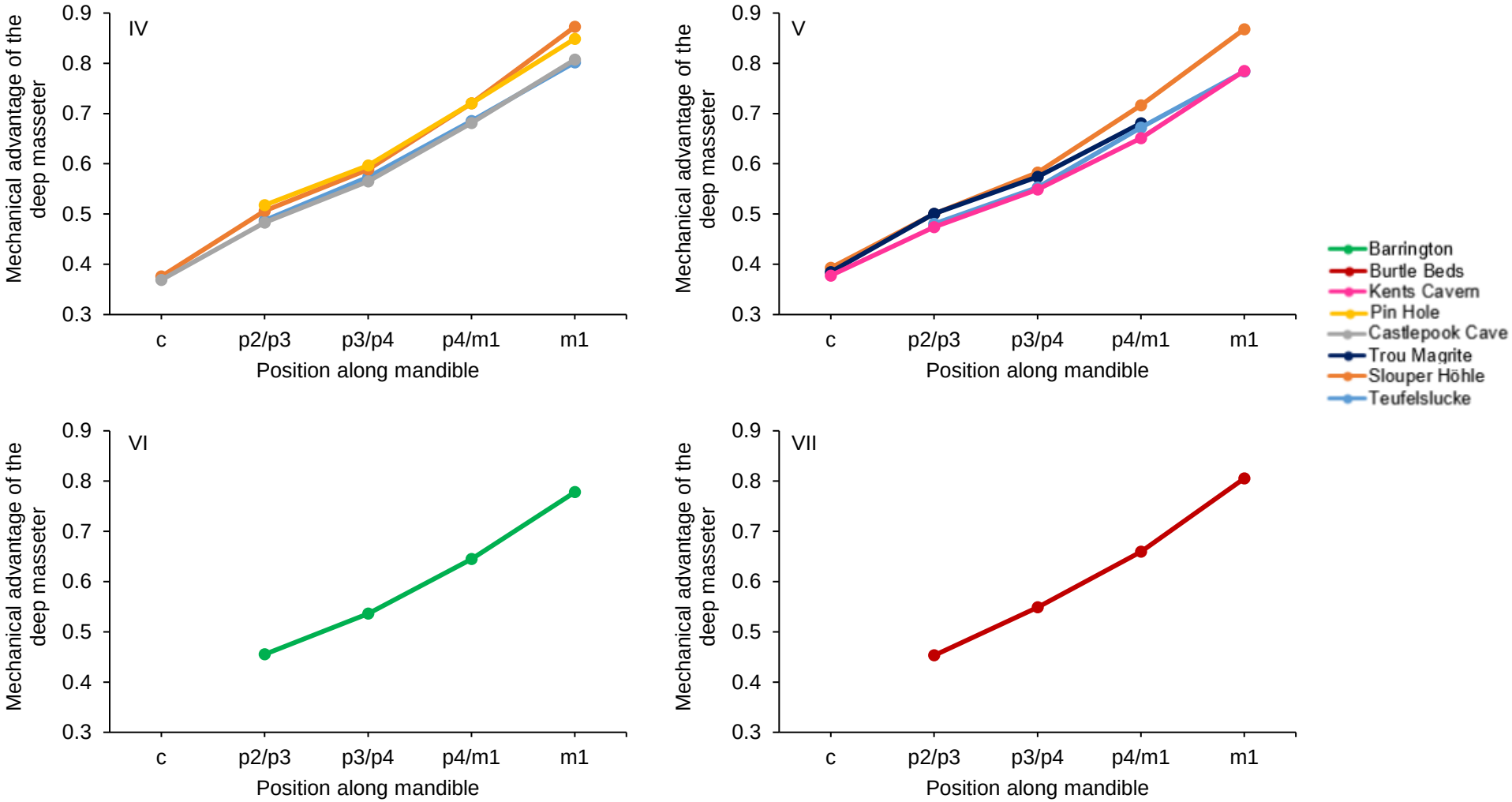

Figure 6.42: Mandibular profiles of the mechanical advantage of the deep masseter of *C. crocuta* from Pleistocene deposits in Europe.

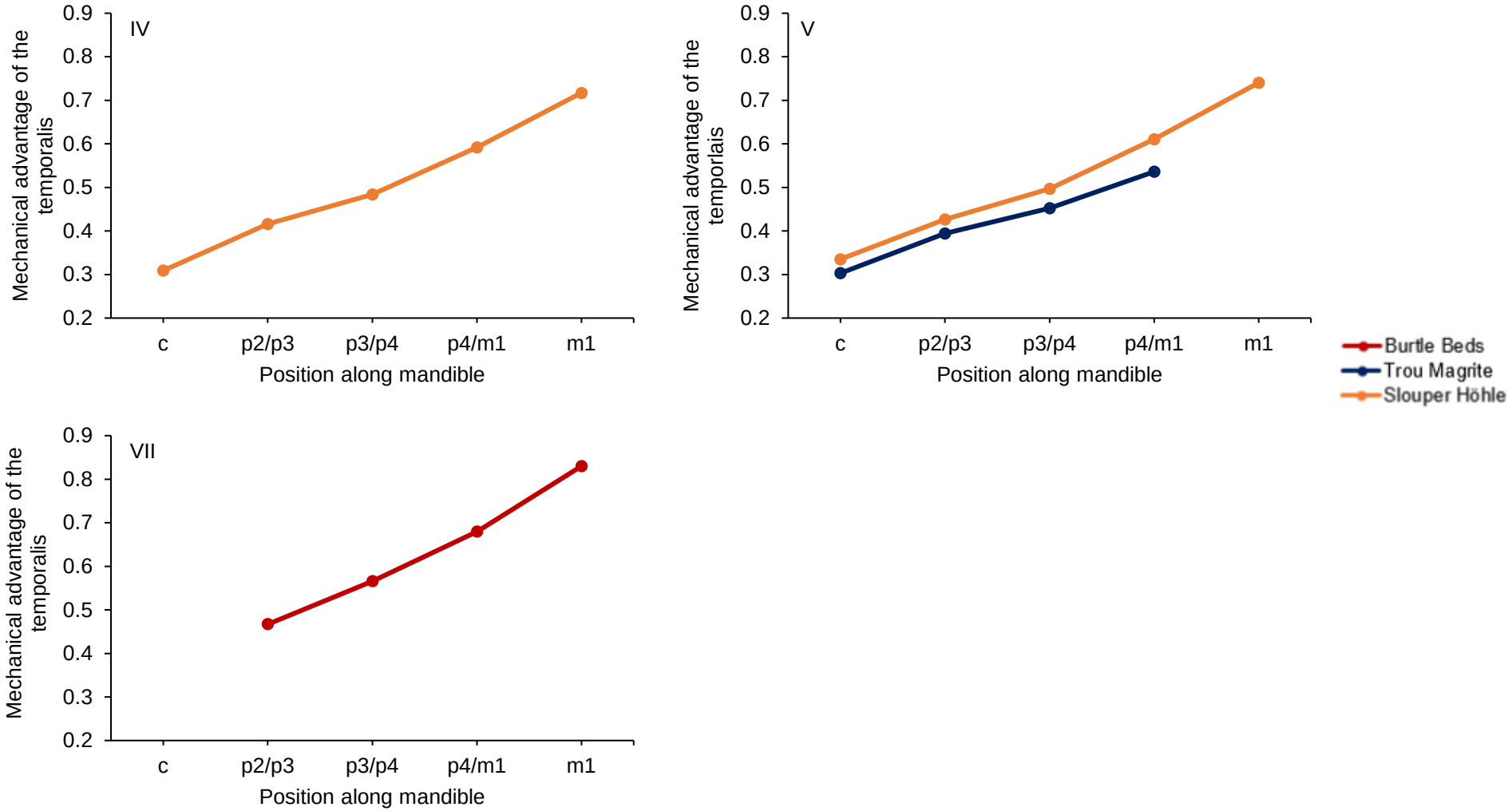

Figure 6.43: Mandibular profiles of the mechanical advantage of the temporalis of *C. crocuta* from Pleistocene deposits in Europe.

6.2.2.2 Post-crania

The post-cranial measurements are presented in Figure 6.44 and Appendix 10.8, Table 10.50 and Figure 10.6.

There is much overlap in the measurements from *C. crocuta* representing different time periods and from different countries. There is clear differentiation between specimens of different ages in a small number of measurements of the humerus and femur. The two greatest length measurements of the humerus from MIS 5e (Barrington) are smaller than those from MIS 3 in Britain and Czech Republic, and Late Pleistocene Slouper Höhle. By contrast, the smallest breadth of the humerus diaphysis is largest in specimens from MIS 7 and MIS 5e, and smallest in MIS 3 specimens from Britain, Ireland and the Czech Republic, in addition to Slouper Höhle.

The femur from MIS 5c Tornewton Lower Hyaena Stratum is shortest, whereas those from MIS 3 in Britain (Caerwent Quarry) and Austria (Höhle Výpustek) are longer, in addition to Late Pleistocene Slouper Höhle. Similarly, the proximal end of the femur is broader from Caerwent Quarry, Höhle Výpustek and Slouper Höhle, and narrowest in all four femora from MIS 5-aged Hoe Grange. The two femora from MIS 9 and MIS 7 have smallest breadths of the diaphysis, whereas the largest are from MIS 3 in (Caerwent Quarry, Höhle Výpustek and San Teodoro), and the Late Pleistocene (Slouper Höhle). The greatest breadth of the distal end of the femur is smallest in specimens from MIS 7, 5 and 5e, whereas the larger specimens are from MIS 3 in Britain and the Czech Republic, in addition to Late Pleistocene Slouper Höhle in the Czech Republic.

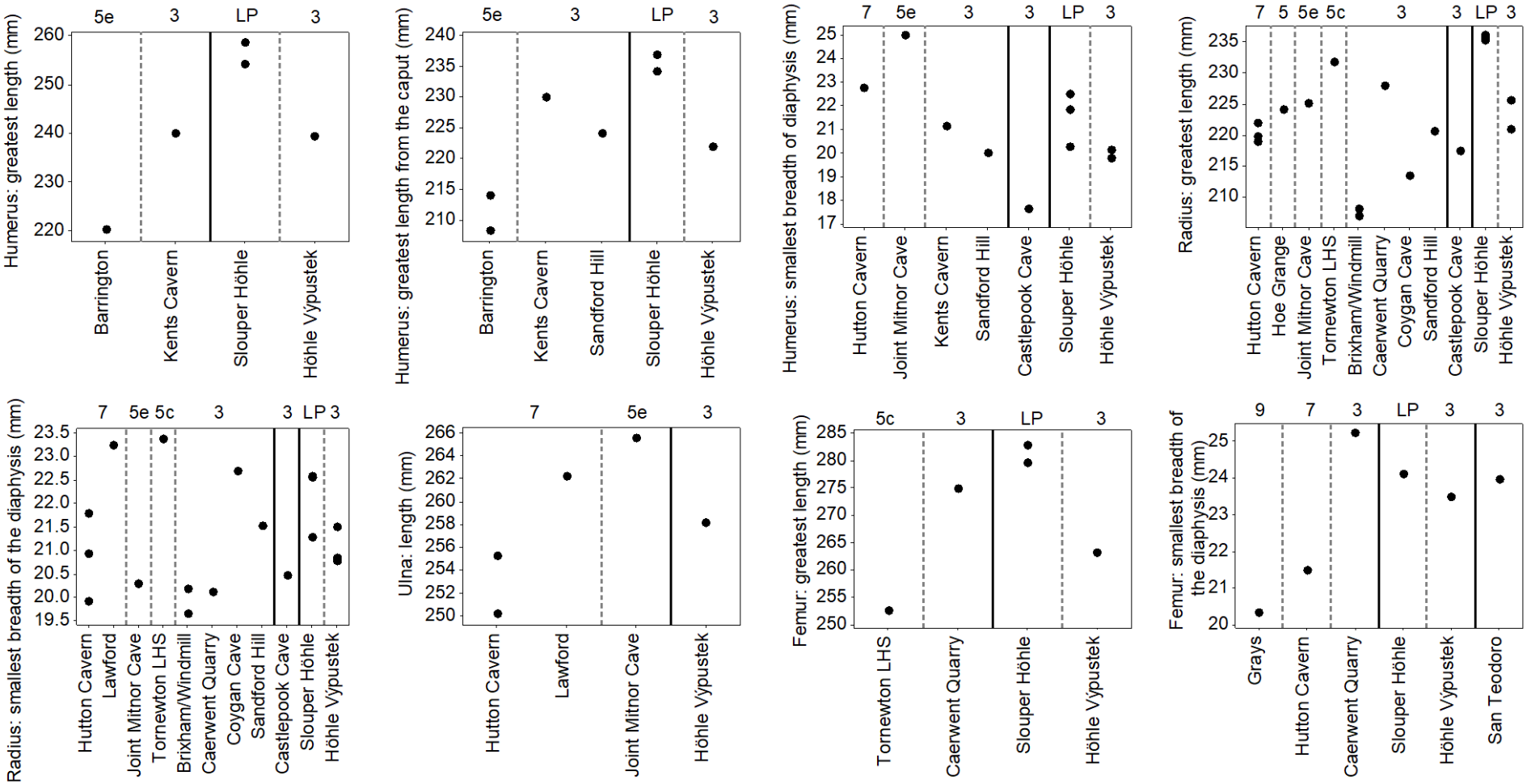

Figure 6.44: Individual value plots and boxplots of Pleistocene *C. crocuta* post-crania measurements from Europe. Numbers on top of the graphs indicate Marine Oxygen Isotope Stages. LP = Late Pleistocene. See Table 6.13 for sample sizes of the boxplots.

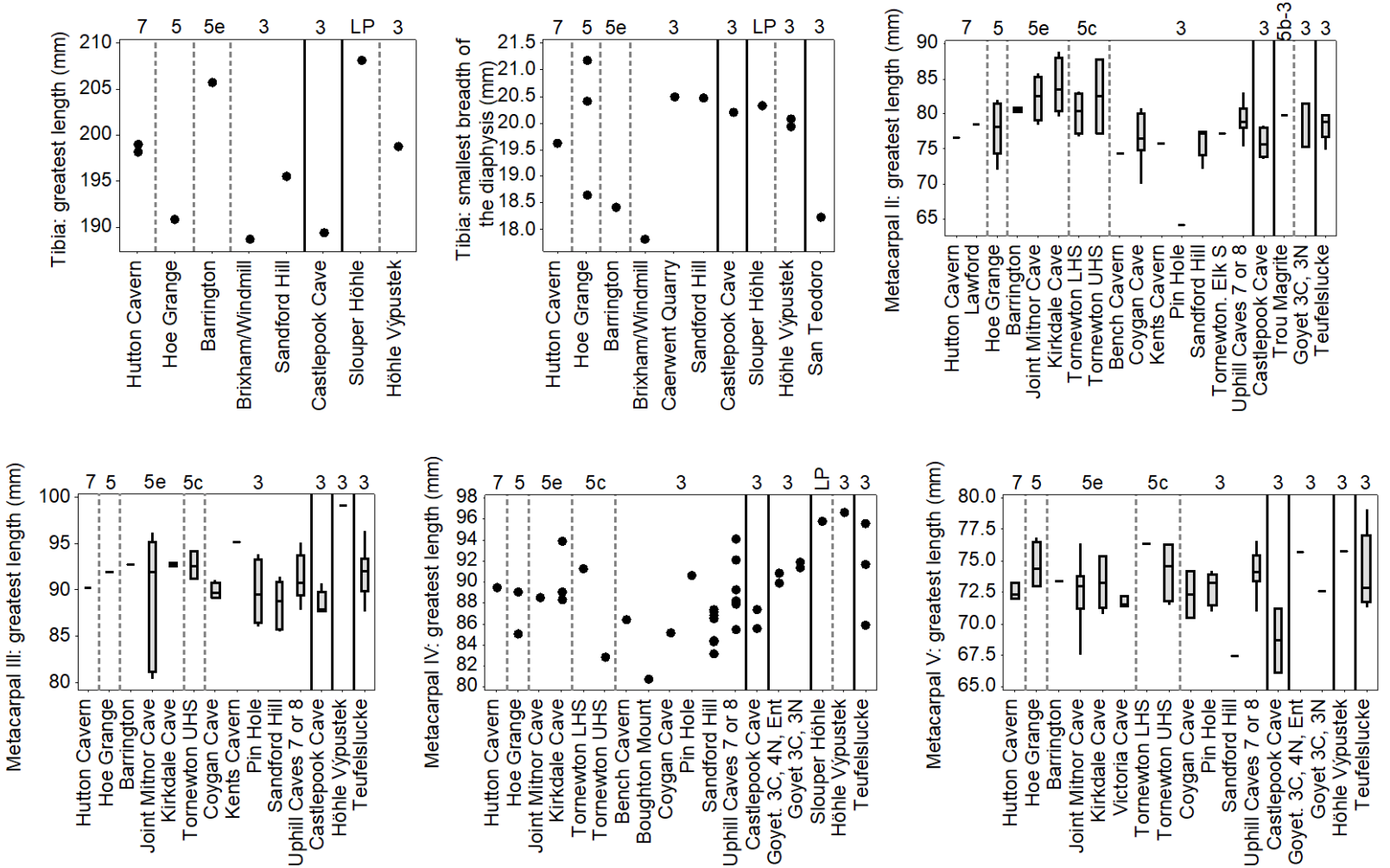
Tibia: greatest length (mm)
Tibia: smallest breadth of the diaphysis (mm)
Metacarpal II: greatest length (mm)
Metacarpal III: greatest length (mm)
Metacarpal IV: greatest length (mm)
Metacarpal V: greatest length (mm)
Hutton Cavern
Lawford
Hoe Grange
Barrington
Joint Mitnor Cave
Kirkdale Cave
Victoria Cave
Tornewton LHS
Tornewton UHS
Tornewton. Elk S
Bench Cavern
Coygan Cave
Kents Cavern
Pin Hole
Sandford Hill
Uphill Caves 7 or 8
Castlepook Cave
Trou Magrite
Goyet 3C, 3N
Teufelslucke
Brixham/Windmill
Caerwent Quarry
Slouper Höhle
Höhle Výpustek
San Teodoro
Boughton Mount
Goyet. 3C, 4N, Ent

Table 6.13: Sample sizes of sites included in the boxplots in Figure 6.44.

Site	Metacarpal II: greatest length	Metacarpal III: greatest length	Metacarpal V: greatest length
Hutton Cavern	1	1	3
Lawford	1		
Hoe Grange	5	1	4
Barrington	2	1	1
Joint Mitnor Cave	4	5	8
Kirkdale Cave	4	2	5
Victoria Cave			3
Tornewton. LHS	4		1
Tornewton. UHS	2	3	4
Bench Cavern	1		
Coygan Cave	7	4	2
Kents Cavern	1	1	
Pin Hole	1	4	5
Sandford Hill	5	8	1
Tornewton. Elk Stratum	1		
Uphill Caves 7 or 8	11	12	13
Castlepook Cave	4	5	2
Trou Magrite	1		
Goyet. 3eme Caverne, 4eme Niveau Ossifère, Galleries Voisines de l'Entrée			1
Goyet. 3eme Caverne, 3eme Niveau	3		1
Höhle Výpustek		1	1
Teufelslucke	8	7	9

Indices and total limb lengths were calculated from combined averages for each chronological 'bin' in each country. Only Britain (MIS 5e, 5c and 3) and the Czech Republic (MIS 3) had sufficient data to calculate the indices and limb lengths. These are compared in Table 6.14.

Czech Republic specimens have the greatest crural index and the forelimb length. Specimens from MIS 3 Britain are also greater than those from MIS 5e in the brachial index, humerus/metacarpal III lengths, and forelimb length. In addition, the femur/metatarsal IV length is greater in the specimens from MIS 3 Britain than MIS 5c. The specimens from MIS 5e Britain have a humerus/metacarpal III index that is between that of MIS 3 in Britain and MIS 3 in the Czech Republic.

Table 6.14: Pleistocene *C. crocuta* post-cranial indices.

	Brachial index: radius length/ humerus length (mm)	**Crural index: tibia length/ femur length (mm)**	**Humerus length/ metacarpal III length (mm)**	**Femur length/ metatarsal IV length (mm)**	**Forelimb length (mm)**	**Hindlimb length (mm)**
Britain MIS 5e	1.022		2.435		535.239	
Britain MIS 5c				3.171		
Britain MIS 3	0.898	0.698	2.66	3.393	545.314	547.816
Czech Republic MIS 3	0.93	0.756	2.413		560.493	

6.2.3 Discussion

6.2.3.1 Crania and dentition

As with the *C. crocuta* body mass reconstructions, there is considerable overlap in the craniodental morphometrics between assemblages of different Marine Oxygen Isotope Stages through the Pleistocene, and from different locations across Europe. Differences are clearer in some of the cranial measurements than the dental measurements, although some of these may be a product of small sample size.

In modern *C. crocuta*, the two measurements that exhibited the strongest relationship to environmental conditions are condylobasal length and the length between the c to the m1 alveoli (Section 5.4.2.2). Both measurements have positive relationships with temperature of the warmest month, closed vegetation cover, and semi-open vegetation cover. They both have negative relationships with open vegetation cover, and weaker relationships with precipitation of the driest month and precipitation of the coolest month. Both measurements are also thought to reflect overall body size (Section 5.4.2.2; Van Valkenburgh, 1990).

There are only five measurements of Pleistocene condylobasal length. The two largest, from Slouper Höhle, unfortunately lack more precise age attribution than 'Late Pleistocene'. Unfortunately, there are no available palaeotemperatures or vegetation information that might allow testing of whether higher summer temperatures at Slouper Höhle and closed or semi-open vegetation had led to expanded condylobasal length. This would be expected if the Pleistocene *C. crocuta* followed the pattern of the modern *C. crocuta*, although the presence of *C. antiquitatis* and *M. primigenius* (Diedrich, 2012a) at the site would suggest otherwise, since these taxa are generally indicative of cold and open conditions (Kahlke and Lacombat, 2008; Boeskorov *et al.*, 2011; Markova *et al.*, 2013).

It was suggested in Section 5.4 that the distance between the c and m1 alveoli is isometrically related to overall body mass. Again, there is much overlap in values between Pleistocene c-m1 length from the different sites, although the largest values generally derive from MIS 3-aged specimens. Furthermore, the Oreston Cave specimen (MIS 7) is large both in c-m1 length and body mass, while the opposite is true of San Teodoro (MIS 3). There are some differences with the body mass reconstruction, in that Castlepook Cave and Teufelslucke specimens are not consistently among the smallest and largest measurements, respectively, possibly a function of the overall smaller sample size of the c-m1 length data. Additionally, when assessing the Castlepook Cave data, the specimens with m1 length and c-m1 alveoli length data exhibit small values for both, whereas those with only c-m1 data have larger values (see Spreadsheet 7). This

indicates that the *C. crocuta* from Castlepook Cave were not consistently small, as suggested in Section 6.1.

A number of the measurements can be assessed in light of functional significance and aid reconstruction of palaeodiet. First, like many of the other morphometric results, there are no clear distinctions in the canine measurements between deposits of different ages. However, the significant difference tests indicate that the lower canines and the anteroposterior diameter of the upper canines from some MIS 3-aged deposits are significantly larger than those from MIS 5e and 5c. The larger canines are notably from Teufelslucke, Kents Cavern and Coygan Cave. This relationship does not hold for the mediolateral diameter of the upper canine with some deposits, such as Pin Hole, significantly smaller than others from MIS 3 and from MIS 5e and 5c.

Although sample sizes were too small to run statistical tests, the canines were also notably large from MIS 7, in particular in the anteroposterior diameter of the upper canine, and both measurements of the lower canine. The mediolateral diameter of the upper canine, and both measurements of the lower canine are notably small from San Teodoro.

Canines are used when killing prey, breaking bone (Van Valkenburgh and Ruff, 1987) and the consumption of muscle with attached bone (Van Valkenburgh, 1996). More robust canines are more able to resist bending stresses incurred when biting and ripping flesh, and upon accidental contact with bone (Van Valkenburgh and Ruff, 1987).

As dental morphology is less influenced than bones by phenotypic plasticity (Caumul and Polly, 2005), it is difficult to assess whether these changes in canine size were a result of the environmental conditions at the time, or a reflection of the overall size of the *C. crocuta*. Nevertheless, the results allow some inference of the capabilities of the species.

The generally larger canines from some MIS 3-aged deposits from Britain and Austria may have been consistent with *C. crocuta* targeting larger prey, for example *C. antiquitatis* (Section 6.1), which would have caused greater bending stresses on the canines. Similarly, the smaller canines from San Teodoro may reflect the reduced size of many of their prey species (Mangano, 2011).

Rapid feeding of carcasses, such as occurs during periods of lower food availability or elevated competition, may increase accidental contact between canines and bone, potentially leading to canine breakage (Van Valkenburgh, 1996). If these conditions occurred during MIS 7 or MIS 3, the larger canines from some deposits may have reduced the likelihood of accidental breakage and associated loss of function of the canine teeth. A notable exception is the small size of the canines from MIS-3 aged deposits of Pin Hole.

The morphology of the mandible, particularly its bending strength, is also important in facilitating predation. Mandibles that are wider and shorter are better able to resist labiolingual loads (Hildebrand, 1974). This is particularly important anteriorly along the mandible as torsion occurs from struggling prey (Biknevicius and Ruff, 1992; Therrien, 2005). Most specimens from San Teodoro exhibited among the narrowest mandibular corpuses at the p2/p3 position, suggesting that these specimens have the weakest labiolingual bending strengths and again highlighting their relatively modest strength requirement in the face of prey of reduced size. Mandibles that are wider at p2/p3 derive from many sites, with no pattern associated with age or geographical location. However, bending strength is best determined through modelling the mandible as a beam, with the zy/L values indicating labiolingual bending strengths.

The zy/L values increase in size with age (Section 5.2). It would therefore be hypothesised that the oldest individuals would have the greatest labiolingual bending strengths. This is not the case for the specimens from the Last Interglacial sites of Barrington (wear stage VI) and Burtle Beds (wear stage VII) at anterior points along the mandible. These zy/L values are lower than some mandibles of younger individuals from Trou Magrite, Pin Hole and Slouper Höhle, although the other Slouper Höhle specimen does not have notably high values.

As labiolingual bending strength is important in resisting torsion when biting struggling prey (Biknevicius and Ruff, 1992; Therrien, 2005), the narrow mandibles from San Teodoro and the low zy/L values from Barrington and Burtle Beds suggest that individuals from these sites were consuming either smaller or less vigorous prey. At San Teodoro, the presence of dwarf prey species (Mangano, 2011), supports the former explanation. The Burtle Beds and Barrington contain a wide range of potential prey species, including megaherbivores such a straight-tusked elephant (*Palaeoloxodon antiquus*) and hippopotamus (*Hippopotamus amphibius*), large bovids and smaller cervids, notably fallow deer (*Dama dama*) (Bulleid and Jackson, 1938; Gibbard and Stuart, 1975). Although Gibbard and Stuart (1975) stated that some bones discovered in the deposits at Barrington had likely been gnawed by *C. crocuta*, the authors did not specify the species. It is therefore difficult at present to assess whether the *C. crocuta* from these sites were consuming smaller prey than those requiring greater mandibular labiolingual bending strengths. The Burtle Beds assemblage contains no specimens with obvious hyaena gnawing (D. Schreve pers. comm.).

The Burtle Beds and Barrington are the only MIS 5e assemblages from which bending strengths were calculated. As mentioned, many MIS 5e-aged *C. crocuta* had smaller canines than those from MIS 3. No canines were available from the Burtle Beds, and there were insufficient data to perform significant difference tests on the Barrington canines, although these represented some of the smallest across all sites, particularly in the anteroposterior diameter of the upper canine.

Therefore, the conclusions from the low labiolingual bending strengths and the small canines are also in support of one another. Although there were insufficient canine data from Slouper Höhle and Trou Magrite to allow tests for significant differences, the anteroposterior diameter of the upper canine and the mediolateral diameter of the lower canines from Slouper Höhle are among the largest, again supporting the greater labiolingual bending strength of the mandible. However, large canines are not a uniform feature of last cold stage *C. crocuta*. Only data of the mediolateral diameter of the upper canine is available from Trou Magrite but this canine is among the smallest across all sites. Additionally, the mediolateral diameters of the Pin Hole upper canines are significantly smaller than those from some MIS 5e and 5c-aged sites. This disparity between the canines and zy/L values from Trou Magrite and Pin Hole may reflect the ability of the mandible to respond to conditions during life via phenotypic plasticity, which is not the case for teeth (Caumul and Polly, 2005).

Given that *C. crocuta* from Trou Magrite and Pin Hole had small canines but were apparently targeting larger prey or were engaged in more frequent predation, it may be hypothesised that these canines were at greater risk of breakage. This will be explored in Section 6.4. Indeed, prey consumption at Pin Hole is evidenced by gnaw marks on most bones, including *C. antiquitatis*, potentially requiring elevated levels of labiolingual bending strength of the mandible, with stresses also applied to the canines. However, it must be noted that these bones may equally have been scavenged rather than hunted.

At present the evidence is insufficient to conclude whether the reason for the larger canines and elevated mandibular labiolingual bending strength from some deposits was due to predation on larger or more vigorous species, or more frequent predation (relative to frequency of scavenging).

The results of m1 length are very similar to those of the body mass reconstructions, which they were used to calculate, and so will not be discussed here. In contrast to the length of the m1, there are no significant differences in P4 lengths between any deposits. Where there are significant differences in the width of the P4 blade, the specimens from MIS 3-aged deposits in Britain and Austria are larger than some from MIS 5e and 5c. Similarly, the width of the m1s from many MIS 3-aged deposits from Britain, Austria, Belgium and Serbia were larger than those from MIS 5e and 5c, suggesting they were more robust. Carnassials are used for removing skin and thus facilitating rapid consumption of a carcass, particularly in times of elevated competition (Van Valkenburgh, 1996, 2007). Similar to the canines, these more robust carnassials may have prevented accidental breakage during rapid carcass consumption during MIS 3.

The P4s, in particular the cusps, may be used for cracking bone (Kurtén and Werdelin, 1988; Van Valkenburgh, 1996). The greatest width of the P4 across the cusps was larger in MIS 3 in Britain, Austria and Belgium, suggesting that the *C. crocuta* from MIS 3 were more capable of consuming bone than those from MIS 5e and 5c. This is further investigated through analysis of the other premolars.

In light of the size differences seen in the lower premolars in different climatic periods (the p3 and p4 were generally larger in MIS 3 while the p2 were larger during MIS 5e), allometric relationships were assessed. The lengths of the p3 and p4 have a likely isometric relationship. The lengths of the p2 and p4 have a hypoallometric relationship, so that as the p4 becomes longer, the p2 increases at a greater rate. The widths of the p2 and p4, and the p3 and p4 have isometric relationships. The widths of the p2 and p3 have a hyperallometric relationship, again meaning that the p2 becomes wider at a greater rate than the p3. By contrast, the lengths of the p2 and p3 have a very weak and insignificant positive relationship with little indication of an allometric relationship, meaning that when the p3 increases in length, the p2 does not necessarily lengthen. This suggests that there are different influences upon the p2 and p3, although it is unclear whether there is a functional reason for this. Nevertheless, this result reflects the difference seen in the sizes of p2 and p3 between *C. crocuta* from MIS 5e and 3.

Premolar robustness was assessed as these teeth are used when consuming bone (Van Valkenburgh, 1996). Increasingly wide premolars are associated with bone-cracking (Van Valkenburgh, 1989; Werdelin and Solounias, 1991). Although the premolars are always longer than wider, a relative increase in width should lead to a more robust tooth shape.

First, the allometric relationships between the lengths and widths of each premolar were assessed to determine whether robustness increased or decreased with length. The lengths and widths of each premolar are positively correlated. There are isometric relationships between the lengths and widths of the P3 and p2, indicating that these teeth become neither more nor less robust with increasingly size. By contrast, there is a hyperallometric relationship between the widths and lengths of the P2, p3 and p4, indicating that when these teeth become longer, the widths increase at a greater rate. These teeth therefore become more robust with increasing size. This results in less slender teeth therefore making them less prone to breakage when consuming bone or other hard materials. In no cases did premolars become less robust with increasing size. The individuals with larger premolars should therefore have a greater capacity for bone consumption without risk of tooth breakage and therefore loss of tooth function.

The next step was to plot the lengths against widths of premolars of different ages in Britain. This was to assess whether there was any pattern in premolar robustness over time. For all premolars, the length/width relationship does not exhibit a clear separation of *C. crocuta* from different periods in Britain, especially in the P3. However, the general pattern is that most of the largest P2, p3 and p4 are from MIS 3-aged individuals, while the smallest P2, p3 and p4 are from MIS 5e and 5c. This is particularly clear for the width of the p4, with the widest teeth being of MIS 3 age. Interestingly, these are the teeth that exhibit increased robustness with size. This therefore suggests that the individuals from MIS 3 were more capable than those of MIS 5 of consuming hard foods such as bone.

Additional indications of bone consumption come in the form of mandibular dorsoventral bending strength. Increased depth of the mandibular corpus is associated with greater dorsoventral bending strength (Hildebrand, 1974). Specimens with notably small depths of the mandible include those from San Teodoro and the Burtle Beds, while notably deep mandibles are from Teufelslucke. Again, modelling the mandible as a beam is a more suitable method of assessing bending strength.

The mandibles exhibit increasing resistance to dorsoventral bending at posterior positions, as also observed by Therrien (2005) and Palmqvist *et al.* (2011). This is because bending stress exerted by bone cracking is greatest posterior to the premolars, which are the bone-cracking teeth (Biknevicius and Ruff, 1992; Therrien, 2005).

The mandible from the Last Interglacial (MIS 5e) Burtle Beds has the shallowest zx/L bending strength profile, and thus the shallowest increase in resistance to dorsoventral bending strength along the mandible. Overall, this specimen also exhibits the lowest resistance to dorsoventral bending, despite it being the oldest individual at wear stage VII. The Last Interglacial specimen from Barrington (wear stage VI) also exhibits relatively low bending strength variables. Younger individuals (wear stage IV) that exhibit particularly great resistance to dorsoventral bending include those from Trou Magrite, Slouper Höhle and Teufelslucke. This is perhaps unexpected as zx/L values have been shown to increase through the life of *C. crocuta* (Section 5.2).

The low zx/L values of the older specimens from the Burtle Beds and Barrington suggest that these individuals may have undergone less dorsoventral bending stress than the younger individuals. If phenotypic plasticity is the cause of these lower values, this may indicate that *C. crocuta* from the Burtle Beds and Barrington consumed less hard food such as bone, or at least were less able to do so. The lower dorsoventral bending strength pairs with the findings of premolar robustness, in that the MIS 5e premolars from Britain have some of the least robust

premolars, and are therefore less suitable for consuming bone. Potential reasons for this are discussed below.

The younger individuals with similar or greater zx/L values than the older individuals are from the last cold stage, including Slouper Höhle, Pin Hole, Teufelslucke and Trou Magrite. The difference between these specimens and those from MIS 5e is particularly striking for the posterior of the mandible, which is the area that undergoes most bending stress when consuming bone (Biknevicius and Ruff, 1992; Therrien, 2005). The results suggest that these individuals were undergoing greater dorsoventral bending stresses than those from temperate MIS 5e, indicating greater hard food consumption.

The zx/zy indices reflect the cross-section of the mandible (Therrien, 2005; Palmqvist *et al.*, 2011). All values for all interdental gaps along all mandibles are greater than one, indicating a deeper than wide mandibular corpus. This indicates a greater resistance to dorsoventral stresses than to labiolingual stresses (Therrien, 2005; Palmqvist *et al.*, 2011). The three mandibles from San Teodoro have notably lower zx/zy values than other specimens, even in the older individuals (wear stages VIII and IX). The results indicate that the San Teodoro individuals had mandibles less suited to resistance of dorsoventral bending stresses, and thus bone consumption.

Bone consumption is increased with low food availability (Kruuk, 1972; Egeland *et al.*, 2008). The results from San Teodoro, the Burtle Beds and Barrington may imply that there was sufficient food to sustain the populations, so the carcasses were not completely consumed. This may have occurred due to high prey abundance during the interglacial, or lower competition, as elevated levels of interspecific competition may increase bone consumption (Egeland *et al.*, 2008). An alternative explanation for the *C. crocuta* from San Teodoro is that the mandibles may have incurred low dorsoventral bending stress due to the smaller size of the dwarfed bones of their prey relative to the mainland prey species.

The increased ability to consume bone may have been useful if there were periods of food scarcity during MIS 3, as *C. crocuta* may have been able to survive by utilising more of a carcass, including the bones. Alternatively, the colder stadial conditions during MIS 3 may have resulted in frozen carcasses, the consumption of which may have placed stress upon teeth in a similar fashion to bone.

Some measurements of the cranium are indicative of muscle size and bite force. For example, the temporal fossa length is an indication of the size of the temporalis muscle (Emerson and Radinsky, 1980). This measurement was only available for two specimens, and was greatest in a

specimen from Slouper Höhle than one from Höhle Výpustek, indicating that the former had a larger temporalis muscle.

A better indication of bite force is to model the mandible as a lever. The relationship between the in-levers, and the out-levers was calculated, providing information about the mechanical advantage of the adductor muscles at each bite point, which is indicative of bite force (Emerson and Radinsky, 1980; Kiltie, 1982; Alexander, 1983; Van Valkenburgh and Ruff, 1987)

Mechanical advantage of the temporalis, deep masseter and superficial masseter were calculated. The greatest mechanical advantage of the superficial masseter occurs in the mandible from Teufelslucke, suggesting that this individual has greater bite strength.

The mechanical advantage of the deep masseter may increase with age in males, but decreases with age in females (Section 5.2). At wear stage IV, differences are seen at the p4/m1 and post-m1 positions with the greatest values in mandibles from Pin Hole and Slouper Höhle, and lower values from Castlepook Cave and Teufelslucke. This suggests that the Teufelslucke specimen has one of the lowest bite forces, in contrast to the results of the superficial masseter. At wear stage V, the Slouper Höhle specimen also has greatest mechanical advantage of the deep masseter. It is difficult to draw conclusions about the Barrington (wear stage VI) and Burtle Beds (wear stage VII) specimens in light of the different ontogenetic changes between males and females, and as these are the only specimens from their respective age classes.

In present-day *C. crocuta*, the mechanical advantage of the temporalis in males may increase with age, yet does not change in females (Section 5.2). The Burtle Beds specimen has the greatest bite force, which is difficult to interpret as it may be due its older age (wear stage VII). Both Slouper Höhle specimens (wear stages IV and V) have greater mechanical advantages of the temporalis muscle than the specimen from Trou Magrite (wear stage V).

In the Carnivora, the temporalis is larger than the masseter (Turnbull, 1970). As force exerted is greater with greater mass (Tseng and Binder, 2010), the temporalis is the dominant jaw closing muscle (see Section 3.3.6.1 for more detail).

In light of the apparent importance of the temporalis muscle, the results of the mechanical advantage of this muscle should be most indicative of bite force of *C. crocuta*. Unfortunately, this has the smallest sample size. The only conclusion that can be drawn is that the Slouper Höhle specimen has a greater bite force than the Trou Magrite specimen within the same age class.

This difference between the Slouper Höhle and Trou Magrite specimens is greater posteriorly along the mandibles. This may be indicative of greater ability to consume hard foods, such as

bone in the Slouper Höhle specimen (following Ferretti, 2007). This reflects the greater dorsoventral bending strength observed in the Slouper Höhle specimens.

It must be borne in mind that additional morphological features conducive to bite force and resisting bending stresses have not been measured, so changes in the cranium may have occurred to facilitate prey capture or hard food consumption that have not been observed. These include vaulted forehead and sinus expansion (Werdelin and Solounias, 1991; Joeckel, 1998), and gape (Binder and Van Valkenburgh, 2000, and see Section 3.3.6).

There are other measurements of the cranium that are functionally important. These include measurements of the orbits, which are related to the eyes and thus to vision (Radinsky, 1981a). The neurocranium breadth is a measurement of the braincase (Ewer, 1973; Thomason, 1991), and the auditory bullae is important for hearing (Hildebrand, 1974).

Unfortunately, due to poor preservation of many specimens, there are small sample sizes of each of the aforementioned features. This makes it difficult to interpret the results with confidence, however, the measurements of specimens from different deposits appear to reflect the trend seen in condylobasal length, an indication of body size (Van Valkenburgh, 1990), and other measurements of skull length. Overall there is little indication that the measurements relating to brain size or the senses were larger or smaller than expected given the body size of the individuals.

6.2.3.2 Post-crania

As with the Pleistocene *C. crocuta* body mass reconstructions (Section 6.1.2.2) and craniodental morphometrics (Section 6.2.2.1), the post-crania reveal much overlap in size between deposits of different ages and from different geographic areas across Europe. The exceptions to this are some measurements of the humerus and femur, both of which may have functional implications.

The humeri are shortest from temperate MIS 5e-aged deposits and longest from MIS 3-aged deposits in Britain and the Czech Republic, in addition to Slouper Höhle. The diaphyses of the humeri from the interglacial assemblages of MIS 7 and 5e are broadest, and they are narrowest from MIS 3 in Britain, Ireland and the Czech Republic, in addition to Slouper Höhle.

The femora are similarly shortest from MIS 5c, and longest from MIS 3 in Britain and the Czech Republic, in addition to Slouper Höhle. However, the femoral diaphyses are narrowest from MIS

9 and 7, and are broadest from MIS 3-aged deposits in Britain, Italy and the Czech Republic, in addition to Slouper Höhle.

The length and breadth of limb bones are related to stride length, which increases with greater effective limb length. This is brought about by lengthening the metapodials and distal long bones (Hildebrand, 1974). Along with shorter and thicker proximal limb bones, this allows for endurance of high-speed locomotion (Hildebrand and Hurley, 1985). The shorter yet thicker humeri in specimens from periods of temperate conditions in Britain may therefore indicate that these *C. crocuta* were capable of fast pursuits for longer periods of time than *C. crocuta* from MIS 3 in Britain and the Czech Republic. However, while the length of the femur is smallest in those from MIS 5c, the diaphyses are also narrowest in temperate MIS 9 and 7, which does not follow the pattern of the humerus. Furthermore, the lack of distinction between other limb measurements from different climatic periods suggests that there is little actual difference in locomotion. In light of this disparity, it is pertinent to assess the post-cranial indices.

The post-cranial indices were calculated from pooled measurements from different deposits dating to MIS 5e, to 5c and to 3 in Britain, and to MIS 3 in the Czech Republic. The lack of post-cranial material from individual sites necessitated this pooling of data.

Data were insufficient to calculate total hindlimb length from all but MIS 3 in Britain. Total forelimb length was greatest in MIS 3 Czech Republic, followed by MIS 3 in Britain and finally shortest in MIS 5e in Britain. This implies that *C. crocuta* from MIS 5e had the shortest stride lengths, and were thus potentially covering shorter distances when hunting. This may, however, be related to the overall body size of an individual; Christiansen (2002) found closer relationships between speed and total limb length when body mass was taken into account. That *C. crocuta* from MIS 3 were on average, but not consistently, larger than those from MIS 5e may explain this result.

The metatarsal/femur ratio is indicative of speed, with lower values associated with greater speed across carnivore species (Van Valkenburgh, 1985). As such, the lower values from MIS 5c *C. crocuta* when compared to those of than MIS 3 in Britain suggest that the latter were capable of slower speeds. Similarly, the metacarpal/humerus ratio was lower in *C. crocuta* from MIS 5e than MIS 3 in Britain, supporting the above point. However, the metacarpal/humerus ratio was lowest overall from MIS 3 in the Czech Republic, suggesting that these individuals were faster than those from both MIS 5e and 3 in Britain.

The final indices are the brachial and crural indices, which are greater in cursorial carnivorans (Meachen *et al.*, 2016). Both indices are greater from the Czech Republic than MIS 3 in Britain. Data only allowed calculation of the brachial index for MIS 5e *C. crocuta*, which was greater than

the MIS 3 values for both Britain and the Czech Republic. This suggests that *C. crocuta* were more cursorial during MIS 5e.

Overall, the results from the limb measurements and ratios are not consistent, which may in part be due to the small amount of available data. However, there is some indication that *C. crocuta* from Britain were more cursorial and capable of higher speeds during MIS 5e and 5c than MIS 3. This may suggest that *C. crocuta* from MIS 5e and 5c were engaged in more frequent predation than scavenging.

Meachen *et al.* (2016) found that the brachial index (reflecting cursoriality) was positively associated with mean annual temperatures and negatively associated with mean annual precipitation. The authors suggested that this was due to the more open vegetation cover of dry climates. Indeed, Polly (2010) found that cursorial carnivorans are mostly found in open habitats. In terms of temperature, this matches well with the apparent greater cursoriality of *C. crocuta* during temperate MIS 5e and 5c compared with reduced cursoriality during cooler MIS 3. The lack of palaeoprecipitation data from assemblages used to calculate the indices mean that the link with the brachial index cannot be determined at this time.

The link between the brachial index and vegetation is also difficult to interpret. Mammals from Höhle Výpustek are indicative of a mixture of forest and much of the vegetation during MIS 3 in Britain was open grassland (Lewis, 2011; Bocherens, 2014). Pollen from the Tornewton Hyaena Stratum (Britain, MIS 5c) indicates open vegetation with some woodland locally or regionally (Lewis, 2011). By contrast, forest was present in Britain during MIS 5e but this is complicated by the presence of open vegetation brought about by grazing and trampling by large herbivores, particularly on river floodplains (Gibbard and Stuart, 1975; Sandom *et al.*, 2014). As the indices were calculated from pooled data from different deposits of a similar age, the local vegetation conditions may have been different at each site, particularly problematic for MIS 5e.

These findings may be contrary to the analyses of the size of the canines and labiolingual mandibular bending strength (Section 6.2.3.1). The interpretation of that data was that during MIS 3, *C. crocuta* were engaged in more frequent predation (relative to scavenging) or targeted larger prey than during MIS 5e. There is one explanation that reconciles the post-cranial and craniodental data. During MIS 5e, *C. crocuta* in Britain may have engaged in more frequent predation (relative to scavenging), explaining the apparently greater cursorial ability. During MIS 3, *C. crocuta* may have scavenged more frequently, but their prey were of a larger size, explaining the larger size of the canines and the greater mandibular resistance to labiolingual bending.

6.3 Age profiles of assemblages

6.3.1 Introduction

Prior to assessing the variation in tooth breakage between assemblages, the age profile of each assemblage must be reconstructed. This is because greater frequency of tooth breakage is found in older *C. crocuta* (Van Valkenburgh, 2009, and see Section 5.5). Failure to pick up on variations in age profiles may lead to erroneous interpretation of tooth breakage results. For example, if a sample with predominantly old-aged individuals contains more broken teeth than a sample with younger individuals, this may be reflective of the age profile, rather than any environmental drivers.

Only permanent and fully formed dentition were considered and juveniles did not, therefore, factor into discussion of the age profiles.

The research questions are as follows:

- What are the age profiles of the assemblages?
- Do any age profiles indicate a dominance of young or old *C. crocuta* that may influence the tooth breakage results?

6.3.2 Results

The *C. crocuta* P3/p3 wear stages for each deposit are plotted in Figure 6.45. For samples with fewer than ten P3/p3 data points, the figure was repeated showing slight, medium and heavy wear of all teeth (Figure 6.46). See Section 4.3.2 for an explanation of the tooth wear stages.

Differences between the two figures are particularly apparent for King Arthur's Cave and Tornewton (Elk Stratum), which have 100 % P3/p3 wear classed as stage III (the youngest class considered in this study). However, when all the teeth are considered, it is evident that there are teeth classed as having slight, medium and heavy wear. Similarly, 100 % of Trou Magrite's P3/p3 teeth were classed as wear stage V, yet has teeth with slight, slight/medium, medium and heavy wear. Cueva de las Hienas has 100 % of P3/p3 teeth classed as wear stage VI, yet assessing all the teeth indicates that the assemblage is predominantly made up of those with slight wear (96.15 %).

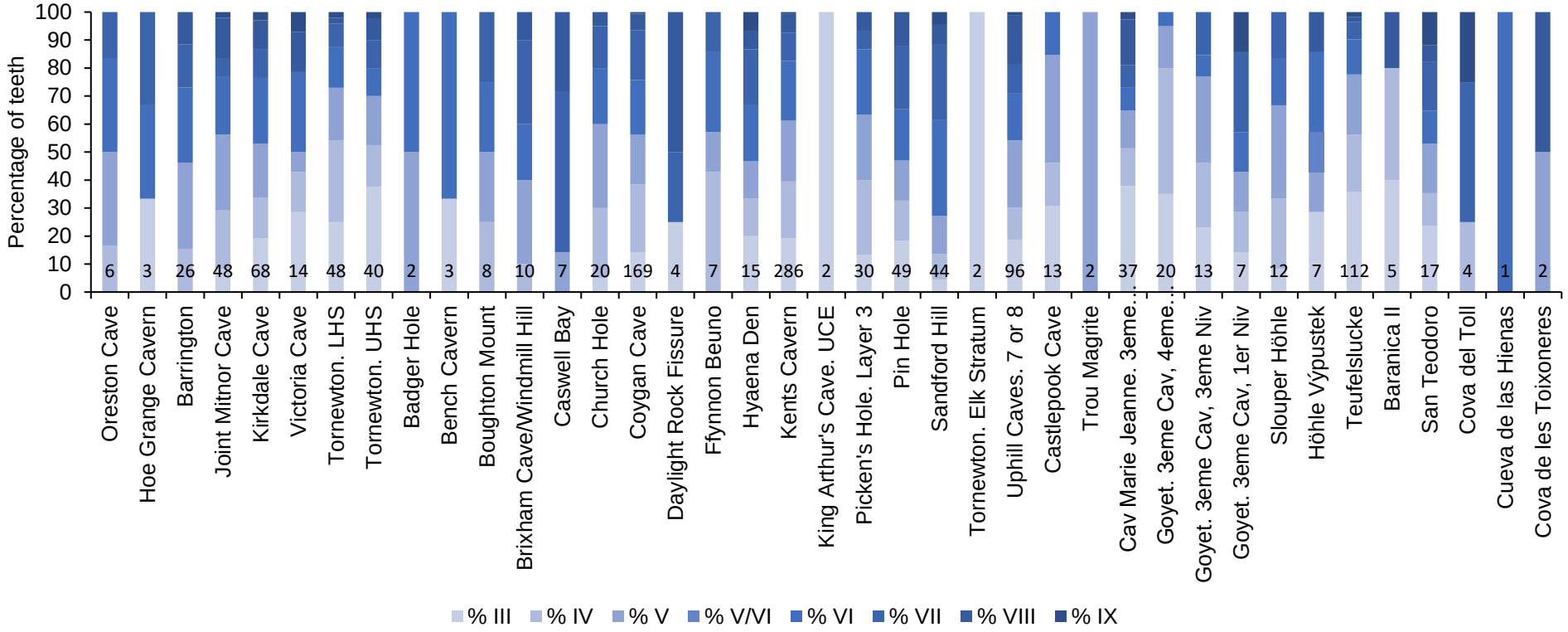

Figure 6.45: Percentage of *C. crocuta* P3/p3 wear stages from Pleistocene deposits. Numbers along the base of the bars are sample sizes.

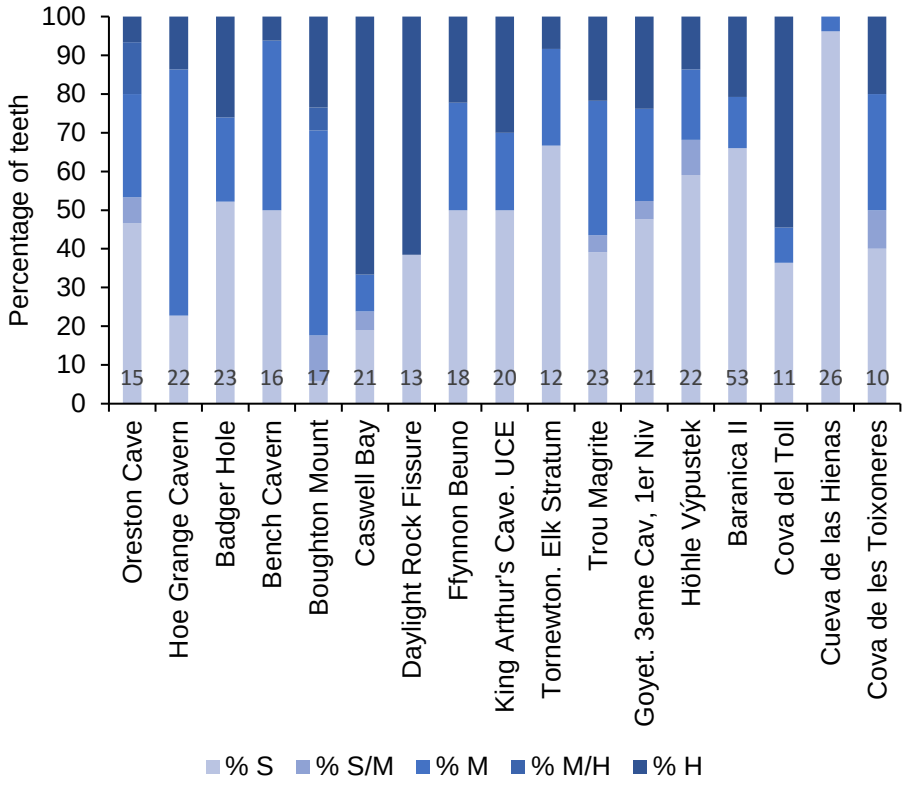

Figure 6.46: Percentage of wear stages of all *C. crocuta* teeth from Pleistocene deposits. S = slight wear. S/M = slight/medium wear. M = medium wear. M/H = medium/heavy wear. H = heavy wear. Numbers along the base of the bars are sample sizes.

The figures indicate that the assemblages have different age profiles of *C. crocuta*. Cueva de las Hienas has the highest proportion of slight wear. Goyet (3eme Cavern, 4eme Niveau Ossifère, Galleries Voisines de l'Entrée) and Baranica II also have a large proportion of teeth at wear stages III and IV. By contrast, at 25 %, Cova del Toll has the greatest proportion of teeth classified as the oldest wear stage, IX, followed by Goyet (3eme Caverne, 1er Niveau) at 14.29 %.

When all teeth are taken into account, Broughton Mount has the lowest proportion of slightly worn teeth. Caswell Bay (66.67 %), Daylight Rock Fissure (61.54 %) and Cova del Toll (54.54%) have the greatest proportions of heavily worn teeth.

6.3.3 Discussion

While tooth wear is an indication of the age of an individual (Stiner, 2004), it may also be influenced by the type of food consumed (Van Valkenburgh, 1988). However, the method is useful in the present study in highlighting the relative proportions of elderly individuals to younger individuals.

Given the evidence that incidences of tooth breakage tend to increase with age (Van Valkenburgh, 2009, and see Section 5.5), it may be expected that the deposits with a large proportion of younger individuals would have low proportions of broken teeth. These deposits include Cueva de las Hienas, Goyet (3eme Caverne, 4eme Niveau Ossifère, Galleries Voisines de L'Entrée) and Baranica II.

Similarly, deposits with a high proportion of older *C. crocuta* may be expected to have high proportions of broken teeth. These deposits include Cova del Toll, Caswell Bay and Daylight Rock Fissure. In particular, it may be expected that these assemblages with greater proportions of older individuals may exhibit greater proportions of broken canines, as these teeth tend to be the tooth most frequently broken at later life stages (Section 5.5). However, environmental and dietary factors may cause a divergence from this prediction.

6.4 Tooth breakage

6.4.1 Introduction

Teeth may be broken due to bone consumption and struggling prey (Van Valkenburgh, 1988, 2009). Bone cracking in particular may hold some important information about ecological considerations as increased bone breakage may be indicative of periods of low food availability (Kruuk, 1972; Egeland *et al.*, 2008).

The research questions are as follows:

- How does the degree of tooth breakage vary between assemblages?
- What information can this provide about the palaeodiet of *C. crocuta*?
- Is this variation in palaeodiet related to changes in environmental conditions?

6.4.2 Results

The percentage of broken and partially or fully healed alveoli were calculated for all deposits with a sample size of at least ten (Figure 6.47). None of the teeth from Badger Hole, Bench Cavern, Boughton Mount, Caswell Bay, Hyaena Den and Tornewton (Elk Stratum) are broken (Table 6.15). None of these deposits contained specimens that exhibited healed alveoli, although only isolated teeth were assessed from Badger Hole.

The other site without broken teeth is San Teodoro, however, 1.96 % of specimens exhibit partially or fully healed alveoli; a feature also present on specimens from Barrington, Kents Cavern, Sandford Hill and Teufelslucke.

The deposit with the greatest proportion of broken teeth is Cova del Toll with 30.77 % broken teeth. The next largest proportions of broken teeth are from Cova de les Toixoneres (15.38 %) Trou Magrite (13.79 %) and Höhle Výpustek (13.73 %).

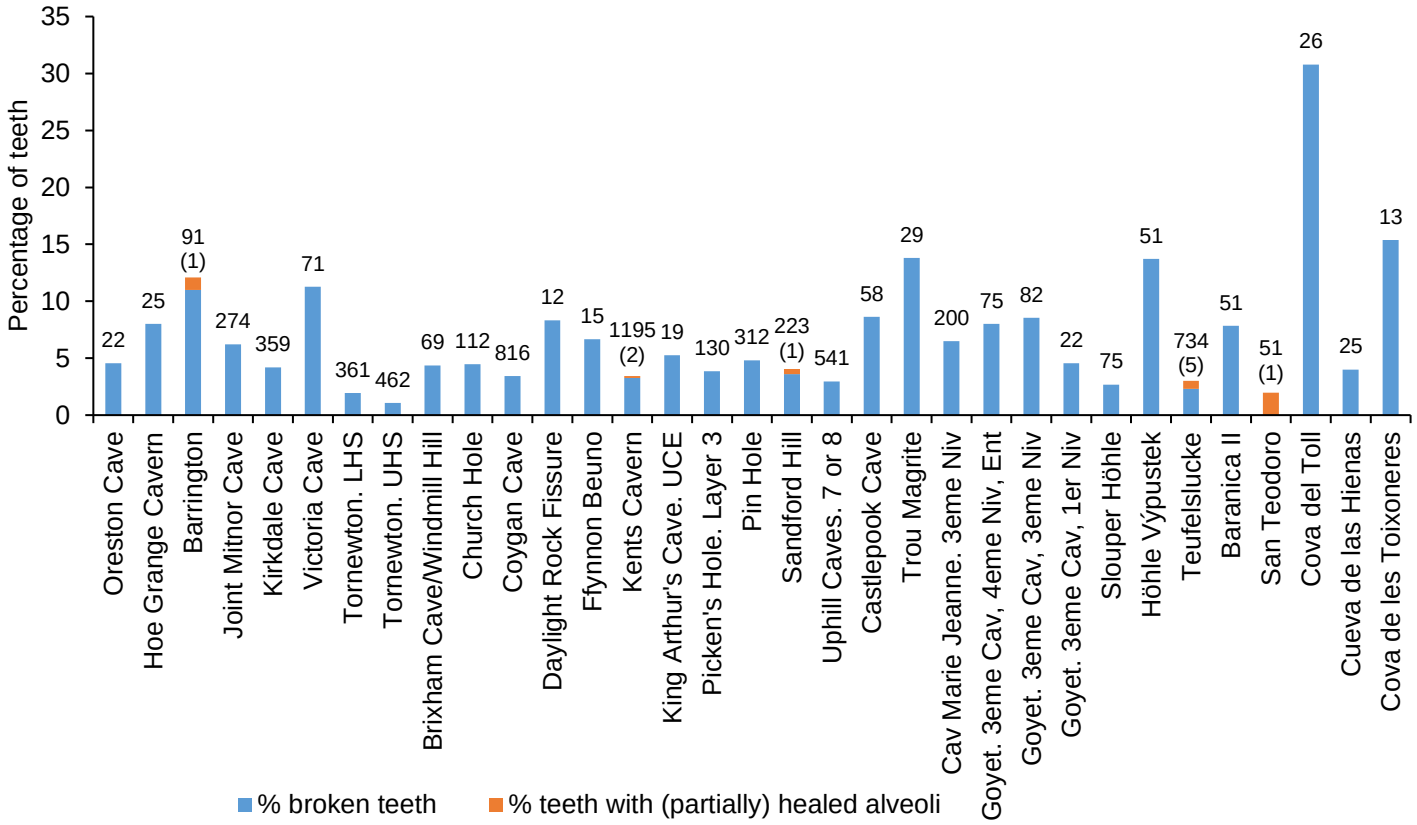

Figure 6.47: Percentage of *C. crocuta* teeth that are broken, and alveoli that are fully or partially healed, from Pleistocene deposits. Values above the bars are the total number of teeth of known condition: unbroken, broken and (partially) healed alveoli. Values in brackets are the number of (partially) healed alveoli that make up the total number of observations.

Table 6.15: Sites without broken teeth or partially healed alveoli. The number of teeth of known condition are stated.

All teeth		**Incisors**		**Canines**		**Premolars**		**Carnassials**	
Site	***No.***	***Site***	***No.***	***Site***	***No.***	***Site***	***No.***	***Site***	***No.***
Badger Hole	23	Oreston Cave	1	Oreston Cave	3	Hoe Grange Cavern	7	Oreston Cave	3
Bench Cavern	18	Tornewton LHS	108	Hoe Grange Cavern	3	Badger Hole	6	Tornewton LHS	73
Boughton Mount	30	Tornewton UHS	182	Badger Hole	8	Bench Cavern	8	Tornewton UHS	61
Caswell Bay	26	Badger Hole	1	Bench Cavern	3	Boughton Mount	17	Badger Hole	8
Hyaena Den	69	Bench Cavern	4	Boughton Mount	5	Caswell Bay	14	Bench Cavern	3
Tornewton Elk Stratum	13	Boughton Mount	3	Caswell Bay	6	Hyaena Den	30	Boughton Mount	5
		Brixham Cave/Windmill Hill	6	Church Hole	24	Tornewton Elk Stratum	7	Brixham Cave/Windmill Hill	12
		Caswell Bay	3	Daylight Rock Fissure	1	Trou Magrite	6	Caswell Bay	3
		Ffynnon Beuno	1	Ffynnon Beuno	4	Goyet. 3eme Cav, 4eme Niv	36	Daylight Rock Fissure	4
		Hyaena Den	5	Hyaena Den	13	Goyet. 3eme Cav, 3eme Niv	36	Ffynnon Beuno	1
		King Arthur's Cave. UCE	6	King Arthur's Cave. UCE	2	Goyet. 3eme Cav, 1er Niv	9	Hyaena Den	21
		Picken's Hole. Layer 3	22	Picken's Hole. Layer 3	22	San Teodoro	30	King Arthur's Cave. UCE	4
		Tornewton Elk Stratum	1	Tornewton Elk Stratum	2			Tornewton Elk Stratum	3
		Castlepook Cave	10	Castlepook Cave	8			Goyet. 3eme Cav, 1er Niv	4
		Goyet. 3eme Cav, 3eme Niv	7	San Teodoro	8			Slouper Höhle	14
		Goyet. 3eme Cav, 1er Niv	3	Cueva de las Hienas	1			Höhle Výpustek	7
		Slouper Höhle	10	Cova de les Toixoneres	1			Baranica II	11
		Cueva de las Hienas	19					San Teodoro	7
		Cova de les Toixoneres	2					Cueva de las Hienas	1

The percentages of broken teeth and healed alveoli were also calculated for each tooth type (incisors, canines, premolars and carnassials; Figure 6.48). Of the deposits with broken incisors, the greatest proportions are from Goyet (3eme Caverne, 4eme Niveau Ossifère, Galleries Voisines de l'Entrée, n=4) and Höhle Výpustek (n=8), both with 25 % broken incisors. Following this is Church Hole (n=20) at 15 %. San Teodoro (n=6) has the greatest proportion of partially or fully healed alveoli at 16.67 %, while a smaller proportion (2.03 %) of specimens from Teufelslucke (n=246) also exhibited this feature. Of the deposits that yielded incisors, 18 sites did not have broken incisors or healed incisal alveoli (Table 6.15).

The deposit with the greatest proportion of broken canines is Cova del Toll at 33.33 % (n=3). This is followed by Barrington at 23.08 % (n=13). Of the sites that yielded canines, 16 did not have broken canines (Table 6.15). No deposits have specimens with partially or fully healed canine alveoli.

Cova del Toll has the greatest proportion of broken premolars (31.25 %, n=16) followed by Cueva de las Hienas (25 %, n=4). Three sites contained specimens with partially or fully healed alveoli, all at low proportions: Barrington (1.61 %, n=62), Sandford Hill (0.8 %, n=125) and Kents Cavern (0.31 %, n=643). Eleven deposits do not have specimens with broken premolars, or healed premolar alveoli (Table 6.15).

Finally, 17 deposits did not yield broken carnassials (Table 6.15). Partially or completely healed carnassial alveoli are not present from any deposit. Trou Magrite yielded the greatest proportion of broken carnassials at 66.67 % (n=3). This is followed by Goyet (3eme Caverne, 3eme Niveau, n=5), Cova de les Toixoneres (n=3) and Cova del Toll (n=7). All four of these deposits have only small sample sizes. Of the deposits with larger sample sizes, Picken's Hole has the greatest proportion of broken carnassials at 16.67 % (n=24).

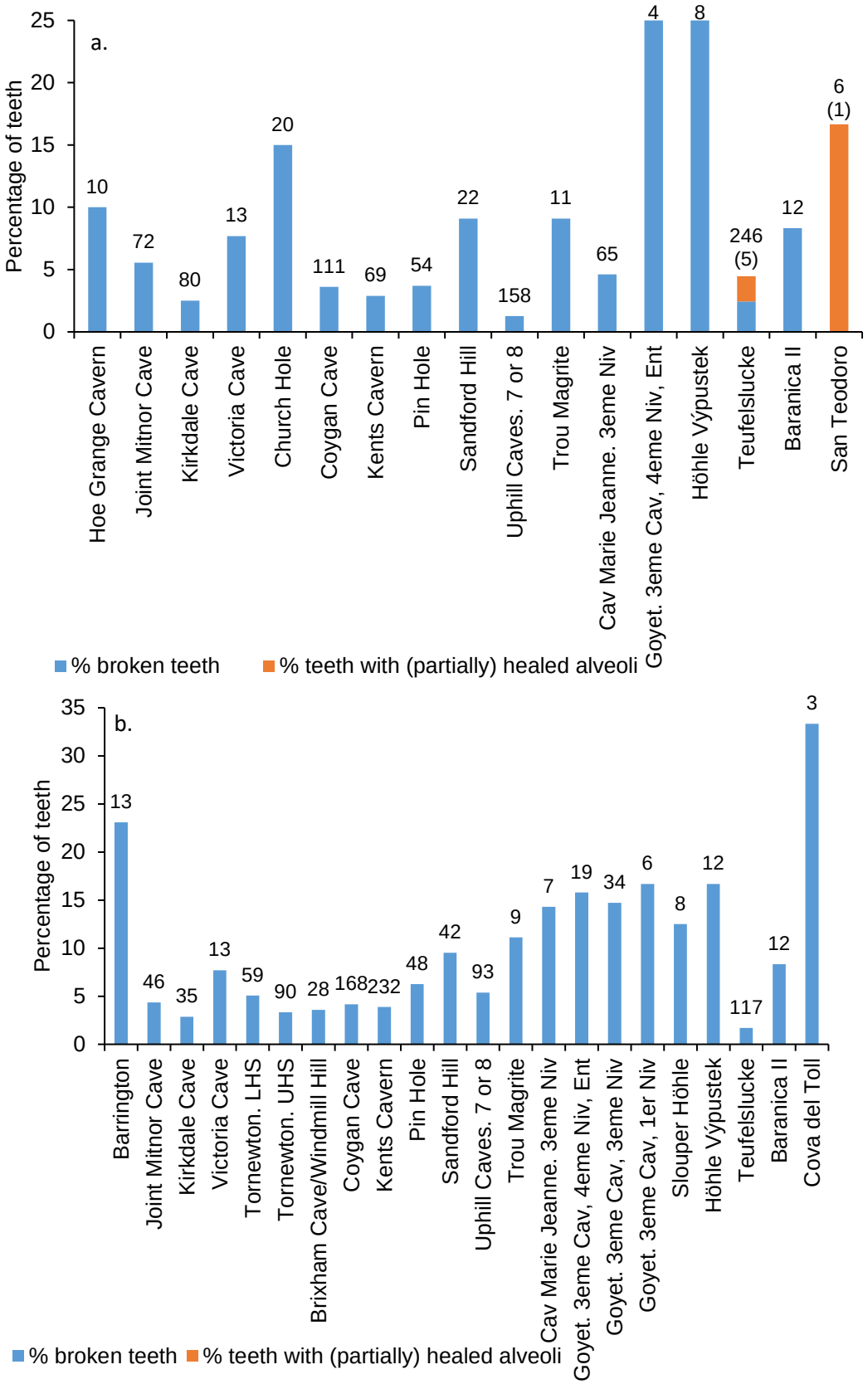

Figure 6.48: Percentage of Pleistocene *C. crocuta* teeth that are broken, and alveoli that are fully or partially healed. a. incisors. b. canines. c. premolars. d. carnassials. Values above the bars are the total number of teeth of known condition. Values in brackets are the number of (partially) healed alveoli that make up the total number of observations.

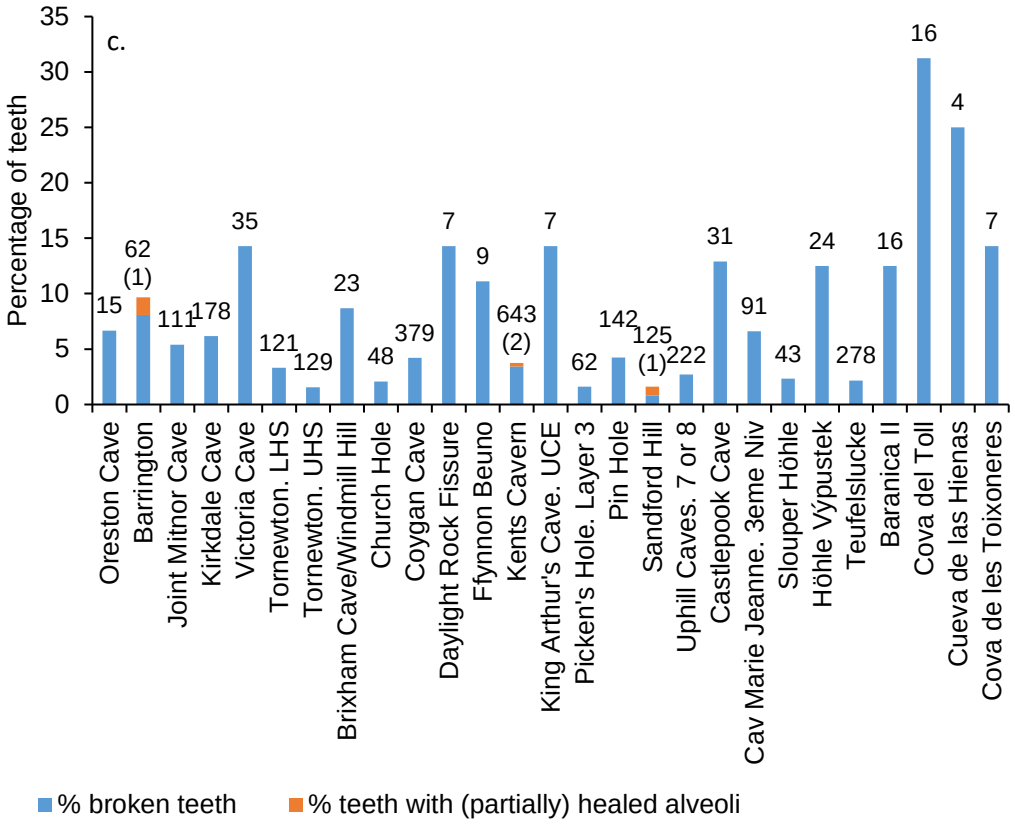

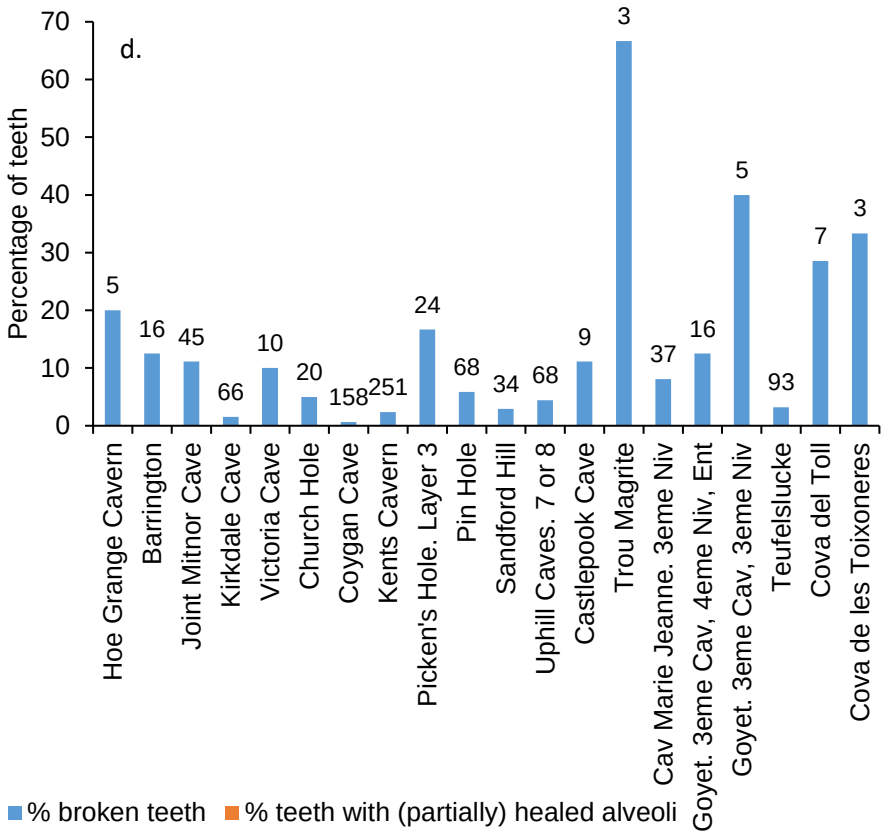

Figure 6.48 continued.

6.4.3 Discussion

The number of partially or fully healed alveoli present in the deposits is likely not representative of the true number. This is because maxillae and mandibles are required for the observation of these features, yet for many sites, the vast majority of teeth are isolated rather than present in jaws. However, it was deemed appropriate to include healed alveoli as their presence may be indicative of bone consumption if the tooth was initially broken and subsequently became infected (Losey *et al.*, 2014), although teeth may also be lost through inflammation of the gum and subsequent infection (Pekelharing, 1974).

When all teeth are considered, Cova del Toll yielded the greatest proportion of broken teeth. This assemblage has a high proportion of old-aged individuals with one of the largest proportions of P3/p3 wear stage IX, and a high proportion of heavily worn teeth (Section 6.3).It is likely, therefore, that the high degree of tooth breakage from Cova del Toll is a consequence of the old age profile of the assemblage (see also Section 5.5 and Van Valkenburgh, 2009).

Other sites that yielded a large proportion of broken teeth are Barrington, Victoria Cave, Trou Magrite, Höhle Výpustke and Cova de les Toixoneres. All of these deposits have age profiles that contain a mixture of young, prime aged and old individuals, so while the result may be due to the age profiles, it may also be due to variations in diet. More information can be derived by assessing each tooth type individually.

Goyet (3eme Caverne, 4eme Niveau Ossifère, Galleries Voisines de l'Entrée, n=4) and Höhle Výpustek (n=8) have the greatest proportions of broken incisors. This is perhaps unexpected for Goyet as from this level, there are only young and prime-aged adults; however, the high percentage is likely a result of the small sample size (n=4). Church Hole (n=20) has the next greatest proportion of broken teeth. San Teodoro (n=8) has a similar proportion of fully or partially healed alveoli. The age profiles of Höhle Výpustek, Church Hole and San Teodoro all include some older aged individuals, although they do not dominate the assemblage.

The incisors are utilised in killing prey (Biknevicius *et al.*, 1996), and cutting skin, subcutaneous tissue and muscle (Van Valkenburgh, 1996). The greater incisor breakage at the aforementioned sites may suggest that *C. crocuta* were engaged in more frequent predation, as opposed to scavenging, leading to breakage of incisors when the prey were attacked. Alternatively, the *C. crocuta* may have been targeting larger prey.

As mentioned in Section 6.2, there is some evidence from the craniodental morphological analysis that *C. crocuta* from MIS 3 were consuming larger prey or potentially preying more

frequently. This may explain the greater proportion of broken incisors at Church Hole and Höhle Výpustek as opposed to sites dating to MIS 5e and 5c. However, this does not explain the differences between these sites and others dating to MIS 3. Some deposits yielded a small number of broken incisors, such as Uphill Caves, and many MIS 3-aged deposits did not yield any broken incisors.

The prey species found in Church Hole and Höhle Výpustek are similar to those from other assemblages dating to MIS 3 (see Appendix 10.1, Table 10.1 and Table 10.3), so there is no evidence to suggest that they were preying on different taxa. The explanation may lie in the oscillating environmental conditions during MIS 3. As previously mentioned (Section 6.1.3.2), errors in radiocarbon dating do not currently allow each deposit to be assigned confidently to a specific stadial or interstadial but, for example, the conditions prevalent during the life of the *C. crocuta* from Church Hole and Höhle Výpustek may have been conducive to more frequent predation rather than scavenging. For Church Hole, this is supported by the small proportion of broken premolars, which will be discussed in more detail below.

As previously discussed, many prey species from San Teodoro were dwarf species (Mangano, 2011) therefore, the theory that incisor loss was caused by targeting of larger prey can be refuted. The question of more frequent predation is difficult to assess. The narrow mandibular corpuses of the San Teodoro *C. crocuta* suggest that these individuals engaged in predation less frequently than those elsewhere (Section 6.2), although the width of the mandible may be a reflection of the size of the individuals.

Cova del Toll has the greatest proportion of broken canines, likely due to the predominance of elderly individuals. Following this is Barrington, which includes some elderly *C. crocuta*, although they do not dominate the assemblage. Except for Barrington, most British deposits from MIS 5e, 5c and 3 have low proportions (2.9-9.5 %) of broken canines. The proportions of broken canines from the Czech and Belgian sites are relatively high (11.1-16.7 %).

Canines are utilised in killing prey (Biknevicius *et al.*, 1996), consumption of muscle with attached bone (Van Valkenburgh, 1996), and sometimes cracking bone (Van Valkenburgh and Ruff, 1987). The canines may be broken through accidental contact with bone, especially when rapidly feeding during times of elevated competition (Van Valkenburgh, 1996). The greater proportion of broken canines from Barrington, and to a lesser extent the Belgian and Czech sites, may again suggest either more frequent predation, or consumption of larger prey, more frequent bone consumption, or elevated levels or competition.

As discussed in Section 6.2, evidence is lacking for the specific prey species targeted by the *C. crocuta* at Barrington. However, evidence from the assemblage indicates that except for *B. primigenius*, the potential prey species present at Barrington are similar to those at other MIS 5e-aged sites of Joint Mitnor, Kirkdale and Victoria Caves: *P. antiquus, S. hemitoechus, H. amphibius, M. giganteus, D. dama, C. elaphus, B. priscus* (Buckland, 1822; Fisher, 1879; Gibbard and Stuart, 1975; Boylan, 1981; Currant and Jacobi, 2011; O'Connor and Lord, 2013). Therefore, there is no evidence to suggest that *C. crocuta* were preying on larger species. Indeed the evidence from mandibular bending strength and post-cranial indices (Section 6.2), suggest that *C. crocuta* from both Barrington and Burtle Beds were potentially preying on smaller prey than those from MIS 3, although data were insufficient to compare with other MIS 5e−aged sites. The post-cranial indices indicated that during MIS 5, *C. crocuta* in Britain were potentially engaged in more frequent predation than those during MIS 3, which may explain the elevated canine breakage at Barrington compared to MIS 3-aged deposits. However, this does not explain why Barrington has greater tooth breakage than other deposits from MIS 5e. Although the Barrington assemblage has some elderly *C. crocuta* (proportion of wear stage VIII = 11.54 %, Section 6.3), this likely is not sufficient to explain the elevated proportion of tooth breakage at this site.

As mentioned, canines accidentally contact bone during rapid feeding due to elevated competition (Van Valkenburgh, 1996). The potential competitor species found at Barrington were *C. lupus, P. leo* (*spelaea*) and *U. arctos* (Fisher, 1879; Gibbard and Stuart, 1975), which were also found at Joint Mitnor Cave and Kirkdale Cave (Buckland, 1822; Boylan, 1981; Currant and Jacobi, 2011), while only *U. arctos* and *P. leo* (*spelaea*) were found at Victoria Cave (O'Connor and Lord, 2013).This suggests that at least in terms of range of competitors, *C. crocuta* at Barrington were not subject to increased competition. There may have been an increase in population of competitors, leading to greater intraspecific or interspecific competition at Barrington, and thus to more rapid consumption of carcasses and accidental contact with bone. Determination of abundance is difficult to reconstruct from Pleistocene deposits.

Another potential explanation lies in the use of canines to breakage bone (Van Valkenburgh and Ruff, 1987). However, increased bone consumption is not supported by an elevated proportion of broken premolars, suggesting that bone breakage was an infrequent activity. This will be explored in more detail below.

A final explanation is the size of the canines. As discussed in Section 6.2, the canines from Barrington are among the smallest across all sites. This may have rendered them more vulnerable to stresses placed upon them and thus more likely to break.

In Section 6.2, it was hypothesised that the canines from Pin Hole would be at greater risk of breakage because of their small size, while the mandibular bending strength and post-cranial indices were suggestive of predation on larger species. Pin Hole does have some broken canines, but the proportion is less than other sites.

As mentioned, all sites from Belgium and the Czech Republic have consistently elevated levels of tooth breakage, above that of most other sites. One of these Belgian sites is Trou Magrite, the canines from which were also suggested to be of greater breakage risk, for the same reasons as those from Pin Hole. This explains the proportion of broken teeth from Trou Magrite, but not from the other Belgian or Czech deposits. There are some cases where the canines from these sites are notably small, such as the mediolateral diameter of the upper canine from Höhle Výpustek and Goyet (3^{eme} Caverne, 1^{er} Niveau). Equally, there are some cases where canines from these deposits are among the largest, such as the anteroposterior diameter of the upper canine from Goyet (3eme Caverne, 3eme Niveau) and the anteroposterior diameter of the lower canines from Höhle Výpustek. Overall, canines from these sites are not consistently small, suggesting that this is not the cause of the fairly high proportions of broken canines. Of these sites, only Höhle Výpustek has a relatively high proportion of broken premolars, and many of these deposits did not yield any broken premolars, suggesting that bone consumption was not the cause of the broken canines. The species present at these sites are similar to other assemblages, such as MIS 3–aged sites at Britain (see Appendix 10.1, Table 10.1 and Table 10.3). This suggests that prey species themselves were also not the cause if the prey were of similar size and similarly vigorous in all sites. More frequent predation or elevated competition may have influenced canine breakage, yet the data are insufficient to assess this.

Cova del Toll has the highest degree of premolar breakage, although this is again expected due to its age profile. Cueva de las Hienas also has a high proportion of broken premolars but this statistic is based on only four premolars so may not be reliable. Other sites with elevated proportions of broken premolars include Victoria Cave, Daylight Rock Fissure, Ffynnon Beuno, King Arthur's Cave (Lower Cave Earth), Castlepook Cave, Höhle Výpustek, Baranica II and Cova de les Toixoneres. As mentioned above, Church Hole has a low proportion of broken premolars, and Barrington has a larger proportion of broken premolars, but still a lower proportion than the other deposits mentioned above.

Premolars are used to consume muscle with attached bone, and to consume bone (Van Valkenburgh, 1996) It is these teeth, therefore, that are particularly useful in determining

periods of elevated bone consumption. Today, *C. crocuta* consume more bone when food availability is low (Kruuk, 1972; Egeland *et al.*, 2008).

Except for Victoria Cave, all sites with elevated premolar breakage are dated to MIS 3. However, there are also a number of other sites from MIS 3, such as Church Hole, Picken's Hole and Sandford Hill that have low proportions of broken premolars. These differences may stem from shorter periods of low availability, such as seasonally harsh conditions. As mentioned, dating resolution is insufficient to allocate the MIS 3 deposits to specific stadials or interstadials, so more specific resolution of this matter is difficult. The dates of these sites also span across a large duration of MIS 3 (see Figure 4.7), so it is not necessarily the case that there were more broken teeth, and therefore lower food availability, around the time of *C. crocuta*'s extirpation from Europe.

An alternative explanation is that the premolars were broken during consumption of frozen carcasses. The deposits with a greater proportion of broken premolars may have been from colder periods. However, the limits with the chronology again make this difficult to confirm at present.

Interestingly, individuals from Slouper Höhle and Teufelslucke have relatively strong mandibular dorsoventral bending strength, suggesting elevated levels of bone consumption (Section 6.2). However, the percentage of tooth breakage from these sites are low. This may be because the premolars from these assemblages tend to be amongst the largest specimens for most measurements. Indeed, some premolar measurements from Teufelslucke are significantly larger than those from other assemblages. This suggests that premolars from Teufelslucke and Slouper Höhle were robust against frequent breakage, even with potentially elevated levels of bone consumption.

Victoria Cave is the site from MIS 5e with the greatest proportion of broken premolars. As mentioned, the potential prey and competitor species in the assemblage are similar to those from Joint Mitnor Cave, Kirkdale Cave and Barrington. This alone is does not suggest lack of food from elevated levels of competition, or reduced prey populations.

The difference between the MIS 5e-aged sites may stem from the climate, as peak warmth occurred for only a short period (less than 1,200 years) of the interglacial (Candy *et al.*, 2016), although dating resolution is insufficiently precise to phase sites within MIS 5e. If the Victoria Cave *C. crocuta* post-dated that climatic optimum conditions would have been cooling towards the early Devensian. The location of Victoria Cave is towards the northern limit of *C. crocuta*'s known range in northwest Europe. Due to its potential placement at the edge of its range, there may have been periods of food instability for *C. crocuta* during sub-optimal conditions.

Trou Magrite has by far the greatest proportion of broken carnassials at 66.67 %. although the sample size is small (n=3). Other sites with relatively large proportions of broken carnassials are Goyet (3eme Caverne, 3eme Niveau, n=5), Cova del Toll (n=3) and Cova de les Toixoneres (n=3). Again, the large proportion of broken carnassials from Cova del Toll is likely a reflection of its age profile. In addition, all of these sites have small sample sizes.

Of the deposits with larger sample sizes, the greatest proportions of broken teeth are from Picken's Hole, followed by lower proportions in Barrington, Joint Mitnor Cave, Victoria Cave, Castlepook Cave and Goyet (3eme Caverne, 4eme Niveau, Galleries Voisines de l'Entrée).

The carnassials, particularly the blades, are used for removing skin from carcasses (Werdelin, 1989; Van Valkenburgh, 1996), while the P4 cones are used in bone consumption (Kurtén and Werdelin, 1988; Van Valkenburgh, 1996). Some of these broken carnassials may therefore stem from bone breakage, as discussed above. However, Picken's Hole had a low proportion of broken premolars, and Goyet (3eme Cavern, 4eme Niveau) yielded none. Therefore, for these deposits at least, the broken carnassials likely derived from a different activity.

One explanation may be the consumption of frozen or partially frozen carcasses. The individuals may have attempted to tear flesh from such carcasses, resulting in broken carnassials. Today, carcass availability is dependent upon factors such as disease, drought and kills by other predators (Henschel and Skinner, 1990; Gasaway *et al.*, 1991). Furthermore, carcasses that are not fresh contain less energy, nutrients and water than fresh kills (Cooper *et al.*, 1999). However, frozen carcasses may have been better preserved, and therefore may have been a viable food source for *C. crocuta* during colder periods of MIS 3 if prey were scarcer. This scarcity may also have been due to seasonal migrations of prey, such as observed in *R. tarandus* in southwestern France during stadial conditions in MIS 3 (Discamps, 2014).

A final factor to bear in mind is that female *C. crocuta* have elevated levels of tooth breakage compared with males (Section 5.2). There is therefore the possibility that assemblages with greater proportions of broken teeth may have more females than assemblages with fewer broken teeth. However, given the lack of SSD in *C. crocuta*, the relative proportions of males and females in each assemblage could not currently be determined in order to test this.

6.5 Conclusion

This section considered both the morphological and palaeodietary variation of *C. crocuta* in response to palaeoenvironmental variation across Europe and through the Pleistocene. First, a variation of the traditional method of body mass reconstruction was proposed, in order to allow reconstruction of Pleistocene *C. crocuta* body masses. The regression model of m1 lengths and body masses of *C. crocuta* from across Africa has good predictive ability and is therefore judged suitable for reconstruction of Pleistocene body masses. The reconstructions indicate that there is much overlap in the body mass estimates from different climatic periods across Europe. There is some indication of *C. crocuta* following Bergmann's Rule, however, this is not a consistent response. It has been suggested that the overall lack of consistent body mass response to environmental changes may in part be due to the behavioural plasticity of *C. crocuta*, particularly elevated bone consumption and the ability to out-compete other carnivores.

The body mass estimates suggest that *C. crocuta* from San Teodoro were consistently small, indicating an influence of the Island Rule.

As with the body mass estimates, the craniodental and post-cranial data show overlaps in measurements between different time periods. Taken together, the data indicate that during MIS 5e and 5c in Britain, *C. crocuta* were hunting more frequently than during MIS 3. By contrast, during MIS 3, *C. crocuta* may have been preying less frequently upon larger or more vigorous species.

The craniodental data are also indicative of bone consumption, which was likely more frequent during MIS 3. This may indicate periods of dietary stress, necessitating the more complete consumption of carcasses and is also reflected by the tooth breakage data. The data also suggest that frozen carcasses may have been consumed and may have been an important food source during periods of harsher conditions of MIS 3.

Overall, this chapter has determined how *C. crocuta* responded to Pleistocene environmental changes in Europe. A number of scenarios have been suggested to explain these responses. In many cases, there is currently insufficient evidence to establish causal mechanisms, although improvements in chronology and more detailed palaeoenvironmental reconstructions, including temperature, precipitation and vegetation, would allow a better understanding of their responses to the local and regional environment, without relying on climatic signals from further afield. Finally, palaeodiet could be further assessed through dietary isotopes and a more thorough analysis of the evidence of *C. crocuta* damage to bones in many of the assemblages.

The implications of the findings in this chapter for *C. crocuta* extirpation will be explored in Chapter 7.

7 Extirpation of *Crocuta crocuta* from Europe

7.1 Introduction

As outlined in the previous chapters, *C. crocuta* are adaptable generalists, with the ability to alter their behaviour in response to changing environmental conditions. However, despite demonstrating resilience over much of the Pleistocene, they ultimately were extirpated from Europe during the Late Pleistocene.

This chapter will first reassess the chronology of *C. crocuta* during MIS 3 in Europe in order to understand the timing of extirpation from different regions in Europe. This will be compared with chronological models of presence/absence of a potential competitor (*P. leo* (*spelaea*)) and three known key prey species (*C. antiquitatis*, *C. elaphus* and *R. tarandus*).

Secondly, palaeoenvironmental information from the literature will be paired with results discussed in Sections 5 and 6 to assess the possible reasons behind *C. crocuta*'s eventual disappearance from Europe. Three areas will be focussed on: environmental conditions (temperature, precipitation and vegetation), food availability (presence of prey species and competition) and competition for shelter.

The research questions for this chapter are as follows:

- When did *C. crocuta* become extirpated from different areas of Europe?
- Did palaeoenvironmental changes influence the extirpation of *C. crocuta*?
- Did food availability influence the extirpation of *C. crocuta*?
- Did competition for shelter influence the extirpation of *C. crocuta*?

7.2 Results

7.2.1 Chronology of Crocuta crocuta during MIS 3

The new model of *C. crocuta* chronology was created by applying a strict selection criteria to the database of radiocarbon dates compiled by Stuart and Lister (2014) and more recently published dates (Section 4.2.5). The dates were calibrated in OxCal 4.3 (Bronk Ramsey, 2009) using the IntCal13 calibration curve (Reimer *et al*., 2013, Section 4.4.3). The model is displayed in Figure 7.1. Full details of all radiocarbon dates can be found in Appendix 10.9, Table 10.56 and Table 10.57.

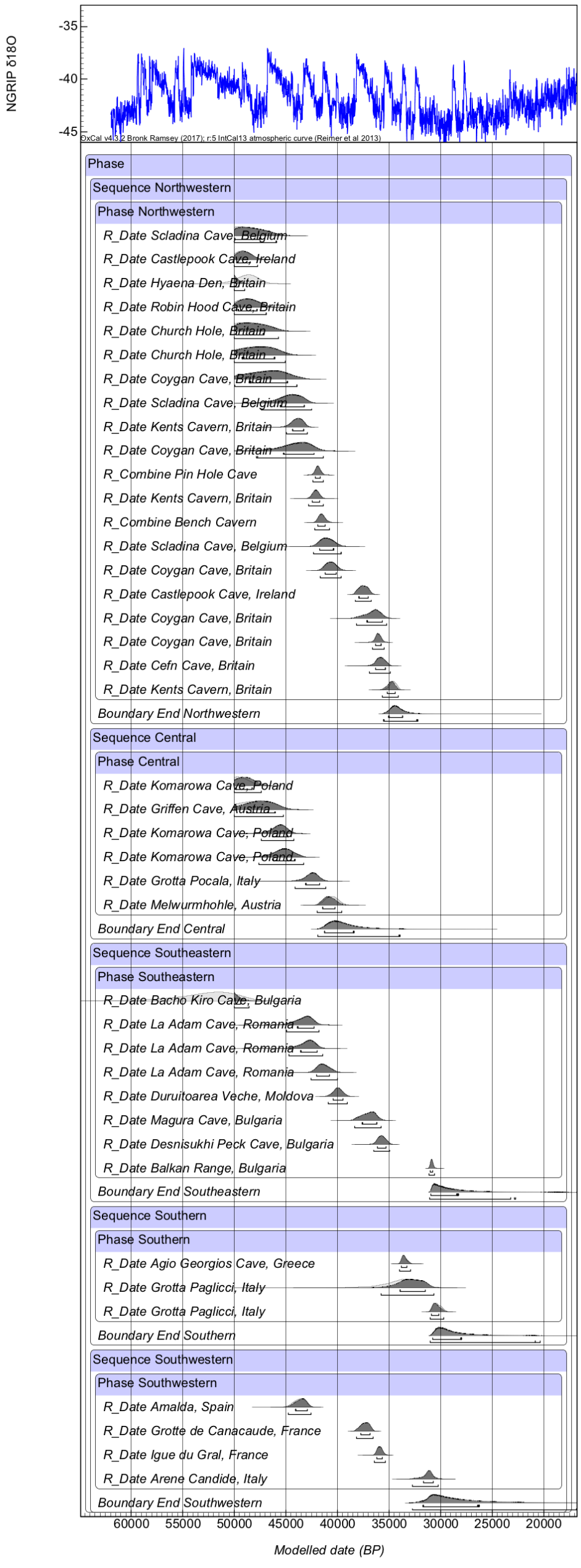

Figure 7.1: Model of radiocarbon dates on *C. crocuta* specimens across Europe. Dates have been split into regions using overlapping phases. Calibrated values show the 68.2 and 95.4 % confidence ranges. Model run using OxCal 4.3 (Bronk Ramsey, 2009) and the IntCal13 calibration curve (Reimer *et al.*, 2013). The NGRIP $\delta^{18}O$ record (Andersen *et al.*, 2004) is displayed.

The chronology indicates that *C. crocuta* disappeared from the Central region (including dates from Austria, Italy and Poland) first. Although the end boundary's 95.4 % confidence range is large (41,880-33,898 cal BP), the confidence at 68.2 % range is more constrained at 41,259-38,375 cal BP.

The next apparent event of consequence is a gap in the dates of *C. crocuta* across all regions. Taking into account the 95.4 % confidence range, the gap dates to between 39,036 and 38,341 cal BP, with only the modelled end boundary of the Central region falling within this period.

The final known appearance of *C. crocuta* in the Northwestern region (Belgium, Britain and Ireland) has an end boundary modelled at 35,523-32,217 cal BP (95.4 % confidence) or 35,018-33,666 cal BP (68.2 % confidence).

The end boundaries of the Southwestern (France, Italy and Spain), Southeastern (Bulgaria, Moldova and Romania) and Southern (Italy and Greece) regions have similar modelled ages. The 95.4 % confidence range of the Southwestern region end boundary is large at 32,722-8898 cal BP. The more constrained 68.2 % confidence end boundary gives dates of 31,691-26,233 cal BP. The end boundary of the Southeastern region is 31,073-22,741 cal BP at 95.4 % confidence interval, or 30,944-28,237 cal BP at 68.2 % confidence. Finally, the end boundary estimates for the Southern region are 31,024-20,330 cal BP (95.4 % confidence) and 30,769-27,954 cal BP (68.2 % confidence).

7.2.2 Chronology of Panthera leo (spelaea) and prey species during MIS 3

A new radiocarbon model was also generated for *P. leo* (*spelaea*) (Figure 7.2, with full details in Appendix 10.9, Table 10.58 and Table 10.59), which shows that the species persisted in Europe until at least 14,764 cal BP. The 68.2 % and 95.4 % confidence ranges for the end boundaries of the Northwestern, Central and Southwestern regions are large, with all extending into at least the Holocene, and some extending into the future. A difference is, however, seen in the Southeastern region, with earlier end boundaries at 35,913-25,202 cal BP (95.4 % confidence) or 35,451-31,997 cal BP (68.2 % confidence).

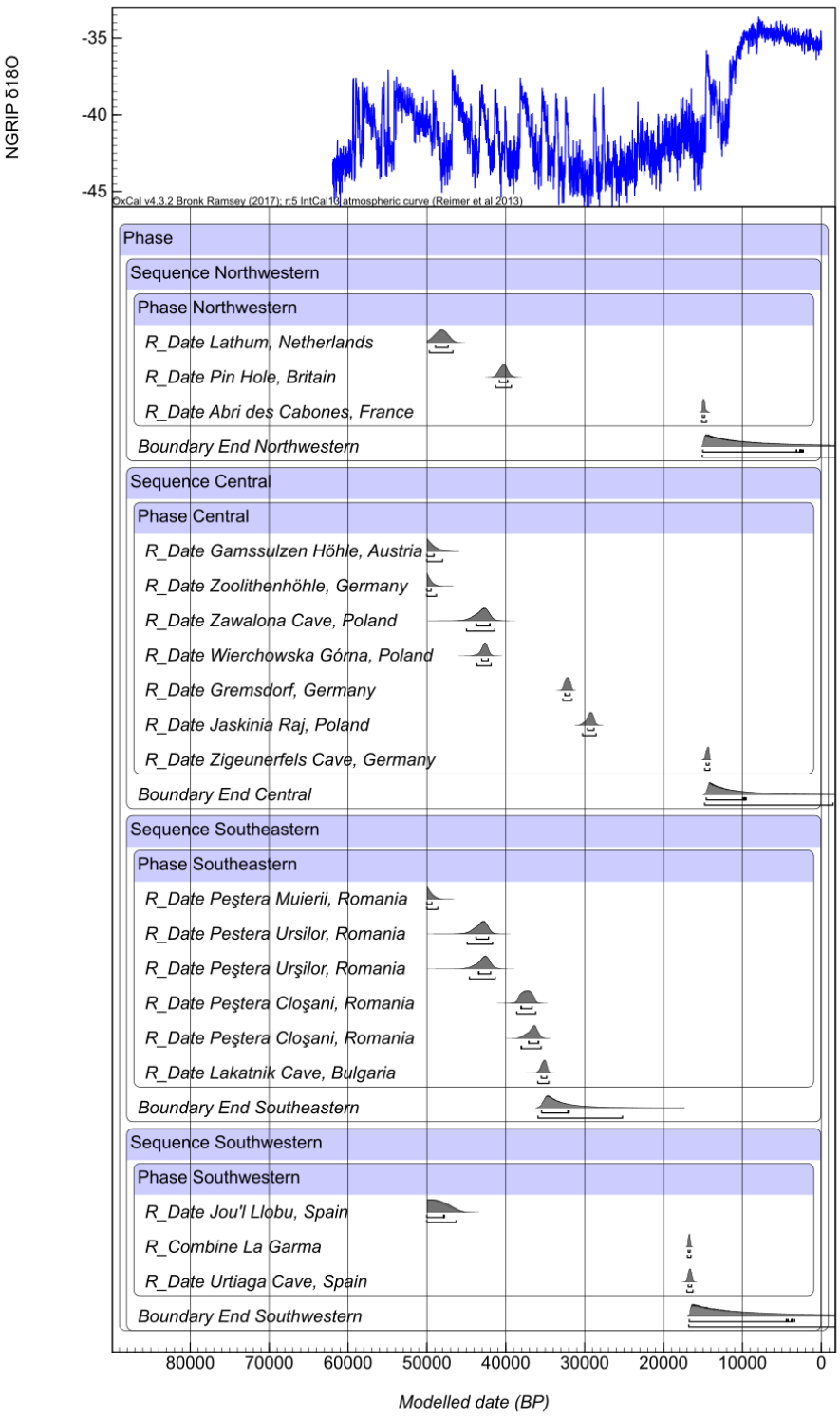

Figure 7.2: Model of radiocarbon dates on *P. leo* (*spelaea*) specimens across Europe. Dates have been split into regions using overlapping phases. Calibrated values show the 68.2 and 95.4 % confidence ranges. Model run using OxCal 4.3 (Bronk Ramsey, 2009) and the IntCal13 calibration curve (Reimer et al., 2013). The NGRIP $\delta^{18}O$ record (Andersen et al., 2004) is displayed.

There is a gap in the *P. leo (spelaea)* dates with a 95.4 % confidence interval between 39,280 and 38,606 cal BP. There are also other gaps in the dates, the most striking of which is the gap before the youngest dates (<20 ka). In the Southwestern region, the gap in the dates at 95.4 % confidence spans 46,295-16,959 cal BP (95.4 % confidence). Similarly, the gap in the dates in the Northwestern region spans 39,280-15,149 cal BP (95.4 % confidence). The gap in the dates in the Central region is shorter, between 28,559-14,764 cal BP at 95.4 % confidence.

Radiocarbon models were also made for three known prey species (*C. antiquitatis*, *R. tarandus*, *C. elaphus*). There are many dates on *C. antiquitatis* from the Northwestern region and only seven acceptable dates from the Central region (Figure 7.3 and Appendix 10.9, Table 10.60 and Table 10.61). The other regions have just one date each. The only dates from these regions are calibrated at 95.4 % confidence to 49,412-42,625 (Southwestern), 43,340-41,925 (Southeastern) and 33,183-31,600 (Northern) cal BP.

The end boundaries of *C. antiquitatis* occurrence in the Northwestern and Central regions are similar, although those for the Central region have a larger span of dates. The Northwestern region's end boundaries are 16,846-14,613 cal BP (95.4 % confidence) and 16,677-15,819 cal BP (68.2 % confidence). Similarly, the Central region's end boundaries are 17,794-1,898 cal BP (95.4 % confidence) and 17,583-12,543 cal BP (68.2 % confidence).

In the Northwestern region, there is a gap in the *C. antiquitatis* dates at 95.4 % confidence between 37,628 and 35,444 cal BP. The gap is larger in the Central region, between 40,037 and 25,493 cal BP. There is an additional gap in *C. antiquitatis* dates in the Northwestern region from 27,351 to 16,855 cal BP.

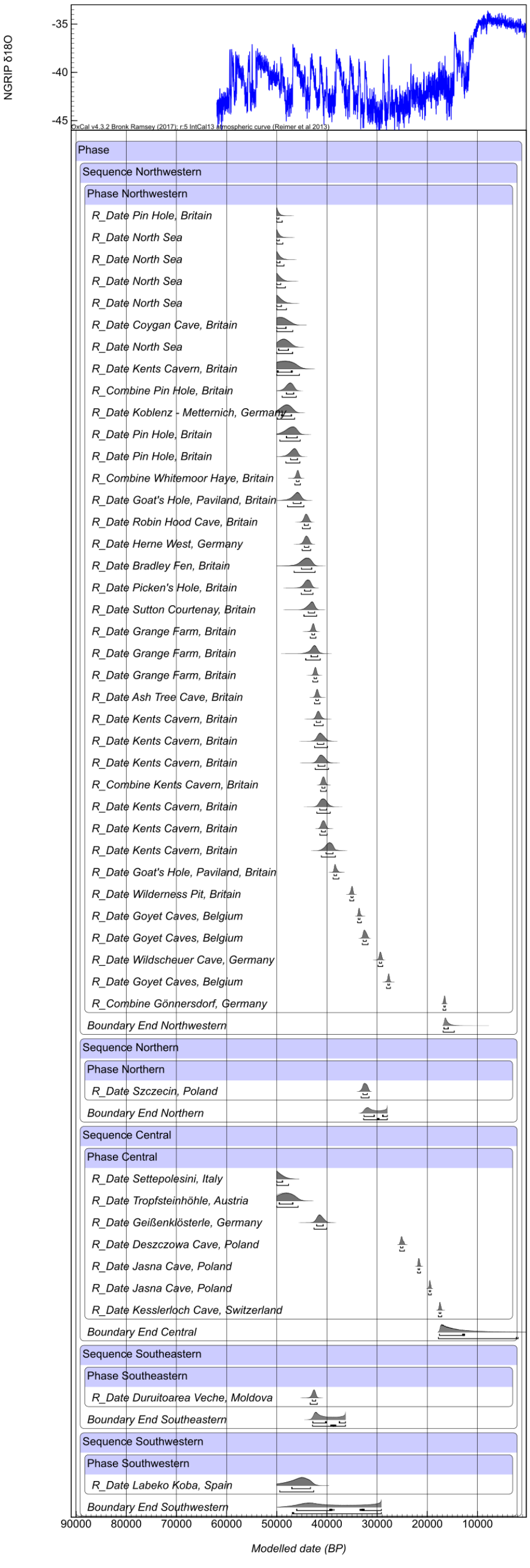

Figure 7.3: Model of radiocarbon dates on *C. antiquitatis* specimens across Europe. Dates have been split into regions using overlapping phases. Calibrated values show the 68.2 and 95.4 % confidence ranges. Model run using OxCal 4.3 (Bronk Ramsey, 2009) and the IntCal calibration curve (Reimer et al., 2013). The NGRIP $\delta^{18}O$ record (Andersen et al., 2004) is displayed.

For the new *C. elaphus* and *R. tarandus* models, no dates younger than 18 ^{14}C BP were included. Furthermore, as the species are both extant in Europe today, end boundaries were not modelled.

The *C. elaphus* model is shown in Figure 7.4, with additional information in Appendix 10.9, Table 10.62. The Southeastern region also has one *C. elaphus* date calibrated to 47,266-42,415 cal BP, while the Central region's sole date is 45,418-41,816 cal BP (both 95.4 % confidence).

There is an absence of *C. elaphus* dates across Europe between 38,433 and 37,532 cal BP. In the Southwestern region, there is also a gap in *C. elaphus* dates from 31,423 to 26,099 cal BP, after which there are a number of dates until the cut-off point for dates included in the model. The youngest date of *C. elaphus* from the Northwestern region is 34,445-33,747 cal BP (all at 95.4 % confidence).

Across Europe, there is one short gap in the *R. tarandus* dates at 95.4 % confidence between 35,469 and 34,694 cal BP (Figure 7.5 and Appendix 10.9, Table 10.63). However, within each region, there are longer intervals during which there is an absence of *R. tarandus* dates at 95.4 % confidence. In the Northwestern region, these occur at 36,925 to 36,289 cal BP and 31,294 to 29,586 cal BP. In the Central region, the gaps in the dates occur at 36,045 to 32,862 cal BP and 31,364 to 25,226 cal BP. In the Southwestern region, the first gap is between 36,390 to 32,966 cal BP, and the second gap is between 31,346 and 23,134 cal BP.

In the Northwestern region, the youngest date of *R. tarandus* in the model is calibrated at 95.4 % confidence to 28,371-27,811 cal BP. In the Central and Southwestern regions, the dates extend until the cut-off point for the dates included in the model.

Going forwards, as the 95.4 % end boundary estimates are often very large, and in some cases unrealistic (such as the end boundaries of *P. leo* (*spelaea*) extending into the future), the 68.2 % estimate will be used. When discussing individual calibrated dates and gaps in the dates, the 95.4 % figures will be used.

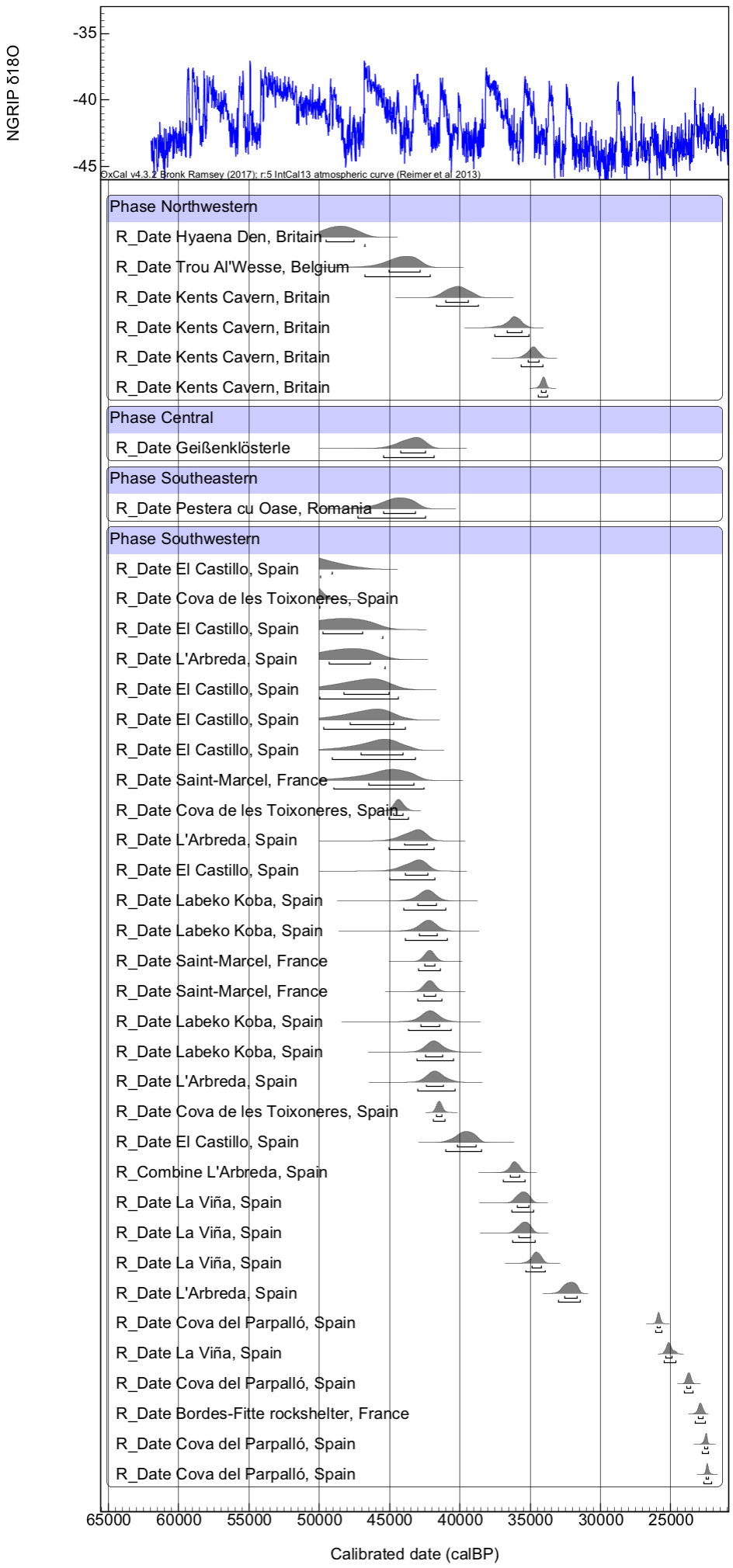

Figure 7.4: Model of radiocarbon dates on *C. elaphus* specimens across Europe. Dates have been split into regions using overlapping phases. Calibrated values show the 68.2 and 95.4 % confidence ranges. Model run using OxCal 4.3 (Bronk Ramsey, 2009) and the IntCal13 calibration curve (Reimer et al., 2013). The NGRIP $\delta^{18}O$ record (Andersen et al., 2004) is displayed.

Figure 7.5: Model of radiocarbon dates on *R. tarandus* specimens across Europe. Dates have been split into regions using overlapping phases. Calibrated values show the 68.2 and 95.4 % confidence ranges. Model run using OxCal 4.3 (Bronk Ramsey, 2009) and the IntCal13 calibration curve (Reimer et al., 2013). The NGRIP $\delta^{18}O$ record (Andersen et al., 2004) is displayed.

7.3 Discussion

7.3.1 Palaeoenvironmental conditions

The first potentially important factors for the extirpation of *C. crocuta* from Europe are the palaeoenvironmental conditions, in particular temperature, precipitation and vegetation cover.

C. crocuta populations today are larger in areas where winter temperatures are warmer, and to a lesser extent where summer temperatures are cooler (Section 5.1). It may therefore be expected that periods of cold conditions may have negatively impacted *C. crocuta* populations, potentially leading to their extirpation from an area.

The new *C. crocuta* chronological model indicates a number of important events in this respect. The first of these is the apparent disappearance of the species from the Central region around 41.3-38.4 ka. This period is covered by Greenland ice core events Greenland Interstadial-10 (GI-10) to Greenland Stadial-9 (GS-9) (Rasmussen *et al.*, 2014), meaning that the last appearance of *C. crocuta* in the Central region cannot be placed within a cold (stadial) or warm (interstadial) period. Similarly, the timing of disappearance from the Northwestern region (35-33.7 ka) spans GI-7b, GI-7a, GS-7 and GI-6 (Rasmussen *et al.*, 2014), and thus cannot be placed within a stadial or interstadial either. However, *C. crocuta* may have been affected by the continental climates in the Central region, resulting in extreme cold winters, and thus potentially explaining the early extirpation from this region.

The gap in *C. crocuta* dates (39 to 38.3 ka) suggests a potential absence of *C. crocuta* across much of Europe at this time. This was also noted by Dinnis *et al.* (2016) for Britain. In southwestern France, *C. crocuta* (as dated from contemporary material) disappeared from the northern part of the Aquitaine Basin at this time (Discamps, 2014). This period falls within GS-9, a prolonged cold period lasting around 1,680 years, longer than any other stadial since the end of GS-18 at 59,440 b2k (Rasmussen *et al.*, 2014). It also coincides with Heinrich Stadial (HS) 4, between 40.2 and 38.3 ka (Sanchez Goñi and Harrison, 2010).

A previous prolonged, but slightly shorter stadial (GS-13 lasting 1,480 years) occurred between 48,340-46,860 b2k (Rasmussen *et al.*, 2014). However, this is towards the limit of the radiocarbon method and the calibrated radiocarbon ages of this age have large confidence intervals (Figure 7.1), making it difficult to assess the response of *C. crocuta* to this event.

The modelled end dates of the Southwestern, Southeastern and Southern regions are similar, indicating the later persistence of *C. crocuta*. With dates of 31.7-26.2, 30.9-28.2 and 30.8-28 ka, the dates fall within GS-5.2 to GS-3. Within this period, GI-5.1, GI-4 and GI-3 were short, lasting only around 240, 300 and 240 years respectively. Meanwhile, the stadials (which seemingly

impacted most on *C. crocuta*) were longer, with GS-5.2 lasting around 1,200 years, GS−5.1 lasting 1,700 years, GS-4 lasting 820 years, and GS-3 lasting 4,200 years (Rasmussen *et al.*, 2014). HS 3 also occurred between 32.7-31.3 ka (Sanchez Goñi and Harrison, 2010).

Overall, there seems to be a temperature relationship with the absence of *C. crocuta* from much of Europe around 39-38.3 ka (GS-9 and HS 4) and the disappearance of *C. crocuta* from the southern regions around 31.7-26.2 ka (GS-5.2 to GS-3 and HS 3).

Unfortunately, there are limited quantitative palaeotemperature reconstructions from sites in which *C. crocuta* have been found. The largely qualitative palaeotemperature reconstructions available for MIS 3 (Table 7.1) range from 'cold' and 'cool' to 'temperate' and 'warm' but unfortunately, come from sites lacking direct dates on *C. crocuta*.

Some of the few quantitative estimations are from Caverne Marie Jeanne, with mean annual temperatures ranging from 4.22°C in the 6eme Niveau to 3.35°C in the 4eme Niveau (López-García *et al.*, 2017). Mean temperature of the warmest month reconstructed from Levels I-III in Cova del Gegant was 20.1±1°C, and mean temperature of the coolest month was 2.6±0.7°C (López-García *et al.*, 2008). This temperature of the warmest month reconstruction falls below the range of those recorded in the sites used in the present-day *C. crocuta* biomass models (25.1-35.4°C, Section 5.1 and Spreadsheet 1). The annual temperatures from Caverne Marie Jeanne and the coolest month temperature from Cova del Gegant fall towards the lower range of the temperature of the coolest month records included in the biomass model (0.3-15.9°C). As temperature of the coolest month has a stronger association with *C. crocuta* biomass than does temperature of the warmest month (Section 5.1), this suggests that the populations of *C. crocuta* may have been small in these areas, although the temperatures were likely not beyond those tolerated by the species. Unfortunately, there are no dates directly upon *C. crocuta* from these sites, so it is unknown whether these conditions occurred close to the point of *C. crocuta* extirpation from the Northwestern region (in the case of Caverne Marie Jeanne) or the Southwestern region (in the case of Cova de Gegant).

If declining temperature were a direct cause of *C. crocuta* absence and extirpation, then the reasons for this may lie in the species' lack of consistent body size change in response to temperature change. Larger body size may allow for increased heat conservation (Mayr, 1956). As discovered in Section 6.1, while some of the largest *C. crocuta* occurred during MIS 3, there was no consistent increase in body mass in this period compared to interglacials. This was assumed to have been due to behavioural and dietary adaptations instead. However, this may have meant that *C. crocuta* was unable to conserve enough body heat in the harshest conditions.

Table 7.1: Climatic conditions and vegetation reconstructed from assemblages in which *C. crocuta* were found. All assemblages are MIS 3 of age, with the exception of Cova del Gegant, which has been dated to MIS 4-3 (Daura et al., 2010). Radiocarbon dates are the modelled dates on *C. crocuta* included in Figure 7.1.

Site	**Dates (cal BP)**	**Climate**	**Dominant vegetation**			**References**
			Open/grassland	***Semi-open/mixed***	***Closed/forested***	
Cave Earth, Kents Cavern, Britain	44,947-42,882 42,788-41,381 35,622-34,075		x			Bocherens *et al.* (1995), Bocherens (2014)
Grange Farm, Britain		Cool, dry climate	x			Cooper *et al.* (2012)
Lower Cave Earth, Pin Hole, Britain	42,388-41,381		x			Jacobi *et al.* (2006), Jacobi and Higham (2011), Lewis (2011)
4eme Niveau, Caverne Marie Jeanne, Belgium		Mean annual temperature = 3.35°C. Mean annual precipitation = 1018 mm		x		Ballmann *et al.* (1980), Brace *et al.* (2012), López-García *et al.* (2017)
5eme Niveau, Caverne Marie Jeanne, Belgium		Mean annual temperature = 4.1°C. Mean annual precipitation = 1023 mm		x		Ballmann *et al.* (1980), Brace *et al.* (2012), López-García *et al.* (2017)
6eme Niveau, Caverne Marie Jeanne, Belgium		Mean annual temperature = 4.22°C. Mean annual precipitation = 1000 mm		x		Ballmann *et al.* (1980), Brace *et al.* (2012), López-García *et al.* (2017)
Höhle Výpustek, Czech Republic				x		Liebe, (1879), Hofreiter *et al.* (2004), Rohland *et al.* (2005)
Dzeravá skala (Pálffy Cave), Slovakia				x		Kaminská *et al.* (2006)

Unit T2, Trapeznyi Chamber, Bukovynka Cave, Ukraine		Relatively warm and dry interstadial		x		Ridush (2009), Gerasimenko *et al.* (2014)
Branica II, Serbia		Cold climate	x			Argant and Dimitrijević (2007), Dimitrijević (2011), Stuart and Lister (2014)
Couche 4, Redaka II, Bulgaria		Cold climate (but not Arctic conditions)	x			Fernandez and Guadelli (2008), Guadelli *et al.* (2013), Raynal *et al.* (2013)
Couche VI, Secteur II, Temnata, Bulgaria		Cool climate with some precipitation	x			Tsanova (2006) and references therein
Couche 4, Secteur I, Temnata, Bulgaria		Cool and dry climate	x			Tsanova (2006) and references therein
Couche 11a, Bacho Kiro, Bulgaria		Dry and warming climate				Kozłowski (1982) cited in Tsanova (2006), Tsanova (2006)
Couche 11, Bacho Kiro, Bulgaria		Humid and warming climate				Kozłowski (1982) cited in Tsanova (2006), Tsanova (2006)
Couche 10, Bacho Kiro, Bulgaria		Warming climate				Kozłowski (1982) cited in Tsanova (2006), Tsanova (2006)
Couche 9, Bacho Kiro, Bulgaria		Dry and cold climate				Kozłowski (1982) cited in Tsanova (2006), Tsanova (2006)
Couche 6c, Bacho Kiro, Bulgaria		Dry and cold climate				Kozłowski (1982) cited in Tsanova (2006), Tsanova (2006)
Couche 6b, Bacho Kiro, Bulgaria		Dry climate				Kozłowski (1982) cited in Tsanova (2006), Tsanova (2006)
Couche 7/6a, Bacho Kiro, Bulgaria		Dry climate				Kozłowski (1982) cited in Tsanova (2006), Tsanova (2006)
Unità Stratigrafica 8, Tana delle Iena, Italy				x		Conti *et al.* (2012), Gatta *et al.* (2016)
SU 11, Area 3, Cava Muracci, Italy				x		Gatta *et al.* (2016), Gatta and Rolfo (2017)
Level 8. Jonzac, France		Temperate climate	x			Richards *et al.* (2008), Bocherens (2015)

Cova del Gegant, Spain		Cooler and wetter than today. Mean annual temperature = 10±2.6°C. Mean temperature of coolest month = 2.6±0.7°C. Mean temperature of warmest month = 20.1±1°C. Mean annual precipitation = 850±150 mm.		x		López-García *et al.* (2008), Daura *et al.* (2010)
Chamber X, Level III, Cova de les Toixoneres, Spain		Humid and temperate climate.		x		López-García *et al.* (2012), Talamo *et al.* (2016)
Chamber X, Level II, Cova de les Toixoneres, Spain		Drier and cooler climate than Level III.		x		López-García *et al.* (2012), Talamo *et al.* (2016)

The potential relationship between temperature and *C. crocuta* absence during MIS 3 may help to explain why *C. crocuta* was absent from Britain during MIS 11 (Schreve, 2001) and possibly from the rest of Europe too (Stuart and Lister, 2014). This absence may have been due to the preceding MIS 12, one of the most severe glacial periods in Middle and Late Pleistocene (Shackleton, 1987). In light of the apparent adverse impact of cold temperatures upon *C. crocuta* populations, MIS 12 may have caused populations to contract far south, meaning that they were then unable to recolonise Europe during the following interglacial. Similarly, the absence of *C. crocuta* in Britain during MIS 5a (Turner, 2009) may have been due to the cold conditions of preceding MIS 5b (Currant and Jacobi, 2011).

The second potentially important palaeoclimatic variable for *C. crocuta* extirpation is precipitation. Today, *C. crocuta* abundance is also greatest where precipitation of the driest month is greater, i.e. in less arid conditions (Section 5.1). Unfortunately, there are few quantitative precipitation records reconstructed from assemblages in which *C. crocuta* have been found. One exception is the mean annual palaeoprecipitation reconstruction from Caverne Marie Jeanne, with estimates of 1,018 mm from the 4eme Niveau, 1,023 mm from the 5eme Niveau and 1,000 mm from the 6eme Niveau (López-García *et al.*, 2017). However, this does not allow for an assessment of whether there were any arid periods during the year. Most of the MIS 3-aged assemblages within which *C. crocuta* has been found (Table 7.1) indicate dry conditions, although some indicate wetter or humid climates. The precipitation of the driest month records of sites included in the biomass analyses range from 0 to 29 mm (Spreadsheet 1), so although *C. crocuta* can tolerate periods of drought, their populations are smaller (Section 5.1).

During periods of aridity, *C. crocuta* will acquire water from fresh carcasses (Cooper, 1990). However, water is limited with increasing desiccation and lack of prey may reduce *C. crocuta* populations (Gasaway *et al.*, 1991). The availability of prey will be explored in more detail in Section 7.3.2.

By contrast, precipitation may have had a negative impact upon *C. crocuta* if it fell as snow, which was likely given the cold conditions of MIS 3. *C. lupus* can successfully hunt ungulates in snow cover, even that over 40 cm depth (Bobek *et al.*, 1992; Gula, 2004), and so was likely able to cope with any periods of elevated snow cover during MIS 3. However, given that snowfall does not appear to be a feature of *C. crocuta* habitats today, it is unclear whether *C. crocuta* would have struggled in deep snow during MIS 3.

A further environmental factor of interest is vegetation. Today, semi-open vegetation cover is positively associated with *C. crocuta* biomass, whereas open vegetation has a negative association (Section 5.1). It may be expected that an expansion of open grassland may have reduced *C. crocuta* biomass and led to their extirpation.

The MIS 3-age assemblages in Table 7.1 all indicate that *C. crocuta* inhabited landscapes that had predominantly open/grassland and semi-open/mixed vegetation cover. Unfortunately, very few of those deposits with reconstructed vegetation also yielded *C. crocuta* dates that were also included in the model. Of those that did, Pin Hole yielded one date (42,388-41,381 cal BP), which is prior to the extirpation of *C. crocuta* from much of Europe. Kents Cavern yielded three dates (44,947-42,882, 42,788-41,381 and 35,622-34,075 cal BP). If open steppe tundra were present (as suggested by Bocherens, 2014) during these three time periods, then vegetation may not have influenced the extirpation of *C. crocuta* as the first two dates are prior to the absence of the species from much of Europe.

Overall, it is difficult to draw conclusions about the influence of local palaeoenvironmental conditions upon *C. crocuta* extirpation because of the limited number of environmental reconstructions associated with dated *C. crocuta* material, and due to limited direct dates on material. Future work could involve collating well-dated palaeoenvironmental records from nearby sites such as lakes, and tying these to the inferred *C. crocuta* presence/absence events, in addition to improving the chronology of *C. crocuta* itself.

In contrast to *C. crocuta*, the final records of *P. leo (spelaea)* occur much later in the Pleistocene. The last dated record is 14,583-14,221 cal BP, with the end boundaries of the Northwestern, Central and Southeastern regions suggesting that the species may have persisted beyond this date. However, there is a gap in the dates between 28.6 and 15.1 ka, which covers most of the Last Glacial Maximum (26.5-19 ka, Clark *et al.*, 2009). If this gap is a true reflection of *P. leo (spelaea)* absence, and not a consequence of sampling bias or lack of preservation under extreme conditions, the species may have temporarily disappeared from Europe or become restricted to refugia before recolonising, which *C. crocuta* apparently failed to do. The conditions during the Last Glacial Maximum may have been too severe for *P. leo* (*spelaea*), thus causing the temporary absence of the species from Europe.

Within the individual regions, *P. leo (spelaea)* may have been absent prior to the extirpation of *C. crocuta*. The end boundary of the Southeastern region is 35.5-32 ka compared with *C. crocuta*'s end boundary of 31-28.2 ka. In the Northwestern region, although there are only three dates, there is a potential absence of *P. leo (spelaea)* from 39.3 to 15.1 ka, prior to the

extirpation of *C. crocuta* at 35-33.7 ka. Finally, in the Southwestern region, there are again only three dates, indicating a potential absence of *P. leo (spelaea)* between 46.3 and 17 ka, again prior to the extirpation of *C. crocuta* to this region at 31.7-26.2 ka. This pattern might change if additional *P. leo (spelaea)* specimens are dated. However, at present the models suggest that *P. leo (spelaea)* were absent from the Southeastern, Southwestern and Northwestern regions long before the final disappearances of *C. crocuta*.

In the Central region, there is a different pattern, with two hiatuses in *P. leo* (*spelaea*). The earlier one is between 41,859 to 32,763 cal BP, a period within which *C. crocuta* likely disappeared from the region. Additionally, both species appear to have been absent from Europe during a similar time period, around 39-38.3 ka for *C. crocuta* and 39.3-38.6 in *P. leo* (*spelaea*).

In contrast to present-day *C. crocuta* biomass, modern *P. leo* biomass does not appear to be as strongly influenced by environmental conditions (Section 5.1). However, this does not match the evidence during the Pleistocene, given that *P. leo* (*spelaea*) were absent from three regions prior to the extirpation of *C. crocuta*, and both species were absent from Europe during the cold conditions around 39.3-38.3 ka. The reason for the difference between the biomass responses of *C. crocuta* and *P. leo* in the present-day, and the absence of *C. crocuta* and *P. leo* (*spelaea*) during the Pleistocene may actually lie in competition, which will be discussed in Section 7.3.2.

7.3.2 Diet and competition

A further potential cause of extirpation is food availability, which may be influenced by the population biomass of prey species and degree of competition for food with other carnivores.

The findings from Section 5.1 indicate that biomasses of Périquet *et al.*'s (2015) medium-sized prey class (120-400 kg) have the greatest positive influence upon *C. crocuta* biomass in Africa today. This is followed by very small-sized (<20 kg) and small-sized prey (20-120 kg).

Based on Collinge's (2001) body mass reconstructions of Pleistocene species from Britain, *C. elaphus* would be classed as medium-sized prey. Some smaller *E. ferus* and larger *R. tarandus* also fall into this size category. None of the species included in Collinge's (2001) study fall into the very small-sized prey category, although the smallest weight of *C. capreolus* was estimated to be 20 kg, which is on the border between the very small- and small-sized prey. It may therefore be expected that the presence of these species were most important for *C. crocuta* populations during the Pleistocene.

Table 7.2 lists the species found in MIS 3-age assemblages that are assumed to have been *C. crocuta* dens. The assemblages included are those that interpreted as *C. crocuta* dens and where the stratigraphic detail is provided as to the level. Also included are likely *C. crocuta* dens that lack stratigraphic information, but with evidence of damage to bones that was likely caused by *C. crocuta*. It is acknowledged that there are limitations to this information. For example, where a site was used by more than one carnivore, a species other than *C. crocuta* may have accumulated some of the bones, or a different species may have damaged the bones.

At least 17 herbivore species were found in the *C. crocuta* dens listed in Table 7.2. There is direct evidence of *C. crocuta* damage on a number of these, including *M. primigenius*, *C. antiquitatis*, *Equus* sp., *R. tarandus*, *C. elaphus*, *M. giganteus* and *Bos*/*Bison*. There is also evidence of damage to bones of other species, including *U. arctos*, *G. gulo* and humans.

Given the range of species present in Pleistocene assemblages and the range of species for which there is direct evidence of consumption, it appears that *C. crocuta* were generalists in their diet, as far as diversity of species targeted. A broad diet of diverse prey is also suggested by dietary isotopes of MIS 3 *C. crocuta* from the Ardennes, Belgium, which targeted most of the prey species present (Bocherens *et al.*, 2011; Bocherens, 2015). This flexibility is seen today, with *C. crocuta* preferentially targeting species depending upon their local availability and ease of capture (Mills, 1990; Holekamp *et al.*, 1997; Hayward, 2006). This leads to different species making up different proportions of *C. crocuta*'s diet in different areas (see review in Section 2.3.3).

Taphonomic and dietary isotopic evidence has pointed to the most important species in Pleistocene *C. crocuta*'s diet in different areas in Europe. For example, the most important species for *C. crocuta* in many sites in Late Pleistocene Italy was *C. elaphus* (Stiner, 2004). Reanalysis of the dietary isotopes of MIS 3-aged fauna from Level 8, Jonzac, France revealed that *C. crocuta* were consuming mostly *M. giganteus*, *Bos*/*Bison* and some *Equus* sp (Richards *et al.*, 2008; Bocherens, 2015).

Table 7.2: Potential competitors and large potential prey species of *C. crocuta*. All assemblages are assumed to be accumulations in dens by the authors, or inferred from the presence of coprolites, juvenile *C. crocuta* or carnivore-damaged bones. All assemblages are dated to MIS 3. Domestic species were not included. Where there is no indication of a stratigraphic level, only species exhibiting clear *C. crocuta* damage are listed. Where only the genus is listed, a number indicates how many species were present, where known. P = present, including sub-species. p = presence of remains identified to same genus or family. ? = uncertainty about identification. A = human presence known only through artefacts or damage to bones. G = specimens gnawed or otherwise damaged, potentially by *C. crocuta*. I = isotopic evidence of consumption of species by *C. crocuta*. *Some uncertainty over contemporaneity with *C. crocuta*.

Site	***P. leo (spelaea)***	***Lynx* sp.**	***C. lupus***	***U. arctos***	***U. spelaeus***	***G. gulo***	***Homo* sp.**	***M. primigenius***	***Equus* sp.**	***C. antiquitatis***	***S. hemitoechus***	***S. scrofa***	***A. alces***	***C. capreolus***	***R. tarandus***	***D. dama***	***C. elaphus***	***M. giganteus***	***B. primigenius***	***B. priscus***	***Ovibos* sp.**	***C. ibex***	***R. rupicapra***	**References**
Layer A2, Badger Hole, Britain				P					1						P ?			P						Campbell (1977)
Brixham Cave/Windmill Hill, Britain				G				G		G														Falconer, (1858), cited in Prestwich, (1873), Prestwich (1873), McFarlane *et al.* (2010)
Caerwent Quarry, Britain								G																Locke (1970)
Ffynnon Beuno, Britain								G	G	G					G		G							Hicks (1885), Aldhouse-Green *et al.* (2015)
Grange Farm, Britain						G		G		G														Cooper *et al.* (2012)
Goat's Hole Paviland, Britain										G														Turner (2000)
Cave Earth, Kents Cavern, Britain				G		G		G	G	G					G		G	G	G					Wilson (2010)
Unit 3c, King Arthur's Cave, Britain				P			A	P	1	P							P							ApSimon *et al.* (1992)

Site	*P. leo (spelaea)*	*Lynx* sp.	*C. lupus*	*U. arctos*	*U. spelaeus*	*G. gulo*	*Homo* sp.	*M. primigenius*	*Equus* sp.	*C. antiquitatis*	*S. hemitoechus*	*S. scrofa*	*A. alces*	*C. capreolus*	*R. tarandus*	*D. dama*	*C. elaphus*	*M. giganteus*	*B. primigenius*	*B. priscus*	*Ovibos sp.*	*C. ibex*	*R. rupicapra*	References
Unit 3d, King Arthur's Cave, Britain				P *			A	P	1	P					P		P		p					Currant (n.d.), cited in ApSimon *et al.* (1992), ApSimon *et al.* (1992)
Unit 3e, King Arthur's Cave, Britain				P			A	P	1	P					P		P		p		P			ApSimon *et al.* (1992)
Layer 3, Picken's Hole, Britain	P		P *	P *			P	P	1	P					P		P	P ?	p					Tratman (1964)
Lower Cave Earth, Pin Hole, Britain	P		P	P			P	P	1	G					P			P		P				Busk (1875), Currant and Jacobi (2011)
Laminated Clay, Priory Farm Cave, Britain			P	P				G	1						P				p					Cowley (1933), Grimes (1933)
Castlepook Cave, Ireland				G *				G							G			G						Ussher, (1906), Scharff *et al.* (1918), Sutcliffe (unpublished data) cited in Woodman *et al.* (1997), Woodman *et al.* (1997), Stuart and Lister (2014)
4eme Niveau, Caverne Marie Jeanne, Belgium	P	1	P		P			P	1	P					P		P		p			P	P	Ballmann *et al.* (1980), Gautier (1980), Brace *et al.* (2012)
5eme Niveau, Caverne Marie Jeanne, Belgium								P	1						P							P	P	Ballmann *et al.* (1980), Gautier (1980), Brace *et al.* (2012)
6eme Niveau, Caverne Marie Jeanne, Belgium			P						1	P				P	P		P		p			P		Ballmann *et al.* (1980), Gautier (1980), Brace *et al.* (2012)
Unit T2, Trapeznyi Chamber, Bukovynka Cave, Ukraine					P				1	P		P						P	P	P				Bondar and Ridush (2015)

Site	*P. leo (spelaea)*	*Lynx* sp.	*C. lupus*	*U. arctos*	*U. spelaeus*	*G. gulo*	*Homo* sp.	*M. primigenius*	*Equus* sp.	*C. antiquitatis*	*S. hemitoechus*	*S. scrofa*	*A. alces*	*C. capreolus*	*R. tarandus*	*D. dama*	*C. elaphus*	*M. giganteus*	*B. primigenius*	*B. priscus*	*Ovibos sp.*	*C. ibex*	*R. rupicapra*	References
Couche 4, Redaka II, Bulgaria	P	1	P		P		A	P ?	2								P	P		P		p		Fernandez and Guadelli (2008), Guadelli *et al.* (2013), Raynal *et al.* (2013)
Couche VI, Secteur II, Temnata, Bulgaria			P				A		2				P	P			P	p ?		p		p	P	Tsanova (2006) and references therein
Unità Stratigrafica 8, Tana delle Iena, Italy			P				A		2 G			P		P		P	P		G					Conti *et al.* (2012)
SU 11, Area 3, Cava Muracci, Italy			P						1		P	P		P		P	P		P					Gatta and Rolfo (2017)
Level J, Les Roches-de-Villeneuve, France	P		P	P ?			G		G											p G				Beauval *et al.* (2005)
Lower assemblage, La Chauverie, France							A		1						P		P		p					Discamps *et al.* (2012a)
Upper assemblage, La Chauverie, France							A		1						P		P		p					Discamps *et al.* (2012a)
Couche 6, Gallerie II, La Grotte de Bourdette, France									P						P			p	p					Discamps *et al.* (2012b)
Couche 7, Gallerie II, La Grotte de Bourdette, France			P		P				P	p		P			P				p					Discamps *et al.* (2012b)
Couche 8, Gallerie II, La Grotte de Bourdette, France			P		P			P	G			P			P			p	p					Discamps *et al.* (2012b)

Despite the frequency with which *C. antiquitatis* occurred in *C. crocuta* dens (Table 7.2), and therefore its apparent importance as food, there is no clear association between the episodes of absence of the species and the absence of *C. crocuta* in the Northwestern region. The chronological model indicates two potential absences of *C. antiquitatis* from the Northwestern region (around 37.6-35.4 and 27.3-16.8 ka), which occur after the apparent brief absence of *C. crocuta* from this region (39.6-38.3 ka), and before and after the extirpation of *C. crocuta* from this region (modelled to be around 35-33.6 ka). The reason for this may lie in the fact that the minimum reconstructed body masses of *C. antiquitatis* from MIS 3 in Britain is 1808±360 kg (Collinge, 2001), falling within Périquet *et al.*'s (2015) very large-size prey class, which has little influence upon present-day *C. crocuta* biomass (Section 5.1), although juvenile *C. antiquitatis* were targeted, as shown in Kents Cavern (Wilson, 2010). So while *C. antiquitatis* appears to have been an important prey as evidenced by the presence of its bones in *C. crocuta* dens in British and Belgian (Northwestern region) assemblages (Table 7.2), the presence of other prey species may have prevented the extirpation of *C. crocuta* during the absence of *C. antiquitatis* around 37.6-35.4 ka. However, populations of *C. antiquitatis* may have been affected by periods of increased snow cover during MIS 3, in light of the species' intolerance of deep snow (Schreve *et al.*, 2013), potentially leading to reduced food availability for *C. crocuta*. Future research on dietary isotopes from well-dated deposits in the Northwestern region may help determine when *C. antiquitatis* made up an important proportion of *C. crocuta*'s diet.

There is only one date on *C. antiquitatis* from the Southwestern region and one from the Southeastern region, which are both more than 10,000 years prior to the extirpation of *C. crocuta* from these regions. More dates are needed from these regions before a conclusion can be drawn about the relationship between the timing of the extirpation of both species.

In the Central region. *C. antiquitatis* may have been absent from this region from 40 to 25.5 ka, potentially affected by the more continental climate of this region. *C. crocuta* became extirpated around 41.3-38.4 ka. If the actual last occurrence of *C. crocuta* was towards the younger range of this end boundary, this may imply that the absence of an important food source contributed to the extirpation of *C. crocuta*.

As mentioned, *C. elaphus* and *R. tarandus* belong to the prey size classes that are most influential in dictating present-day *C. crocuta* biomass. It may therefore be expected that there is some link between the chronology of these species and that of *C. crocuta*. There is one date on *C. elaphus* material from the Central and Southeastern regions but both pre-date the extirpation of *C. crocuta* from these regions, thereby highlighting the need for additional dating.

There is a potential link between *C. elaphus* and *C. crocuta* in the Northwestern region. *C. elaphus* was absent from 34.4 to 33.7 ka, while *C. crocuta* disappeared around 35-33.7 ka. If the later estimate of *C. crocuta* extirpation is true, it may have occurred at the time of *C. elaphus* absence. Interestingly, in Britain, *C. elaphus* was one of the two species with a body mass that increased in line with *C. crocuta*, although it is difficult to determine whether the covariation was causal, or whether both species were responding in a similar way to environmental changes. Nevertheless, the trend suggests that *C. crocuta* were still able to prey upon the large *C. elaphus* during MIS 3 (Section 6.1). This, linked with the importance of medium-sized prey such as *C. elaphus*, and evidence of carnivore damage to the bones of this species from sites such as Kents Cavern (Wilson, 2010) and Ffynnon Beuno (Aldhouse-Green *et al.*, 2015), points to the possible importance of *C. elaphus* as a food source in the Northwestern region. Therefore, the absence of *C. elaphus* may have contributed to the extirpation of *C. crocuta*. A further consideration is that in Britain, *C. elaphus* were already restricted in their range during MIS 3 as they were only found in southern Britain (Currant and Jacobi, 2011). This highlights that a potentially important food source was not available to more northern populations of *C. crocuta*, perhaps increasing their vulnerability.

Similarly, in the Southwestern region, *C. elaphus* were potentially absent between 31.4 and 26.1 ka. *C. crocuta* likely became extirpated from this region between 31.7 and 26.2 ka. There is evidence of *C. elaphus* in MIS 3-aged *C. crocuta* assemblages in this region such as La Chauverie, France (Discamps *et al.*, 2012a). In southwestern France from assemblages of MIS 3 age, isotopic evidence indicates that important prey species in this area were *C. elaphus* in addition to *R. tarandus*, *Bos*/*Bison*, *M. giganteus* and *E. ferus* (Bocherens *et al.*, 2005).

The final new chronological model was produced on dates of *R. tarandus*. This species may have been absent for a short period in the Northwestern region between 35.5 and 34.7 ka, which is similar to the timing of extirpation of *C. crocuta* in this region (35-33.7 ka). However, the absence of *R. tarandus* was unlikely to have been due to cold conditions, given the northern habitats of the species today, some of which are within the Arctic Circle (Gunn, 2016). Remains of *R. tarandus* were present in many *C. crocuta* assemblages in the Northwestern region, including bones that exhibit carnivore damage (Table 7.2). *C. crocuta* from the Kents Cavern Cave Earth displayed a wide range of isotopic values (Bocherens *et al.*, 1995), which the author suggested may have been due to some individuals becoming more specialist and relying on a smaller range of species, such as *R. tarandus*, during periods of reduced prey availability. *C. crocuta* may therefore have become extirpated in response to the absence of both *R. tarandus* and *C. elaphus* in this region.

In the Southwestern region, there are two potential periods of absence of *R. tarandus*, the second of which occurred between 31.3 and 23.1 ka. This is around the time of the modelled extirpation of *C. crocuta* from this region (31.7-26.2 ka). As mentioned, *R. tarandus* was an important prey species in southwestern France during MIS 3 (Bocherens *et al.*, 2005). Again, *C. crocuta* may have been responding to the absence of both *R. tarandus* and *C. elaphus* in this region. By contrast, the periods of absence of *R. tarandus* from the Central region occur after the extirpation of *C. crocuta* from this region.

Finally, Discamps (2014) assessed reconstructed prey biomass in southwestern France. As mentioned, *C. crocuta* appear to be largely absent from Europe between 39-38.3, around the time that Discamps (2014) found that *C. crocuta* disappeared from the north of the Aquitaine basin, where prey biomass was generally low, coupled with seasonal migrations of *R. tarandus* that resulted in only seasonally available resources. It is unclear at present whether these conditions occurred elsewhere in Britain to cause the widespread absence of *C. crocuta*. Migrations of species such as *R. tarandus* might prohibit occupation of *C. crocuta* from an area if sufficient residential prey were unavailable, although this may be difficult to detect in the available records.

Overall, the extirpation of *C. crocuta* from the Central region may be in response to the absence of *C. antiquitatis*. The extirpation of *C. crocuta* from the Northwestern and Southwestern regions may be in response to the absence of *R. tarandus* and *C. elaphus*. However, since there were also cold climate conditions around the time of *C. crocuta* extirpation from the Southwestern region (Section 7.3.1), these may have been a contributing, if not the key, driving factor in *C. crocuta* decline.

Further radiocarbon dates are needed to clarify the timing of the presence and absence of these species, in particular in the Southern and Southeastern regions.

The second potential influence upon food availability is competition. Today, competition has a negligible influence upon *C. crocuta* biomass, which is evidenced through the weak correlation with other large carnivore biomasses (Section 5.1). Indeed, while exploitation and interference competition exists between *C. crocuta* and other large carnivores (e.g Kruuk, 1972; Mills, 1990; Cooper *et al.*, 1999; Breuer, 2005), there is evidence of environmental partitioning allowing multiple carnivores to inhabit the same area. This environmental partitioning may involve the carnivores occupying different types of vegetation (e.g. Schaller, 1972, Section 5.1), hunting at different times of the day (Schaller, 1972; Hofer, 1998; Mills, 1998; Périquet *et al.*, 2015), or targeting different species or age classes of prey (Mills, 1990; Périquet *et al.*, 2015).

Although competition does not appear to influence *C. crocuta* populations today, this may not have been the case during the Pleistocene, since not only were there different species coexisting but different environmental conditions may have prevented or disrupted some of the environmental partitioning seen today.

As outlined in Table 7.2, during the Pleistocene there were multiple large carnivores that may have competed with *C. crocuta* for food. Taphonomic evidence and dietary isotopes have shed some light upon competition between these species.

In Late Pleistocene Italy, taphonomic evidence indicated that *C. crocuta* and hominins had similar prey preferences, with *C. elaphus* as the most important prey. *C. crocuta* targeted slightly more *Equus* sp. and *B. primigenius*, and hominins targeted slightly more small ungulates. The main difference was with *C. lupus*, which targeted more *C. ibex* and *C. capreolus* in addition to smaller species (Stiner, 1992, 2004). However, *C. crocuta* and *C. lupus* targeted mostly the oldest and youngest prey individuals whereas hominins preyed on prime-aged adults (Stiner, 2004).

There were also similarities in the diets of *C. crocuta* and *H. neanderthalensis* during MIS 4 and 3 in France, with both species consuming bovids, equids and cervids. However, *H. neanderthalensis* consumed more cervids. *C. crocuta* consumed more bovids and equids, and a more diverse range of fauna, including other carnivores (Dusseldorp, 2013a). A similar pattern was seen in Level 8 at Jonzac, France with *C. crocuta* and *H. neanderthalensis* both consuming *Bos*/*Bison* and *E. caballus*, although *C. crocuta* preferentially targeted *M. giganteus* (Richards *et al.*, 2008; Bocherens, 2014). Similarly, in MIS 3-aged assemblages from Les Rochers-de-Villeneuve, bones of *Bison* sp. and *Equus* sp. exhibited damage caused by both *C. crocuta* and *H. neanderthalensis*, indicating competition (Beauval *et al.*, 2005). Again, dietary isotopes indicated that in southwestern France during MIS 3, *C. crocuta* and *H. neanderthalensis* consumed similar amounts of *Bos*/*Bison*, *M. giganteus*, *C. elaphus* and *E. ferus*. More *R. tarandus* was consumed by *C. crocuta*, whereas more *C. antiquitatis* and *M. primigenius* were consumed by *H. neanderthalensis* (Bocherens *et al.*, 2005).

By contrast, Naito *et al.* (2016) analysed dietary isotopes of fauna from Spy Cave (Belgium), finding similarities between *C. lupus* and *H. neanderthalensis*, and differences between *H. neanderthalensis* and *C. crocuta*. One *H. neanderthalensis* individual did not preferentially consume any herbivore species, while the other individual relied most heavily upon *R. tarandus*, *E. caballus* and Bovidae sp. The diet of *H. neanderthalensis* was supplemented by intake of plants. These authors suggested that the different isotopic signature of *C. crocuta* may have been due to the consumption of juvenile herbivores, other carnivores, or of different parts of

the carcass in comparison to Neanderthals. Whatever the reason, Naito *et al.* (2016) concluded that *C. crocuta* and *H neanderthalensis* were not competing for food.

Yeakel *et al.* (2013) calculated the degree of dietary specialisation of predators in the Ardennes (Belgium) and Swabian Jura (Germany) during MIS 3 from dietary isotopes. In the Ardennes, *C. crocuta* consumed a wider range of prey species than both *C. lupus* and *H. neanderthalensis*. By contrast, in the Swabian Jura, *H. neanderthalensis* consumed a wider range of prey species than *C. crocuta*.

C. crocuta and *P. leo* (*spelaea*) from MIS 3-aged assemblages Ziegeleigrube Coenen, Germany exhibited separate niches, exhibited by dietary isotopes (Wißing *et al.*, 2015). This separation of *C. crocuta* and *P. leo* (*spelaea*) was also observed in the Belgian Ardennes, while the diets of *G. gulo, P. pardus* and some *U. arctos* overlapped with those of *C. crocuta*. While *C. crocuta* likely consumed most of the prey species present, *C. lupus* relied upon *R. rupicapra*, *C. elaphus* and *M. giganteus* due to being outcompeted by *C. crocuta* for other prey species such as *M. primigenius*, *C. antiquitatis* and *E. ferus*. Likewise, *P. leo (spelaea)* were apparently restricted to *R. tarandus* and *Ursus* sp. cubs. The only *P. spelaea* individual with values overlapping those of *C. crocuta* post-dated the extirpation of *C. crocuta* from Europe, suggesting that *C. crocuta* had previously outcompeted *P. spelaea* (Bocherens *et al.*, 2011; Yeakel *et al.*, 2013; Bocherens, 2015). The reliance of *P. leo (spelaea)* on *R. tarandus* and bear cubs when *C. crocuta* was present was also observed in the Swabian Jura, Germany (Bocherens *et al.*, 2011).

P. leo (*spelaea*) may have been solitary hunters, based on a review of *P. leo* (*spelaea*) dietary isotopes, which indicated each individual was consuming different prey, rather than all *P. leo* (*spelaea*) exhibiting similar isotopic values (Bocherens *et al.*, 2011). If *P. leo* (*spelaea*) were indeed solitary hunters, large groups of *C. crocuta* may have easily outcompeted them, explaining the different diets of both species outlined above. In contrast, the large size of adult *U. arctos* may have tempered competition from *C. crocuta*, while *P. pardus* may have cached their food to safeguard it from *C. crocuta* (Bocherens *et al.*, 2011).

The lack of competition of between *C. crocuta* and *P. leo (spelaea)* is also indicated by the timing of the presence of both species. In the Southeastern region, *P. leo (spelaea)* disappeared earlier than *C. crocuta*. Additionally, *P. leo (spelaea)* were apparently absent from the Northwestern and Southwestern prior to the extirpation of *C. crocuta*. Unless these dates do not cover the entirety of *P. leo (spelaea)* occupation, it is likely that lions did not outcompete *C. crocuta* and contribute to its extirpation. The exception is the Central region, where *C. crocuta* became extirpated while *P. leo (spelaea)* persisted, although *P. leo (spelaea)* may have been absent for a short period around the time of *C. crocuta*'s extirpation. However, as mentioned, *P. leo*

(spelaea) were out-competed by *C. crocuta* in the Swabian Jura in the Central region during MIS 3 (Bocherens *et al.*, 2011).

The above evidence suggests that there was some competition between *H. neanderthalensis* and *C. crocuta* for food. Except for uncertainties with dates from southern Iberia, the last *H. neanderthalensis* in Europe were around 41-39 ka (Higham *et al.*, 2014). This is prior to the extirpation of *C. crocuta* from Northwestern, Southwestern, Southeastern and Southern Europe, meaning that competition with *H. neanderthalensis* would not have contributed to their extirpation from these areas. The youngest *H. neanderthalensis* date does overlap with the absence of *C. crocuta* from much of Europe, and the extirpation of *C. crocuta* from the Central region. The dates therefore do not preclude competition with *H. neanderthalensis* as contributing to these two *C. crocuta* events.

Overall, the evidence suggests that there was limited competition for food between *C. crocuta* and *C. lupus*. Some competition occurred between *C. crocuta* and *U. arctos, G. gulo* and *P. pardus*. However, today, *C. crocuta* will often out-compete *P. pardus* in direct competitive interactions (Mills, 1990). When *G. gulo* consumes ungulates, it usually does so by scavenging (Abramov, 2016). Today, *C. crocuta* is the dominant species in direct competitive interaction with another frequent scavenger, *P. brunnea* (Mills, 1990). This suggests that *P. pardus* and *G. gulo* likely did not outcompete *C. crocuta* for food. Therefore, unless prey became increasingly scarce towards the times of *C. crocuta* extirpation, it appears unlikely that *C. crocuta* populations were limited by the presence of other carnivores.

The final species of interest is modern humans. The first arrival of modern humans in Italy and Greece was just before 45 ka (Douka *et al.*, 2014), prior to the extirpation of *C. crocuta* from any of the regions. The first evidence of modern humans in Britain is dated to 42,350-40,760 cal BP (Higham *et al.*, 2011; Proctor *et al.*, 2017), prior to the extirpation of *C. crocuta* from the Northwestern region (35-33.7 ka). This means that the arrival of modern humans did not immediately cause the extirpation of *C. crocuta*. However, it is difficult to assess the size of populations of both species and the relationship between them. Unfortunately, there are also no isotopic studies comparing the species consumed by *C. crocuta* and modern humans.

Improved knowledge would come both from further dating and from further isotopic and taphonomic studies. This would allow an assessment of competition in a greater area of Europe and an evaluation of whether competition increased as certain herbivores became scarcer in different regions.

The assessment of bone consumption in this thesis has highlighted periods of increase in this behaviour. While this cannot shed light on whether prey biomass was low or competition was high, it does point to periods of low food availability. The craniodental morphometrics (Section 6.2) indicate that *C. crocuta* in Britain, Belgium (Northwestern region of Europe), Austria and the Czech Republic (Central region of Europe) had greater ability to consume bone during MIS 3 than *C. crocuta* in Britain during MIS 5e and 5c. This is supported by the frequency of broken premolars (Section 6.4); with one exception, all assemblages with elevated levels of broken premolars are of MIS 3 age. Some MIS 3-aged assemblages had lower proportions of broken premolars, suggesting that there were both periods of increased food stress and periods when there was sufficient food. Unfortunately, dating resolution is not sufficient to determine the climatic conditions that occurred during these periods of food stress, e.g. stadials/interstadials, or periods when prey species were absent or seasonally unavailable.

Similarly, dating resolution is not currently sufficient to determine whether these periods of elevated bone consumption occurred towards the end of *C. crocuta* presence in the Northwestern and Central regions, nor whether they can be linked to the absence of *C. crocuta* from most of Europe around 39-38.3 ka. If the periods of food stress occurred during these events in the *C. crocuta* chronology, this may link to the absence of *R. tarandus* and *C. elaphus* from the Northwestern region, and the absence of *C. antiquitatis* from the Central region.

Food stress may be linked to a lack of water during periods of aridity, as discussed above. Indeed, the Mammoth Steppe, which was present over much of Europe during the last glacial, occurred in arid conditions (Guthrie, 2001). Lower food availability would also mean fewer opportunities for the *C. crocuta* to obtain water from carcasses.

Further dating of the assemblages included in the tooth breakage study (Section 6.4) would help link the record of tooth breakage to the chronologies of *C. crocuta* and its prey, and to precipitation records. Particularly beneficial would be to date the broken teeth themselves.

7.3.3 Competition for shelter

The final factor to consider is competition for shelter, which may have been important during the harsher climatic periods of MIS 3. Today, dens are used by *C. crocuta* for sheltering the young, with a female and her cubs residing in natal dens (Boydston *et al.*, 2006), and older cubs inhabiting communal dens (East *et al.*, 1989; Holekamp and Smale, 1998), although the entrance to dens and hollows in the ground may be used to shelter adults during the day (Henschel *et al.*, 1979; Korb, 2000). During the Pleistocene, periods of colder climate conditions may have necessitated the use of dens as shelter for both adults and cubs. There is abundant evidence of

this across Europe, with remains of cubs, juveniles, prime-aged adults and old-aged adults found within caves (Diedrich, 2011a). This is further illustrated by the age profiles of the cave assemblages (Section 6.3), many yielding young, prime-aged and old adult *C. crocuta*.

Many caves were also used by other predators, leading to the potential for competition for shelter. This is indicated in Table 7.3, with some sites showing evidence of occupation by *U. spelaeus*, *C. lupus*, *P. leo (spelaea)* and humans, in addition to *C. crocuta*. At Cova de les Toixoneres, there is even evidence that *C. crocuta* may have inhabited in the interior of the cave at the same time as *H. neanderthalensis* occupied the front of the cave (Talamo *et al.* 2016).

Except for Cova de les Toixoneres, limitations of chronological resolution usually prevent assessment of the time between occupations of different species. This is illustrated by the occupations of sites by both *C. crocuta* and *H. neanderthalensis* in southwestern France (Discamps et al., 2012a, and references therein). However, Discamps et al. (2012a) suggested that in light of the apparent abundance of *C. crocuta* and *H. neanderthalensis* in southwestern France, both species likely competed for the use of caves. However, given that *H. neanderthalensis* disappeared from Europe around 41-39 ka (Higham *et al.*, 2014), competition for shelter with this species would not have prompted the later extirpation of *C. crocuta* from the Southwestern region.

As with the competition for food discussed above, it is unlikely that competition for shelter with *P. leo (spelaea)* was the cause of *C. crocuta* extirpation as the former species was absent prior to *C. crocuta* extirpation. The potential exception for this is the Central region.

In Serbia, there are very few known *C. crocuta* dens. Some caves had been occupied by humans, and many by *Ursus* sp. (Dimitrijević, 2011; Cvetković and Dimitrijević, 2014). As mentioned, *C. crocuta* became extirpated from the Southeastern region during a long period of cold conditions. If *C. crocuta* were outcompeted by *Ursus* sp. and humans for shelter, this may have contributed to its extirpation from this region.

Overall, competition for cave sites may have contributed to the extirpation of *C. crocuta* from Europe, particularly during the colder climatic conditions around the time of its final occurrences. Again, further dating of *C. crocuta* and other cave users could allow a better idea of the temporal separation of different occupations of caves.

Table 7.3: Cave sites used by *C. crocuta* and another species. All sites are dated to MIS 3.

Site	Use of cave	References
Höhle Výpustek, Czech Republic	*C. crocuta* and *U. spelaeus* den	Liebe (1879), Hofreiter *et al.* (2004), Rohland *et al.* (2005)
Couche 4, Redaka II, Bulgaria	Use of cave by *C. crocuta*, *V. vulpes* and *Homo* sp.	Fernandez and Guadelli (2008), Guadelli *et al.* (2013), Raynal *et al.* (2013)
Couche VI, Secteur II, Temnata, Bulgaria	Accumulation of assemblage by *C. crocuta* and *H. neanderthalensis*	Tsanova (2006) and references therein
Unità Stratigrafica 8, Tana delle Iena, Italy	Used by *C. crocuta, C. lupus, V. vulpes* and humans	Conti *et al.* (2012), Gatta *et al.* (2016)
Level J, Rochers-de-Villeneuve, France	Occupied by *C. crocuta* and *H. neanderthalensis*, with a short period of time between occupations	Beauval *et al*. (2005)
La Grotte de Bourdette, France	Occupied by *C. crocuta* and *U. spelaeus*	Discamps *et al*. (2012b).
Chamber X, Level III, Cova de les Toixoneres, Spain	*C. crocuta* occupied the interior of the cave (Chamber Y, Level 1) during approximately the same period that *H. neanderthalensis* occupied the front of the cave (Chamber X, Level III)	Talamo *et al.* (2016)

7.4 Conclusion

This chapter has presented new chronological models for *C. crocuta*, its competitor (*P. leo* (*spelaea*)) and three prey species (*C. antiquitatis*, *C. elaphus* and *R. tarandus*) in Europe during MIS 3.

The extirpation of *C. crocuta* from the Central region of Europe around 41.3-38.3 ka is too broad an estimate to attribute to a single stadial or interstadial period. However, the cold, continental nature of the climate may have contributed to the disappearance of *C. crocuta* from the region. The event may be linked to an absence of *C. antiquitatis* (a species often found in *C. crocuta* dens) from this region.

The second event noted is the potential absence of *C. crocuta* from much of Europe around 39-38.3 ka, which occurred during a prolonged stadial. This may also have been linked to low prey

biomass and seasonal availability of *R. tarandus*, as suggested by (Discamps, 2014) for southwest France.

C. crocuta became extirpated from the Northwestern region around 35-33.7 ka, potentially linked to the absence of *R. tarandus* and *C. elaphus*.

Finally, *C. crocuta* became extirpated from the Southwestern, Southern and Southeastern regions at around the same time (31.7-26.2 ka). This occurred during a period of stadials and short interstadials, which may have been exacerbated in the Southeastern region by competition for shelter with bears and humans. Absences of *R. tarandus* and *C. elaphus* may also have contributed to the extirpation of *C. crocuta* from the Southwestern region.

In the light of these new chronological models, this chapter has therefore presented some suggestions regarding the reasons for *C. crocuta* extirpation from Europe. Further dating is needed to assess more confidently the links between *C. crocuta* extirpation and *P. leo* (*spelaea*) presence, prey presence in Southeastern and Southern regions, periods of limited food availability, and competition for dens. Additionally, the *C. crocuta* chronological model should be compared with well-dated regional palaeoenvironmental records to assess further the influences of temperature, precipitation (particularly periods of aridity) and vegetation cover.

8 Conclusion

8.1 Overview

C. crocuta first appeared in Europe from around 850 to 780 ka (Garcia and Arsuaga, 2001). They eventually became widespread across Eurasia, particularly during the Late Pleistocene (when they are frequently the dominant carnivore in terms of numbers of remains), and were present during both warm and cold climatic periods (e.g. Currant and Jacobi, 2011) until their eventual extirpation around 31.7-26.2 ka.

This thesis set out to determine how the body size, morphology and palaeodiet responses of *C. crocuta* varied in response to Pleistocene environmental changes in Europe, as well as examining the possible causes of the extirpation of *C. crocuta* from Europe. This was paired with a study on the influence of climate, vegetation cover, food availability and competition upon present-day *C. crocuta* biomass, body size and morphometrics. The study of modern *C. crocuta* also highlighted any influences of age and sex on body size, morphometrics and tooth breakage to inform analytical methods and interpretation of the Pleistocene data.

The aims were as follows:

- To assess the body mass and morphometric responses of *C. crocuta* to Pleistocene environmental changes in Europe
- To assess the palaeodiet of *C. crocuta* from Pleistocene Europe, with a particular focus on bone consumption and frequency of predation versus scavenging
- To reassess the timing and potential reasons for the extirpation of *C. crocuta* from Europe

The present study expanded upon previous investigations of body mass and morphometrics of *C. crocuta* in Britain (Turner, 1981; Collinge, 2001) by increasing the temporal and spatial range of sites and including additional methods such as reconstructing mandibular bending strength and bite force, and the creation of a new model for reconstructing Pleistocene body mass. Fossil *C. crocuta* was therefore assessed across much of its chronological occupation of Britain, from the early Middle Pleistocene to MIS 3. In addition, the present study encompassed Late Pleistocene *C. crocuta* from Austria, Belgium, the Czech Republic, Ireland, Italy, Serbia and Spain in order to provide a more robust dataset for investigating any spatially distinctive trends.

8.2 Body size and morphometrics

The investigation of body size and morphometrics began with an assessment of present-day *C. crocuta*. This indicated that many cranial features measured were not fully grown in *C. crocuta* with P3/p3 wear stage III (the youngest age group considered in the study). This necessitated the exclusion of cranial measurements of individuals with wear stage III from future analyses. Additionally, some features continue growing through the life of an individual. This meant that prior to analysing the Pleistocene material, the data pertaining to these features were split into their different age classes. This was important to avoid mistaking an influence of ontogenetic age for an influence of environmental change.

Further assessment was undertaken on SSD in modern *C. crocuta*. This demonstrated that while there was predominantly female-dominated SSD in modern *C. crocuta* body masses, the degree of SSD is lower than other carnivores such as *P. leo*. For most of the craniodental and post-cranial measurements, there was no consistent direction in SSD. Furthermore, there were no environmental correlates with the degree of SSD, thus suggesting that the degree of SSD would not increase with changes in environmental conditions during the Pleistocene. Together, these observations indicated that the relative proportion of males and females in a Pleistocene assemblage should not influence the average body mass or morphometric measurement values. The results of the ontogeny and SSD investigations demonstrate the importance of assessing these characteristics in present-day individuals prior to an investigation of any Pleistocene material.

An assessment was made into the environmental influences upon craniodental and post-cranial measurements. Most measurements showed poor relationships with environmental variables. Two measurements (condylobasal length and length between the c-m1 alveoli) demonstrated similar signals, and further investigation determined that these measurements likely gave a robust indication of overall body size.

The investigation into Pleistocene *C. crocuta* began with a variation of the traditional method of reconstructing Pleistocene *C. crocuta* body masses. This method regressed average body masses of present-day *C. crocuta* from locations in Africa against average m1 lengths sourced close to the body mass study sites. The statistical results of this model indicated that the relationship between body mass and m1 length was significant and that the model was therefore suitable for reconstruction of Pleistocene body masses.

Pleistocene *C. crocuta* body masses were not consistently larger or smaller in either periods of cold or warm climate, nor was there any pattern observed with vegetation. This pattern was checked against the craniodental measurements, in particular those demonstrating body size

(condylobasal length and length between the c-m1 alveoli), which also showed overlaps in values between warm and cold periods.

The lack of consistent response in body mass and many of the morphometrics is in contrast to other carnivores, which exhibited size differences during the Pleistocene. *C. lupus* was particularly large during MIS 5a due to cold conditions and the absence of competition, whereas during MIS 3, the presence of competitors forced *C. lupus* to subsist on smaller prey resulting in body mass decrease (Flower and Schreve, 2014; Flower, 2016). *P. leo* (*spelaea*) was smaller in MIS 5e than MIS 3, due to the forested environment during MIS 5e leading to sub-optimal foraging and subsistence on smaller prey (Collinge, 2001). Finally, *U. arctos* was largest in MIS 5a, medium-sized in MIS 6, 5e, 5c and 3, and smallest during MIS 9 and 7. The larger sizes during MIS 6, 5a and 3 may have been due a reduction in plant biomass and resultant switch to a more carnivorous diet. No explanation was given for the medium-sized forms in MIS 5e and 5c (Collinge, 2001).

The lack of body size change in *C. crocuta* may have been due to behavioural responses, in particular fully consuming carcasses including the bones, which occurs today when there is low food availability (Kruuk, 1972). Additionally, *C. crocuta* out-competed other species such as *P. leo* (*spelaea*) and *C. lupus* (Bocherens *et al.*, 2011; Yeakel *et al.*, 2013; Flower and Schreve, 2014; Bocherens, 2015; Flower, 2016), and thus was not forced to subsist on smaller prey species, which may otherwise have resulted in body size change.

The exception to the lack of consistent body size change is the small size of *C. crocuta* from San Teodoro Cave in Sicily, indicating conformation to the Island Rule. Once Sicily was isolated from mainland Italy between 40 and 27 ka (Antonioli *et al.*, 2015), *C. crocuta* likely became smaller relative to mainland populations, likely a result of subsisting upon dwarf species on the island.

8.3 Palaeodiet

The investigation into the palaeodiet of *C. crocuta* focused on bone consumption and predation behaviour. A number of lines of evidence were used to interpret palaeodiet, including craniodental morphology, post-cranial morphology, body mass and tooth breakage.

Some of the craniodental morphometrics were used in the calculation of two mechanical principles. Mandibular bending strength was calculated by modelling the mandible as a beam, while bite force was measured through calculating the mechanical advantage of the mandible from the ratios of the in-lever and out-lever arms. When these principles had been previously applied to *C. crocuta*, it was usually in interspecific studies and using modern populations to

examine bending strength (Radinsky, 1981b; Van Valkenburgh and Ruff, 1987; Biknevicius and Ruff, 1992; Therrien, 2005; Ferretti, 2007; Meloro *et al.*, 2008; Palmqvist *et al.*, 2011). This was therefore the first study to attempt to assess changes in fossil *C. crocuta* mandible bending strength and bite force in this way.

Prior to assessing Pleistocene tooth breakage, the frequency of tooth breakage was assessed in modern *C. crocuta*. This was coupled with an assessment of tooth loss, which may occur through breakage of teeth (Losey *et al.*, 2014). Tooth loss overall made up a small proportion of the total teeth in modern populations. As jaws are often fragmented and thus loss of teeth cannot be identified in Pleistocene populations, the results indicated that missing lost teeth should not influence the overall assessment of bone consumption in Pleistocene assemblages.

Reconstructed *C. crocuta* body masses from Britain were correlated with those of potential predators and with potential prey species. Most importantly, correlations were observed with *C. elaphus* and Rhinocerotidae (*S. hemitoechus* and *C. antiquitatis*), with *C. crocuta* body masses increasing in line with these herbivores. This suggested that even though these prey individuals became larger in MIS 3, *C. crocuta* were still able to predate them, although in the case of Rhinocerotidae, the focus would have likely been juveniles. This was supported by the morphometric results, which indicated that *C. crocuta* in Britain may have been targeting larger prey during MIS 3, relative to MIS 5e and 5c.

The morphometric results also indicated that in Britain, *C. crocuta* were more cursorial and capable of locomotion at higher speeds during the temperate periods of MIS 5e (Last Interglacial) and 5c (Early Devensian interstadial) than during MIS 3 (Middle Devensian). This potentially indicates that *C. crocuta* in MIS 5e and 5c were engaged in more frequent predation than scavenging (relative to frequency of scavenging). This apparent reliance on scavenged food by MIS 3-aged *C. crocuta* may have been disadvantageous as scavenged food is an unreliable food source, which contains less energy, nutrients and water than fresh kills (Cooper *et al.*, 1999).

During MIS 3, bone consumption was more frequent, as indicated by the craniodental morphometrics and tooth breakage data. This suggested that there may have been periods of food stress. Frozen carcasses may also have been consumed during MIS 3, which may have been an important food source in times of harsher conditions.

8.4 Extirpation

The assessment of the extirpation of *C. crocuta* from Europe focussed on three main areas: environment (temperature, precipitation and vegetation), palaeodiet (prey presence, competition, food stress and scavenging frequency) and the use of caves for shelter.

First, an investigation was made into the environmental influences upon present-day *C. crocuta* population biomasses. This was compared with that of an important competitor, *P. leo*, and concluded that *P. leo* biomass is less influenced by environmental conditions. By contrast, *C. crocuta* biomass is greatest in areas with greater biomass of very small-, small- and medium-size prey, warmer winters and cooler summers, lack of arid conditions, and greater areas of semi-open vegetation cover. Moreover, competition seems to have a negligible influence upon *C. crocuta* biomass.

A new chronological model was constructed of *C. crocuta*, using quality-controlled published radiocarbon dates from MIS 3. Further models were also constructed of a potential competitor (*P. leo* (*spelaea*)) and three prey species (*C. antiquitatis*, *C. elaphus* and *R. tarandus*). The age models invoked a more stringent selection criteria of radiocarbon dates than in previously published studies of *C. crocuta*, *P. leo* (*spelaea*) and *C. antiquitatis* (Stuart and Lister, 2011, 2012, 2014). In addition, a new calibration curve, IntCal13 (Reimer *et al.*, 2013) was used in the models. In addition, as the youngest dates in a region may not be the final appearance of a species in a region, end boundaries were modelled for those species that are totally extinct or locally extinct from Europe.

The first event identified was the extirpation of *C. crocuta* from the Central region of Europe around 41.3-38.4 ka, which spans GI−10 to GS-9. Without tighter chronological control, *C. crocuta* disappearance cannot be attributed to either a stadial or interstadial. However, the continental climates in this region may have resulted in extreme cold winters, which may have impacted upon *C. crocuta* populations. Equally, this event may have been in response to the apparent absence of *C. antiquitatis*, a key prey species, from this region, although the radiocarbon models suggest that *R. tarandus* and *C. elaphus* were both still present in the region when *C. crocuta* disappeared. The combination of cold winters and *C. antiquitatis* absence may therefore have led to *C. crocuta* extirpation from the Central region.

Of particular note is the potential absence of *C. crocuta* across much of Europe from 39 to 38.3 ka, which may be attributed to the extreme cold conditions during GS-9 and HS 4. This may have been exacerbated by low prey biomass and seasonal migrations of *R. tarandus*, thereby limiting resources.

The extirpation of *C. crocuta* from the Northwestern region occurred around 35-33.7 ka. This period spans both stadials and interstadials and again, the chronological resolution is insufficient to pinpoint a single climatic period. However, additional information comes from the contemporary prey species. *C. crocuta* extirpation from the Northwestern region may have been in response to the absence of *C. elaphus* and *R. tarandus*.

The extirpation of *C. crocuta* from the Southwestern, Southern and Southeastern regions occurred around 31.7-26.2 ka, which corresponds with an intense period of short interstadials and long stadials (GS-5.2 to GS-3) and H-3. *C. crocuta* from the Southwestern region may also have been negatively impacted by an absence of *C. elaphus* and *R. tarandus*, although there was insufficient records of dated prey remains from the Southern and Southeastern regions to examine whether *C. crocuta* in these regions might have been similarly affected. Competition for shelter may nevertheless have played a significant role, with *C. crocuta* in the Southeastern region potentially influenced by competition for shelter with humans and bears.

In summary, the new chronological models of the presence and absence of *C. crocuta* and key prey species have advanced our knowledge both of apparent gaps in the records and of final known appearances. Nevertheless, there remains significant challenges in establishing whether climate or prey availability is the main driver or whether (perhaps more likely), both played a significant contributing factor.

8.5 Limitations

One of the major limitations of the study was the lack of chronological resolution for most of the assemblages. While this is of less significant when comparing the broad pattern across different interglacials, this was particularly problematic for MIS 3, which was characterised by multiple episodes of rapidly fluctuating temperatures. Many of the assemblages could only be given a broad MIS 3 attribution and even when reliable, quality-controlled radiocarbon dates were available, the current resolution does not always allow for identification of an individual interstadial or stadial. As a result, the lack of resolution is currently masking potential responses in *C. crocuta* morphology and diets to abrupt climatic changes.

Resolution was also limiting in the development of the new chronological models of *C. crocuta*, *P. leo* (*spelaea*), *C. antiquitatis*, *C. elaphus* and *R. tarandus*. For *C. crocuta*, there were large areas of Europe with no or very few dates, such as the Iberian Peninsula, Poland and Italy. For *P. leo* (*spelaea*), there are a lack of dates from the Northwestern region, particularly France and Britain. For the prey species, the main areas lacking dates are the Southern and Southeastern regions.

A further limitation of the study is that there is a lack of detailed, quantitative palaeoenvironmental reconstructions for sites in which *C. crocuta* were found. In particular, quantitative records of temperature and precipitation (although difficult to produce) are absent. This is unfortunate as *C. crocuta* biomass records appeared to be influenced by these climatic variables today.

There was a clear collecting and taphonomic bias towards skulls and dental remains, resulting in limited post-cranial material of modern and Pleistocene *C. crocuta* respectively. This meant that the changes seen in post-crania with ontogeny, and the manifestation of SSD could not be adequately explored. Furthermore, the post-cranial indices, useful in providing predation information, were based on small sample sizes, and data from the same Marine Oxygen Isotope Stage had to be pooled, in order to improve sample size, thereby concealing the potential effects of any short-term fluctuations in climate.

A further limitation is the use of the vegetation data in the analyses of present-day *C. crocuta*. These data were collected between 1981 and 1994 (Hansen *et al.*, 1998, 2000), and did not take in to account the fact that the vegetation may have changed in some areas. Nevertheless, it provided a standardised classification that could be applied throughout the whole dataset.

8.6 Further study

An important area for further study is to date more *C. crocuta* specimens. This would aid in interpretation of the morphological and dietary patterns seen in MIS 3, particularly whether *C. crocuta* were responding to stadial/interstadial climatic fluctuations, as well as allowing an assessment of whether body size and diet change around the time of the species' extirpation from Europe. Dates on the m1s used in the body mass reconstructions would be particularly beneficial. Dates could also be taken from broken *C. crocuta* premolars, in order to understand better the temporal patterns in food availability.

Additional dates on *C. crocuta* would strengthen the chronological model. As stated, there are large areas of Europe that have few or no radiocarbon dates and obtaining new dated material from the Iberian Peninsula, France and Germany should be a target for further research. As *C. crocuta* appeared to retreat towards the south of Europe during MIS 3, dates should also focus on Italy and Greece. Dates of *P. leo* (*spelaea*) should focus on the Northwestern region. Moreover, additional dates of *C. antiquitatis*, *C. elaphus* and *R. tarandus* are needed, particularly to underpin the Southeastern and Southern regions of the models.

Further dates on other species that occupied cave sites would also be beneficial. This would improve the understanding of competition for shelter during MIS 3.

Due to few palaeoenvironmental records constructed from *C. crocuta* assemblages, comparison of long palaeoenvironmental records with robust chronologies, such as those from lakes, could be compared with the *C. crocuta* chronological model. This could strengthen the relationship between *C. crocuta* absences and temperature, precipitation and aridity and vegetation cover.

Further study could also incorporate additional analyses of palaeodiet. In the present study, the palaeodietary information largely focussed on bone breakage. This could be supplemented by dental microwear analyses. This technique allows differentiation of types of food consumed by individuals, including meat and bone (Van Valkenburgh *et al.*, 1990; Solounias and Semprebon, 2002; Bastl *et al.*, 2012), which are of particular relevance to *C. crocuta*. This can therefore highlight elevated levels of bone consumption, and thus dietary stress, which could be coupled with the existing tooth breakage, mandibular bending strength and bite force data.

Additionally, dietary isotope analysis could be carried out to supplement those already published. Dietary isotopes can indicate the relative importance of different prey species in the diet of *C. crocuta*. Furthermore, if dietary isotopes are also analysed from other carnivores, an assessment can be made about competition between these species and *C. crocuta*. This has been carried out on material from sites in Belgium, France and Germany, highlighting diets of *C. crocuta* and those of other carnivores including *P. leo* (*spelaea*), *C. lupus* and *H. neanderthalensis* (e.g. Bocherens *et al.*, 2005; Yeakel *et al.*, 2013; Wißing *et al.*, 2015). The results of additional palaeodietary studies on well-dated material could be used to further determine the influence of prey species presence and competition on *C. crocuta* extirpation from Europe.

The palaeodietary and morphometric responses of Pleistocene spotted hyaena (*Crocuta crocuta* Erxleben, 1777) to environmental changes in Europe

Volume II

Angharad Kathrine Jones

Royal Holloway University of London

PhD Geography

Contents (Volume II)

9 References

Abouheif, E. and Fairbairn, D. J. (1997) 'A comparative analysis of allometry for sexual size dimorphism: assessing Rensch's Rule', *The American Naturalist*, 149(3), pp. 540–562.

Abramov, A. V (2016) *Gulo gulo. The IUCN Red List of Threatened Species 2016: e.T9561A45198537*.

Adam, K. D. (1966) 'IV. Die Mammutreste', *Denkschriften der Akademie der Wissenschaften. Die Teufels- oder Fuchsenlucken bei Eggenburg (NÖ)*, 112, pp. 39–60.

Aldhouse-Green, S., Scott, K., Schwarcz, H., Grün, R., Housley, R., Rae, A., Bevins, R. and Redknap, M. (1995) 'Coygan Cave, Laugharne, South Wales, a Mousterian site and hyaena den: a report on the excavations of the University of Cambridge excavations', *Proceedings of the Prehistoric Society*, 61, pp. 37–79.

Aldhouse-Green, S., Dinnis, R., Scott, K. and Walker, E. A. (2015) 'The nature of human activity at Cae Gwyn and Ffynnon Beuno caves and the dating of prey and predator presences', in Ashton, N. and Harris, C. (eds) *No Stone Unturned: papers in honour of Roger Jacobi*. London: Lithics Studies Society, pp. 77–92.

Alexander, R. M. (1983) *Animal Mechanics: Second Edition*. Oxford: Blackwell Scientific Publications.

Allen, J. A. (1877) 'The influence of physical conditions on the genesis of species', *Radical Review*, 1, pp. 108–140.

Allen, J. A. (1924) 'Carnivora collected By the American Museum Congo Expedition', *Bulletin of the American Museum of Natural History*, 47(8), pp. 73–281.

Allué, E., Burjachs, F., Vernet, J.-L., Morales, J. I., Rodríguez-Hidalgo, A., Cebrià, A. and Rosell, J. (2013) 'Cova del Toll (Moià, Bages): Perspectiva paleoambiental i arqueobotànica del Plistocè i Holocè', *Quadern de Prehistòria Catalana*, (21), pp. 21–38.

Andersen, K. K. *et al.* (2004) 'High-resolution record of Northern Hemisphere climate extending into the last interglacial period', *Nature*, 431(7005), pp. 147–151.

Anderson, P. S. L., Renaud, S. and Rayfield, E. J. (2014) 'Adaptive plasticity in the mouse mandible', *BMC Evolutionary Biology*, 14, pp. 1–9.

Andersson, K. (2004) 'Elbow-joint morphology as a guide to forearm function and foraging behaviour in mammalian carnivores', *Zoological Journal of the Linnean Society*, 142(1), pp. 91–

104.

Ansorge, H. (1994) 'Intrapopular skull variability in the red fox, *Vulpes vulpes*, (Mammalia, Carnivora, Canidae)', *Zoologische Abhandlungen, Staatliches Museum für Tierkunde*, 48, pp. 103–123.

Antonioli, F., Presti, V. L., Morticelli, M. G., Bonfiglio, L., Mannino, M. A., Palombo, M. R., Sannino, G., Ferranti, L., Furlani, S., Lambeck, K., Canese, S., Catalano, R., Chiocci, F. L., Mangano, G., Scicchitano, G. and Tonielli, R. (2015) 'Timing of the emergence of the Europe-Sicily bridge (40-17 cal ka BP) and its implications for the spread of modern humans', *Geological Society, London, Special Publications*, 411, pp. 111–144.

Anyonge, W. (1993) 'Body mass in large extant and extinct carnivores', *Journal of Zoology*, 231(2), pp. 339–350.

ApSimon, A. M., Smart, P. L., MacPhail, R., Scott, K. and Taylor, H. (1992) 'King Arthur's Cave, Whitchurch, Herefordshire: reassessment of a Middle and Upper Palaeolithic, Mesolithic and beaker site', *The Proceedings of the University of Bristol Speleological Society*, 19(2), pp. 183–249.

Argant, J. and Dimitrijević, V. (2007) 'Pollen analyses of Pleistocene hyaena coprolites from Montenegro and Serbia', *Geoloski anali Balkanskog poluostrva*, (68), pp. 73–80.

Argot, C. (2010) 'Morphofunctional analysis of the postcranium of *Amphicyon major* (Mammalia, Carnivora, Amphicyonidae) from the Miocene of Sansan (Gers, France) compared to three extant carnivores: *Ursus arctos*, *Panthera leo*, and *Canis lupus*', *Geodiversitas*, 32(1), pp. 65–106.

Armstrong, R. A. (2014) 'When to use the Bonferroni correction', *Ophthalmic & physiological optics : the journal of the British College of Ophthalmic Opticians (Optometrists)*, 34(5), pp. 502–508.

Arnold-Bemrose, H. H. and Newton, E. T. (1905) 'On an ossiferous cavern of Pleistocene age at Hoe-Grange Quarry, Longcliffe, near Brassington (Derbyshire)', *Quarterly Journal of the Geological Society*, 61, pp. 43–63.

Arsznov, B. M., Lundrigan, B. L., Holekamp, K. E. and Sakai, S. T. (2011) 'Sex and the frontal cortex: a developmental CT study in the spotted hyena', *Brain, Behavior and Evolution*, 76(3–4), pp. 185–197.

Ashton, K. G., Tracy, M. C. and Queiroz, A. D. (2000) 'Is Bergmann's Rule Valid for Mammals?', *The American Naturalist*, 156(4), pp. 390–415.

Aubry, T., Dimuccio, L. A., Almeida, M., Buylaert, J. P., Fontana, L., Higham, T., Liard, M., Murray, A. S., Neves, M. J., Peyrouse, J. B. and Walter, B. (2012) 'Stratigraphic and technological evidence from the middle palaeolithic-Châtelperronian-Aurignacian record at the Bordes-Fitte rockshelter (Roches d'Abilly site, Central France)', *Journal of Human Evolution*. Elsevier Ltd, 62(1), pp. 116–137.

Bailey, T. N. (1993) *The African Leopard: ecology and behavior of a solitary felid*. New York: Columbia University Press.

Balch, H. E. (1937) *Mendip, its Swallet Caves and Rock Shelters*. Wells: Clare Son & Co. Ltd., The Cathedral Press.

Ballmann, P., de Coninck, J., de Heinzelin, J., Gautier, A., Geets, S. and Rage, J.-C. (1980) 'La Caverne Marie-Jeanne (Hastière-Lavaux, Belgique). I - Les dépôts quaternaires; inventaire paléontologique et archéologique', *Institut Royal des Sciences Naturelles de Belgique Mémoires*, 117, pp. 5–24.

Barnett, R., Shapiro, B., Barnes, I., Ho, S. Y. W., Burger, J., Yamaguchi, N., Higham, T. F. G., Wheeler, H. T., Rosendahl, W., Sher, A. V., Sotnikova, M., Kuznetsova, T., Baryshnikov, G. F., Martin, L. D., Harington, C. R., Burns, J. A. and Cooper, A. (2009) 'Phylogeography of lions (*Panthera leo* ssp.) reveals three distinct taxa and a late Pleistocene reduction in genetic diversity', *Molecular Ecology*, 18(8), pp. 1668–1677.

Baryshnikov, G. (1995) 'Cave hyena, *Crocuta spelaea* (Carnivora, Hyaenidae) from Palaeolithic fauna of the Crimea', *Trudy Zoologicheskogo iIstituta Rossiiskoi Akademii Nauk*, 263, pp. 3–45.

Baryshnikov, G. (1999) 'Chronological and geographical variability of *Crocuta spelaea* (Carnivora, Hyaenidae) from the Pleistocene of Russia', in Haynes, G., Klimowicz, J., and Reumer, J. W. F. (eds) *Mammoths and the Mammoth Fauna: studies of an extinct ecosystem*. Rotterdam: The Natural History Museum Rotterdam, pp. 155–174.

Bastl, K., Semprebon, G. and Nagel, D. (2012) 'Low-magnification microwear in Carnivora and dietary diversity in Hyaenodon (Mammalia: Hyaenodontidae) with additional information on its enamel microstructure', *Palaeogeography, Palaeoclimatology, Palaeoecology*, 348–349, pp. 13–20.

Bearder, S. K. (1977) 'Feeding habits of spotted hyaenas in a woodland habitat', *East African Wildlife Journal*, 15, pp. 263–280.

Beauval, C., Maureille, B., Lacrampe-Cuyaubère, F., Serre, D., Peressinotto, D., Bordes, J.-G., Cochard, D., Couchoud, I., Dubrasquet, D., Laroulandie, V., Lenoble, A., Mallye, J.-B., Pasty, S., Primault, J., Rohland, N., Pääbo, S. and Trinkaus, E. (2005) 'A late Neandertal femur from Les

Rochers-de-Villeneuve, France', *Proceedings of the National Academy of Sciences of the United States of America*, 102(20), pp. 7085–7090.

Benson-Amram, S., Dantzer, B., Stricker, G., Swanson, E. M. and Holekamp, K. E. (2016) 'Brain size predicts problem-solving abilities in mammalian carnivores', *Proceedings of the National Academy of Sciences*, 113(9), pp. 2532–2537.

Berg, F. (1966) 'X. Die prähistorischen Funde', *Denkschriften der Akademie der Wissenschaften. Die Teufels- oder Fuchsenlucken bei Eggenburg (NÖ)*, 112, pp. 123–135.

Bergmann, C. (1847) 'Ueber die Verhältnisse der Wärmeökonomie der Thiere zu ihrer Grösse', *Gottinge studies*, 3(1), pp. 595–708.

Biewener, A. A. (1989) 'Scaling body support in mammals: limb posture and muscle mechanics', *Science*, 245(4913), pp. 45–48.

Biknevicius, A. R. (1996) 'Functional discrimination in the masticatory apparatus of juvenile and adult cougars (Puma concolor) and spotted hyenas (*Crocuta crocuta*)', *Canadian Journal of Zoology*, 74, pp. 1934–1942.

Biknevicius, A. R. and Ruff, C. B. (1992) 'The structure of the mandibular corpus and its relationship to feeding behaviours in extant carnivorans', *Journal of Zoology*, 228(3), pp. 479–507.

Biknevicius, A. R., Van Valkenburgh, B. and Walker, J. (1996) 'Incisor size and shape: implications for feeding behaviors in saber-toothed "cats"', *Journal of Vertebrate Paleontology*, 16(3), pp. 510–521.

Binder, W. J. and Van Valkenburgh, B. (2000) 'Development of bite strength and feeding behaviour in juvenile spotted hyenas (*Crocuta crocuta*)', *Journal of Zoology*, 252, pp. 273–83.

Binder, W. J. and Van Valkenburgh, B. (2010) 'A comparison of tooth wear and breakage in Rancho La Brea sabertooth cats and dire wolves across time', *Journal of Vertebrate Paleontology*, 30(1), pp. 255–261.

Bird, D. J., Amirkhanian, A., Pang, B. and Van Valkenburgh, B. (2014) 'Quantifying the cribriform plate: influences of allometry, function and phylogeny in Carnivora', *The Anatomical Record*, 297, pp. 2080–2092.

Bishop, M. J. (1982) *The Mammal Fauna of the Early Middle Pleistocene Cavern Infill Site of Westbury-Sub-Mendip, Somerset*. London: The Palaeontological Association.

Blackwell, B., Chu, S., Chaity, I., Huang, Y. E. W., Mihailović, D., Roksandić, M., Dimitrijević, V., Blickstein, J., Huang, A. and Skinner, A. R. (2014) 'ESR Dating Ungulate Tooth Enamel from the

Mousterian Layers at Pešturina, Serbia', in Mihailović, D. (ed.) *Palaeolithic and Mesolithic Research in the Central Balkans*. Belgrade: Serbian Archaeological Society, pp. 21–38.

Blasco, R., Rosell, J., van der Made, J., Rodríguez, J., Campeny, G., Arsuaga, J. L., Bermúdez de Castro, J. M. and Carbonell, E. (2011) 'Hiding to eat: The role of carnivores in the early Middle Pleistocene from the TD8 level of Gran Dolina (Sierra de Atapuerca, Burgos, Spain)', *Journal of Archaeological Science*. Elsevier Ltd, 38(12), pp. 3373–3386.

Blockley, S. P. E. and Pinhasi, R. (2011) 'A revised chronology for the adoption of agriculture in the Southern Levant and the role of Lateglacial climatic change', *Quaternary Science Reviews*. Elsevier Ltd, 30(1–2), pp. 98–108.

Bobek, B., Perzanowski, K. and Smietana, W. (1992) 'The influence of snow cover on wolf *Canis lupus* and red deer *Cervus elaphus* relationships in Bieszczady Mountains', in Bobek, B., Perzanowski, K., and Regelin, W. (eds) *Global trends in wildlife management. Transactions of the 18th IUCB Congress, Krakow 1987*. Krakow-Warszawa: Swiat Press, pp. 341–348.

Bocherens, H., Fogel, M. L., Tuross, N. and Zeder, M. (1995) 'Trophic structure and climatic information from isotopic signatures in Pleistocene cave fauna of Southern England', *Journal of Archaeological Science*, 22, pp. 327–340.

Bocherens, H., Drucker, D. G., Billiou, D., Patou-Mathis, M. and Vandermeersch, B. (2005) 'Isotopic evidence for diet and subsistence pattern of the Saint-Césaire I Neanderthal: Review and use of a multi-source mixing model', *Journal of Human Evolution*, 49, pp. 71–87.

Bocherens, H., Drucker, D. G., Bonjean, D., Bridault, A., Conard, N. J., Cupillard, C., Germonpré, M., Höneisen, M., Münzel, S. C., Napierala, H., Patou-Mathis, M., Stephan, E., Uerpmann, H. P. and Ziegler, R. (2011) 'Isotopic evidence for dietary ecology of cave lion (*Panthera spelaea*) in North-Western Europe: prey choice, competition and implications for extinction', *Quaternary International*, 245(2), pp. 249–261.

Bocherens, H. (2014) 'Diet and ecology of the Scladina I-4A Neandertal child: insights from stable isotopes', in Toussaint, M. and Bonjean, D. (eds) *The Scladina I-4A Juvenile Neandertal, Andenne, Belgium: palaeoanthropology and context*. Andenne: études et Recherches Archéologiques de l'Université de Liège, pp. 351–362.

Bocherens, H. (2015) 'Isotopic tracking of large carnivore palaeoecology in the mammoth steppe', *Quaternary Science Reviews*, 117, pp. 42–71.

Bocherens, H., Drucker, D. G., Germonpré, M., Lázničková-Galetová, M., Naito, Y. I., Wissing, C., Brůžek, J. and Oliva, M. (2015) 'Reconstruction of the Gravettian food-web at Předmostí I using multi-isotopic tracking (13C, 15N, 34S) of bone collagen', *Quaternary International*, 359–

360, pp. 211–228.

Bocherens, H., Díaz-Zorita Bonilla, M., Daujeard, C., Fernandes, P., Raynal, J.-P. and Moncel, M.-H. (2016) 'Direct isotopic evidence for subsistence variability in Middle Pleistocene Neanderthals (Payre, southeastern France)', *Quaternary Science Reviews*, 154, pp. 226–236.

Boeskorov, G. G., Lazarev, P. A., Sher, A. V, Davydov, S. P., Bakulina, N. T., Shchelchkova, M. V, Binladen, J., Willerslev, E., Buigues, B. and Tikhonov, A. N. (2011) 'Woolly rhino discovery in the lower Kolyma River', *Quaternary Science Reviews*. Elsevier Ltd, 30(17–18), pp. 2262–2272.

Bohm, T. and Höner, O. R. (2015) *Crocuta crocuta. The IUCN Red List of Threatened Species 2015*.

Bollen, K. A. and Jackman, R. W. (1990) 'Regression Diagnostics: an expository treatment of outliers and influential cases', in Fox, J. and Long, J. S. (eds) *Modern Methods of Data Data Analysis*. Newbury Park: Sage Publications, pp. 257–291.

Bon, C., Berthonaud, V., Maksud, F., Labadie, K., Poulain, J., Artiguenave, F., Wincker, P., Aury, J.-M. and Elalouf, J.-M. (2012) 'Coprolites as a source of information on the genome and diet of the cave hyena', *Proceedings of the Royal Society B: Biological Sciences*, 279, pp. 2825–2830.

Bondar, K. and Ridush, B. (2015) 'Rockmagnetic and palaeomagnetic studies of unconsolidated sediments of Bukovynka Cave (Chernivtsi region, Ukraine)', *Quaternary International*, 357, pp. 125–135.

Bonfiglio, L., Marra, A. C., Masini, F. and Petruso, D. (2001) 'Depositi a vertebrati e ambienti costieri pleistocenici della Sicilia e della Calabria meridionale', *Biogeographia*, 22, pp. 29–43.

Bonfiglio, L., Esu, D., Mangano, G., Masini, F., Petruso, D., Soligo, M. and Tuccimei, P. (2008) 'Late Pleistocene vertebrate-bearing deposits at San Teodoro Cave (North-Eastern Sicily): Preliminary data on faunal diversification and chronology', *Quaternary International*, 190(1), pp. 26–37.

Boucher, S., Crête, M., Ouellet, J.-P., Daigle, C. and Lesage, L. (2004) 'Large-scale trophic interactions: White-tailed deer growth and forest understory', *Ecoscience*, 11(3), pp. 286–295.

Bourke, J., Wroe, S., Moreno, K., McHenry, C. and Clausen, P. (2008) 'Effects of gape and tooth position on bite force and skull stress in the dingo (*Canis lupus dingo*) using a 3-dimensional finite element approach', *PLoS ONE*, 3(5), pp. 1–5.

Bout, N., Born, C. and Spohr, C. (2010) 'Evidence that the spotted hyena is present in the rainforest-savannah mosaic of south-east Gabon', *Mammalian Biology*, 75, pp. 175–179.

Bowen, D. Q., Sykes, G. A., Reeves, A., Miller, G. H., Andrews, J. T., Brew, J. S. and Hare, P. E.

(1985) ‘Amino acid geochronology of raised beaches in south west Britain’, *Quaternary Science Reviews*, 4, pp. 279–318.

Boydston, E. E., Kapheim, K. M., Watts, H. E., Szykman, M. and Holekamp, K. E. (2003) ‘Altered behaviour in spotted hyenas associated with increased human activity’, *Animal Conservation*, 6(3), pp. 207–219.

Boydston, E. E., Kapheim, K. M. and Holekamp, K. E. (2006) ‘Patterns of den occupation by the spotted hyaena (*Crocuta crocuta*)’, *African Journal of Ecology*, 44(1), pp. 77–86.

Boydston, E. E., Morelli, T. L. and Holekamp, K. E. (2001) ‘Sex differences in territorial behavior exhibited by the spotted hyena (Hyaenidae, *Crocuta crocuta*)’, *Ethology*, 107(5), pp. 369–385.

Boylan, P. J. (1981) ‘A new revision of the Pleistocene mammalian fauna of Kirkdale Cave, Yorkshire’, *Proceedings of the Yorkshire Geological Society*, 43(3), pp. 253–280.

Brace, S., Palkopoulou, E., Dalén, L., Lister, A. M., Miller, R., Otte, M., Germonpré, M., Blockley, S. P. E., Stewart, J. R. and Barnes, I. (2012) ‘Serial population extinctions in a small mammal indicate Late Pleistocene ecosystem instability’, *Proceedings of the National Academy of Sciences of the United States of America*, 109(50), pp. 20532–6.

Breuer, T. (2005) ‘Diet choice of large carnivores in northern Cameroon’, *African Journal of Ecology*, 43(2), pp. 97–106.

Briant, R. M., Brock, F., Demarchi, B., Langford, H. E., Penkman, K. E. H., Schreve, D. C., Schwenninger, J. L. and Taylor, S. (2018) ‘Improving chronological control for environmental sequences from the last glacial period’, *Quaternary Geochronology*. Elsevier, 43(October 2017), pp. 40–49.

Brody, S. (1945) *Bioenergetics and growth with special reference to the efficiency complex in domestic animals*. New York: Reinhold Publishing Corporation.

Bronk Ramsey, C., Higham, T. F. G., Owen, D. C., Pike, A. W. G. and Hedges, R. E. M. (2002) ‘Radiocarbon dates from the Oxford AMS system: Archaeometry datelist 31’, *Archaeometry*, 44(3), pp. 1–149.

Bronk Ramsey, C., Thomas Higham, B., Angela Bowles, B. and Robert Hedges, B. (2004) ‘Improvements to the pretreatment of bone at Oxford’, *Radiocarbon*, 46(1), pp. 155–163.

Bronk Ramsey, C. (2009) ‘Bayesian analysis of radiocarbon dates’, *Radiocarbon*, 51(1), pp. 337–360.

Bronk Ramsey, C., Higham, T. F. G., Brock, F., Baker, D. and Ditchfield, P. (2009) ‘Radiocarbon dates from the Oxford AMS system: Archaeometry datelist 33’, *Archaeometry*, 51(2), pp. 323–

349.

Bronk Ramsey, C., Higham, T. F. G., Brock, F., Baker, D., Ditchfield, P. and Staff, R. A. (2015) 'Radiocarbon dates from the Oxford AMS system: Archaeometry datelist 35', *Archaeometry*, 57(1), pp. 177–216.

Brown, C., Balisi, M., Shaw, C. A. and Van Valkenburgh, B. (2017) 'Skeletal trauma reflects hunting behaviour in extinct sabre-tooth cats and dire wolves', *Nature Ecology & Evolution*, 1(5), pp. 1–7.

Buckland, W. (1822) 'Account of an assemblage of fossil teeth and bones of elephant, rhinoceos, hippopotamus, bear, tiger, and hyaena, and sixteen other animals; discovered in a cave at Kirkdale, Yorkshire, in the year 1821: with a comparative view of five similar caverns in', *Philosophical Transactions of the Royal Society of London*, 112, pp. 171–236.

Bulleid, A. and Jackson, J. W. (1938) 'The Burtle Sand Beds of Somerset', *Proceedings of the Somerset Archaeology and Natural History Society*, 83, pp. 171–195.

Busk, G. (1875) 'List of the mammalian remains collected by the Rev. J. M. Mello in the Rock-Fissure Cavern in Creswell Crags, Derbyshire', *Quarterly Journal of the Geological Society*, 31, pp. 683–691.

Calderone, J. B., Reese, B. E. and Jacobs, G. H. (2003) 'Topography of photoreceptors and retinal ganglion cells in the spotted hyena (*Crocuta crocuta*)', *Brain, Behavior and Evolution*, 62(4), pp. 182–192.

Campbell, J. B. (1977) *The Upper Palaeolithic of Britain: a study of man and nature in the late Ice Age*. Oxford: Clarendon Press.

Candy, I., White, T. S. and Elias, S. (2016) 'How warm was Britain during the Last Interglacial? A critical review of Ipswichian (MIS 5e) palaeotemperature reconstructions', *Journal of Quaternary Science*, 31(8), pp. 857–868.

Carbone, C. and Gittleman, J. L. (2002) 'A common rule for the scaling of carnivore density', *Science*, 295, pp. 2273–2276.

Carbone, C., Pettorelli, N. and Stephens, P. A. (2011) 'The bigger they come, the harder they fall: body size and prey abundance influence predator-prey ratios', *Biology letters*, 7(November 2010), pp. 312–315.

Carbone, C., Teacher, A. and Rowcliffe, J. M. (2007) 'The costs of carnivory', *PLoS Biology*, 5(2), pp. 0363–0368.

Caro, T. M., Holt, M. E., FitzGibbon, C. D., Bush, M., Hawkey, C. M. and Kock, R. A. (1987)

'Health of adult free-living cheetahs', *Journal of Zoology, London*, 212, pp. 573–584.

Carrascal, L. M., Galván, I. and Gordo, O. (2009) 'Partial least squares regression as an alternative to current regression methods used in ecology', *Oikos*, 118, pp. 681–690.

Caumul, R. and Polly, P. D. (2005) 'Phylogenetic and environmental components of morphological variation: skull, mandible, and molar shape in marmots (*Marmota*, Rodentia).', *Evolution; international journal of organic evolution*, 59(11), pp. 2460–2472.

Celesia, G. G., Townsend Peterson, A., Kerbis Peterhans, J. C. and Gnoske, T. P. (2010) 'Climate and landscape correlates of African lion (*Panthera leo*) demography', *African Journal of Ecology*, 48(1), pp. 58–71.

Charles, R., Jacobi, R. M., Cook, J. and Beasley, M. J. (1994) 'The Lateglacial Fauna from the Robin Hood Cave, Creswell Crags: a re-assessment', *Oxford Journal of Archaeology*, 13(1), pp. 1–32.

Christiansen, P. (2002) 'Locomotion in terrestrial mammals: the influence of body mass, limb length and bone proportions on speed', *Zoological Journal of the Linnean Society*, 136(4), pp. 685–714.

Christiansen, P. and Adolfssen, J. S. (2005) 'Bite forces, canine strength and skull allometry in carnivores (Mammalia, Carnivora)', *Journal of Zoology*, 266, pp. 133–151.

Christiansen, P. and Wroe, S. (2007) 'Bite forces and evolutionary adaptations to feeding ecology in carnivores', *Ecology*, 88(2), pp. 347–358.

Clark, P. U., Dyke, A. S., Shakun, J. D., Carlson, A. E., Clark, J., Wohlfarth, B., Mitrovica, J. X., Hostetler, S. W. and McCabe, A. M. (2009) 'The Last Glacial Maximum', *Science*, 325(5941), pp. 710–714.

Collinge, S. E. (2001) *Body size and community structure in British Pleistocene mammals*. University College London.

Comeyne, A. (2013) *Taphonomy, osteometry and archaeozoology of the Pleistocene herbivores from the third horizon of the Goyet cave, Belgium*. Universiteit Gent.

Conti, N., Coppola, D., Petronio, C., Petrucci, M., Sardella, R. and Salari, L. (2012) 'La fauna del Pleistocene superiore di Tana delle Iene (Ceglie Messapica, Brindisi, Italia meridionale)', *Bollettino del Museo Civico di Storia Naturale di Verona*, 36, pp. 63–76.

Cook, R. D. (1977) 'Detection of influential observation in linear regression', *Technometrics*, 19(1), pp. 15–18.

Cook, R. D. and Weisberg, S. (1980) 'Characterizations of an empirical influence function for

detecting influential cases in regression', *Techometrics*, 22(4), pp. 495–508.

Cooper, L. P., Thomas, J. S., Beamish, M. G., Gouldwell, A., Collcutt, S. N., Williams, J., Jacobi, R. M., Currant, A. and Higham, T. F. G. (2012) 'An Early Upper Palaeolithic Open-air Station and Mid-Devensian Hyaena Den at Grange Farm, Glaston, Rutland, UK', *Proceedings of the Prehistoric Society*, 78, pp. 73–93.

Cooper, S. M. (1989) 'Clan sizes of spotted hyaenas in the Savuti region of the Chobe National Park, Botswana', *Botswana Notes and Records*, 21, pp. 121–133.

Cooper, S. M. (1990) 'The hunting behaviour of spotted hyaenas (*Crocuta crocuta*) in a region containing both sedentary and migratory populations of herbivores', *African Journal of Ecology*, 28, pp. 131–141.

Cooper, S. M. (1993) 'Denning behaviour of spotted hyaenas (*Crocuta crocuta*) in Botswana', *African Journal of Ecology*, 31, pp. 178–180.

Cooper, S. M., Holekamp, K. E. and Smale, L. (1999) 'A seasonal feast: Long-term analysis of feeding behaviour in the spotted hyaena (*Crocuta crocuta*)', *African Journal of Ecology*, 37, pp. 149–160.

Cowley, L. F. (1933) 'Priory Farm Cave, Monkton, Pembrokeshire. The human and animal remains', *Archaeologia Cambrensis1*, 88, pp. 99–100.

Cox, P. G. (2008) 'A quantitative analysis of the Eutherian orbit: correlations with masticatory apparatus', *Biological Reviews*, 83(1), pp. 35–69.

Crezzini, J., Boscato, P., Ricci, S., Ronchitelli, A., Spagnolo, V. and Boschin, F. (2016) 'A spotted hyaena den in the Middle Palaeolithic of Grotta Paglicci (Gargano promontory, Apulia, Southern Italy)', *Archaeological and Anthropological Sciences*, 8, pp. 227–240.

Cueto, M., Camarós, E., Castaños, P., Ontañón, R. and Arias, P. (2016) 'Under the skin of a lion: Unique evidence of upper Paleolithic exploitation and use of cave lion (*Panthera spelaea*) from the Lower Gallery of La Garma (Spain)', *PLoS ONE*, 11(10), pp. 1–19.

Currant, A. and Jacobi, R. (2001) 'A formal mammalian biostratigraphy for the Late Pleistocene of Britain', *Quaternary Science Reviews*, 20(16–17), pp. 1707–1716.

Currant, A. P. (1998) 'Tornewton Cave', in Campbell, S. *et al*. (eds) *Quaternary of South-West England*. London: Chapman and Hall, pp. 138–145.

Currant, A. P. (2004) 'The Quaternary mammal collections at the Somerset County Museum, Taunton', in Schreve, D. C. (ed.) *The Quaternary Mammals of Southern & Eastern England*. London: Quaternary Research Association, pp. 101–109.

Currant, A. P. and Jacobi, R. (2011) 'The Mammal Faunas of the British Late Pleistocene', in Ashton, N., Lewis, S., and Stringer, C. (eds) *The Ancient Human Occupation of Britain*. Amsterdam: Elsevier, pp. 165–180.

Curtis, A. A. and Van Valkenburgh, B. (2014) 'Beyond the sniffer: Frontal sinuses in carnivora', *Anatomical Record*, 297(11), pp. 2047–2064.

Cusack, J. J., Dickman, A. J., Kalyahe, M., Rowcliffe, J. M., Carbone, C., MacDonald, D. W. and Coulson, T. (2017) 'Revealing kleptoparasitic and predatory tendencies in an African mammal community using camera traps: a comparison of spatiotemporal approaches', *Oikos*, 126, pp. 812–822.

Cvetković, N. J. and Dimitrijević, V. M. (2014) 'Cave bears (Carnivora, Ursidae) from the Middle and Late Pleistocene of Serbia: a revision', *Quaternary International*, 339–340, pp. 197–208.

Damasceno, E. M., Hingst-Zaher, E. and Astúa, D. (2013) 'Bite force and encephalization in the Canidae (Mammalia: Carnivora)', *Journal of Zoology*, 290(4), pp. 246–254.

Damuth, J. (1981) 'Population density and body size in mammals', *Nature*, pp. 699–700.

Damuth, J. (1987) 'Interspecific allometry of population density in mammals and other animals: the independence of body mass and population energy-use', *Biological Journal of the Linnean Society*, 31, pp. 193–246.

Daujeard, C., Moncel, M.-H., Rivals, F., Fernandez, P., Aureli, D., Auguste, P., Bocherens, H., Crégut-Bonnoure, É., Debard, É. and Liouville, M. (2011) 'Quel type d'occupation dans l'ensemble F de Payre (Ardèche, France) ? Halte de chasse spécialisée ou campement de courte durée ? Un exemple d'approche multidisciplinaire', in Bon, F., Costamagno, S., and Valdeyron, N. (eds) *Haltes de chasse en Préhistoire. Quelles réalités archéologiques ? Actes du colloque international du 13 au 15 mai 2009, université Toulouse II - Le Mirail*. Toulouse: P@lethnologie, pp. 77–101.

Daura, J., Sanz, M., Subirá, M. E., Quam, R., Fullola, J. M. and Arsuaga, J. L. (2005) 'A Neandertal mandible from the Cova del Gegant (Sitges, Barcelona, Spain)', *Journal of Human Evolution*, 49, pp. 56–70.

Daura, J., Sanz, M., Pike, A. W. G., Subirà, M. E., Fornós, J. J., Fullola, J. M., Julià, R. and Zilhão, J. (2010) 'Stratigraphic context and direct dating of the Neandertal mandible from Cova del Gegant (Sitges, Barcelona)', *Journal of Human Evolution*. Elsevier Ltd, 59(1), pp. 109–122.

Davies, J. A. (1926) 'Notes on Upper Palaeolithic implements from some Mendip Caves', *Proceedings of the University of Bristol Spelaeological Society*, 2(3), pp. 261–273.

Davies, M. (1989) 'Recent advances in cave archaeology in southwest Wales', in Ford, T. D. (ed.) *Limestones and Caves of Wales*. Cambridge: Cambridge University Press, pp. 79–91.

Davies, W. and Gollop, P. (2003) 'The human presence in europe during the Last Glacial Period II: climate tolerance and climate preferences of Mid- and Late Glacial hominids', in van Andel, T. H. and Davies, W. (eds) *Neanderthals and Modern Humans in the European Landscape of the Last Glaciation - Archaeological Results of the Stage 3 Project*. Cambridge: McDonald Institute for Archaeological Research, pp. 131–146.

Davis, S. J. M., Robert, I. and Zilhão, J. (2007) 'Caldeirão cave (Central Portugal) - whose home? Hyaena, man, bearderd vulture...', *Courier Forschungsinstitut Senckenberg*, 259, pp. 213–226.

Dawkins, W. B. (1862) 'On a hyaena-den at Wookey Hole, near Wells', *Quarterly Journal of the Geological Society*, 18, pp. 115–126.

Dawkins, W. B. (1863) 'On a hyaena-den at Wookey Hole, near Wells. No. II', *Quarterly Journal of the Geological Society*, 19, pp. 260–274.

Dawkins, W. B. (1869) 'On the distribution of the British postglacial mammals', *Quarterly Journal of the Geological Society*, 25, pp. 192–217.

Dawkins, W. B. (1877) 'On the mammal-fauna of the caves of Creswell Crags', *Quarterly Journal of the Geological Society*, 33, pp. 589–612.

Dayan, T. and Simberloff, D. (1998) 'Size patterns among competitors: ecological character displacement and character release in mammals, with special reference to island populations', *Mammal Review*, 28(3), pp. 99–124.

Debenham, N. C., Atkinson, T., Grün, R., Higham, T., Housley, R., Pettitt, P., Rowe, P. and Zhou, L. P. (2012) '11. Dating', in Aldhouse-Green, S. H. R., Peterson, R., and Walker, E. A. (eds) *Neanderthals in Wales: Pontnewydd and the Elwy Valley*. Cardiff: Oxbow Books in association with The National Museum of Wales, pp. 302–320.

von den Driesch, A. (1976) *A Guide to the Measurement of Animal Bones from Archaeological Sites*. Cambridge, Massachusettes: Peabody Museum, Harvard University.

DeVault, T. L., Rhodes Jr., O. E. and Shivik, J. A. (2003) 'Scavenging by vertebrates : and evolutionary on an important perspectives in terrestrial transfer energy pathway ecosystems', *Oikos*, 102, pp. 225–234.

Diedrich, C. (2015) 'Late Pleistocene spotted hyena den sites and specialized rhinoceros scavengers in the karstified Zechstein areas of the Thuringian Mountains (Central Germany)', *Quaternary Science Journal*, 64(1), pp. 29–45.

Diedrich, C. G. (2006) 'The *Crocuta crocuta spelaea* (Goldfuss 1823) population fromthe early Late Pleistocene hyena open air prey deposit site Biedensteg (Bad Wildungen, Hess, NW Germany)', *Cranium*, 23(2), pp. 39–53.

Diedrich, C. G. (2011a) 'A clan of Late Pleistocene hyenas, *Crocuta crocuta spelaea* (Goldfuss 1823), from the Rösenbeck Cave (Germany) and a contribution to cranial shape variability', *Biological Journal of the Linnean Society*, 103, pp. 191–220.

Diedrich, C. G. (2011b) 'Periodical use of the Balve Cave (NW Germany) as a Late Pleistocene *Crocuta crocuta spelaea* (Goldfuss 1823) den: Hyena occupations and bone accumulations vs. human Middle Palaeolithic activity', *Quaternary International*, 233(2), pp. 171–184.

Diedrich, C. G. (2011c) 'The Late Pleistocene spotted hyena *Crocuta crocuta spelaea* (Goldfuss 1823) population with its type specimens from the Zoolithen Cave at Gailenreuth (Bavaria, South Germany): a hyena cub raising den of specialised cave bear scavengers in boreal forest env', *Historical Biology*, 23(4), pp. 335–367.

Diedrich, C. G. (2012a) 'An Ice Age spotted hyena *Crocuta crocuta spelaea* (Goldfuss 1823) population, their excrements and prey from the Late Pleistocene hyena den of the Sloup Cave in the Moravian Karst, Czech Republic', *Historical Biology*, 24(2), pp. 161–185.

Diedrich, C. G. (2012b) 'Europe's first Upper Pleistocene *Crocuta crocuta spelaea* (Goldfuss 1823) skeleton from the Koněprusy Caves: A hyena cave prey depot site in the Bohemian Karst (Czech Republic)', *Historical Biology*, 24(1), pp. 63–89.

Dimitrijević, V. M. (2011) 'Late Pleistocene hyaena *Crocuta crocuta spelaea* (Goldfuss, 1823) from Baranica Cave (southeast Serbia): competition for a den site', in Toškan, B. (ed.) *Fragments of Ice Age Environments: Proceedings in Honour of Ivan Turk's Jubilee*. Ljubljana: Inštitut za arheologijo ZRC SAZU, pp. 69–84.

Dimitrijević, V. M., Dulić, I. A. and Cvetković, N. J. (2014) 'The Janda cavity at Fruška Gora, the first cave assemblage from the southeast Pannonian lowland (Vojvodina, Serbia)', *Quaternary International*, 339–340, pp. 97–111.

Dinnis, R., Pate, A. and Reynolds, N. (2016) 'Mid-to-late Marine Isotope Stage 3 mammal faunas of Britain: a new look', *Proceedings of the Geologists' Association*. The Geologists' Association, 127(4), pp. 435–444.

Discamps, E. (2011) *Hommes et hyènes face aux recompositions des communautés d'Ongulés (MIS5-3): éléments pour un cadre paléoécologique des sociétés du Paléolithique moyen et supérieur ancien d'Europe de l'Ouest*. L'Université Bordeaux.

Discamps, E., Delagnes, A., Lenoir, M. and Tournepiche, J.-F. (2012) 'Human and hyena co-occurrences in Pleistocene sites: insights from spatial, faunal and lithic analyses at Camiac and La Chauverie (SW France)', *Journal of taphonomy*, 10(3–4), pp. 291–316.

Discamps, E., Boudadi-Maligne, M., Chagneau, J., Armand, D., Guadelli, J.-L. and Lenoir, M. (2012) 'Ours, hommes, hyenes: qui a occupé la grotte de Bourdette (Sainte-Colombe-en-Bruilhois, Lot-et-Garonne, France)?', *Paleo*, 23, pp. 117–136.

Discamps, E. (2014) 'Ungulate biomass fluctuations endured by Middle and Early Upper Paleolithic societies (SW France, MIS 5-3): the contributions of modern analogs and cave hyena paleodemography', *Quaternary International*. Elsevier Ltd and INQUA, 337, pp. 64–79.

Dodge, D. R., Bouwman, A. S., Pettitt, P. B. and Brown, T. A. (2012) 'Mitochondrial DNA haplotypes of Devensian hyaenas from Creswell Crags, England', *Archaeological and Anthropological Sciences*, 4, pp. 161–166.

Domingo, M. S., Alberdi, M. T., Sánchez-Chillón, B. and Cerdeño, E. (2005) 'La fauna cuaternaria de la cornisa cantábrica en las colecciones del Museo Nacional de Ciencias Naturales', *Munibe*, 57, pp. 325–350.

Donovan, D. T. (1988) 'The Late Pleistocene sequence at Wells, Somerset', *Proceedings of the University of Bristol Spelaeological Society*, 18(2), pp. 241–257.

Douka, K., Higham, T. F. G., Wood, R., Boscato, P., Gambassini, P., Karkanas, P., Peresani, M. and Ronchitelli, A. M. (2014) 'On the chronology of the Uluzzian', *Journal of Human Evolution*. Elsevier Ltd, 68(1), pp. 1–13.

Duan, N. (1983) 'Smearing estimate: a nonparametric retransformation method', *Journal of the American Statistical Association*, 78(383), pp. 605–610.

Dunbar, R. I. M. (1998) 'The social brain hypothesis', *Evolutionary Anthropology*, 6(5), pp. 178–190.

Dunbar, R. I. M. (2009) 'The social brain hypothesis and its implications for social evolution', *Annals of Human Biology*, 36(5), pp. 562–72.

Dupont, E. (1873) *L'Homme Pendant les Ages de la Pierre dans les Environs de Dinant-sur-Meuse*. Deuxieme E. Bruxelles: Muquartdt.

Dusseldorp, G. L. (2013a) 'Chapter 12. Neanderthals and cave hyenas: co-existence, competition or conflict?', in Clark, J. L. and Speth, J. D. (eds) *Zooarchaeology and Modern Human Origins: Human Hunting Behaviour During the Later Pleistocene*. Dordrecht: Springer Science+Business Media, pp. 191–208.

Dusseldorp, G. L. (2013b) 'Neanderthals and cave hyenas: co-existence, competition or conflict?', in Clark, J. L. and Speth, J. D. (eds) *Zooarchaeology and Modern Human Origins: Human Hunting Behaviour During the Later Pleistocene*. Dordrecht: Springer Science+Business Media, pp. 191–208.

Earp, J. R., Magraw, D., Poole, E. G., Land, D. H. and Whiteman, A. J. (1961) *Geology of the Country Around Clitheroe and Nelson (one-inch geological sheet, 68, new series)*. London: Her Majesty's Stationery Office.

East, M., Hofer, H. and Turk, A. (1989) 'Functions of birth dens in spotted hyaenas (*Crocuta crocuta*)', *Journal of The Zoological Society of London*, 219, pp. 690–697.

East, M. L. and Hofer, H. (1993) 'Male spotted hyenas (*Crocuta crocuta*) queue for status in social groups dominated by females', *Behavioral Ecology*, 12(5), pp. 558–68.

East, M. L., Hofer, H. and Wickler, W. (1993) 'The erect "penis" is a flag of submission in a female-dominated society: greetings in Serengeti hyenas', *Behavioral Ecology and Sociobiology*, 33(6), pp. 355–370.

Eaton, R. L. (1974) *The Cheetah: the biology, ecology and behavior of an endangered species*. New York: Van Nostrand Reinhold Company.

Egeland, A., Egeland, C. P. and Bunn, H. (2008) 'Taphonomic analysis of a modern spotted hyaena (Crocuta crocuta) den from Nairobi, Kenya', *Journal Of Taphonomy*, 6(3–4), pp. 275–299.

Ehrenberg, K. (1966a) 'I. Die bisher veröffentlichten Ergebnisse über die Erforschung der Höhle und die Untersuchung ihrer Funde nebst einigen Ergänzungen', in Ehrenberg, K. (ed.) *Denkschriften der Akademie der Wissenschaften.- Die Teufels- oder Fuchsenlucken bei Eggenburg (NÖ)*. Wien: Verlag der Österreichischen Akademie der Wissenschaften, pp. 7–14.

Ehrenberg, K. (1966b) 'I. Die bisher veröffentlichten Ergebnisse über die Erforschung der Höhle und die Untersuchung ihrer Funde nebst einigen Ergänzungen', *Denkschriften der Akademie der Wissenschaften. Die Teufels- oder Fuchsenlucken bei Eggenburg (NÖ)*, 112, pp. 7–14.

Ehrenberg, K. (1966c) 'XI. Der Fundbestand in seiner Gesamtheit. Eine biospeläologisch-biohistorische Schlußbetrachtung', *Denkschriften der Akademie der Wissenschaften. Die Teufels- oder Fuchsenlucken bei Eggenburg (NÖ)*, 112, pp. 137–158.

Ellis, J. L., Thomason, J., Kebreab, E., Zubair, K. and France, J. (2009) 'Cranial dimensions and forces of biting in the domestic dog', *Journal of Anatomy*, 214(3), pp. 362–373.

Emerson, S. B. and Radinsky, L. (1980) 'Functional analysis of sabertooth cranial morphology',

Paleobiology, 6(3), pp. 295–312.

Esri (2006) *Living Atlas of the World: light gray canvas*.

Estes, R. D. (1991) *The Behavior Guide to African Mammals: including hoofed mammals, carnivores, primates*. Berkeley and Los Angeles: University of California Press.

Ewer, R. F. (1973) *The Carnivores*. London: Cox & Wyman Ltd.

Fairbairn, D. J. (1997) 'Allometry for sexual size dimorphism: pattern and process in the coevolution of body size in males and females', *Annual Review of Ecology and Systematics*, 28, pp. 659–687.

Faith, J. T. (2007) 'Sources of variation in carnivore tooth-mark frequencies in a modern spotted hyena (*Crocuta crocuta*) den assemblage, Amboseli Park, Kenya', *Journal of Archaeological Science*, 34(10), pp. 1601–1609.

Falconer, H. (1858) 'Letter to the Secretary of the Geological Society'.

Falconer, H. (1860) 'On the ossiferous caves of the peninsula of Gower, in Glamorganshire, South Wales', *Quarterly Journal of the Geological Society*, 16, pp. 487–491.

Faurby, S. and Svenning, J.-C. (2016) 'Resurrection of the Island Rule: Human-Driven Extinctions Have Obscured a Basic Evolutionary Pattern', *The American Naturalist*, 187(6), pp. 812–820.

Fernández-García, M. (2014) 'Paleoecología y biocronología mediante el estudio de los roedores del Pleistoceno Superior-Holoceno de la cueva del Toll (Moià, Cataluña, NE de la península Ibérica)', *Treballs del Museu de Geologia de Barcelona*, 20, pp. 73–97.

Fernandez, P. and Guadelli, J.-L. (2008) 'Étude préliminaire des grands mammifères du repaire d'hyènes de Redaka II (Bulgarie du nord-ouest)', *Quaternaire*, 19(1), pp. 43–68.

Ferretti, M. P. (2007) 'Evolution of bone-cracking adaptations in hyaenids (Mammalia, Carnivora)', *Swiss Journal of Geosciences*, 100(1), pp. 41–52.

Figueirido, B., MacLeod, N., Krieger, J., De Renzi, M., Pérez-Claros, J. A. and Palmqvist, P. (2011) 'Constraint and adaptation in the evolution of carnivoran skull shape', *Paleobiology*, 37(3), pp. 490–518.

Figueirido, B., Tseng, Z. J. and Martín-Serra, A. (2013) 'Skull shape evolution in durophagous carnivorans', *Evolution*, 67(7), pp. 1975–1993.

Finarelli, J. A. and Flynn, J. J. (2009) 'Brain-size evolution and sociality in Carnivora', *PNAS*, 106(23), pp. 9345–9349.

Fisher, O. (1879) 'On a mammaliferous deposit at Barrington, near Cambridge', *Quarterly Journal of the Geological Society*, 35, pp. 670–677.

Flower, L. O. H. (2016) 'New body mass estimates of British Pleistocene wolves: Palaeoenvironmental implications and competitive interactions', *Quaternary Science Reviews*, 149(January), pp. 230–247.

Flower, L. O. H. and Schreve, D. C. (2014) 'An investigation of palaeodietary variability in European Pleistocene canids', *Quaternary Science Reviews*, 96, pp. 188–203.

Fosbrooke, H. A. (1963) 'The Stomoxys plague in Ngorongoro, 1962', *African Journal of Ecology*, 1(1), pp. 124–126.

Foster, J. B. (1964) 'Evolution of mammals on islands', *Nature*, 202, pp. 234–235.

Fourvel, J.-B., Fosse, P., Fernandez, P. and Antoine, P.-O. (2015) 'Large mammals of Fouvent-Saint-Andoche (Haute-Saône, France): a glimpse into a Late Pleistocene hyena den', *Geodiversitas*, 37(2), pp. 237–266.

Fourvel, J.-B., Fosse, P. and Avery, G. (2015) 'Spotted, striped or brown? Taphonomic studies at dens of extant hyaenas in eastern and southern Africa', *Quaternary International*. Elsevier Ltd, 369, pp. 38–50.

Fourvel, J. B., Fosse, P., Brugal, J. P., Cregut-Bonnoure, E., Slimak, L. and Tournepiche, J. F. (2014) 'Characterization of bear remains consumption by Pleistocene large carnivores (Felidae, Hyaenidae, Canidae)', *Quaternary International*, 339–340, pp. 232–244.

Frank, L. G. (1986) 'Social organization of the spotted hyaena *Crocuta crocuta*. II. Dominance and reproduction', *Animal Behaviour*, 34(5), pp. 1510–1527.

Frank, L. G., Glickman, S. E. and Zabel, C. J. (1989) 'Ontogeny of female dominance in the spotted hyaena: perspectives from nature and captivity', in Jewell, P. A. and Maloiy, G. M. O. (eds) *Zoological Society of London Symposia 61: The Biology of Large African Mammals in their Environment*. Oxford: Clarendon Press, pp. 127–146.

Freedman, J. (2015) 'William Buckland's connections to the last surviving Pleistocene collections from Yealm Bridge Caverns, Devon', *The Geological Curator*, 10(4), pp. 147–158.

Garcia, N. and Arsuaga, J. L. (2001) 'Les carnivores (Mammalia) des sites du Pleistocene ancien et moyen d'Atapuerca (Espagne)', *L'Anthropologie*, 105, pp. 83–93.

Garn, S. M., Osborne, R. H. and McCabe, K. D. (1979) 'The effect of prenatal factors on crown dimensions', *American Journal of Physical Anthropology*, 51, pp. 665–678.

Gasaway, W. C., Mossestad, K. T. and Stander, P. E. (1991) 'Food acquisition by spotted

hyaenas in Etosha National Park, Namibia: predation versus scavenging', *African Journal of Ecology*, 29, pp. 64–75.

Gatta, M., Sinopoli, G., Giardini, M., Giaccio, B., Hajdas, I., Pandolfi, L., Bailey, G., Spikins, P., Rolfo, M. F. and Sadori, L. (2016) 'Pollen from Late Pleistocene hyena (*Crocuta crocuta spelaea*) coprolites: An interdisciplinary approach from two Italian sites', *Review of Palaeobotany and Palynology*, 233, pp. 56–66.

Gatta, M. and Rolfo, M. F. (2017) 'Cava Muracci: a new middle-upper palaeolithic site in west-central Italy', *Mediterranean Archaeology and Archaeometry*, 17(2), pp. 105–116.

Gautier, A. (1980) 'La Caverne Marie-Jeanne (Hastière-Lavaux, Belgique). II - Notes sur les mammifères', *Institut Royal des Sciences Naturelles de Belgique Mémoires*, 117, pp. 27–42.

Gautier, A., Cordy, J.-M., Straus, L. G. and Otte, M. (1997) 'Taphonomic, chronostratigraphic, palaeoenvironmental and anthropogenic implications of the Upper Pleistocene faunas from Le Trou Magrite, Belgium', *Anthropozoologica*, 25–26, pp. 343–354.

Gay, S. W. and Best, T. L. (1996) 'Age-related variation in the skulls of the puma (*Puma concolor*)', *Journal of Mammalogy*, 77(1), pp. 191–198.

van der Geer, A., Lyras, G., De Vos, J. and Dermitzakis, M. (2010) *Evolution of Island Mammals*. Chichester: John Wiley & Sons Ltd.

Gerasimenko, N., Ridush, B. and Korzun, J. (2014) 'Pollen and lithological data from the Bukovynka Cave deposits as recorders of the Late Pleistocene and Holocene climatic change in the eastern foothills of the Carpathian Mountains (Ukraine)', in Mindrescu, M. (ed.) *Late Pleisotcene and Holocene Climate Variability in the Carpathian-Balkan Region*. Cluj-Napoca: Ştefan cel Mare University Press, pp. 54–58.

Germonpre, M. (1997) 'The Magdalenian upper horizon of Goyet and the late Upper Palaeolithic recolonisation of the Belgian Ardennes', *Bulletin de l'Institut Royal des Sciences Naturelles de Belqique, Sciences de la Terre*, 67, pp. 167–182.

Germonpré, M. (2001) 'A reconstruction of the spatial distribution of the faunal remains of Goyet, Belgium', *Notae Praehistoricae*, pp. 57–65.

Germonpré, M., Sablin, M. V, Stevens, R. E., Hedges, R. E. M., Hofreiter, M., Stiller, M. and Després, V. R. (2009) 'Fossil dogs and wolves from Palaeolithic sites in Belgium, the Ukraine and Russia: osteometry, ancient DNA and stable isotopes', *Journal of Archaeological Science*, 36, pp. 473–490.

Germonpré, M. and Hämäläinen, R. (2007) 'Fossil bear bones in the Belgian Upper Paleolithic:

the possibility of a proto bear-ceremonialism', *Arctic Anthropology*, 44(2), pp. 1–30.

Germonpré, M. and Sablin, M. V (2001) 'Cave bear (*Ursus spelaeus*) from Chamber B of the Goyet Cave in Belgium', *Bulletin de l'Institut Royal des Sceiences Naturelles de Belgique, Sciences de la Terre*, 71, pp. 209–233.

Gibbard, P. L. and Stuart, A. J. (1975) 'Flora and vertebrate fauna of the Barrington Beds', *Geological Magazine*, 112(5), pp. 493–501.

Gienapp, P., Teplitsky, C., Alho, J. S., Mills, J. A. and Merilä, J. (2008) 'Climate change and evolution: disentangling environmental and genetic responses', *Molecular Ecology*, 17, pp. 167–178.

Gilmour, M., Currant, A., Jacobi, R. and Stringer, C. (2007) 'Recent TIMS dating results from British Late Pleistocene vertebrate faunal localities: context and interpretation', *Journal of Quaternary Science*, 22(8), pp. 793–800.

Gittleman, J. L. (1986) 'Carnivore brain size, behavioral ecology, and phylogeny', *Journal of Mammalogy*, 67(1), pp. 23–36.

Gittleman, J. L. and Van Valkenburgh, B. (1997) 'Sexual dimorphism in the canines and skulls of carnivores: effects of size, phylogeny, and behavioural ecology', *Journal of Zoology*, 242(1), pp. 97–117.

Goillot, C., Blondel, C. and Peigné, S. (2009) 'Relationships between dental microwear and diet in Carnivora (Mammalia) - implications for the reconstruction of the diet of extinct taxa', *Palaeogeography, Palaeoclimatology, Palaeoecology*, 271(1–2), pp. 13–23.

Grant-Dalton, S. (1917) 'Untitled note', in Rhŷs, J. et al. (eds) *An Inventory of the Ancient Monuments in Wales and Monmouthshire. V - County of Carmarthen*. London: His Majesty's Stationery Office, p. 281.

Gray, H. (2003) *Gray's Anatomy*. Bath: Parragon.

Green, A. H., Miall, L. C., Brigg, J. and Davis, J. W. (1880) 'Report of the Raygill Fissure exploration committee', *Proceedings of the Yorkshire Geological and Polytechnic Society*, 7, pp. 300–306.

Green, B., Anderson, J. and Whateley, T. (1984) 'Water and sodium turnover and estimated food consumption in free-living lions (*Panthera leo*) and spotted hyaenas (*Crocuta crocuta*)', *Journal of Mammalogy*, 65(4), pp. 593–599.

Grimes, W. F. (1933) 'Priory Farm Cave, Monkton, Pembrokeshire', *Archaeologia Cambrensis*, 88, pp. 88–98.

Grimes, W. F. and Cowley, L. F. (1935) 'Coygan Cave, Llansadyrnin, Carmarthenshire', *Archaeologia Cambrensis*, 90, pp. 95–111.

Guadelli, A., Guadelli, J.-L., Fernandez, P. and Sirakov, N. (2013) 'Preliminary GIS and intra-site spatial analysis of the faunal remains from Redaka II cave', in *Second European SCGIS Conference 'Conservation of natural and cultural heritage for sustainable development: GIS-based approach'*, pp. 54–61.

Gula, R. (2004) 'Influence of snow cover on wolf Canis lupus predation patterns in Bieszczady Mountains, Poland', *Wildlife Biology*, 10, pp. 17–23.

Gunn, A. (2016) *Rangifer tarandus. The IUCN Red List of Threatened Species 2016: e.T29742A22167140*.

Guthrie, D. R. (2001) 'Origin and causes of the mammoth steppe: A story of cloud cover, woolly mammal tooth pits, buckles, and inside-out Beringia', *Quaternary Science Reviews*, 20, pp. 549–574.

Hammer, Ø., Harper, D. A. T. and Ryan, P. D. (2001) 'PAST: Paleontological Statistics software package for education and data analysis', *Palaeontologia Electronica*, 4(1), p. 9.

Hancock, G. R. and Klockars, A. J. (1996) 'The Quest for α: Developments in Multiple Comparison Procedures in the Quarter Century Since Games (1971)', *Review of Educational Research*, 66(3), pp. 269–306.

Hansen, M., DeFries, R., Townshend, J. R. G. and Sohlberg, R. (1998) *UMD Global Land Cover Classification, 1 Kilometer, 1.0*. College Park, Maryland, 1981-1994: Department of Geography, University of Maryland.

Hansen, M. C., Defries, R., Townshend, J. R. G. and Sohlberg, R. (2000) 'Global land cover classification at 1 km spatial resolution using a classification tree approach', *International Journal of Remote Sensing*, 21(6&7), pp. 1331–1364.

Harris, M. A. and Steudel, K. (1997) 'Ecological correlates of hind-limb length in the Carnivora', *Journal of Zoology*, 241, pp. 381–408.

Harrison, R. A. (1977) 'The Uphill Quarry Caves, Weston-super-Mare, A Reappraisal', *The Proceedings of the University of Bristol Speleological Society*, pp. 233–54.

Hartová-Nentvichová, M., Anděra, M. and Hart, V. (2010) 'Cranial ontogenetic variability, sex ratio and age structure of the red fox', *Central European Journal of Biology*, 5(6), pp. 894–907.

Hatton, I. A., McCann, K. S., Fryxell, J. M., Davies, T. J., Smerlak, M., Sinclair, A. R. E. and Loreau, M. (2015) 'The predator-prey power law: biomass scaling across terrestrial and aquatic

biomes', *Science*, 349(6252), pp. 1–13.

Hayward, M. W. (2006) 'Prey preferences of the spotted hyaena (*Crocuta crocuta*) and degree of dietary overlap with the lion (*Panthera leo*)', *Journal of Zoology*, 270, pp. 606–614.

Hayward, M. W. and Hayward, G. J. (2007) 'Activity patterns of reintroduced lion *Panthera leo* and spotted hyaena *Crocuta crocuta* in the Addo Elephant National Park, South Africa', *African Journal of Ecology*, 45(2), pp. 135–141.

Hayward, M. W. and Kerley, G. I. H. (2008) 'Prey preferences and dietary overlap amongst Africa's large predators', *South African Journal of Wildlife Research*, 38(2), pp. 93–108.

Hayward, M. W. and Slotow, R. (2009) 'Temporal Partitioning of Activity in Large African Carnivores: Tests of Multiple Hypotheses', *South African Journal of Wildlife Research*, 39(2), pp. 109–125.

Helsel, D. R. and Hirsch, R. M. (2002) *Statistical Methods in Water Resources: Techniques of Water-Resources Investigations of the United States Geological Survey. Book 4, Hydrologic Analysis and Interpretation*. U.S. Geological Survey.

Henschel, J. R. (1986) *The Socio-ecology of a Spotted Hyaena Crocuta crocuta Clan in the Kruger National Park*. University of Pretoria.

Henschel, J. R. and Skinner, J. D. (1990) 'The diet of the spotted hyaenas (*Crocuta crocuta*) in Kruger National Park', *African Journal of Ecology*, 28, pp. 69–82.

Henschel, J. R., Tilson, R. and Von Blottnitz, F. (1979) 'Implications of a Spotted Hyaena Bone Assemblage in the Namib Desert', *The South African Archaeological Bulletin*, 34(130), pp. 127–131.

Herring, S. W. (1993) 'Functional morphology of mammalian mastication', *American Zoologist*, 33(3), pp. 289–299.

Hicks, H. (1867) 'Discovery of a hyaena-den, near Laugharne, Carmarthenshire', *Geological Magazine*, 4(37), pp. 307–309.

Hicks, H. (1885) 'Results of recent researches in some bone-caves in North Wales (Ffynnon Beuno and Cae Gwyn).', *Proceedings of the Geologists' Association*, 9(1), pp. 3–17.

Higham, T., Jacobi, R., Basell, L., Bronk Ramsey, C., Chiotti, L. and Nespoulet, R. (2011) 'Precision dating of the Palaeolithic: A new radiocarbon chronology for the Abri Pataud (France), a key Aurignacian sequence', *Journal of Human Evolution*. Elsevier Ltd, 61(5), pp. 549–563.

Higham, T., Compton, T., Stringer, C., Jacobi, R., Shapiro, B., Trinkaus, E., Chandler, B., Gröning,

F., Collins, C., Hillson, S., O'Higgins, P., FitzGerald, C. and Fagan, M. (2011) 'The earliest evidence for anatomically modern humans in northwest Europe', *Nature*, 479, pp. 521–524.

Higham, T., Basell, L., Jacobi, R., Wood, R., Ramsey, C. B. and Conard, N. J. (2012) 'Testing models for the beginnings of the Aurignacian and the advent of figurative art and music: the radiocarbon chronology of Geißenklösterle', *Journal of Human Evolution*, 62(6), pp. 664–676.

Higham, T. *et al.* (2014) 'The timing and spatiotemporal patterning of Neanderthal disappearance', *Nature*, 512(7514), pp. 306–309.

Higham, T. F. G., Bronk Ramsey, C., Brock, F., Baker, D. and Ditchfield, P. (2011) 'Radiocarbon dates from the Oxford AMS system: Archaeometry datelist 34', *Archaeometry*, 53(5), pp. 1067–1084.

Higham, T. F. G., Jacobi, R. M. and Bronk Ramsey, C. (2006) 'AMS radiocarbon dating of ancient bone using ultrafiltration', *Radiocarbon*, 48(2), pp. 179–195.

Hijmans, R. J., Cameron, S. E., Parra, J. L., Jones, P. G. and Jarvis, A. (2005) 'Very high resolution interpolated climate surfaces for global land areas', *International Journal of Climatology*, 25, pp. 1965–1978.

Hildebrand, M. (1974) *Analysis of Vertebrate Structure*. New York: John Wiley & Sons.

Hildebrand, M. and Hurley, J. P. (1985) 'Energy of the oscillating legs of a fast-moving cheetah, pronghorn, jackrabbit, and elephant', *Journal of morphology*, 184, pp. 23–31.

Hillson, S. (2005) *Teeth. Second Edition*. Cambridge: Cambridge University Press.

Hofer, H. (1998a) 'Chapter 3: species accounts - spotted hyaena *Crocuta crocuta* (Erxleben, 1777)', in Mills, G. and Hofer, H. (eds) *Hyaenas: Status survey and conservation action plan*. Gland, Switzerland and Cambridge: IUCN, p. 155.

Hofer, H. (1998b) 'Stripped hyaena *Hyaena* (*hyaena*) *hyaena* (Linnaeus, 1758)', in Hofer, H. and Mills, G. (eds) *Hyaenas: Status survey and conservation action plan*. Gland, Switzerland and Cambridge: IUCN, pp. 21–26.

Hofer, H. (2000) 'Serengeti spotted hyaenas and the El Niño 1997/98', *IUCN Hyaena Specialist Group Newsletter*, 7, pp. 19–21.

Hofer, H. and East, M. (1995) 'Population dynamics, population size, and the commuting system of Serengeti spotted hyenas', in Sinclair, A. R. E. and Arcese, P. (eds) *Serengeti II. Dynamics, Management, and Conservation of an Ecosystem*. Chicago and London: The University of Chicago Press, pp. 332–363.

Hofer, H. and Mills, G. (1998a) 'Chapter 4: Worldwide distribution of hyaenas', in Mills, G. and

Hofer, H. (eds) *Hyaenas: Status survey and conservation action plan*. Gland, Switzerland and Cambridge: IUCN, p. 155.

Hofer, H. and Mills, G. (1998b) 'Chapter 5: Population size, threats and conservation status of hyaenas', in Mills, G. and Hofer, H. (eds) *Hyaenas: Status survey and conservation action plan*. Gland, Switzerland and Cambridge: IUCN, pp. 64–79.

Hofreiter, M., Serre, D., Rohland, N., Rabeder, G., Nagel, D., Conard, N., Münzel, S. and Pääbo, S. (2004) 'Lack of phylogeography in European mammals before the last glaciation', *Proceedings of the National Academy of Sciences of the United States of America*, 101(35), pp. 12963–12968.

Holekamp, K. E., Smale, L., Berg, R. and Cooper, S. M. (1997) 'Hunting rates and hunting success in the spotted hyena (*Crocuta crocuta*)', *Journal of The Zoological Society of London*, 242, pp. 1–15.

Holekamp, K. E. and Dloniak, S. M. (2010) 'Intraspecific variation in the behavioral ecology of a tropical carnivore, the spotted hyena', *Advances in the Study of Behavior*, 42(C), pp. 189–229.

Holekamp, K. E. and Smale, L. (1998) 'Behavioral development in the spotted hyena', *BioScience*, 48(12), pp. 997–1005.

Höner, O. P., Wachter, B., East, M. L. and Hofer, H. (2002) 'The response of spotted hyaenas to long-term changes in prey populations: functional response and interspecific kleptoparasitism', *Journal of Animal Ecology*, 71(2), pp. 236–246.

Höner, O. P., Wachter, B., East, M. L., Runyoro, V. A. and Hofer, H. (2005) 'The effect of prey abundance and foraging tactics on the population dynamics of a social, territorial carnivore, the spotted hyena', *Oikos*, 108(3), pp. 544–554.

Höner, O. P., Wachter, B., Speck, S., Wibbelt, G., Ludwig, A., Fyumagwa, R. D., Wohlsein, P., Lieckfeldt, D., Hofer, H. and East, M. L. (2006) 'Severe *Streptococcus* infection in spotted hyenas in the Ngorongoro Crater, Tanzania', *Veterinary Microbiology*, 115(1–3), pp. 223–228.

Höner, O. P., Wachter, B., Goller, K. V, Hofer, H., Runyoro, V., Thierer, D., Fyumagwa, R. D., Müller, T. and East, M. L. (2012) 'The impact of a pathogenic bacterium on a social carnivore population', *Journal of Animal Ecology*, 81, pp. 36–46.

Hopcraft, G. (2008) 'Official Map: Serengeti - Masai Mara, Ngorongoro, Oldupai'. Doune: Harvey.

Hopkins, R. J. A., Snoeck, C. and Higham, T. F. G. (2016) 'When Dental Enamel is Put to the Acid Test: Pretreatment Effects and Radiocarbon Dating', *Radiocarbon*, 58(4), pp. 893–904.

Howes, C. J. (1988) 'The Dillwyn diaries 1817-1852, Buckland, and caves of Gower (South Wales)', *Proceedings of the University of Bristol Spelaeological Society*, 18(2), pp. 298–305.

Hoyos, M. (1979) *El karst de Asturias durante de Pleistoceneo superior y Holoceno*. Universidad Complutense de Madrid.

Hunt, R. M. (1974) 'The auditory bulla in Carnivora: an anatomical basis for reappraisal of carnivore evolution', *Journal of Morphology*, 143, pp. 21–76.

Hylander, W. L. (1979) 'Mandibular function in *Galago crassicaudatus* and *Macaca fascicularis*: an in vivo approach to stress analysis of the mandible', *Journal of morphology*, 159(2), pp. 253–296.

Image Landsat Google Earth Pro (2013) *Google Earth Pro, version 7.1.5.1557*.

Iñigo, C. (1995) 'El rinoceronte del Pleistoceno Superior de la Cueva del Búho (Segovia)', *Boletín Geológico y Minero*, 106(2), pp. 107–110.

Iñigo, C., Molero, G. and Maldonado, E. (1998) 'Los carnívoros del yacimiento del Pleistoceno de Cueva del Buho (Segovia, España) y sus huellas de actividad', *Estudios Geológicos*, 54, pp. 65–73.

Irving, L. (1957) 'The usefulness of Scholander's views on adaptive insulation of animals', *Evolution*, 11(2), pp. 257–259.

Isaac, J. L. (2005) 'Potential causes and life-history consequences of sexual size dimorphism in mammals', *Mammal Review*, 35(1), pp. 101–115.

Ivanova, S., Gurova, M., Spassov, N., Hristova, L., Tzankov, N., Popov, V., Marinova, E., Makedonska, J., Smith, V., Ottoni, C. and Lewis, M. (2016) 'Magura Cave, Bulgaria: a multidisciplinary study of Late Pleistocene human palaeoenvironment in the Balkans', *Quaternary International*. Elsevier Ltd, 415, pp. 86–108.

Jacobi, R., Debenham, N. and Catt, J. (2007) 'A collection of early Upper Palaeolithic artefacts from Beedings, near Pulborough, West Sussex, and the context of similar finds from the British Isles', *Proceedings of the Prehistoric Society*, 73, pp. 229–326.

Jacobi, R. and Higham, T. (2011) '11 The British earlier Upper Palaeolithic: settlement and chronology', in Ashton, N., Lewis, S. G., and C, S. (eds) *The Ancient Human Occupation of Britain*. Amsterdam and Oxford: Elsevier, pp. 181–222.

Jacobi, R. M., Rowe, P. J., Gilmour, M. A., Grün, R. and Atkinson, T. C. (1998) 'Radiometric dating of the Middle Palaeolithic tool industry and associated fauna of Pin Hole Cave, Creswell Crags, England', *Journal of Quaternary Science*, 13, pp. 29–42.

Jacobi, R. M. (2007) 'The Stone Age archaeology of Church Hole, Creswell Crags, Nottinghamshire', in Pettitt, P. B., Bahn, P., and Ripoll, S. (eds) *Palaeolithic Cave Art at Creswell Crags in European Context*. Oxford: Oxford University Press, pp. 71–111.

Jacobi, R. M., Rose, J., MacLeod, A. and Higham, T. F. G. (2009) 'Revised radiocarbon ages on woolly rhinoceros (*Coelodonta antiquitatis*) from western central Scotland: significance for timing the extinction of woolly rhinoceros in Britain and the onset of the LGM in central Scotland', *Quaternary Science Reviews*. Elsevier Ltd, 28(25–26), pp. 2551–2556.

Jacobi, R. M., Higham, T. F. G., Haesaerts, P., Jadin, I. and Basell, L. S. (2010) 'Radiocarbon chronology for the early Gravettian of Northern Europe: new AMS determinations for Maisières-Canal, Belgium', *Antiquity*, 84, pp. 26–40.

Jacobi, R. M. and Hawkes, C. J. (1993) 'Archaeological notes: work at the Hyaena Den, Wookey Hole', *Proceedings of the University of Bristol Spealaeological Society*, 19(3), pp. 369–371.

Jacobi, R. M. and Higham, T. F. G. (2008) 'The "Red Lady" ages gracefully: new ultrafiltration AMS determinations from Paviland', *Journal of Human Evolution*. Elsevier Ltd, 55(5), pp. 898–907.

Jacobi, R. M., Higham, T. F. G. and Bronk Ramsey, C. (2006) 'AMS radiocarbon dating of Middle and Upper Palaeolithic bone in the British Isles: improved reliability using ultrafiltration', *Journal of Quaternary Science*, 21, pp. 557–573.

Jacobi, R. M. and Pettitt, P. B. (2000) 'An Aurignacian point from Uphill Quarry (Somerset) and the earliest settlement of Britain by *Homo sapiens sapiens*', *Antiquity*, 74, pp. 513–518.

James, F. C. (1970) 'Geographic size variation in birds and its relationship to climate', 51(3), pp. 365–390.

Jenks, S. M. and Werdelin, L. (1998) 'Chapter 2: Taxonomy and systematics of living hyaenas (Family Hyaenidae)', in Mills, G. and Hofer, H. (eds) *Hyaenas: Status survey and conservation action plan*. Gland, Switzerland and Cambridge: ICUN.

Joeckel, R. M. (1998) 'Unique frontal sinuses in fossil and living Hyaenidae (Mammalia, Carnivora): description and interpretation', *Journal of Vertebrate Paleontology*, 18(3), pp. 627–639.

Jones, M. (1997) 'Character displacement in Australian Dasyurid carnivores: size relationships and prey size patterns', *Ecology*, 78(8), pp. 2569–2587.

Juste, J. and Castroveijo, J. (1992) 'Unusual record of the spotted hyena (*Crocuta crocuta*) in Rio Muni, Equatorial Guinea (Central Africa)', *Zeitschrift für Säugetierkunde*, 57, pp. 380–381.

Kahlke, R. D. and Lacombat, F. (2008) 'The earliest immigration of woolly rhinoceros (*Coelodonta tologoijensis*, Rhinocerotidae, Mammalia) into Europe and its adaptive evolution in Palaearctic cold stage mammal faunas', *Quaternary Science Reviews*, 27(21–22), pp. 1951–1961.

Kaminská, L., Kozłowski, J. K. and Svoboda, J. A. (2006) 'The Dzerava Skala Cave, West Slovakia Excavations 2003-2004', in Cracovie, L. d'Archeologie de l'Universite de (ed.) *Recherches Archeologiques de 1999-2003*. Kraków: L'Institut d'Archeologie de l'Universite de Cracovie, pp. 299–306.

Kay, R. F. and Kirk, E. C. (2000) 'Osteological evidence for the evolution of activity pattern and visual acuity in primates', *American Journal of Physical Anthropology*, 113(2), pp. 235–262.

Kibanya, P. K. (1996) *Characterization of Mammal Hairs and their Application in Determining Diet Composition of Lion (Panthera Leo Massaica Neuman) in the Salient Region of Aberdare National Park, Kenya.* University of Nairobi.

Kiltie, R. A. (1982) 'Bite force as a basis for niche differentiation between rain forest peccaries (*Tayassu tajacu* and *T. percari*)', *Biotropica*, 14(3), pp. 188–195.

Kissui, B. M. and Packer, C. (2004) 'Top-down population regulation of a top predator: lions in the Ngorongoro Crater', *Proceedings of the Royal Society of London, B*, 271, pp. 1867–1874.

Klein, R. G. (1986) 'Carnivore size and Quaternary climatic change in southern Africa', *Quaternary Research*, 26, pp. 153–170.

Klein, R. G. and Scott, K. (1989) 'Glacial/interglacial size variation in fossil spotted hyenas (*Crocuta crocuta*) from Britain', *Quaternary Research*, 32, pp. 88–95.

Koepfli, K.-P., Jenks, S. M., Eizirik, E., Zahirpour, T., Van Valkenburgh, B. and Wayne, R. K. (2006) 'Molecular systematics of the Hyaenidae: relationships of a relictual lineage resolved by a molecular supermatrix', *Molecular Phylogenetics and Evolution*, 38, pp. 603–620.

Korb, J. (2000) 'Methods to study elusive hyenas in the Comoé National Park, Côte d'Ivoire', *IUCN Hyaena Specialist Group Newsletter*, 7, pp. 3–12.

Kozłowski, J. K. (1982) *Excavation in Bacho Kiro cave (Bulgaria). Final report*. Warszawa: Państwowe Wydawnictwo Naukowe.

Kruuk, H. (1972) *The Spotted Hyena: a study of predation and social behavior*. Chicago: The University of Chicago.

Kucera, M. and Malmgren, B. A. (1998) 'Logratio transformation of compositional data - A resolution of the constant sum constraint', *Marine Micropaleontology*, 34(1–2), pp. 117–120.

Kuhn, B. F. (2012) 'Bone accumulations of spotted hyaenas (*Crocuta crocuta*, Erxleben, 1777) as indicators of diet and human conflict; Mashatu, Botswana', *International Journal of Ecology*, 2012.

Kurtén, B. (1956) 'The Status and Affinities of *Hyaena sinensis* Owen and Hyaena ultima Matsumoto', *American Museum Novitates*, (1764), pp. 1–48.

Kurtén, B. and Werdelin, L. (1988) 'A review of the genus *Chasmaporthetes* Hay, 1921 (Carnivora, Hyaenidae)', *Journal of Vertebrate Paleontology*, 8(1), pp. 46–66.

Lacaille, A. D. and Grimes, W. F. (1955) 'The prehistory of Caldey, part 1', *Archaeologia Cambrensis*, 104, pp. 85–165.

Lacaille, A. D. and Grimes, W. F. (1961) 'The prehistory of Caldey, part 2', *Archaeologia Cambrensis*, 110, pp. 30–70.

Laing, R. (1890) 'On the bone caves of Cresswell, and discovery of an extinct Pleiocene feline (*Felis brevirostris*) new to Great Britain', *Report of the British Association for the Advancement of Science*, 59, pp. 582–584.

Lansing, S. W., Cooper, S. M., Boydston, E. E. and Holekamp, K. E. (2009) 'Taphonomic and zooarchaeological implications of spotted hyena (*Crocuta crocuta*) bone accumulations in Kenya: a modern behavioral ecological approach', *Paleobiology*, 35(2), pp. 289–309.

Laws, E. (1888) *The History of Little England Beyond Wales and the Non-Kymric Colony Settled in Pembrokeshire*. London: George Bell.

Legendre, S. and Roth, C. (1988) 'Correlation of carnassial tooth size and body weight in recent carnivores (Mammalia)', *Historical Biology*, 1, pp. 85–98.

Lehmann, U. (1966) 'VI. Die Boviden', *Denkschriften der Akademie der Wissenschaften. Die Teufels- oder Fuchsenlucken bei Eggenburg (NÖ)*, 112, pp. 83–88.

Lewis, M. D. (2011) 'Pleistocene hyaena coprolite palynology in Britain: implications for the environments of early humans', in Ashton, N., Lewis, S. G., and Stringer, C. (eds) *The Ancient Human Occupation of Britain*. Amsterdam: Elsevier, pp. 263–278.

Lewis, M., Pacher, M. and Turner, A. (2010) 'The larger Carnivora of the West Runton Freshwater Bed', *Quaternary International*, 228(1–2), pp. 116–135.

Lewis, S. G., Ashton, N. and Jacobi, R. (2011) 'Testing human presence during the Last Interglacial (MIS 5e): a review of the British evidence', in Ashton, N., Lewis, S. G., and Stringer, C. (eds) *The Ancient Human Occupation of Britain*. London: Elsevier Science, pp. 125–164.

Liebe, K. T. (1879) 'Die fossile Fauna der Höhle Vypustek in Mähren nebst Bemerkungen

betreffs einiger Knochenreste aus der Kreuzberghöhle in Krain', *Sitzungsberichte der Akademie der Wissenschaften mathematisch-naturwissenschaftliche Klasse*, 79, pp. 472–490.

Lindenfors, P., Gittleman, J. L. and Jones, K. E. (2007) 'Sexual size dimorphism in mammals', in Fairbairn, D. J., Blanckenhorn, W. U., and Székely, T. (eds) *Sex, size and gender roles: evolutionary studies of sexual size dimorphism*. Oxford: Oxford University Press, pp. 16–26.

Lindeque, M. (1981) *Reproduction in the Spotted Hyaena, Crocuta crocuta (Erxleben)*. University of Pretoria.

Lister, A. M. (2001) 'Age profile of mammoths in a Late Pleistocene hyaena den at Kent's Cavern, Devon, England', in *Anthropological papers of the University of Kansas*, pp. 35–43.

Locke, S. (1970) 'A Late Pleistocene mammal fauna from Caerwent Quarry, Monmouthshire', *Proceedings of the Bristol Naturalists' Society*, 32(1), pp. 84–87.

Lomolino, M. V (1985) 'Body size of mammals on islands: the Island Rule reexamined', *The American naturalist*, 125(2), pp. 310–316.

Lomolino, M. V, Van der Geer, A. A., Lyras, G. A., Palombo, M. R., Sax, D. F. and Rozzi, R. (2013) 'Of mice and mammoths: generality and antiquity of the island rule', *Journal of Biogeography*, 40, pp. 1427–1439.

López-García, J. M., Blain, H. A., Cuenca-Bescós, G. and Arsuaga, J. L. (2008) 'Chronological, environmental, and climatic precisions on the Neanderthal site of the Cova del Gegant (Sitges, Barcelona, Spain)', *Journal of Human Evolution*, 55, pp. 1151–1155.

López-García, J. M., Blain, H. A., Burjachs, F., Ballesteros, A., Allué, E., Cuevas-Ruiz, G. E., Rivals, F., Blasco, R., Morales, J. I., Hidalgo, A. R., Carbonell, E., Serrat, D. and Rosell, J. (2012) 'A multidisciplinary approach to reconstructing the chronology and environment of southwestern European Neanderthals: the contribution of Teixoneres cave (Moià, Barcelona, Spain)', *Quaternary Science Reviews*, 43, pp. 33–44.

López-García, J. M., Blain, H.-A., Lozano-Fernández, I., Luzi, E. and Folie, A. (2017) 'Environmental and climatic reconstruction of MIS 3 in northwestern Europe using the small-mammal assemblage from Caverne Marie-Jeanne (Hastière-Lavaux, Belgium)', *Palaeogeography, Palaeoclimatology, Palaeoecology*. Elsevier B.V., 485, pp. 622–631.

Lorenc, M. (2013) 'Radiocarbon ages of bones from Vistulian (Weichselian) cave deposits in Poland and their stratigraphy', *Acta Geologica Polonica*, 63(3), pp. 399–424.

Lorenzen, E. D. *et al.* (2011) 'Species-specific responses of Late Quaternary megafauna to climate and humans', *Nature*, 479(7373), pp. 359–364.

Losey, R. J., Jessup, E., Nomokonova, T. and Sablin, M. (2014) 'Craniomandibular trauma and tooth loss in northern dogs and wolves: Implications for the archaeological study of dog husbandry and domestication', *PLoS ONE*, 9(6).

Lovich, J. E. and Gibbons, J. W. (1992) 'A review of techniques for quantifying sexual size dimorphism', *Growth, Development and Aging*, 56, pp. 269–281.

Lucas, P. W. (2015) 'The masticatory system and its function', in Irish, J. D. and Scott, G. R. (eds) *A Companion to Dental Anthropology*. Chichester: John Wiley & Sons, pp. 108–119.

Lucas, P. W. and Peters, C. R. (2007) 'Function of postcanine tooth crown shape in mammals', in Teaford, M. F., Smith, M. M., and Ferguson, M. W. J. (eds) *Development, Function and Evolution of Teeth*. Cambridge: Cambridge University Press, pp. 282–289.

Luke, D. A., Tonge, C. H. and Reid, D. J. (1979) 'Metrical analysis of growth changes in the jaws and teeth of normal, protein deficient and calorie deficient pigs', *Journal of Anatomy*, 129(3), pp. 449–457.

Lyras, G. A., van der Geer, A. A. E. and Rook, L. (2010) 'Body size of insular carnivores: evidence from the fossil record', *Journal of Biogeography*, 37, pp. 1007–1021.

Macrini, T. E. (2012) 'Comparative Morphology of the Internal Nasal Skeleton of Adult Marsupials Based on X-ray Computed Tomography', *Bulletin of the American Museum of Natural History*, (365), pp. 1–91.

Magniez, P. and Boulbes, N. (2014) 'Environment during the Middle to Late Palaeolithic transition in southern France: The archaeological sequence of Tournal Cave (Bize-Minervois, France)', *Quaternary International*. Elsevier Ltd and INQUA, 337, pp. 43–63.

Maldonado, E. (1996) *Revisión de los équidos del Pleistoceno Medio y Superior de España*. Universidad Complutense de Madrid.

Mangano, G. (2011) 'An exclusively hyena-collected bone assemblage in the Late Pleistocene of Sicily: Taphonomy and stratigraphic context of the large mammal remains from San Teodoro Cave (North-Eastern Sicily, Italy)', *Journal of Archaeological Science*. Elsevier Ltd, 38(12), pp. 3584–3595.

Markova, A. K., Puzachenko, A. Y., Van Kolfschoten, T., Van der Plicht, J. and Ponomarev, D. V. (2013) 'New data on changes in the European distribution of the mammoth and the woolly rhinoceros during the second half of the Late Pleistocene and the early Holocene', *Quaternary International*, 292, pp. 4–14.

Marra, A. C., Villa, P., Beauval, C., Bonfiglio, L. and Goldberg, P. (2004) 'Same predator, variable

prey: taphonomy of two Upper Pleistocene hyena dens in Sicily and SW France', *Revue de Paléobiologie*, 23(2), pp. 787–801.

Marra, A. C. (2009) 'Pleistocene mammal faunas of Calabria (Southern Italy): biochronology and palaeobiology', *Bollettino della Società Paleontologica Italiana*, 48(2), pp. 113–122.

Martín-Serra, A., Figueirido, B. and Palmqvist, P. (2016) 'In the pursuit of the predatory behavior of borophagines (Mammalia, Carnivora, Canidae): inferences from forelimb morphology', *Journal of Mammalian Evolution*, 23(3), pp. 237–249.

Martin, C. and Sanchiz, B. (1989) 'Anuros Pleistocénicos de la Cueva de las Hienas (Las Caldas, Asturias)', *Munibe Ciencias Naturales*, 41, pp. 75–77.

Martin, R. A. (1990) 'Estimating body mass and correlated variables in extinct mammals: travels in the fourth dimension', in Damuth, J. and MacFadden, B. J. (eds) *Body Size in Mammalian Paleobiology: Estimation and Biological Implications*. Cambridge: Cambridge University Press, pp. 49–68.

Matthews, L. H. (1939) 'The subspecies and variation of the spotted hyaena, *Crocuta crocuta* Erxl.', *Proceedings of the Zoological Society of London*, 109, pp. 237–260.

Mayr, E. (1956) 'Geographical character gradients and climatic adaptation', *Evolution*, 10(1), pp. 105–108.

McDonough, T. J. and Christ, A. M. (2012) 'Geographic variation in size, growth, and sexual dimorphism of Alaska brown bears, *Ursus arctos*', *Journal of Mammalogy*, 93(3), pp. 686–697.

McFarlane, D. A. and Ford, D. C. (1998) 'The age of the Kirkdale Cave palaeofauna', *Cave and Karst Science*, 25(1), pp. 3–6.

McFarlane, D. A., Lundberg, J. and Roberts, W. (2010) 'A Geographic Information Systems approach to the 19th Century excavation of Brixham Cavern, Devon, England', *Studies in Speleology*, 17, pp. 1–11.

McNab, B. K. (1971) 'On the ecological significance of Bergmann's Rule', *Ecology*, 52(5), pp. 845–854.

McNab, B. K. (2010) 'Geographic and temporal correlations of mammalian size reconsidered: a resource rule', *Oecologia*, 164(1), pp. 13–23.

Meachen, J. A., Dunn, R. H. and Werdelin, L. (2016) 'Carnivoran postcranial adaptations and their relationships to climate', *Ecography*, 39(6), pp. 553–560.

Meers, M. B. (2002) 'Maximum bite force and prey size of *Tyrannosaurus rex* and their relationships to the inference of feeding behavior', *Historical Biology*, 16(1), pp. 1–12.

Meinertzhagen, R. (1938) 'Some weights and measurements of large mammals', *Proceedings of the Zoological Society of London*, A108(3), pp. 433–439.

Meiri, M., Lister, A. M., Higham, T. F. G., Stewart, J. R., Straus, L. G., Obermaier, H., González Morales, M. R., Marín-Arroyo, A. B. and Barnes, I. (2013) 'Late-glacial recolonization and phylogeography of European red deer (*Cervus elaphus* L.)', *Molecular Ecology*, 22(18), pp. 4711–4722.

Meiri, S., Dayan, T., Simberloff, D. and Grenyer, R. (2009) 'Life on the edge: carnivore body size variation is all over the place', *Proceedings. Biological sciences / The Royal Society*, 276(1661), pp. 1469–1476.

Meiri, S. (2011) 'Bergmann's Rule - what's in a name?', *Global Ecology and Biogeography*, 20, pp. 203–207.

Meiri, S., Cooper, N. and Purvis, A. (2008) *The island rule: made to be broken?*, *Proceedings of the Royal Society B: Biological Sciences*.

Meiri, S. and Dayan, T. (2003) 'On the validity of Bergmann's rule', *Journal of Biogeography*, 30(3), pp. 331–351.

Meiri, S., Dayan, T. and Simberloff, D. (2004) 'Carnivores, biases and Bergmann's rule', *Biological Journal of the Linnean Society*, 81, pp. 579–588.

Meiri, S., Yom-Tov, Y. and Geffen, E. (2007) 'What determines conformity to Bergmann's rule?', *Global Ecology and Biogeography*, 16(6), pp. 788–794.

Mello, J. M. (1875) 'On some bone-caves in Creswell Crags', *Quartarpalaontologie*, 31, pp. 679–683.

Mello, J. M. (1877) 'The bone-caves of Creswell Crags - 3rd paper', *Quarterly Journal of the Geological Society*, 33, pp. 579–588.

Meloro, C., Raia, P., Piras, P., Barbera, C. and O'Higgins, P. (2008) 'The shape of the mandibular corpus in large fissiped carnivores: allometry, function and phylogeny', *Zoological Journal of the Linnean Society*, 154, pp. 832–845.

Merilä, J. and Hendry, A. P. (2014) 'Climate change, adaptation, and phenotypic plasticity: the problem and the evidence', *Evolutionary Applications*, 7, pp. 1–14.

Millar, A. J. S. and Hickling, G. J. (1990) 'Fasting endurance and the evolution of mammalian body size', *Functional Ecology*, 4(1), pp. 5–12.

Mills, G. (1998) 'Brown hyaena *Hyaena* (*Parahyaena*) *brunnea* (Thunberg, 1820)', in Hofer, H. and Mills, G. (eds) *Hyaenas: Status survey and conservation action plan*. Gland, Switzerland

and Cambridge: IUCN, pp. 26–29.

Mills, M. G. L. (1990) *Kalahari Hyenas: comparative behavioral ecology of two species*. Caldwell, New Jersey: The Blackburn Press.

Mills, M. G. L. and Mills, M. E. J. (1977) 'An analysis of bones collected at hyaena breeding dens in the Gemsbok National Parks (Mammalia: Carnivora)', *Annals of the Traansvaal Museum*, 30(14), pp. 145–159.

Minitab Inc. (2010) 'Minitab 17 Statistical Software'. State College, PA.

Molero, G., Maldonado, E., Iñigo, C., Sánchez, F. and Díez, A. (1989) 'El yacimiento el Pleistoceno superior de la Cueva del Búho (Perogordo, Segovia) y su fauna de vertebrados', in *Volumen de Comunicaciones de las V Jornadas de Paleontología*. Valencia, pp. 101–102.

Moore, W. J. (1981) *The Mammalian Skull*. Cambridge: Cambridge University Press.

Morris, J. (1850) 'On the occurrence of mammalian remains at Brentford', *Quarterly Journal of the Geological Society*, 6, pp. 201–204.

Myers, P., Lundrigan, B. L., Gillespie, B. W. and Zelditch, M. L. (1996) 'Phenotypic plasticity in skull and dental morphology in the prairie deer mouse (*Peromyscus maniculatus bairdii*)', *Journal of Morphology*, 229, pp. 229–237.

Nadachowski, A., Żarski, M., Urbanowski, M., Wojtal, P., Miękina, B., Lipecki, G., Ochman, K., Krawczyk, M., Jakubowski, G. and Tomek, T. (2009) *Late Pleistocene Environment of the Częstochowa Upland (Poland) Reconstructed on the Basis of Faunistic Evidence from Archaeological Cave Sites*. Kraków: Institute of Systematics and Evolution of Animals, PAS.

Naito, Y. I., Chikaraishi, Y., Drucker, D. G., Ohkouchi, N., Semal, P., Wißing, C. and Bocherens, H. (2016) 'Ecological niche of Neanderthals from Spy Cave revealed by nitrogen isotopes of individual amino acids in collagen', *Journal of Human Evolution*. Elsevier Ltd, 93(April), pp. 82–90.

Mac Nally, R. (1996) 'Hierarchical partitioning as an interpretative tool in multivariate inference', *Australian Journal of Ecology*, 21, pp. 224–228.

Mac Nally, R. (2000) 'Regression and model-building in conservation biology, biogeography and ecology: the distinction between – and reconciliation of – "predictive" and "explanatory" models', *Biodiversity and Conservation*, 9, pp. 655–71.

Neaves, W. B., Griffin, J. E. and Wilson, J. D. (1980) 'Sexual dimorphism of the phallus in spotted hyena', *Journals of Reproduction Fertility*, 59, pp. 509–513.

van Nédervelde, J. and Davies, M. (1975) *Caldey Island cave excavations 1975*.

Neruda, P. and Nerudová, Z. (2013) 'The Middle-Upper Palaeolithic transition in Moravia in the context of the Middle Danube region', *Quaternary International*, 294, pp. 3–19.

Nummela, S., Pihlström, H., Puolamäki, K., Fortelius, M., Hemilä, S. and Reuter, T. (2013) 'Exploring the mammalian sensory space: co-operations and trade-offs among senses', *Journal of Comparative Physiology A: Neuroethology, Sensory, Neural, and Behavioral Physiology*, 199(12), pp. 1077–1092.

O'Connor, T. and Lord, T. (2013) 'Cave palaeontology', in Waltham, T. and Lowe, D. (eds) *Caves and Karst of the Yorkshire Dales*. British Cave Research Association, pp. 225–238.

Olea, P. P., Mateo-Tomás, P. and de Frutos, Á. (2010) 'Estimating and modelling bias of the hierarchical partitioning public-domain software: Implications in environmental management and conservation', *PLoS ONE*, 5(7), pp. 1–7.

ORAU (no date) *University of Oxford ORAU Database*.

Orford, H. J. L., Perrin, M. R. and Berry, H. H. (1988) 'Contraception, reproduction and demography of free-ranging Etosha lions (*Panthera leo*)', *Journal of Zoology*, 729, pp. 717–733.

Palmqvist, P., Martínez-Navarro, B., Pérez-Claros, J. A., Torregrosa, V., Figueirido, B., Jiménez-Arenas, J. M., Patrocinio Espigares, M., Ros-Montoya, S. and De Renzi, M. (2011) 'The giant hyena *Pachycrocuta brevirostris*: modelling the bone-cracking behavior of an extinct carnivore', *Quaternary International*, 243(1), pp. 61–79.

Panciroli, E., Janis, C., Stockdale, M. and Martín-Serra, A. (2017) 'Correlates between calcaneal morphology and locomotion in extant and extinct carnivorous mammals', *Journal of Morphology*, 278(10), pp. 1333–1353.

Parfitt, S. A. (1999) '4. Mammalia', in Roberts, M. B. and Parfitt, S. A. (eds) *Boxgrove: a Middle Pleistocene hominid site at Eartham Quarry, Boxgrove, West Sussex*. English Heritage, pp. 197–290.

Parfitt, S. A. *et al.* (2005) 'The earliest record of human activity in northern Europe', *Nature*, 438(December), pp. 1008–1012.

Peigné, S., Goillot, C., Germonpré, M., Blondel, C., Bignon, O. and Merceron, G. (2009) 'Predormancy omnivory in European cave bears evidenced by a dental microwear analysis of Ursus spelaeus from Goyet, Belgium', *Proceedings of the National Academy of Sciences of the United States of America*, 106, pp. 15390–15393.

Pekelharing, C. J. (1974) 'Paradontal disease as a cause of tooth loss in a population of chamois (*Rupicapra rupicapra* L.) in New Zealand', *Zeitschrift für Säugetierkunde*, 39, pp. 250–255.

Pengelly, W. (1865) ‘First report of the committee for exploring Kent’s Cavern, Devonshire’, *British Association for the Advancement of Science*, 35, pp. 16–25.

Pengelly, W. (1866) ‘Second report of the committee for exploring Kent’s Cavern, Devonshire’, *British Association for the Advancement of Science*, 36, pp. 1–11.

Pengelly, W. (1867) ‘Third report of the committee for exploring Kent’s Cavern, Devonshire’, *British Association for the Advancement of Science*, 37, pp. 24–34.

Pengelly, W. (1868) ‘Fourth report of the committee for exploring Kent’s Cavern, Devonshire’, *British Association for the Advancement of Science*, 38, pp. 45–58.

Pengelly, W. (1869) ‘Fifth report of the committee for exploring Kent’s Cavern, Devonshire’, *British Association for the Advancement of Science*, 39, pp. 189–208.

Pengelly, W. (1870) ‘Sixth report of the committee for exploring Kent’s Cavern, Devonshire’, *British Association for the Advancement of Science*, 40, pp. 16–29.

Pengelly, W. (1872) ‘Eighth report of the committee for exploring Kent’s Cavern, Devonshire’, *British Association for the Advancement of Science*, 42, pp. 28–47.

Pengelly, W. (1874) ‘Tenth report of the committee for exploring Kent’s Cavern, Devonshire’, *British Association for the Advancement of Science*, 44, pp. 1–17.

Pengelly, W. (1888) ‘Recent researches in Bench Cavern, Brixham, Devon’, *Transactions of the Edinburgh Geological Society*, pp. 507–512.

Pérez-Barbería, F. J., Shultz, S. and Dunbar, R. I. M. (2007) ‘Evidence for coevolution of sociality and relative brain size in three orders of mammals’, *Evolution*, 61(12), pp. 2811–2821.

Périquet, S., Mapendere, C., Revilla, E., Banda, J., Macdonald, D. W., Loveridge, A. J. and Fritz, H. (2016) ‘A potential role for interference competition with lions in den selection and attendance by spotted hyaenas’, *Mammalian Biology*, 81, pp. 227–234.

Périquet, S., Fritz, H. and Revilla, E. (2015) ‘The Lion King and the Hyaena Queen: large carnivore interactions and coexistence’, *Biological Reviews*, 90(4), pp. 1197–1214.

Pollard, A. M., Blockley, S. P. E. and Lane, C. S. (2006) ‘Some numerical considerations in the geochemical analysis of distal microtephra’, *Applied Geochemistry*, 21(10), pp. 1692–1714.

Polly, P. D. (2010) ‘Tiptoeing through the trophics: Geographic variation in carnivoran locomotor ecomorphology in relation to environment’, in Goswami, A. and Friscia, A. (eds) *Carnivoran Evolution: New Views on Phylogeny, Form, and Function*. Cambridge: Cambridge University Press, pp. 347–410.

Prestwich, J. (1873) ‘Report on the exploration of Brixham Cave, conducted by a committee of the Geological Society, and under the superintendence of WM. Pengelly, Esq., F.R.S., aided by a local committee; with descriptions of the animal remains by George Busk, Esq., F.R.S., a’, *Philosophical Transactions of the Royal Society of London*, 163, pp. 471–572.

Proctor, C., Douka, K., Proctor, J. W. and Higham, T. (2017) ‘The Age and Context of the KC4 Maxilla, Kent’s Cavern, UK’, *European Journal of Archaeology*, 20(1), pp. 74–97.

R Core Team (2016) ‘R: A language and environment for statistical computing’. Vienna: R Foundation for Statistical Computing.

Radinsky, L. B. (1981a) ‘Evolution of skull shape in carnivores 1. Representative modern carnivores’, *Biological Journal of the Linnean Society*, 15, pp. 369–388.

Radinsky, L. B. (1981b) ‘Evolution of skull shape in carnivores 2 . Additional modern carnivores’, *Biological Journal of the Linnean Society*, 16, pp. 337–355.

Radinsky, L. B. (1982) ‘Evolution in skull shape in carnivores 3. The origin and early radiation of the modern carnivore families’, *Paleobiology*, 8(3), pp. 177–195.

Rahmat, S. J. and Koretsky, I. A. (2015) ‘Diversity of mandibular morphology in some carnivorans’, *Vestnik Zoologii*, 49(3), pp. 267–284.

Raia, P. (2004) ‘Morphological correlates of tough food consumption in large land carnivores’, *Italian Journal of Zoology*, 71(1), pp. 45–50.

Raia, P. and Meiri, S. (2006) ‘The island rule in large mammals: paleontology meets ecology’, *Evolution*, 60(8), pp. 1731–1742.

Ralls, K. (1976) ‘Mammals in which females are larger than males’, *The Quarterly Review of Biology*, 51, pp. 245–276.

Ralls, K. and Harvey, P. (1985) ‘Geographic variation in size and sexual dimorphism of North American weasels’, *Biological Journal of the Linnean Society*, 25(2), pp. 119–167.

Randau, M., Goswami, A., Hutchinson, J. R., Cuff, A. R. and Pierce, S. E. (2016) ‘Cryptic complexity in felid vertebral evolution: shape differentiation and allometry of the axial skeleton’, *Zoological Journal of the Linnean Society*, 178(1), pp. 183–202.

Rasmussen, S. O. *et al.* (2014) ‘A stratigraphic framework for abrupt climatic changes during the Last Glacial period based on three synchronized Greenland ice-core records: Refining and extending the INTIMATE event stratigraphy’, *Quaternary Science Reviews*. Elsevier Ltd, 106, pp. 14–28.

Rautenbach, I. L. (1978) *The mammals of the Transvaal*. University of Natal.

Rautenbach, I. L. (1982) *Mammals of the Transvaal (ECOPLAN Monograph 1)*. Pretoria: ECOPLAN.

Raynal, J.-P., Guadelli, J.-L., Aujoulat, N., Barbazza, M., D'Errico, F., Jaubert, J., El Graoui, M., Ferrier, C., Kervazo, B., Konik, S., Moncel, M.-H., Piperno, M., Sirakov, N., Daujeard, C., Douze, K. and Gallotti, R. (2013) *Origines II : espaces et expressions. Rapport scientifique 2008-2012*. Contrat Région Aquitaine.

Reimer, P. *et al.* (2013) 'IntCal13 and Marine13 Radiocarbon Age Calibration Curves 0–50,000 Years cal BP', *Radiocarbon*, 55(4), pp. 1869–1887.

Rensberger, J. M. and Wang, X. (2005) 'Microstructural reinforcement in the canine enamel of the hyaenid *Crocuta crocuta*, the felid *Puma concolor* and the late Miocene canid *Borophagus secundus*', *Journal of Mammalian Evolution*, 12(3–4), pp. 379–403.

Rensch, B. (1950) 'Die Abhängigkeit der relativen Sexualdifferenz von der Körpergrösse', *Bonner Zoologische Beiträge*, 1, pp. 58–69.

Richards, M. P., Taylor, G., Steele, T., McPherron, S. P., Soressi, M., Jaubert, J., Orschiedt, J., Mallye, J. B., Rendu, W. and Hublin, J. J. (2008) 'Isotopic dietary analysis of a Neanderthal and associated fauna from the site of Jonzac (Charente-Maritime), France', *Journal of Human Evolution*, 55, pp. 179–185.

Ridush, B. (2009) '"Bear Caves" in Ukraine', *Slovenský Kras Acta Carsologica Slovaca*, 47, pp. 67–84.

Roberts, A. (1951) *The Mammals of South Africa*. South Africa: 'The Mammals of South Africa' Book Fund.

Roberts, M. B. and Parfitt, S. A. (1999) '5.9 Biostratigraphy and summary', in Roberts, M. B. and Parfitt, S. A. (eds) *Boxgrove: a Middle Pleistocene hominid site at Eartham Quarry, Boxgrove, West Sussex*. English Heritage, pp. 303–307.

Rode, K. D., Amstrup, S. C. and Regehr, E. V (2010) 'Reduced body size and cub recruitment in polar bears associated with sea ice decline', *Ecological Applications*, 20(3), pp. 768–782.

Rohland, N., Pollack, J. L., Nagel, D., Beauval, C., Airvaux, J., Pääbo, S. and Hofreiter, M. (2005) 'The population history of extant and extinct hyenas', *Molecular Biology and Evolution*, 22(12), pp. 2435–2443.

Rougier, H., Crevecoeur, I., Beauval, C., Posth, C., Flas, D., Wißing, C., Furtwängler, A., Germonpré, M., Gómez-Olivencia, A., Semal, P., Van Der Plicht, J., Bocherens, H. and Krause, J. (2016) 'Neandertal cannibalism and Neandertal bones used as tools in Northern Europe',

Scientific Reports. Nature Publishing Group, 6(June), pp. 1–11.

Rychlik, L., Ramalhinho, G. and Polly, P. D. (2006) 'Response to environmental factors and competition: skull, mandible and tooth shapes in Polish water shrews (*Neomys*, Soricidae, Mammalia)', *Journal of Zoological Systematics and Evolutionary Research*, 44(4), pp. 339–351.

Sabol, M., Čeklovský, T., Beňuš, R., Kováčová, M., Joniak, P., Zervanova, J. and Putiška, R. (2013) 'Fossil assemblages from Neanderthal sites of Slovakia - preliminary results', in Filippi, M. and Bosák, P. (eds) *16th International Congress of Speleology*. Brno: Czech Speleological Society and SPELEO2013, pp. 192–195.

Sanchez Goñi, M. F. and Harrison, S. P. (2010) 'Millennial-scale climate variability and vegetation changes during the Last Glacial: Concepts and terminology', *Quaternary Science Reviews*, 29(21–22), pp. 2823–2827.

Sandom, C. J., Ejrnaes, R., Hansen, M. D. D. and Svenning, J.-C. (2014) 'High herbivore density associated with vegetation diversity in interglacial ecosystems', *Proceedings of the National Academy of Sciences*, 111(11), pp. 4162–4167.

Santana, S. E. (2016) 'Quantifying the effect of gape and morphology on bite force: biomechanical modelling and *in vivo* measurements in bats', *Functional Ecology*, 30(4), pp. 557–565.

Sardella, R. and Petrucci, M. (2012) 'The earliest Middle Pleistocene *Crocuta crocuta* (Erxleben, 1777) at Casal Selce (Rome, Italy)', *Quaternary International*, 267, pp. 103–110.

Savage, R. J. G. (1977) 'Evolution in carnivorous mammals', *Palaeontology*, pp. 237–271.

Schaller, G. B. (1972) *The Serengeti Lion: a study of predator-prey relations*. Chicago: The University of Chicago Press.

Scharff, R. F., Seymour, H. J. and Newton, E. T. (1918) 'The exploration of Castlepook Cave, County Cork, being the third report from the committee appointed to explore Irish cave', *Proceedings of the Royal Irish Academy. Section B: Biological, Geological, and Chemical Science*, 34, pp. 33–72.

Scholander, P. F. (1955) 'Evolution of Climatic Adaptation in Homeotherms', *Evolution*, 9(1), pp. 15–26.

Schreve, D., Howard, A., Currant, A., Brooks, S., Buteux, S., Coope, R., Crocker, B., Field, M., Greenwood, M., Greig, J. and Toms, P. (2013) 'A Middle Devensian woolly rhinoceros (*Coelodonta antiquitatis*) from Whitemoor Haye Quarry, Staffordshire (UK): Palaeoenvironmental context and significance', *Journal of Quaternary Science*, 28(2), pp. 118–

130.

Schreve, D. C. (1997) *Mammalian biostratigraphy of the later Middle Pleistocene in Britain*. University College London.

Schreve, D. C. (2001) 'Differentiation of the British late Middle Pleistocene interglacials: the evidence from mammalian biostratigraphy', *Quaternary Science Reviews*, 20, pp. 1693–1705.

Schreve, D. C. (2007) 'Mammalian assemblages from the Trent', in White, T. S. et al. (eds) *The Quaternary of the Trent Valley and Adjoining Regions Field Guide*. London: Quaternary Research Association, pp. 49–61.

Schreve, D. C. (2012) 'The vertebrate assemblage from Lynford: taphonomy, biostratigraphy and implications for Middle Palaeolithic subsistence strategies', in Boismier, W. A., Gamble, C., and Coward, F. (eds) *Neanderthals Among Mammoths. Excavations at Lynford Quarry, Norfolk*. Swindon: English Heritage, pp. 157–204.

Schubert, B. W., Ungar, P. S. and DeSantis, L. R. G. (2010) 'Carnassial microwear and dietary behaviour in large carnivorans', *Journal of Zoology*, 280, pp. 257–263.

Schultz, A. H. (1940) 'The size of the orbit and of the eye in primates', *American Journal of Physical Anthropology*, 26(1), pp. 389–408.

Seierstad, I. K. *et al.* (2014) 'Consistently dated records from the Greenland GRIP, GISP2 and NGRIP ice cores for the past 104ka reveal regional millennial-scale δ18O gradients with possible Heinrich event imprint', *Quaternary Science Reviews*, 106, pp. 29–46.

Senter, P. and Moch, J. G. (2015) 'A critical survey of vestigial structures in the postcranial skeletons of extant mammals', *PeerJ*, 3, pp. 2–48.

Serrat, M. A. (2013) 'Allen's Rule revisited: temperature influences bone elongation during a critical period of postnatal development', *The Anatomical Record*, 296, pp. 1534–1545.

Serrat, M. A., King, D. and Lovejoy, C. O. (2008) 'Temperature regulates limb length in homeotherms by directly modulating cartilage growth', *Proceedings of the National Academy of Sciences of the United States of America*, 105(49), pp. 19348–19353.

Serrat, M. A., Williams, R. M. and Farnum, C. E. (2010) 'Exercise mitigates the stunting effect of cold temperature on limb elongation in mice by increasing solute delivery to the growth plate', *Journal of Applied Physiology*, 109, pp. 1869–1879.

Shackleton, N. J. (1987) 'Oxygen isotopes, ice volume and sea level', *Quaternary Science Reviews*, 6, pp. 183–190.

Sheng, G. L., Soubrier, J., Liu, J. Y., Werdelin, L., Llamas, B., Thomson, V. A., Tuke, J., Wu, L. J.,

Hou, X. D., Chen, Q. J., Lai, X. L. and Cooper, A. (2014) 'Pleistocene Chinese cave hyenas and the recent Eurasian history of the spotted hyena, *Crocuta crocuta*', *Molecular Ecology*, 23, pp. 522–533.

Shortridge, G. C. (1934a) *The Mammals of South West Africa: a biological account of the forms occurring in that region. Volume I*. London: William Heinemann Ltd.

Shortridge, G. C. (1934b) *The Mammals of South West Africa: a biological account of the forms occurring in that region. Volume II*. London: William Heinemann Ltd.

Sillero-Zubiri, C. and Gottelli, D. (1991) 'Threats to Aberdare rhinos: predation versus poaching', *Pachyderm*, 14, pp. 37–38.

Sillero-Zubiri, C. and Gottelli, D. (1992) 'Population ecology of spotted hyaena in an equatorial mountain forest', *African Journal of Ecology*, 30(4), pp. 292–300.

Silva, M. and Downing, J. A. (1995) *Mammalian Body Masses*. London: CRC Press.

Skinner, J. D. (1976) 'Ecology of the brown hyaena *Hyaena brunnea* in the Transvaal with a distribution map for Southern Africa', *South African Journal of Science*, 72, pp. 262–269.

Skinner, J. D. (2006) 'Bone collecting by hyaenas: a review', *Transactions of the Royal Society of South Africa*, 61(1), pp. 4–7.

Skinner, J. D. and Chimimba, C. T. (2005) *The Mammals of the Southern African Sub-Region*. Third Edit. Cambridge: Cambridge University Press.

Skinner, J. D. and Ilani, G. (1979) 'The striped hyaena, *Hyaena hyaena* of the Judean and Negev Deserts and a comparison with the brown hyaena *H. brunnea*', *Israel Journal of Zoology*, 28, pp. 229–232.

Slater, G. J., Dumont, E. R. and Van Valkenburgh, B. (2009) 'Implications of predatory specialization for cranial form and function in canids', *Journal of Zoology*, 278, pp. 181–188.

Slater, G. J. and Van Valkenburgh, B. (2009) 'Allometry and performance: the evolution of skull form and function in felids', *Journal of Evolutionary Biology*, 22, pp. 2278–2287.

Smith, R. J. (1984) 'Allometric scaling in comparative biology: problems of concept and method.', *The American journal of physiology*, 246(2 Pt 2), pp. R152–R160.

Smith, R. J. (1993) 'Logarithmic transformation bias in allometry', *American Journal of Physical Anthropology*, 90(2), pp. 215–228.

Smith, R. J. (1996) 'Biology and body size in human evolution: statistical inference misapplied', *Current Anthropology*, 37(3), pp. 451–481.

Smith, R. J. (1999) ‘Statistics of sexual size dimorphism’, *Journal of Human Evolution*, 36(4), pp. 423–458.

Smith, R. J. (2009) ‘Use and misuse of the reduced major axis for line-fitting’, *American Journal of Physical Anthropology*, 140(3), pp. 476–486.

Smith, T. D. and Rossie, J. B. (2008) ‘Nasal fossa of mouse and dwarf lemurs (primates, Cheirogaleidae)’, *Anatomical Record*, 291(8), pp. 895–915.

Smithers, R. H. N. (1971) *The Mammals of Botswana*. University of Pretoria.

Smithers, R. H. N. (1983) *The Mammals of the Southern African Subregion*. First. Pretoria: Pretoria University Press.

Smuts, G. L., Robinson, G. A. and Whyte, I. J. (1980) ‘Comparative growth of wild male and female lions (*Panthera leo*)’, *Journal of Zoology*, 190, pp. 365–373.

Snowdon, P. (1991) ‘A ratio estimator for bias correction in logarithmic regressions’, *Canadian Journal of Forest Research*, 21(5), pp. 720–724.

Solounias, N. and Semprebon, G. (2002) ‘Advances in the Reconstruction of Ungulate Ecomorphology with Application to Early Fossil Equids’, *American Museum Novitates*, (3366), pp. 1–49.

Stanley, S. M. (1973) ‘An explanation for Cope’s Rule’, *Evolution*, 27(1), pp. 1–26.

Stefen, C. and Rensberger, J. M. (1999) ‘The specialized structure of Hyaenid enamel: description and development with the lineage - including perocrocutids’, *Scanning Microscopy*, 13(2), pp. 363–380.

Steudel, K., Porter, W. P. and Sher, D. (1994) ‘The biophysics of Bergmann’s rule: a comparison of the effects of pelage and body size variation on metabolic rate’, *Canadian Journal of Zoology*, 72(1), pp. 70–77.

Stevens, R. E., Germonpré, M., Petrie, C. A. and O’Connell, T. C. (2009) ‘Palaeoenvironmental and chronological investigations of the Magdalenian sites of Goyet Cave and Trou de Chaleux (Belgium), via stable isotope and radiocarbon analyses of horse skeletal remains’, *Journal of Archaeological Science*, 36, pp. 653–662.

Stevenson-Hamilton, J. (1947) *Wild Life in South Africa*. Cassell an. London.

Stewart, J. R. (2008) ‘The progressive effect of the individualistic response of species to Quaternary climate change: an analysis of British mammalian faunas’, *Quaternary Science Reviews*. Elsevier Ltd, 27(27–28), pp. 2499–2508.

Stiner, M. C. (1992) 'Overlapping species "choice" by Italian Upper Pleistocene predators', *Current Anthropology*, 33(4), pp. 433–451.

Stiner, M. C. (2004) 'Comparative ecology and taphonomy of spotted hyenas, humans, and wolves in Pleistocene Italy', *Revue de Paleobiologie*, 23, pp. 771–785.

Stuart, A. J. (1982) *Pleistocene vertebrates in the British Isles*. Essex: Longman Group Limited.

Stuart, A. J. and Lister, A. M. (2001) 'The mammalian faunas of Pakefield/Kessingland and Corton, Suffolk, UK: Evidence for a new temperate episode in the British early Middle Pleistocene', *Quaternary Science Reviews*, 20, pp. 1677–1692.

Stuart, A. J. and Lister, A. M. (2011) 'Extinction chronology of the cave lion *Panthera spelaea*', *Quaternary Science Reviews*. Elsevier Ltd, 30(17–18), pp. 2329–2340.

Stuart, A. J. and Lister, A. M. (2012) 'Extinction chronology of the woolly rhinoceros *Coelodonta antiquitatis* in the context of late Quaternary megafaunal extinctions in northern Eurasia', *Quaternary Science Reviews*. Elsevier Ltd, 51, pp. 1–17.

Stuart, A. J. and Lister, A. M. (2014) 'New radiocarbon evidence on the extirpation of the spotted hyaena (*Crocuta crocuta* (Erxl.)) in northern Eurasia', *Quaternary Science Reviews*, 96, pp. 108–116.

Stuart, C. T. (1981) 'Notes on the mammalian carnivores of the Cape Province, South Africa', *Bontebok*, 1, pp. 1–58.

Sutcliffe, A. J. (1970) 'Spotted hyaena: crusher, gnawer, digester and collector of bones', *Nature*, 227, pp. 1110–1113.

Sutcliffe, A. J. (1981) 'Progress report on exavations in Minchin Hole, Gower', *Quaternary Newsletter*, 33, pp. 1–17.

Sutcliffe, A. J. (1986) *On the Track of Ice Age Mammals*. London: British Museum (Natural History).

Sutcliffe, A. J., Currant, A. P. and Stringer, C. B. (1987) 'Evidence of sea-level change from coastal caves with raised beach deposits, terrestrial faunas and dated stalagmites', *Progress in Oceanography*, 18, pp. 243–271.

Sutcliffe, A. J. and Kowalski, K. (1976) 'Pleistocene rodents of the British Isles', *Bulletin of the British Museum (Natural History), Geology*, 27(2), pp. 33–147.

Sutcliffe, A. J. and Zeuner, F. E. (1962) 'Excavations in the Torbryan Caves. I. Tornewton', *Proceedings of the Devon Archaeological Exploration Society*, 5, pp. 127–145.

Swanson, A., Arnold, T., Kosmala, M., Forester, J. and Packer, C. (2016) 'In the absence of a "landscape of fear": how lions, hyenas, and cheetahs coexist', *Ecology and Evolution*, 6, pp. 8534–8545.

Swanson, E. M., Holekamp, K. E., Lundrigan, B. L., Arsznov, B. M. and Sakai, S. T. (2012) 'Multiple determinants of whole and regional brain volume among terrestrial carnivorans', *PLoS ONE*, 7(6).

Swanson, E. M., McElhinny, T. L., Dworkin, I., Weldele, M. L., Glickman, S. E. and Holekamp, K. E. (2013) 'Ontogeny of sexual size dimorphism in the spotted hyena (*Crocuta crocuta*)', *Journal of Mammalogy*, 94(6), pp. 1298–1310.

Szmidt, C. C., Moncel, M. H. and Daujeard, C. (2010) 'Nouvelles données sur le Moustérien final de la France méditerranéenne: premières datations radiocarbone (SMA) à la Grotte de Saint-Marcel (Ardèche)', *Comptes Rendus - Palevol*. Academie des sciences, 9(4), pp. 185–199.

Talamo, S., Blasco, R., Rivals, F., Picin, A., Chacón, M. G., Iriarte, E., López-García, J. M., Blain, H.-A., Arilla, M., Rufà, A., Sánchez-Hernández, C., Andrés, M., Camarós, E., Ballesteros, A., Cebrià, A., Rosell, J. and Hublin, J.-J. (2016) 'The radiocarbon approach to Neanderthals in a carnivore den site: a well-defined chronology for Teixoneres Cave (Moià, Barcelona, Spain)', *Radiocarbon*, pp. 1–19.

Talbot, L. and Talbot, M. (1962) 'Flaxedil and other drugs in field immobilization and translocation of large mammals in East Africa', *Journal of Mammalogy*, 43, pp. 76–88.

Tanner, J. B., Dumont, E. R., Sakai, S. T., Lundrigan, B. L. and Holekamp, K. E. (2008) 'Of arcs and vaults: The biomechanics of bone-cracking in spotted hyenas (*Crocuta crocuta*)', *Biological Journal of the Linnean Society*, 95, pp. 246–255.

Tanner, J. B., Zelditch, M. L., Lundrigan, B. L. and Holekamp, K. E. (2010) 'Ontogenetic change in skull morphology and mechanical advantage in the spotted hyena (*Crocuta crocuta*)', *Journal of Morphology*, 271(3), pp. 353–365.

Taylor, M. E. (1989) 'Locomotor adaptations by carnivores', in Gittleman, J. L. (ed.) *Carnivore Behavior, Ecology, and Evolution*. Ithaca: Cornell University Press, pp. 382–409.

Tejero, J. M., Christensen, M. and Bodu, P. (2012) 'Red deer antler technology and early modern humans in Southeast Europe: An experimental study', *Journal of Archaeological Science*. Elsevier Ltd, 39(2), pp. 332–346.

Thackeray, J. F. and Kieser, J. A. (1992) 'Body mass and carnassial length in modern and fossil carnivores', *Annals of the Transvaal Museum*, 35(24), pp. 337–341.

Thenius, E. (1966) 'V. Die Cervidae und Perissodactyla (Equidae, Rhinocerotidae)', *Denkschriften der Akademie der Wissenschaften. Die Teufels- oder Fuchsenlucken bei Eggenburg (NÖ)*, 112, pp. 61–82.

Therrien, F. (2005) 'Mandibular force profiles of extant carnivorans and implications for the feeding behaviour of extinct predators', *Journal of Zoology*, 267, pp. 249–270.

Thomason, J. J. (1991) 'Cranial strength in relation to estimated biting forces in some mammals', *Canadian Journal of Zoology*, 69, pp. 2326–2333.

Tilson, R., von Blottnitz, F. and Henschel, J. (1980) 'Prey selection by spotted hyaena (*Crocuta crocuta*) in the Namib Desert', *Madoqua*, 12(1), pp. 41–49.

von Toldt, C. (1905) 'Die Winkelforsatz des Unterkiefers biem Menschen und bei den Säugetieren und die Beziehungen der Kaumuskein zu demselben II Teil', *Sitzungsberichte / Akademie der Wissenschaften in Wien, Mathematisch-Naturwissenschaftliche Klasse Bd*, 114, pp. 315–476.

Tratman, E. K. (1964) 'Picken's Hole, Crook Peak, Somerset. A Pleistocene Site', *Proceedings of the University of Bristol Spelaeological Society*, pp. 112–115.

Tratman, E. K., Donovan, D. T. and Campbell, J. B. (1971) 'The Hyaena Den (Wookey Hole), Mendip Hills, Somerset', *Proceedings of the University of Bristol Spelaeological Society*, 12(3), pp. 245–279.

Trimmer, W. K. (1813) 'An account of some organic remains found near Brentford, Middlesex', *Philosophical Transactions of the Royal Society of London*, 103, pp. 131–137.

Tsanova, T. (2006) *Les débuts du Paléolithique supérieur dans l'Est des Balkans: réflexion à partir de l'étude taphonomique et techno-économique des ensembles lithiques des sites de Bacho Kiro (couche 11), Temnata (couches VI et 4) et Kozarnika (niveau VII)*. L'Université Bordeaux 1.

Tseng, Z. J. (2009) 'Cranial function in a late Miocene *Dinocrocuta gigantea* (Mammalia: Carnivora) revealed by comparative finite element analysis', *Biological Journal of the Linnean Society*, 96, pp. 51–67.

Tseng, Z. J., Antón, M. and Salesa, M. J. (2011) 'The evolution of the bone-cracking model in carnivorans: cranial functional morphology of the Plio-Pleistocene cursorial hyaenid *Chasmaporthetes lunensis* (Mammalia: Carnivora)', *Paleobiology*, 37(1), pp. 140–156.

Tseng, Z. J. and Binder, W. J. (2010) 'Mandibular biomechanics of *Crocuta crocuta*, *Canis lupus*, and the late Miocene *Dinocrocuta gigantea* (Carnivora, Mammalia)', *Zoological Journal of the*

Linnean Society, 158(3), pp. 683–696.

Turnbull, W. D. (1970) *Mammalian Masticatory Apparatus*, *Fieldiana: Geology*.

Turner, A. (1981) *Aspects of the palaeoecology of large predators, including man, during the British Upper Pleistocene, with particular emphasis on predator-prey relationships*. University of Sheffield.

Turner, A. (1984) 'The interpretation of variation in fossil specimens of spotted hyaena (*Crocuta crocuta* Erxleben, 1777) from Sterkfontein valley sites (Mammalia, Carnivora)', *Annals of the Transvaal Museum*, 33(27), pp. 399–418.

Turner, A. (1999) '8 Larger carnivores (Mammalia, Carnivora) from Westbury Cave', in Andrews, P. et al. (eds) *Westbury Cave: the Natural History Museum Excavations 1976 - 1984*. Bristol: Western Academic & Specialist Press Limited, pp. 175–193.

Turner, A. (2000) 'The Paviland mammalian fauna', in Aldhouse-Green, S. (ed.) *Paviland Cave and the 'Red Lady': a definitive report*. Bristol: Western Academic and Specialist Press Limited, pp. 133–140.

Turner, A. (2009) 'The evolution of the guild of large Carnivora of the British Isles during the Middle and Late Pleistocene', *Journal of Quaternary Science*, 24(8), pp. 991–1005.

Ussher, R. J. (1906) 'The hyaena-dens of the Mammoth Cave near Doneraile, Co. Cork', *The Irish Naturalist*, 15(11), pp. 237–249.

Van Valen, L. (1973) 'Pattern and the balance of nature', *Evolutionary Theory*, 1(1), pp. 31–49.

Van Valkenburgh, B. (1985) 'Locomotor diversity within past and present guilds of large predatory mammals', *Paleobiology*, 11(4), pp. 406–428.

Van Valkenburgh, B. (1987) 'Skeletal indicators of locomotor behavior in living and extinct carnivores', *Journal of Vertebrate Paleontology*, 7(2), pp. 162–182.

Van Valkenburgh, B. (1988) 'Incidence of tooth breakage among large, predatory mammals', *The American Naturalist*, 131(2), pp. 291–302.

Van Valkenburgh, B. (1989) 'Carnivore dental adaptations and diet: a study of trophic diversity within guilds', in Gittleman, J. L. (ed.) *Carnivore Behavior, Ecology, and Evolution*. Ithaca: Cornell University Press, pp. 410–436.

Van Valkenburgh, B. (1990) 'Skeletal and dental predictors of body mass in carnivores', in Damuth, J. and MacFadden, B. J. (eds) *Body Size in Mammalian Paleobiology: Estimation and Biological Implications*. Cambridge: Cambridge University Press, pp. 181–205.

Van Valkenburgh, B. (1996) 'Feeding behavior in free-ranging, large African carnivores', *Journal of Mammalogy*, 77(1), pp. 240–254.

Van Valkenburgh, B. (2007) '*Déjà vu* : the evolution of feeding morphologies in the Carnivora', *Integrative and Comparative Biology*, 47(1), pp. 147–163.

Van Valkenburgh, B. (2009) 'Costs of carnivory: Tooth fracture in Pleistocene and recent carnivorans', *Biological Journal of the Linnean Society*, 96, pp. 68–81.

Van Valkenburgh, B. and Hertel, F. (1993) 'Tough times at La Brea: tooth breakage in large carnivores of the Late Pleistocene', *Science*, 261(5120), pp. 456–459.

Van Valkenburgh, B. and Koepfli, K. (1993) 'Cranial and dental adaptations to predation in canids', in Dunstone, N. and Gorman, M. L. (eds) *Mammals as Predators: Symposia of the Zoological Society of London Number 65*. Oxford: Clarendon Press, pp. 15–37.

Van Valkenburgh, B. and Ruff, C. B. (1987) 'Canine tooth strength and killing behaviour in large carnivores', *Journal of Zoology, London*, 212, pp. 379–397.

Van Valkenburgh, B., Sacco, T. and Wang, X. M. (2003) 'Pack hunting in Miocene borophagine dogs: evidence from craniodental morphology and body size', *Bulletin of the American Museum of Natural History*, 279, pp. 147–162.

Van Valkenburgh, B., Teaford, M. F. and Walker, A. (1990) 'Molar microwear and diet in large carnivores: inferences concerning diet in the sabretooth cat, *Smilodon fatalis*', *Journal of Zoology*, 222, pp. 319–340.

Van Valkenburgh, B., Wang, X. and Damuth, J. (2004) 'Cope's rule, hypercarnivory, and extinction in North American canids', *Science (New York, N.Y.)*, 306, pp. 101–104.

Van Valkenburgh, B. and Wayne, R. K. (2010) 'Carnivores', *Current Biology*, 20(21), pp. R915–R919.

Varela, S., Lobo, J. M., Rodríguez, J. and Batra, P. (2010) 'Were the Late Pleistocene climatic changes responsible for the disappearance of the European spotted hyena populations? Hindcasting a species geographic distribution across time', *Quaternary Science Reviews*, 29(17–18), pp. 2027–2035.

Villa, P., Sánchez Goñi, M. F., Cuenca Bescós, G., Grün, R., Ajas, A., García Pimienta, J. C. and Lees, W. (2010) 'The archaeology and paleoenvironment of an Upper Pleistocene hyena den: An integrated approach', *Journal of Archaeological Science*, 37, pp. 919–935.

de Villalta, J. F. (1972) 'Presencia de la *Marmota* y otros elementos de la fauna esteparia en el Pleistocene catalán', *Acta Geológica Hispánica*, 6, pp. 170–173.

Volmer, R. and Hertler, C. (2016) 'The effect of competition on shared food resources in carnivore guilds', *Quaternary International*, 413, pp. 32–43.

Walsh, C. and Mac Nally, R. (2004) 'heir.part: Heirarchical Partitioning. R package version 1.0'.

Walsh, C. and Mac Nally, R. (2005a) 'heir.part: Heirarchical Partitioning. R package version 1.0-1'.

Walsh, C. and Mac Nally, R. (2005b) '"'The hier.part Package'" version 1.0-1. Hierarchical Partitioning. Documentation for R: A language and environment for statistical computing'. Vienna: R Foundation for Statistical Computing.

Walsh, C. and Mac Nally, R. (2007a) 'heir.part: Heirarchical Partitioning. R package version 1.0-2'.

Walsh, C. and Mac Nally, R. (2007b) '"'The hier.part Package'" version 1.0-2. Hierarchical Partitioning. Documentation for R: A language and environment for statistical computing'. Vienna: R Foundation for Statistical Computing.

Walsh, C. and Mac Nally, R. (2013) 'heir.part: Heirarchical Partitioning. R package version 1.0-4'.

Walsh, C. and Mac Nally, R. (2015) 'Package "hier.part": Heirarchical Partitioning. Version 1.0-2. Documentation for R: A language and environment for statistical computing', p. 11.

Weaver, M. E. and Ingram, D. L. (1969) 'Morphological changes in swine associated with environmental temperature', *Ecology*, 50(4), pp. 710–713.

Weinstein, K. J. (2011) 'Climatic and altitudinal influences on variation in Macaca limb morphology', *Anatomy Research International*, 2011, pp. 1–18.

Werdelin, L. (1989) 'Constraint and adaptation in the bone-cracking canid *Osteoborus* (Mammalia: Canidae)', *Paleobiology*, 15(4), pp. 387–401.

Werdelin, L. and Solounias, N. (1991) 'The Hyaenidae: taxonomy, systematics and evolution', *Fossils and Strata*, 30, p. 104.

Whateley, A. (1980) 'Comparative body measurements of male and female spotted hyaenas from Natal', *Lammergyer*, 28, pp. 40–43.

Whitman, D. W. and Agrawal, A. A. (2009) 'What is phenotypic plasticity and why is it important?', in Whitman, D. W. and Ananthakrishnan, T. N. (eds) *Phenotypic Plasticity of Insects: Mechanisms and Consequences*. Enfield: Science Publishers, pp. 1–63.

Widger, J. L. (1892) 'The Torbryan Caves', *The Torquay Directory and South Devon Journal*.

Wigginton, J. D. and Dobson, F. S. (1999) 'Environmental influences on geographic variation in body size of western bobcats', *Canadian Journal of Zoology*, 77(5), pp. 802–813.

Wilson, E. and Reynolds, S. H. (1901) 'Uphill bone-caves', *Proceedings of the Bristol Naturalists' Society*, 9, pp. 152–160.

Wilson, H. C. A. (2010) *The Middle Devensian (MIS 3) mammals of Kents Cavern: an analysis of a small and large vertebrate assemblage recovered from the Great Chamber*. Royal Holloway University of London.

Wilson, V. J. (1968) 'Weights of some mammals from eastern Zambia', *Arnoldia*, 3, pp. 1–20.

Wilson, V. J. (1975) *Mammals of the Wankie National Park, Rhodesia*. Salisbury: National Museums and Monuments of Rhodesia, Museum memoir no.5.

Wißing, C., Matzerath, S., Turner, E. and Bocherens, H. (2015) 'Paleoecological and climatic implications of stable isotope results from late Pleistocene bone collagen, Ziegeleigrube Coenen, Germany', *Quaternary Research (United States)*. University of Washington, 84(1), pp. 96–105.

Wojtal, P. (2007) *Zooarchaeological studies of the Late Pleistocene sites in Poland*. Kraków: Institute of Systematics and Evolution of Animals, PAS.

Wood, R., Bernaldo de Quirós, F., Maíllo-Fernández, J. M., Tejero, J. M., Neira, A. and Higham, T. (2018) 'El Castillo (Cantabria, northern Iberia) and the Transitional Aurignacian: Using radiocarbon dating to assess site taphonomy', *Quaternary International*, 474, pp. 56–70.

Wood, R. E., Arrizabalaga, A., Camps, M., Fallon, S., Iriarte-Chiapusso, M. J., Jones, R., Maroto, J., De la Rasilla, M., Santamaría, D., Soler, J., Soler, N., Villaluenga, A. and Higham, T. F. G. (2014) 'The chronology of the earliest Upper Palaeolithic in northern Iberia: New insights from L'Arbreda, Labeko Koba and La Viña', *Journal of Human Evolution*. Elsevier Ltd, 69(1), pp. 91–109.

Woodman, P., McCarthy, M. and Monaghan, N. (1997) 'The Irish Quaternary fauna project', *Quaternary Science Reviews*, 16(96), pp. 129–159.

Wroe, S., McHenry, C. and Thomason, J. (2005) 'Bite club: comparative bite force in big biting mammals and the prediction of predatory behaviour in fossil taxa', *Proceedings of the Royal Society B: Biological Sciences*, 272, pp. 619–625.

Yeakel, J. D., Guimarães, P. R., Bocherens, H. and Koch, P. L. (2013) 'The impact of climate change on the structure of Pleistocene food webs across the mammoth steppe', *Proceedings of the Royal Society B: Biological Sciences*, 280, p. 20130239.

Yll, R., Carrión, J. S., Marra, A. C. and Bonfiglio, L. (2006) 'Vegetation reconstruction on the basis of pollen in Late Pleistocene hyena coprolites from San Teodoro Cave (Sicily, Italy)', *Palaeogeography, Palaeoclimatology, Palaeoecology*, 237(1), pp. 32–39.

Zapfe, H. (1966a) 'II. Die Höhlenbärenreste', *Denkschriften der Akademie der Wissenschaften. Die Teufels- oder Fuchsenlucken bei Eggenburg (NÖ)*, 112, pp. 15–22.

Zapfe, H. (1966b) 'III. Die übrigen Carnivoren (außer Höhlenhyäne und Höhlenbär)', *Denkschriften der Akademie der Wissenschaften. Die Teufels- oder Fuchsenlucken bei Eggenburg (NÖ)*, 112, pp. 23–38.

Zedrosser, A., Dahle, B. and Swenson, J. E. (2006) 'Population density and food conditions determine adult female body size in brown bears', *Journal of Mammalogy*, 87(3), pp. 510–518.

Zhou, Y., Wang, S.-R. and Ma, J.-Z. (2017) 'Comprehensive species set revealing the phylogeny and biogeography of Feliformia (Mammalia, Carnivora) based on mitochondrial DNA', *PLoS ONE*, 12(3), pp. 1–19.

10 Appendices

10.1 Pleistocene sites

Table 10.1: Details of sites included in the Pleistocene morphological and palaeodietary studies. Where stratigraphic information is available, only layers that had included the *C. crocuta* specimens included in this study are detailed. Where necessary, species names have been changed to follow the current nomenclature. Where marine oxygen isotope stages of British assemblages were not specified in the literature, the mammal species were compared to those of mammal assemblage zones in Schreve (2001) and Currant and Jacobi (2011) to determine the age of the deposits.

Site	Age	Environmental reconstruction	Large mammal species	Further information	References
Britain					
Pakefield, Suffolk	**Red-brown ferruginous sand and gravel**: Early Middle Pleistocene	**Red-brown ferruginous sand and gravel**: mixed forest and open vegetation. Temperate period.	**Red-brown ferruginous sand and gravel**: C. crocuta, scimitar-toothed cat (Homotherium sp.), Ursus sp., steppe mammoth (Mammuthus trogontherii), Palaeoloxodon antiquus, Equus sp. (large), (horse) Equus altidens, rhinoceros (Stephanorhinus hundscheimensis), H. amphibius, S. scofa, deer (Megaloceros verticornis), deer (Megaloceros savini), deer (Megaloceros dawkinsi), C. elaphus, Bison sp.		Stuart and Lister (2001) and references therein
Grays, Essex	MIS 9	Temperate climate, possibly warmer than today. Summer temperatures at least 18°C, winter	*C. lupus, V. vulpes, U. arctos,* otter (Lutrinae sp.), *P. antiquus,* Elephantidae sp., *E. ferus,* narrow-nosed rhinoceros (*Stephanorhinus hemitoechus*), Merck's rhinoceros (*Stephanorhinus kirkchbergensis*), *S. scrofa,* hippopotamus		Schreve (1997), Schreve (2001)

		temperatures at least 5°C. Woodland with some open grassland.	(*Hippopotamus amphibius*), *M. giganteus, D. dama* spp., *C. elaphus,* elk (*Alces* cf. *alces*), *C. capreolus, B. primigenius,* Bovidae sp., Barbary macaque (*Macacus sylvanus*)		
Bleadon, Somerset	Later MIS 7	Temperate climate. Open grassland with some areas of deciduous or mixed woodland	*C. lupus*, *V. vulpes*, *U. arctos*, polecat (*Mustela putorius*), wild cat (*Felis silvestris*), *P. leo*, *P. pardus*, straight-tusked elephant (*Palaeoloxodon antiquus*), *Mammuthus primigenius*, Elephantidae sp., *E. ferus*, Rhinocerotidae sp., *S. scrofa, C. elaphus, C. capreolus, B. primigenius, B. cf. priscus,* Bovidae sp.	Used as a *P. leo* den	Schreve (1997), Schreve (2001)
Hutton Cavern, Somerset	Later MIS 7	Temperate climate with onset of colder conditions. Open grassland.	*C. lupus, V. vulpes, F. silvestris, P. leo, M. primigenius,* Elephantidae sp., *E. ferus, S. scrofa, C. elaphus*		Schreve (1997), Schreve (2001)
Lawford, Warwickshire	Possibly later MIS 7		*R. tarandus, B. primigenius*(?), *B. priscus*(?), *C. antiquitatis, P. antiquus, M. primigenius*		Dawkins (1869)
Oreston Cave, Devon	Later MIS 7	Temperate climate, with warm summers and cold winters. Open grassland with some woodland.	*C. lupus, U. arctos, P. leo, M. primigenius, E. ferus, Equus hydruntinus* (stenonid ass), *C. antiquitatis, S. scrofa, C. elaphus, C. capreolus, B. primigenius,* Bovidae sp.		Schreve (1997), Schreve (2001)
Prissen's Tor Cave = Spritsail Tor, Swansea	**Cave Earth**: Possibly Later MIS 7		**Cave Earth**: *C. crocuta, P. spelaea, U. spelaeus* (probably actually *U. arctos*), *C. lupus, V. vulpes, M. meles, P. antiquus, M.*	*C. crocuta* den. Bones of Cervidae sp., *Bos* sp. and	Falconer (1860)

			primigenius, C. antiquitatis, Equus sp., *Sus* sp., *Bos* sp., Cervidae sp.	*Equus* sp. gnawed, likely by *C. crocuta.*	
Barrington, Cambridgeshire	MIS 5e	River floodplain with local open grassland, areas with herbaceous species and damp meadows. Mixed temperate oak forest further from the river.	*C. lupus, V. vulpes, U. arctos,* badger (*Meles meles*), *P. leo, P. antiquus, S. hemitoechus, H. amphibius, M. giganteus, D. dama, C. elaphus, B. priscus, B. primigenius*	Some bones with gnaw marks, possibly by *C. crocuta*	Fisher (1879), Gibbard and Stuart (1975), Currant and Jacobi (2011)
Brentford, London	MIS 5e		*C. crocuta, P. spelaea, H. amphibius, P. antiquus, S. hemitoechus, B. priscus, B. primigenius, R. tarandus, C. elaphus*	May correspond to remains found at one of two sites (one at Kew Bridge and one west of Kew Bridge). Later excavations near Kew Bridge revealed similar deposits. *C. crocuta* not listed by Trimmer (1813) or Morris, (1850). *C. crocuta* is listed by Dawkins (1869), but this species list not trusted by Lewis *et al.* (2011)	Trimmer (1813), Morris, (1850), Dawkins (1869), Lewis *et al.* (2011)
Burtle Beds, Somerset	Possibly MIS 5e		*C. crocuta, C. lupus,* Elephantidae sp., *S. hemitoechus, H. amphibius, D. dama, C. elaphus,* cf. *C. capreolus, B. primigernius,* Bovini sp.		Bulleid and Jackson (1938) Currant and Jacobi (2011)
Eastern Torrs Quarry, Devon	MIS 5e		*C. crocuta, H. amphibius*		Sutcliffe (1986)

Hoe Grange, Derbyshire	MIS 5	Interglacial conditions	*C. crocuta, P. leo, F. silvestris, C. lupus,* Arctic fox (*Alopex lagopus*?), *U. arctos*(?), *M. meles, Bos/Bison, M. giganteus, C. elaphus, D. dama, C. capreolus, S. scrofa, S. hemitoechus, P. antiquus*		Arnold-Bemrose and Newton (1905), Lewis *et al.* (2011)
Joint Mitnor Cave, Devon	MIS 5e		*C. crocuta, C. lupus, V. vulpes, U. arctos, M. meles, F. silvestris, P. leo, P. antiquus, S. hemitoechus, S. scrofa, H. amphibius, C. elaphus, D. dama, M. giganteus, B. priscus*		Currant and Jacobi (2011)
Kirkdale Cave, Yorkshire	MIS 5e See Table 10.4		*C. crocuta, Canis cf. lupus, V. vulpes, Ursus cf. arctos, Panthera cf. leo, P. antiquus, H. amphibious, C. elaphus, Dama cf. dama, M. giganteus, Bison cf. priscus, S. hemitoechus, Sus sp.(?), Equus sp.(?)*	Many bones (including those of *C. crocuta*) gnawed, possibly by *C. crocuta*. Probably *C. crocuta* den	Buckland (1822), Boylan (1981), McFarlane and Ford (1998)
Little Syke, Lincolnshire	MIS 5e	Presence of still or slow-flowing water. Riparian vegetation. Summer temperatures slightly highly than present day	*C. crocuta, H. amphibius, B. priscus, P. antiquus, S. hemitoechus*		Schreve (2007)
Milton Hill, Somerset	MIS 5e		*C. crocuta, H. amphibius, P. antiquus, B. primigenius, B. priscus, C. elaphus, D. dama, C. capreolus?,* Hominidae sp. (artefacts – later unconfirmed)		Balch (1937), Donovan (1988), Lewis *et al.* (2011)
Minchin Hole, Outer Beach, Glamorgan	MIS 5 See Table 10.4	Small mammals indicate temperate woodland	**Neritoides beach**: *C. crocuta, P. leo, D. dama, S. scrofa*. **Earthy Breccia Series**: *C. crocuta, P. leo, V. vulpes, S. hemitoechus, E.*		Sutcliffe (1981) Bowen *et al.* (1985), Sutcliffe *et al.* (1987)

			ferus, P. antiquus, C. elaphus, D. dama, S. scrofa		
Raygill Fissure, Yorkshire	MIS 5e		*C. crocuta, P. antiquus, S. hemitoechus, H. amphibius, B. priscus, C. capreolus.* Additional species towards base of fissure: *Ursus* sp.*, P. leo*	Pitfall trap	Green *et al.* (1880), Earp *et al.* (1961), Currant and Jacobi (2011), O'Connor and Lord (2013)
Tornewton Cave, Devon	See Table 10.2				
Victoria Cave, Yorkshire	MIS 5e See Table 10.4	Mammals suggest open vegetation.	*C. crocuta, V. vulpes, U. arctos, P. leo, P. antiquus, Mammuthus* sp.*, S. hemitoechus, H. amphibius, M. giganteus, C. elaphus, D. dama, C. capreolus, B. priscus*	Bones show damage by *C. crocuta*	Gilmour *et al.* (2007), Currant and Jacobi (2011), O'Connor and Lord (2013)
Badger Hole, Wookey Hole, Somerset	**Layer A2**: MIS 3 See Table 10.4		**Layer A2**: *C. crocuta, Felis* sp.*,* otter (*Lutra lutra*), *Vulpes/Alopex, Ursus* cf. *arctos, E. ferus, M. giganteus, R. tarandus?*	Many gnawed bones present in Layer A2.	Campbell (1977), Jacobi *et al.* (2006)
Bench Cavern, Devon	MIS 3 See Table 10.4		Dyke: *C. lupus, V. vulpes*, *A. lagopus*, *U. spelaeus* (possibly actually *U. arctos*), possibly *B. primigenius,* possibly *R. tarandus*, Cervidae sp., *C. antiquitatis,* Hominidae sp. (artefact). Cave earth within tunnel: *V. vulpes*.	No bones of any species had gnaw marks, except for one *C. crocuta* mandible. However, site is a fissure into which material had fallen, rather than a den.	Pengelly (1888), Jacobi *et al.* (2006)
Boughton Mount, Kent	MIS 3		*R. tarandus, C. elaphus, B. primigenius, E. caballus, C. antiquitatis, M. primigenius*		Dawkins (1869)
Brixham Cave/ Windmill Hill, Devon	MIS 3		*U. arctos* (*U. spelaeus* also mentioned by earlier authors)*, P. spelaea, V. vulpes, M. meles, R. tarandus, B. primigenius, C. capreolus, C. elaphus, C. antiquitatis, E. ferus, M. primigenius, Homo* sp. (artefacts)	Lack of juveniles, no coprolites. Many bones gnawed in Third and Fourth Beds, perhaps by *C. crocuta.* Gnawed bones include *U.*	Falconer, (1858), cited in Prestwich, (1873), Prestwich (1873), McFarlane *et al.* (2010)

			arctos, M. primigenius and *C. antiquitatis*. *B. primigenius*, *C. capreolus, C. elaphus, C. antiquitatis, E. ferus* and some *M. primigenius* were all found in similar locations to *C. crocuta*, so may have been their prey. Subsequent to *C. crocuta*, cave used by *U. arctos*	
Caerwent Quarry, Monmouthshire	MIS 3	*P. spelaea, M. meles, U. arctos, M. primigenius, S. scrofa, M. giganteus, R. tarandus, Bos/Bison*	No gnaw marks on bones, but fragmentary condition of bones and presence of juvenile *M. primigenius* suggests assemblage accumulated by *C. crocuta*	Locke (1970)
Caswell Bay, Swansea	MIS 3	*V. vulpes, P. spelaea, R. tarandus, C. elaphus, B. primigenius, B. priscus?, E. ferus, C. antiquitatis*	Material in thesis likely to be from Hyaena Den, Caswell Bay	Dawkins (1869), Howes (1988)
Church Hole, Creswell Crags, Nottinghamshire	MIS 3. See Table 10.4	**Upper beds at front of cave, and Chambers A and B**: *C. crocuta, U. arctos, C. antiquitatis, Mammuthus* sp., *Equus* sp., *R. tarandus, B. priscus*. **Talus red earth/sand**: *C. crocuta, M. meles, Canis* sp., *Ursus* sp., Rhinocerotidae sp., *Equus* sp., *M. giganteus, R. tarandus*. **Chamber A – Breccia (1)**: *C. crocuta*, Hominidae sp. (artefacts). **Reddish loamy cave earth (2)**: *C. crocuta, R. tarandus,* Hominidae sp. (artefacts). **Light cave earth (3)**: *C. crocuta, Ursus* sp., *Canis* sp., *C. antiquitatis, R.*	Some bones gnawed by C. crocuta and some broken by humans	Dawkins (1877), Mello (1877), Higham *et al.* (2006), Jacobi and Higham (2011)

			tarandus, M. giganteus, Hominidae sp. (artefact). **Mottled bed (4)**: *C. crocuta, Canis* sp., *Ursus* sp., *C. antiquitatis, R. tarandus, Mammuthus* sp., *E. ferus,* Hominidae sp. (artefacts). **Red sand (5)**: *C. crocuta, Canis* sp., *Ursus* sp., *C. antiquitatis, Mammuthus* sp., *Equus* sp., *B. priscus, R. tarandus,* Hominidae sp. (artefacts). **Chamber B** – similar species to Chamber A		
Coygan Cave, Carmarthenshire	MIS 3 See Table 10.4	Mammal species suggest extensive grassland	**Northerly compartment, reddish earthy soil**: *C. crocuta, C. antiquitatis, M. primigenius, Equus* sp., *R. tarandus.* Central dome to western branch, below stalagmite: *C. crocuta, U. arctos* (*U. spelaeus* also mentioned), *P. spelaea, V. vulpes*, *M. primigenius, C. antiquitatis, Equus* sp., *M. giganteus, R. tarandus, B. primigenius, B. priscus,* Hominidae sp. (artefact). **Southern half of main chamber, below stalagmite**: similar to above, with *D. dama*. **Central area, stony clay, below thin stalagmite**: *C. crocuta, C. antiquitatis, M. primigenius, E. caballus, B. primigenius, M. giganteus.* **Central area, cave earth, above thin stalagmite**: *C. crocuta Ursus* sp. (identified as *U. spelaeus*), *C. antiquitatis, M. primigenius, E. caballus, B. primigenius, R. tarandus*?	Most bones (including those of *C. crocuta, C. antiquitatis* and *E. ferus*) gnawed by *C. crocuta*. Human occupation short, later used as *C. crocuta* den.	Hicks (1867), Laws (1888), Grant-Dalton (1917), Grimes and Cowley (1935), Aldhouse-Green *et al.* (1995), Higham *et al.* (2006), Jacobi and Higham (2011)

		North Passage: *C. crocuta, V. vulpes, U. arctos, E. ferus, Sus* sp., *C. elaphus, R. tarandus.* **Outer Chamber**: *C. crocuta, C. lupus, A. lagopus, M. primigenius, C. antiquitatis, E. ferus, C. elaphus, R. tarandus, M. giganteus, Bos/Bison.* **Inner Chamber**: *C. crocuta, C. lupus, M. primigenius, C. antiquitatis, E. ferus, R. tarandus, M. giganteus, Bos/Bison.* **Example distribution of species by spit in Trench 2, Outer Chamber. Layer 2**: *C. crocuta, Vulpes/Alopex, M. primigenius, E. ferus, M. giganteus, Bos.Bison.* **Layer 4**: *C. crocuta, C. lupus, A. lagopus, M. primigenius, C. antiquitatis, E. ferus, R. tarandus, Bos/Bison,* Hominidae sp. (artefacts). **Layer 5**: *C. crocuta, A. lagopus, U. arctos, M. primigenius, C. antiquitatis, E. ferus, R. tarandus, M. giganteus, C. elaphus.*		
Daylight Rock Fissure, Pembrokeshire	MIS 3 See Table 10.4	*P. spelaea, Ursus* sp., *C. antiquitatis, Equus* sp., *Mammuthus* sp., *R. tarandus Bos/Bison, M. giganteus*	Some bones gnawed by *C. crocuta*	Lacaille and Grimes (1955) and Lacaille and Grimes (1961) both cited in Davies (1989), Davies (1989), Aldhouse-Green (n.d.), cited in Jacobi and Higham (2011)

Ffynnon Beuno Cave, Denbighshire	MIS 3 See Table 10.4		*C. crocuta, Vulpes/Alopex, C. antiquitatis, M. primigenius, Equus* sp., Bovidae sp., *R. tarandus, C. elaphus, D. dama, Homo* sp. (artefacts)	Occupied by *C. crocuta*. Bones of *C. antiquitatis, M. primigenius*, *Equus* sp., *C. elaphus* and *R. tarandus* gnawed by *C. crocuta*	Hicks (1885), Jacobi and Higham (n.d.) cited in Aldhouse-Green *et al.* (2015), Aldhouse-Green *et al.* (2015)
Goat's Hole Paviland, Swansea	MIS 3 See Table 10.4		*C. crocuta, C. lupus, V. vulpes* (may be recent)*, Vulpes/Alopex, U. arctos, M. primigenius, E. ferus, C. antiquitatis, S. scrofa, R. tarandus, C. elephas, M. giganteus*(?), *B. priscus* (some material possibly recent)*, O. aries* (domestic sheep, possibly recent), *Homo* sp. (artefacts), later *Homo sapiens*	Aurignacian occupation possibly alternated with *C. crocuta* occupation of the caves, however, many of the bones likely accumulated by humans. *U. arctos* may have later used the cave. The Red Lady was buried later. Gnawing by *C. crocuta* evident on *C. antiquitatis* long bones and shed, male *R. tarandus* antlers.	Turner (2000), Jacobi *et al.* (2006), Jacobi and Higham (2008)
Hyaena Den, Wookey Hole, Somerset	**Cave Earth**: MIS 3 See Table 10.4		*C. crocuta, P. spelaea, U. arctos* (*U. spelaeus* also mentioned), *C. lupus, A. lagopus*?*, V. vulpes, M. meles* (possibly intrusive)*, M. primigenius, C. antiquitatis, B. primigenius, B. priscus, E. caballus, S. scrofa, M. giganteus, C. elaphus, D. dama*?*, R. tarandus,* Hominidae sp.	Human artefacts in contact with *C. crocuta* teeth. Damage to bones (including those of carnivores) and antlers, probably by *C. crocuta*	Dawkins (1862), Dawkins (1863), Balch (1937), Tratman *et al.* (1971), Donovan (1988), Jacobi and Hawkes (1993), Jacobi *et al.* (2006)
Kents Cavern, Devon	**Red cave earth**: MIS 3 See Table 10.4	Isotopic values from herbivores indicate open vegetation.	**Granular Stalagmite**: *C. crocuta, Ursus* sp., *C. antiquitatis,* Elephantidae sp., Cervidae sp., Hominidae sp. (artefacts) **Black band (in Vestibule)**: *C. crocuta, Vulpes/Alopex, M. meles, Ursus* sp., *C.*	Cave has many chambers and passages, and the same stratigraphy is observed in most places: limestone blocks at the top, black	Pengelly (1865), Pengelly (1866), Pengelly (1867), Pengelly (1868), Dawkins (1868)

		antiquitatis, Equus sp., Cervidae spp., Bovidae sp., Hominidae sp. (artefacts) **Red cave earth**: *C. crocuta, U. arctos, P. spelaea, F. silvestris*?, *C. lupus, V. vulpes, M. meles, G. gulo, E. caballus*, *M. primigenius* (mostly juveniles), *C. antiquitatis, B. primigenius, B. priscus, M. giganteus, C. elaphus, R. tarandus, Ovis* sp. (potentially intrusive) Hominidae (artefacts), *H. sapiens* (mandible from Vestibule) **Talus external to North Sally-port**: *C. crocuta, Ursus* sp., *Equus* sp., Rhinocerotidae sp., Hominidae sp. (artefacts)	mould, granular stalagmite, red cave earth. In some areas, red cave earth lies below black mould. In the Vestibule, a black band also lies beneath the granular stalagmite. Little stratigraphy within the red cave earth. Breccia present in some areas, but did not contain *C. crocuta*. The talus external to North Sally-port was fine silt. The same species were found in all four of the foot-deep layers excavated by Pengelly. Bone gnawed by *C. crocuta* included *U. arctos*, *G. gulo*, *M. primigenius* (many juveniles), *Equus* sp., *C. antiquitatis* (many juveniles), *R. tarandus*, *C. elaphus*, *M. giganteus* and *B. primigenius*	cited in Pengelly (1869), Pengelly (1870), Pengelly (1872), Pengelly (1874), Lister (2001), (Bocherens *et al.*, 1995), Jacobi *et al.* (2006), Jacobi (2007) cited in Stuart and Lister (2014), Wilson (2010), Higham *et al.* (2011), Jacobi and Higham (2011), Bocherens (2014), Proctor *et al.* (2017) and references therein
King Arthur's Cave, Herefordshire	**Unit 3**: MIS 3	Species from 1925-1929 University of Bristol Spelaeological Society excavations. **Unit 3c**: *C. crocuta, U. arctos, M. primigenius, E. ferus, C. antiquitatis, C. elaphus,* Hominidae sp. (artefacts). **Unit 3d**: *C. crocuta, U. arctos, M. primigenius, E. ferus, C. antiquitatis, C. elaphus, R. tarandus, Bos/Bison,* Hominidae sp.	Unit 3e in the Passage is also called Upper Cave Earth. Unit 3d: ungnawed *U. arctos* humerus and femur may indicate this species occupied cave later than *C. crocuta* and burrowed into deposits. Unit 3e: *C. elaphus*	Currant (n.d.), cited in ApSimon *et al.* (1992), ApSimon *et al.* (1992)

			(artefacts). **Unit 3e**: *C. crocuta, U. arctos, M. primigenius, E. ferus, C. antiquitatis, C. elaphus, R. tarandus, Bos/Bison, Ovis sp.* (sheep), Hominidae sp. (artefacts).	bones ungnawed may indicate that this species may have been brought in after *C. crocuta* occupied the cave. Units 3c, 3d and 3e: likely *C. crocuta* dens	
Lewes Castle Cave, Swansea	MIS 3		*C. crocuta, C. lupus, Mammuthus* sp., *C. antiquitatis, R. tarandus*		Davies (1989)
Nanna's Cave, Caldey Island, Pembrokeshire	MIS 3 See Table 10.4				Aldhouse-Green (n.d.) cited in Jacobi and Higham (2011)
Picken's Hole, Somerset	**Layer 3**: MIS 3		**Layer 3**: *C. crocuta, P. spelaea, F. silvestris, C. lupus* (may have been derived from Layer 5), *Canis* sp., *A. lagopus, V. vulpes, U. arctos* (base of layer), *E. caballus, C. antiquitatis, M. primigenius, R. tarandus, C. elaphus, M. giganteus*?, *Bos* sp., Hominidae sp.	Layer 3: *C. crocuta* is most abundant carnivore. Most bones gnawed by *C. crocuta*	Tratman (1964)
Pin Hole, Creswell Crags, Derbyshire	**Lower Cave Earth**: MIS 3 See Table 10.4	Pollen from *C. crocuta* coprolite from Level 10', east passage (sediments continuation of Lower Cave Earth or main passage): 1 % arboreal pollen, 99 % non-arboreal pollen, indicating open grassland	**Lower Cave Earth**: *C. crocuta*, *C. lupus, V. vulpes, U. arctos, P. spelaea, M. primigenius, E. ferus, C. antiquitatis, M. giganteus, R. tarandus, B. priscus, Homo* sp.	Nearly all bones, including *C. antiquitatis* gnawed by *C. crocuta*. Damage may also have been caused to a bone of *M. giganteus*. Early Gravettian industry found near base of Upper Cave Earth. Cave Earth largely comprised of sediment that fell from aven and fissures in the roof of the cave, with reworked older deposits.	Busk (1875), Mello (1875), Jacobi *et al.* (1998), Jacobi *et al.* (2006), Currant and Jacobi (2011), Jacobi and Higham (2011), Lewis (2011)

			However, lower Cave Earth stratigraphy maintained	
Priory Farm Cave, Pembrokeshire	**Laminated Clay**: MIS 3	**Laminated Clay**: *C. crocuta, U. arctos, C. lupus*, *R. tarandus, E. caballus,* Bovidae sp., *M. primigenius* **Uncertain stratigraphic provenance**: *Vulpes/Alopex, M. meles, C. elaphus, Sus* sp., Caprinae sp.	Some bones including *M. primigenius* gnawed by *C. crocuta.* Flint artefacts found in Gravel, but uncertain relationship to Laminated Clay. Site occupied by *C. crocuta*	Cowley (1933), Grimes (1933)
Sandford Hill, Somerset	MIS 3 (specimens with dense preservation)	*C. crocuta, P. spelaea, V. vulpes, C. lupus, U. arctos, E. ferus, C. antiquitatis, R. tarandus, C. elaphus, B. priscus*	Two types of preservation. One group: dense bone, gnawing by *C. crocuta*. Other group: light weight, including *R. tarandus, P. spelaea*, some *C. antiquitatis*	Currant (2004)
Uphill Caves, Somerset	MIS 3 See Table 10.4	**Caves 7 and 8**: *C. crocuta, P. spelaea, V. vulpes, Ursus* sp.*, M. meles* (possibly intrusive), *M. primigenius, C. antiquitatis, Equus* sp., *B. priscus, Cervus* (*elaphus*?), *R. tarandus, M. giganteus*? **Cave 8**: Hominidae sp. (artefacts)	Potential mixing of deposits by water	Wilson and Reynolds (1901), Davies (1926), Sutcliffe (n.d.) cited in Harrison (1977), Harrison (1977), Jacobi and Pettitt (2000), (Jacobi *et al.*, 2006)
Yealm Bridge, Devon	MIS 3	*C. crocuta, C. lupus, V. vulpes, Ursus* sp., *E. caballus, C. antiquitatis, C. elaphus, R. tarandus, Bos* sp., *B. priscus, O. aries, M. primigenius*		Freedman (2015)

Robin Hood Cave, Creswell Crags, Derbyshire	**Red clay and yellow sand**: MIS 5e. **Silty sand from southwestern corner of Western Chamber**, excavated in 1981: MIS 3. **Layers USB, OB, LSB, B/A and A** from 1969 excavation: MIS 3 See Table 10.4	Mammal remains suggest cold conditions, interrupted by milder conditions	**Red clay and yellow sand**: *C. crocuta, C. lupus, Ursus* sp., *H. amphibius, S. hemitoechus, B. priscus,* Cervidae sp., *S. scrofa.* 1969 excavations (layers listed higher to lower) **Layer USB**: *C. crocuta* (may be derived from lower layers)*, C. lupus, U. arctos, C. antiquitatis, E. ferus, R. tarandus,* Hominidae sp. (artefacts). **Layer OB**: *C. crocuta* (may be derived from lower layers)*, C. lupus, V. vulpes, U. arctos, C. antiquitatis, E. ferus, C. elaphus, M. giganteus, R. tarandus,* Hominidae sp. (artefacts). **Layer LSB**: *C. crocuta* (may be derived from lower layers)*, A. lagopus, C. antiquitatis, E. ferus, R. tarandus,* Hominidae sp. (artefacts). **Layer B/A**: *C. crocuta* (may be derived from lower layers)*, A. lagopus, C. antiquitatis, E. ferus, R. tarandus, C. ibex,* Hominidae sp. (artefacts). **Layer A**: *C. crocuta, V. vulpes, C. lupus, M. primigenius, C. antiquitatis, Equus* cf. *germanicus* (horse), *C. elaphus,* Hominidae sp. (artefacts)		Laing (1890), Campbell (1977), Charles *et al.* (1994), Jacobi *et al.* (2006), Higham *et al.* (2006), Jacobi and Higham (2011)
Austria					
Teufelslucke, Eggenburgh	MIS 3 See Table 10.4		*C. crocuta, U. spelaeus, C. lupus, V. vulpes, A. lagopus, G. gulo, M. meles, P. spelaea, M. primigenius, B. priscus, Bison bonasus* (European bison), *C. elaphus, M. giganteus, R. tarandus, Equus* cf. *chosaricus* (horse)*, E.*	Inhabited by *C. crocuta*, *U. spelaeus* and humans	Adam (1966), Berg (1966), Ehrenberg (1966a), Ehrenberg (1966b) Lehmann (1966), Thenius (1966), Zapfe

			hydruntinus, C. antiquitatis, Hominidae sp. (artefacts)		(1966a), Zapfe (1966b), Hofreiter *et al.* (2004), Rohland *et al.* (2005)
Belgium					
Goyet caves, Namur Province	See Table 10.3				
Caverne Marie-Jeanne, Hastière, Namur Province	**4eme Niveau**: MIS 3 See Table 10.4	**4eme Niveau**: based on fauna, mean annual temperature = 3.35°C; mean annual precipitation = 1018 mm. Cool temperatures. Open dry meadows and woodland dominant, with areas of open humid meadows, rocky environments and areas of running water	**4eme Niveau**: *C. crocuta, L. lynx, P. spelaea, M. meles, C. lupus, V. vulpes/A. lagopus, U. spelaeaus, M. primigenius, C. antiquitatis, Equus* cf. *remagensis* (horse), *C. elaphus, R. tarandus, R. rupicapra, C. ibex, B. priscus* (possibly also *B. primigenius*), Hominidae sp. (artefacts)	Used as *C. crocuta* den. Evidence of *C. crocuta* damage to large herbivore bones. Although artefacts are present, no evidence of humans inhabiting the cave	Ballmann *et al.* (1980), Gautier (1980), Brace *et al.* (2012), López-García *et al.* (2017)
Trou Magrite, Pont-à-Lesse, Namur	Late Pleistocene (probably MIS 5b to 3)		**Fluvial silt (lower levels)**: *C. crocuta, P. spelaea, Lynx* sp., *F. silvestris, Canis* sp., *V. vulpes, U. spelaeus, M. meles, Mammuthus* sp., Rhinocerotidae sp., *S. scrofa, Equus* sp.,	Dupont's 'Âge du Mammoth'	Dupont (1873), Gautier *et al.* (1997), RBINS museum label

			R. rupicapra, R. tarandus, C. capreolus, C. ibex, Bovidae sp., Hominidae sp. (artefacts, including carved reindeer antlers)		
Czech Republic					
Höhle Výpustek	MIS 3 See Table 10.4	Large and small mammals indicate mixture of forest and steppe vegetation	*C. crocuta, U. spelaeus, P. spelaea, L. lynx, F. silvestris, Canis* sp., *C. familiaris, V. vulpes, A. lagopus, G. gulo, C. antiquitatis, M. primigenius, Equus* sp., *R. tarandus, C. elaphus, M. giganteus, C. capreolus, C. ibex, B. priscus*	Likely used as a den for predators, including *C. crocuta* and *U. spelaeus*. Potentially some mixing of deposits, including introduction of domestic species (*C. familiaris*, domestic goose, *Ancer* sp., and chicken, *Gallus gallus domesticus*). However, complete skeletons of *C. crocuta* and *U. spelaeus* present	Liebe, (1879), Hofreiter *et al.* (2004), Rohland *et al.* (2005)
Slouper Höhle	Late Pleistocene		*C. crocuta*, possibly *P. spelaea, C. antiquitatis, B. primigenius, M. primigenius, R. tarandus*	*U. spelaeus* also present in cave, but may not have been contemporary with *C. crocuta*.	Diedrich (2012)
Ireland					
Castlepook Cave, County Cork	MIS 3 See Table 10.4		*C. crocuta, U. arctos* (may not have been contemporaneous with *C. crocuta*), *V. vulpes, A. lagopus, C. lupus, M. primigenius* (many juveniles), *R. tarandus* (including male, female and juvenile antlers), *M. giganteus* (some juveniles)	*C. crocuta* and *U. arctos* used cave as den. Gnawed bones of *R. tarandus* (although many were not gnawed), *M. primigenius*, *M. giganteus*, *U. arctos* and *C. crocuta*	Ussher, (1906), Scharff *et al.* (1918), Sutcliffe (unpublished data) cited in Woodman *et al.* (1997), Woodman *et al.*

					(1997), Stuart and Lister (2014)
Italy					
San Teodoro, Acquedolci, Sicily	**Unit B**: MIS 2-3 See Table 10.4	Trench α: cool climate becoming colder and arid. Open, steppe vegetation. Trench β, Squares A-C: cool climate becoming colder and arid. Trench β, Squares D-G: more humid climate, indicated by molluscs. Unit B: open, steppe vegetation with some trees. Cool summers, indicated by pollen from *C. crocuta* coprolites.	**Unit B**: *C. crocuta, C. lupus, V. vulpes, Palaeoloxodon mnaidriensis* (dwarf elephant), *E. hydruntinus, Bos primigenius siciliae* (Sicilian aurochs), *Bison priscus siciliae* (Sicilian bison), *Cervus elaphus siciliae* (Sicilian red deer), *S. scrofa*	Used as *C. crocuta* den. *C. crocuta* damage to bones including *C. crocuta, P. mnaidriensis, C. e. siciliae, S. scrofa, E. hydruntinus, B. p. siciliae/B. p. sicilae*	Marra *et al.* (2004), Yll *et al.* (2006), Bonfiglio *et al.* (2008) Mangano (2011), Antonioli *et al.* (2015)
Serbia					
Baranica I	**Layer 2**: MIS 2 **Layer 3**: MIS 3 See Table 10.4	Cold climate	*C. crocuta, C. lupus, V. vulpes, U. spelaeus, M. meles, P. spelaea, C. antiquitatis, E. ferus, E. hydruntinus, M. giganteus, C. elaphus, B. priscus, C. ibex, R. rupicapra, Homo* sp. (Layer 2)	*C. crocuta* gnawing on *C. crocuta* remains. *C. crocuta* den. Many remains accumulated by *C. crocuta*	Argant and Dimitrijević (2007), Dimitrijević (2011)

Baranica II	MIS 3 See Table 10.4	Cold climate. Open vegetation with steppe species	*C. crocuta, C. lupus, V. vulpes, U. spelaeus, P. spelaea, P. pardus, F. silvestris, M. primigenius, C. antiquitatis, E. ferus, E. hydruntinus, M. giganteus, C. elaphus, B. priscus, C. ibex, R. rupicapra*	*C. crocuta* gnawing on *C. crocuta. C. crocuta* den. Most remains accumulated by *C. crocuta*	Argant and Dimitrijević (2007), Dimitrijević (2011), Stuart and Lister (2014)
Spain					
Cova de les Toixoneres = Cova de les Teixoneres, Barcelona	MIS 3 See Table 10.4	**Chamber X, Level III**: open forest dominated, temperate and humid climate. **Chamber X, Level II**: open forest dominated with increase in meadows, drier and cooler climate than Level III.	**Chamber X, Level IIIb**: *C. crocuta, U. spelaeus, V. vulpes, Lynx* sp., *M. meles,* Proboscidea sp., Rhinocerotidae Sp., *E. ferus, E. hydruntinus, Bos/Bison, C. elaphus, C. capreolus, S. scrofa, Castor* sp., *H. neanderthalensis* (artefacts). **Chamber X, Level IIIa**: *C. crocuta*, *U. spelaeus*, *C. lupus*, *M. meles*, Rhinocerotidae sp., *E. ferus, Bos/Bison,* Caprinae sp., *C. elaphus, S. scrofa, Castor* sp*., H. neanderthalensis* (artefacts). **Chamber X, Level IIb**: *C. crocuta, U. spelaeus, V. vulpes, Lynx* sp., *M. meles,* Rhinocerotidae sp., *E. ferus, Bos/Bison,* Caprinae sp. *C. elaphus, S. scrofa, Homo* sp. (artefacts). **Chamber X, Level IIa**: *C. crocuta, U. spelaeus, Lynx* sp., Rhinocerotidae sp., *E. ferus, Bos/Bison,* Caprinae sp. *C. elaphus, S. scrofa, Homo* sp. (artefacts). **Chamber Y, Level 1**: *C. crocuta*.	Radiocarbon dates suggest that *C. crocuta* occupied the interior of the cave (Chamber Y, Level 1) during approximately the same period that *H. neanderthalensis* occupied the front of the cave (Chamber X, Level III). Evidence of carnivore damage to ungulate bones in Chamber A, Levels IIa, IIb, IIIa and IIIb.	López-García *et al.* (2012), Talamo *et al.* (2016)
Cova del Toll, Barcelona	Late Pleistocene	**Levels D, E and F**: cold and wet climate. **Level H**: very cold and wet climate.	**Level D**: *C. crocuta, U. spelaeus, C. lupus, M. meles, Lynx pardinus* (Iberian lynx), *C. elaphus, C. capreolus.* **Level E**: *C. crocuta.* **Level F**: *C. crocuta, U. spelaeus, C. elaphus, C. capreolus, S. scrofa*		Allué *et al.* (2013)

		Level I: cool climate.	**Level H**: *C. crocuta, U. spelaeus, Canis* sp., *P. spelaea, F. silvestris, L. pardinus, B. priscus, B. primigenius, C. ibex, R. rupicapra, C. elaphus, S. scrofa, E. caballus, C. antiquitatis.* **Level I**: *C. crocuta, U. spelaeus, E. caballus, B. priscus, Hippopotamus major* (giant European hippopotamus), *Stephanorhinus kirchbergensis* (Merck's rhinoceros)		
Cova del Gegant, Barcelona	MIS 4-3 See Table 10.4	Fauna indicates a mixture of open vegetation and open forest. Mean annual temperature = 10±2.6°C (cooler than today). Mean temperature of coolest month = 2.6±0.7°C. Mean temperature of warmest month = 20.1±1°C. Mean annual precipitation = 850±150 mm (wetter than today).	*C. crocuta, C. lupus, Cuon alpinus europaeus* (European dhole), *F. silvestris, L. pardinus, U. arctos, V. vulpes, M. meles, P. pardus, Bos/Bison, Capra pyrenaica* (Iberian ibex), *C. elaphus, S. scrofa, S. kirchbergensis, S. hemitoechus, E. caballus, H. neanderthalensis*	Fauna found in Levels III, IIa and I, however, stratigraphic provenance information of specimens is lacking	Daura *et al.* (2005), López-García *et al.* (2008), Daura *et al.* (2010), Fernández-García (2014)

Cova B d'Olopte	MIS 3	**Stratum 6**: *C. crocuta, P. spelaea, C. antiquitatis, Equus* sp., *S. scrofa, C. elaphus, B. primigenius*		de Villalta (1972), Fernández-García (2014)
Cueva de las Hienas (= Las Caldas), Asturias	MIS 5b-3	*C. crocuta, Canis* sp., *V. vulpes, E. ferus, S. hemitoechus, S. scrofa, C. elaphus, Bos/Bison, R. rupicapra, Capra* sp.		Sesé and Morales (n.d.), cited in Martin and Sanchiz (1989), Hoyos (1979), cited in Martin and Sanchiz (1989), Martin and Sanchiz (1989), Domingo *et al.* (2005)
Cueva del Búho, Segovia	MIS 5d-3	*C. crocuta, Lynx spelaea* (cave lynx), possibly *Panthera* sp., *C. lupus, V. vulpes, M. meles, Equus ferus antunesi* (horse), *E. hydruntinus, C. elaphus, S. scrofa, Bos* cf. *primigenius, S. hemitoechus*	Used as *C. crocuta* den. Gnaw marks and evidence of acid digestion on *Equus* sp., Bovidae sp. and Cervidae sp. bones, probably by *C. crocuta*.	Iñigo (1995), Molero *et al.* (1989) and Maldonado (1996) both cited in Iñigo *et al.* (1998), Iñigo *et al.* (1998)

Table 10.2: Details of Tornewton, Devon, Britain. References: Widger (1892) and Sutcliffe and Zeuner (1962) both cited in Currant (1998) and Gilmour et al. (2007), Sutcliffe and Kowalski (1976), Currant (1998), Gilmour et al. (2007), Lewis (2011).

Stratigraphic unit	**Age**	**Palaeoenvironmental reconstruction**	**Large mammal species**	**Further information**
Vivian's Vault	MIS 6 & 5e			
Great Bone Bed = Hyaena Stratum = Unit I = gritty cave earth	MIS 5c See Table 10.4	Pollen from *C. crocuta* coprolite thought to be from this unit: non-arboreal pollen most abundant, some woodland locally or regionally, lack of thermophilous species.	*C. crocuta, C. lupus, V. vulpes, P. leo, Ursus* sp., *S. hemitoechus, H. amphibius, D. dama, C. elaphus,* large bovid	*C. crocuta* den. Mostly teeth and foot bone present – *C. crocuta* consumed most parts of *C. crocuta* and other species
Elk Stratum	MIS 3		*C. crocuta, C. antiquitatis, E. ferus, R. tarandus, C. elaphus*	
Glutton Stratum	End of MIS 3, but mixed with other fauna		*U. arctos, G. gulo, C. lupus, V. vulpes, P. leo. M. meles, R. tarandus, E. ferus, S. hemitoechus, H. amphibius, D. dama, C. capreolus,* small bovid	

Table 10.3: Details of Goyet caves, Namur Province, Belgium. References: Dupont (1873), Germonpre (1997), Germonpré (2001), Germonpré and Sablin (2001), Germonpré and Hämäläinen (2007), Germonpré *et al.* (2009), Peigné *et al.* (2009), Stevens *et al.* (2009), Stuart and Lister (2012), Germonpré (unpublished) cited in Comeyne (2013), Comeyne (2013), Rougier *et al.* (2016), supplemented by museum labels from RBINS.

Stratigraphic unit	**Age**	**Palaeoenvironmental reconstruction**	**Large mammal species**	**Further information**
3eme Caverne, Chamber A, 1er Niveau Ossifère	MIS 3 See Table 10.4	Mammals indicate open steppe vegetation and dry climate, and reflect the hilly topography	*C. crocuta, C. lupus* , *V. vulpes, A. lagopus*, *U. arctos, U. spelaeus, M. meles, Mammuthus* sp.*, C. antiquitatis, Equus caballus arcelini* (domestic horse), *R. tarandus, C. ibex, R. rupicapra, O. moschatus, S. scrofa,* Bovidae sp.*,* Hominidae sp. (damage to bone, artefacts)	Carnivore remains found at back of Chamber, and bone accumulated by humans found at front of chamber. Humans responsible for accumulation of most *Equus* sp. remains
3eme Caverne, Chamber A, 3eme Niveau	MIS 3 See Table 10.4		*C. crocuta, C. lupus, U. spelaeus, U. arctos R. tarandus*, *Equus* sp. *H. neanderthalensis*	Large carnivores found at back of chamber and bone accumulated by humans found at front of chamber. *C. crocuta* gnaw marks confined to specimens from the rear half of the chamber, and cut-marks confined to the front, with little spatial overlap. Carnivore damage to *Equus* sp. and *R. tarandus* remains is rare. Cut-marks evidence on *H. neanderthalensis*, *Equus* sp. and *R. tarandus* bones. Some *U. spelaeus* bones shown human modification, but there is no evidence of this on *C. crocuta* remains, although both species found towards the back of the chamber
3eme Caverne, Chamber A, 4eme Niveau Ossifère, Galleries Voisines de l'Entrée	MIS 3 See Table 10.4		*C. crocuta, C. lupus, A. lagopus, V. vulpes, U. spelaeus, L. lynx, M. primigenius, C. antiquitatis, E. germanicus, C. elaphus, R. tarandus, B. priscus, R. rupicapra, C. ibex*	Level located mainly at the back of the chamber.

Table 10.4: Dating of sites included in this study. U-Th = uranium-thorium dating. UF = ultrafiltrated gelatin, radiocarbon pre-treatment. 14C = radiocarbon date. OSL = Optically stimulated luminescence Radiocarbon dates calibrated using OxCal 4.3 and IntCal13, with 95.4 % confidence range (Bronk Ramsey, 2009; Reimer et al., 2013). For references see Table 10.1 to Table 10.3. Where possible, the radiocarbon dates displayed are only those that included the ultrafiltrated radiocarbon pre-treatment. There are additional, younger dates from Goyet, 3eme Caverne, 1er Niveau Ossifère, in Chamber A on *E. c. arcelini*, *O. moschatus*, *Canis* sp. (likely wolf) and *C. antiquitatis*, which range from 16,320±140 ^{14}C BP = 20,070-19,337 cal BP to 12,560±50 ^{14}C BP = 15,142-14,529 cal BP.

Site	Stratigraphy	Dating method	Species	Date	Calibrated date (cal BP)	Further information
Kirkdale Cave	Capping bone-bearing sediment	U-Th	Flowstone	121.4+4.8/-4.6 ka		
Minchin Hole		U-Th	Flowstone	127-107 ka		
Minchin Hole		Amino acid		MIS 5		
Victoria Cave		U-Th	Flowstone encasing *S. hemitoechus* tooth	115.69+2.68/-2.64 ka		
Victoria Cave		U-Th	Flowstone encasing *S. hemitoechus* tooth	111.97+2.42/-2.38 ka		
Tornewton	Dark Earth	U-Th	Stalagmite	100.447 ka		
Tornewton	Dark Earth	U-Th	Stalagmite	104.928 ka		
Tornewton	Dark Earth	U-Th	Stalagmite	98.370 ka		
Tornewton	Capping Dark Earth	U-Th	Stalagmite	77.552 ka		Minimum age for Dark Earth
Tornewton	Capping Dark Earth	U-Th	Stalagmite	76.290 ka		Minimum age for Dark Earth
Tornewton	Hyaena Stratum		Stalagmite	134.519 ka		Maximum age for Hyaena Stratum
Badger Hole	Grid Gc 5’	UF ^{14}C	*E. ferus*	36,000±450 ^{14}C BP	41,563-39,706	
Bench Cavern		UF ^{14}C	*C. crocuta*	36,800±450 ^{14}C BP	42,114-40,510	
Church Hole		UF ^{14}C	*C. crocuta*	>40,000 ^{14}C BP		
Coygan Cave		UF ^{14}C	*C. crocuta*	32,140±250 ^{14}C BP	36,580-35,465	

Coygan Cave	Trench IIB, Spit 5	UF ^{14}C	*C. crocuta*	32,400±550 ^{14}C BP	38,145-35,231	
Coygan Cave		UF ^{14}C	*C. crocuta*	36,000±550 ^{14}C BP	41,721-39,516	
Coygan Cave	Trench IIB, Spit 7	UF ^{14}C	*C. crocuta*	39,700±1700 ^{14}C BP	47,894-41,331	Date may extend out of range
Coygan Cave	Trench IIB, Spit 1	UF ^{14}C	*C. crocuta*	43,000±2,100 ^{14}C BP	= ?-43,944	Date may extend out of range
Coygan Cave		^{14}C	*C. crocuta*	>37,700 ^{14}C BP		
Coygan Cave	Trench IIB, Spit 4	^{14}C	*C. crocuta*	>41,300 ^{14}C BP		
Coygan Cave		UF ^{14}C	*C. antiquitatis*	45,800±320 ^{14}C BP	?-48,510	Date may extend out of range
Daylight Rock Fissure		^{14}C	*C. crocuta*	46,400±3800 ^{14}C BP	?-45,053	Date may extend out of range
Ffynnon Beuno Cave		^{14}C	*C. crocuta*	18,520±130 ^{14}C BP	22,681-22,001	Date likely inaccurate due to conservation
Ffynnon Beuno Cave		^{14}C	*C. antiquitatis*	28,030±340 ^{14}C BP	32,865-31,225	
Ffynnon Beuno Cave		^{14}C	*Bos/Bison*	24,450±400 ^{14}C BP	29,368-27,762	
Ffynnon Beuno Cave		^{14}C	*M. primigenius* (gnawed)	27,860±340 ^{14}C BP	32,697-31,129	
Goat's Hole Paviland		UF ^{14}C	*C. crocuta*	23,120±130 ^{14}C BP	27,656-27,169	Date likely inaccurate due to conservation
Goat's Hole Paviland		UF ^{14}C	*C. antiquitatis* (gnawed by *C. crocuta*)	32,870±200 ^{14}C BP	37,701-36,302	
Goat's Hole Paviland		UF ^{14}C	*C. antiquitatis* (gnawed by *C. crocuta*)	33,800±200 ^{14}C BP	38,770-37,634	

Goat's Hole Paviland		UF ^{14}C	*C. antiquitatis* (gnawed by *C. crocuta*)	42,650±800 ^{14}C BP	47,869-44,594	
Goat's Hole Paviland		UF ^{14}C	*R. tarandus* (gnawed by *C. crocuta*)	31,990±180 ^{14}C BP	36,298-35,469	
Goat's Hole Paviland		UF ^{14}C	*R. tarandus* (gnawed by *C. crocuta*)	37,350±320 ^{14}C BP	42,296-41,315	
Goat's Hole Paviland		UF ^{14}C	*R. tarandus* (gnawed by *C. crocuta*)	40,570±370 ^{14}C BP	44,869-43,380	
Goat's Hole Paviland		UF ^{14}C	*R. tarandus*	23,700±140 ^{14}C BP	28,058-27,548	Repeated date
Goat's Hole Paviland		UF ^{14}C	*R. tarandus*	24,240±110 ^{14}C BP	28,601-27,957	Repeated date
Goat's Hole Paviland		UF ^{14}C	Cervidae sp.	21380±170 ^{14}C BP	25997-25337	
Goat's Hole Paviland		UF ^{14}C	*U. arctos*	28,750±600 ^{14}C BP	33,972-31,437	
Goat's Hole Paviland		UF ^{14}C	*Equus* sp.	26,170±150 ^{14}C BP	30,858-29,970	
Goat's Hole Paviland		UF ^{14}C	*M. primigenius*	22,210±160 ^{14}C BP	26,964-26,059	Repeated date
Goat's Hole Paviland		UF ^{14}C	*M. primigenius*	21,710±120 ^{14}C BP	26,179-25,743	Repeated date
Goat's Hole Paviland		UF ^{14}C	*H. sapiens*	28,870±180 ^{14}C BP	33,586-32,513	
Goat's Hole Paviland		UF ^{14}C	*H. sapiens*	29,490±210 ^{14}C BP	34,074-33,245	
Hyaena Den	Unit 2 (Cave Earth)	UF ^{14}C	*C. crocuta*	48,600±1,000 ^{14}C	50,940-46,790	Date out of range
Hyaena Den	Unit 2 (Cave Earth)	UF ^{14}C	*C. elaphus*	45,100±1,000 ^{14}C BP	?-46,740	Date may extend out of range
Hyaena Den	Unit 2 (Cave Earth)	UF ^{14}C	Bone fragment	47,000±1,700 ^{14}C	?-49,811	Date probably out of range
Hyaena Den	Unit 1 (Fine Silt)	UF ^{14}C	Bone fragment	52,700±2,000 ^{14}C BP	58,841-49,261	Date out of range
Hyaena Den		UF ^{14}C	Antler/bone point artefact	31,550±340 ^{14}C BP	36,164-34,784	
Kents Cavern		UF ^{14}C	*C. crocuta*	40,200±600 ^{14}C BP	44,945-42,881	
Kents Cavern		UF ^{14}C	*C. crocuta*	37,750±500 ^{14}C BP	42,785-41,379	
Kents Cavern		UF ^{14}C	*C. crocuta*	30,630±380 ^{14}C BP	35,346-33,933	

Kents Cavern		UF ^{14}C	Bone fragment (damaged by *C. crocuta*)	36,750±450 ^{14}C BP	42,080-40,460	
Kents Cavern	C13’-3”	UF ^{14}C	*P. leo*	43,600±3,600 ^{14}C BP	?-43,322	Date may extend out of range
Kents Cavern	C5'-9"	UF ^{14}C	cf. *P. leo*	38,380±340 ^{14}C BP	42,954-42,007	
Kents Cavern	C5'-0	UF ^{14}C	*C. lupus*	29,840±330 ^{14}C BP	34,598-33,431	
Kents Cavern	C9'-0	UF ^{14}C	*U. arctos*	35,600±700 ^{14}C BP	41,611-38,806	
Kents Cavern	C14'-0	UF ^{14}C	*C. antiquitatis*	45,000±2,200 ^{14}C BP	?-45,465	Date may extend out of range
Kents Cavern	C9'-6"	UF ^{14}C	*C. antiquitatis*	37,200±550 ^{14}C BP	42,530-40,750	
Kents Cavern	Trench C, C9-10'0?"	UF ^{14}C	*C. antiquitatis*	36,700±750 ^{14}C BP	42,470-39,880	
Kents Cavern	Trench C, 9'9"	UF ^{14}C	*C. antiquitatis*	36,500±750 ^{14}C BP	42,341-39,676	
Kents Cavern	Trench C, C10-11'	UF ^{14}C	*C. antiquitatis*	36,100±700 ^{14}C BP	42,004-39,333	
Kents Cavern	C8'-3"	UF ^{14}C	*C. antiquitatis*	36,370±320 ^{14}C BP	41,645-40,310	Repeated date
Kents Cavern	C8'-3"	UF ^{14}C	*C. antiquitatis*	35,650±330 ^{14}C BP	41,088-39,522	Repeated date
Kents Cavern	C8'-3"	UF ^{14}C	*C. antiquitatis*	36,040±330 ^{14}C BP	41,409-39,960	
Kents Cavern	Trench C, C10'0"	UF ^{14}C	*C. antiquitatis*	34,950±650 ^{14}C BP	41,111-38,316	
Kents Cavern	C12'-13'-0	UF ^{14}C	*C. antiquitatis* (heated)	35,150±330 ^{14}C BP	40,501-38,895	
Kents Cavern	C19'-20'-0	UF ^{14}C	*R. tarandus*	49,600±220 ^{14}C BP	50,053-49,172	Date out of range
Kents Cavern	C15'-0	UF ^{14}C	*R. tarandus*	40,000±700 ^{14}C BP	44,976-42,655	
Kents Cavern	Trench C, C10'0"	UF ^{14}C	*R. tarandus*	35,100±650 ^{14}C BP	41,176-38,457	
Kents Cavern	Trench C, 9'90"	UF ^{14}C	*R. tarandus*	34,850±600 ^{14}C BP	40,911-38,285	
Kents Cavern	C7'-3"	UF ^{14}C	*C. elaphus*	35,550±750 ^{14}C BP	41,654-38,700	
Kents Cavern	Entrance to NE Gallery trench, 6'6"-7"	UF ^{14}C	*C. elaphus*	33,150±550 ^{14}C BP	38,716-36,094	
Kents Cavern	Trench C, C12'9-13'8"	UF ^{14}C	*C. elaphus*	32,200±450 ^{14}C BP	37,532-35,100	

Kents Cavern	Entrance to NE Gallery trench, 6'6"-7"	UF ^{14}C	*C. elaphus*	30,850±400 ^{14}C BP	35,629-34,066	
Kents Cavern	C4'-4"--4'-8"	UF ^{14}C	*C. elaphus*	30,000±180 ^{14}C BP	34,445-33,747	
Kents Cavern	Trench C, C12'6"-13'8"	UF ^{14}C	Bovidae sp.	38,900±1,100 ^{14}C BP	45,073-41,467	
Kents Cavern	B8'-0	^{14}C	Bovidae sp.	36,400±1400 ^{14}C BP	43,746-38,402	
Kents Cavern	B6'-0	UF ^{14}C	Bovidae sp.	31,400±380 ^{14}C BP	39,615-37,545	
Kents Cavern	Trench C, C10'9"	UF ^{14}C	Bovidae sp.	32,800±800 ^{14}C BP	38,986-35,192	
Nanna's Cave		UF ^{14}C	*C. crocuta*	27,100±750 ^{14}C BP	33,108-29,692	
Pin Hole		UF ^{14}C	*C. crocuta*	>35,500 ^{14}C BP		
Pin Hole		UF ^{14}C	*C. crocuta*	37,800±500 ^{14}C BP	42,815-41,419	Repeated date
Pin Hole		UF ^{14}C	*C. crocuta*	37,150±450 ^{14}C BP	42,359-40,895	Repeated date
Pin Hole	64/11' - 0"	UF ^{14}C	*C. antiquitatis* (gnawed by *C. crocuta*)	58,800±3,700 ^{14}C BP	77,703-53,623	Date out of range
Pin Hole	42/11' - 6"	UF ^{14}C	*C. antiquitatis*	55,900±4,000 ^{14}C BP	77,074-50,625	Date out of range
Pin Hole	50/10' - 0"	UF ^{14}C	*C. antiquitatis*	54,000±2,900 ^{14}C BP	66,391-49,341	Date out of range
Pin Hole	48/8' - 6"	UF ^{14}C	*C. antiquitatis*	52,500±2,800 ^{14}C BP	64,070-47,945	Repeated date. Date out of range
Pin Hole	48/8' - 6"	UF ^{14}C	*C. antiquitatis*	>43,000 ^{14}C BP		Repeated date
Pin Hole	50/7' - 0"	UF ^{14}C	*C. antiquitatis*	45,000±750 ^{14}C BP	49,969-46,935	Date may extend out of range
Pin Hole	44/8' - 6"	UF ^{14}C	*C. antiquitatis*	43,350±650 ^{14}C BP	48,199-45,384	
Pin Hole	37/9' - 6"	UF ^{14}C	*M. primigenius*	48,400±110 ^{14}C BP	48,622-48,183	Date may extend out of range
Pin Hole	62/9' - 0"	UF ^{14}C	*E. ferus*	53,000±1,900 ^{14}C BP	58,636-49,721	Date out of range
Pin Hole	64/9' - 0"	UF ^{14}C	*E. ferus*	49,600±1,000 ^{14}C BP	51,940-47,790	Date out of range
Pin Hole	50/8' - 0"	UF ^{14}C	*E. ferus*	47,000±1,200 ^{14}C BP	?-49,897	Date probably out of range
Pin Hole	64/7' - 0"	UF ^{14}C	*R. tarandus*	44,200±800 ^{14}C BP	49,453-45,952	Date may extend out of range

Pin Hole	65/8' - 0"	UF ^{14}C	*R. tarandus*	40,650±500 ^{14}C BP	45,145-43,286	
Pin Hole	70/7 - 0"	UF ^{14}C	*R. tarandus*	37,760±340 ^{14}C BP	42,578-41,599	
Pin Hole	53/7' - 6"	UF ^{14}C	Bovidae sp.	48,000±1,000 ^{14}C BP	?-49,976	Date probably out of range
Pin Hole	65/9' - 0"	UF ^{14}C	Bovidae sp.	40,720±390 ^{14}C BP	45,040-43,475	
Uphill Caves	Possibly Cave 8	UF ^{14}C	Aurignacian bone or antler point	31,730±250 ^{14}C BP	36,183-35,055	
Robin Hood Cave		UF ^{14}C	*C. crocuta*	>49,800 ^{14}C BP		1969 excavation
Robin Hood Cave	Southwestern corner, Western Chamber, Spit 9	UF ^{14}C	*C. crocuta*	>42,000 ^{14}C BP		1981 excavation
Robin Hood Cave	Southwestern corner, Western Chamber, A, Spit 26	UF ^{14}C	*C. crocuta*	>52,800 ^{14}C BP		1981 excavation
Robin Hood Cave	Southwestern corner, Western Chamber, Spit 12	UF ^{14}C	*C. crocuta*	45,300±1,000 ^{14}C	?-46,910	1981 excavation. Date may extend out of range
Robin Hood Cave	Southwestern corner, Western Chamber, Spit 7	UF ^{14}C	*P. leo*	>38,500 ^{14}C BP		1981 excavation
Robin Hood Cave	Southwestern corner, Western Chamber, Spit 19	UF ^{14}C	*R. tarandus*	47,300±1,200 ^{14}C BP	?-49,932	1981 excavation. Date probably out of range
Teufelslucken		^{14}C	*C. crocuta*	40,170+920/-830 ^{14}C BP	45,555-42,534	
Teufelslucken		^{14}C	*C. crocuta*	38,060+900/-910 ^{14}C BP	43,952-40,961	
Caverne Marie-Jeanne	Couche 4	UF ^{14}C	*Dicrostonyx torquatus* (Arctic lemming)	47,600±3300 ^{14}C BP	?-49,682	Date probably out of range
Caverne Marie-Jeanne	Couche 4	UF ^{14}C	*D. torquatus*	>43,900 ^{14}C BP		
Caverne Marie-Jeanne	Couche 4	UF ^{14}C	*D. torquatus*	43,000±1900 ^{14}C BP	?-44,124	Date may extend out of range
Goyet	3eme Caverne, 1er Niveau Ossifère, in Chamber A	^{14}C	*C. crocuta*	27,230±260 ^{14}C BP	31,521-30,849	

Goyet	3eme Caverne, 1er Niveau Ossifère, in Chamber A	^{14}C	*C. crocuta*	35,000±400 ^{14}C BP	40,474-38,667	
Goyet	3eme Caverne, 1er Niveau Ossifère, in Chamber A	^{14}C	*U. spelaeus*	38,770+1,180/-1,030 ^{14}C BP	45,209-41,238	
Goyet	3eme Caverne, 1er Niveau Ossifère, in Chamber A	UF ^{14}C	*C. antiquitatis* (with cut marks)	23,560±230 ^{14}C BP	28,126-27,352	
Goyet	3eme Caverne, 1er Niveau Ossifère, in Chamber A	UF ^{14}C	*C. antiquitatis*	28,470±140 ^{14}C BP	32,951-31,810	
Goyet	3eme Caverne, 1er Niveau Ossifère, in Chamber A	UF ^{14}C	*C. antiquitatis*	29,330±160 ^{14}C BP	33,891-33,150	
Goyet	3eme Caverne, 1er Niveau Ossifère, in Chamber A (front of cave)	UF ^{14}C	*E. c. arcelini*	31,750±200 ^{14}C BP	45,209-41,238	
Goyet	3eme Caverne, 1er Niveau Ossifère, in Chamber A	^{14}C	*H. neanderthalensis*	41,200+500/-410 ^{14}C BP	45,627-43,752	
Goyet	3eme Caverne, 1er Niveau Ossifère, in Chamber A	^{14}C	*H. neanderthalensis*	41,200+500/-410 ^{14}C BP	42,893-41,925	
Goyet	3eme Caverne, 1er Niveau Ossifère, in Chamber A	^{14}C	*H. neanderthalensis*	41,200+500/-410 ^{14}C BP	41,791-40,570	
Goyet	3eme Caverne, 3eme Niveau, in Chamber A (back of cave)	^{14}C	*U. arctos*	10,640±50 ^{14}C BP	12,714-12,535	May be intrusive
Goyet	3eme Caverne, 3eme Niveau, in Chamber A (back of cave)	^{14}C	*U. arctos*	32,580+250/-230 ^{14}C BP	37,432-35,922	
Goyet	3eme Caverne, 3eme Niveau, in Chamber A (back of cave)	^{14}C	*U. spelaeus* (with ochre staining)	23,580±130 ^{14}C BP	27,918-27,485	Repeated date
Goyet	3eme Caverne, 3eme Niveau, in Chamber A (back of cave)	^{14}C	*U. spelaeus* (with ochre staining)	27,920+160/-150 ^{14}C BP	32,236-31,270	Repeated date
Goyet	3eme Caverne, 3eme Niveau, in Chamber A (back of cave)	^{14}C	*U. spelaeus*	27,440±170 ^{14}C BP	31,531-31,040	

Goyet	3eme Caverne, 3eme Niveau, in Chamber A (back of cave)	^{14}C	*U. spelaeus*	32,900+240/-220 ^{14}C BP	37,885-36,282	
Goyet	3eme Caverne, 3eme Niveau, in Chamber A (front of cave)	^{14}C	*R. tarandus* (with ochre staining)	27,590±170 ^{14}C BP	31,674-31,097	
Goyet	3eme Caverne, 3eme Niveau, in Chamber A (front of cave)	^{14}C	*R. tarandus*	34,670+900/-810 ^{14}C BP	41,332-37,040	
Goyet	3eme Caverne, 3eme Niveau, in Chamber A	^{14}C	*H. neanderthalensis*	40,690+480/-400 ^{14}C BP	45,146-43,339	
Goyet	3eme Caverne, 3eme Niveau, in Chamber A	^{14}C	*H. neanderthalensis*	39,870+400/-350 ^{14}C BP	44,330-42,874	
Goyet	3eme Caverne, 3eme Niveau, in Chamber A	^{14}C	*H. neanderthalensis*	39,140+390/-340 ^{14}C BP	43,641-42,393	
Goyet	3eme Caverne, 3eme Niveau, in Chamber A	^{14}C	*H. neanderthalensis*	38,440+340/-300 ^{14}C BP	42,992-42,043	
Goyet	3eme Caverne, 3eme Niveau, in Chamber A	^{14}C	*H. neanderthalensis*	37,860+350/-310 ^{14}C BP	42,650-41,660	
Goyet	3eme Caverne, 3eme Niveau, in Chamber A	^{14}C	*H. neanderthalensis*	37,250+320/-280 ^{14}C BP	42,235-41,235	
Goyet	3eme Caverne, 4eme Niveau Ossifère, Galleries Voisines de l'Entrée, in Chamber A	^{14}C	*Canis* sp. (Palaeolithic dog)	31,680±250	36,140-35,009	
Höhle Výpustek		^{14}C	*C. crocuta*	46,000+2,400/-1,820 ^{14}C BP	?-45,942	Date may extend out of range
Castlepook Cave	Elephant Hall	^{14}C	*C. crocuta*	>45,000 ^{14}C BP		
Castlepook Cave		UF ^{14}C	*C. crocuta*	45,700±700 ^{14}C BP	?-47,754	Date may extend out of range
Castlepook Cave	Gallery of the Aged Carnivores	UF ^{14}C	*C. crocuta*	33,240±220 ^{14}C BP	38,291-36,700	
San Teodoro	Trench β	U-Th	Flowstone	32±4 ka		
San Teodoro	Trench β, Level B-II	^{14}C	*E. hydruntinus*	18,330±400 ^{14}C BP	23,125-21,149	
Baranica I	Layer 2	^{14}C	*M. giganteus*	23,520±110 ^{14}C BP	27,854-27,470	

Baranica I	Layer 4	^{14}C	*U. spelaeus*	35,780±320 ^{14}C BP	41,184-39,695	
Baranica II		UF ^{14}C	*C. crocuta*	>53,100 ^{14}C BP		
Cova de les Toixoneres	Chamber Y, Unit 1	UF ^{14}C	*C. crocuta*	43,100±400	47,243-45,493	
Cova de les Toixoneres	Chamber Y, Unit 1	UF ^{14}C	*Pinus t. sylvestris* (Scots pine)	28,390±80	32,759-31,821	
Cova de les Toixoneres	Chamber Y, Unit 1	UF ^{14}C	Small size ungulate	10,343±29	12,384-12,022	
Cova de les Toixoneres	Chamber X, Unit II	UF ^{14}C	*C. elaphus* (human modified)	40,800±320	45,011-43,651	
Cova de les Toixoneres	Chamber X, Unit II	UF ^{14}C	*C. elaphus* (human modified)	36,850±211	41,871-41,037	
Cova de les Toixoneres	Chamber X, Unit II	UF ^{14}C	Large size	34,940±173	39,956-38,963	
Cova de les Toixoneres	Chamber X, Unit II	UF ^{14}C	Medium size	39,320±263	43,542-42,635	
Cova de les Toixoneres	Chamber X, Unit II	UF ^{14}C	Medium size	34,900±175	39,913-38,918	
Cova de les Toixoneres	Chamber X, Unit II	UF ^{14}C	Medium size	30,780±110	34,978-34,437	
Cova de les Toixoneres	Chamber X, Unit II	UF ^{14}C	Small size (human modified)	39,000±260	43,266-42,458	
Cova de les Toixoneres	Chamber X, Unit III	UF ^{14}C	*C. elaphus*	>51,000		
Cova de les Toixoneres	Chamber X, Unit III	UF ^{14}C	*C. elaphus* (human modified)	47,200±670	?-49,973	Date probably out of range
Cova de les Toixoneres	Chamber X, Unit III	UF ^{14}C	*C. elaphus* (human modified)	40,610±340	44,860-43,450	
Cova de les Toixoneres	Chamber X, Unit III	UF ^{14}C	Medium size (human modified)	42,020±370	46,073-44,695	
Cova de les Toixoneres	Chamber X, Unit III	UF ^{14}C	Medium size	41,560±337	45,640-44,375	
Cova de les Toixoneres	Chamber X, Unit III	UF ^{14}C	Medium size	41,270±327	45,410-44,135	
Cova de les Toixoneres	Chamber X, Unit III	UF ^{14}C	Unidentified	42,250±359	46,257-44,895	
Cova del Gegant	Overlying sequence	U-Th	Speleothem	49.3±1.9 ka		
Cova del Gegant		U-Th	*H. neanderthalensis*	52.3±2.3 ka		
Cova del Gegant	Base of deposits	OSL	Speleothem	60±6.9 ka		

10.2 **Crocuta crocuta and Panthera leo biomass**

Table 10.5: Spearman Rank Order correlations between variables included in PLS 1-4 with *C. crocuta* and *P. leo* biomass as the dependent variable. Top value is the r_s statistic. Bottom value is the p-value. Yellow shaded boxes show correlations significant at 95 % confidence, and thus indicating multicollinearity.

Spearman rank order statistic, p-value	**Other predator biomass**	**Very small prey biomass**	**Small prey biomass**	**Medium prey biomass**	**Large prey biomass**	**Very large prey biomass**	**Min. temperature of coldest month**	**Max. temperature of warmest month**	**Temperature seasonality**	**Rainfall of the driest month**	**Rainfall of the wettest month**	**Rainfall seasonality**	**Closed vegetation cover**	**Semi-open vegetation cover**	**Open vegetation cover**
***C. crocuta* biomass**	0.663 <0.05	0.768 <0.05	0.604 <0.05	0.815 <0.05	0.595 0.001	0.122 0.519	-0.121 0.522	-0.546 0.002	-0.259 0.168	0.19 0.314	0.498 0.005	-0.062 0.743	0.431 0.017	-0.119 0.531	-0.379 0.039
***P. leo* biomass**	0.712 <0.05	0.833 <0.05	0.551 0.002	0.64 <0.05	0.615 <0.05	0.057 0.763	0.125 0.509	-0.536 0.002	-0.507 0.004	0.299 0.108	0.576 0.001	-0.149 0.431	0.388 0.034	-0.418 0.022	-0.248 0.187
Other predator biomass		0.81 <0.05	0.648 <0.05	0.709 <0.05	0.447 0.013	0.055 0.774	-0.219 0.246	-0.474 0.008	-0.069 0.717	0.186 0.326	0.409 0.025	0.002 0.99	0.416 0.022	-0.203 0.282	-0.336 0.07
Very small prey biomass			0.608 <0.05	0.803 <0.05	0.581 0.001	-0.045 0.812	-0.009 0.964	-0.695 <0.05	-0.452 0.012	0.219 0.245	0.715 <0.05	-0.044 0.818	0.349 0.059	-0.26 0.166	-0.272 0.146
Small prey biomass				0.498 0.005	0.499 0.005	0.186 0.325	-0.106 0.579	-0.552 0.002	-0.448 0.013	0.675 <0.05	0.174 0.359	-0.541 0.002	0.267 0.154	-0.09 0.636	-0.081 0.67
Medium prey biomass					0.341 0.065	-0.14 0.461	-0.103 0.589	-0.607 <0.05	-0.25 0.182	0.14 0.459	0.598 <0.05	0.065 0.732	0.204 0.28	-0.133 0.483	-0.189 0.317

Table 10.5 continued.

Large prey biomass						0.374 0.042	0.088 0.644	-0.384 0.036	-0.372 0.043	0.274 0.143	0.315 0.09	-0.217 0.25	0.539 0.002	-0.36 0.051	-0.394 0.031
Very large prey biomass							0.148 0.434	0.338 0.068	0.117 0.537	0.154 0.416	-0.245 0.191	-0.228 0.226	0.356 0.054	-0.042 0.826	-0.16 0.397
Minimum temperature of coldest month								-0.017 0.93	-0.396 0.03	0.201 0.288	0.352 0.057	-0.237 0.207	-0.177 0.351	-0.671 <0.05	0.513 0.004
Maximum temperature of warmest month									0.698 <0.05	-0.425 0.019	-0.64 <0.05	0.221 0.24	-0.056 0.767	0.314 0.091	-0.072 0.704
Temperature seasonality										-0.601 <0.05	-0.452 0.012	0.53 0.003	0.088 0.642	0.362 0.049	-0.275 0.141
Rainfall of the driest month											-0.147 0.439	-0.957 <0.05	-0.094 0.621	-0.292 0.117	0.408 0.025
Rainfall of the wettest month												0.314 0.091	0.241 0.199	-0.421 0.021	-0.13 0.495
Rainfall seasonality													0.139 0.462	0.238 0.204	-0.434 0.017
Closed vegetation cover														-0.315 0.09	-0.835 <0.05
Semi-open vegetation cover															-0.09 0.637
Open vegetation cover															

10.3 Repeated linear measurements

Table 10.6: Sub-sample 1 of randomly sub-sampled repeated linear measurements from a C. crocuta cranium held in the Department of Geography, Royal Holloway University of London. A = total length of the cranium. B = length of the m1. C = width of the m1. D = depth of the mandible at the p2/p3 interdental gap. E = width of the mandible at the p2/p3 interdental gap. F = distance from the mandibular articular condyle to the p2/p3 interdental gap.

A (mm)	B (mm)	C (mm)	D (mm)	E (mm)	F (mm)
256.64	29.4	12.33	33	19.39	127.35
256.41	29.4	12.49	33.18	19.57	126.65
256.56	29.4	12.49	33.01	19.88	127.6
256.47	29.41	12.43	33.02	19.65	126.74
256.54	29.41	12.5	32.98	19.74	126.66
256.55	29.4	12.51	32.89	19.8	126.55
256.5	29.4	12.48	32.86	19.52	126.81
256.49	29.45	12.45	32.99	19.99	126.92
256.45	29.39	12.31	32.95	19.95	126.48
256.57	29.4	12.35	32.94	19.48	126.37
256.44	29.43	12.3	33.08	19.93	126.59
256.37	29.45	12.38	32.77	19.76	126.52
256.58	29.38	12.41	32.78	19.92	127.36
256.5	29.39	12.4	32.71	19.94	126.6
256.53	29.4	12.33	32.81	19.85	126.18

Table 10.7: Sub-sample 2 of randomly sub-sampled repeated linear measurements from a C. crocuta cranium held in the Department of Geography, Royal Holloway University of London. A = total length of the cranium. B = length of the m1. C = width of the m1. D = depth of the mandible at the p2/p3 interdental gap. E = width of the mandible at the p2/p3 interdental gap. F = distance from the mandibular articular condyle to the p2/p3 interdental gap.

A (mm)	B (mm)	C (mm)	D (mm)	E (mm)	F (mm)
256.54	29.38	12.44	33.1	19.7	127.39
256.52	29.45	12.42	32.97	19.55	126.51
256.52	29.4	12.32	32.98	19.46	126.74
256.49	29.4	12.47	33.07	19.8	126.52
256.46	29.38	12.43	32.9	19.83	126.96
256.48	29.45	12.39	32.99	19.79	126.09
256.52	29.43	12.55	32.77	19.96	126.95
256.48	29.39	12.57	32.97	20	126.68
256.54	29.4	12.32	32.9	19.52	126.74
256.46	29.39	12.42	32.97	19.59	126.25
256.56	29.44	12.44	32.92	19.96	126.69
256.5	29.43	12.39	33.06	19.85	126.47
256.35	29.37	12.38	32.57	19.91	126.58
256.57	29.38	12.54	32.88	19.46	125.64
256.63	29.38	12.4	32.89	19.61	126.55

10.4 Modern Crocuta crocuta ontogenetic size change

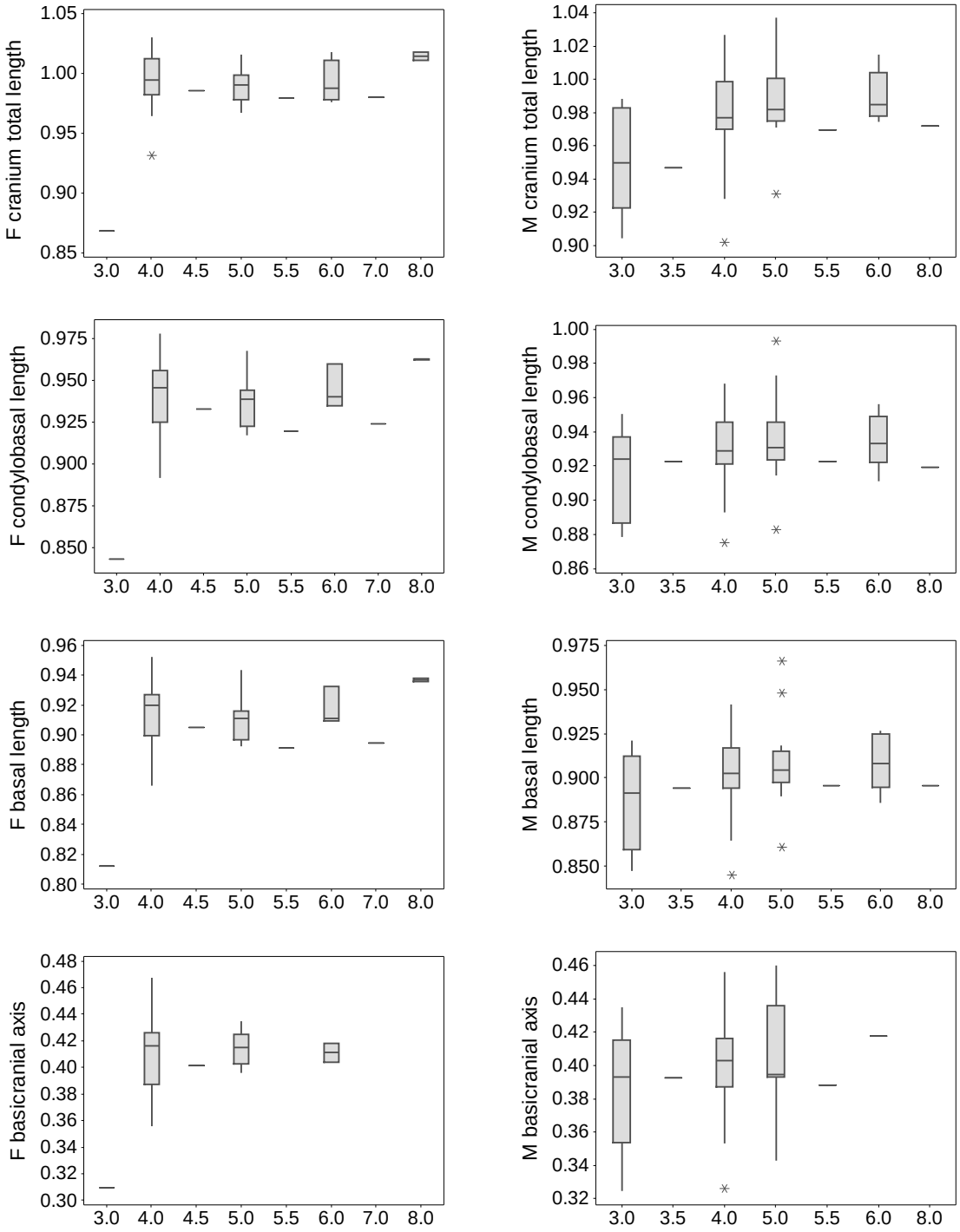

Figure 10.1: Boxplots of female (F) and male (M) *C. crocuta* cranial measurements divided by m1 length, base-10 logarithmically transformed. x-axis numbers are P3/p3 wear stages. See Table 10.8 for sample sizes.

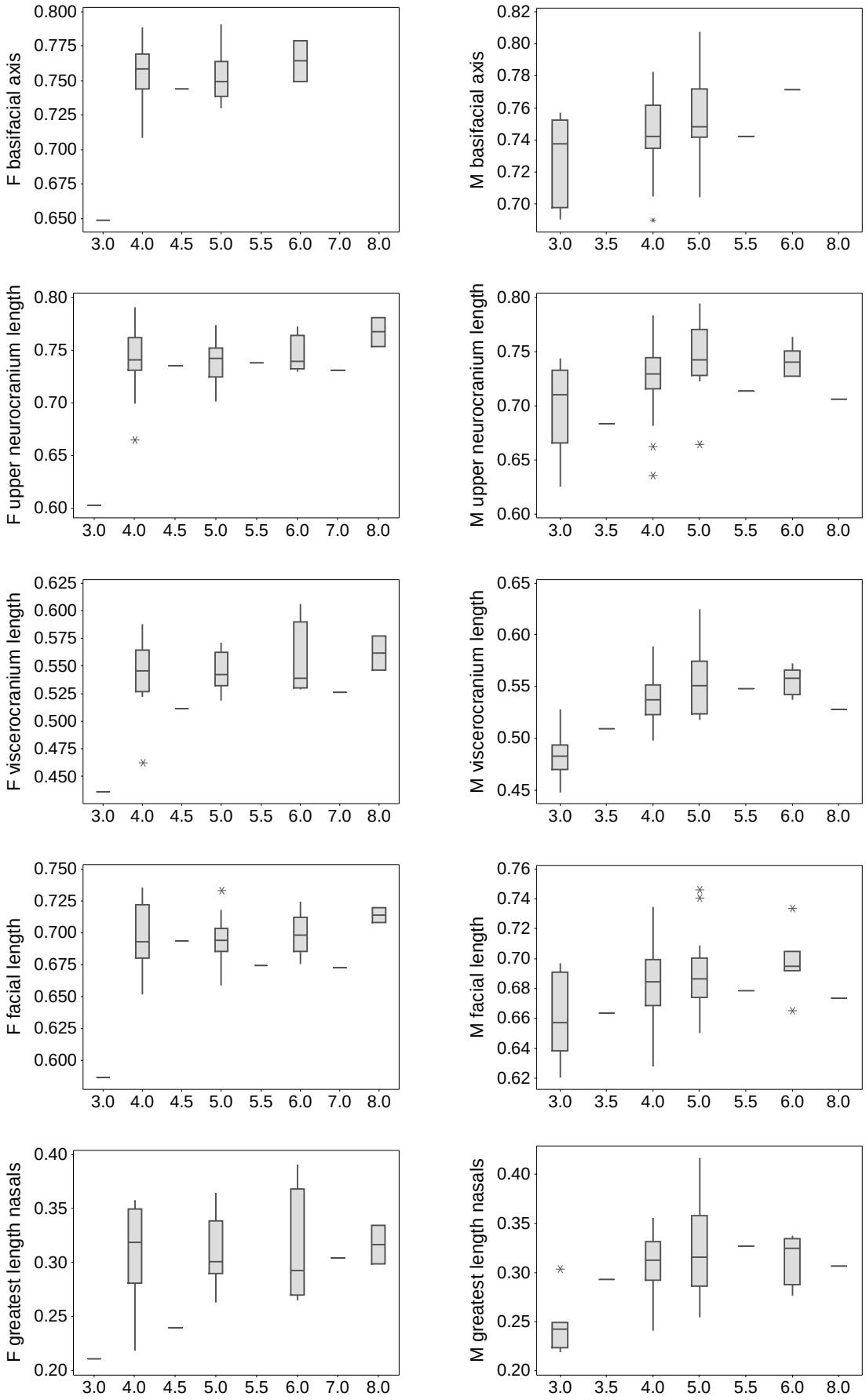

Figure 10.1 continued.

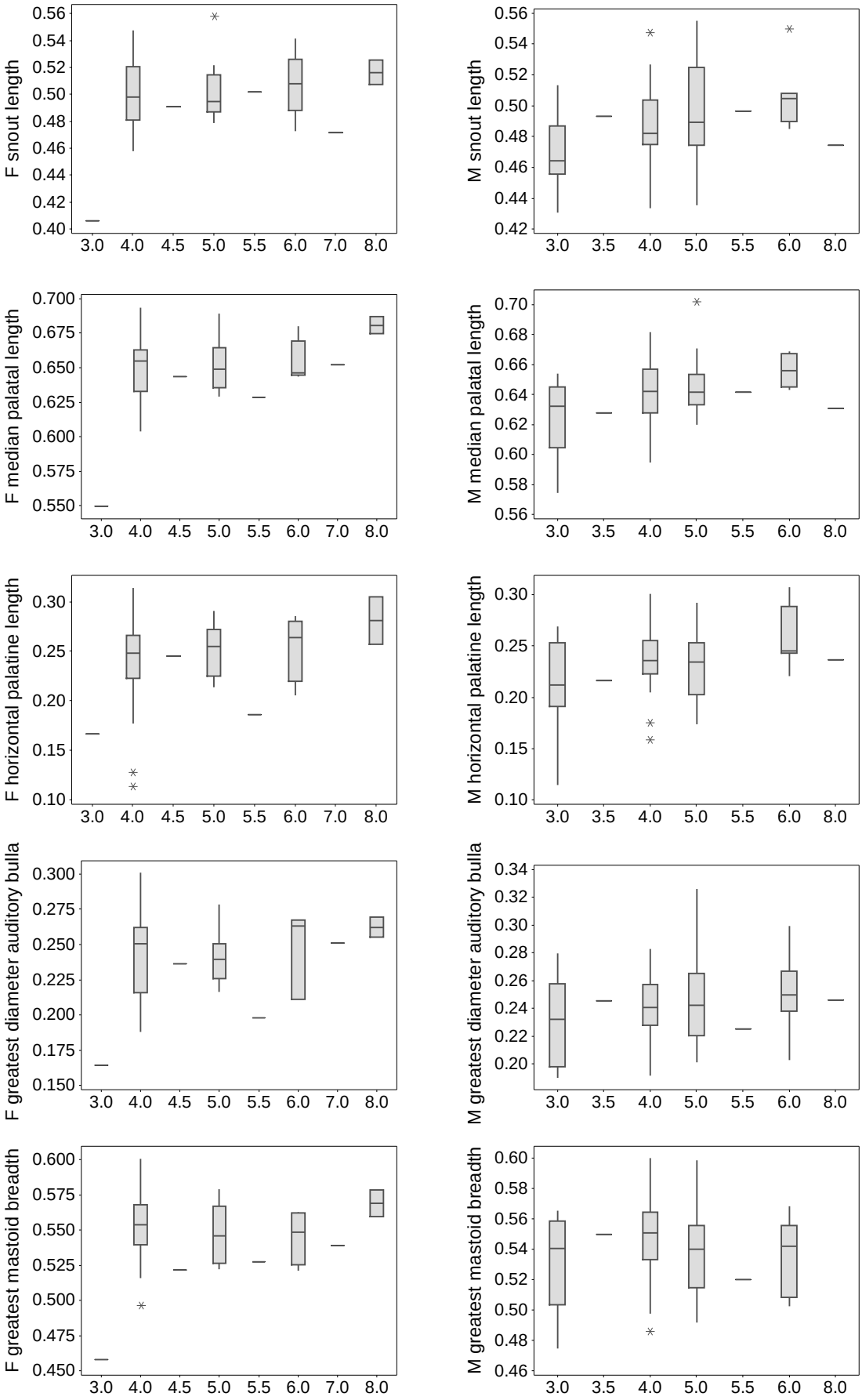

Figure 10.1 continued.

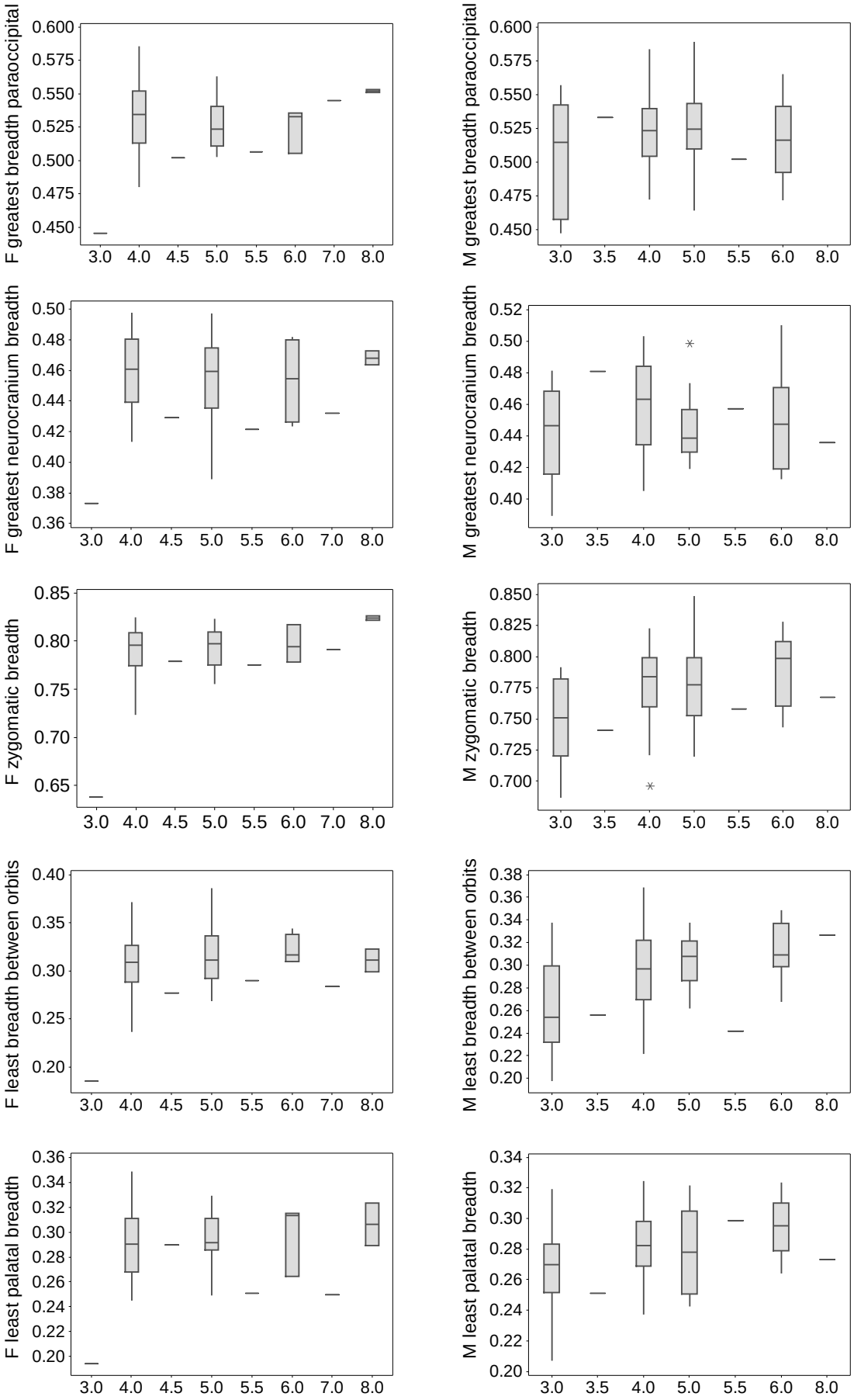

Figure 10.1 continued.

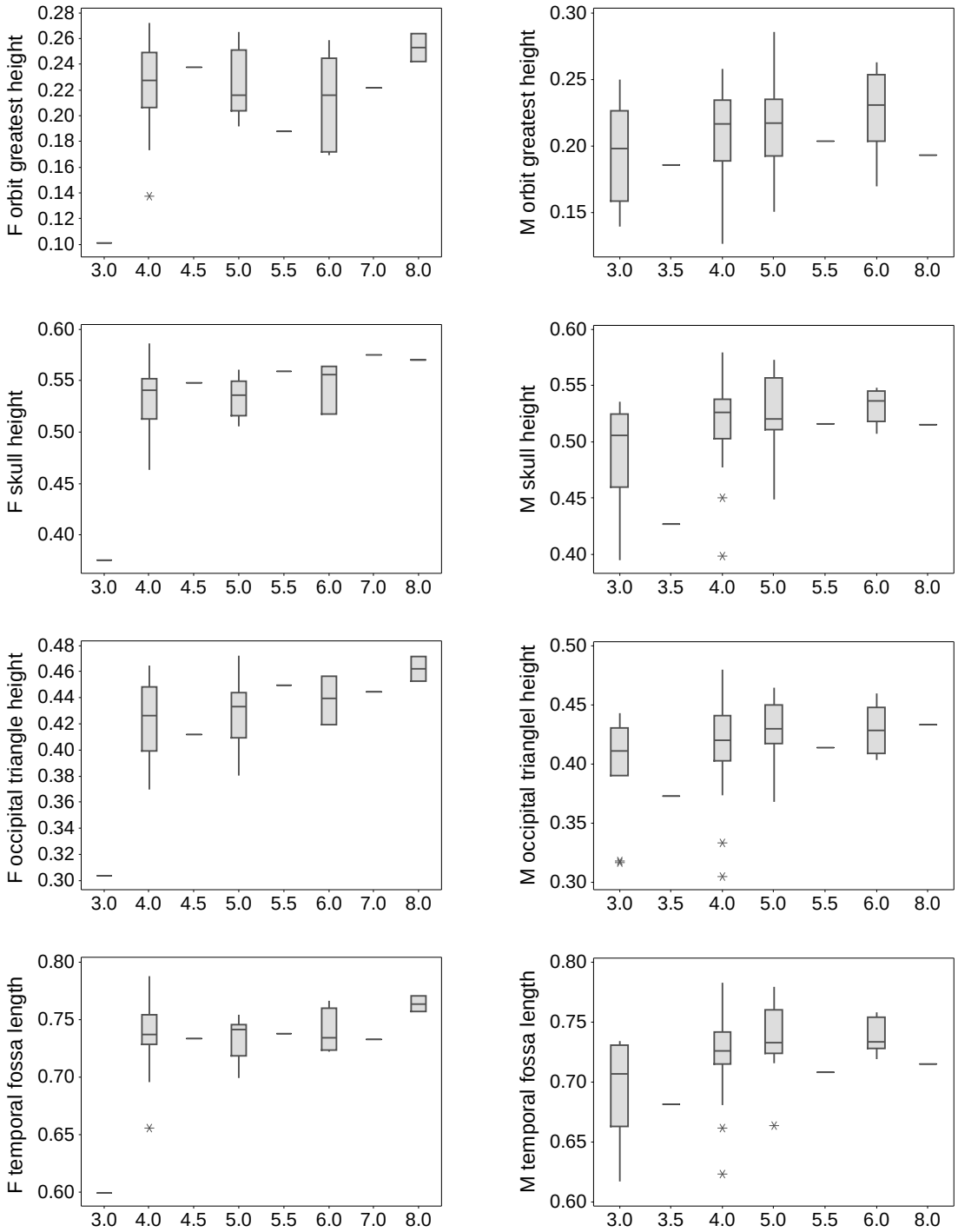

Figure 10.1 continued.

Table 10.8: Sample sizes of boxplots in Figure 10.1. F = female. M = male.

P3/p3 wear stage and sex	Total length of cranium	Condylobasal length	Basal length	Basicranial axis	Basifacial axis	Upper neurocranium length	Viscerocranium length	Facial length	Greatest length of nasals	Snout length	Median palatal length	Greatest diameter of auditory bulla	Greatest mastoid breadth	Greatest breadth of paraoccipital	Greatest neurocranium breadth	Zygomatic breadth	Least breadth between orbits	Least palatal breadth	Greatest height of orbits	Skull height	Height of occipital triangle	Temporal fossa length
3 F	1	1	1	1	1	1	1	1	1	1	1	1	1	1	1	1	1	1	1	1	1	1
4 F	19	19	19	16	13	20	14	17	15	18	18	22	22	22	22	20	21	22	22	22	21	21
4.5 F	1	1	1	1	1	1	1	1	1	1	1	1	1	1	1	1	1	1	1	1	1	1
5 F	16	15	15	8	8	16	10	17	10	16	15	16	16	16	16	16	17	15	17	16	16	16
5.5 F	1	1	1			1		1		1	1	1	1	1	1	1	1	1	1	1	1	1
6 F	4	3	3	2	2	4	4	5	4	5	5	3	4	3	4	3	4	3	5	3	3	4
7 F	1	1	1			1	1	1	1	1	1	1	1	1	1	1	1	1	1	1	1	1
8 F	2	2	2			2	2	2	2	2	2	2	2	2	2	2	2	2	2	2	2	2
3 M	10	12	11	12	10	11	8	11	8	11	11	14	14	12	14	12	12	14	12	12	12	11
3.5 M	1	1	1	1		1	1	1	1	1	1	1	1	1	1	1	1	1	1	1	1	1
4 M	31	30	28	30	26	31	24	32	24	31	28	33	31	30	33	30	32	30	32	30	31	32
5 M	14	13	14	9	10	14	9	15	9	15	13	15	15	14	15	15	15	14	15	13	14	14
5.5 M	1	1	1	1	1	1	1	1	1	1	1	1	1	1	1	1	1	1	1	1	1	1
6 M	7	7	7	1	1	7	5	7	4	8	7	7	6	5	6	6	7	6	8	7	7	7
8 M	1	1	1			1	1	1	1	1	1	1			1	1	1	1	1	1	1	1

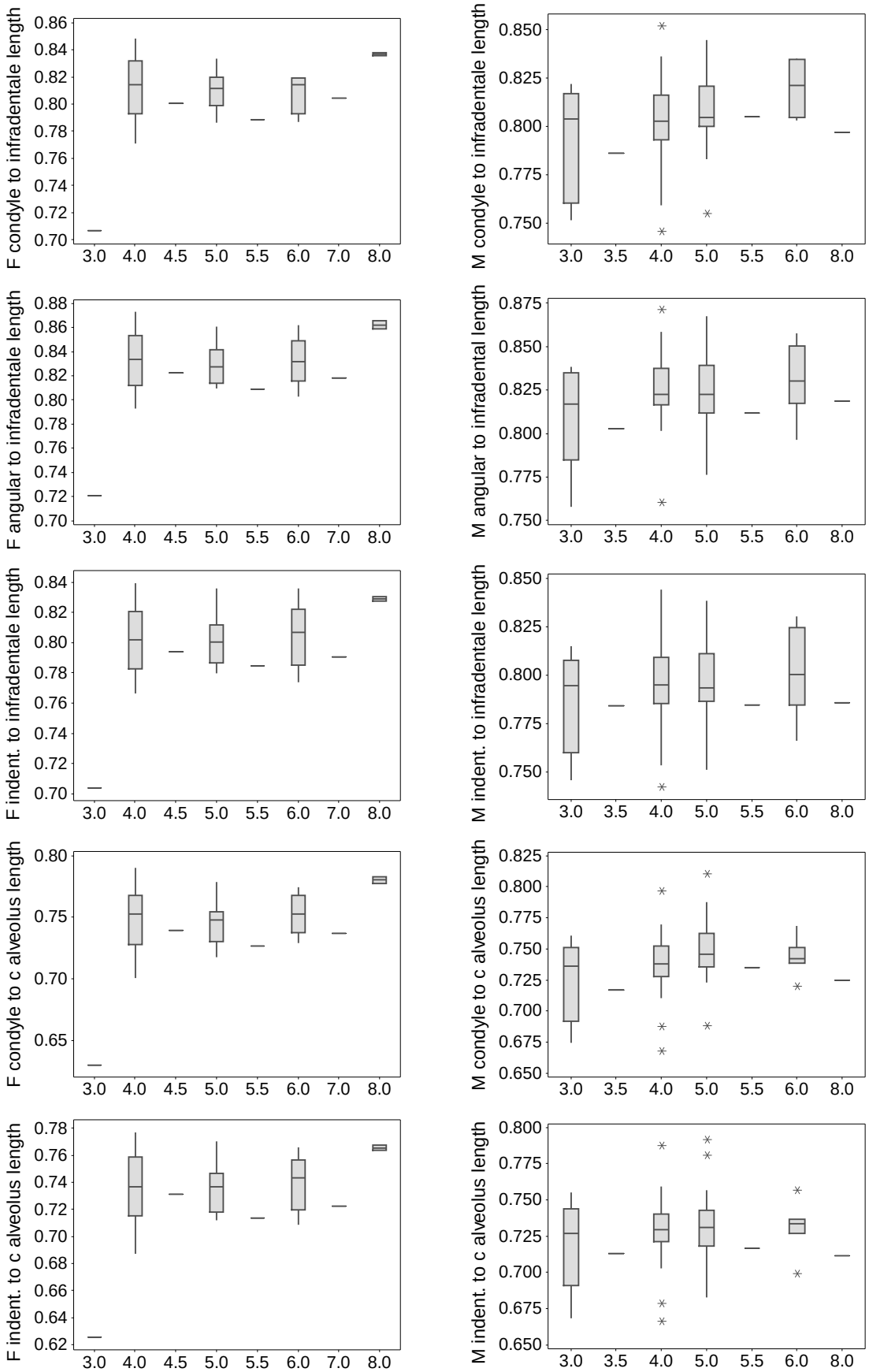

Figure 10.2: Boxplots of female (F) and male (M) *C. crocuta* mandibular measurements divided by m1 length, base-10 logarithmically transformed. x-axis numbers are P3/p3 wear stages. See Table 10.9 for sample sizes.

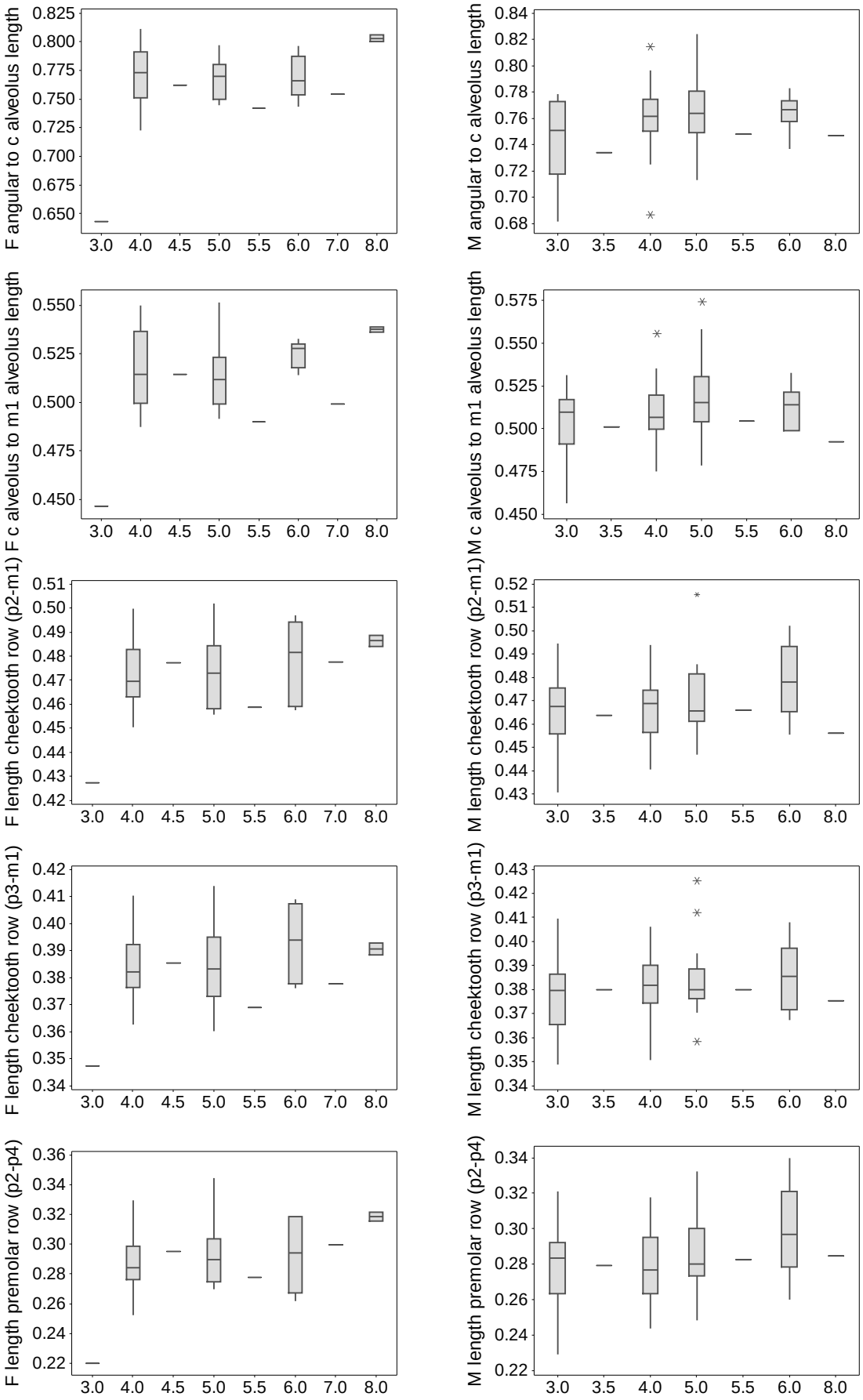

Figure 10.2 continued

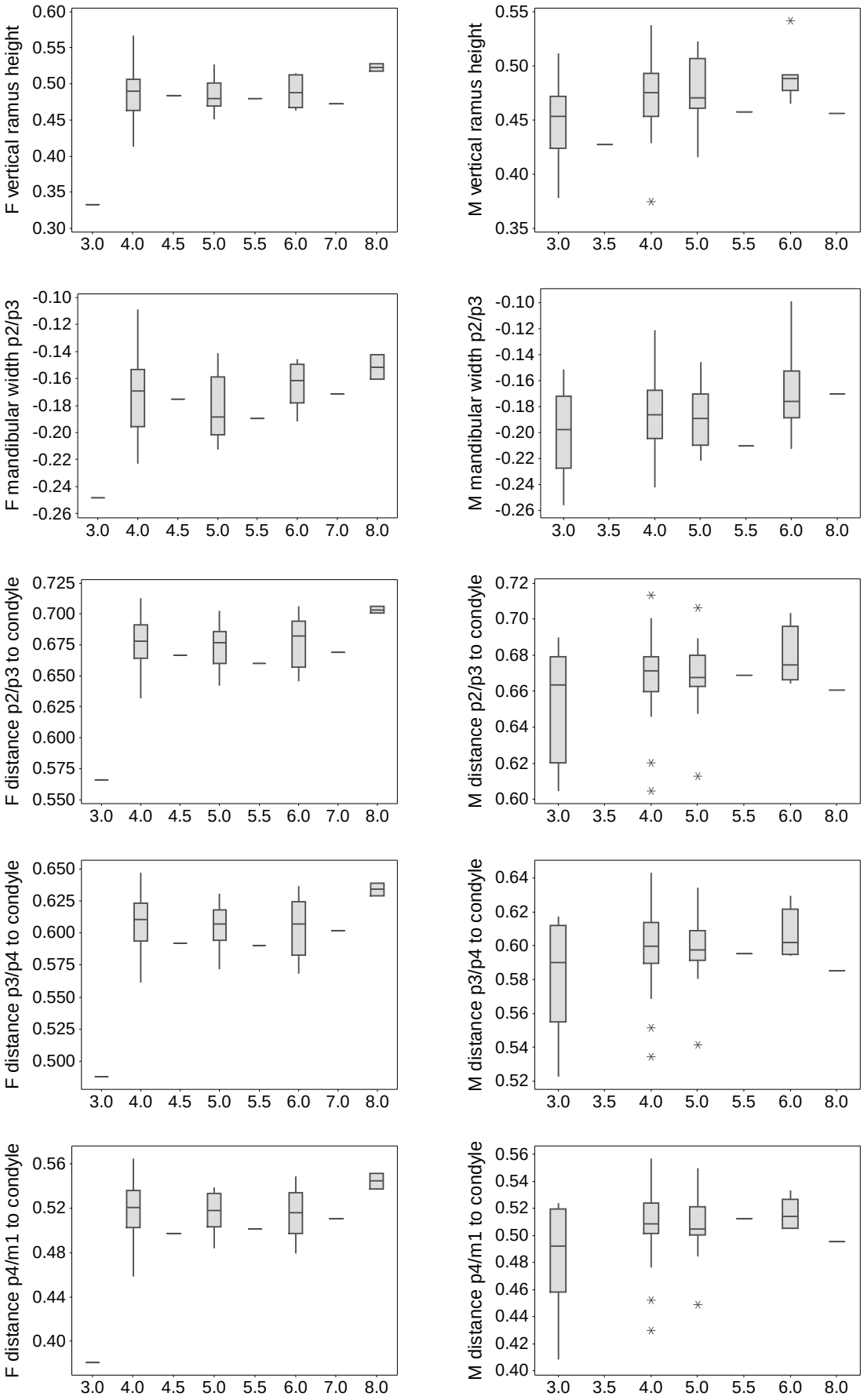

Figure 10.2 continued.

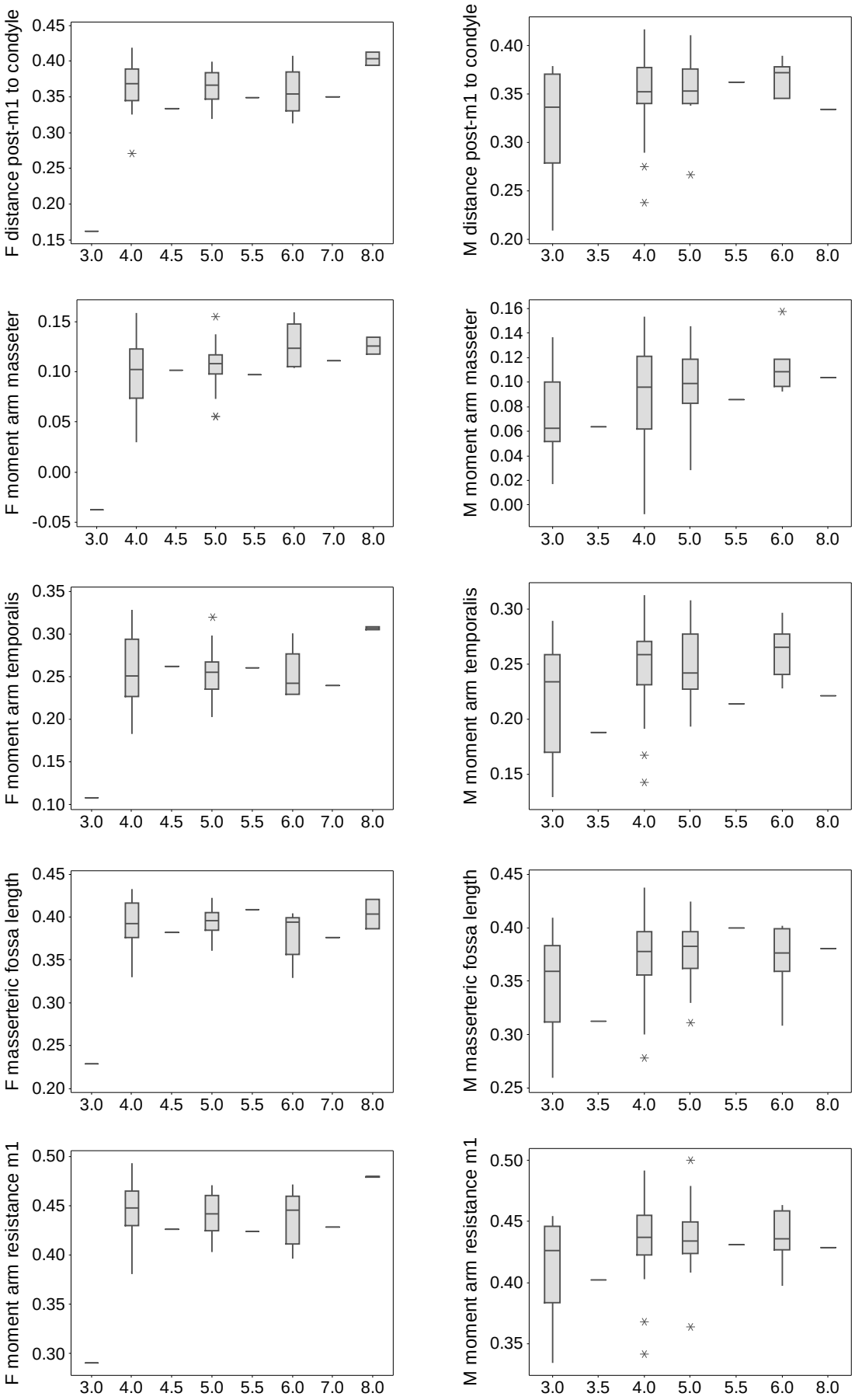

Figure 10.2 continued.

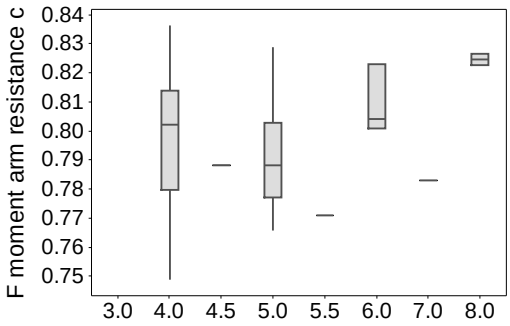

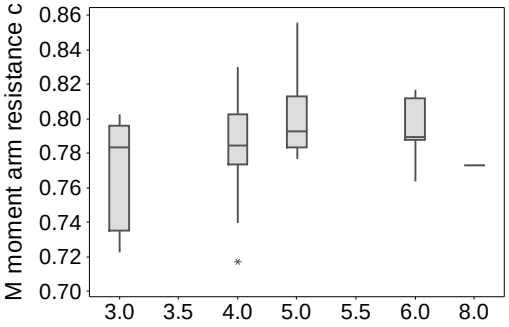

Figure 10.2 continued.

Table 10.9: Sample sizes of boxplots in Figure 10.2. F = female. M = male.

P3/p3 wear stage and sex	Condyle to infradental length	Angular to infradental length	Indent to infradental length	Condyle to c alveolus length	Indent to c alveolus length	Angular to c alveolus length	c alveolus to m1 alveolus length	Length of cheektooth row (p2-m1)	Length of cheektooth row (p3-m1)	Length of premolar row (p2-p4)	Vertical ramus height	Mandibular width p2/p3	Distance from p2/p3 to condyle	Distance from p3/p4 to condyle	Distance from p4/m1 to condyle	Distance from post-m1 to condyle	Moment arm of masseter	Moment arm of temporalis	Masseteric fossa length	Moment arm of resistance at m1	Moment arm of resistance at c
3 F	1	1	1	1	1	1	1	1	1	1	1	1	1	1	1	1	1	1	1	1	1
4 F	18	19	19	21	21	21	21	22	22	22	21	22	22	22	22	22	21	21	22	22	21
4.5 F	1	1	1	1	1	1	1	1	1	1	1	1	1	1	1	1	1	1	1	1	1
5 F	12	16	16	15	15	15	15	15	17	16	17	15	15	15	15	15	17	17	17	17	13
5.5 F	1	1	1	1	1	1	1	1	1	1	1	1	1	1	1	1	1	1	1	1	1
6 F	4	5	5	5	5	5	5	5	5	5	5	5	5	5	5	5	5	5	5	5	3
7 F	1	1	1	1	1	1	1	1	1	1	1	1	1	1	1	1	1	1	1	1	1
8 F	2	2	2	2	2	2	2	2	2	2	2	2	2	2	2	2	2	2	2	2	2
3 M	10	14	14	13	14	14	14	14	14	14	13	12	12	12	12	12	14	13	13	13	12
3.5 M	1	1	1	1	1	1	1	1	1	1	1						1	1	1	1	
4 M	31	32	32	30	31	31	31	33	35	33	31	32	33	33	33	33	32	32	33	33	29
5 M	12	14	14	15	15	15	15	15	15	15	14	14	14	14	14	1	15	14	15	15	12
5.5 M	1	1	1	1	1	1	1	1	1	1	1	1	1	1	1	1	1	1	1	1	
6 M	4	6	6	7	7	7	7	8	8	8	8	7	7	7	7	7	8	8	8	8	7
8 M	1	1	1	1	1	1	1	1	1	1	1	1	1	1	1	1	1	1	1	1	1

10.5 Modern Crocuta crocuta body mass and sexual size dimorphism

Table 10.10: Recent *C. crocuta* mean female and male body mass (BM) values, and associated calculations of sexual size dimorphism SSD. Positive SSD values indicate that females are larger.

Country	Location	Mean female BM (kg)	Mean male BM (kg)	SSD	BM reference
Botswana		70.99	80.06	-0.052	Smithers (1971)
Kenya	Aberdare National Park	51.80	47.4	0.039	Sillero-Zubiri and Gottelli (1992)
Kenya	Maasai Mara National Reserve	59.39	53.67	0.044	Swanson *et al*. (2013)
Kenya	Narok District	50.7	43.6	0.066	Neaves *et al*. (1980)
South Africa		61.1	56.2	0.036	Skinner (1976)
South Africa	Hluhluwe-iMfolozi Park	70	66.6	0.022	Whateley (1980)
South Africa	iMfolozi Game Reserve	57.75	47.5	0.085	Green *et al*. (1984)
South Africa	Kalahari Gemsbok National Park	70.9	59	0.08	Mills (1990)
South Africa	Kruger National Park	70.76	58.06	0.086	Stevenson-Hamilton (1947)
South Africa	Kruger National Park	68.2	62.5	0.038	Henschel (1986, cited in Skinner and Chimimba 2005)
South Africa and Zimbabwe	Transvaal and Zimbabwe	64.8	57.8	0.05	Rautenbach (1978, cited in Smithers 1983); Smithers (1983)
Southern Africa		47.18	46.87	0.003	Thackeray and Kieser (1992)
Tanzania	Serengeti	55.3	48.7	0.055	Kruuk (1972)
Zambia		68.2	67.7	0.003	Wilson (1975, cited in Silva and Downing 1995)

Table 10.11: Recent *P. leo* mean female and male body mass (BM) values, and associated calculations of sexual size dimorphism SSD. Positive SSD values indicate that males are larger.

Country	Location	Mean female BM (kg)	Mean male BM (kg)	SSD	BM reference
Botswana	Pandamatenga	223.51	284.4	0.105	Best (unpublished data, cited in Smithers, 1971)
Botswana	Tshabong	106.14	149.69	0.149	Parris (n.d. cited in Smithers, 1971)
Kenya		151.05	174.81	0.063	Meinertzhagen (1938)
Kenya and Tanzania		119.5	174.9	0.165	Smuts *et al*. (1980, and references within)
Namibia	Etosha National Park	141	190	0.13	Orford *et al*. (1988)
South Africa	iMfolozi Game Reserve	136.33	193	0.151	Green *et al*. (1984)
South Africa	Kalahari National Park	139.80	188.40	0.13	Smuts *et al*. (1980, and references within)
South Africa	Kruger National Park	124.2	187.5	0.179	Smuts *et al*. (1980);
Southern Africa		178.00	189.98	0.028	Thackeray and Kieser (1992)
Zimbabwe		133.6	193.3	0.16	Smuts *et al*. (1980, and references within)
Zimbabwe	Pandamatenga	136.53	153.77	0.052	Johnstone (n.d., cited in Smithers, 1971)

Table 10.12: Recent *P. pardus* mean female and male body mass (BM) values, and associated calculations of sexual size dimorphism SSD. [a]Old-aged adults; [b]Prime-aged adults. Positive SSD values indicate that males are larger.

Country	Location	Mean female BM (kg)	Mean male BM (kg)	SSD	BM reference
Kenya		49.67	62.14	0.097	Meinertzhagen (1938)
South Africa	Cape Province	21.2	30.9	0.164	Stuart (1981)
South Africa[a]	Sabie River, Kruger National Park	37.2	63.1	0.23	Bailey (1993)
South Africa[b]	Sabie River, Kruger National Park	37.5	58.2	0.191	Bailey (1993)
South Africa	Transvaal	27.3	50.3	0.265	Rautenbach (1982, cited in Silva and Downing 1995)
Southern Africa		38.6	56.4	0.165	Thackeray and Kieser (1992)
Zimbabwe	Matetsi	31.52	59.68	0.277	Johnstone (n.d., cited in Smithers, 1971)

Table 10.13: Recent *A. jubatus* mean female and male body mass (BM) values, and associated calculations of sexual size dimorphism SSD. Positive SSD values indicate that males are larger.

Country	Location	Mean female BM (kg)	Mean male BM (kg)	SSD	BM reference
Kenya		43	53.9	0.098	Meinertzhagen (1938)
South Africa	Near Kruger National Park	57.6	52.62	-0.039	Roberts (1951, cited in Eaton 1974)
Southern Africa		45.5	51.55	0.054	Thackeray and Kieser (1992)
Tanzania	Serengeti ecosystem	37.25	43.38	0.066	Caro *et al*. (1987)

Table 10.14: Recent *P. brunnea* mean female and male body mass (BM) values, and associated calculations of sexual size dimorphism SSD. Positive SSD values indicate that males are larger.

Country	Location	Mean female BM (kg)	Mean male BM (kg)	SSD	BM reference
South Africa	Kalahari National Park	37.6	40.2	0.03	Mills (1990)
South Africa	Transvaal	42	47.1	0.05	Skinner and Ilani (1979)
South Africa	Transvaal	27.9	36.5	0.12	Rautenbach (1982, cited in Silva and Downing 1995)
South Africa		40.9	43.9	0.03	Skinner (1976)
Southern Africa		37.05	38.85	0.02	Thackeray and Kieser (1992)
Zimbabwe		39.96	38.1	-0.02	Smithers (1983)

Table 10.15: Recent *L. pictus* mean female and male body mass (BM) values, and associated calculations of sexual size dimorphism SSD. The positive SSD values indicates that males are larger.

Country	Location	Mean female BM (kg)	Mean male BM (kg)	SSD	BM reference
Botswana		21.32	21.77	0.009	Smithers (1971)

10.6 Modern Crocuta crocuta geographical variation

Table 10.16: Spearman Rank Order correlations on variables included in the PLS regressions with present-day *C. crocuta* craniodental measurements as the dependent variables. Top figure is r_s statistic. Bottom figure is p-value. Yellow shaded boxes show correlations significant at 95 % confidence, and thus indicating multicollinearity.

	Minimum temperature coolest month	Maximum temperature warmest month	Precipitation driest month	Precipitation wettest month	Closed vegetation cover	Semi-open vegetation cover	Open vegetation cover
Minimum temperature coolest month		0.215 0.084	0.377 0.002	0.353 0.004	0.103 0.41	-0.001 0.994	-0.142 0.255
Maximum temperature warmest month			-0.468 <0.05	-0.07 0.578	-0.093 0.457	0.458 <0.05	-0.349 0.004
Precipitation driest month				0.113 0.367	0.13 0.299	-0.325 0.008	0.138 0.268
Precipitation wettest month					0.419 <0.05	-0.000 1	-0.284 0.021
Closed vegetation cover						-0.241 0.051	-0.673 <0.05
Semi-open vegetation cover							-0.452 <0.05
Open vegetation cover							

Table 10.17: Leverage values of PLS regressions run on tooth measurements of present-day *C. crocuta*. LRL = leverage reference line. Difference = the difference between the maximum leverage value and the LRL. Shaded values are maximum, extreme values that were excluded from subsequent PLS reruns.

Site	Anteroposterior diameter of C	Mediolateral diameter of C	Length of P1	Width of P1	Length of P2	Width of P2	Length of P3	Width of P3	Length of P4	Greatest width of P4	Width of P4
PLS	39	40	41	42	43	44	45	47	48	49	50
1.1	0.039	0.024	0.026	0.020	0.027	0.020	*	0.019	0.019	0.022	0.018
2.1	*	*	*	*	*	0.021	0.121	*	0.019	0.026	0.018
3.1	*	0.023	0.116	0.026	0.048	0.101	0.047	0.098	0.060	0.017	0.040
3.2	0.041	0.076	*	0.050	*	0.056	0.072	0.030	0.019	0.036	0.031
4.1	*	0.026	*	*	0.021	0.020	*	0.023	0.021	0.021	0.023
5.1	*	*	0.039	0.020	0.021	*	0.039	0.029	0.020	0.020	0.019
5.2	*	*	0.026	0.030	*	0.018	*	*	0.027	0.019	0.025
5.3	*	0.052	0.026	0.034	*	0.019	0.043	0.019	0.023	0.044	0.035
6.1	*	0.030	0.031	0.020	0.020	0.023	0.031	*	0.019	0.026	0.020
6.2	0.071	0.069	0.026	0.041	0.036	0.018	0.077	0.020	0.028	0.061	0.041
6.3	*	0.054	0.026	0.030	0.027	0.018	0.055	0.019	0.023	0.039	0.031
6.4	*	0.045	*	0.027	0.024	0.018	0.039	0.019	0.022	0.031	0.029
6.5	*	*	*	0.064	0.067	0.023	0.205	*	*	0.125	0.072
6.6	0.040	0.032	0.034	0.021	0.021	0.022	0.056	0.023	0.019	0.030	0.020
6.7	0.039	0.024	0.038	0.021	0.021	0.026	0.052	0.027	0.021	0.020	0.018
6.8	0.041	0.021	0.070	0.026	0.022	0.028	0.121	0.035	0.027	0.022	0.020
6.9	0.064	0.029	0.043	0.046	0.045	0.033	0.080	0.039	0.042	0.024	0.037
6.10	*	0.022	*	0.030	*	0.023	*	0.025	0.033	0.029	0.027
6.11	*	0.033	0.035	0.042	0.040	0.035	0.042	0.040	0.046	0.029	0.035

6.12	*	*	*	0.053	0.053	*	*	*	*	*	*
6.13	*	*	*	*	0.029	0.025	*	*	*	0.018	*
6.14	0.046	0.025	0.026	0.022	0.021	0.019	*	0.019	0.020	0.020	0.022
6.15	0.047	0.024	0.041	0.030	*	0.036	*	0.035	0.030	0.018	0.022
7.1	0.090	0.062	0.036	0.070	0.060	0.041	0.085	0.044	0.052	0.049	0.049
9.1	*	*	0.057	0.056	0.056	0.045	*	*	*	0.037	0.053
9.2	0.040	0.023	0.029	0.020	0.020	0.022	0.027	0.021	0.019	0.020	0.020
10.1	*	*	*	*	*	*	*	0.028	*	0.030	0.030
10.2	0.079	0.060	0.083	0.074	0.050	0.044	0.075	0.054	0.059	0.025	0.048
10.3	0.125	0.046	0.026	0.054	0.087	0.046	0.126	0.045	0.050	0.089	0.067
10.4	0.083	0.040	0.039	0.053	*	0.050	0.060	0.048	0.049	0.040	0.043
10.6	0.187	0.144	0.073	0.163	0.152	0.083	0.164	0.088	0.123	0.115	0.115
11.1	*	0.039	0.057	0.036	0.030	0.025	0.054	0.032	0.037	0.020	0.034
12.1	0.233	0.050	0.119	0.064	0.123	0.150	0.089	0.140	0.119	0.055	0.088
12.2	*	*	*	0.033	*	0.038	*	*	0.019	0.030	0.027
13.1	0.053	0.039	0.056	0.050	0.044	0.033	0.050	0.036	0.041	0.022	0.031
13.2	*	0.034	0.045	0.047	0.036	0.023	0.068	0.027	0.035	0.019	0.028
14.1	*	*	0.166	0.038	0.039	0.086	0.110	0.097	*	0.016	*
15.1	0.041	0.030	0.029	0.022	0.020	0.026	0.114	0.020	0.019	0.017	0.025
16.1	*	*	*	*	*	*	0.122	*	0.035	0.066	0.058
16.2	*	*	*	*	*	*	*	0.034	*	0.065	*
17.1	0.045	0.178	*	*	*	0.033	0.593	0.020	0.026	0.016	0.038
17.2	*	0.061	*	*	*	0.027	0.080	0.038	0.046	0.026	0.048
18.1	0.086	0.038	0.110	0.037	0.025	0.038	0.116	0.056	0.048	0.016	0.039
19.1	*	*	0.148	0.024	0.020	0.075	*	0.072	*	*	*
19.2	0.118	0.061	*	*	0.057	0.060	0.082	0.074	0.083	0.025	0.058
19.3	*	0.028	*	0.042	0.050	0.050	0.137	0.057	0.061	0.019	*
20.1	*	0.033	*	*	*	0.019	*	0.025	0.026	0.017	*
21.1	*	*	*	0.053	0.048	0.034	0.049	0.036	0.043	0.024	0.031
21.2	*	*	*	*	0.028	0.022	0.032	0.029	0.035	0.021	0.030

21.3	*	0.042	*	*	0.056	*	0.065	*	0.039	0.048	0.047
21.4	*	0.029	*	0.021	0.022	0.018	0.030	0.020	0.019	0.020	0.019
21.5	*	0.022	*	*	*	0.025	*	0.025	*	*	0.018
21.6	*	0.034	0.039	0.041	0.028	0.024	0.035	0.032	0.039	0.020	0.032
21.7	*	0.024	0.029	*	0.034	*	0.035	0.029	0.028	0.021	0.025
21.8	*	0.035	0.028	0.024	*	0.026	*	*	*	0.029	0.027
21.9	*	*	*	0.025	0.024	0.018	0.047	0.020	0.021	0.033	0.030
21.10	*	0.021	*	0.020	0.022	0.020	0.024	0.020	0.019	0.016	0.018
21.11	0.055	0.028	*	0.025	0.024	0.018	0.035	0.019	0.022	0.030	*
21.12	0.068	0.050	0.059	0.054	0.045	0.029	0.082	0.037	0.043	0.028	0.046
22.1	*	*	0.026	0.025	0.043	0.045	0.095	0.035	0.027	0.030	0.023
22.2	*	*	*	*	0.022	*	*	*	*	0.017	*
23.1	*	0.024	0.026	0.020	0.021	*	*	*	0.019	0.017	0.019
23.2	0.040	0.025	0.026	0.020	0.021	0.020	0.031	0.020	0.019	0.016	0.019
24.1	0.110	0.049	0.058	0.066	0.058	0.042	0.069	0.053	0.069	0.036	0.056
24.2	0.122	0.044	0.035	0.073	0.089	0.047	0.142	0.050	0.077	0.063	0.062
25.1	*	*	*	*	*	*	*	*	*	*	*
LRL value	0.077	0.043	0.051	0.040	0.041	0.036	0.128	0.038	0.037	0.032	0.036
Max. leverage	0.233	0.178	0.166	0.163	0.152	0.150	0.593	0.140	0.123	0.125	0.115
Difference	0.156	0.135	0.115	0.123	0.111	0.115	0.465	0.102	0.086	0.093	0.079

Site	**Anteroposterior diameter of c**	**Mediolateral diameter of c**	**Length of p2**	**Width of p2**	**Length of p3**	**Width of p3**	**Length of p4**	**Width of p4**	**Length of m1**	**Width of m1**	
PLS	51	53	54	56	58	59	60	61	62	63	
1.1	0.064	0.038	0.105	0.024	0.019	0.025	0.024	0.017	0.019	0.025	
2.1	*	*	*	*	0.019	*	*	*	0.020	*	

3.1	0.048	0.029	0.122	0.069	0.020	0.068	0.025	0.057	0.059	0.061	
3.2	0.094	0.074	0.081	0.045	0.064	0.019	*	0.017	0.019	0.021	
4.1	0.050	*	0.032	0.024	0.019	*	*	0.018	0.020	0.026	
5.1	*	*	0.068	0.024	0.028	0.021	0.026	0.017	0.019	0.025	
5.2	*	*	*	*	0.040	*	0.034	0.023	*	*	
5.3	*	*	0.033	0.022	0.043	0.026	0.049	0.020	0.022	0.025	
6.1	*	*	*	*	*	*	0.027	0.017	0.019	0.019	
6.2	0.130	0.107	0.103	0.032	0.044	0.036	0.059	0.021	0.024	0.040	
6.3	0.096	0.071	0.092	0.027	0.029	0.029	0.042	0.018	0.020	0.030	
6.4	*	*	0.049	*	*	*	*	0.018	0.019	0.025	
6.5	*	*	*	0.072	*	*	*	0.033	*	*	
6.6	0.060	0.051	0.098	0.021	0.021	0.020	0.029	0.017	0.019	0.021	
6.7	0.043	0.034	0.093	0.021	0.019	0.020	0.024	0.022	0.024	0.019	
6.8	0.039	0.032	0.134	0.047	0.022	0.021	0.024	0.025	0.026	0.019	
6.9	0.055	0.045	0.109	0.034	0.051	0.038	0.040	0.046	0.051	0.031	
6.10	*	*	0.159	0.062	0.043	0.027	*	0.035	0.051	0.028	
6.11	0.048	0.045	0.056	0.047	0.036	0.035	0.044	0.034	0.049	0.045	
6.12	*	*	0.079	*	0.047	0.055	0.063	0.038	*	*	
6.13	*	*	0.034	*	0.021	*	*	0.021	*	*	
6.14	0.041	0.035	0.034	0.020	0.024	0.020	*	0.018	0.020	0.019	
6.15	*	*	0.038	0.033	0.022	0.030	*	0.026	0.030	0.033	
7.1	0.123	0.081	0.069	0.063	0.051	0.057	0.066	0.042	0.050	0.070	
9.1	*	*	0.063	*	*	0.062	*	0.049	0.048	0.055	
9.2	0.039	0.035	0.034	0.019	0.023	0.019	0.025	0.017	0.019	0.020	
10.1	*	*	*	0.034	0.033	0.035	*	0.030	0.032	*	
10.2	0.087	0.053	0.073	0.069	0.049	0.047	0.062	0.042	0.046	0.049	
10.3	*	0.124	0.150	0.094	0.075	0.091	0.057	0.075	0.077	0.077	
10.4	*	0.064	0.068	0.063	0.043	0.058	*	0.048	0.055	0.063	
10.6	0.292	0.205	0.192	0.136	0.124	0.132	0.155	0.094	0.111	0.159	
11.1	*	0.040	0.044	0.042	0.031	0.030	0.040	0.026	0.029	0.028	

12.1	*	0.078	0.169	0.142	0.048	0.139	0.059	0.110	0.124	0.145	
12.2	*	*	*	0.063	*	0.019	*	*	*	*	
13.1	0.063	0.046	0.046	0.040	0.037	0.034	0.045	0.031	0.035	0.036	
13.2	*	0.043	0.031	0.031	0.043	0.026	0.044	0.028	0.032	0.025	
14.1	*	*	*	0.099	*	0.055	*	0.042	*	0.059	
15.1	*	*	0.065	0.065	0.035	0.019	0.030	0.017	0.019	*	
16.1	*	*	*	*	*	*	0.080	0.043	*	*	
16.2	*	*	*	0.092	*	*	*	0.051	*	*	
17.1	0.099	0.040	0.406	0.309	0.040	0.020	0.097	0.023	0.025	0.019	
17.2	*	0.057	*	0.067	0.056	0.039	0.060	0.036	0.037	0.034	
18.1	0.044	0.029	0.148	0.088	0.026	0.033	0.035	0.031	0.033	0.029	
19.1	*	*	0.216	0.067	0.047	0.025	0.036	0.021	0.021	0.024	
19.2	0.069	0.052	0.098	0.075	0.048	0.053	0.069	0.049	0.062	0.062	
19.3	*	0.037	0.079	0.043	0.042	0.040	0.041	0.050	0.060	0.035	
20.1	*	*	*	0.048	*	0.023	0.034	0.023	*	0.020	
21.1	*	*	0.045	0.037	0.043	0.034	0.047	0.034	0.043	0.039	
21.2	0.040	0.037	0.055	0.026	0.036	0.025	0.040	0.026	0.036	0.027	
21.3	*	*	*	*	*	*	*	*	*	*	
21.4	*	0.039	0.066	0.025	0.020	0.022	0.025	0.017	0.019	0.020	
21.5	*	*	*	*	0.019	*	*	*	0.019	0.022	
21.6	0.041	0.037	*	0.028	0.036	0.025	0.043	0.027	0.036	0.028	
21.7	*	*	0.051	0.032	0.030	0.029	0.030	0.029	0.034	0.030	
21.8	0.057	*	*	*	*	*	*	*	0.019	0.019	
21.9	*	*	*	0.026	0.026	0.028	*	0.019	0.020	*	
21.10	*	*	*	0.019	0.019	0.020	*	0.017	*	*	
21.11	*	0.049	0.047	*	*	*	*	*	0.024	0.022	
21.12	0.093	0.061	0.053	0.057	0.054	0.044	0.051	0.041	0.039	0.033	
22.1	*	*	0.073	0.083	0.020	0.043	0.026	0.030	0.035	0.055	
22.2	*	*	*	0.097	*	*	*	0.028	0.029	0.020	
23.1	*	0.030	0.039	0.028	0.019	0.019	0.023	0.017	0.020	0.019	

23.2	0.040	0.030	0.031	0.033	0.019	0.019	0.024	0.017	0.020	0.020	
24.1	0.067	0.067	0.073	0.050	0.064	0.049	0.068	0.052	0.068	0.053	
24.2	0.078	0.104	*	0.086	0.090	0.061	0.079	0.070	0.097	0.069	
25.1	*	*	*	*	0.026	0.032	*	0.040	*	*	
LRL value	0.074	0.057	0.130	0.075	0.038	0.038	0.047	0.033	0.037	0.038	
Max. leverage	0.292	0.205	0.406	0.309	0.124	0.139	0.155	0.110	0.124	0.159	
Difference	0.218	0.148	0.275	0.234	0.087	0.100	0.109	0.077	0.087	0.121	
Site	**Length of P3**	**Anteroposterior diameter of c**	**Length of p2**	**Width of p2**							
PLS	46	52	55	57							
Without Site	17.1	10.6	17.1	17.1							
1.1	*	0.092	0.024	0.024							
2.1	0.025	*	*	*							
3.1	0.028	0.050	0.080	0.063							
3.2	0.026	0.139	0.023	0.025							
4.1	*	0.055	0.025	0.024							
5.1	0.023	*	0.022	0.025							
5.2	*	*	*	*							
5.3	0.039	*	0.026	0.022							
6.1	0.024	*	*	*							
6.2	0.049	0.157	0.024	0.032							
6.3	0.034	0.113	0.022	0.025							
6.4	0.030	*	0.023	*							
6.5	0.083	*	*	0.069							
6.6	0.025	0.065	0.026	0.020							

6.7	0.022	0.044	0.033	0.020							
6.8	0.022	0.041	0.042	0.019							
6.9	0.046	0.069	0.066	0.033							
6.10	*	*	0.053	0.033							
6.11	0.040	0.046	0.053	0.045							
6.12	*	*	0.049	*							
6.13	*	*	0.025	*							
6.14	*	0.041	0.025	0.019							
6.15	*	*	0.032	0.033							
7.1	0.056	0.175	0.052	0.062							
9.1	*	*	0.060	*							
9.2	0.023	0.040	0.022	0.020							
10.1	*	*	*	0.033							
10.2	0.048	0.113	0.057	0.043							
10.3	0.084	*	0.086	0.078							
10.4	0.054	*	0.056	0.061							
10.6	0.146	*	0.101	0.136							
11.1	0.033	*	0.036	0.026							
12.1	0.081	*	0.134	0.143							
12.2	*	*	*	0.023							
13.1	0.043	0.077	0.037	0.033							
13.2	0.041	*	0.036	0.024							
14.1	0.026	*	*	0.052							
15.1	0.026	*	0.024	0.026							
16.1	0.083	*	*	*							
16.2	*	*	*	0.063							
17.1	*	0.125	*	*							
17.2	0.044	*	*	0.029							
18.1	0.025	0.042	0.056	0.026							
19.1	*	*	0.033	0.025							

19.2	0.053	0.064	0.072	0.055							
19.3	0.047	*	0.072	0.036							
20.1	*	*	*	0.020							
21.1	0.048	*	0.043	0.038							
21.2	0.032	0.039	0.046	0.027							
21.3	0.058	*	*	*							
21.4	0.024	*	0.024	0.019							
21.5	*	*	*	*							
21.6	0.032	0.040	*	0.027							
21.7	0.032	*	0.040	0.031							
21.8	*	0.062	*	*							
21.9	0.028	*	*	0.023							
21.10	0.022	*	*	0.020							
21.11	0.031	*	0.030	*							
21.12	0.049	0.129	0.051	0.030							
22.1	0.031	*	0.033	0.057							
22.2	*	*	*	0.019							
23.1	*	*	0.023	0.020							
23.2	0.022	0.041	0.023	0.021							
24.1	0.063	0.064	0.077	0.051							
24.2	0.100	0.077	*	0.072							
25.1	*	*	*	*							
LRL value	0.043	0.077	0.044	0.038							

Table 10.18: Leverage values of PLS regressions run on cranial measurements of present-day *C. crocuta*. LRL = leverage reference line. Difference = the difference between the maximum leverage value and the LRL. Shaded values are maximum, extreme values that were excluded from subsequent PLS reruns.

Site	Total length of cranium	Condylobasal length	Basal length	Basicranial axis	Basifacial axis	Upper neurocranium length	Viscerocranium length	Facial length	Greatest length of the nasals	Snout length	Median palatal length	Length of the horizontal part of the palatine	Length of the cheektooth row (P1-P4)	Length of the cheektooth row (P1-P3)	Greatest diameter of the auditory bulla
PLS	64	65	66	67	68	69	70	71	72	73	74	75	76	78	80
1.1	0.023	0.024	0.025	*	*	0.027	*	0.023	*	0.021	0.020	0.025	0.020	0.158	0.020
2.1	*	*	*	*	0.030	*	0.025	0.021	0.034	0.020	0.021	*	0.029	0.146	*
3.1	0.084	0.095	0.112	0.103	0.142	0.070	0.096	0.083	0.048	0.076	0.125	0.117	0.119	0.210	0.099
3.2	0.020	0.023	0.025	0.028	0.048	0.023	0.023	0.021	0.024	0.020	0.027	0.044	0.039	0.345	0.022
4.1	*	*	*	*	*	*	*	*	*	*	*	*	*	*	*
5.1	*	*	0.034	*	*	*	*	0.028	*	0.023	0.034	0.045	*	*	0.028
5.3	0.022	0.022	0.023	0.036	*	0.031	*	0.023	*	0.025	0.020	0.021	0.022	0.073	0.019
6.2	0.028	0.027	0.026	0.050	0.032	0.043	0.042	0.030	0.073	0.031	0.020	0.023	0.020	0.124	0.021
6.3	0.027	0.027	0.027	*	0.033	*	0.035	*	0.052	0.029	0.020	0.023	0.021	0.104	0.022
6.4	0.025	0.025	0.027	0.039	0.032	0.034	0.031	0.025	0.040	0.028	0.021	*	0.021	0.073	0.022
6.5	0.048	*	*	*	*	0.083	0.086	0.057	0.156	0.053	0.023	0.038	0.022	0.271	0.031
6.6	0.020	0.022	0.024	0.029	0.033	0.022	0.023	0.020	0.034	0.020	0.027	0.023	0.028	0.099	0.021
6.7	*	0.025	0.027	0.028	*	*	0.023	0.022	0.025	0.022	0.031	0.025	0.033	0.087	0.025
6.9	0.037	0.036	0.039	0.045	0.049	0.036	0.041	0.034	0.033	0.037	0.041	0.031	0.059	0.103	0.037
6.10	0.020	0.021	0.022	0.030	0.030	0.022	0.030	0.021	0.034	0.021	0.020	0.022	0.108	0.183	0.019
6.11	0.033	0.035	0.034	*	0.049	0.034	0.051	0.039	0.053	0.036	0.034	0.039	0.039	0.118	0.031
6.12	0.046	0.046	0.043	*	*	0.057	0.074	0.054	0.093	0.050	0.035	0.046	0.035	0.117	0.037

6.13	0.023	0.026	0.025	*	*	0.024	0.027	0.024	0.028	0.023	0.023	0.028	*	*	0.022
6.14	0.020	0.021	0.022	0.029	0.031	*	0.024	*	0.025	0.021	0.020	0.022	0.020	0.060	0.019
6.15	0.034	0.038	0.038	0.044	0.057	0.031	0.037	0.035	0.032	0.032	0.037	0.041	0.037	0.057	0.034
7.1	0.055	0.057	*	0.080	*	0.059	0.072	0.060	0.081	0.055	*	0.054	0.043	*	0.045
9.1	0.068	0.067	0.071	0.084	0.084	0.070	*	0.062	*	0.064	0.064	0.057	0.063	0.094	0.062
10.1	0.031	0.031	0.031	*	*	0.035	0.038	0.032	0.039	0.031	0.029	0.030	0.033	0.050	0.028
10.2	0.069	0.073	0.075	0.082	0.095	0.060	0.065	0.064	0.054	0.069	0.066	0.061	0.067	0.115	0.065
10.3	0.051	0.045	0.044	0.077	0.054	0.070	0.083	0.054	0.087	0.049	0.043	0.042	0.099	0.267	0.042
10.4	0.051	0.053	0.051	0.072	0.073	0.053	0.067	0.055	0.066	0.049	0.048	0.055	0.054	0.079	0.046
11.1	0.038	0.039	0.044	0.051	0.051	0.038	*	0.036	*	0.041	0.036	0.034	0.033	0.076	0.037
12.1	0.129	0.139	0.147	0.186	0.197	0.127	0.183	0.141	0.140	0.124	0.149	0.167	0.151	0.193	0.134
12.2	0.022	0.021	0.022	0.029	0.033	*	0.023	*	0.026	0.023	0.022	0.027	0.055	0.168	0.019
13.1	0.042	0.045	0.045	0.053	0.063	0.039	0.042	0.040	0.041	0.042	0.038	0.040	0.036	0.156	0.039
13.2	0.030	0.031	0.032	0.038	0.044	0.029	0.030	0.028	0.030	0.032	0.028	0.026	*	*	0.029
14.1	0.103	0.119	0.137	*	*	0.078	*	0.097	*	0.097	0.135	0.129	0.158	0.172	0.114
15.1	0.020	*	*	*	*	0.023	0.023	0.021	0.024	0.021	0.020	*	0.021	0.258	*
16.1	0.027	0.023	0.024	*	*	0.039	0.033	0.024	0.043	0.031	0.020	*	0.063	0.229	0.022
16.2	*	*	*	*	*	0.050	*	*	*	*	*	0.036	0.073	*	0.031
17.1	0.052	0.053	0.055	0.052	0.047	0.044	0.028	0.040	0.028	0.061	0.033	0.025	0.439	0.642	0.036
17.2	0.056	0.054	0.059	0.063	0.065	0.053	0.049	0.048	0.041	0.057	0.051	0.038	0.052	0.091	0.050
18.1	0.063	0.067	*	0.070	*	0.050	0.055	0.055	0.031	0.065	*	0.058	0.096	0.129	0.068
19.1	0.060	0.078	0.100	0.059	0.129	0.035	0.045	0.053	*	*	0.117	0.104	0.172	0.323	0.081
19.2	0.078	0.086	0.091	0.105	0.116	0.068	*	0.079	*	0.085	0.081	*	0.071	0.167	0.079
21.1	0.035	0.038	0.036	0.048	0.054	0.033	0.041	0.037	0.043	0.036	0.033	0.036	0.038	0.146	0.033
21.2	0.025	0.026	0.027	0.037	0.036	0.026	0.034	0.027	0.034	0.029	0.026	0.026	0.029	0.103	0.024
21.3	0.041	0.038	0.038	*	*	0.049	0.052	0.040	0.054	0.040	0.035	*	0.052	0.090	0.035
21.4	0.023	0.023	0.024	0.031	0.031	0.026	0.024	0.021	0.027	0.022	0.020	0.022	0.024	0.124	0.020
21.6	0.029	0.030	0.031	0.042	*	0.029	0.037	0.031	0.035	0.033	0.030	0.029	0.028	0.097	0.028
21.7	0.027	*	*	*	*	*	0.033	0.028	0.031	0.027	0.029	0.029	0.037	0.052	0.026
21.8	0.020	0.022	0.023	*	*	0.023	0.023	0.020	0.026	0.020	0.022	0.028	0.025	0.112	0.019

21.9	*	*	*	*	*	*	*	*	*	*	*	*	0.022	*	0.022
21.10	0.021	*	*	*	*	0.021	0.023	0.020	0.023	*	0.021	*	*	*	0.020
21.11	0.021	0.021	*	0.030	*	0.025	*	0.021	*	*	*	0.021	0.031	0.079	0.019
21.12	0.052	0.049	0.056	0.060	0.061	0.053	0.048	0.044	0.040	0.052	0.047	0.036	0.046	0.127	0.049
22.1	0.032	0.035	0.032	0.049	0.053	0.034	0.049	0.038	0.051	0.028	0.032	0.048	0.040	0.171	0.029
23.1	0.021	0.022	0.024	*	*	0.023	0.023	0.020	0.024	0.021	0.020	0.021	0.027	0.073	0.019
23.2	0.020	0.021	0.023	0.028	0.030	0.023	*	0.020	*	0.021	0.020	0.022	0.024	0.070	0.019
24.1	0.049	0.049	0.050	0.072	0.065	0.050	0.068	0.052	0.066	0.056	0.047	0.046	0.055	0.117	0.047
25.1	0.030	0.032	0.035	0.041	0.051	0.028	0.040	0.031	0.031	0.031	0.040	0.038	0.070	0.102	0.034
LRL value	0.040	0.043	0.044	0.056	0.061	0.043	0.045	0.040	0.047	0.040	0.040	0.043	0.078	0.250	0.038
Max. leverage	0.129	0.139	0.147	0.186	0.197	0.127	0.183	0.141	0.156	0.124	0.149	0.167	0.439	0.642	0.134
Difference	0.089	0.097	0.103	0.131	0.137	0.084	0.137	0.101	0.110	0.084	0.109	0.124	0.361	0.392	0.096

Site	**Greatest mastoid breadth**	**Greatest breadth of bases of paraoccipital processes**	**Greatest breadth of the foramen magnum**	**Height of the foramen magnum**	**Greatest neurocranium breadth**	**Zygomatic breadth**	**Least breadth of the skull**	**Least breath between the orbits**	**Greatest palatal breadth**	**Least palatal breadth**	**Greatest height of the orbit**	**Skull height**	**Height of the occipital triangle**	**Temporal fossa length**	
PLS	81	82	83	84	86	88	89	91	92	93	94	95	96	97	
1.1	0.029	0.025	0.023	0.168	0.053	0.033	0.023	0.022	0.031	0.025	0.021	0.026	0.024	0.024	
2.1	*	*	*	*	0.059	0.028	0.060	0.024	0.027	0.021	0.019	*	*	*	
3.1	0.021	0.026	0.088	0.202	0.076	0.042	0.100	0.062	0.051	0.110	0.124	0.055	0.076	0.082	
3.2	0.046	0.077	0.023	0.337	0.134	0.023	0.058	0.021	0.024	0.031	0.067	0.027	0.028	0.020	
4.1	*	*	*	*	*	*	0.027	*	*	*	*	*	*	*	
5.1	0.022	0.040	*	0.148	0.023	0.023	0.029	0.022	*	*	0.054	*	*	*	
5.3	0.056	0.083	*	*	0.024	0.038	0.019	0.024	0.036	0.021	0.026	0.036	0.032	0.024	

6.2	0.086	0.115	0.026	0.179	0.046	0.067	0.026	0.035	0.058	0.022	0.021	0.056	0.042	0.032	
6.3	0.061	0.074	*	0.144	0.033	0.053	0.021	0.027	0.046	0.023	0.019	0.050	0.038	0.030	
6.4	0.047	0.056	0.026	0.100	0.025	0.040	0.021	0.023	0.037	0.022	0.019	0.042	0.036	0.028	
6.5	0.172	*	*	*	0.101	0.145	0.052	0.069	0.128	0.035	0.019	*	*	0.061	
6.6	0.043	0.066	0.024	0.139	0.032	0.032	0.023	0.019	0.027	0.023	0.029	0.027	0.022	0.020	
6.7	0.029	0.043	0.027	0.119	0.026	0.024	0.024	0.019	0.022	0.026	0.030	0.022	0.021	*	
6.9	0.022	0.021	0.036	0.134	0.033	0.025	0.036	0.037	0.030	0.033	0.027	0.027	0.033	0.036	
6.10	0.022	0.033	0.023	0.186	0.040	0.021	0.080	0.033	0.022	0.022	0.021	0.021	0.021	0.020	
6.11	0.030	0.032	0.036	0.135	0.037	0.036	0.045	0.046	0.036	0.031	0.024	0.037	0.032	0.032	
6.12	0.069	0.075	0.042	0.160	0.059	0.073	0.052	0.060	0.071	0.040	0.023	*	0.056	0.049	
6.13	0.020	0.020	0.026	0.065	0.031	0.024	0.027	0.025	0.024	*	0.023	0.023	0.022	0.022	
6.14	0.023	0.029	0.023	0.064	0.024	*	0.018	0.019	0.022	0.021	0.021	0.023	0.023	0.020	
6.15	0.021	0.020	0.038	0.060	0.032	*	0.033	0.032	0.030	0.041	0.039	0.029	0.028	0.031	
7.1	0.056	0.047	0.054	*	0.060	0.069	0.053	0.060	0.070	0.054	0.031	0.063	0.055	0.054	
9.1	0.044	0.029	0.063	0.093	0.062	0.057	0.062	0.053	0.065	0.065	0.046	0.062	0.071	0.068	
10.1	0.030	0.027	0.030	0.049	0.032	0.033	0.031	0.032	0.036	0.031	0.022	0.030	0.033	0.032	
10.2	0.035	0.024	0.081	0.111	0.060	0.051	0.065	0.050	0.053	0.067	0.054	0.069	0.059	0.061	
10.3	0.070	0.068	0.033	0.230	0.071	0.064	0.087	0.072	0.081	0.042	0.022	0.042	0.065	0.061	
10.4	0.040	0.031	0.048	0.090	0.059	0.054	0.059	0.059	0.058	0.053	0.037	0.046	0.047	0.051	
11.1	0.028	0.026	0.043	0.085	0.032	0.034	0.034	0.031	0.033	0.033	0.029	0.046	0.039	0.036	
12.1	0.059	0.032	0.117	0.196	0.144	0.109	0.158	0.141	0.121	0.147	0.123	0.107	0.121	0.133	
12.2	0.050	0.060	0.024	0.184	0.062	0.031	0.066	0.020	0.030	0.021	0.031	0.036	0.035	0.022	
13.1	0.028	0.023	0.047	0.143	0.040	0.037	0.034	0.038	0.037	0.041	0.035	0.042	0.033	0.038	
13.2	0.023	0.022	0.035	0.177	0.027	0.026	0.024	0.029	0.026	*	0.023	0.030	0.025	0.028	
14.1	0.023	0.025	0.130	0.178	0.102	0.053	0.134	0.058	0.056	0.130	0.143	0.091	0.090	0.090	
15.1	0.022	*	*	*	0.029	*	0.035	0.020	0.021	0.025	0.025	*	*	0.020	
16.1	0.060	0.088	0.024	*	0.027	0.033	0.023	0.031	0.039	*	0.030	0.031	0.036	0.031	
16.2	0.049	0.047	0.026	0.244	0.054	0.049	0.075	0.052	*	*	0.021	0.030	0.046	0.044	
17.1	0.045	0.033	0.103	0.649	0.424	0.045	0.395	0.019	0.036	0.038	0.021	0.125	0.074	0.037	
17.2	0.035	0.026	0.062	0.107	0.061	0.040	0.060	0.036	0.044	0.046	0.033	0.057	0.056	0.051	

18.1	0.021	0.022	0.082	0.149	0.104	0.030	0.104	0.032	0.033	0.063	0.066	0.059	0.063	0.055	
19.1	0.038	0.115	0.087	0.354	0.085	*	0.128	0.024	*	0.106	0.171	0.034	0.044	0.048	
19.2	0.038	0.027	0.095	0.159	0.067	0.060	0.070	0.068	0.058	0.075	0.067	0.089	0.067	0.069	
21.1	0.027	0.024	*	*	0.042	0.034	0.036	0.041	*	0.034	0.028	0.034	0.028	0.032	
21.2	0.023	0.027	0.029	0.104	0.027	0.024	0.026	0.030	0.025	0.023	0.019	0.028	0.026	0.024	
21.3	0.045	0.042	0.033	0.094	0.044	0.043	0.043	0.045	0.051	0.034	0.022	0.037	0.046	0.044	
21.4	0.029	0.027	0.024	0.132	0.023	0.030	0.021	0.019	0.028	0.023	0.019	0.027	0.026	0.023	
21.6	0.024	0.026	0.035	0.098	0.032	0.026	0.027	0.031	0.027	0.026	0.021	0.034	0.029	0.027	
21.7	0.021	0.021	*	*	0.026	0.025	0.031	0.030	0.027	0.028	0.023	*	*	0.026	
21.8	*	*	*	0.155	0.021	*	0.019	*	0.023	0.026	*	0.024	0.025	0.020	
21.9	*	*	*	*	0.028	*	0.023	*	*	*	*	*	*	*	
21.10	0.020	0.022	*	*	0.022	*	0.018	0.019	*	*	0.022	*	*	0.020	
21.11	0.031	0.045	0.023	0.078	0.020	0.025	0.023	0.022	*	0.021	0.024	0.024	0.025	0.021	
21.12	0.035	0.027	0.051	0.168	0.043	0.039	0.047	0.037	0.044	0.043	0.033	0.048	0.053	0.051	
22.1	0.028	0.023	0.030	0.218	0.051	0.041	0.062	0.043	0.044	0.042	0.031	0.028	0.030	0.033	
23.1	0.023	0.023	0.023	0.090	0.021	0.023	0.026	0.019	0.023	0.021	0.019	0.026	0.025	0.021	
23.2	0.022	0.024	0.023	0.095	0.023	0.022	0.028	0.019	0.021	0.021	0.019	0.024	0.024	0.020	
24.1	0.040	0.041	0.051	0.122	0.050	0.045	0.050	0.060	0.047	0.039	0.029	0.054	0.046	0.047	
25.1	0.019	0.020	0.031	0.111	0.037	0.022	0.047	0.038	0.024	0.031	0.034	0.024	0.025	0.029	
LRL value	0.038	0.040	0.045	0.267	0.073	0.042	0.036	0.038	0.042	0.042	0.038	0.043	0.042	0.039	
Max. leverage	0.172	0.115	0.130	0.649	0.424	0.145	0.395	0.141	0.128	0.147	0.171	0.125	0.121	0.133	
Difference	0.133	0.075	0.085	0.382	0.351	0.104	0.359	0.103	0.086	0.105	0.134	0.082	0.079	0.094	

Site	Length of the cheektooth row (P1-P4)	Length of the cheektooth row (P1-P3)	Height of the foramen magnum	Greatest neurocranium breadth	Least breadth of the skull										
PLS	77	79	85	87	90										
Without Site	17.1	17.1	17.1	17.1	17.1										
1.1	0.021	0.171	0.024	0.119	0.022										
2.1	0.020	0.147	*	0.119	0.024										
3.1	0.115	0.223	0.088	0.161	0.091										
3.2	0.040	0.515	0.023	0.476	0.046										
4.1	*	*	*	*	0.021										
5.1	*	*	0.041	0.098	0.026										
5.3	0.021	0.073	*	0.065	0.018										
6.2	0.020	0.124	0.026	0.117	0.022										
6.3	0.020	0.104	0.025	0.091	0.020										
6.4	0.020	0.073	0.024	0.060	0.019										
6.5	0.021	0.272	*	0.225	0.040										
6.6	0.028	0.099	0.025	0.092	0.019										
6.7	0.035	0.087	0.029	0.076	0.022										
6.9	0.050	0.107	0.040	0.081	0.037										
6.10	0.025	0.218	0.023	0.132	0.033										
6.11	0.033	0.122	0.043	0.080	0.040										
6.12	0.031	0.122	0.050	0.109	0.046										
6.13	*	*	0.030	0.040	0.025										
6.14	0.020	0.060	0.023	0.048	0.018										

6.15	0.038	0.059	0.045	0.044	0.034										
7.1	0.039	*	*	0.118	0.047										
9.1	0.059	0.095	0.068	0.076	0.049										
10.1	0.030	0.050	0.035	0.040	0.030										
10.2	0.056	0.153	0.088	0.106	0.041										
10.3	0.055	0.303	0.043	0.204	0.070										
10.4	0.051	0.079	0.061	0.063	0.057										
11.1	0.032	0.076	0.038	0.061	0.027										
12.1	0.150	0.214	0.134	0.181	0.166										
12.2	0.029	0.237	0.023	0.211	0.033										
13.1	0.039	0.159	0.052	0.098	0.034										
13.2	*	*	0.036	0.082	0.025										
14.1	0.098	0.196	0.124	0.179	0.066										
15.1	0.020	0.277	*	0.237	0.022										
16.1	0.024	0.244	*	0.204	0.021										
16.2	0.040	*	0.033	0.185	0.055										
17.2	0.042	0.119	0.061	0.100	0.028										
18.1	0.057	0.157	0.071	0.152	0.031										
19.1	0.084	0.326	0.076	0.247	0.042										
19.2	0.068	0.185	0.097	0.116	0.059										
21.1	0.037	0.149	*	0.062	0.037										
21.2	0.026	0.110	0.031	0.051	0.025										
21.3	0.040	0.097	0.038	0.080	0.041										
21.4	0.020	0.124	0.023	0.084	0.018										
21.6	0.027	0.113	0.037	0.052	0.025										
21.7	0.032	0.052	*	0.039	0.030										
21.8	0.022	0.116	0.026	0.096	0.020										
21.9	0.020	*	*	0.046	0.020										
21.10	*	*	*	0.044	0.019										
21.11	0.020	0.084	0.023	0.066	0.019										

21.12	0.048	0.128	0.048	0.117	0.033										
22.1	0.035	0.171	0.042	0.116	0.048										
23.1	0.020	0.074	0.023	0.036	0.019										
23.2	0.020	0.070	0.023	0.049	0.019										
24.1	0.049	0.117	0.055	0.053	0.051										
25.1	0.052	0.147	0.032	0.118	0.049										
LRL value	0.040	0.255	0.045	0.185	0.036										

Table 10.19: Leverage values of PLS regressions run on mandibular measurements of present-day *C. crocuta*. LRL = leverage reference line. Difference = the difference between the maximum leverage value and the LRL. Shaded values are maximum, extreme values that were excluded from subsequent PLS reruns.

Site	c alveolus to m1 alveolus length	Length of cheektooth row (p2 – m1)	Length of cheektooth row (p3 – m1)	Length of premolar row (p2 – p4)	Mandibular width at p3/p4	Mandibular width at p4/m1	Mandibular width at post-m1	Distance from p3/p4 to middle of articular condyle	Distance from p4/m1 to middle of articular condyle	Distance from post-m1 to middle of articular condyle	Moment arm of the temporalis	Moment arm of the superficial masseter	Momement arm of the deep masseter	Moment arm of resistance at m1
PLS	98	99	101	103	104	106	107	108	109	110	111	113	115	116
1.1	0.021	0.146	0.143	0.023	0.033	0.029	0.038	0.024	0.025	0.028	0.064	0.142	0.026	0.026
2.1	0.020	0.133	0.132	0.020	0.070	0.035	0.050	0.021	0.021	0.022	0.061	0.122	0.034	0.021
3.1	0.096	0.189	0.138	0.047	0.102	0.093	0.062	0.092	0.102	0.103	0.100	0.146	0.037	0.087
3.2	0.020	0.320	0.295	0.029	0.038	0.052	0.032	0.021	0.024	0.028	0.038	0.293	0.022	0.024
4.1	*	0.101	0.047	0.025	*	*	*	*	*	*	*	*	0.029	0.027
5.1	*	0.096	0.095	0.019	0.032	0.031	0.026	0.027	0.030	0.036	0.028	0.085	0.019	0.033
5.2	0.021	0.134	0.118	0.021	0.021	0.020	0.021	0.020	0.020	0.022	0.034	0.122	0.020	0.020
6.2	0.029	0.170	0.161	0.047	0.051	0.033	0.072	0.038	0.033	0.035	0.061	0.170	0.074	0.032
6.3	0.028	0.136	0.129	0.037	0.032	0.027	0.051	0.034	0.031	0.034	0.047	0.137	0.049	0.030
6.4	0.026	0.090	0.084	0.033	0.026	0.023	0.035	0.030	0.027	0.029	0.036	0.087	0.036	0.026
6.5	*	*	*	0.092	*	*	*	*	*	*	*	*	*	*
6.6	0.020	0.131	0.125	0.022	0.037	0.021	0.036	0.021	0.020	0.021	0.045	0.128	0.033	0.020
6.7	0.022	0.109	0.105	0.019	0.031	0.020	0.025	0.020	0.021	0.020	0.039	0.107	0.023	0.020
6.9	0.038	0.105	0.103	0.037	0.036	0.030	0.022	0.031	0.031	0.026	0.036	0.100	0.025	0.030
6.10	0.021	0.167	0.150	0.023	0.064	0.030	0.029	0.021	0.021	0.020	0.021	0.139	0.031	0.020
6.11	0.038	0.112	0.095	0.036	0.048	0.044	0.050	0.040	0.038	0.034	0.037	0.073	0.052	0.035
6.12	0.053	0.129	0.125	0.060	*	*	*	*	*	*	0.066	0.127	0.095	0.053

6.13	0.023	0.045	0.033	0.022	0.026	0.028	0.027	0.023	0.024	0.024	0.022	0.030	0.024	0.025
6.14	0.021	0.047	0.040	0.021	0.021	0.020	0.020	0.021	0.020	0.020	0.020	0.039	0.021	0.020
6.15	0.033	0.045	0.040	0.027	0.034	0.036	0.031	0.033	0.034	0.035	0.033	0.039	0.026	0.037
7.1	0.056	0.104	0.102	0.063	0.062	0.058	0.075	0.061	0.058	0.058	0.057	0.090	0.080	0.061
9.1	0.067	0.087	0.072	0.065	0.064	0.051	0.049	0.066	0.065	0.063	0.068	0.066	0.050	0.064
10.1	0.031	0.043	0.037	0.034	0.036	0.032	0.033	0.031	0.031	0.029	0.035	0.039	0.034	0.030
10.2	0.067	0.094	0.073	0.060	0.073	0.040	0.037	0.062	0.060	0.061	0.077	0.083	0.044	0.067
10.3	0.056	0.217	0.116	0.073	0.128	0.077	0.088	0.058	0.057	0.045	0.138	0.144	0.083	0.048
10.4	0.052	0.067	0.067	0.053	0.065	0.063	0.067	0.055	0.055	0.052	0.058	0.065	0.061	0.056
11.1	0.040	0.071	0.058	0.036	0.039	0.028	0.029	0.039	0.037	0.037	0.038	0.068	0.030	0.037
12.1	0.148	0.189	0.173	0.105	0.185	0.189	0.181	0.159	0.166	0.163	0.181	0.185	0.124	0.148
12.2	0.021	0.175	0.141	0.031	0.034	0.032	0.021	0.021	0.020	0.020	0.020	0.119	0.022	0.020
13.1	0.039	0.114	0.066	0.038	0.038	0.034	0.031	0.038	0.037	0.038	0.040	0.092	0.033	0.043
13.2	0.028	0.130	0.065	0.031	0.028	0.023	0.021	0.026	0.025	0.024	0.038	0.112	0.024	0.028
14.1	0.111	0.165	0.164	0.055	0.140	0.072	0.054	0.107	0.113	0.126	0.118	0.167	0.040	0.108
15.1	0.020	0.230	0.226	0.022	0.028	0.030	0.033	0.020	0.021	0.022	0.021	0.167	0.021	0.021
16.1	0.027	0.216	0.215	0.052	0.032	0.020	0.021	0.024	0.022	0.020	0.027	0.192	0.036	0.021
16.2	0.039	0.222	0.092	*	0.115	0.066	0.077	0.043	0.044	0.037	0.133	0.154	0.064	*
17.1	0.046	0.637	0.604	0.052	0.383	0.051	0.031	0.040	0.031	0.040	0.340	0.581	0.026	0.040
17.2	0.054	0.086	0.085	0.054	0.062	0.025	0.023	0.047	0.044	0.041	0.061	0.085	0.032	0.046
18.1	*	0.126	0.125	0.041	0.109	0.028	0.022	0.058	0.058	0.058	0.095	0.119	0.023	0.053
19.1	0.064	0.308	0.270	0.020	0.131	0.042	0.022	0.056	0.069	0.083	0.081	0.278	0.021	0.062
19.2	0.085	0.152	0.086	0.065	0.086	0.060	0.059	0.083	0.080	0.082	0.093	0.100	0.061	0.083
21.1	0.034	0.110	0.047	0.036	0.034	0.036	0.034	0.033	0.033	0.031	0.036	0.061	0.037	0.037
21.2	0.029	0.093	0.077	0.028	0.029	0.025	0.025	0.027	0.026	0.023	0.036	0.069	0.030	0.024
21.4	0.021	0.117	0.111	0.023	0.021	0.021	0.024	0.022	0.022	0.024	0.035	0.102	0.021	0.023
21.6	0.033	0.088	0.065	0.030	0.033	0.025	0.025	0.031	0.029	0.026	0.046	0.060	0.032	0.027
21.7	0.028	0.047	0.046	0.027	0.031	0.029	0.026	0.026	0.026	0.024	0.027	0.047	0.026	0.026
21.8	0.020	0.101	0.087	0.024	*	*	*	*	*	*	0.024	0.068	0.021	0.020
21.9	*	*	0.060	*	*	*	*	*	*	*	*	*	*	*

21.10	0.020	0.041	0.039	0.019	0.020	0.021	0.020	0.020	0.020	0.021	0.020	0.043	0.019	*
21.11	0.022	0.065	0.055	0.025	0.033	0.021	0.025	0.022	0.021	0.020	0.028	0.059	0.028	0.020
21.12	0.050	0.120	0.120	0.052	0.046	0.029	0.025	0.044	0.042	0.039	0.044	0.106	0.030	0.044
22.1	0.033	0.134	0.117	0.030	0.072	0.065	0.074	0.039	0.042	0.042	0.070	0.136	0.050	0.040
23.1	0.021	0.070	0.051	0.020	0.021	0.020	0.021	0.022	0.021	0.023	0.025	0.045	0.019	0.020
23.2	0.021	0.065	0.054	0.020	0.022	0.021	0.020	0.021	0.020	0.021	0.021	0.041	0.019	0.020
24.1	0.056	0.111	0.076	0.054	0.057	0.049	0.051	0.054	0.050	0.043	0.052	0.079	0.059	0.048
25.1	0.034	*	*	*	0.042	0.042	0.029	0.031	0.032	0.028	0.031	0.090	0.024	0.029
LRL value	0.040	0.231	0.189	0.038	0.080	0.040	0.040	0.040	0.040	0.040	0.077	0.192	0.038	0.039
Max. leverage	0.148	0.637	0.604	0.105	0.383	0.189	0.181	0.159	0.166	0.163	0.340	0.581	0.124	0.148
Difference	0.108	0.407	0.416	0.067	0.303	0.149	0.141	0.119	0.126	0.123	0.263	0.389	0.087	0.109

Site	**Length of cheektooth row (p2 – m1)**	**Length of cheektooth row (p3 – m1)**	**Mandibular width at p3/p4**	**Moment arm of the temporalis**	**Moment arm of the superficial masseter**									
PLS	100	102	105	112	114									
Without Site	17.1	17.1	17.1	17.1	17.1									
1.1	0.020	0.019	0.025	0.031	0.159									
2.1	0.020	0.021	0.024	0.024	0.133									
3.1	0.083	0.074	0.095	0.102	0.204									
3.2	0.022	0.028	0.028	0.027	0.486									
4.1	0.027	0.024	*	*	*									
5.1	0.021	0.021	0.026	0.026	0.103									
5.3	0.023	0.024	0.021	0.020	0.130									
6.2	0.028	0.024	0.035	0.038	0.171									

6.3	0.025	0.023	0.030	0.034	0.138									
6.4	0.025	0.024	0.026	0.029	0.092									
6.6	0.020	0.021	0.021	0.021	0.131									
6.7	0.024	0.025	0.021	0.020	0.109									
6.9	0.046	0.047	0.037	0.031	0.108									
6.10	0.024	0.021	0.029	0.021	0.190									
6.11	0.037	0.035	0.045	0.033	0.114									
6.12	0.049	0.043	*	0.059	0.138									
6.13	0.022	0.021	0.025	0.023	0.046									
6.14	0.022	0.021	0.021	0.020	0.049									
6.15	0.030	0.030	0.034	0.032	0.047									
7.1	0.054	0.054	0.059	0.054	0.129									
9.1	0.070	0.069	0.062	0.068	0.088									
10.1	0.034	0.032	0.034	0.034	0.043									
10.2	0.064	0.074	0.051	0.046	0.123									
10.3	0.070	0.054	0.079	0.087	0.249									
10.4	0.052	0.048	0.061	0.058	0.067									
11.1	0.038	0.039	0.035	0.032	0.070									
12.1	0.131	0.109	0.181	0.179	0.210									
12.2	0.022	0.025	0.022	0.020	0.236									
13.1	0.037	0.040	0.037	0.032	0.121									
13.2	0.030	0.033	0.026	0.022	0.139									
14.1	0.086	0.093	0.084	0.085	0.187									
15.1	0.022	0.023	0.021	0.020	0.241									
16.1	0.041	0.039	0.027	0.025	0.229									
16.2	0.047	0.035	0.061	0.069	0.249									
17.2	0.059	0.069	0.037	0.036	0.109									
18.1	0.064	0.075	0.042	0.040	0.154									
19.1	0.044	0.048	0.044	0.051	0.317									
19.2	0.073	0.079	0.073	0.058	0.160									

21.1	0.034	0.036	0.036	0.028	0.115									
21.2	0.030	0.031	0.029	0.022	0.096									
21.4	0.020	0.020	0.021	0.025	0.115									
21.6	0.033	0.036	0.030	0.023	0.100									
21.7	0.030	0.029	0.030	0.026	0.047									
21.8	0.021	0.021	*	0.020	0.103									
21.9	*	0.025	*	*	*									
21.10	0.020	0.019	0.021	0.020	0.045									
21.11	0.023	0.022	0.024	0.022	0.070									
21.12	0.056	0.059	0.040	0.042	0.121									
22.1	0.030	0.025	0.049	0.050	0.136									
23.1	0.020	0.020	0.021	0.022	0.072									
23.2	0.020	0.020	0.020	0.020	0.066									
24.1	0.057	0.056	0.059	0.043	0.106									
25.1	*	*	0.042	0.032	0.136									
LRL value	0.039	0.038	0.041	0.039	0.235									

10.7 Pleistocene Crocuta crocuta body mass reconstruction

Table 10.20: Body mass and m1 lengths of recent *C. crocuta* used in the ordinary least squares regression model. [1]Kruuk (1972), [2]Wilson (1968), cited in Bailey (1993), [3]Wilson (1975), cited in Silva and Downing (1995), [4]Smithers (1971), [5]Sillero-Zubiri and Gottelli (1992), [6]Swanson et al. (2013), [7]Powell-Cotton (n.d.), cited in Shortridge (1934).

Body mass location	m1 length location	Sex	Body mass (n)	m1 (n)	Body mass (kg)	m1 length (mm)	Body mass (Log10)	m1 length (Log10)
Serengeti, Tanzania[1]	Ngorongoro Conservation Area, Tanzania	F	8	19	55.30	26.73	1.74	1.43
Serengeti, Tanzania[1]	Ngorongoro Conservation Area, Tanzania	M	12	15	48.70	26.51	1.69	1.42
Zambia[2,3]	Lundazi District, Zambia	F	?	1	68.20	30.01	1.83	1.48
Zambia[2,3]	Fort Jameson District; Kabompo District, Zambia	M	?	3	67.70	30.03	1.83	1.48
Botswana[4]	Tsane; Joverega, Botswana	F	4	2	73.48	28.09	1.87	1.45
Botswana[4]	Mababe Flats, Botswana	M	2	3	80.06	30.83	1.9	1.49
Salient area of the Aberdare National Park, Kenya[5]	Mount Kenya, Kenya	F	9	1	51.80	25.98	1.71	1.41
Salient area of the Aberdare National Park, Kenya[5]	Mount Kenya, Kenya	M	5	1	47.40	26.08	1.68	1.42
Masai Mara National Reserve, Kenya[6]	Sotik, Kenya	F	631 (F&M)	4	59.39	27.91	1.77	1.45
Masai Mara National Reserve, Kenya[6]	Sotik, Kenya	M	631 (F&M)	9	53.67	26.71	1.73	1.43
Ethiopia[7]	Argobba, south Harrar, Ethiopia	F	1	1	35.83	25.69	1.55	1.41

10.8 Pleistocene Crocuta crocuta craniodental and post-cranial morphology

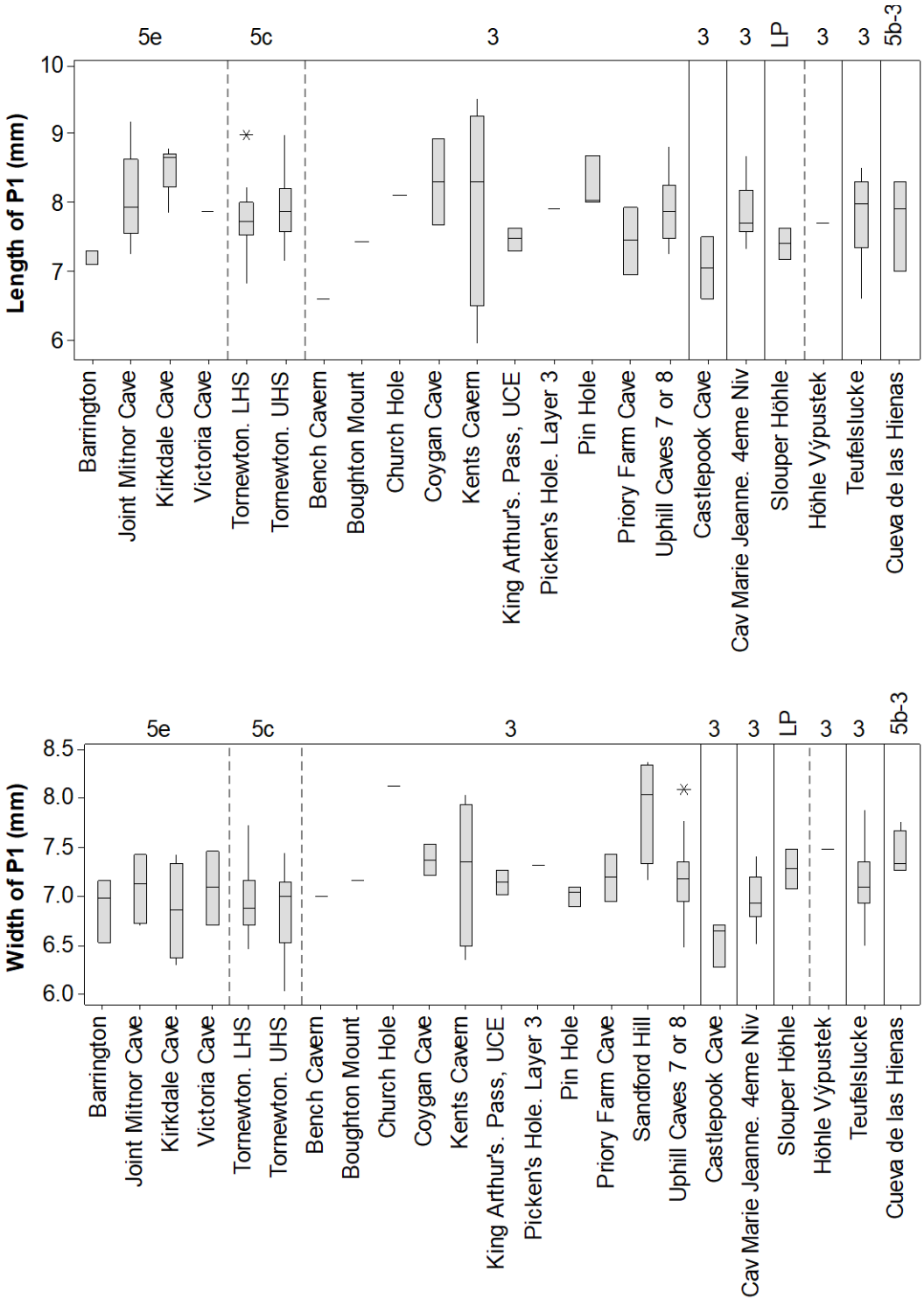

Figure 10.3: Boxplots of *C. crocuta* dental measurements. Numbers along the top indicate marine oxygen isotope stages. LP = Late Pleistocene. See Table 10.21 for sample sizes.

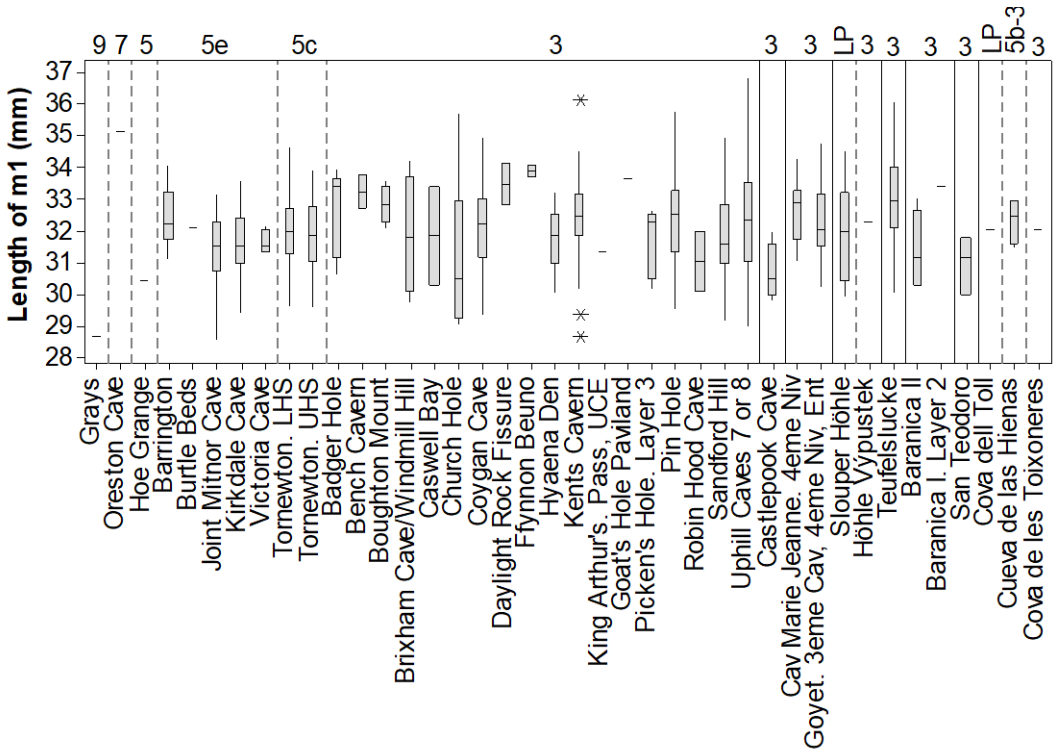

Figure 10.3 continued.

Table 10.21: Sample sizes of boxplots in Figure 10.3.

Site	P1 L	P1 W	m1 L
Grays			1
Oreston			1
Hoe Grange			1
Barrington	3	3	7
Burtle Beds			1
Joint Mitnor Cave	5	4	19
Kirkdale Cave	7	6	31
Victoria Cave	1	2	4
Tornewton. LHS	11	11	33
Tornewton. UHS	21	28	34
Badger Hole			5
Bench Cavern	1	1	2
Boughton Mount	1	1	4
Brixham Cave/Windmill Hill			4
Caswell Bay			2
Church Hole	1	1	7
Coygan Cave	2	2	74
Daylight Rock Fissure			2
Ffynnon Beuno			2
Goat's Hole Paviland			1
Hyaena Den			8
Kents Cavern	4	7	109
King Arthur's Cave. The Passage, Upper Cave Earth	2	2	1
Picken's Hole. Layer 3	1	1	9
Pin Hole	3	3	34
Priory Farm Cave	2	2	
Robin Hood Cave			2
Sandford Hill		4	22
Uphill Caves 7 or 8	15	15	35
Castlepook Cave	2	3	4
Caverne Marie-Jeanne. 4eme Niveau	12	14	21
Goyet. 3eme Caverne, 4eme Niveau Ossifère, Galleries Voisines de l'Entrée			8
Slouper Höhle	2	2	10
Höhle Výpustek	1	1	1
Teufelslucke	26	30	47
Baranica II			7
Baranica I. Layer 2			1
San Teodoro			3
Cova del Toll			1
Cueva de las Hienas	3	4	4
Cova de les Toixoneres			1

Table 10.22: Results of ANOVA with post-hoc Tukey's tests for Pleistocene upper dentition measurements. Sites that do not share a letter are significantly different.

Site	Anteroposterior diameter of C	Length of P1	Width of P1	Length of P2	With of P2	Length of P3	Width of P3	Length of P4	Greatest width of P4	Width of P4
Joint Mitnor Cave	C			B		A B	A		B C D	A B
Kirkdale Cave				A B	A B	A				
Tornewton LHS		A	A		B	B	A	A	C D	B
Tornewton UHS	B C	A				A B		A	D	B
Coygan Cave				A	A B	A B	A	A		A
Kents Cavern	A B			A	A	A	A	A	B C	A
Pin Hole					A B		A	A	A B C	A
Sandford Hill	A B									
Uphill Caves 7 or 8		A	A		A B	A	A		A B C D	A B
Teufelslucke	A		A	A	A B		A	A	A	A
Caverne Marie Jeanne. 4eme Niveau		A	A	A	A B		A		A B	A B
p-value	<0.05	0.928	0.195	<0.05	0.029	<0.05	0.105	0.686	<0.05	<0.05

Table 10.23: Results of ANOVA with post-hoc Tukey's tests for Pleistocene lower dentition measurements. Sites that do not share a letter are significantly different.

Site	Anteroposterior diameter of c	Mediolateral diameter of c	Length of p2	With of p2	Length of p3	Width of p3	Length of P4	Width of P4	Length of m1	Width of m1
Barrington						A B				
Joint Mitnor Cave		C	A		D	B	A	C		B C D E G H I J
Kirkdale Cave			A	A	C D	A B	A	C	B	C D E H I J
Tornewton LHS	B C	B C			D	B	A	C	B	J
Tornewton UHS	C	C	A B	A	C D	A B	A	C	B	F G H I J
Brixham Cave/Windmill Hill		A B C								
Church Hole		A B C								
Coygan Cave	A	A B	A B	A	B C D	A B	A		A B	A
Kents Cavern	A	A B		A	A B C	A B	A	B		A E
Picken's Hole. Layer 3		A B C	A B			A B		A B C		
Pin Hole		A B C	A B	A	A B C D	A B	A	B C	A B	A B C D E F G H I
Sandford Hill		A B C	B	A	A B C D	B		B C	B	D E I J
Uphill Caves 7&8	A B	A B C	B			A B	A	A B	A B	A
Caverne Marie Jeanne. 4eme Niveau				A	A B		A	A B	A B	A B C D E
Goyet. 3eme Caverne, 4eme Niveau Ossifère, Galleries Voisines de l'Entrée						A B				A B C D E F G H I
Goyet. 3eme Caverne, 3eme Niveau		A B C						A B		
Slouper Höhle								A B	A B	A B C D E F G H I J
Teufelslucke	A	A	A B	A	A	A		A	A	A
Baranica II										A B C D
p-value	<0.05	<0.05	0.001	0.1	<0.05	<0.05	0.052	<0.05	<0.05	<0.05

Table 10.24: Results of t-tests on the mediolateral diameter of C from Pleistocene deposits in Europe. Top values are t-values, bottom values are p-values. Shaded cells indicate significant differences at 95 % confidence.

t-value p-value	Teufelslucke	Joint Mitnor	Tornewton UHS	Coygan Cave	Kents Cavern	Pin Hole	Sandford Hill	Uphill Caves 7&8
Teufelslucke	-	1.8 0.085	0.16 0.877	1.4 0.169	1 0.325	5.88 <0.05	3.08 0.004	1.51 0.143
Joint Mitnor	-	-	1.83 0.079	2.93 0.008	2.62 0.016	2.54 0.021	0.4 0.695	0.57 0.577
Tornewton UHS	-	-	-	1.1 0.277	0.74 0.463	5.48 <0.05	2.94 0.006	1.54 0.134
Coygan Cave	-	-	-	-	0.41 0.68	7.88 <0.05	4.88 <0.05	2.93 0.006
Kents Cavern	-	-	-	-	-	7.33 <0.05	4.38 <0.05	2.53 0.017
Pin Hole	-	-	-	-	-	-	3.17 <0.04	3.98 0.001
Sandford Hill	-	-	-	-	-	-	-	1.29 0.21
Uphill Caves 7&8	-	-	-	-	-	-	-	-

Table 10.25: Mann-Whitney test results on Pleistocene dental measurements from Europe. Shaded cells indicate significant differences at 95 % confidence.

		Anteroposterior diameter of C	**Greatest width of P4**	**Width of p4**
Coygan Cave vs. Joint Mitnor Cave	W-value p-value	1256.5 <0.05	1673.5 0.988	4411 <0.05
Coygan Cave vs. Kirkdale Cave	W-value p-value			4422.5 <0.05
Coygan Cave vs. Tornewton LHS	W-value p-value	1242.5 <0.05	2079.5 0.279	5315.5 <0.05
Coygan Cave vs. Tornewton UHS	W-value p-value	1155 0.124	1734 0.023	5453 <0.05
Coygan Cave vs. Kents Cavern	W-value p-value	1401.5 0.66	2852.5 0.087	8767 0.628
Coygan Cave vs. Picken's Hole. Layer 3	W-value p-value			3484.5 0.468
Coygan Cave vs. Pin Hole	W-value p-value		1580 0.045	4809.5 0.004
Coygan Cave vs. Sandford Hill	W-value p-value	1048.5 0.855		4362.5 0.002
Coygan Cave vs. Uphill Caves 7 or 8	W-value p-value		1570 0.118	4586 0.807
Coygan Cave vs. Caverne Marie Jeanne. 4eme Niveau	W-value p-value		1661 0.025	3943 0.902
Coygan Cave vs. Goyet. 3eme Cavern, 3eme Niveau	W-value p-value			3514 0.56
Coygan Cave vs. Slouper Höhle	W-value p-value			3433.5 0.935
Coygan Cave vs. Teufelslucke	W-value p-value	968 0.212	1879 <0.05	4650.5 0.004

Table 10.26: Mann-Whitney test results on Pleistocene dental measurements from Europe. Shaded cells indicate significant differences at 95 % confidence.

		Width of P1
Tornewton UHS vs. Tornewton LHS	W-value p-value	542 0.585
Tornewton UHS vs. Uphill Caves 7&8	W-value p-value	524.5 0.02
Tornewton UHS vs. Teufelslucke	W-value p-value	659 0.01
Tornewton UHS vs. Caverne Marie Jeanne. 4eme Niveau	W-value p-value	568.5 0.379

Table 10.27: Mann-Whitney test results on Pleistocene dental measurements from Europe. Shaded cells indicate significant differences at 95 % confidence.

Sites		Anteroposterior diameter of C	Mediolateral diameter of C
Tornewton LHS vs. Joint Mitnor Cave	W-value p-value	143.5 0.514	216.5 0.313
Tornewton LHS vs. Tornewton UHS	W-value p-value	102 0.004	203 0.005
Tornewton LHS vs. Coygan Cave	W-value p-value	135.5 <0.05	278 <0.05
Tornewton LHS vs. Kents Cavern	W-value p-value	106.5 <0.05	299 0.001
Tornewton LHS vs. Pin Hole	W-value p-value		290.5 0.028
Tornewton LHS vs. Sandford Hill	W-value p-value	80.5 <0.05	270 0.743
Tornewton LHS vs. Uphill Caves 7&8	W-value p-value		212.5 0.146
Tornewton LHS vs. Teufelslucke	W-value p-value	78 <0.05	190.5 0.001

Table 10.28: Mann-Whitney test results on Pleistocene dental measurements from Europe. Shaded cells indicate significant differences at 95 % confidence.

Sites		Width of P3	Width of P4
Kirkdale Cave vs. Joint Mitnor Cave	W-value p-value	127 0.076	130.5 0.364
Kirkdale Cave vs. Tornewton LHS	W-value p-value	211 0.453	270 0.183
Kirkdale Cave vs. Tornewton UHS	W-value p-value		187 0.204
Kirkdale Cave vs. Coygan Cave	W-value p-value	461 0.225	221 0.018
Kirkdale Cave vs. Kents Cavern	W-value p-value	441 0.746	342.5 0.072
Kirkdale Cave vs. Pin Hole	W-value p-value	175.5 0.015	112.5 0.043
Kirkdale Cave vs. Uphill Caves 7&8	W-value p-value	253 0.034	205.5 0.784
Kirkdale Cave vs. Teufelslucke	W-value p-value	277.5 0.98	215 0.008
Kirkdale Cave vs. Caverne Marie Jeanne. 4eme Niveau	W-value p-value	190.5 0.15	128.5 0.217

Table 10.29: Mann-Whitney test results on Pleistocene dental measurements from Europe. Shaded cells indicate significant differences at 95 % confidence.

Sites		Length of P1	Length of p4
Teufelslucke vs. Joint Mitnor Cave	W-value p-value		826 0.364
Teufelslucke vs. Kirkdale Cave	W-value p-value		1055 0.007
Teufelslucke vs. Tornewton UHS	W-value p-value	618.5 0.915	1265 0.027
Teufelslucke vs. Tornewton LHS	W-value p-value	498.5 0.894	1050.5 0.273
Teufelslucke vs. Coygan Cave	W-value p-value		2009.5 0.001
Teufelslucke vs. Kents Cavern	W-value p-value		2536.5 0.194
Teufelslucke vs. Pin Hole	W-value p-value		892 0.246
Teufelslucke vs. Uphill Caves 7&8	W-value p-value	529.5 0.665	1016 0.159
Teufelslucke vs. Caverne Marie Jeanne. 4eme Niveau	W-value p-value	499 0.814	749 0.673

Table 10.30: Mann-Whitney test results on Pleistocene dental measurements from Europe. Shaded cells indicate significant differences at 95 % confidence.

Sites		Length of p2	Length of m1
Kents Cavern vs. Joint Mitnor Cave	W-value p-value	1613.5 0.009	7566.5 <0.05
Kents Cavern vs. Kirkdale Cave	W-value p-value	1812.5 0.02	8439 <0.05
Kents Cavern vs. Tornewton LHS	W-value p-value		8326.5 0.01
Kents Cavern vs. Tornewton UHS	W-value p-value	1690 0.233	8429.5 0.006
Kents Cavern vs. Coygan Cave	W-value p-value	2264 0.329	10573.5 0.121
Kents Cavern vs. Picken's Hole. Layer 3	W-value p-value	1748.5 0.912	
Kents Cavern vs. Pin Hole	W-value p-value	2017 0.554	7867.5 0.928
Kents Cavern vs. Sandford Hill	W-value p-value	1871.5 0.119	7561.5 0.024
Kents Cavern vs. Uphill Caves 7&8	W-value p-value	2279 0.347	8088.5 0.388
Kents Cavern vs. Caverne Marie Jeanne. 4eme Niveau	W-value p-value	1900.5 0.363	7030.5 0.492
Kents Cavern vs. Slouper Höhle	W-value p-value		6679.5 0.183
Kents Cavern vs. Teufelslucke	W-value p-value	2691.5 0.123	7888.5 0.01

Table 10.31: Mann-Whitney test results on Pleistocene dental measurements from Europe. Shaded cells indicate significant differences at 95 % confidence.

Sites		Width of p2	Length of p3
Uphill Caves 7 or 8 vs. Joint Mitnor Cave	W-value p-value		1333.5 <0.05
Uphill Caves 7 or 8 vs. Kirkdale Cave	W-value p-value	399.5 0.82	1341 0.007
Uphill Caves 7 or 8 vs. Tornewton LHS	W-value p-value		1210 0.001
Uphill Caves 7 or 8 vs. Tornewton UHS	W-value p-value	360.5 0.387	1238.5 0.006
Uphill Caves 7 or 8 vs. Coygan Cave	W-value p-value	740 0.852	2097.5 0.132
Uphill Caves 7 or 8 vs. Kents Cavern	W-value p-value	1139 0.673	2671 0.959
Uphill Caves 7 or 8 vs. Picken's Hole. Layer 3	W-value p-value		
Uphill Caves 7 or 8 vs. Pin Hole	W-value p-value	608.5 0.244	1217 0.324
Uphill Caves 7 or 8 vs. Sandford Hill	W-value p-value	509 0.118	1226 0.444
Uphill Caves 7 or 8 vs. Caverne Marie Jeanne. 4eme Niveau	W-value p-value	393 0.294	960.5 0.014
Uphill Caves 7 or 8 vs. Teufelslucke	W-value p-value	638.5 0.228	1405 0.006

Table 10.32: Mann-Whitney test results on Pleistocene dental measurements from Europe. Shaded cells indicate significant differences at 95 % confidence.

Sites		Length of m1
Joint Mitnor Cave vs. Kirkdale Cave	W-value p-value	469.5 0.772
Joint Mitnor Cave vs. Tornewton LHS	W-value p-value	434 0.19
Joint Mitnor Cave vs. Tornewton UHS	W-value p-value	450.5 0.25
Joint Mitnor Cave vs. Coygan Cave	W-value p-value	657 0.025
Joint Mitnor Cave vs. Kents Cavern	W-value p-value	689.5 <0.05
Joint Mitnor Cave vs. Pin Hole	W-value p-value	370 0.008
Joint Mitnor Cave vs. Sandford Hill	W-value p-value	363.5 0.36
Joint Mitnor Cave vs. Uphill Caves 7&8	W-value p-value	412.5 0.047
Joint Mitnor Cave vs. Caverne Marie Jeanne. 4eme Niveau	W-value p-value	270.5 0.001
Joint Mitnor Cave vs. Slouper Höhle	W-value p-value	269.5 0.491
Joint Mitnor Cave vs. Teufelslucke	W-value p-value	359 <0.05

Table 10.33: Mann-Whitney test results on Pleistocene dental measurements from Europe. Shaded cells indicate significant differences at 95 % confidence.

Sites		**Length of p2**	**Width of p3**
Caverne Marie Jeanne. 4eme Niveau vs. Barrington	W-value p-value		321 0.503
Caverne Marie Jeanne. 4eme Niveau vs. Joint Mitnor Cave	W-value p-value	227.5 0.114	370.5 0.193
Caverne Marie Jeanne. 4eme Niveau vs. Kirkdale Cave	W-value p-value	300 0.207	351 1
Caverne Marie Jeanne. 4eme Niveau vs. Tornewton LHS	W-value p-value		371.5 0.988
Caverne Marie Jeanne. 4eme Niveau vs. Tornewton UHS	W-value p-value	256 0.829	331 0.728
Caverne Marie Jeanne. 4eme Niveau vs. Coygan Cave	W-value p-value	477.5 0.859	634.5 0.077
Caverne Marie Jeanne. 4eme Niveau vs. Kents Cavern	W-value p-value	727.5 0.363	1251 0.047
Caverne Marie Jeanne. 4eme Niveau vs. Picken's Hole. Layer 3	W-value p-value	273 0.581	309 0.547
Caverne Marie Jeanne. 4eme Niveau vs. Pin Hole	W-value p-value	369.5 0.255	440.5 0.945
Caverne Marie Jeanne. 4eme Niveau vs. Sandford Hill	W-value p-value	311 0.069	549 0.201
Caverne Marie Jeanne. 4eme Niveau vs. Uphill Caves 7&8	W-value p-value	473.5 0.105	474.5 0.198
Caverne Marie Jeanne. 4eme Niveau vs. Goyet. 3eme Caverne, 4eme Niveau Ossifère, Galleries Voisines de l'Entrée	W-value p-value		282 0.234
Caverne Marie Jeanne. 4eme Niveau vs. Teufelslucke	W-value p-value	640 0.83	438.5 0.002

Table 10.34: Mann-Whitney test results on Pleistocene dental measurements from Europe. Shaded cells indicate significant differences at 95 % confidence.

Sites		**Width of m1**
Picken's Hole. Layer 3 vs. Joint Mitnor Cave	W-value p-value	177 0.067
Picken's Hole. Layer 3 vs. Kirkdale Cave	W-value p-value	193 0.051
Picken's Hole. Layer 3 vs. Tornewton LHS	W-value p-value	304 0.028
Picken's Hole. Layer 3 vs. Tornewton UHS	W-value p-value	307 0.022
Picken's Hole. Layer 3 vs. Coygan Cave	W-value p-value	386 0.639
Picken's Hole. Layer 3 vs. Kents Cavern	W-value p-value	585 0.686
Picken's Hole. Layer 3 vs. Pin Hole	W-value p-value	241 0.664
Picken's Hole. Layer 3 vs. Sandford Hill	W-value p-value	213 0.053
Picken's Hole. Layer 3 vs. Uphill Caves 7&8	W-value p-value	213 0.491
Picken's Hole. Layer 3 vs. Caverne Marie Jeanne. 4eme Niveau	W-value p-value	175 0.737
Picken's Hole. Layer 3 vs. Goyet. 3eme Caverne, 4eme Niveau Ossifère, Galleries Voisines de l'Entrée	W-value p-value	100.5 0.526
Picken's Hole. Layer 3 vs. Slouper Höhle	W-value p-value	105 1
Picken's Hole. Layer 3 vs. Teufelslucke	W-value p-value	253 0.211
Picken's Hole. Layer 3 vs. Baranica II	W-value p-value	91.5 0.326

Table 10.35: Summary of significant difference tests on Pleistocene C. crocuta C anteroposterior diameter measurements. Y = significant difference at 95 %. Numbers next to Y indicate which assemblage's average value is larger. Blank cells = no significant difference.

Site	1. Joint Mitnor Cave	2. Tornewton LHS	3. Tornewton UHS	4. Coygan Cave	5. Kents Cavern	6. Sandford Hill	7. Teufelslucke
1. Joint Mitnor Cave				4Y	5Y	6Y	7Y
2. Tornewton LHS			3Y	4Y	5Y	6Y	7Y
3. Tornewton UHS							7Y
4. Coygan Cave							
5. Kents Cavern							
6. Sandford Hill							
7. Teufelslucke							

Table 10.36: Summary of significant difference tests on Pleistocene C. crocuta C mediolateral diameter measurements. Y = significant difference at 95 %. Numbers next to Y indicate which assemblage's average value is larger. Blank cells = no significant difference.

Site	1. Joint Mitnor Cave	2. Tornewton LHS	3. Tornewton UHS	4. Coygan Cave	5. Kents Cavern	6. Pin Hole	7. Sandford Hill	8. Uphill Caves 7 or 8	9. Teufelslucke
1. Joint Mitnor Cave				4Y	5Y	1Y			
2. Tornewton LHS			3Y	4Y	5Y	2Y			9Y
3. Tornewton UHS						3Y	3Y		
4. Coygan Cave						4Y	4Y	4Y	
5. Kents Cavern						5Y	5Y	5Y	
6. Pin Hole							7Y	8Y	9Y
7. Sandford Hill									9Y
8. Uphill Caves 7 or 8									
9. Teufelslucke									

Table 10.37: Summary of significant difference tests on Pleistocene C. crocuta c anteroposterior diameter measurements. Y = significant difference at 95 %. Numbers next to Y indicate which assemblage's average value is larger. Blank cells = no significant difference.

Site	1. Tornewton LHS	2. Tornewton UHS	3. Coygan Cave	4. Kents Cavern	5. Uphill Caves 7 or 8	6. Teufelslucke
1. Tornewton LHS			3Y	4Y		6Y
2. Tornewton UHS			3Y	4Y	5Y	6Y
3. Coygan Cave						
4. Kents Cavern						
5. Uphill Caves 7 or 8						
6. Teufelslucke						

Table 10.38: Results of significant difference tests on Pleistocene C. crocuta c mediolateral diameter measurements. Y = significant difference at 95 %. Numbers next to Y indicate which assemblage's average value is larger. Blank cells = no significant difference.

Site	1. Joint Mitnor Cave	2. Tornewton LHS	3. Tornewton UHS	4. Brixham/ Windmill	5. Church Hole	6. Coygan Cave	7. Kents Cavern	8. Picken's Hole	9. Pin Hole	10. Sandford Hill	11. Uphill Caves 7 or 8	12. Goyet. 3eme Cav, 3eme Niv	13. Teufelslucke
1. Joint Mitnor Cave						6Y	7Y						13Y
2. Tornewton LHS													13Y
3. Tornewton UHS						6Y	7Y						13Y
4. Brixham/ Windmill													
5. Church Hole													
6. Coygan Cave													
7. Kents Cavern													
8. Picken's Hole													
9. Pin Hole													
10. Sandford Hill													
11. Uphill Caves 7 or 8													
12. Goyet. 3eme Cav, 3eme Niv													
13. Teufelslucke													

Table 10.39: Summary of significant difference tests on Pleistocene C. crocuta P2 length measurements. Y = significant difference at 95 %. Numbers next to Y indicate which assemblage's average value is larger. Blank cells = no significant difference.

Site	1. Joint Mitnor Cave	2. Kirkdale Cave	3. Coygan Cave	4. Kents Cavern	5. Teufelslucke	6. Caverne Marie Jeanne
1. Joint Mitnor Cave			3Y	4Y	5Y	6Y
2. Kirkdale Cave						
3. Coygan Cave						
4. Kents Cavern						
5. Teufelslucke						
6. Caverne Marie Jeanne						

Table 10.40: Summary of significant difference tests on Pleistocene C. crocuta P2 width measurements. Y = significant difference at 95 %. Numbers next to Y indicate which assemblage's average value is larger. Blank cells = no significant difference.

Site	1. Kirkdale Cave	2. Tornewton LHS	3. Coygan Cave	4. Kents Cavern	5. Pin Hole	6. Uphill Caves 7 or 8	7. Teufelslucke	8. Caverne Marie Jeanne
1. Kirkdale Cave								
2. Tornewton LHS				4Y				
3. Coygan Cave								
4. Kents Cavern								
5. Pin Hole								
6. Uphill Caves 7 or 8								
7. Teufelslucke								
8. Caverne Marie Jeanne								

Table 10.41: Summary of significant difference tests on Pleistocene C. crocuta P3 length measurements. Y = significant difference at 95 %. Numbers next to Y indicate which assemblage's average value is larger. Blank cells = no significant difference.

Site	1. Joint Mitnor Cave	2. Kirkdale Cave	3. Tornewton LHS	4. Tornewton UHS	5. Coygan Cave	6. Kents Cavern	7. Uphill Caves 7 or 8
1. Joint Mitnor Cave		2Y				6Y	7Y
2. Kirkdale Cave							
3. Tornewton LHS							
4. Tornewton UHS							
5. Coygan Cave							
6. Kents Cavern							
7. Uphill Caves 7 or 8							

Table 10.42: Summary of significant difference tests on Pleistocene C. crocuta P3 width measurements. Y = significant difference at 95 %. Numbers next to Y indicate which assemblage's average value is larger. Blank cells = no significant difference.

Site	1. Joint Mitnor Cave	2. Kirkdale Cave	3. Tornewton LHS	4. Coygan Cave	5. Kents Cavern	6. Pin Hole	7. Uphill Caves 7 or 8	8. Teufelslucke	9. Caverne Marie Jeanne
1. Joint Mitnor Cave									
2. Kirkdale Cave						2Y	2Y		
3. Tornewton LHS									
4. Coygan Cave									
5. Kents Cavern									
6. Pin Hole									
7. Uphill Caves 7 or 8									
8. Teufelslucke									
9. Caverne Marie Jeanne									

Table 10.43: Summary of significant difference tests on Pleistocene C. crocuta p2 length measurements. Y = significant difference at 95 %. Numbers next to Y indicate which assemblage's average value is larger. Blank cells = no significant difference.

Site	1. Joint Mitnor Cave	2. Kirkdale Cave	3. Tornewton UHS	4. Coygan Cave	5. Kents Cavern	6. Picken's Hole. Layer 3	7. Pin Hole	8. Sandford Hill	9. Uphill Caves 7 or 8	10. Caverne Marie Jeanne	11. Teufelslucke
1. Joint Mitnor Cave					1Y			1Y	1Y		
2. Kirkdale Cave					2Y			2Y	2Y		
3. Tornewton UHS											
4. Coygan Cave											
5. Kents Cavern											
6. Picken's Hole. Layer 3											
7. Pin Hole											
8. Sandford Hill											
9. Uphill Caves 7 or 8											
10. Caverne Marie Jeanne											
11. Teufelslucke											

Table 10.44: Summary of significant difference tests on Pleistocene C. crocuta p3 length measurements. Y = significant difference at 95 %. Numbers next to Y indicate which assemblage's average value is larger. Blank cells = no significant difference.

Site	1. Joint Mitnor Cave	2. Kirkdale Cave	3. Tornewton LHS	4. Tornewton UHS	5. Coygan Cave	6. Kents Cavern	7. Pin Hole	8. Sandford Hill	9. Uphill Caves 7 or 8	10. Caverne Marie Jeanne	11. Teufelslucke
1. Joint Mitnor Cave						6Y			9Y	10Y	11Y
2. Kirkdale Cave									9Y	10Y	11Y
3. Tornewton LHS						6Y			9Y	10Y	11Y
4. Tornewton UHS									9Y	10Y	11Y
5. Coygan Cave											11Y
6. Kents Cavern											
7. Pin Hole											
8. Sandford Hill											
9. Uphill Caves 7 or 8										10Y	11Y
10. Caverne Marie Jeanne											
11. Teufelslucke											

Table 10.45: Results of significant difference tests on Pleistocene C. crocuta p3 width measurements. Y = significant difference at 95 %. Numbers next to Y indicate which assemblage's average value is larger. Blank cells = no significant difference.

Site	1. Barrington	2. Joint Mitnor Cave	3. Kirkdale Cave	4. Tornewton LHS	5. Tornewton UHS	6. Coygan Cave	7. Kents Cavern	8. Picken's Hole	9. Pin Hole	10. Sandford Hill	11. Uphill Caves	12. Caverne Marie Jeanne	13. Goyet. 3eme Cav 4eme Niv	14. Teufelslucke
1. Barrington														
2. Joint Mitnor Cave														14Y
3. Kirkdale Cave														
4. Tornewton LHS														14Y
5. Tornewton UHS														
6. Coygan Cave														
7. Kents Cavern												7Y		
8. Picken's Hole														
9. Pin Hole														
10. Sandford Hill														14Y
11. Uphill Caves														
12. Caverne Marie Jeanne														14Y
13. Goyet. 3eme Cav, 4eme Niv														
Teufelslucke														

Table 10.46: Summary of significant difference tests on Pleistocene C. crocuta p4 length measurements. Y = significant difference at 95 %. Numbers next to Y indicate which assemblage's average value is larger. Blank cells = no significant difference.

Site	1. Joint Mitnor Cave	2. Kirkdale Cave	3. Tornewton LHS	4. Tornewton UHS	5. Coygan Cave	6. Kents Cavern	7. Pin Hole	8. Uphill Caves 7 or 8	9. Caverne Marie Jeanne	10. Teufelslucke
1. Joint Mitnor Cave										
2. Kirkdale Cave										10Y
3. Tornewton LHS										
4. Tornewton UHS										10Y
5. Coygan Cave										10Y
6. Kents Cavern										
7. Pin Hole										
8. Uphill Caves 7 or 8										
9. Caverne Marie Jeanne.										
10. Teufelslucke										

Table 10.47: Summary of significant difference tests on Pleistocene C. crocuta p4 width measurements. Y = significant difference at 95 %. Numbers next to Y indicate which assemblage's average value is larger. Blank cells = no significant difference.

Site	1. Joint Mitnor Cave	2. Kirkdale Cave	3. Tornewton LHS	4. Tornewton UHS	5. Coygan Cave	6. Kents Cavern	7. Picken's Hole	8. Pin Hole	9. Sandford Hill	10. Uphill Caves	11. Caverne Marie Jeanne	12. Goyet. 3eme Cave, 3eme Niv	13. Slouper Höhle	14. Teufelslucke
1. Joint Mitnor Cave					5Y	6Y				10Y	11Y	12Y	13Y	14Y
2. Kirkdale Cave					5Y	6Y				10Y	11Y	12Y	13Y	14Y
3. Tornewton LHS					5Y	6Y				10Y	11Y	12Y	13Y	14Y
4. Tornewton UHS					5Y	6Y				10Y	11Y	12Y	13Y	14Y
5. Coygan Cave								5Y	5Y					14Y
6. Kents Cavern														14Y
7. Picken's Hole														
8. Pin Hole														14Y
9. Sandford Hill														14Y
10. Uphill Caves														
11. Caverne Marie Jeanne														
12. Goyet. 3eme Cav, 3eme Niv														
13.Slouper Höhle														
14. Teufelslucke														

Table 10.48: Summary of significant difference tests on Pleistocene C. crocuta P4 greatest width measurements. Y = significant difference at 95 %. Numbers next to Y indicate which assemblage's average value is larger. Blank cells = no significant difference.

Site	1. Joint Mitnor Cave	2. Tornewton LHS	3. Tornewton UHS	4. Coygan Cave	5. Kents Cavern	6. Pin Hole	7. Uphill Caves 7 or 8	8. Teufelslucke	9. Caverne Marie Jeanne
1. Joint Mitnor Cave								8Y	
2. Tornewton LHS								8Y	9Y
3. Tornewton UHS				4Y	5Y	6Y		8Y	9Y
4. Coygan Cave						6Y		8Y	9Y
5. Kents Cavern								8Y	
6. Pin Hole									
7. Uphill Caves 7 or 8									
8. Teufelslucke									
9. Caverne Marie Jeanne									

Table 10.49: Summary of significant difference tests on Pleistocene C. crocuta P4 width measurements. Y = significant difference at 95 %. Numbers next to Y indicate which assemblage's average value is larger. Blank cells = no significant difference.

Site	1. Kirkdale Cave	2. Joint Mitnor Cave	3. Tornewton LHS	4. Tornewton UHS	5. Coygan Cave	6. Kents Cavern	7. Pin Hole	8. Uphill Caves 7 or 8	9. Teufelslucke	10. Caverne Marie Jeanne
1. Kirkdale Cave					5Y		7Y		9Y	
2. Joint Mitnor Cave										
3. Tornewton LHS					5Y	6Y	7Y		9Y	
4. Tornewton UHS					5Y	6Y	7Y		9Y	
5. Coygan Cave										
6. Kents Cavern										
7. Pin Hole										
8. Uphill Caves 7 or 8										
9. Teufelslucke										
10. Caverne Marie Jeanne										

Table 10.50: Summary of significant difference tests on Pleistocene C. crocuta m1 width measurements. Y = significant difference at 95 %. Numbers next to Y indicate which assemblage's average value is larger. Blank cells = no significant difference.

Site	1. Joint Mitnor Cave	2. Kirkdale Cave	3. Tornewton LHS	4. Tornewton UHS	5. Coygan Cave	6. Kents Cavern	7. Picken's Hole. Layer 3	8. Pin Hole	9. Sandford Hill	10. Uphill Caves 7 or 8	11. Caverne Marie Jeanne	12. Goyet. 3eme Cav, 4eme Niv	13. Slouper Höhle	14. Teufelslucke	15. Baranica II
1. Joint Mitnor Cave					5Y					10Y				14Y	
2. Kirkdale Cave					5Y					10Y				14Y	
3. Tornewton LHS					5Y	6Y	7Y	8Y		10Y	11Y	12Y		14Y	15Y
4. Tornewton UHS					5Y	6Y	7Y			10Y	11Y			14Y	15Y
5. Coygan Cave									5Y	10Y				14Y	
6. Kents Cavern															
7. Picken's Hole. Layer 3															
8. Pin Hole															
9. Sandford Hill										10Y				14Y	
10.Uphill Caves 7 or 8															
11. Caverne Marie Jeanne															
12. Goyet. 3eme Cav, 4eme Niv															
13. Slouper Höhle															
14. Teufelslucke															
15. Baranica II															

Table 10.51: Cranial measurements of Pleistocene *C. crocuta* from Europe. Measurement included are those with fewer than four data values. The measurements are in mm. [a]Both specimens have been categorised into P3/p3 wear stage V.

Site	Median palatal length (mm)	Breadth dorsal to the external auditory meatus (mm)	Greatest palatal breadth (mm)	Least palatal breadth (mm)	Skull height (mm)	Height of the occipital triangle (mm)
Barrington		95.49[a]	110.08			68.99
Barrington					103	
Slouper Höhle	144.24	105.42[a]	123.47	65.41	112.97	82.89
Slouper Höhle			125.64	64.67		
Höhle Výpustek	135.11				102.07	80.89

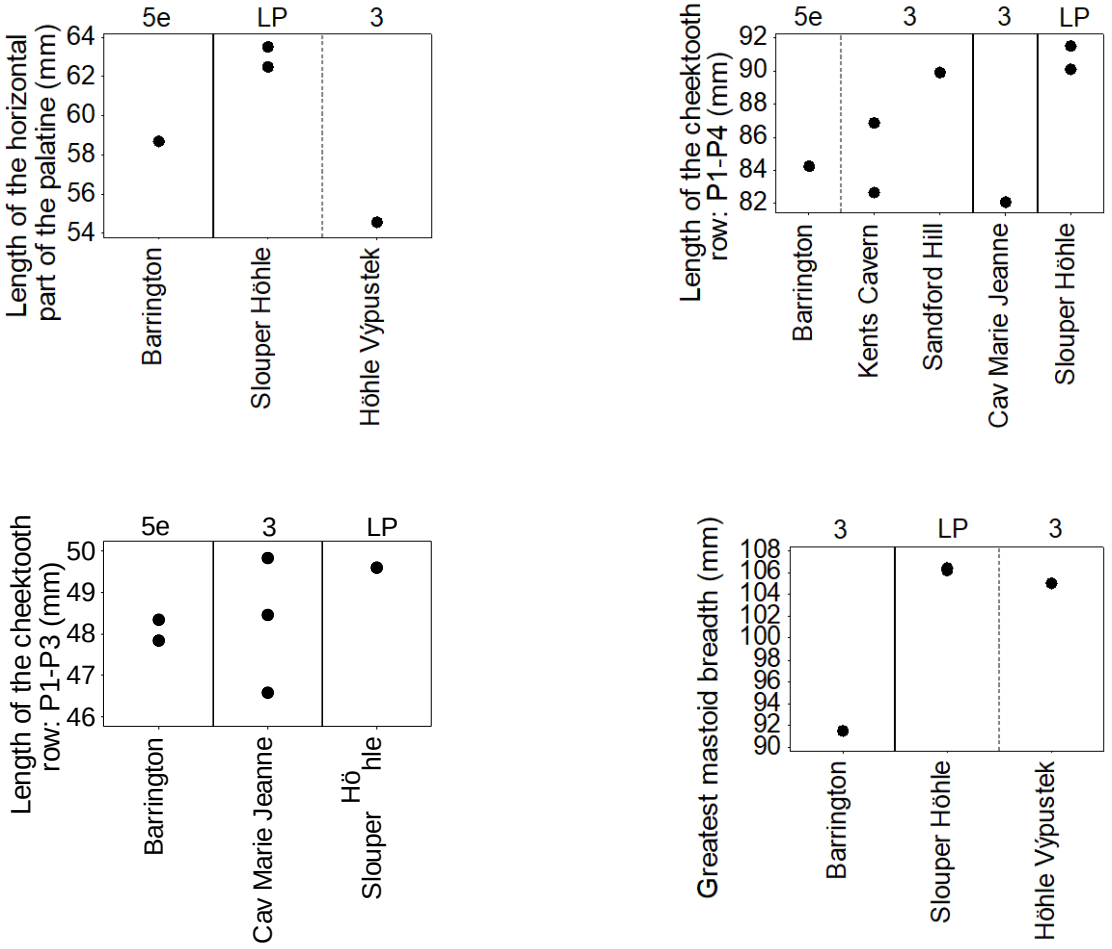

Figure 10.4: Individual value plots of Pleistocene *C. crocuta* cranial measurements. Numbers along the top of the graphs indicate marine oxygen isotope stages. LP = Late Pleistcene.

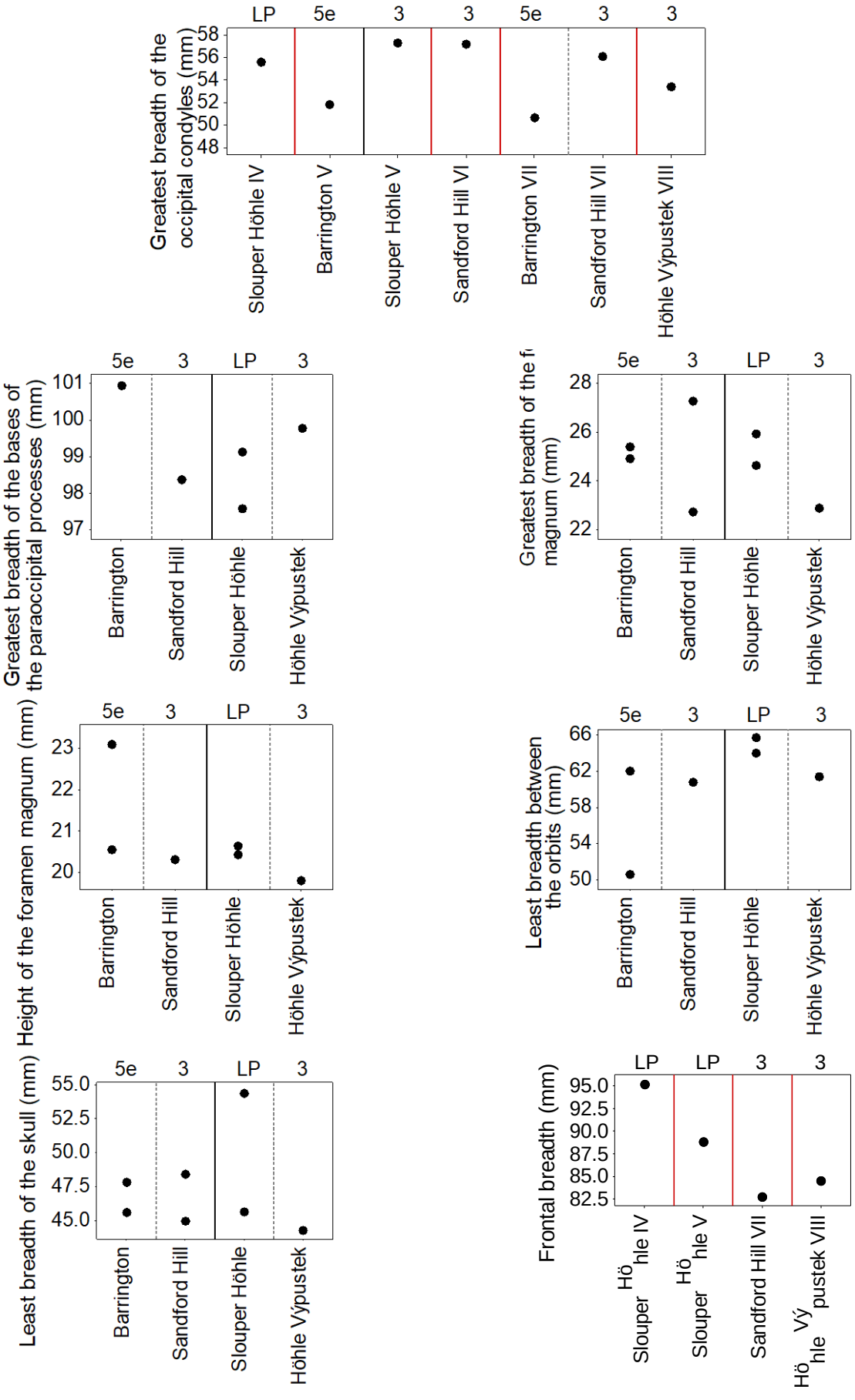

Figure 10.4 continued.

Table 10.52: Measurements of the height of the vertical ramus of Pleistocene *C. crocuta* from Europe.

	Height of the vertical ramus (mm)
Trou Magrite	100.13
Slouper Höhle	96.78
Slouper Höhle	93.13

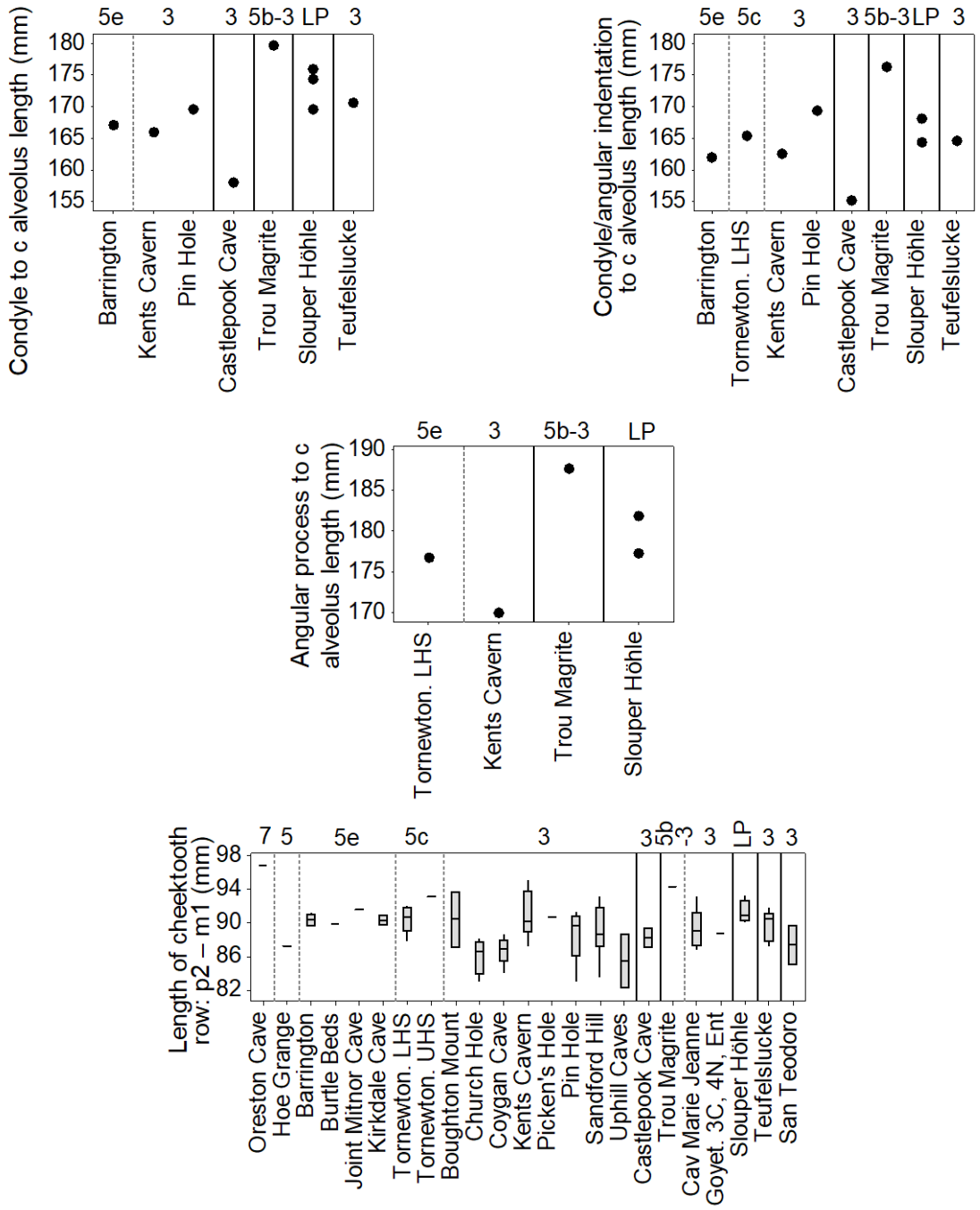

Figure 10.5: Boxplots and individual value plots of Pleistocene *C. crocuta* mandibular measurements. Numbers along the top of the graphs indicate marine oxygen isotope stages. LP = Late Pleistocene. See Table 10.53 for sample sizes in the boxplots.

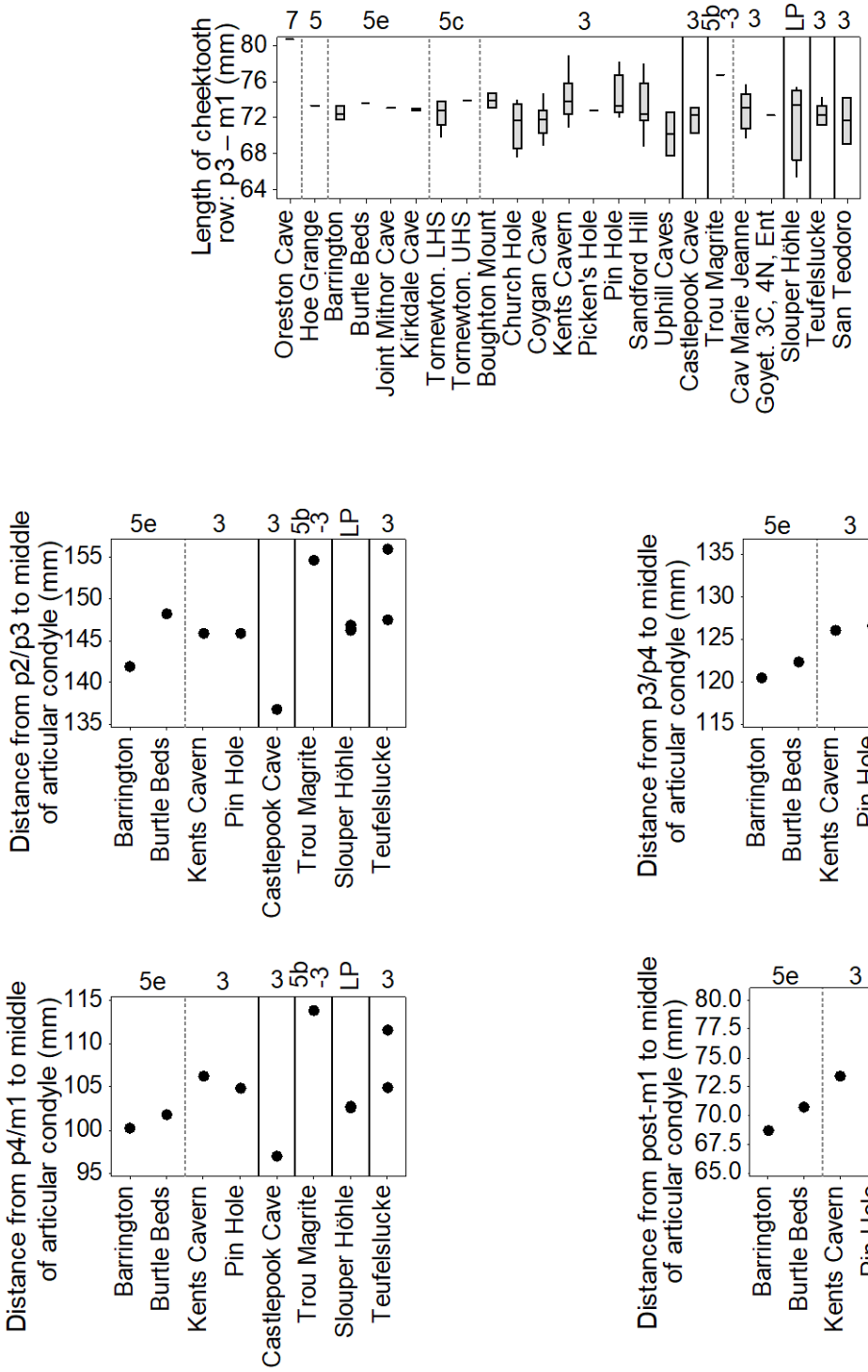

Figure 10.5 continued.

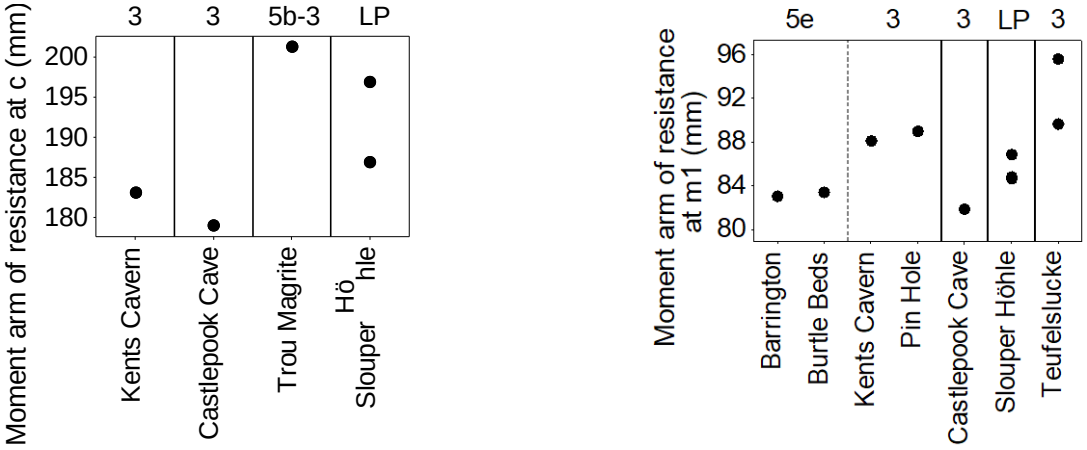

Figure 10.5 continued.

Table 10.53: Sample sizes of the boxplots in Figure 10.5.

Site	Length of cheektooth row (p2-m1)	Length of cheektooth row (p3-m1)
Oreston	1	1
Hoe Grange	1	1
Barrington	4	4
Burtle Beds	1	1
Joint Mitnor Cave	1	1
Kirkdale Cave	2	2
Tornewton. LHS	5	5
Tornewton. UHS	1	1
Boughton Mount	2	2
Church Hole	4	4
Coygan Cave	6	7
Kents Cavern	12	13
Picken's Hole. Layer 3	1	1
Pin Hole	6	7
Sandford Hill	8	8
Uphill Caves 7 or 8	2	2
Castlepook Cave	3	3
Trou Magrite	1	1
Caverne Marie-Jeanne. 4eme Niveau	5	5
Goyet. 3eme Caverne, 4eme Niveau Ossifère, Galleries Voisines de l'Entrée	1	1
Slouper Höhle	5	4
Teufelslucke	7	6
San Teodoro	2	2

Table 10.54: *C. crocuta* post-cranial measurements from Pleistocene deposits. All values are in mm.

	Atlas: greatest length	Sacrum: physiological length	Sacrum: greatest breadth of the cranial articular surface	Sacrum: greatest height of the cranial articular surface	Humerus: greatest breadth of the proximal end
Hutton		83.77	31.22	18.97	
Hoe Grange		85.71	32.67	18.88	69.94
Hoe Grange					73.39
Joint Mitnor Cave					65.5
Tornewton LHS	57.53				
Uphill Caves 7 or 8			30.84	20.55	
Slouper Höhle	72.42				

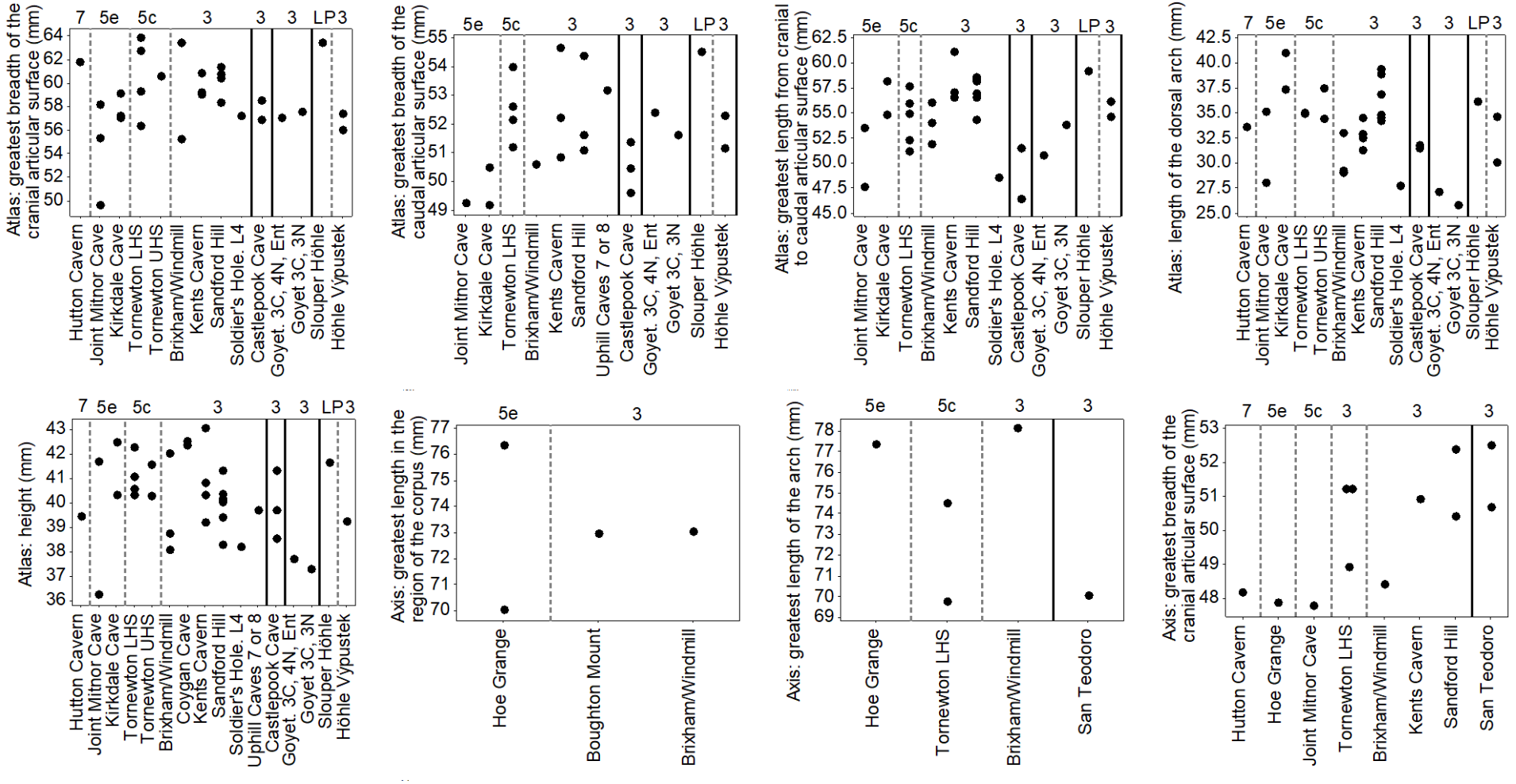

Figure 10.6: Boxplots and individual value plots of Pleistocene *C. crocuta* post-cranial measurements. Numbers along the top of the graphs indicate marine oxygen isotope stages. LP = Late Pleistocene. See Table 10.55 for sample sizes of the boxplots.

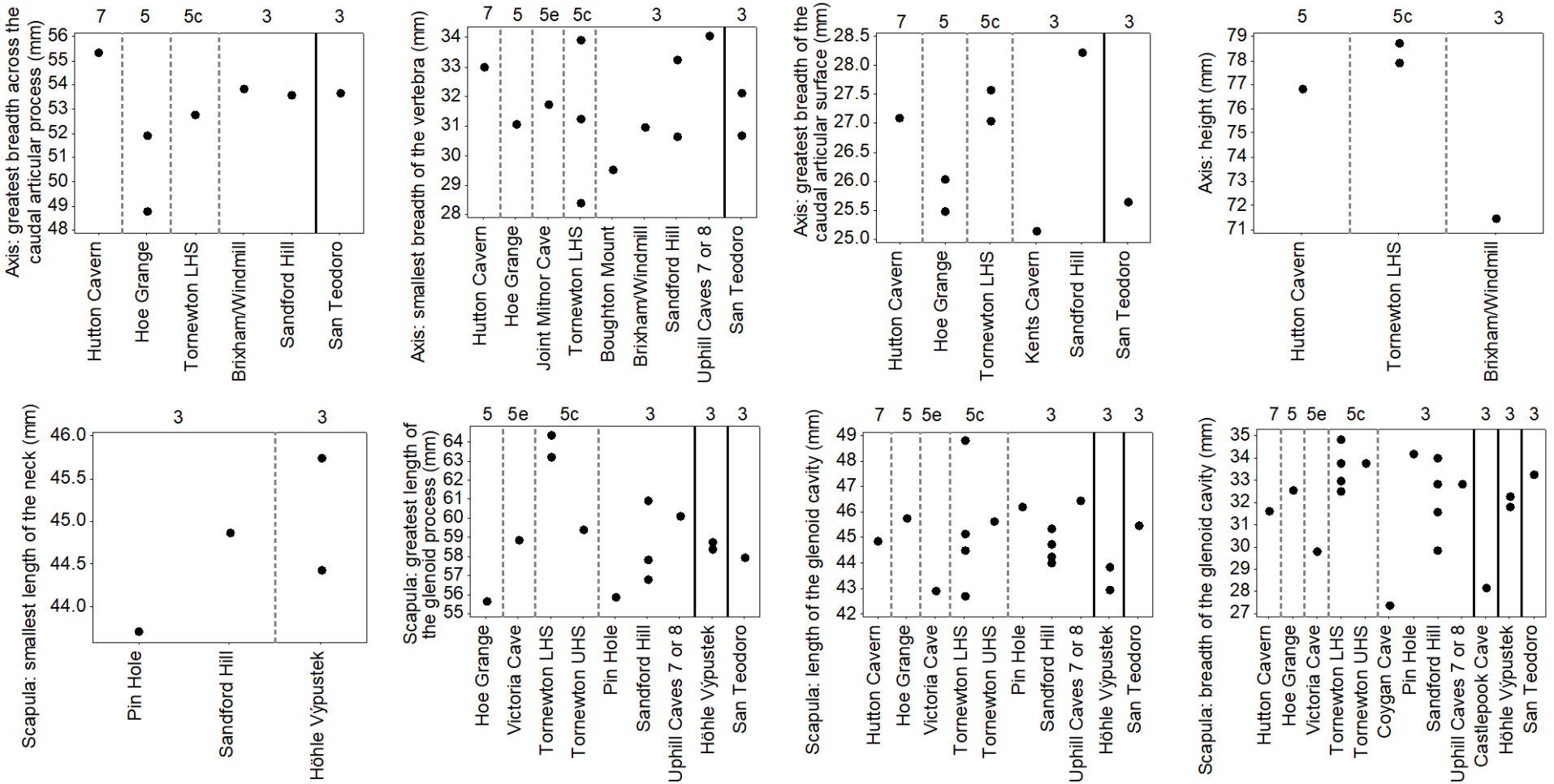

Figure 10.6 continued.

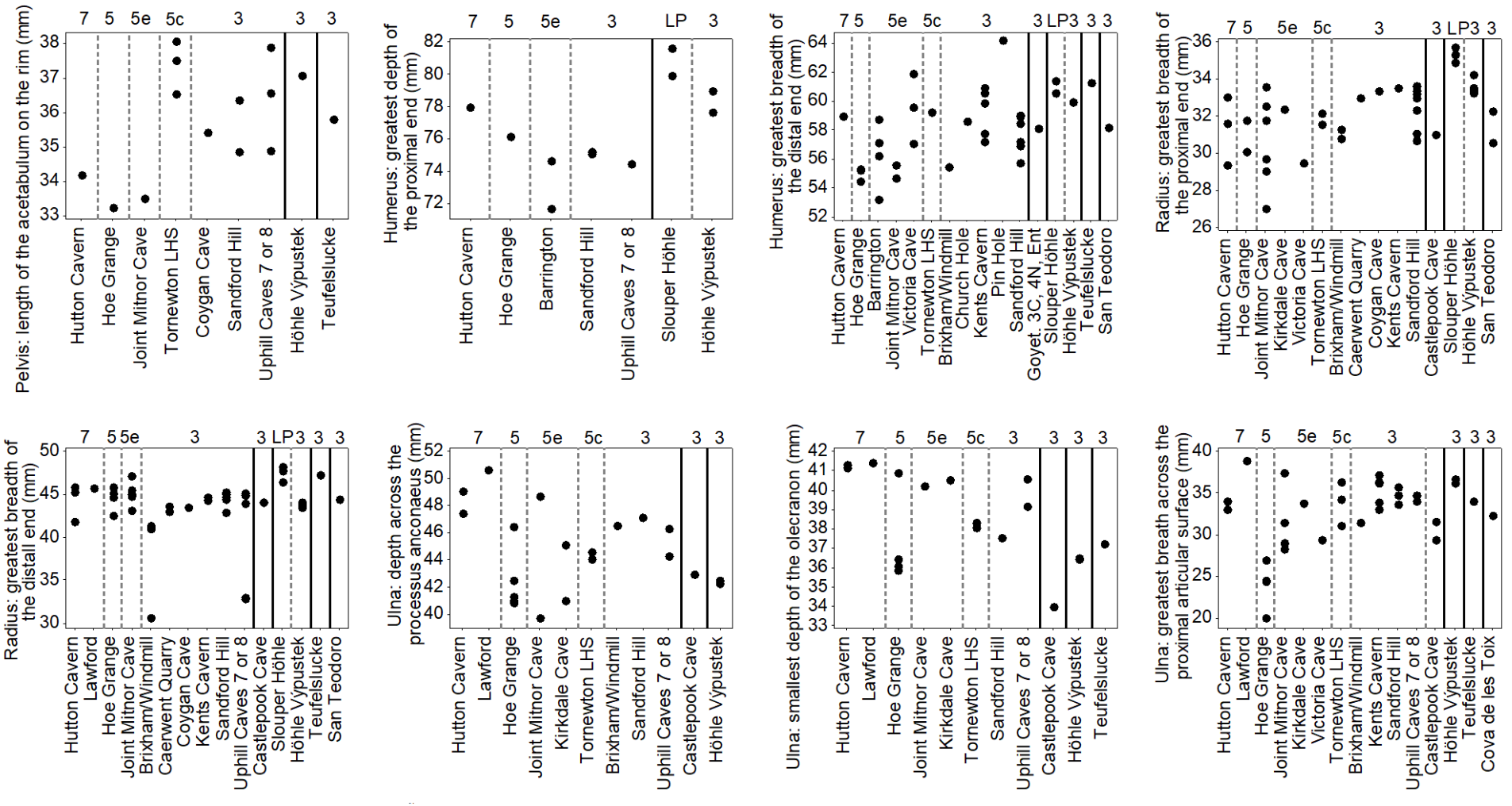

Figure 10.6 continued.

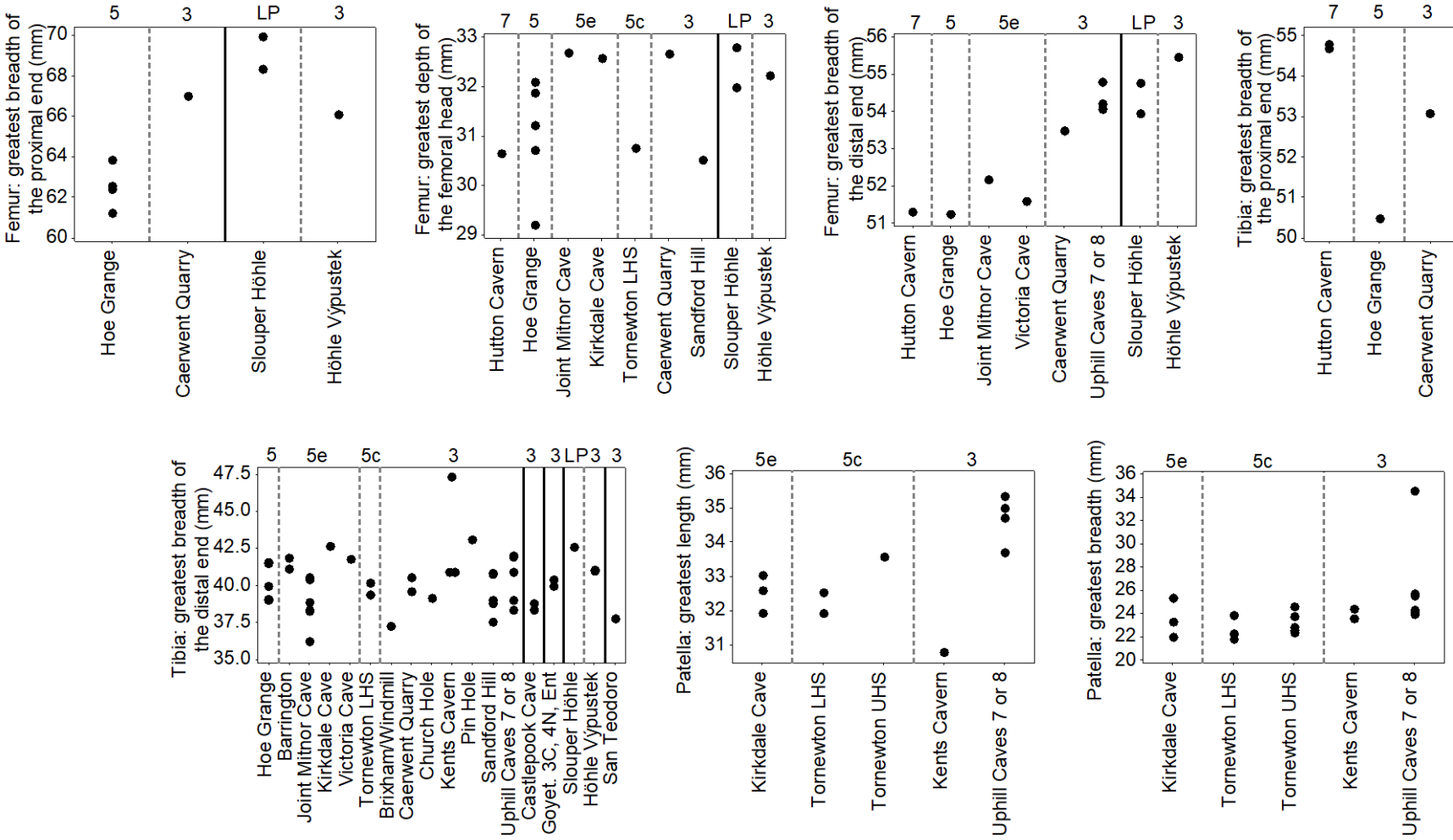

Figure 10.6 continued.

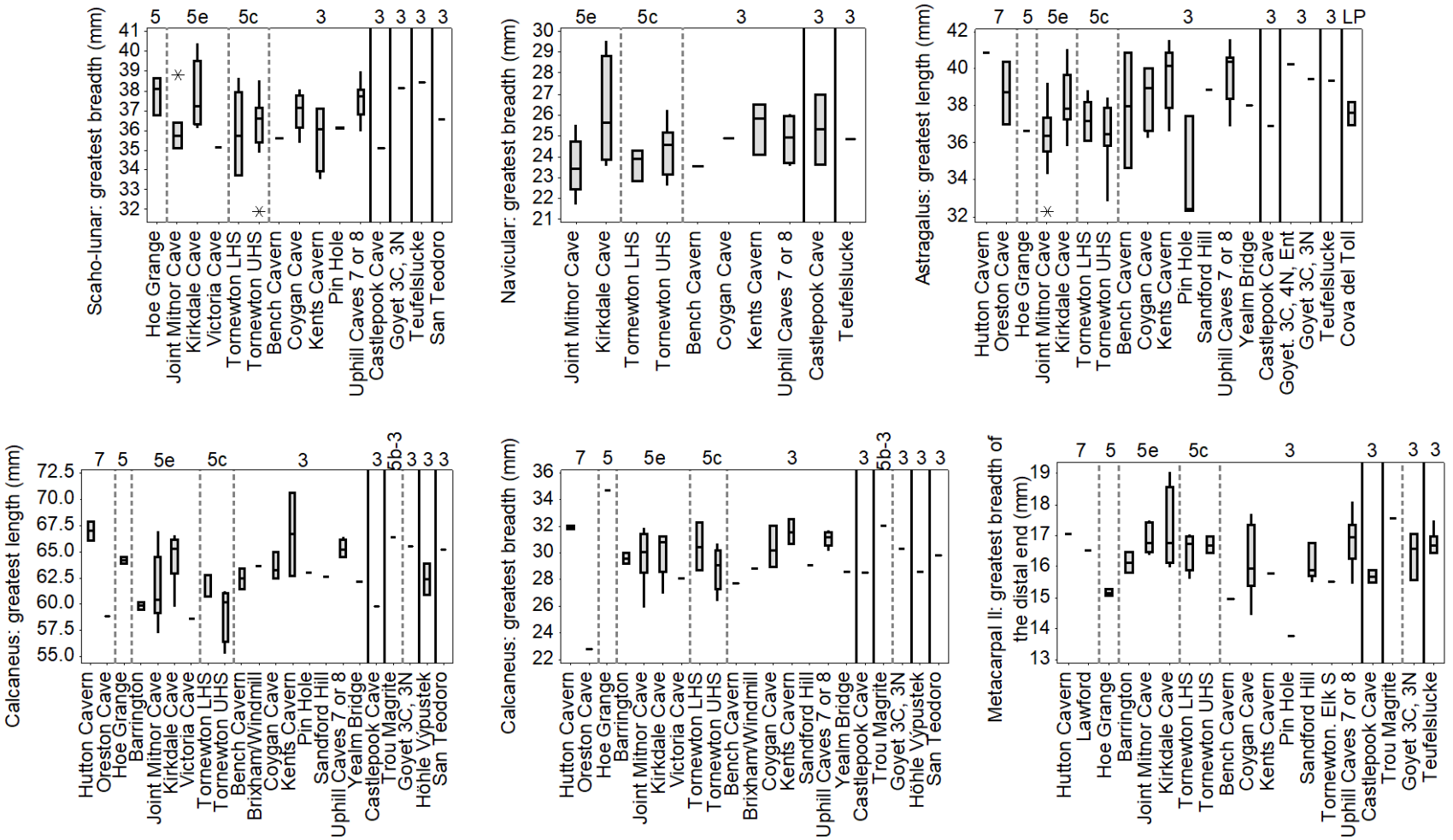

Figure 10.6 continued.

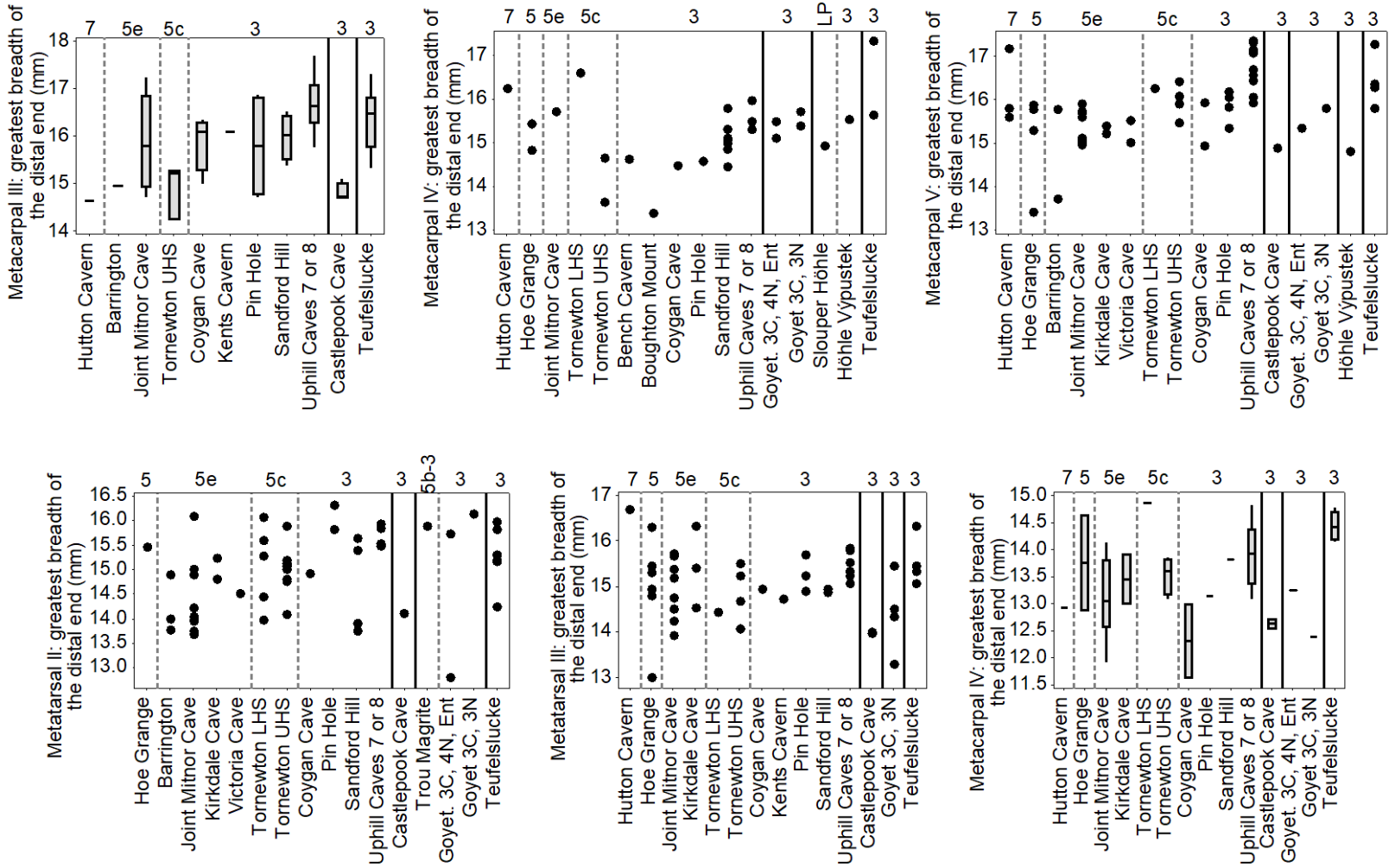

Figure 10.6 continued.

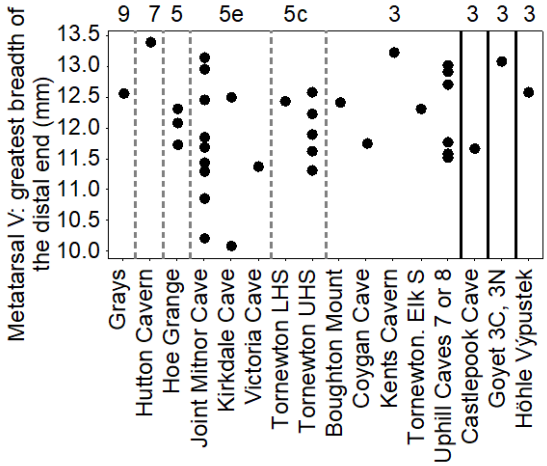

Figure 10.6 continued.

Table 10.55: Sample sizes of the boxplots in Figure 10.6.

Site	Scapho-lunar greatest breadth	Navicular greatest breadth	Astragalus greatest length	Calcaneus greatest length	Calcaneus greatest breadth	Metacarpal II greatest breadth of distal end	Metacarpal III greatest breadth of distal end	Metatarsal IV greatest breadth of distal end
Hutton Cavern			1	2	2	1	1	1
Lawford						1		
Oreston			2	1	1			
Hoe Grange	3		1	2	1	4		2
Barrington				2	2	2	1	
Joint Mitnor Cave	7	13	16	12	12	5	6	9
Kirkdale Cave	5	4	11	8	5	4		2
Victoria Cave	1			1	1			
Tornewton. LHS	7	3	7	3	3	4		1
Tornewton. UHS	19	19	14	4	5	2	3	4
Bench Cavern	1	1	3	2	1	1		
Brixham Cave/Windmill Hill				1	1			
Coygan Cave	6	1	4	3	3	7	4	2
Kents Cavern	4	3	5	2	2	1	1	
Pin Hole	2		3	1		1	4	1
Sandford Hill			1	1	1	5	9	1
Tornewton. Elk Stratum.						1		
Uphill Caves 7 or 8	16	6	11	8	6	10	9	8
Yealm Bridge			1	1	1			
Castlepook Cave	1	2	1	1	1	3	4	2
Trou Magrite				1	1	1		
Goyet. 3eme Caverne, 4eme Niveau Ossifère, Galleries Voisines de l'Entrée			1					1
Goyet. 3eme Caverne, 3eme Niveau	1		1	1	1	3		1
Höhle Výpustek				2	1			
Teufelslucke	1	1	1			7	7	4
San Teodoro	1			1	1			
Cova del Toll			2					

10.9 Radiocarbon models

Table 10.56: Radiocarbon dates on *C. crocuta* specimens used in the new chronology model. Original database compiled by Stuart and Lister (2014) with additional dates sourced from the literature. All dates are from specimens subjected to ultrafiltration pre-treatment. Dates modelled and calibrated using OxCal 4.3 (Bronk Ramsey, 2009) and the IntCal13 calibration curve (Reimer *et al*., 2013). 'Region' refers to the regions of Europe used in the model. NW = northwestern. C = central. SE = southwestern. S = southern. SW = southwestern. 68.2 % and 95.4 % are confidence intervals.

Site	Country	Region	Lab no.	14C BP		Modelled cal BP (68.2 %)		Modelled cal BP (95.4 %)		Reference
				Date	Error	From	To	From	To	
Bacho Kiro Cave	Bulgaria	SE	OxA-11421	51,500	2,400	50,003	49,406	50,003	48,548	Stuart and Lister (2014)
Hyaena Den	Britain	NW	OxA-13917	48,600	1,000	50,003	49,559	50,003	48,995	Jacobi *et al.* (2006)
Komarowa Cave	Poland	C	OxA-11062	46,100	900	49,823	48,284	50,003	47,399	Stuart and Lister (2014)
Scladina Cave	Belgium	NW	OxA-23789	46,000	2,400	49,935	47,487	50,003	45,917	Stuart and Lister (2014)
Castlepook Cave	Ireland	NW	OxA-19532	45,700	700	49,767	48,451	50,003	47,739	Stuart and Lister (2014)
Church Hole	Britain	NW	OxA-21996	45,400	2,200	49,815	47,132	50,003	45,732	Dodge *et al.* (2012)
Robin Hood Cave	Britain	NW	OxA-12771	45,300	1,000	49,624	47,766	50,003	46,884	Jacobi *et al.* (2006), Jacobi and Higham (2011)
Griffen Cave	Austria	C	VERA-1835	44,300	1,800/ 1,500	48,817	46,026	49,979	45,248	Hofreiter *et al.* (2004), Rohland *et al.* (2005)
Church Hole	Britain	NW	OxA-21995	44,200	2,000	49,252	46,069	50,003	45,057	Dodge *et al.* (2012)
Coygan Cave	Britain	NW	OxA-14401	43,000	2,100	48,539	44,828	49,953	43,897	Jacobi and Higham (2011), Higham *et al.* (2006)
Komarowa Cave	Poland	C	OxA-11158	42,200	800	46,278	44,814	47,386	44,196	Stuart and Lister (2014)
Komarowa Cave	Poland	C	OxA-11161	41,700	1,100	46,193	44,123	47,623	43,283	Stuart and Lister (2014)
Scladina Cave	Belgium	NW	OxA-23790	40,800	1,300	45,521	43,216	47,351	42,489	Stuart and Lister (2014)
Kents Cavern	Britain	NW	OxA-19509	40,200	600	44,363	43,272	44,947	42,882	Jacobi and Higham (2011)
Coygan Cave	Britain	NW	OxA-14403	39,700	1,700	45,212	42,266	47,858	41,345	Higham *et al.* (2006), Jacobi and Higham (2011)
Amalda	Spain	SW	OxA-10398	39,900	700	44,061	42,909	44,758	42,524	Stuart and Lister (2014)

La Adam Cave	Romania	SE	OxA-22128	39,100	1,000	43,867	42,283	44,962	41,749	Stuart and Lister (2014)
La Adam Cave	Romania	SE	OxA-22127	38,700	1,000	43,543	41,982	44,669	41,435	Stuart and Lister (2014)
Grotta Pocala	Italy	C	VERA-2532	38,220	920/820	43,069	41,746	44,126	41,140	Hofreiter *et al.* (2004), Rohland *et al.* (2005)
Pin Hole Cave	Britain	NW	OxA-15518	37,800	500	42,139	41,645	42,388	41,381	Jacobi and Higham (2011)
Pin Hole Cave	Britain	NW	OxA-15520	37,150	450					Jacobi and Higham (2011)
Kents Cavern	Britain	NW	OxA-11152	37,750	500	42,430	41,745	42,788	41,381	Stuart and Lister (2014)
Bench Quarry	Britain	NW	OxA-13324	37,500	900	41,874	41,207	42,170	40,781	Jacobi *et al.* (2006), Jacobi and Higham (2011)
Bench Quarry	Britain	NW	OxA-13512	36,800	450					Jacobi *et al.* (2006), Jacobi and Higham (2011)
La Adam Cave	Romania	SE	OxA-22129	36,850	750	42,034	40,748	42,569	40,019	Stuart and Lister (2014)
Scladina Cave	Belgium	NW	OxA-23791	36,450	750	41,734	40,359	42,306	39,633	Stuart and Lister (2014)
Coygan Cave	Britain	NW	OxA-14402	36,000	500	41,183	40,135	41,641	39,606	Higham *et al.* (2006), Jacobi and Higham (2011)
Melwurmhöhle	Austria	C	VERA-2540	35,900	600/560	41,442	40,216	41,931	39,558	Hofreiter *et al.* (2004), Rohland *et al.* (2005)
Duruitoarea Veche	Moldova	SE	OxA-11691	35,350	380	40,396	39,480	40,876	39,036	Stuart and Lister (2014)
Castlepook Cave	Ireland	NW	OxA-19531	33,240	220	37,932	37,003	38,291	36,698	Stuart and Lister (2014)
Grotte de Canacaude	France	SW	OxA-16691	33,130	220	37,727	36,825	38,168	36,550	Stuart and Lister (2014)
Magura Cave	Bulgaria	SE	OxA-31115	32,750	500	37,592	36,174	38,341	35,773	Ivanova *et al.* (2016)
Coygan Cave	Britain	NW	OxA-14473	32,400	550	37,131	35,647	38,149	35,252	Higham *et al.* (2006), Jacobi and Higham (2011)
Coygan Cave	Britain	NW	OxA-14400	32,140	250	36,296	35,765	36,579	35,465	Jacobi *et al.* (2006)
Igue du Gral	France	SW	OxA-20763	31,990	240	36,166	35,641	36,389	35,331	Stuart and Lister (2014)
Cefn Cave	Britain	NW	OxA-9698	31,900	450	36,270	35,315	36,883	34,844	Aldhouse-Green (n.d.) cited in Jacobi and Higham (2011)
Desnisukhi Peck Cave	Bulgaria	SE	OxA-11552	31,810	370	36,108	35,309	36,455	34,912	Stuart and Lister (2014)
Kents Cavern	Britain	NW	OxA-30351	30,630	380	35,148	34,371	35,622	34,075	Proctor *et al.* (2017)
Agios Georgios Cave	Greece	S	OxA-17009	29,340	240	33,797	33,282	33,957	32,931	Stuart and Lister (2014)

Grotta Paglicci	Italy	S	OxA-10657	29,100	1,600	33,917	31,465	35,758	30,631	Stuart and Lister (2014)
Arene Candide	Italy	SW	OxA-10658	27,050	550	31,639	30,672	32,753	30,223	Stuart and Lister (2014)
Balkan Range	Bulgaria	SE	OxA-11551	26,600	170	30,990	30,731	31,105	30,575	Stuart and Lister (2014)
Grotta Paglicci	Italy	S	OxA-10523	26,120	330	30,852	30,137	31,013	29,670	Stuart and Lister (2014)

Table 10.57: End boundaries of *C. crocuta* presence in each region of Europe. Boundaries modelled using OxCal 4.3 (Bronk Ramsey, 2009) and the IntCal13 calibration curve (Reimer *et al*., 2013). 68.2 % and 95.4 % are confidence intervals.

Region	**No. dates in region**	**End boundary (68.2 %)**		**End boundary (95.4 %)**	
		From	**To**	**From**	**To**
Northwestern	20	35,018	33,666	35,523	32,217
Central	6	41,259	38,375	41,880	33,898
Southeastern	8	30,944	28,237	31,073	22,741
Southern	3	30,769	27,954	31,024	20,330
Southwestern	4	31,691	26,233	32,722	8,898

Table 10.58: Radiocarbon dates on *P. leo* (*spelaea*) specimens used in the new chronology model. Original database compiled by Stuart and Lister (2011) with additional dates sourced from the literature. All dates are from specimens subjected to ultrafiltration pre-treatment. Dates modelled and calibrated using OxCal 4.3 (Bronk Ramsey, 2009) and the IntCal13 calibration curve (Reimer *et al*., 2013). 'Region' refers to the regions of Europe used in the model. NW = northwestern. C = central. SE = southwestern. SW = southwestern. 68.2 % and 95.4 % are confidence intervals.

Site	**Country**	**Region**	**Lab no.**	**14C BP**		**Modelled cal BP (68.2 %)**		**Modelled cal BP (95.4 %)**		**Reference and notes**
				Date	**Error**	**From**	**To**	**From**	**To**	
Emine-Bair-Khosar Cave	Ukraine	SE	OxA-17044	56400	2100					Excluded from model as too old. Stuart and Lister (2011)
Gamssulzen Höhle	Austria	C	OxA-13110	49900	2500	50003	49104	50003	48022	Barnett *et al.* (2009)
Zoolithenhöhle	Germany	C	OxA-14863	47600	900	50003	49477	50003	48803	Barnett *et al.* (2009)
Peştera Muierii	Romania	SE	OxA-16380	47500	900	50003	49379	50003	48629	Bronk Ramsey *et al.* (2009)
Jou'l Llobu	Spain	SW	OxA-10186	46400	2100	50003	47775	50003	46295	Stuart and Lister (2011)
Lathum	Netherlands	NW	OxA-16715	44850	650	48932	47312	49687	46713	Stuart and Lister (2011)
Peştera Urşilor	Romania	SE	OxA-22122	39000	1000	43788	42192	44897	41674	Stuart and Lister (2011)
Zawalona Cave	Poland	C	OxA-11156	38800	1100	43772	41994	44987	41392	Stuart and Lister (2011)
Wierchowska Górna	Poland	C	OxA-10087	38650	600	43058	42234	43655	41859	Barnett *et al.* (2009)
Peştera Urşilor	Romania	SE	OxA-22123	38600	1000	43453	41922	44608	41344	Stuart and Lister (2011)
Pin Hole	Britain	SW	OxA-19092	35650	450	40810	39764	41299	39280	Stuart and Lister (2011)
Peştera Cloşani	Romania	SE	OxA-22124	33150	500	38087	36660	38606	36193	Stuart and Lister (2011)
Peştera Cloşani	Romania	SE	OxA-22125	32500	450	37101	35849	38032	35515	Stuart and Lister (2011)
Lakatnik Cave	Bulgaria	SE	OxA-11422	31200	330	35500	34808	35930	34556	Stuart and Lister (2011)
Gremsdorf	Germany	C	OxA-14862	28310	150	32506	31863	32763	31627	Barnett *et al.* (2009)
Jaskinia Raj	Poland	C	OxA-11096	25190	350	29641	28825	30270	28559	Stuart and Lister (2011)
La Garma	Spain	SW	OxA-18698	13830	55	16864	16627	16959	16521	Cueto *et al.* (2016)
La Garma	Spain	SW	OxA-18699	13832	41					Cueto *et al.* (2016)

Urtiaga Cave	Spain	SW	OxA-10121	13770	120	16864	16443	17035	16274	Stuart and Lister (2011)
Abri des Cabones	France	NW	OxA-12021	12565	50	15064	14779	15149	14554	Stuart and Lister (2011)
Zigeunerfels Cave	Germany	C	OxA-17268	12375	50	14583	14221	14764	14135	Stuart and Lister (2011)

Table 10.59: End boundaries of *P. leo* (*spelaea*) presence in each region of Europe. Boundaries modelled using OxCal 4.3 (Bronk Ramsey, 2009) and the IntCal13 calibration curve (Reimer *et al*., 2013).

Region	**No. dates in region**	**End date (68.2 %)**		**End date (95.4 %)**	
		From	**To**	**From**	**To**
Northwestern	3	15024	2272	15078	-21847
Central	7	14580	9519	14783	-1495
Southeastern	6	35451	31997	35913	25202
Southwestern	3	16732	-18572	16790	-18575

Table 10.60: Radiocarbon dates on *C. antiquitatis* specimens used in the new chronology model. Original database compiled by Stuart and Lister (2012) with additional dates sourced from the literature. All dates are from specimens subjected to ultrafiltration pre-treatment. Dates modelled and calibrated using OxCal 4.3 (Bronk Ramsey, 2009) and the IntCal13 calibration curve (Reimer *et al*., 2013). 'Region' refers to the regions of Europe used in the model. NW = northwestern. N = Northern. C = central. SE = southwestern. SW = southwestern. 68.2 % and 95.4 % are confidence intervals.

Site	**Country**	**Region**	**Lab no.**	**14C BP**		**Modelled cal BP (68.2 %)**		**Modelled cal BP (95.4 %)**		**Reference and notes**
				Date	**Error**	**From**	**To**	**From**	**To**	
Pin Hole	Britain	NW	OxA-14197	55900	4000	50003	49679	50003	49214	Removed from figure as date out of range Jacobi *et al.* (2006)
Pin Hole	Britain	NW	OxA-12808	54000	2900	50003	49685	50003	49211	Removed from figure as date out of range Jacobi *et al.* (2006), Jacobi *et al.* (2009)
Pin Hole	Britain	NW	OxA-14211	53400	1700					Excluded from model as too old Higham *et al.* (2006)
Pin Hole	Britain	NW	OxA-14212	50200	1400					Excluded from model as too old Higham *et al.* (2006)
Pin Hole	Britain	NW	OxA-14720	53300	3400	50003	49491	50003	48716	Removed from figure as date out of range Jacobi *et al.* (2009)
Pin Hole	Britain	NW	OxA-14717	52900	1900	50003	49878	50003	49792	Removed from figure as date out of range Jacobi *et al.* (2009)
Pin Hole	Britain	NW	OxA-13880	52500	2800	50003	49534	50003	48842	Removed from figure as date out of range Jacobi *et al.* (2006)
Clifford Hill	Britain	NW	OxA-19559	49800	1000	50003	49791	50003	49475	Removed from figure as date out of range

										Jacobi *et al.* (2009)
Settepolesini	Italy	C	OxA-10522	49100	2300	50003	48817	50003	47641	Stuart and Lister (2012)
Pin Hole	Britain	NW	OxA-14719	49000	1300	50003	49569	50003	48925	Jacobi *et al.* (2009)
North Sea		NW	OxA-16297	48100	1100	50003	49492	50003	48800	Lorenzen *et al.* (2011)
North Sea		NW	OxA-16296	47900	1200	50003	49360	50003	48559	Lorenzen *et al.* (2011)
North Sea		NW	OxA-16294	47400	1200	50003	49200	50003	48274	Lorenzen *et al.* (2011)
North Sea		NW	OxA-16299	47100	1200	50003	49065	50003	48065	Lorenzen *et al.* (2011)
Coygan Cave	Britain	NW	OxA-16647	45800	1400	50003	48144	50003	46803	Jacobi *et al.* (2009)
North Sea		NW	OxA-16295	45200	1000	49651	47656	50003	46826	Lorenzen *et al.* (2011)
Kents Cavern	Britain	NW	OxA-14761	45000	2200	49936	46903	50003	45482	Higham *et al.* (2006), Jacobi *et al.* (2006)
Pin Hole	Britain	NW	OxA-13881	45000	750	48104	46614	48933	46105	Higham *et al.* (2006), Jacobi *et al.* (2006)
Pin Hole	Britain	NW	OxA-13682	41900	900					Jacobi *et al.* (2009)
Tropfsteinhöhle Kugelstein	Austria	C	OxA-10737	44900	1800	49503	46773	50003	45751	Stuart and Lister (2012)
Koblenz - Metternich	Germany	NW	OxA-10893	44700	900	49097	47032	49917	46438	Stuart and Lister (2012)
Pin Hole	Britain	NW	OxA-15521	43700	1000	48101	45922	49387	45323	Jacobi *et al.* (2009)
Pin Hole	Britain	NW	OxA-13592	43350	650	47266	45852	48193	45388	Jacobi *et al.* (2006)
Whitemoor Haye Quarry	Britain	NW	OxA-15843	43350	500	46095	45546	46403	45280	Schreve *et al.* (2013)
Whitemoor Haye Quarry	Britain	NW	OxA-15844	42850	450					Schreve *et al.* (2013)
Whitemoor Haye Quarry	Britain	NW	OxA-15845	41690	400					Schreve *et al.* (2013)
Goat's Hole, Paviland	Britain	NW	OxA-13657	42650	800	46718	45170	47860	44595	Jacobi and Higham (2008)
Labeko Koba	Spain	SW	OxA-10102	41500	2000	47016	43278	49412	42625	Stuart and Lister (2012)
Robin Hood Cave	Britain	NW	OxA-15484	40550	400	44519	43691	44895	43325	Jacobi *et al.* (2009)
Herne West	Germany	NW	OxA-15798	40500	450	44500	43608	44940	43242	Lorenzen *et al.* (2011)

Bradley Fen	Britain	NW	OxA-31962	40400	1200	45079	43035	46549	42362	Briant *et al.* (2018)
Picken's Hole	Britain	NW	OxA-10804	40200	700	44449	43216	45123	42783	Jacobi *et al.* (2007) cited in Jacobi *et al.* (2009)
Sutton Courtenay	Britain	NW	OxA-20989	39200	800	43716	42440	44581	42047	Hopkins *et al.* (2016)
Grange Farm	Britain	NW	OxA-21310	38800	390	43001	42459	43323	42197	Cooper *et al.* (2012)
Duruitoarea Veche	Moldova	SE	OxA-11690	38550	500	42912	42240	43340	41925	Stuart and Lister (2012)
Grange Farm	Britain	NW	OxA-22149	38400	900	43187	41854	44242	41324	Cooper *et al.* (2012)
Grange Farm	Britain	NW	OxA-21309	38120	360	42560	42065	42821	41827	Cooper *et al.* (2012)
Ash Tree Cave	Britain	NW	OxA-14196	37540	370	42207	41675	42480	41395	Jacobi *et al.* (2009)
Kents Cavern	Britain	NW	OxA-13965	37200	550	42127	41289	42533	40754	Higham *et al.* (2006), Jacobi *et al.* (2006)
Geißenklösterle	Germany	C	OxA-21744	36850	750	42042	40748	42574	40037	Higham *et al.* (2012)
Kents Cavern	Britain	NW	OxA-27527	36700	750	41919	40615	42471	39872	Proctor *et al.* (2017)
Kents Cavern	Britain	NW	OxA-30161	36500	750	41778	40402	42341	39690	Proctor *et al.* (2017)
Kents Cavern	Britain	NW	OxA-14210	36370	320	41000	40406	41266	40138	Higham *et al.* (2006), Jacobi *et al.* (2006)
Kents Cavern	Britain	NW	OxA-14701	35650	330					Higham *et al.* (2006), Jacobi *et al.* (2006)
Kents Cavern	Britain	NW	OxA-27444	36100	700	41435	40062	42013	39346	Proctor *et al.* (2017)
Kents Cavern	Britain	NW	OxA-13921	36040	330	41081	40313	41411	39961	Higham *et al.* (2006), Jacobi *et al.* (2006)
Kents Cavern	Britain	NW	OxA-30274	34950	650	40192	38784	41109	38313	Proctor *et al.* (2017)
Goat's Hole, Paviland	Britain	NW	OxA-13377	33800	200	38587	38071	38770	37628	Jacobi and Higham (2008)
Wilderness Pit	Britain	NW	OxA-19560	31140	170	35200	34809	35444	34659	Jacobi *et al.* (2009)
Goyet Caves	Belgium	NW	OxA-12120	29330	160	33754	33413	33891	33145	Stuart and Lister (2012)
Goyet Caves	Belgium	NW	OxA-12119	28470	140	32775	32151	32950	31810	Stuart and Lister (2012)
Szczecin	Poland	N	OxA-11059	28450	250	32820	31955	33183	31600	Stuart and Lister (2012)
Wildscheuer Cave	Germany	NW	OxA-10892	25290	170	29555	29104	29808	28887	Stuart and Lister (2012)
Goyet Caves	Belgium	NW	OxA-11291	23560	230	27863	27519	28122	27351	Stuart and Lister (2012)
Deszczowa Cave	Poland	C	OxA-11060	20800	150	25347	24854	25493	24560	Wojtal (2007) and Nadachowski *et al.* (2009) cited in Lorenc (2013)
Jasna Cave	Poland	C	OxA-11095	17880	100	21820	21527	21935	21355	Stuart and Lister (2012)

Jasna Cave	Poland	C	OxA-11159	16140	90	19604	19340	19741	19203	Stuart and Lister (2012)
Kesslerloch Cave	Switzerland	C	OxA-10238	14330	110	17627	17300	17794	17125	Stuart and Lister (2012)
Gönnersdorf	Germany	NW	OxA-10200	13810	90	16699	16408	16855	16313	Stuart and Lister (2012)
Gönnersdorf	Germany	NW	OxA-10201	13610	80					Stuart and Lister (2012)

Table 10.61: End boundaries of *C. antiquitatis* presence in each region of Europe. Boundaries modelled using OxCal 4.3 (Bronk Ramsey, 2009) and the IntCal13 calibration curve (Reimer *et al*., 2013).

Region	**No. dates in region**	**End date (68.2 %)**		**End date (95.4 %)**	
		From	**To**	**From**	**To**
Northwestern	43	16677	15819	16846	14613
Northern	1	32618	27958	32692	27958
Central	7	17583	12543	17794	1898
Southeastern	1	42841	36303	42868	36303
Southwestern	1	46038	29153	46904	29153

Table 10.62: Radiocarbon dates on *C. elaphus* specimens used in the new chronology model. All dates are from specimens subjected to ultrafiltration pre-treatment. Dates modelled and calibrated using OxCal 4.3 (Bronk Ramsey, 2009) and the IntCal13 calibration curve (Reimer *et al*., 2013). 'Region' refers to the regions of Europe used in the model. NW = northwestern. C = central. SE = southwestern. SW = southwestern. 68.2 % and 95.4 % are confidence intervals.

Site	**Country**	**Region**	**Lab no.**	**14C BP**		**cal BP (68.2 %)**		**cal BP (95.4 %)**		**Reference and notes**
				Date	**Error**	**From**	**To**	**From**	**To**	
El Castillo	Spain	SW	OxA-22205	49400	3700	...	49083	...	49875	Wood *et al.* (2018)
Cova de les Toixoneres	Spain	SW	MAMS-18671	47200	670	...	49795	...	49973	Talamo *et al.* (2016)
Hyaena Den	Britain	NW	OxA-13915	45100	1000	49523	47544	...	46740	Jacobi *et al.* (2006)
El Castillo	Spain	SW	OxA-21974	44900	2100	49759	46918	...	45488	Wood *et al.* (2018)
L'Arbreda	Spain	SW	OxA-21702	44400	1900	49305	46340	...	45310	Wood *et al.* (2014)
El Castillo	Spain	SW	OxA-22202	43100	1700	48249	45049	49945	44359	Wood *et al.* (2018)
El Castillo	Spain	SW	OxA-22403	42700	1600	47825	44695	49690	43895	Wood *et al.* (2018)
El Castillo	Spain	SW	OxA-22203	42000	1500	47035	44063	49051	43181	Wood *et al.* (2018)
Saint-Marcel	France	SW	OxA-19624	41300	1700	46464	43270	48946	42570	Szmidt *et al.* (2010)
Cova de les Toixoneres	Spain	SW	MAMS-18669	40800	320	44695	44021	45011	43651	Talamo *et al.* (2016)
Pestera cu Oase	Romania	SE	OxA-22097	40700	1300	45426	43163	47266	42415	Meiri *et al.* (2013)
Trou Al'Wesse	Belgium	NW	OxA-22098	40200	1300	45020	42848	46731	42099	Meiri *et al.* (2013)
Geißenklösterle	Germany	C	OxA-21657	39400	1100	44208	42446	45418	41846	Higham *et al.* (2012)
L'Arbreda	Spain	SW	OxA-21704	39200	1000	43939	42350	45029	41825	Wood *et al.* (2014)
El Castillo	Spain	SW	OxA-22201	39100	1000	43855	42275	44960	41750	Wood *et al.* (2018)
Labeko Koba	Spain	SW	OxA-22562	38100	900	42970	41676	43990	41010	Wood *et al.* (2014)
Labeko Koba	Spain	SW	OxA-22561	38000	900	42903	41607	43890	40886	Wood *et al.* (2014)
Saint-Marcel	France	SW	OxA-19623	37850	550	42521	41779	42923	41384	Szmidt *et al.* (2010)
Saint-Marcel	France	SW	OxA-19625	37850	600	42556	41745	43010	41305	Szmidt *et al.* (2010)
Labeko Koba	Spain	SW	OxA-22563	37800	900	42776	41462	43665	40637	Wood *et al.* (2014)
Labeko Koba	Spain	SW	OxA-22560	37400	800	42447	41237	43046	40446	Wood *et al.* (2014)

L'Arbreda	Spain	SW	OxA-21662	37300	800	42385	41149	42968	40353	Wood *et al.* (2014)
Cova de les Toixoneres	Spain	SW	MAMS-17600	36850	211	41675	41266	41871	41037	Talamo *et al.* (2016)
Kents Cavern	Britain	NW	OxA-13457	35550	750	41005	39395	41651	38700	Higham *et al.* (2011), Jacobi and Higham (2011)
El Castillo	Spain	SW	OxA-21713	35000	600	40187	38871	40988	38433	Tejero *et al.* (2012), Wood *et al.* (2018)
L'Arbreda	Spain	SW	OxA-21703	32300	450	36423	35732	36914	35348	Wood *et al.* (2014)
L'Arbreda	Spain	SW	OxA-21663	32100	450					Wood *et al.* (2014)
Kents Cavern	Britain	NW	OxA-27443	32200	450	36625	35561	37532	35100	Proctor *et al.* (2017)
La Viña	Spain	SW	OxA-21678	31600	400	35912	35066	36309	34734	Wood *et al.* (2014)
La Viña	Spain	SW	OxA-21689	31500	400	35800	34967	36231	34671	Wood *et al.* (2014)
Kents Cavern	Britain	NW	OxA-30352	30850	400	35166	34385	35629	34066	Proctor *et al.* (2017)
La Viña	Spain	SW	OxA-21687	30600	370	34868	34204	35285	33922	Wood *et al.* (2014)
Kents Cavern	Britain	NW	OxA-21106	30000	180	34225	33885	34445	33747	Higham *et al.* (2011), Jacobi and Higham (2011)
L'Arbreda	Spain	SW	OxA-21781	28260	280	32553	31679	32977	31423	Wood *et al.* (2014)
Cova del Parpalló	Spain	SW	OxA-26345	21580	140	25983	25748	26099	25615	Bronk Ramsey *et al.* (2015)
La Viña	Spain	SW	OxA-21686	20820	130	25348	24925	25487	24611	Wood *et al.* (2014)
Cova del Parpalló	Spain	SW	OxA-22890	19690	110	23876	23567	24026	23412	Bronk Ramsey *et al.* (2015)
Bordes-Fitte rockshelter	France	NW	OxA-22315	19020	110	23057	22722	23262	22555	Aubry *et al.* (2012)
Cova del Parpalló	Spain	SW	OxA-26342	18640	100	22599	22393	22780	22312	Bronk Ramsey *et al.* (2015)
Cova del Parpalló	Spain	SW	OxA-26343	18520	100	22500	22300	22638	22118	Bronk Ramsey *et al.* (2015)

Table 10.63: Radiocarbon dates on *R. tarandus* specimens used in the new chronology model. All dates are from specimens subjected to ultrafiltration pre-treatment. Dates modelled and calibrated using OxCal 4.3 (Bronk Ramsey, 2009) and the IntCal13 calibration curve (Reimer *et al*., 2013). 'Region' refers to the regions of Europe used in the model. NW = northwestern. C = central. SW = southwestern. 68.2 % and 95.4 % are confidence intervals.

Site	Country	Region	Lab no.	14C BP		cal BP (68.2 %)		cal BP (95.4 %)		Reference and notes
				Date	Error	From	To	From	To	
Kents Cavern	Britain	NW	OxA-14714	49600	2200	...	49674	...	49959	Higham *et al.* (2006), Jacobi *et al.* (2006)
La Chauverie	France	SW	OxA-23693	49000	3400	...	49055	...	49869	Discamps (2011) cited in Discamps *et al.* (2012)
Robin Hood Cave	Britain	NW	OxA-12772	47300	1200	...	49534	...	49932	Jacobi *et al.* (2006)
Jaskinia Mamutowa	Poland	C	OxA-14405	46400	1200	...	48722	...	47538	Wojtal (2007) cited in Lorenc (2013)
Pin Hole	Britain	NW	OxA-11796	44200	800	48397	46545	49453	45952	Higham *et al.* (2006), Jacobi *et al.* (2006)
Pontnewydd	Britain	NW	OxA-14055	41400	1400	46207	43560	48313	42793	Debenham *et al.* (2012)
Bordes-Fitte rockshelter	France	NW	OxA-22316	41200	1300	45884	43493	47804	42739	Aubry *et al.* (2012)
Pin Hole	Britain	NW	OxA-11797	40650	500	44683	43710	45145	43286	Higham *et al.* (2006), Jacobi *et al.* (2006)
Goat's Hole, Paviland	Britain	NW	OxA 13439	40570	370	44515	43744	44869	43380	Jacobi and Higham (2008)
Kents Cavern	Britain	NW	OxA-13888	40000	700	44275	43076	44976	42655	Higham *et al.* (2006), Jacobi *et al.* (2006)
Pontnewydd	Britain	NW	OxA-14052	39600	900	44150	42690	45082	42195	Debenham *et al.* (2012)
Čertova díra	Czech Republic	C	OxA-22448	39500	1100	44282	42516	45486	41913	Neruda and Nerudová (2013)
Jaskinia Mamutowa	Poland	C	OxA-14404	38250	550	42759	42031	43192	41671	Wojtal (2007) cited in Lorenc (2013)
Pin Hole	Britain	NW	OxA-11980	37760	340	42330	41847	42578	41599	Jacobi *et al.* (2006)
Jaskinia Mamutowa	Poland	C	OxA-14408	37550	450	42269	41631	42596	41292	Wojtal (2007) cited in Lorenc (2013)

Goat's Hole, Paviland	Britain	NW	OxA 13658	37350	320	42061	41580	42296	41315	Jacobi and Higham (2008)
Geißenklösterle	Germany	C	OxA-21746	36850	800	42067	40709	42650	39935	Higham *et al.* (2012)
Geißenklösterle	Germany	C	OxA-21745	36650	750	41884	40559	42437	39830	Higham *et al.* (2012)
Geißenklösterle	Germany	C	OxA-21743	36100	700	41429	40057	42004	39333	Higham *et al.* (2012)
Abri Pataud	France	SW	OxA-21578	35750	700	41150	39680	41731	38946	Higham *et al.* (2011)
Kents Cavern	Britain	NW	OxA-30272	35100	650	40351	38921	41176	38457	Proctor *et al.* (2017)
Geißenklösterle	Germany	C	OxA-21659	35050	600	40243	38917	41021	38475	Higham *et al.* (2012)
Abri Pataud	France	SW	OxA-21579	35000	600	40240	38826	41129	38368	Higham *et al.* (2011)
Abri Pataud	France	SW	OxA-21597	35000	650	40187	38871	40988	38433	Higham *et al.* (2011)
Kents Cavern	Britain	NW	OxA-30162	34850	600	40029	38738	40911	38285	Proctor *et al.* (2017)
Abri Pataud	France	SW	OxA-21599	34850	600	40029	38738	40911	38285	Higham *et al.* (2011)
Bordes-Fitte rockshelter	France	NW	Lyon-6920 (SacA18936)	34520	850	40186	38181	41095	36925	Aubry *et al.* (2012)
Abri Pataud	France	SW	OxA-21596	34500	600	39749	38435	40581	37576	Higham *et al.* (2011)
Kůlna Cave	Czech Republic	C	OxA-25297	34350	600	39672	38281	40365	37240	Bronk Ramsey *et al.* (2015)
Abri Pataud	France	SW	OxA-21671	34300	600	39640	38212	40285	37139	Higham *et al.* (2011)
Abri Pataud	France	SW	OxA-21600	34200	550	39475	38118	40055	37120	Higham *et al.* (2011)
Abri Pataud	France	SW	OxA-21581	33550	550	38545	37066	39160	36385	Higham *et al.* (2011)
Abri Pataud	France	SW	OxA-21670	33450	500	38415	37036	38885	36390	Higham *et al.* (2011)
Geißenklösterle	Germany	C	OxA-21661	32900	450	37669	36364	38371	36045	Higham *et al.* (2012)
Goat's Hole, Paviland	Britain	NW	OxA-13438	31990	180	36120	35691	36298	35469	Jacobi and Higham (2008)
Pontnewydd	Britain	NW	OxA-13993	30240	230	34485	34045	34694	33869	Debenham *et al.* (2012)
Champ de Fouilles	Belgium	NW	OxA-18010	28650	200	33121	32393	33388	31935	Jacobi *et al.* (2010)
Abri Pataud	France	SW	OxA-21588	28250	280	32539	31666	32966	31417	Higham *et al.* (2011)
Abri Pataud	France	SW	OxA-21586	28230	290	32520	31636	32966	31393	Higham *et al.* (2011)

Čertova díra	Czech Republic	C	OxA-22449	28160	280	32412	31569	32862	31364	Neruda and Nerudová (2013)
Abri Pataud	France	SW	OxA-21587	28150	290	32411	31554	32876	31346	Higham *et al.* (2011)
Champ de Fouilles	Belgium	NW	OxA-18007	27950	170	31883	31419	32339	31294	Jacobi *et al.* (2010)
Pontnewydd	Britain	NW	OxA-13984	25210	120	29430	29078	29586	28916	Debenham *et al.* (2012)
Goat's Hole, Paviland	Britain	NW	OxA-17560	24240	110	28197	27916	28371	27811	Jacobi and Higham (2008)
Goat's Hole, Paviland	Britain	NW	OxA-16602	23700	140					Jacobi and Higham (2008)
Jaskinia Mamutowa	Poland	C	OxA-14409	20650	100	25070	24653	25226	24505	Wojtal (2007) cited in Lorenc (2013)
Kastelhöhle	Switzerland	C	OxA-9738	19620	140	23841	23461	24016	23230	Bronk Ramsey *et al.* (2002)
Kastelhöhle	Switzerland	C	OxA-9739	19200	150	23356	22935	23550	22730	Bronk Ramsey *et al.* (2002)
Les Harpons	France	SW	OxA-26878	18960	110	22976	22659	23134	22507	Bronk Ramsey *et al.* (2015)
Kastelhöhle	Switzerland	C	OxA-9737	18530	150	22565	22231	22746	21975	Bronk Ramsey *et al.* (2002)
Les Harpons	France	SW	OxA-26876	18450	100	22454	22223	22524	21999	Bronk Ramsey *et al.* (2015)

10.10 Spreadsheet details

The data in the spreadsheets (on disc) are as follows:

- Spreadsheet 1 – present-day predator and prey biomass, climatic conditions and vegetation cover
- Spreadsheet 2 – present-day *C. crocuta* body mass, body mass sexual size dimorphism, predator density, prey biomass, climatic conditions and vegetation cover
- Spreadsheet 3 – present-day morphometric sites with climate data and vegetation cover
- Spreadsheet 4 – present-day craniodental morphometrics and calculations of mandibular bending strength, mandibular mechanical advantage, ontogeny and sexual size dimorphism
- Spreadsheet 5 – present-day post-cranial morphometrics and calculations of post-cranial indices, ontogengy and sexual size dimorphism
- Spreadsheet 6 – present-day tooth breakage data
- Spreadsheet 7 – Pleistocene crandiodental morphometrics and calculations of mandibular bending strength and mandibular mechanical advantage
- Spreadsheet 8 – Pleistocene post-cranial morphometrics and calculations of post-cranial indices
- Spreadsheet 9 – Pleistocene body mass reconstructions
- Spreadsheet 10 – Pleistocene tooth wear and breakage data